

HYDROLOGIC ANALYSIS OF THE RIO GRANDE BASIN NORTH  
OF EMBUDO, NEW MEXICO, COLORADO AND NEW MEXICO

By Glenn A. Hearne and Jack D. Dewey

---

U.S. GEOLOGICAL SURVEY

Water-Resources Investigations Report 86-4113



Denver, Colorado  
1988

DEPARTMENT OF THE INTERIOR  
DONALD PAUL HODEL, Secretary  
U.S. GEOLOGICAL SURVEY  
Dallas L. Peck, Director

---

For additional information  
write to:

Colorado District Chief  
U.S. Geological Survey  
Water Resources Division  
Box 25046, Mail Stop 415  
Denver Federal Center  
Denver, CO 80225

Copies of this report can  
be purchased from:

U.S. Geological Survey  
Books and Open-File Reports  
Federal Center, Bldg. 41  
Box 25425  
Denver, CO 80225  
[Telephone: (303) 236-7476]

# CONTENTS

	Page
Abstract-----	1
Introduction-----	2
Purpose of the study-----	2
Scope of report-----	2
Geographic setting-----	5
Geohydrologic setting-----	7
History of agricultural development-----	11
Significance of water resources-----	12
The San Juan Mountains-----	14
Water-budget model of the San Juan Mountains-----	15
Temperature-----	20
Precipitation-----	21
Snowmelt-----	23
Sublimation-----	24
Evapotranspiration-----	24
Water stored in the snowpack-----	27
Water stored in the root zone-----	27
Flow from the San Juan Mountains to the Alamosa Basin-----	28
The Sangre de Cristo Mountains-----	30
Regression model of water yield from the Sangre de Cristo Mountains-----	31
Flow from the Sangre de Cristo Mountains to the Alamosa Basin and the Costilla Plains-----	33
The San Luis Hills-----	33
The Taos Plateau-----	35
Regression model of water yield from the Taos Plateau-----	36
Flow from the Taos Plateau to the Rio Grande-----	38
The Costilla Plains-----	38
Calculated evapotranspiration for the Costilla Plains-----	39
Water budget for the Costilla Plains-----	40
The Alamosa Basin-----	42
Calculated evapotranspiration for the Alamosa Basin-----	44
Water budget for the Alamosa Basin-----	49
Digital models of ground-water flow-----	50
Evaluation of representation using a two-dimensional model-----	51
Evaluation of initial condition using a two-dimensional model--	60
Initial steady-state condition-----	60
1950 condition-----	61
Aquifer characteristics in the three-dimensional model-----	63
Alamosa Formation, not including clay series-----	65
Clay series of Alamosa Formation-----	65
Santa Fe Formation, above 1,300 feet-----	65
Santa Fe Formation, with intercalated volcanic rocks-----	67
Santa Fe Formation, below 1,300 feet-----	67
Fault zone-----	67
Representation of change in recharge and discharge-----	73
Ground-water withdrawals-----	75
Return flow from irrigation-----	87
Evapotranspiration salvage-----	91
Streamflow capture-----	93

	Page
Analysis of 1950-80 changes: calibration-----	94
Analysis of 1950-80 changes: sensitivity-----	100
Priorities for data collection-----	104
Projected response to withdrawals in nonirrigated areas-----	106
Summary-----	109
Selected references-----	113
Supplemental data	
Attachment 1. Input file to define aquifer characteristics and hydraulic-head-dependent boundaries-----	122
Attachment 2. Input file for the 1950-79 transient simulation-----	167

## PLATE

Plate 1. Map showing location of the study area and flows calculated from mountain water-budget model and regression models of water yield-----In pocket

## FIGURES

	Page
Figure 1. Map showing location of the eastern part of the Southwest Alluvial Basins study area-----	3
2. Map showing physiographic subdivisions of the study area-----	6
3-7. Diagrams showing:	
3. Modes of occurrence of ground water-----	8
4. Generalized west-to-east section across the Alamosa Basin-----	9
5. Generalized west-to-east section across the Taos Plateau and the Costilla Plains-----	10
6. Movement of water as represented in the water-budget model of the San Juan Mountains-----	16
7. Flow chart of the water-budget model of the San Juan Mountains-----	18
8. Map showing example subarea in the Goose Creek drainage basin-----	19
9. Graph showing relation assumed between evapotranspiration from ground water and depth to water-----	45
Figures 10-15. Graphs showing section model:	
10. With three layers-----	54
11. Having equal layers 100 feet thick, equivalent to three-layer model-----	55
12. With seven layers-----	56
13. Having equal layers 100 feet thick, equivalent to seven-layer model-----	57
14. With nine layers-----	58
15. Having equal layers 100 feet thick, equivalent to nine-layer model-----	59
16. Transmissivity representing the unconfined aquifer, layer seven (top layer) of the three-dimensional model-----	64
17. Hydraulic conductivity represented in row 26 of the three-dimensional model-----	66
18. Hydraulic conductivity represented in column 11 from row 25 to row 49 of the three-dimensional model-----	68



Figures 19-22.	Graphs showing hydraulic conductivity of the upper confined aquifer, represented in the three-dimensional model as:	
19.	Layer six-----	69
20.	Layer five-----	70
21.	Layer four-----	71
22.	Layer three-----	72
23.	Graph showing ground-water withdrawals and surface-water diversions for irrigation-----	76
24.	Irrigated area represented in the three-dimensional model-----	78
25.	Graph showing subareas where irrigation was supplemented by ground-water withdrawals-----	80
26-30.	Graphs showing ground-water withdrawals represented in the three-dimensional model in:	
26.	Layer seven-----	82
27.	Layer six-----	83
28.	Layer five-----	84
29.	Layer four-----	85
30.	Layer three-----	86
31-33.	Graphs showing recharge to layer seven of the three-dimensional model representing:	
31.	Return flow from irrigation-----	88
32.	Return flow from sprinkler irrigation-----	89
33.	Return flow from gravity irrigation-----	90
34-38.	Graphs showing:	
34.	Comparison between simulated and measured decline of water level in the shallow aquifer for 1970-79-----	96
35.	Simulated decline in water level in the shallow aquifer for 1970-79-----	97
36.	Measured decline in water level in the shallow aquifer for 1970-79-----	98
37.	Simulated source of water withdrawn from the Alamosa Basin-----	99
38.	Simulated decline in hydraulic head after 10 years of withdrawals shown in table 28-----	108

## TABLES

Table 1.	Discharge and drainage area for selected stations along the Rio Grande-----	13
2.	Weather Bureau stations used to establish regression relations for temperature and precipitation-----	17
3.	Regression relations between altitude and mean monthly temperature-----	21
4.	Regression relations between mean winter precipitation and mean monthly precipitation during summer months-----	23
5.	Coefficients for estimating daily potential evapotranspiration from daily potential evaporation-----	26
6.	Capacity of the root zone to store water-----	28

	Page
Table 7. Streamflow and estimated ground-water flow to the Alamosa Basin from drainage basins in the San Juan Mountains with measured streamflow-----	29
8. Comparison of published estimates of flow from the San Juan Mountains to the Alamosa Basin-----	30
9. Comparison of published estimates of flow from the San Juan Mountains to the closed basin-----	30
10. Streamflow-gaging stations in the Sangre de Cristo Mountains that were used in the regression model of mountain water yield-----	32
11. Comparison of published estimates of flow from the Sangre de Cristo Mountains to the closed basin and the Alamosa Basin--	33
12. Streamflow-gaging stations in New Mexico that were used in the regression model of the Taos Plateau water yield----	37
13. Water budget for the Costilla Plains-----	41
14. Calculated evapotranspiration for nonirrigated areas-----	46
15. Crop type, consumptive use, and evapotranspiration for irrigated areas in the Alamosa Basin-----	48
16. Comparison of published estimates of evapotranspiration from the Alamosa Basin-----	48
17. Water budget for the Alamosa Basin-----	49
18. Sensitivity of simulated hydraulic head to number of layers used to approximate the flow equation-----	53
19. Sensitivity of simulated hydraulic head to representing only the upper 3,200 feet of saturated thickness-----	60
20. Relation between evapotranspiration and depth to water used for nonirrigated areas in the section model-----	61
21. Ground-water withdrawals and surface-water diversions for irrigation-----	74
22. Indexes of ground-water withdrawal, return flow, and evapotranspiration-----	77
23. Large-capacity irrigation wells-----	81
24. Evapotranspiration salvage represented for nonirrigated areas-	92
25. Changes in ground-water withdrawals and irrigation return flows as adjusted during model calibration-----	96
26. Sensitivity of simulated 1980 condition to rates of withdrawal represented prior to 1970-----	101
27. Sensitivity of simulated 1980 condition to the value assumed for individual system characteristics-----	103
28. Withdrawals represented in the model to demonstrate response in nonirrigated areas-----	107
29. Declines in hydraulic head simulated after 10 years of withdrawals in nonirrigated areas-----	109
30. Estimated contribution to flow in the Rio Grande at Embudo, N. Mex., for each hydrologic regime, showing methods of estimation-----	110

## CONVERSION FACTORS

Inch-pound units used in this report may be converted to International System of Units (SI) by the following conversion factors:

<i>Multiply inch-pound units</i>	<i>By</i>	<i>To obtain SI units</i>
acre	0.4047	hectare
acre-foot	0.001233	cubic hectometer
acre-foot per acre	0.003048	cubic hectometer per hectare
cubic foot	0.02831	cubic meter
cubic foot per second	0.02831	cubic meter per second
degree Fahrenheit per foot	0.1693	degree Celsius per meter
foot	0.3048	meter
foot per mile	0.1894	meter per kilometer
foot squared per day	0.0929	meter squared per day
gallon	3.785	liter
gallon per minute	0.06309	liter per second
gallon per minute per foot	0.2070	liter per second per meter
inch	25.40	millimeter
inch per degree Fahrenheit	45.72	millimeter per degree Celsius
kilowatt hour	$3.6 \times 10^6$	joule
mile	1.609	kilometer
square foot	0.0929	square meter
square mile	2.590	square kilometer

To convert degrees Fahrenheit (°F) to degrees Celsius (°C) use the following formula:  $^{\circ}\text{C} = (^{\circ}\text{F} - 32) \times 5/9$ .

# HYDROLOGIC ANALYSIS OF THE RIO GRANDE BASIN NORTH OF EMBUDO, NEW MEXICO, COLORADO AND NEW MEXICO

by Glenn A. Hearne and Jack D. Dewey

## ABSTRACT

Large areas of Colorado, New Mexico, and Texas are connected by the Rio Grande, which is the major channel for surface water and the major drain for a variety of geohydrologic regimes. Five regions represent differing hydrologic regimes in the 10,400 square miles of the Rio Grande basin above Embudo, New Mexico.

For each of the five region's flow regimes, the water yield, or difference between precipitation and evapotranspiration, was estimated. The three regions in which precipitation exceeded evapotranspiration and the estimated water yield of each region for 1950-80 were: the San Juan Mountains, 2,800 cubic feet per second; the Sangre de Cristo Mountains, 780 cubic feet per second; and the Taos Plateau, 28 cubic feet per second. Evapotranspiration exceeded precipitation in the Costilla Plains by 150 cubic feet per second and in the Alamosa Basin by 2,400 cubic feet per second. The sum of these estimated flows and the decrease in storage in the Alamosa Basin (87 cubic feet per second) results in a calculated discharge from the study area (1,145 cubic feet per second) that was 69 percent greater than the measured discharge from the study area (680 cubic feet per second). This difference probably results from inaccuracies in estimating flow rates for the individual regions.

A three-dimensional digital model was constructed to represent the aquifer system in the Alamosa Basin. Conclusions based on a preliminary analysis using a two-dimensional section model had been: (1) A seven-layer model representing 3,200 feet of saturated thickness could accurately simulate the behavior of the flow in the basin; and (2) the 1950 flows and water levels were approximately stable and would be a satisfactory initial condition. For the three-dimensional model, values of aquifer characteristics were assumed or estimated from the work of previous investigators. Recharge and discharge represented in the model included changes since 1950 in ground-water withdrawals, return flow, salvaged evapotranspiration, and captured streamflow. Reasonable modifications to ground-water withdrawals allowed simulated changes to approximate the measured data--small declines in water level from 1950 to 1969 and water-level declines from 1970 to 1979 that were within about 5 feet of measured water-level declines. During 1980, the source of water withdrawn by wells was estimated to be 80 percent salvaged evapotranspiration, 14 percent depleted storage in the aquifer, and 6 percent captured streamflow. Sensitivity tests indicated that salvaged evapotranspiration was the major source, accounting for 69 to 82 percent of the ground-water withdrawals. Simulated hydraulic-head declines were most sensitive to ground-water withdrawals.

The three-dimensional model of ground-water flow was used to estimate the response to withdrawals from the Closed Basin Project (U.S. Bureau of Reclamation, 1963) in the Alamosa Basin. Evapotranspiration salvage was the source of most withdrawals, and hydraulic-head declines of more than 2 feet were simulated in the upper confined aquifer. The reliability of these projections is limited by the lack of calibration data in nonirrigated areas.

## INTRODUCTION

Alluvial basins of the southwestern United States are an important source of water. Historically, development has been possible only where water has been available in adequate quantities and of suitable quality. An understanding of the hydrology of these basins can assist in management of the available water supply. This study is part of the Southwest Alluvial Basins study (fig. 1), which, in turn, is part of a continuing national program of Regional Aquifer-Systems Analysis (Wilkins and others, 1980). The study area is the Rio Grande drainage basin above Embudo, N. Mex., including the closed basin north of low topographic and ground-water divides in Colorado.

### Purpose of the Study

The purposes of this study are to: (1) Provide estimates of water exchange rates between components of the flow system; and (2) improve the ability to estimate the hydrologic changes in the ground-water flow system in response to management alternatives. Other reports produced by this study describe water levels and recent changes in water levels (Crouch, 1983) and characterize the geochemistry of the system (R.S. Williams Jr., U.S. Geological Survey, written commun., 1984). This report describes the development and application of water-budget, regression, and ground-water-flow models. Each major physiographic subdivision of the study area forms a hydrologic regime in which hydrologic phenomena follow a consistent pattern. For each hydrologic regime, inflow and outflow rates were estimated. Where significant ground-water development has occurred or is anticipated, a digital model of ground-water flow was developed.

### Scope of Report

The scope includes describing the methods and presenting the results of hydrologic analyses. The following list includes the purpose and method of analysis for each hydrologic regime:

#### San Juan Mountains

Purpose: Estimate the total flow (ground water and surface water) from the San Juan Mountains to the Alamosa Basin.

Method: Water-budget model.

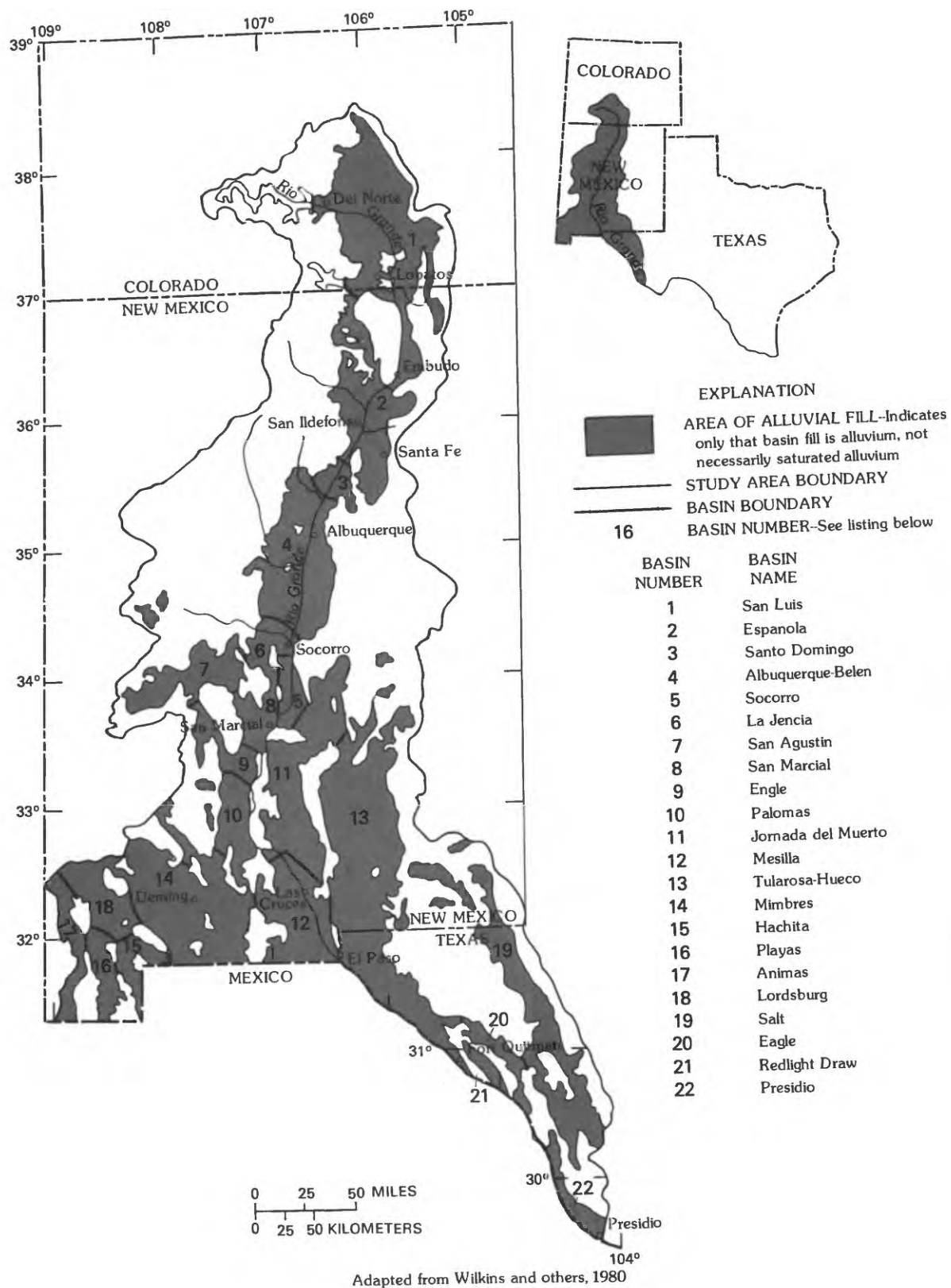


Figure 1.--Location of the eastern part of the Southwest Alluvial Basins study area.

Sangre de Cristo Mountains

Purpose: Estimate the surface-water flow from the Sangre de Cristo Mountains to the Alamosa Basin and the Costilla Plains.

Method: Regression model of water yield.

Taos Plateau

Purpose: Estimate the gain in flow of the Rio Grande due to precipitation on the plateau.

Method: Regression model of water yield.

Alamosa Basin and Costilla Plains

Purpose: Estimate the discharge from these areas by evapotranspiration.

Method: Evapotranspiration calculation.

Alamosa Basin and Costilla Plains

Purpose: Demonstrate that the estimates obtained from the preceding models are compatible with each other.

Method: Water-budget model.

Alamosa Basin

Purpose: (1) Demonstrate that the finite difference grid used for the three-dimensional model of ground-water flow causes only moderate errors in simulation results; and (2) Demonstrate that the 1950 condition is stable and can be used as an initial condition for the three-dimensional model of ground-water flow.

Method: Two-dimensional section model of ground-water flow.

Alamosa Basin

Purpose: (1) Analyze the changes caused by development of ground-water resources from 1950 to 1980; (2) Describe the functioning of the ground-water flow system; (3) Provide guidelines for establishing priorities for data collection; and (4) Project the changes resulting from the Closed Basin Project (U.S. Bureau of Reclamation, 1963).

Method: Three-dimensional model of ground-water flow.

The model used for each analysis is described before it is used. Readers primarily interested in the quantitative description of the flow system provided by the model analysis can skip over the detailed model descriptions. These descriptions are included to permit readers to scrutinize the assumptions made in developing the models.

## Geographic Setting

The study area includes the Rio Grande drainage basin above Embudo, N. Mex., and the closed basin in Colorado. Embudo, a Spanish word meaning "funnel," is an appropriate term, because the intermontane channel narrows to restrict ground-water flow and routes most of the discharge from the study area through the Rio Grande. The total area is about 10,400 square miles, of which about 7,400 square miles is in Colorado (including about 2,900 square miles in a closed basin) and about 3,000 square miles is in New Mexico.

The study area consists of mountain ranges, intermontane valleys, piedmont alluvial plains, and lava plateaus (fig. 2). Boundaries of the study area are the drainage divides in the Sangre de Cristo Mountains to the east and the San Juan Mountains to the west. The intermontane area is divided by the San Luis Hills into a broad flat valley to the north (the Alamosa Basin) and a piedmont alluvial plain (the Costilla Plains) and lava plateau (the Taos Plateau) to the south. The Alamosa Basin contains a low topographic divide that forms a closed basin (no surface-water outflow) north of the Rio Grande drainage basin. San Luis Valley includes the Alamosa Basin and that part of the Costilla Plains in Colorado. Sunshine Valley includes that part of the Costilla Plains between the Colorado-New Mexico State line and the Red River.

Altitude of the study area ranges from about 5,789 feet at streamflow-gaging station 08279500 on the Rio Grande at Embudo, N. Mex., to 14,345 feet on Blanca Peak in the Sangre de Cristo Mountains. Average altitude of the irrigated land in the Alamosa Basin is about 7,700 feet.

Climate and native vegetation vary with latitude and altitude. Average annual temperature is about 42° Fahrenheit in the Alamosa Basin, about 44° at Cerro, N. Mex., and about 47° at Taos, N. Mex. The length of the frost-free period ranges from about 90 to 115 days in the Alamosa Basin, and the length increases southward to an average of about 118 days at Cerro, N. Mex., and about 128 days at Taos, N. Mex.

The intermontane areas are arid; potential evaporation exceeds precipitation. Potential evaporation is greater than 3 feet per year; average annual precipitation ranges from less than 8 inches on the Alamosa Basin to about 12 inches on the Costilla Plains. Away from stream channels, native vegetation in the valleys consists of shrubs and grass.

In the mountains, temperatures are cooler, and precipitation is greater than in the intermontane areas. Average annual precipitation exceeds 30 inches and occurs primarily as winter snow. At Wolf Creek Pass (in the San Juan Mountains, at an altitude of 10,200 feet) average snow depth on April 1 (from 1936 through 1977) was about 79 inches, and the average water content was about 28 inches. Native vegetation is mainly coniferous forests. In the Sangre de Cristo Mountains, precipitation is less than in the San Juan Mountains; winter precipitation (U.S. Weather Bureau, undated, a and b) exceeds 30 inches in the San Juan Mountains but not in the Sangre de Cristo Mountains.

The study area is sparsely populated (about six people per square mile). In 1980, the six counties that are mostly or totally in the study



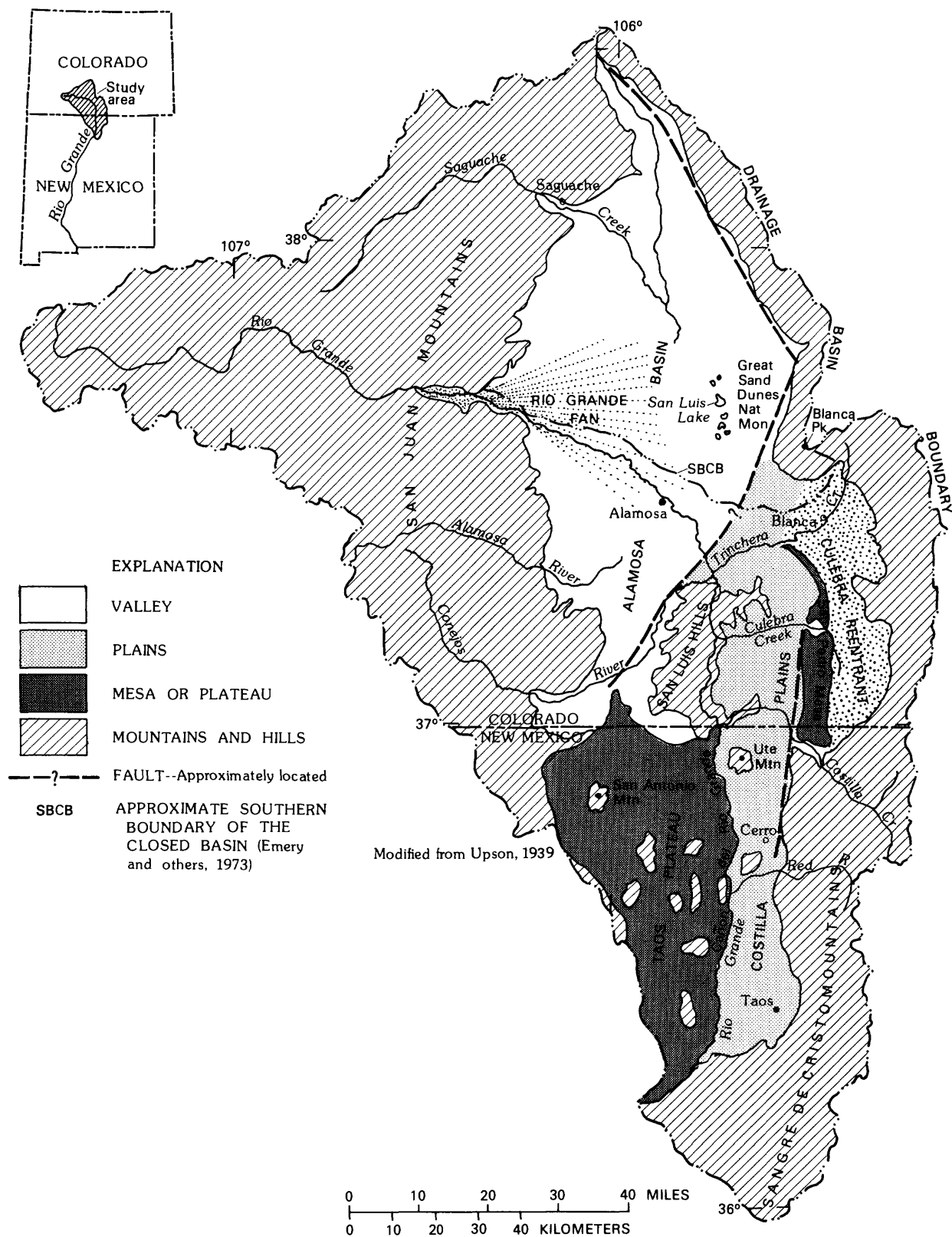


Figure 2.--Physiographic subdivisions of the study area.

area (Saguache, Rio Grande, Alamosa, Costilla, and Conejos in Colorado and Taos in New Mexico) had a total population of 56,566, distributed over 9,515 square miles. Alamosa, with a population of 6,830 (an increase of 10 percent from that of 1960), was the only town with a population of more than 5,000.

Most of the study area is subdivided by U.S. Bureau of Land Management systems in which locations are given by township, range, section, and position within the section. For most of the area, townships are numbered north of the New Mexico base line and east of the New Mexico principal meridian. In the eastern Alamosa Basin, townships are numbered south from the Colorado base line and east of the sixth principal meridian. A local grid system has been established on Sangre de Cristo Grant but is not shown on plate 1.

### Geohydrologic Setting

The study area contains five interrelated flow regimes that correspond approximately with the physiographic subdivisions (fig. 2), the San Juan Mountains, the Sangre de Cristo Mountains, the Taos Plateau, the Costilla Plains, and the Alamosa Basin. Significant ground-water development has occurred only in the Alamosa Basin. The San Juan Mountains and the Sangre de Cristo Mountains are a source of water for the Alamosa Basin and the Costilla Plains. The intermontane area contains several thousand feet of interbedded gravel, sand, silt, clay, and volcanic rocks that form a complex aquifer system. The San Luis Hills form a hydraulic barrier between the Alamosa Basin to the north and the Costilla Plains and the Taos Plateau to the south.

Ground water occurs in a variety of conditions (fig. 3) within the study area. Perched or semiperched conditions occur in aquifers of the Taos Plateau (Winograd, 1959, p. 34), the Costilla Plains (Winograd, 1959, p. 25), and around the perimeter of the Alamosa Basin and indicate that water is flowing from shallow to deeper aquifers of the system. Confined and flowing artesian conditions (Lohman and others, 1972) occur toward the center of the Alamosa Basin (Emery and others, 1975, pl. 6) and indicate that water is flowing from deep to shallower aquifers of the system. In simplified description, the aquifers in the Alamosa Basin consist of an unconfined aquifer and a confined aquifer separated by either a clay series or unfractured volcanic rocks. Although this simplification is useful, the aquifer system is a heterogeneous mixture of aquifers and leaky confining beds, each of limited areal extent and variable hydraulic properties. Details of ground-water flow are as complex as the distribution of aquifers and leaky confining beds and as complex as the distribution of recharge and discharge, which vary both in space and time. However, in aquifers of the Alamosa Basin, the general pattern of flow (fig. 4) shows recharge and downward flow around the perimeter and upward flow and discharge in the central area. In aquifers of the Costilla Plains (fig. 5), recharge from the Sangre de Cristo Mountains moves through the sedimentary rocks to fractured volcanic rocks and discharges along the Rio Grande. In aquifers of the Taos Plateau (fig. 5), recharge moves through fractured volcanic rocks and discharges along the Rio Grande.

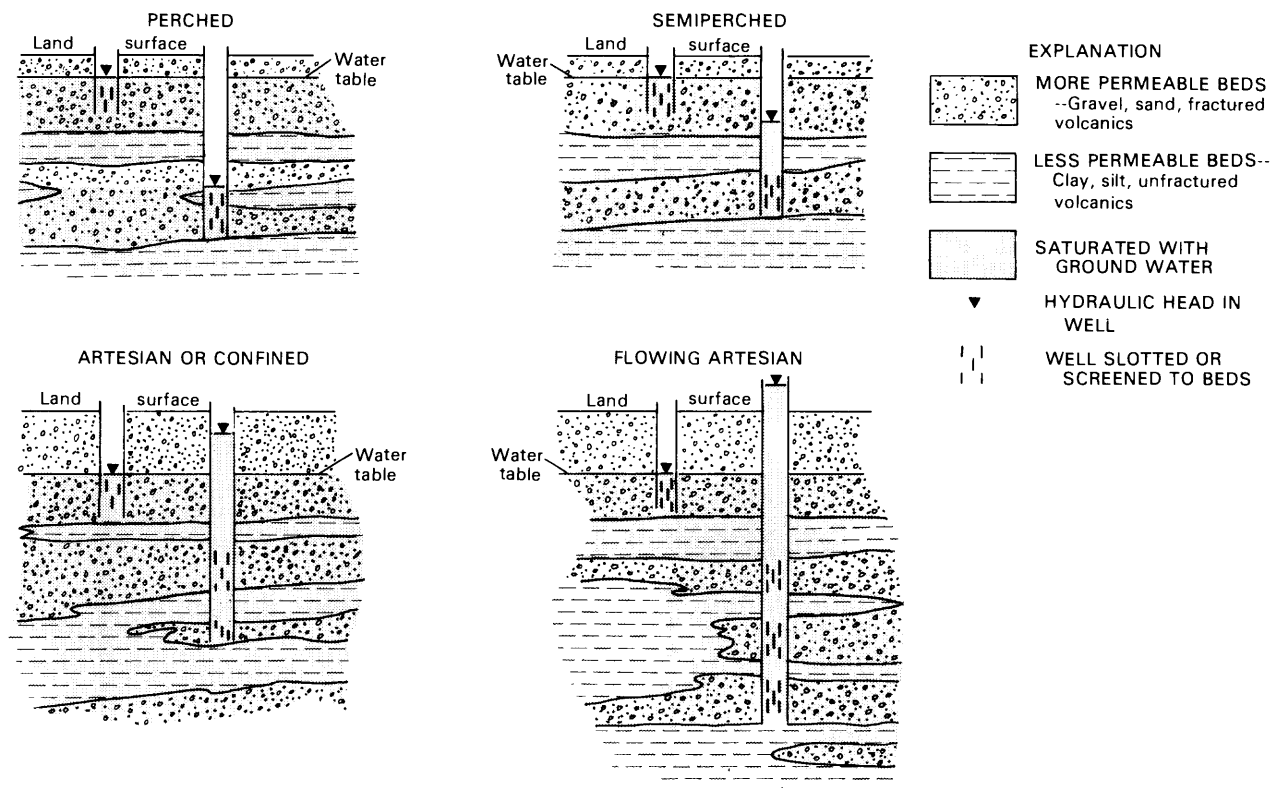


Figure 3.--Modes of occurrence of ground water.

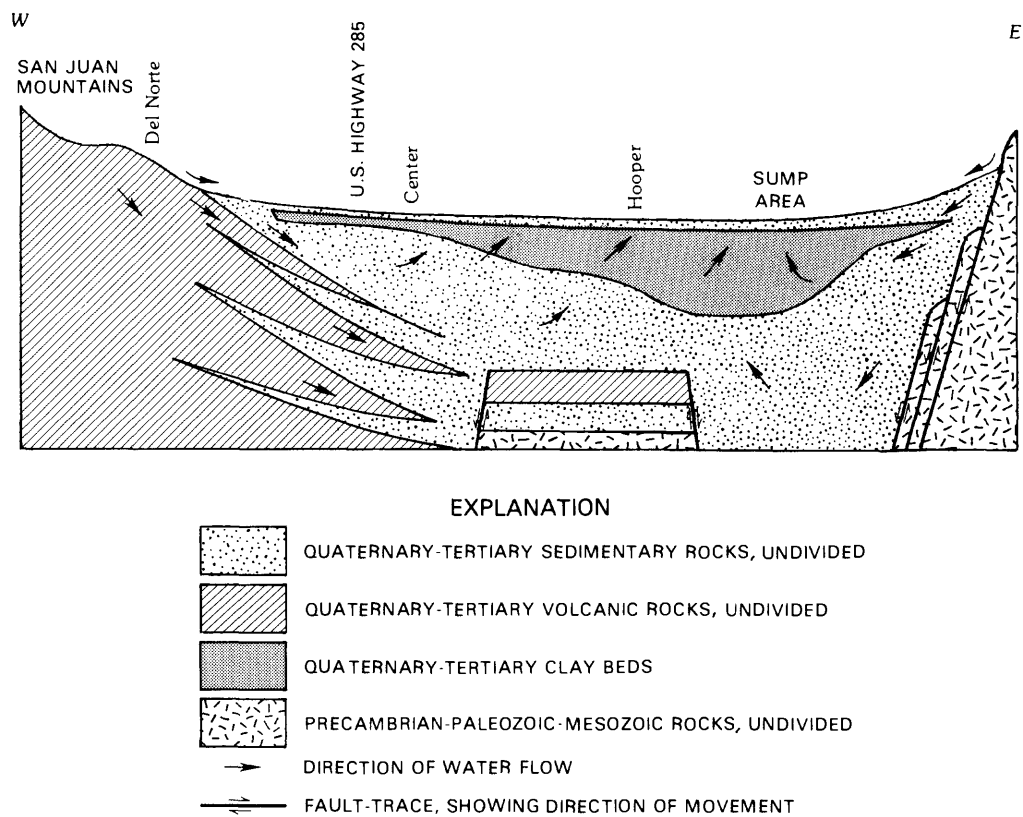


Figure 4.--Generalized west-to-east section across the Alamosa Basin.

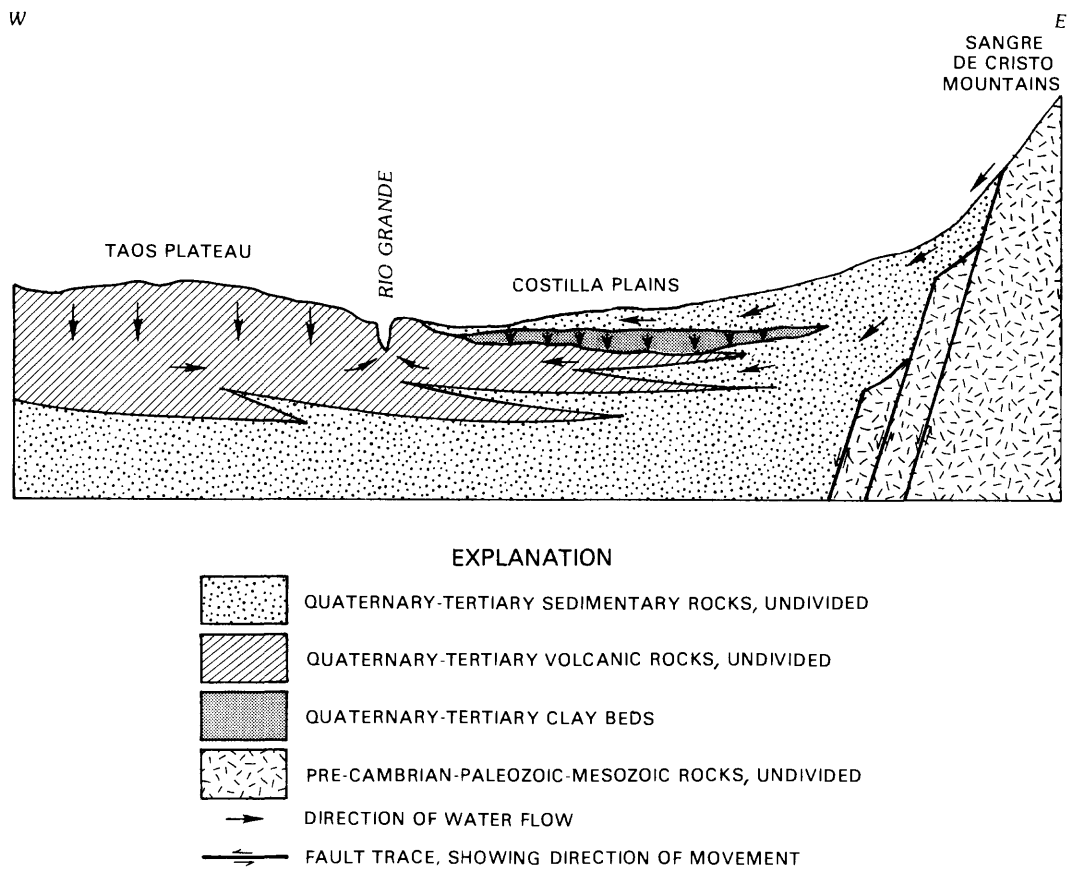


Figure 5.--Generalized west-to-east section across the Taos Plateau and the Costilla Plains.

## History of Agricultural Development

Development of irrigated agriculture in the Alamosa Basin has undergone five basic changes: (1) Extensive diversion of surface water started about 1880; (2) development of confined ground water started about 1890; (3) a shift of irrigated areas from the center of the Alamosa Basin to the west was completed by about 1910; (4) ground water withdrawals by large-capacity irrigation wells (greater than 300 gallons per minute) became significant about 1950; and (5) extensive irrigation by sprinkler systems started about 1970.

The Alamosa Basin has been used for irrigated agriculture since at least the 1630's when the Spanish settlers arrived. However, prior to about 1880, irrigated acreage was small. An extensive network of canals was constructed during about 1880-90 to divert water for irrigation. By 1904, all streams entering the basin were appropriated for irrigation. Irrigation was concentrated in the central part of the Alamosa Basin northeast of Monte Vista, Colo.

Water from confined aquifers in the Alamosa Basin has been used since 1887. Although the number of wells completed in confined aquifers increased, through the 1930's discharge primarily was from small-capacity flowing wells; only two large-capacity, pumped wells completed in confined aquifers were used for irrigation during 1936 (Powell, 1958).

The main concentration of irrigated areas shifted from the center of the Alamosa Basin to the western side (Powell, 1958). Crops were subirrigated by applying enough surface water to raise the level of the water table to the root zone of the growing crops. Higher water levels resulted in waterlogging in the lower areas to the east. Increased evapotranspiration from areas where the water table was near the surface resulted in alkali damage to some areas. Lands to the east were abandoned, and irrigated agriculture shifted to higher land to the west. By about 1910, agricultural areas in the center of the basin were out of production, and irrigation was concentrated on the western side of the Alamosa Basin on the Rio Grande fan (fig. 2).

Extensive development of ground-water resources for irrigation began about 1950. Continued artificial recharge by subirrigation, canal leakage, and flow from wells completed in confined aquifers increased the volume of water stored in the unconfined ground-water reservoir, raising water levels on the western side of the Alamosa Basin by 50 to 100 feet (Powell, 1958). This ground-water resource was developed when the supply of surface water decreased during the drought of the 1930's. However, the rate of ground-water withdrawal prior to 1950 was small compared to the rate of withdrawal after 1950 (Emery and others, 1972). The rate of withdrawal from confined aquifers also increased; Powell (1958) reported 61 large-capacity pumped wells completed in confined aquifers.

Irrigation with sprinkler systems became common during the 1970's. The total number of sprinkler systems increased from 262 in 1973 to 1,541 in 1980 (Davis Engineering Service, Inc., 1981). Most sprinklers irrigated a quarter section (about 160 acres). The greatest density of sprinkler systems was on

the Rio Grande fan north of the river: Townships 39N to 41N and Ranges 7E to 9E (pl. 1). Diversions from surface water and water withdrawn from wells in both unconfined and confined aquifers can supply water for sprinklers.

### Significance of Water Resources

The water resources of the study area are significant because:

(1) Irrigated agriculture is important to the economy of the study area; and  
(2) the study area is a major source area for the water available to downstream uses in New Mexico, Texas, and Mexico. The economy of the area is very dependent on agriculture; because of the arid climate, agriculture requires irrigation. Irrigation in the study area is a major user of water from the Rio Grande basin. During 1950, about 910,000 acres of land were irrigated in the Rio Grande basin above Presidio, Tex.; about 660,000 acres (73 percent) were in the study area. Most of this irrigated acreage was in the Alamosa Basin. Evapotranspiration in the San Luis Valley was estimated (Emery and others, 1973) to transfer water to the atmosphere at the rate of 3,300 cubic feet per second; 1,900 cubic feet per second was from irrigated areas and 1,400 cubic feet per second was from nonirrigated areas.

The study area is a major source of water for the Rio Grande basin. The division of the basin into producing and consuming areas is shown in table 1. The producing area is above Otowi Bridge, near San Ildefonso, N. Mex., (fig. 1), where discharge of the Rio Grande increases as the size of the drainage area increases; the drainage area is producing more water than is being consumed. The consuming area is below Otowi Bridge, where discharge of the Rio Grande decreases as the size of the drainage area increases; the added drainage area is producing less water than is being consumed. The Rio Grande gains streamflow in three major reaches: (1) The San Juan Mountains upstream from the Del Norte, Colo., station (08220000); (2) The Costilla Plains between the Lobatos, Colo., station (08251500) and the Embudo, N. Mex., station (08279500); and (3) the reach between the Embudo station (08279500) and Otowi Bridge station (08313000) where the Rio Chama discharged a 1912-50 average of 605 cubic feet per second into the Rio Grande from a drainage area of 3,200 square miles.

The Rio Grande Compact was adopted in 1939 for the purpose of ". . . effecting an equitable apportionment . . ." of the waters of the Rio Grande above Fort Quitman, Tex. The Rio Grande Compact (Rio Grande Compact Commission, 1981) prescribes the allocation of the water of the Rio Grande among the users in Colorado, New Mexico, Texas, and Mexico by establishing a relation between the amount of water flowing by one streamflow-gaging station and the amount of water that should be available at a downstream streamflow-gaging station. Index stations monitor the amount of streamflow from major streams carrying surface water into the Alamosa Basin, which are the Rio Grande and the Conejos River. Based on these index streamflows, the Rio Grande Compact requires that a varying percentage of streamflow be available at the State line, as measured at the streamflow-gaging station on the Rio Grande near Lobatos, Colo., (08251500). The smaller the index streamflow, the smaller the percentage to be delivered at the State line. By 1965, it was adjudicated that Colorado had delivered about 900,000 acre-feet less than required by the Compact (Radosevich and Rutz, 1979). Streamflow in the Rio

Table 1.--Discharge and drainage area for selected stations along the Rio Grande  
(location shown on figure 1)  
[ft<sup>3</sup>/s, cubic feet per second; mi<sup>2</sup>, square miles]

Station name	Station number	Period of record	Average discharge for period of record through 1950 (ft <sup>3</sup> /s)	Gain (+) or loss (-) in upstream reach (ft <sup>3</sup> /s)	Drainage area above station (mi <sup>2</sup> )
Near Del Norte, Colo.	08220000	1889-1950	959	+959	1,320
Near Lobatos, Colo.	08251500	1899-1950	717	-242	7,700
At Embudo, N. Mex.	08279500	1889-1950	1,139	+422	10,400
At Otowi Bridge near San Ildefonso, N. Mex.	08313000	1895-1905 1909-50	1,699	+560	14,300
At San Marcial, N. Mex.	08358500	1924-50	1,268	-431	27,700
At El Paso, Tex.	08364000	1889-1950	972	-296	29,267
Above Presidio, Tex. (upper Presidio station).	08371500	1900-13 1923-50	486	-486	34,988



Grande at Otowi Bridge near San Ildefonso, N. Mex., (08313000), about 26 miles southwest of Embudo, N. Mex., is used as an index to allocate the water among the downstream users in New Mexico, Texas, and Mexico.

The Closed Basin Project of the U.S. Bureau of Reclamation entails a well field on the east side of the Alamosa Basin (located approximately from T.42N.R.9E to T.37N.R.11E) to pump water into a channel extending to the Rio Grande. The Reclamation Project Authorization Act of 1972 (Public Law 92-514) authorized construction of the project ". . . for the principal purposes of salvaging, regulating, and furnishing water from the closed basin area of Colorado . . ." Water from the project would be used for: (1) Assisting in meeting the delivery required by the Rio Grande Compact at the streamflow-gaging station on the Rio Grande near Lobatos, Colo., (2) maintaining two wildlife refuges in Colorado; (3) eliminating any deficit in deliveries by Colorado; and (4) irrigation or other beneficial uses in Colorado. Most of the water withdrawn by the Closed Basin Project is expected (Emery, 1970) to come from salvaged ground water that would otherwise have been lost to evapotranspiration from nonirrigated areas.

### THE SAN JUAN MOUNTAINS

The San Juan Mountains (fig. 2) cover about 5,000 square miles in southwestern Colorado. They consist of a thick sequence of volcanic rocks. Precipitation increases with altitude from about 8 to 40 inches per year. Streams from about 2.3 million acres drain to the Alamosa Basin. The beds generally dip to the east to underlie and intertongue with sedimentary rocks beneath the Alamosa Basin. However, multiple source areas for the volcanic rock and interbedding of rocks of different character add to the complexity of the hydrogeologic system.

Rocks of the San Juan Mountains vary in permeability; being composed of layers of limited areal extent, they form an aquifer system that is anisotropic and heterogeneous when seen as a whole. Geohydrologic details are complex because of the irregular distribution of aquifers and of water available for recharge. However, the aquifer system is not restricted to shallow depth. For example, ash-flow tuffs that are exposed near the edge of the Alamosa Basin are permeable (Huntley, 1976, p. 55; estimates hydraulic conductivities as high as 140 feet per day) and extend several miles into the valley (Burroughs, 1981), forming a natural conduit for ground-water flow from the San Juan Mountains into the Alamosa Basin. The general pattern of flow is as follows: rainfall, snowmelt, and streamflow recharge permeable units where they are at the surface or are overlain by permeable alluvium; water flows through the aquifer system along the more permeable zones (which probably follow the layering); and water discharges either to a stream draining the mountains or to the aquifers of the Alamosa Basin.

No significant ground-water development has occurred in the San Juan Mountains. Their significance to the hydrology of the study area is as a source of water for the Alamosa Basin. Several streams flow from the San Juan Mountains onto the Alamosa Basin. The largest of these are the Rio Grande and the Conejos River. Periods of wet and dry years result in similar streamflow patterns at the Rio Grande near Del Norte, Colo., (streamflow-gaging station

08220000; map number 200 on pl. 1), and at the Conejos River near Mogote, Colo., (streamflow-gaging station 08246500; map number 465 on pl. 1). These variations in streamflow appear to be the result of variations in precipitation.

Ground-water flow from the San Juan Mountains to the Alamosa Basin is nearly constant. A change in subsurface flow would result only from change in hydraulic head. Hydraulic heads in recharge areas of the San Juan Mountains may fluctuate with seasonal and long-term changes in recharge, and hydraulic heads in the Alamosa Basin have declined in response to ground-water development. However, these fluctuations are small compared to the altitude of the recharge area above the valley.

The water-budget model described in the following section was used to estimate the average flow of water from the San Juan Mountains to the Alamosa Basin. Readers not interested in the detailed description of the model may skip the following section and resume reading at the section "Flow from the San Juan Mountains to the Alamosa Basin."

#### Water-Budget Model of the San Juan Mountains

The average flow of water from the San Juan Mountains to the Alamosa Basin for 1950-80 was estimated using a water-budget model. A regression model of water yield was not appropriate because a significant part of the water yield was anticipated to leave the mountains as ground water rather than streamflow. A water-budget model is a mathematical statement that the rate of outflow must equal the rate of inflow plus the rate at which the volume of water in storage changes. The water-budget model used to represent the San Juan Mountains (fig. 6) required the assumptions that: (1) The long-term change in volume of water in storage from 1950 to 1980 was negligible; (2) precipitation (fig. 6, item 1) was the only inflow; and (3) outflow included sublimation (fig. 6, item 2), evapotranspiration (fig. 6, item 3), and the sum (fig. 6, item 4) of streamflow and ground-water flow to the Alamosa Basin. Therefore, the water budget is expressed as:

$$\hat{Q} = \hat{P} - \hat{S} - E; \quad (1)$$

where

$\hat{Q}$  = sum of streamflow and ground-water flow to the Alamosa Basin (fig. 6, item 4) ( $L^3/T$ );

$\hat{P}$  = precipitation (fig. 6, item 1) ( $L^3/T$ );

$\hat{S}$  = sublimation (fig. 6, item 2) ( $L^3/T$ ); and

$E$  = evapotranspiration (fig. 6, item 3) ( $L^3/T$ ).

Temperature was used to determine whether precipitation was added to storage in the snowpack (fig. 6, item 5) or in the root zone (fig. 6, item 6) and to calculate the volume of snowmelt (fig. 6, item 7) to be moved from the snow-

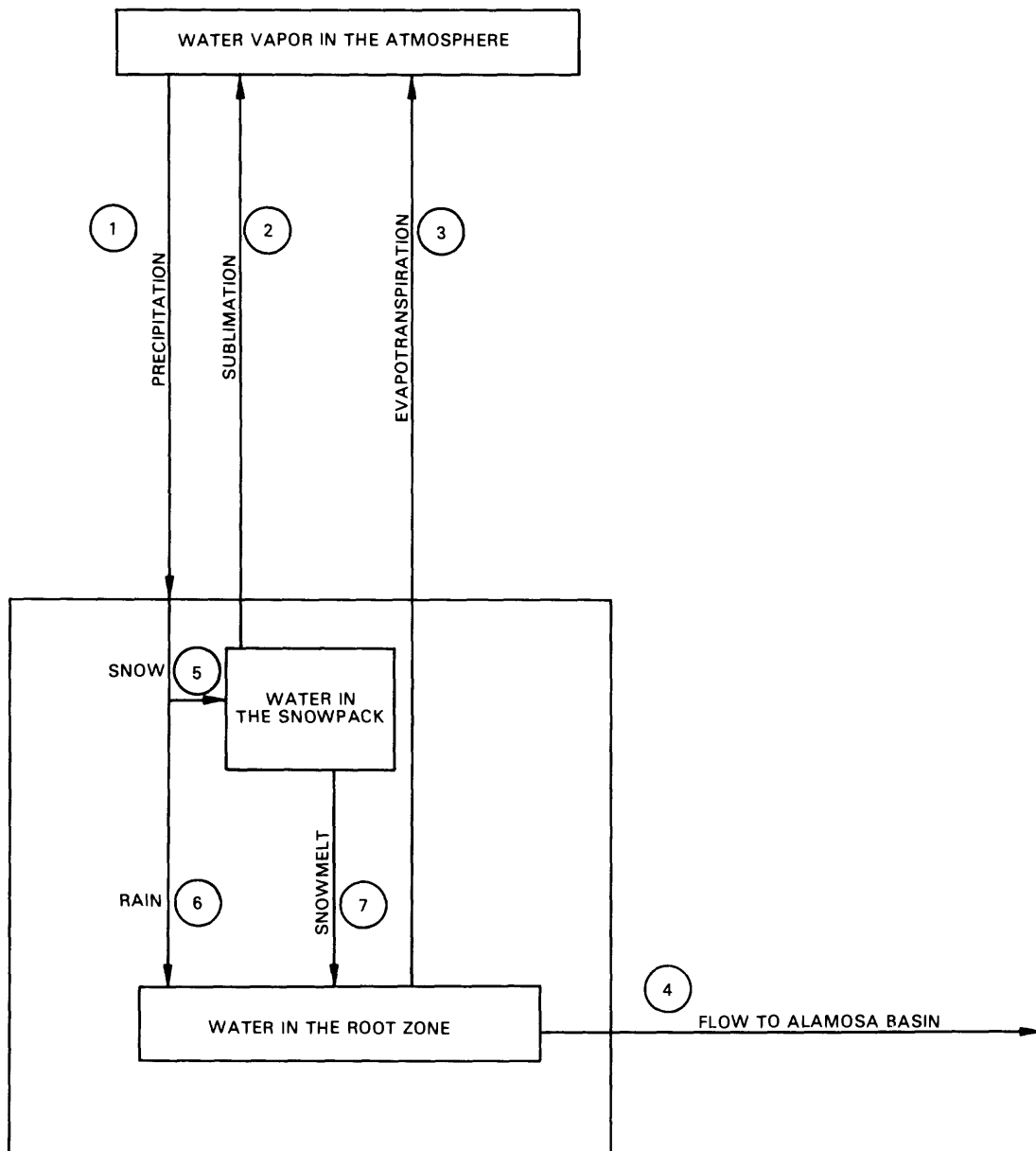


Figure 6.--Movement of water as represented in the water-budget model of the San Juan Mountains.

pack to the root zone. The calculated storage in the snowpack and the root zone affected the rates of sublimation (fig. 6, item 2) and evapotranspiration (fig. 6, item 3). Water in excess of the storage capacity of the root zone was assumed to flow to the Alamosa Basin (fig. 6, item 4) either as streamflow or ground-water flow. The sequence of calculations is shown in figure 7. For example, if the status of the model from the preceding day included a snowpack and a saturated root zone, and the Weather Bureau data indicated no precipitation and a temperature greater than 34° Fahrenheit, then the model subtracted sublimation from the snowpack, subtracted snowmelt from the snowpack, and added snowmelt to available moisture before comparing the volume of available moisture with the storage capacity of the root zone. Water in excess of the storage capacity of the root zone was accumulated as flow to the Alamosa Basin before advancing to the next day.

Each drainage basin in the San Juan Mountains was divided into subareas for which a water budget was calculated. These subareas were defined by mean winter (October through April) precipitation (U.S. Weather Bureau, undated, a and b) and vegetation type (U.S. Soil Conservation Service, 1978). Average altitude and surface area for each subarea were determined from U.S. Geological Survey 1:250,000 maps.

Daily records of temperature and precipitation were obtained (U.S. Weather Bureau, written commun., 1981) for six stations (table 2, fig. 8) with more than 5 years of temperature or precipitation record located in or near the San Juan Mountains. Data from the six stations with more than 5 years of temperature records were used to establish a regression relation between temperature and altitude. Data from the five stations with more than 5 years of precipitation record were used to establish a regression relation between mean monthly summer (May through September) precipitation and mean winter precipitation. Data from the Del Norte station were used with the mean winter precipitation, altitude, area, and vegetation type of each subarea to estimate daily temperature, precipitation, snowmelt, sublimation, and evapotranspiration for each subarea.

Table 2.--Weather Bureau stations used to establish regression relations for temperature and precipitation  
(Location shown in figure 8)

Weather Bureau station identification			Altitude (feet)	Years of record through 1980	
Station name	Division	Index number		Temperature	Precipitation
Del Norte-----	05	2184	7,884	52	58
Hermit-----	05	3951	9,000	72	73
Monte Vista-----	05	5706	7,662	44	43
Rio Grande					
Reservoir-----	05	7050	9,495	9	4
Saguache-----	05	7337	7,697	69	78
Wolf Creek Pass----	05	9181	10,642	25	23

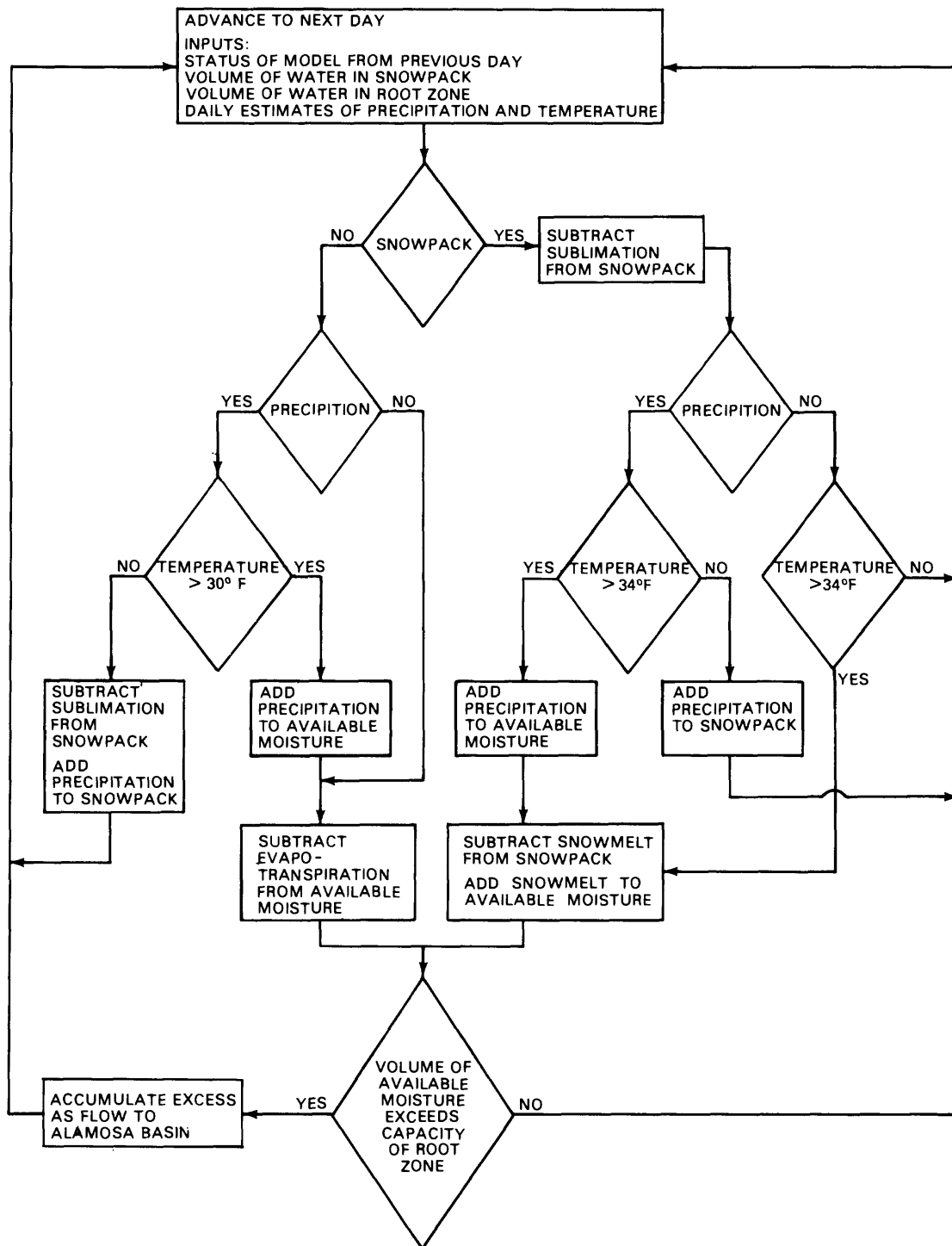


Figure 7.--Flow chart of the water-budget model of the San Juan Mountains.

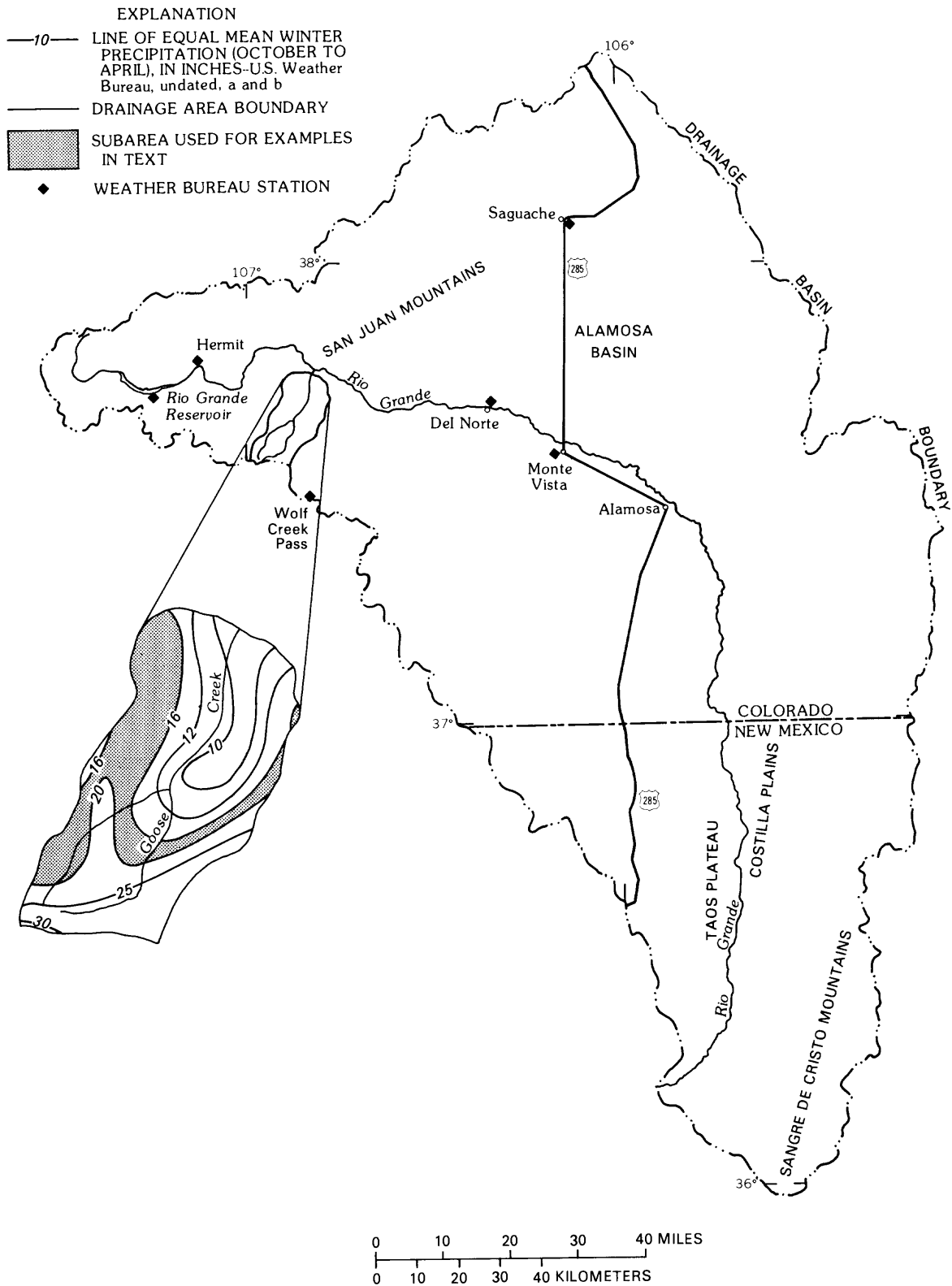


Figure 8.--Example subarea in the Goose Creek drainage basin.

For example, one subarea was defined (fig. 8) as that part of the Goose Creek drainage basin between the contours of 16 inches and 20 inches of mean winter precipitation (U.S. Weather Bureau, undated, a). Mean winter precipitation for the subarea was assumed to be 18 inches. Average altitude was estimated as 11,200 feet. Surface area was estimated as 17,600 acres. Vegetation in the subarea consisted of coniferous forest (U.S. Soil Conservation Service, 1978). Daily values of temperature and precipitation recorded by the Weather Bureau station at Del Norte were used to estimate daily values of temperature and precipitation for the subarea. This subarea of Goose Creek drainage basin is used repeatedly in this section of the report as an example of the method.

### Temperature

The mean daily temperature, which is needed to compute sublimation and evapotranspiration for each subarea, was estimated from the altitude of the subarea and the mean daily temperature recorded at the Weather Bureau station near Del Norte. For each month, a relation (table 3) was established between altitude and mean monthly temperature by a least-squares regression of the six Weather Bureau stations with more than 5 years of temperature record (table 2) located in or near the San Juan Mountains (fig. 8). The mean daily temperature for each subarea was calculated as:

$$T = T_s + R_t (A_a - 7,884); \quad (2)$$

where

$T$  = estimated mean daily temperature for the subarea, in degrees Fahrenheit;

$T_s$  = mean daily temperature recorded at the Del Norte station, in degrees Fahrenheit;

$R_t$  = slope of the regression line between altitude and mean monthly temperature (table 3) for the month in which the daily temperature is being estimated, in degrees Fahrenheit per foot;

$A_a$  = average altitude of the subarea, in feet; and

7,884 = altitude of the Del Norte station, in feet.

For example, on May 12, 1959, mean daily temperature at the Del Norte station ( $T_s$ ) was 57° Fahrenheit. The slope of the regression line ( $R_t$ ) between altitude and temperature for the month of May was -0.00538° Fahrenheit per foot. Equation 2 yields an estimated mean daily temperature ( $T$ ) of 39° Fahrenheit for the example subarea of the Goose Creek drainage basin, where average altitude ( $A_a$ ) is 11,200 feet.

Table 3.--Regression relations between altitude and mean  
monthly temperature  
[°F/ft, degrees Fahrenheit per foot; °F, degrees Fahrenheit]

Month	Regression Coefficients		Correlation coefficient (dimensionless)	Standard error of the estimate (°F)
	Slope, $R_t$ (°F/ft)	Intercept (°F)		
January----	-0.00194	33.4	-0.61	3.4
February---	-.00346	50.6	-.69	4.8
March-----	-.00505	71.1	-.87	3.9
April-----	-.00535	82.5	-.91	3.3
May-----	-.00538	91.8	-.92	3.1
June-----	-.00486	96.0	-.95	2.2
July-----	-.00438	97.3	-.97	1.4
August-----	-.00453	96.3	-.97	1.6
September--	-.00352	82.2	-.95	1.6
October----	-.00336	71.5	-.95	1.6
November---	-.00281	53.1	-.85	2.3
December---	-.00210	37.7	-.70	2.9

#### Precipitation

Daily precipitation (fig. 6, item 1) for each subarea was estimated from mean winter precipitation for the subarea and daily precipitation recorded at the Del Norte station. Because of large seasonal variations in precipitation, different estimates were used for winter (October through April) and each month of summer (May through September).

Daily winter precipitation was calculated as:

$$P_d = (P_a/4.21)P_{sd} ; \quad (3)$$

where

$P_d$  = estimated daily precipitation for the subarea, in inches;

$P_a$  = mean winter precipitation for the subarea, in inches;

4.21 = mean winter precipitation recorded at the Del Norte station 1950-80, in inches; and

$P_{sd}$  = daily precipitation recorded at the Del Norte station, in inches.

The type of precipitation (snow or rain) that was assumed for each subarea on a particular day was determined, based on whether or not a snowpack was simulated by the model and on the mean temperature for the subarea. If the mean daily temperature was 30° Fahrenheit or less, precipitation values used in the model were considered to be snow (fig. 6, item 5), and they were added to the snowpack values. If the mean daily temperature was between 30 to



34° Fahrenheit and a snowpack was simulated, precipitation values used in the model were considered snow (fig. 6, item 5); if a snowpack was not simulated, the precipitation was considered rain (fig. 6, item 6). If the mean daily temperature was greater than 34° Fahrenheit, the precipitation was considered rain (fig. 6, item 6), and it was added to the soil moisture.

For example, on April 9, 1959, the Del Norte station reported a mean daily temperature ( $T_s$ ) of 30° Fahrenheit and a precipitation ( $P_{sd}$ ) of 0.30 inch. For the example subarea of the Goose Creek drainage basin, the mean winter precipitation ( $P_a$ ) of 18 inches yielded (eq. 3) an estimated daily precipitation ( $P_d$ ) of 1.28 inches. The estimated temperature ( $T$ , eq. 2) was 12° Fahrenheit. In the model, precipitation values were added to the snowpack values.

Because of large variations in precipitation during the summer, daily summer (May through September) precipitation was calculated using a different relation for each month. For each of the five summer months, a least-squares regression was used to develop a relation (table 4) between mean winter precipitation and mean monthly precipitation for the five stations with more than 5 years of precipitation record (table 2) located in or near the San Juan Mountains (fig. 8). Daily summer precipitation for each subarea was calculated as:

$$P_d = [P_{sm} + (P_a - 4.21)R_p] \frac{P_{sd}}{P_{sm}}; \quad (4)$$

where

$P_d$  = estimated daily precipitation for the subarea, in inches;

$P_{sm}$  = mean monthly precipitation (table 4) recorded at the Del Norte station 1950-80, in inches;

$P_a$  = mean winter precipitation for the subarea, in inches;

4.21 = mean winter precipitation recorded at the Del Norte station 1950-80, in inches;

$R_p$  = slope of the regression line (table 4) for the summer month for which precipitation is being estimated, dimensionless; and

$P_{sd}$  = daily precipitation recorded at the Del Norte station, in inches.

For example, on August 4, 1959, the Del Norte station reported a mean daily temperature ( $T_s$ ) of 64° Fahrenheit and a precipitation for the day ( $P_{sd}$ ) of 0.34 inch. Precipitation for August ( $P_{sm}$ ) averaged 1.63 inches at the Del Norte station. For August, the slope of the regression line ( $R_p$ ) was 0.113 (table 4). For the example subarea, equation 4 yields an estimated daily precipitation ( $P_d$ ) of 0.66 inch. The estimated mean daily temperature for the subarea ( $T$ , eq. 2) was 49° Fahrenheit; therefore, the model added the precipitation values to soil-moisture values.

Table 4.--Regression relations between mean winter precipitation  
and mean monthly precipitation during summer months  
[in., inches]

Month	Regression coefficients			Standard error of the estimate (in.)	Mean monthly precipitation at Del Norte, $P_{sm}$ (in.)
	Slope, $R_p$	Intercept (in.)	Correlation coefficient		
May-----	0.053	0.58	0.988	0.10	0.85
June-----	.047	.41	.998	.04	.64
July-----	.076	1.30	.954	.27	1.57
August-----	.113	1.03	.985	.02	1.63
September----	.137	.37	.994	.16	.89

#### Snowmelt

Snowpack was assumed to delay transmission of water from precipitation to soil moisture until the estimated daily temperature exceeded 34° Fahrenheit. Moisture from the melting snowpack (fig. 6, item 7) was calculated as:

$$M = R_m(T-34); \quad (5)$$

where

$M$  = daily snowmelt, in inches;

$R_m$  = coefficient of snowmelt, in inches per degree Fahrenheit; and

$T$  = estimated mean daily temperature (eq. 2) for the subarea, in degrees Fahrenheit.

An  $R_m$  value of 0.05 inch per degree Fahrenheit was found by experimentation to simulate snowpack conditions qualitatively similar to those in the San Juan Mountains; if the  $R_m$  value was too small, simulated snowpack remained all year at higher altitudes; if the  $R_m$  value was too large, simulated snowpack melted too early. The  $R_m$  value of 0.05 inch per degree Fahrenheit simulated snowpack all summer for 2 or 3 years at the highest altitude for several subareas.

For example, on June 11, 1959, the Del Norte station reported no precipitation and a mean daily temperature ( $T_s$ ) of 63° Fahrenheit. For the example subarea, the estimated mean temperature of 47° Fahrenheit ( $T$ , eq. 2) resulted in a daily snowmelt ( $M$ ) of 0.6 inch (eq. 5).

## Sublimation

If the model calculates that the subarea is covered with snowpack, loss of moisture to the atmosphere is by sublimation (fig. 6, item 2). Sublimation has been reported as averaging 0.011 inch per day for 24 days at an altitude of 8,800 feet in Utah (Croft and Monninger, 1953) and 0.015 inch per day in an open area at an altitude of 6,900 feet in California (Halverson, 1972). For the study area, sublimation was assumed to occur at the constant rate of 0.011 inch per day. For example, the 17,600 acres of the example subarea was simulated as having a snowpack on December 15, 1958. Sublimation of 0.011 inch per day resulted in 16 acre-feet being subtracted from the snowpack.

## Evapotranspiration

If the model indicates that the subarea is not covered with a snowpack, loss of moisture to the atmosphere is by evapotranspiration (fig. 6, item 3). Daily values of evapotranspiration for each subarea were estimated in three steps from temperature, altitude, solar radiation, vegetation type, and soil moisture. In the first step, potential evaporation from open water was calculated for each subarea from temperature, altitude, and solar radiation data. In the second step, potential evapotranspiration for the vegetation type in the subarea was calculated from potential evaporation from open water. In the third and final step, evapotranspiration was estimated from potential evapotranspiration for the vegetation type and soil moisture available to the vegetation.

Daily potential evaporation from open water for each subarea was calculated using the Jensen-Haise equation (Jensen and Haise, 1963) as modified by Wymore (1974, p. 26) to improve estimates for high-altitude, cold sites. The Jensen-Haise equation was developed using data from arid or semi-arid areas of the Western United States. Equations with similar altitude corrections resulted in accurate water-use estimates (Kruse and Haise, 1974) for wet mountain meadows with water at or near the land surface. Potential evapotranspiration was calculated as:

$$E_w = [0.014T - (0.57 - 0.00004A_a)]R(0.35 + 0.61S_o); \quad (6)$$

where

$E_w$  = daily potential evaporation from open water, in inches per day;

$T$  = estimated mean daily temperature (eq. 2) for the subarea,  
in degrees Fahrenheit;

$A_a$  = average altitude of the subarea, in feet;

$R$  = total solar and sky radiation for a cloudless day converted to  
evapotranspiration equivalent (Jensen and Haise, 1963,  
table 6), in inches per day; and

$S_o$  = estimated average fraction of possible sunshine for the  
subarea, dimensionless.

Monthly values of  $S_o$  reported for Albuquerque, N. Mex., during 1982 and 1983 ranged from 0.61 to 0.92. For the model,  $S_o$  was assumed to be 0.60 because the study area is higher and has more precipitation and, therefore, more cloud cover than Albuquerque.

Potential evapotranspiration for each vegetation type in the subarea was calculated from potential evaporation for the subarea. The relation between daily potential evapotranspiration and daily potential evaporation is shown in table 5 for each of the eight vegetation types in the study area. Potential evapotranspiration was calculated as the product of potential evaporation (eq. 6) and the coefficient from table 5.

The relation between actual evapotranspiration and potential evapotranspiration depends on factors including soil, plant, and atmospheric conditions. However, empirical relations (Zahner, 1967) commonly assume that actual evapotranspiration occurs at the potential rate as long as soil moisture is readily available, and then the rate decreases rapidly. Actual evapotranspiration was assumed to equal potential evapotranspiration only when the soil moisture available to the vegetation exceeded 50 percent of the moisture that the root zone was able to retain. For less than 50 percent, the water was assumed to be released less readily, and actual evapotranspiration was calculated to be less than potential evapotranspiration. When the water simulated by the model as stored in the root zone was less than 50 percent of the volume the root zone was able to retain, actual evapotranspiration was calculated as:

$$E_A = \frac{2M_A}{M_p} E_p; \quad (7)$$

where

$E_A$  = estimated actual evapotranspiration for the vegetation type, in inches per day;

$M_A$  = volume of water simulated as being in the root zone, in inches;

$M_p$  = volume of water the root zone was able to retain, in inches; and

$E_p$  = potential evapotranspiration for the vegetation type, in inches per day.

For example, on June 23, 1959, the station at Del Norte recorded no precipitation and a mean daily temperature ( $T_s$ ) of 65° Fahrenheit. For the example subarea, the mean daily temperature ( $T$ ) was estimated (eq. 2) as 49° Fahrenheit. For June,  $R$  is 0.523 inch per day from Jensen and Haise (1963, table 6); daily potential evaporation ( $E_w$ ) is estimated (eq. 6) as 0.21 inch per day. For the vegetation type in the example subarea (coniferous forest), potential evapotranspiration ( $E_p$ ) is estimated (table 5) as 80 percent of potential evaporation ( $E_w$ ) or 0.17 inch per day. From the preceding day, the root zone contained as much water as it was able to hold ( $M_A = M_p$ ); actual evapotranspiration ( $E_A$ ) was calculated as 0.17 inch per day, equal to potential evapotranspiration ( $E_p$ ). If the simulated volume ( $M_A$ ) had been 10 percent of the volume that the root zone would have been able to hold ( $M_p$ ),

Table 5.--Coefficients for estimating daily potential evapotranspiration  
from daily potential evaporation  
[After Wymore, 1974]

Vegetation type	Value of coefficient (dimensionless) for the month											
	January	February	March	April	May	June	July	August	September	October	November	December
Sagebrush---	0.50	0.50	0.50	0.60	0.80	0.80	0.80	0.71	0.53	0.50	0.50	0.50
Desert shrub-----	.50	.50	.50	.60	.80	.80	.80	.71	.53	.50	.50	.50
Pinon- Juniper---	.65	.65	.65	.70	.80	.80	.80	.80	.69	.65	.65	.65
Mountain shrub-----	.60	.60	.60	.67	.81	.85	.82	.74	.65	.60	.60	.60
Coniferous forest----	.70	.70	.70	.71	.80	.80	.80	.79	.75	.71	.70	.70
Aspen forest----	.60	.60	.60	.67	.85	.90	.86	.75	.65	.60	.60	.60
Rockland and miscellan- eous-----	.50	.50	.50	.60	.65	.65	.65	.60	.50	.50	.50	.50
Grass-----	.50	.50	.50	.80	.80	.80	.80	.71	.53	.50	.50	.50

actual evapotranspiration ( $E_A$ ) would have been calculated (eq. 7) as 0.03 inch per day, 20 percent of potential evapotranspiration ( $E_p$ ).

#### Water Stored in the Snowpack

For each subarea, an accounting was kept of the water simulated as stored in the snowpack; precipitation as snow (fig. 6, item 5) was added to the snowpack; sublimation (fig. 6, item 2) and snowmelt (fig. 6, item 7) were subtracted from the snowpack.

For example, on May 14, 1959, simulated snowpack from the previous day was equivalent to 11.08 inches of water. The station at Del Norte recorded no precipitation and a mean daily temperature ( $T_s$ ) of 57° Fahrenheit. The mean daily temperature for the example subarea ( $T$ ) was estimated (eq. 2) to be 39° Fahrenheit. Sublimation ( $\hat{S}$ ) was estimated as 0.011 inch, and snowmelt ( $M$ ) was estimated (eq. 5) as 0.26 inch, leaving a simulated snowpack of 10.81 inches of water.

#### Water Stored in the Root Zone

For each subarea, an accounting was kept of the water simulated as stored in the root zone; precipitation as rain (fig. 6, item 6) and snowmelt (fig. 6, item 7) were added to soil moisture; evapotranspiration (fig. 6, item 3) was subtracted from soil moisture; when the simulated volume of water exceeded the capacity of the root zone, the excess was subtracted from soil moisture and was assumed to flow to the Alamosa Basin (fig. 6, item 4).

The available water-holding capacity of the root zone was estimated for each of the eight vegetation types recognized in the San Juan Mountains (table 6). Except for grass, the values in table 6 were developed (Wymore, 1974, table 7) by assuming that soil water available to plants is that held within the root zone and, therefore, is a function of the depth of the root zone. The value for grass was obtained by assuming that the capacity of the root zone to store water depends on the depth of the root zone for the vegetation type. Root-density measurements (Brown and Thompson, 1965, p. 758) show that spruce (coniferous forest) roots are scarce below 7 feet, and grass roots are scarce below 4 feet. The value for grass in table 6 was estimated by assuming the same ratio (57 percent) between the water-holding capacity of grass and coniferous forest.

For the example subarea, on May 2, 1959, calculated soil moisture from the previous day was 3.5 inches of water; calculated snowpack from the previous day was equivalent to 8.82 inches of water. The station at Del Norte recorded no precipitation and a mean daily temperature ( $T_s$ ) of 55° Fahrenheit. Mean daily temperature ( $T$ ) for the example subarea was estimated as 37° Fahrenheit (eq. 2, rounded). Because there was a simulated snowpack, evapotranspiration from soil moisture was assumed to be zero, and snowmelt was

estimated as 0.16 inch (eq. 5). Therefore, simulated soil moisture was increased to 3.66 inches, which exceeded the water-holding capacity of the root zone for coniferous forest, 3.5 inches (table 6). Simulated soil moisture was kept at the maximum of 3.5 inches. The remaining 0.16 inch of water over 17,600 acres of coniferous forest resulted in an estimated flow of 230 acre-feet (rounded) from the subarea.

Table 6.--*Capacity of the root zone to store water*

Type of vegetation	Water-holding capacity of root zone (inch)
Sagebrush-----	5.8
Desert shrub-----	6.5
Pinon-Juniper-----	3.0
Mountain shrub-----	4.0
Coniferous forest-----	3.5
Aspen forest-----	5.0
Rockland and miscellaneous-----	3.0
Grass-----	2.0

#### Flow from the San Juan Mountains to the Alamosa Basin

Flow from the San Juan Mountains to the Alamosa Basin was estimated using the water-budget model of the San Juan Mountains. Combined streamflow and ground-water flow (pl. 1) was calculated as 2,800 cubic feet per second (rounded). Streamflow from the San Juan Mountains was subtracted from the total water yield to estimate ground-water flow to the Alamosa Basin from those basins with measured streamflow (table 7). Measured streamflow ranges from 17 percent (Carnero Creek near La Garita, Colo., 08230500) to 113 percent (Conejos River near Mogote, Colo., 08246500) of the water yield calculated by the water-budget model. Most basins appear to lose water to ground water, and streamflow is only part of the water yield to the Alamosa Basin. Exceptions to this general tendency may result from errors in the water-budget model used to calculate water yield or from hydrologic differences among the basins. The two basins (those drained by the Conejos and Los Pinos Rivers) for which ground-water flow is negative may be draining adjacent basins. For example, ground water may be moving from the La Jara Creek basin to the Conejos River basin to appear as streamflow in the Conejos River near Mogote, Colo.

Flows from basins in the San Juan Mountains to the Alamosa Basin were accumulated (pl. 1 and table 7) and compared to similar estimates by Emery and others (1973, pl. 1) in table 8. The major difference is that Emery assumed that ground-water flow was negligible; whereas, in this report, the water-budget model calculated a water yield greater than measured streamflow.

Table 7.--Streamflow and estimated ground-water flow to the Alamosa Basin from drainage basins in the San Juan Mountains with measured streamflow  
[All values are in cubic feet per second]

Station name	Station number	Map number <sup>1</sup>	Total water <sup>2</sup> yield	Streamflow <sup>3</sup>	Ground-water flow <sup>4</sup>
CLOSED BASIN					
Kerber Creek at Ashley Ranch, near Villa Grove, Colo.	08224500	245	43	13	30
Saguache Creek near Saguache, Colo.	08227000	270	241	57	184
Carnero Creek near La Garita, Colo.	08230500	305	63	11	52
La Garita Creek near La Garita, Colo.	08231000	310	55	13	42
UPSTREAM FROM RIO GRANDE NEAR DEL NORTE					
Rio Grande at Wagonwheel Gap, Colo. <sup>5</sup>	08217500	175	889	506	383
Goose Creek at Wagonwheel Gap, Colo. <sup>5</sup>	08218500	185	94	60	34
South Fork Rio Grande at South Fork, Colo. <sup>5</sup>	08219500	195	335	190	145
Rio Grande near Del Norte, Colo. <sup>6</sup>	08220000	200	1,453	771	682
DOWNSTREAM FROM RIO GRANDE NEAR DEL NORTE					
Pinos Creek near Del Norte, Colo.	08220500	205	75	23	52
Alamosa Creek <sup>7</sup> above Terrace Reservoir, Colo.	08236000	360	136	98	38
La Jara Creek at Gallegos Ranch near Capulin, Colo.	08238000	380	57	15	42
CONEJOS RIVER AND TRIBUTARIES					
Conejos River near Mogote, Colo.	08246500	465	259	292	-33
San Antonio River at Ortiz, Colo.	08247500	475	36	13	23
Los Pinos River near Ortiz, Colo.	08248000	480	99	105	-6

<sup>1</sup>Locations shown on plate 1.

<sup>2</sup>Calculated by the water-budget model of the San Juan Mountains for drainage area above the station.

<sup>3</sup>Mean streamflow for 1950-80.

<sup>4</sup>Calculated as a residual. Negative values result from measured streamflow greater than the water yield calculated by the water-budget model of the San Juan Mountains.

<sup>5</sup>Drainage area included in that for station 08220000. Only streamflow past the Del Norte station reaches Alamosa Basin as streamflow.

<sup>6</sup>Drainage area above this station includes the drainage area for the upstream stations 08217500, 08218500, and 08219500.

<sup>7</sup>This station is on Alamosa River.



Table 8.--*Comparison of published estimates of flow from the San Juan Mountains to the Alamosa Basin*  
[All estimates are in cubic feet per second]

Source	Measured streamflow	Estimated total streamflow	Estimated total water yield
This report-----	1,400	( <sup>1</sup> )	2,800
Emery and others (1973)---	( <sup>2</sup> )	1,700	1,700

<sup>1</sup>Not estimated.

<sup>2</sup>Not given separately.

Flow from the San Juan Mountains to the closed basin was accumulated (pl. 1 and table 7) and compared to similar estimates by Emery and others (1973, pl. 1) and by Huntley (1976, table 3) in table 9. Whereas Emery assumed that ground-water flow was negligible, both this report and Huntley's calculated a water yield greater than measured streamflow. The difference between this report and Huntley's results from different estimation methods used in the water-budget models.

Table 9.--*Comparison of published estimates of flow from the San Juan Mountains to the closed basin*  
[All estimates are in cubic feet per second]

Source	Measured streamflow	Total streamflow	Estimated total water yield
This report-----	94	( <sup>1</sup> )	490
Huntley (1976)-----	95	95	760
Emery and others (1973)---	( <sup>2</sup> )	149	149

<sup>1</sup>Not estimated.

<sup>2</sup>Not given separately.

#### THE SANGRE DE CRISTO MOUNTAINS

The Sangre de Cristo Mountains (fig. 2) of the Southern Rocky Mountains consist of two linear fault-block segments that extend from the northern tip of the study area to Santa Fe, N. Mex., (fig. 1). The northern segment extends north-northwest from Blanca Peak to form the eastern border of the Alamosa Basin (fig. 2). The southern unit extends south from Blanca Peak to form the eastern borders of the Costilla Plains (fig. 2) and the Espanola basin (fig. 1). The two units hinge in a zone of complex structure near Blanca Peak.

The Sangre de Cristo Mountains consist largely of Precambrian, Paleozoic, and Mesozoic igneous and metamorphic rocks. Ground water moves through fracture openings and weathered zones, which generally are of small areal extent and shallow depth. Ground-water flow is complex because of the irregular spatial distribution of aquifers; the general pattern of flow is as follows: Rainfall and snowmelt recharge shallow aquifers on hillsides

adjacent to stream valleys; water flows through these shallow aquifers and discharges to the streams draining the valleys. Hillsides adjacent to Alamosa Basin may discharge to shallow aquifers of the basin.

No significant ground-water development has occurred in the Sangre de Cristo Mountains. The significance of the Sangre de Cristo Mountains to the hydrology of the study area is as a source of water for the Alamosa Basin and the Costilla Plains. Several streams flow from the Sangre de Cristo Mountains onto the Alamosa Basin and the Costilla Plains. North of Blanca Peak, the streams enter the closed basin from which there is no surface-water discharge. South of Blanca Peak, the streams enter either the Alamosa Basin or the Costilla Plains and flow to the Rio Grande. However, most of the flow infiltrates through the more permeable valley fill to recharge the ground-water flow system.

The regression model described in the following section was used to estimate the average flow from the Sangre de Cristo Mountains to the Alamosa Basin and the Costilla Plains. Readers not interested in this detailed description may skip the following section and resume reading at the section "Flow from the Sangre de Cristo Mountains to the Alamosa Basin and the Costilla Plains."

#### Regression Model of Water Yield from the Sangre de Cristo Mountains

Water yield from the Sangre de Cristo Mountains for 1950-80 was calculated from a regression model of 16 basins in or adjacent to the study area. Basins were selected that: (1) Had measured streamflow most of 1950-80; (2) had no unmeasured diversions upstream from the gaging station; and (3) overlay crystalline rock. Ground water that left these basins underground was assumed negligible. Therefore, streamflow past these stations (table 10) was assumed to represent the water yield of the basin.

The model was a multiple linear regression of mean annual water yield against mean winter precipitation and drainage area. Mean winter precipitation was determined from a map constructed from data for 1931-60 (U.S. Weather Bureau, undated, a and b). Area of the basin was obtained from U.S. Geological Survey (1969, 1970) descriptions of the gaging stations. The regression equation was:

$$Q = 7.62 \times 10^{-5} A^{0.977} P^{3.596}; \quad (8)$$

where

$Q$  = mean annual water yield, in cubic feet per second;

$A$  = area of the basin, in square miles; and

$P$  = mean winter precipitation, in inches.

This equation is similar to that proposed by Borland (1970) except that latitude and slope of the basin were not retained as independent variables. The regression was made linear by regressing  $\log Q$  against  $\log A$  and  $\log P$ . The correlation coefficient for this logarithmic regression was 0.96.

Table 10.--Streamflow-gaging stations in the Sangre de Cristo Mountains that were used in the regression model of mountain water yield  
[mi<sup>2</sup>, square miles; ft<sup>3</sup>/s, cubic feet per second; in., inches]

Station name	Station number	Map number	Area (mi <sup>2</sup> )	Average discharge (1950-80) (ft <sup>3</sup> /s)	Mean winter precipitation (1930-60) (in.)
Rayado Creek at Sauble Ranch, near Cimarron, N. Mex.	07208500	( <sup>1</sup> )	65	13	8.63
Coyote Creek near Golondrinas, N. Mex.	07218000	( <sup>1</sup> )	215	10	7.09
Mora River at La Cueva, N. Mex.	07215500	( <sup>1</sup> )	173	25	8.58
Ute Creek near Fort Garland, Colo.	08242500	425	32	17	11.4
Red River near Questa, N. Mex. (diversions are added in).	08265000	650	113	42	10.9
Cabresto Creek near Questa, N. Mex. (plus Llano Ditch).	08266000	660	36.7	11	11.2
Rio Hondo near Valdez, N. Mex.	08267500	675	36.2	30	14.0
Rio Pueblo de Taos near Taos, N. Mex.	08269000	690	66.6	<sup>3</sup> ,724	10.6
Rio Lucero near Arroyo Seco, N. Mex.	08271000	710	16.6	<sup>3</sup> ,719	14.7
Rio Grande del Rancho near Talpa, N. Mex.	08275500	755	83	<sup>4</sup> ,720	9.36
Rio Chiquito near Talpa, N. Mex.	08275600	756	37	<sup>5</sup> ,78	9.17
Embudo Creek at Dixon, N. Mex.	08279000	790	305	<sup>6</sup> ,766	9.14
Rio Ojo Caliente at La Madera, N. Mex.	08289000	( <sup>2</sup> )	419	60	7.89
Santa Cruz River at Cundiyo, N. Mex.	08291000	( <sup>1</sup> )	86	26	9.71
Pecos River near Pecos, N. Mex.	08378500	( <sup>2</sup> )	189	88	12.16
Gallinas Creek near Montezuma, N. Mex.	08380500	( <sup>2</sup> )	84	17	9.41

<sup>1</sup>Station is out of the study area and is not shown on plate 1. Refer to U.S. Geological Survey, 1969, for location.

<sup>2</sup>Station is out of the study area and is not shown on plate 1. Refer to U.S. Geological Survey, 1970, for location.

<sup>3</sup>Average discharge estimated for 1952-62.

<sup>4</sup>Average discharge estimated for 1950-51.

<sup>5</sup>Average discharge estimated for 1950-56.

<sup>6</sup>Average discharge estimated for 1955-62.

<sup>7</sup>For periods of missing record, monthly discharge was estimated from a regression relation with monthly discharge from the Santa Cruz River at Cundiyo, N. Mex., (08291000).

Flow from the Sangre de Cristo Mountains to the  
Alamosa Basin and the Costilla Plains

Flow from the Sangre de Cristo Mountains to the Alamosa Basin and the Costilla Plains was estimated using the water-yield model for the Sangre de Cristo Mountains. Total water yield was calculated (using eq. 8) as 780 cubic feet per second (rounded); flows for individual basins are shown on plate 1. Runoff from about 450,000 acres of the Sangre de Cristo Mountains flows onto the Alamosa Basin; combined water yield (pl. 1) was estimated (using eq. 8) to be 340 cubic feet per second (rounded). Runoff from about 900,000 acres of the Sangre de Cristo Mountains flows onto the Costilla Plains; combined water yield (pl. 1) was estimated (using eq. 8) to be 440 cubic feet per second (rounded), 120 cubic feet per second (rounded) in Colorado, and 330 cubic feet per second (rounded) in New Mexico.

Flow from the Sangre de Cristo Mountains to the Alamosa Basin was accumulated (pl. 1) and compared to similar estimates by Emery and others (1973, pl. 1) and Huntley (1976, table 2) in table 11. Differences between estimated total flow to the closed basin primarily are due to the assumption in this report and by Emery and others (1973) that ground-water flow was negligible. Differences between estimated total flow to the Alamosa Basin are due to the different methods of estimation and the different time period during which flows were averaged.

Table 11.--*Comparison of published estimates of flow from the Sangre de Cristo Mountains to the closed basin and the Alamosa Basin*  
[All estimates are in cubic feet per second]

Source	Estimated flow to the closed basin			Estimated flow to the Alamosa Basin		
	Streamflow	Ground-water flow	Total flow	Streamflow	Ground-water flow	Total flow
This report-- <sup>(1)</sup>		<sup>(1)</sup>	260	<sup>(1)</sup>	<sup>(1)</sup>	340
Emery and others (1973)-----	160	0	160	210	0	210
Huntley (1976)-----	260	89	350	<sup>(2)</sup>	<sup>(2)</sup>	<sup>(2)</sup>

<sup>1</sup>Not estimated as a separate item.

<sup>2</sup>Not estimated.

### THE SAN LUIS HILLS

The San Luis Hills (fig. 2) are one of the northeast-trending basement lineaments characteristic of the Rio Grande rift below Alamosa, Colo., (Chapin, 1979). South of the Manassa fault, the San Luis Hills trend along a line extending southwest from the structurally complex area south of Blanca Peak, which separates the northern and southern units of the Sangre de Cristo Mountains. A narrow bridge connecting the San Luis Hills and Blanca Peak is

indicated by a gravity high beneath the northwestern edge of the Costilla Plains (Burroughs, 1978). The upfaulted blocks of the San Luis Hills separate the Alamosa Basin to the north from the Taos Plateau and the Costilla Plains to the south. The volcanic rocks of the San Luis Hills are equivalent to the Conejos Formation of the San Juan Mountains (Burroughs, 1971), which date from about 27 million years ago. To the south and east of the hills, younger age basalts (dating from 3.6 to 4.5 million years ago) are equivalent to those of the Taos Plateau. Structurally, the San Luis Hills are divided into east and west sections along a fault zone near the Rio Grande. Stocks and dikes are found primarily near this fault zone or in the San Luis Hills to the west. In these western San Luis Hills, the strata are nearly horizontal. In contrast, the eastern San Luis Hills are tilted-fault blocks dipping to the southeast about 10 to 15 degrees.

The San Luis Hills are significant to the hydrology of the study area because of their position between the aquifers to the north and south. Ground-water flow from the Alamosa Basin to the Taos Plateau and the Costilla Plains must flow through or around the San Luis Hills. No significant ground-water development has occurred in the San Luis Hills. Flow from the San Luis Hills to the Alamosa Basin or the Costilla Plains probably is small.

The San Luis Hills may be a barrier to ground-water flow from the Alamosa Basin to either the Costilla Plains or the Taos Plateau. However, the data are inconclusive because of the variability of hydraulic conductivity exhibited by materials grouped together as volcanic rock. Both water-budget and water-level data indicate that flow through or around the San Luis Hills is small. Calculation of ground-water flow through or around the San Luis Hills as the residual term of a water budget produces a very uncertain estimate. For example, Emery and others (1973, fig. 1) calculated the ground-water outflow from the San Luis Valley as 69 cubic feet per second. However, because this flow is only 2 percent of the estimated evapotranspiration, a slight error in estimating evapotranspiration would result in a large error in calculated ground-water outflow. A 10 percent error in estimated evapotranspiration would be more than 330 cubic feet per second.

The flow may be small because the basalts are poor aquifers. Alternately, in the western San Luis Hills, stocks and dikes (Burroughs, 1971) may form hydraulic barriers between the permeable strata of the volcanic rocks. In the eastern San Luis Hills, the southeasterly dip of 10 to 15 degrees may severely retard horizontal flow from the Alamosa Basin to the Costilla Plains. Assuming hydraulic conductivities (Huntley, 1976) of 140 feet per day along the beds and 0.0003 foot per day normal to the beds, a dip of 10 degrees would result in an effective horizontal hydraulic conductivity of about 0.01 foot per day (Hearne, 1985a). Horizontal flow would be about 0.01 cubic foot per second or 8 acre-feet per year through an area of the San Luis Hills about 1,000 feet deep and 1 mile wide under a hydraulic gradient of 100 feet per mile. Although flow through the San Luis Hills is small, individual aquifers in the hills may yield significant quantities of water to a well.

Water-level data are consistent with the hypothesis that the San Luis Hills are a barrier to flow, in that: (1) Water-level contours are approximately perpendicular to the hills; and (2) hydraulic-head differences across the San Luis Hills are much greater than those on either side of the hills. In southwestern Alamosa Basin, flow lines bend around the western hills and water-level contours are approximately perpendicular to the hills (pl. 1). Data support the hypothesis that: (1) The western San Luis Hills form a barrier to ground-water flow between the Alamosa Basin and either the Taos Plateau or the Costilla Plains; and (2) this barrier consists of a series of discontinuities between adjacent aquifers; individual aquifers in the San Luis Hills may be permeable.

In the eastern San Luis Hills, water-level contours in the shallow alluvium (pl. 1), although perpendicular to the San Luis Hills, are about the same on either side of the San Luis Hills. The eastern San Luis Hills could be either: (1) An impermeable boundary dividing flow between the Alamosa Basin and the Costilla Plains; or (2) an aquifer comparable to those on either side. However, hydraulic heads in the volcanic rocks south of the San Luis Hills are lower than hydraulic heads in the aquifers of the Alamosa Basin and the shallow alluvium in the Costilla Plains. The most reasonable hydraulic barrier between the Alamosa Basin and the Costilla Plains is the eastern San Luis Hills. The difference in hydraulic head between shallow alluvial aquifers and underlying volcanic rocks of the Costilla Plains will be discussed in the section entitled "The Costilla Plains."

## THE TAOS PLATEAU

The Taos Plateau (fig. 2) is south of the San Luis Hills and west of the Rio Grande. The land is capped with volcanic rocks that erupted between about 2.0 to 4.5 million years ago (Lipman and Mehnert, 1979, p. 289). Volcanic rocks of the plateau extend north to the San Luis Hills and perhaps into the subsurface in southwestern Alamosa Basin. San Pedro Mesa (on the State boundary east of the Costilla Plains and south of Blanca Peak) may be capped with volcanic rocks of the plateau (Upson, 1939, p. 586). The eastern margin of the plateau is near the Rio Grande. The western margin was arbitrarily assumed to be the project boundary. Volcanic plateau basalts dip eastward and extend several miles east of the Rio Grande. East of the Rio Grande, the Costilla Plains are described as a separate area, because these volcanic rocks are covered with alluvial sediments that form an upper aquifer. Hills on the Taos Plateau and the Costilla Plains (fig. 2) represent the topography around which the basalts flowed.

The Taos Plateau is underlain by lava flows and beds of volcanic ash; individual lava flows are generally less than 50 feet thick. As much as 670 feet of volcanic rocks are exposed in the canyon of the Rio Grande. The volcanic rocks are, in turn, underlain by sedimentary rocks of the Santa Fe Group. Ground water moves through fractures in the volcanic rocks or along the zones between individual lava flows. Therefore, although individual rocks may be impermeable, basalt lavas as a group are very permeable to ground-water flow in the plane of the lava flows. However, normal to the plane of the lava flows, water moves through fractures. The anisotropy of the hydraulic conductivity of the basalt lavas as a group is quite variable. Details of

ground-water flow are complex because of the dependence on the topography (unknown but probably complex) around which the basaltic lava flowed and the irregular distribution of fractures permitting vertical flow. The general pattern of flow is irregularly distributed recharge moving through fractures to local perched aquifers and eventually to the deep aquifer system, where it moves to discharge as springflow or seepage flow to the Rio Grande. In the southwestern third of the Taos Plateau, lava flows are above the water table, and water moves through underlying sedimentary rocks. Recharge also may occur as seepage from streams draining highlands west of the Taos Plateau. Recharge to the northern third of the Taos Plateau may originate as seepage loss from surface water that is flowing toward the Alamosa Basin. However, this hypothesis cannot be verified because of the lack of geologic and hydrologic data.

The Taos Plateau has low relief and low-gradient drainage except for steeper channels near several extinct volcanoes and hills of older rock that rise above the flat surface. Numerous depressions with clay or silt bottoms are found on the plateau. Most precipitation appears to: (1) Return to the atmosphere as evapotranspiration; (2) recharge the permeable volcanic rocks directly; or (3) flow to one of the depressions or to an arroyo, where water not lost to the atmosphere recharges the permeable volcanic rocks. Discharge from the Taos Plateau as streamflow is small.

The regression model described in the following section was used to estimate water yield from the Taos Plateau to the Rio Grande. Readers not interested in this detailed description may skip the following section and resume reading at the section "Flow from the Taos Plateau to the Rio Grande."

#### Regression Model of Water Yield from the Taos Plateau

Water yield from the Taos Plateau was calculated from a regression model of 16 basins in New Mexico (table 12). The basins resemble the Taos Plateau because they receive small amounts of precipitation. However, the basins differ from the Taos Plateau in that they overlie rocks of small permeability. Recharge to ground water was assumed to be negligible, and the water yield of the area was assumed to be measured as streamflow. Because of the similarities in precipitation, area, and slope, water yield was assumed to be similar for basins on the Taos Plateau and the basins used in the regression. However, on the Taos Plateau most of the water yield may leave the basin as ground-water outflow.

The model was a multiple regression of mean annual water yield against mean winter precipitation, slope, and drainage area. Mean winter precipitation was determined from a map constructed from data for 1931-60 (U.S. Weather Bureau, undated, a and b). Slope was calculated as the altitude difference, in feet, divided by the length of channel, in miles, between two points along a stream. These two points were measured from the lowest point of the stream in the basin and were located upstream 10 percent and 85 percent of the stream length. The stream length was measured from the lowest to the highest point

Table 12.--Streamflow-gaging stations in New Mexico that were used in the regression model of the Taos Plateau water yield  
[mi<sup>2</sup>, square miles; ft/mi, feet per mile; in., inches; ft<sup>3</sup>/s, cubic feet per second]

Station name	Station number	Map number	Basin area (mi <sup>2</sup> )	Basin slope (ft/mi)	Winter precipitation (1931-60) (in.)	Period of record	Mean discharge (period of record) (ft <sup>3</sup> /s)
Vermejo River near Dawson	07203000	( <sup>1</sup> )	301	62.9	6.02	1916-17, 1920, 1928-80	17.9
Sixmile Creek near Eagle Nest	07205000	( <sup>1</sup> )	10.5	429	9.27	1932, 1959-75	2.51
Ponil Creek near Cimarron	07207500	( <sup>1</sup> )	171	99	7.09	1916-25, 1928, 1951-80	10.8
Rayado Creek at Sauble Ranch, near Cimarron	07208500	( <sup>1</sup> )	65	212	8.63	1912, 1914, 1916-20, 1924, 1928-80	13.7
Mora River at La Cueva	07215500	( <sup>1</sup> )	173	65.2	8.58	1907-10, 1932-86	26.8
Coyote Creek near Golondrinas	07218000	( <sup>1</sup> )	215	45.3	7.09	1928-80	11.2
Rio Fernando De Taos, near Taos	08275000	750	71.7	126	8.67	1913-17, 1928, 1963-80	5.87
Rio Grande Del Rancho, near Talpa	08275500	755	83	194	9.36	1952-80	18.9
Rio Chiquito near Talpa	08275600	756	37	168	9.17	1957-80	7.56
Embudo Creek at Dixon	08279000	790	305	113	9.14	1924, 1925, 1927-55, 1963-80	74.9
Rio Ojo Caliente at La Madera	08289000	( <sup>1</sup> )	419	104	7.89	1932-80	64.9
Santa Cruz River at Cundiyo	08291000	( <sup>1</sup> )	86	320	9.71	1930-80	28.2
Arroyo Chico near Guadalupe	08340500	( <sup>1</sup> )	1,390	21.9	4.27	1943-80	21.3
Gallinas Creek near Montezuma	08380500	( <sup>1</sup> )	84	196	9.41	1915, 1917-80	19.1
Rio Tularosa near Bent	08481500	( <sup>1</sup> )	120	146	8.45	1949-80	9.67
Gila River near Gila	09430500	( <sup>1</sup> )	1,864	37.1	6.88	1928-80	134

<sup>1</sup>Station is out of study area and not shown on plate 1. Refer to U.S. Geological Survey (1971-75b, 1976-82a) for location.



along the stream. Area of the basin was obtained from U.S. Geological Survey (1971-75b, 1976-82a) descriptions of the gaging stations. The regression equation was:

$$Q = 1.074 \times 10^{-5} A^{1.216} P^{2.749} S^{0.535}; \quad (9)$$

where

$Q$  = mean annual water yield, in cubic feet per second;

$A$  = area of the basin, in square miles;

$P$  = mean winter precipitation, in inches; and

$S$  = slope of the basin, in feet per mile.

This equation is similar to that proposed by Borland (1970) except that the latitude of the basin was not retained as an independent variable. The regression was made linear by regressing  $\log Q$  against  $\log A$ ,  $\log P$ , and  $\log S$ . The correlation coefficient for this logarithmic regression was 0.96.

#### Flow from the Taos Plateau to the Rio Grande

The flow calculated by the Taos Plateau water-yield model was 28 cubic feet per second. Because the modeling assumptions were not verified, the confidence in this estimate was minimal. No attempt was made to apportion the recharge among individual basins in the Taos Plateau. However, the estimated flow was small, about 2 percent of the 1950-80 mean streamflow measured at the gaging station on the Rio Grande at Embudo, N. Mex., (08279500).

#### THE COSTILLA PLAINS

The Costilla Plains (fig. 2) are bounded by the Sangre de Cristo Mountains to the east, the Picuris Mountains to the south, the Taos Plateau to the west, and the San Luis Hills to the north. The Rio Grande flows onto the Costilla Plains through a breach in the San Luis Hills, flows along the western margin, and discharges from the plains through a bedrock constriction near Embudo, N. Mex. Along this reach, altitude of the Rio Grande decreases from 7,450 to less than 5,800 feet. The Costilla Plains contain several thousand feet of interbedded gravel, sand, silt, clay, and volcanic rocks. The general description of the aquifer system offered by Winograd (1959) consists of a shallow alluvial aquifer, underlain by volcanic rocks from the Taos Plateau, in turn underlain by several thousand feet of interbedded sedimentary rocks (fig. 5). Within this aquifer system, water typically occurs in perched or semiperched (fig. 3) conditions. Recharge to the alluvial aquifer is by leakage from streams flowing from the Sangre de Cristo Mountains. Discharge from the alluvial aquifer is downward to underlying volcanic rocks. The general flow and nature of discharge are determined by local aquifer characteristics. For discussion of flow and discharge, the Costilla Plains may be divided into three areas: (1) From the San Luis Hills to Ute Mountain; (2) from Ute Mountain to the Red River; and (3) south of the Red River.

From the San Luis Hills to Ute Mountain, the Costilla Plains are in an area of complex structure associated with the San Luis Hills and the hinge for the two segments of the Sangre de Cristo Mountains. Hydraulic conductivity is such that the alluvium above the volcanics is not saturated everywhere, and water levels in the volcanic rocks are below the level of the Rio Grande. Recharge is by seepage from streams as they cross the permeable alluvium. Water flows west through the alluvial aquifer, down to underlying volcanic rocks, and south as subsurface flow through the volcanic rocks.

From Ute Mountain to the Red River, the shallow alluvial aquifer is separated from underlying volcanic rocks by less permeable clay beds. Movement of water down through the clays is slow enough that the shallow alluvium is saturated. Water enters the volcanic rocks as subsurface flow from the north and as flow down from the semiperched alluvial aquifer. Discharge from the volcanic rocks is through springs along the Rio Grande and the Red River.

South of the Red River, a narrow strip of less permeable volcanic rocks forms a hydrologic barrier to movement of ground water from the alluvial aquifer on the east to the Rio Grande on the west. The alluvial aquifer is recharged by seepage from streams as they flow from the Sangre de Cristo Mountains to the east. Ground water discharges from springs along the major streams east of the volcanic rocks.

Although irrigated agriculture is practiced in the Costilla Plains, the significance of the plains to the hydrology of the study area is as a source of water for the Rio Grande. The gain in flow of the Rio Grande as it passes along the western margin of the Costilla Plains prompted Major Powell in 1890 (Siebenthal, 1910, p. 16) to testify that ". . . when the river emerges into the valley at the foot of Embudo Canyon, it is a fine stream and must always be so whatever water is taken out in Colorado above." A water balance of the Costilla Plains will provide estimates of the sources of this gain.

The evapotranspiration model described in the following section was used to estimate evapotranspiration from the Costilla Plains. Readers not interested in this detailed description may skip the following section and resume reading at the section "Water budget for the Costilla Plains."

#### Calculated Evapotranspiration for the Costilla Plains

Evapotranspiration is a complex physical process. However, the calculations here rely on simplifying assumptions that reduce the model to bookkeeping. This section describes the bookkeeping calculations used. Evapotranspiration from the Costilla Plains was assumed to depend on depth to water and land use. Three categories were considered: (1) Water-course and riparian areas; (2) nonirrigated areas; and (3) irrigated areas.

Watercourse and riparian areas include those along the Rio Grande from the San Luis Hills to Embudo, N. Mex., irrigation canals, stock ponds, reservoirs, and streams on the Costilla Plains. For these areas, water is at or near the land surface. For water at the land surface in the Alamosa Basin, Emery and others (1971) estimated an evapotranspiration of 5 feet per year.

For the 4,000 acres (estimated from U.S. Geological Survey topographic maps) of watercourse and riparian areas in the Costilla Plains, evapotranspiration was assumed to be 4.5 feet per year. The resulting loss to the atmosphere was calculated to be 25 cubic feet per second.

For other nonirrigated areas, evapotranspiration was assumed to be limited by precipitation. Away from watercourses and riparian areas, the depth to water was estimated from 1980 water levels to exceed 20 feet (Crouch, 1983). At these depths, Emery and others (1971) estimated evapotranspiration from ground water to be negligible. Therefore, precipitation was assumed to be the only source of water for evapotranspiration. Precipitation from each storm event was assumed to be stored as soil moisture and returned to the atmosphere by evapotranspiration. Precipitation was estimated from isohyetal maps (National Oceanic and Atmospheric Administration, 1980) to average about 1.0 foot per year. Therefore, evapotranspiration from the estimated 340,000 acres of nonirrigated land in the Costilla Plains was calculated to be 470 cubic feet per second.

For irrigated areas, evapotranspiration was estimated from irrigated acreage, average depletion, and precipitation. Of the 72,000 acres of irrigated land in Costilla County, Colorado (U.S. Soil Conservation Service and Colorado State University Experiment Station, 1980a), about 43,000 acres (60 percent) is in the Costilla Plains. For 1950-80, the irrigated area in Taos County, New Mexico (Lansford and others, 1980) has averaged about 41,000 acres including idle and fallow land. Therefore, the total irrigated acreage of the Costilla Plains was estimated to be 84,000 acres.

Precipitation on irrigated acreage was estimated to be 1.0 foot per year, the same as for nonirrigated land. Therefore, precipitation on the 84,000 acres of irrigated land was calculated to be 120 cubic feet per second.

In addition to precipitation, irrigation withdrawals were made from surface and ground-water sources for application to irrigated areas. Irrigation depletion is the amount of water from surface water and ground-water withdrawals that is consumed by crops or lost to the atmosphere during irrigation. During 1979, depletion was estimated as 47,650 acre-feet (Lansford and others, 1980) for 41,900 irrigated acres in Taos County, New Mexico. This rate of 1.14 feet per year was used to calculate a depletion of 130 cubic feet per second for the 84,000 irrigated acres in the Costilla Plains.

In summary, evapotranspiration from the Costilla Plains was estimated to be 740 cubic feet per second (rounded): 25 cubic feet per second from watercourse and riparian areas, 470 cubic feet per second from nonirrigated areas, and 250 cubic feet per second from irrigated areas.

#### Water Budget for the Costilla Plains

The Costilla Plains is described by presenting a water budget (table 13). The change in the volume of water stored beneath the Costilla Plains was assumed to be negligible. Many of the items in the water budget have been estimated in the sections "Flow from the Sangre de Cristo Mountains to the

Alamosa Basin and the Costilla Plains," "Flow from the Taos Plateau to the Rio Grande," and "Calculated Evapotranspiration for the Costilla Plains."

In the section "Calculated Evapotranspiration for the Costilla Plains," precipitation was estimated to average 1.0 foot per year. Precipitation on the 430,000 acres (rounded) of the Costilla Plains was calculated to be 590 cubic feet per second (rounded).

Table 13.--*Water budget for the Costilla Plains*  
[All estimates are in cubic feet per second]

Inflow and outflow	Estimated flow
INFLOW	
Sangre de Cristo Mountains-----	440
Taos Plateau-----	28
Precipitation on the Costilla Plains-----	590
Rio Grande, near Lobatos, Colo.-----	350
Ground-water flow past the San Luis Hills-----	( <sup>1</sup> )
Total inflow-----	1,408
OUTFLOW	
Evapotranspiration from the Costilla Plains-----	740
(Nonirrigated areas--490 (rounded))	
(Irrigated areas-----250)	
Rio Grande, near Embudo, N. Mex.-----	680
Total outflow-----	1,420

<sup>1</sup>Not estimated.

The Rio Grande flows through the Costilla Plains from the San Luis Hills to Embudo, N. Mex. Average streamflow in the Rio Grande from 1950 to 1980 was 350 cubic feet per second near Lobatos, Colo., and 680 cubic feet per second near Embudo, N. Mex.

Ground-water discharge from the study area is assumed to be negligible. The channel narrows at Embudo, N. Mex., and impermeable crystalline rock restricts flow through the permeable sedimentary rocks of the Costilla Plains.

Ground-water inflow to the Costilla Plains through and around the San Luis Hills cannot be measured directly. Also, inadequate definition of the transmissivity of the volcanic rocks of the San Luis Hills precludes an independent estimate of inflow from the hydraulic gradient. Hydraulic heads are higher in the Alamosa Basin. Therefore, flow (if any) must be from the Alamosa Basin to the Costilla Plains. To balance the water budget, inflow should equal outflow. Ground-water inflow was calculated as the residual of the water budget to be about 10 cubic feet per second by subtracting other estimated inflows from the estimated outflow. Because the flow is small relative to the other items in the budget, this estimate is not accurate and was not included in table 13. Although the budget (table 13) indicates that large flows through or around the San Luis Hills are not needed to account for

the observed gains in the Rio Grande, a water budget is not a reliable method for accurately estimating small flows.

## THE ALAMOSA BASIN

The Alamosa Basin (fig. 2) is bounded by the Sangre de Cristo Mountains on the east, the San Juan Mountains on the west, and the San Luis Hills on the south. The Rio Grande flows into the Alamosa Basin from the San Juan Mountains and flows from the valley through a gap in the San Luis Hills. The Alamosa Basin contains several thousand feet of interbedded gravel, sand, silt, clay, and volcanic rocks that form a leaky artesian aquifer system. A common description of the aquifer system is based on the division of the aquifer system into an "unconfined aquifer" and a "confined aquifer" separated by either a clay series or unfractured volcanic rocks. These subdivisions are useful in describing general features of the aquifer system, but they need to be used with caution. The conceptual system accepted here is not of two aquifers separated by an impermeable confining bed but rather of complexly interlayered aquifers and leaky confining beds, each of limited areal extent and variable hydraulic properties. The resulting complex is a heterogeneous, anisotropic aquifer system.

Most deep wells in the Alamosa Basin probably are completed in more than one aquifer of the system. Analysis of water levels from such wells requires supportive data that may or may not be available. Hydraulic head in the well depends on depth of the well, aquifers to which the well is completed, and the hydraulic head and hydraulic conductivity of each aquifer. Wells completed to more than one aquifer may be conduits for flow between aquifers either with or without flow at the surface. Hydraulic head in the well is a composite of hydraulic heads in the aquifers with which the well is in hydraulic connection. For such an aquifer system, hydraulic head in a well completed to more than one stratum may provide little or no information about hydraulic head in an individual stratum. Potentiometric surface is a valid concept only if the particular stratum in the aquifer system is specified; the water table is the potentiometric surface in the uppermost saturated strata of the aquifer system. Surfaces representing water levels in wells of variable depths do not constitute a potentiometric surface.

The Alamosa Basin contains a closed basin to the north of the Rio Grande. The closed basin is separated from the rest of the Alamosa Basin by a low topographic divide and a ground-water divide. For years, the closed basin has discharged neither surface water nor ground water to the Rio Grande (Powell, 1958, pl. 8; Emery and others, 1973). However, both surface and ground-water divides occasionally may be breached. Although the closed basin is not yet integrated with the rest of the Alamosa Basin by aggradation or erosional breaching, a drainage course to the Rio Grande has existed (Siebenthal, 1910, p. 12), and presumably, this drainage flowed during unusually large runoff events. The ground-water divide may have developed because of surface-water irrigation on the alluvial fan of the Rio Grande. Most of the flow of the Rio Grande is diverted to irrigate the fan north of the river. The resultant recharge from unconsumed irrigation water to ground water may have raised the hydraulic head by as much as 50 to 100 feet creating the ground-water divide (Powell, 1958, p. 56). During 1970 to 1979, changes in hydraulic head of less

than 30 feet have transposed the ground-water divide southward to the Rio Grande (Crouch, 1983). This southern boundary of the closed basin probably migrates north and south in response to seasonal and long-term changes in irrigation-return flow and ground-water withdrawals.

Recharge to the closed basin consists of percolation of surface water from streams flowing from the adjacent mountains, percolation of water applied to irrigated areas, and subsurface flow through the permeable volcanic rocks of the San Juan Mountains (fig. 4). Most of the recharge is from the San Juan Mountains on the west; subsurface flow is greater than streamflow. Recharge from precipitation on the closed basin is small because precipitation is less than evapotranspiration. Discharge consists of withdrawals from wells and evapotranspiration. The general pattern of flow is from recharge areas near the perimeter to discharge areas near the center of the Alamosa Basin. However, both recharge and discharge are distributed throughout large overlapping areas, and the detailed flow is complex.

South of the Rio Grande, in central Alamosa Basin, hydrologic conditions differ from those in the closed basin in that: (1) Streamflow dominates recharge from the west; and (2) discharge may include seepage to the Rio Grande. The general pattern of flow is similar to that in the closed basin: ground-water flows from the perimeter to the center of the basin.

In the southern Alamosa Basin, hydrologic conditions are altered further because: (1) The San Luis Hills form a hydraulic barrier and contribute little or no recharge; (2) subsurface volcanic rocks rather than the clay series are the principal confining beds; and (3) subsurface recharge from the San Juan Mountains may be less than in the closed basin. The general pattern of flow is recharge from the San Juan Mountains, flow along permeable beds to the northwest, flow along the border of the San Luis Hills, or discharge to springs along the border of the San Luis Hills.

The Alamosa Basin is significant to the hydrology of the study area as the area of major discharge. Most of the irrigated agriculture in the study area is in the Alamosa Basin. Throughout large areas of the basin, ground water is near enough to the land surface to be available for evapotranspiration. Water is lost to the atmosphere through evapotranspiration by both crops and native vegetation. Emery and others (1973) estimate that the average rate of evapotranspiration was about 3,300 cubic feet per second; 1,900 cubic feet per second was used by crops and 1,400 cubic feet per second was used by native vegetation. By comparison, the average rate of flow of the Rio Grande near Embudo, N. Mex., (08279500), was 680 cubic feet per second for 1950-80, less than half the rate at which water was used by native vegetation in the Alamosa Basin.

The evapotranspiration model described in the following section was used to estimate evapotranspiration from the Alamosa Basin. Readers not interested in this detailed description may skip the following section and resume reading at the section entitled "Water Budget for the Alamosa Basin."

## Calculated Evapotranspiration for the Alamosa Basin

In the Alamosa Basin, evapotranspiration was assumed to depend on land use and depth to water. Evapotranspiration consumes water from both precipitation and ground water. Although the partitioning results from complex physical processes, the calculations here rely on simplifying assumptions that reduce the model to bookkeeping. This section describes the bookkeeping calculations used. For nonirrigated areas, calculated evapotranspiration was dependent on depth to water. Within the irrigated areas, calculated evapotranspiration was dependent on crop type and an assumed depth to water.

For nonirrigated areas, evapotranspiration was assumed to consume ground water to meet part of the demand. Six depth-to-water categories were established and areas were estimated from 1980 water levels (Crouch, 1983). Evapotranspiration of ground water (fig. 9) was assumed to follow the relation of depth to water estimated by Emery and others (1971). Evapotranspiration from ground water in watercourse and riparian areas along the Rio Grande and Conejos River was assumed to be 4.5 feet per year. Evapotranspiration from ground water in other areas where the depth to water was less than 2 feet was assumed to be 3.1 feet per year (69 percent of that from watercourses). Similarly, evapotranspiration from ground water (table 14) was estimated for other depth-to-water zones.

On nonirrigated areas, evapotranspiration was assumed to consume part of the precipitation. Precipitation that is not lost to evapotranspiration was assumed to recharge ground water. The part of precipitation that recharges ground water was assumed to be a function of depth to ground water. Further, the relation was assumed to parallel that for evapotranspiration from ground water. For watercourse and riparian areas, where ground-water levels are near the land surface, all of the precipitation was assumed to recharge ground water. For other areas where the depth to water was less than 2 feet, 69 percent of the precipitation was assumed to recharge ground water; 31 percent of the precipitation (table 14) was assumed lost to evapotranspiration. Similarly, for areas where the depth to water was greater than 12 feet, none of the precipitation was assumed to recharge ground water; all was assumed lost to evapotranspiration. Average precipitation was estimated to be 0.64 foot per year, the mean of long-term precipitation reported for six sites in the Alamosa Basin (Davis Engineering Service, Inc., 1977).

Evapotranspiration from nonirrigated areas was calculated (table 14) as the sum of evapotranspiration from ground water and evapotranspiration of precipitation. For example, in the 6- to 12-foot depth-to-water zone, evapotranspiration of ground water was 0.40 foot per year, 9 percent of watercourse evaporation. Similarly, 9 percent of precipitation was assumed to recharge ground water; 91 percent of precipitation, 0.58 foot per year, was assumed to be lost to evapotranspiration. The total evapotranspiration of 0.98 foot per year results in evapotranspiration of 140 cubic feet per second from the 105,000 acres. Evapotranspiration from 1,000,000 nonirrigated acres (rounded) in the Alamosa Basin was calculated to be 2,000 cubic feet per second (rounded) (table 14).

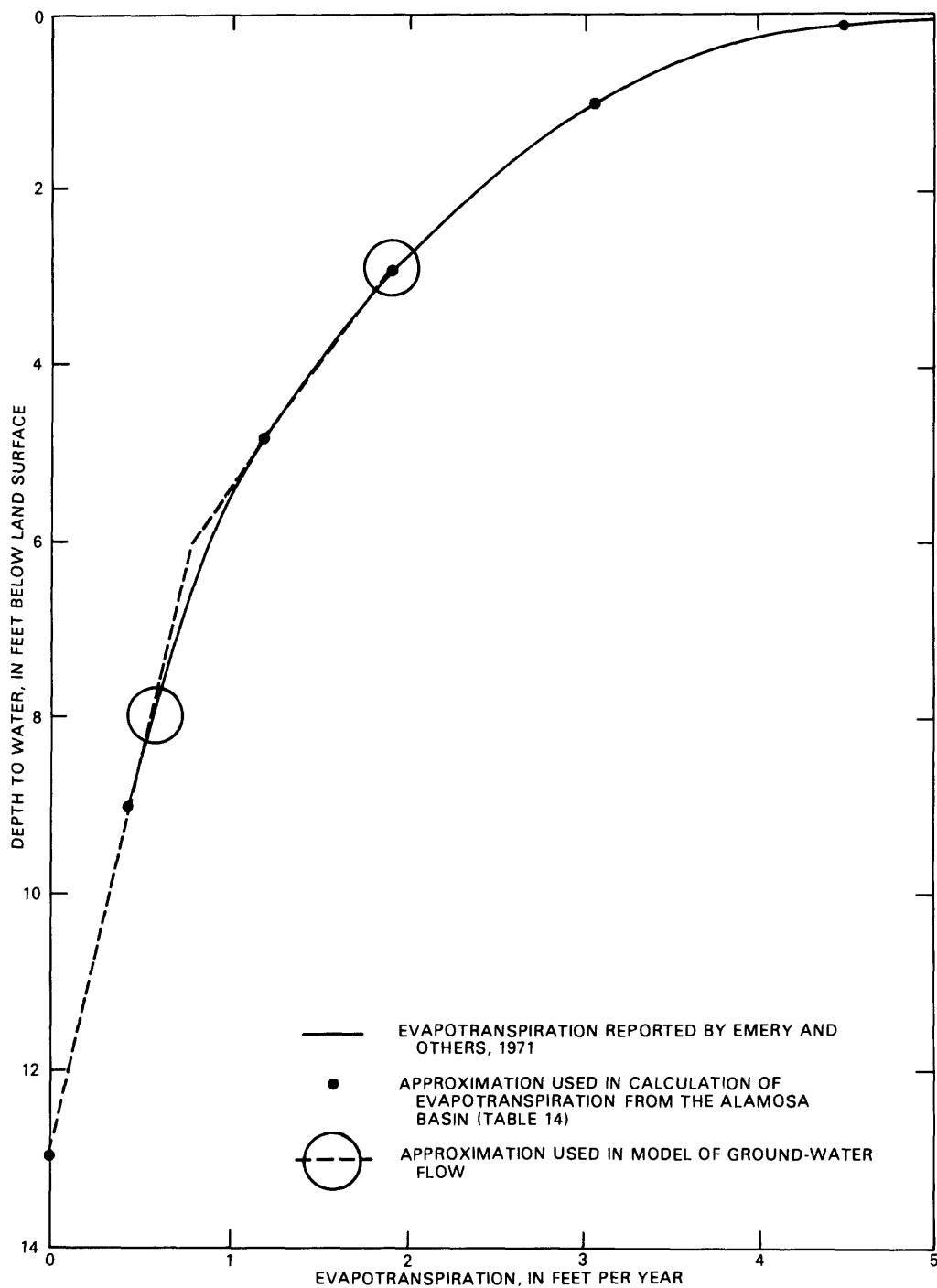


Figure 9.--Relation assumed between evapotranspiration from ground water and depth to water.



Table 14.--Calculated evapotranspiration for nonirrigated areas  
[ft/yr, feet per year; ft<sup>3</sup>/s, cubic feet per second]

Depth-to-water zone	Area (acres)	Evapotranspiration from ground water		Evapotranspiration from precipitation		Total evapotranspiration	
		(ft/yr)	(percent) <sup>1</sup>	(percent) <sup>2</sup>	(ft/yr)	(ft/yr)	(ft <sup>3</sup> /s)
Watercourse and riparian-----	30,000	4.5	100	0	0.0	4.5	190
Less than 2 feet-----	150,000	3.1	69	31	.20	3.3	680
2 to 4 feet-----	85,000	1.9	42	58	.37	2.3	270
4 to 6 feet-----	82,000	1.2	27	73	.47	1.7	190
6 to 12 feet-----	100,000	.40	9	91	.58	.98	140
Greater than 12 feet---	590,000	.0	0	100	.64	.64	520
Total-----	1,000,000 (rounded)						2,000

<sup>1</sup>Percent of watercourse evapotranspiration.

<sup>2</sup>Percent of precipitation.

Irrigated area was estimated from maps prepared by the U.S. Soil Conservation Service and Colorado State University Experiment Station (1979a, b, and c; 1980a and b). The area for each crop type was estimated from harvested, irrigated acreage compiled by Colorado Crop and Livestock Reporting Service (Colorado Department of Agriculture, 1979, 1980, and 1981, and Colorado Water Court, Division 3, Case W3466, 1979, exhibits 24, 26, 30, 32, and 221). However, only part of the area shown as irrigated on the land-use maps was used to produce a harvested crop; the remainder was assumed to be either irrigated or nonirrigated pasture. The extent to which pasture was irrigated was assumed to vary as a function of water availability. For the Alamosa Basin, the annual volume diverted from surface water and withdrawn from ground water for irrigation from 1950 through 1979 ranged from 905,100 acre-feet during 1951 to 2,117,000 acre-feet during 1979 and a mean value of 1,494,000 acre-feet (about 70 percent of the maximum value). This variation in water use was assumed to indicate the extent to which pasture was irrigated. From 1950 through 1979, an average of 70 percent of the irrigated area was assumed to be actively irrigated. The remaining 30 percent was assumed to be nonirrigated pasture. Therefore, the total irrigated area from the land-use maps was assumed to consist of: (1) The average harvested, irrigated acreage; (2) nonirrigated pasture; and (3) the balance of irrigated pasture. Of the 710,000 acres irrigated in the Alamosa Basin, 320,000 acres were harvested; 210,000 acres (30 percent) were assumed to be nonirrigated pasture; and the remaining 180,000 acres were assumed to be irrigated pasture.

For irrigated areas, evapotranspiration includes consumptive use required by the crop. Consumptive use is the amount of water used in transpiration and building of plant tissue and evaporation from adjacent soil. Calculations using a modified Blaney-Criddle formula for six locations in the Alamosa Basin (Davis Engineering Service, Inc., 1977) yield consumptive use for four major crops: alfalfa, grass, spring grains, and potatoes. For each crop, the average consumptive use for the Alamosa Basin was assumed to be the average of the values from the six locations. The consumptive use for grass was used for both "other hay" and "irrigated pasture" crop types (table 15). For non-irrigated pasture, consumptive use was not computed separately but was included in the assumed total evapotranspiration. The consumptive use for each crop was assumed to be supplied by a combination of irrigation, shallow ground water, and precipitation.

All precipitation on irrigated areas was assumed to be returned to the atmosphere by evapotranspiration. That part of precipitation that is available to help meet the consumptive water requirement of the crop is called effective precipitation. The rest of the precipitation was assumed to be returned to the atmosphere without contributing to the production of the crop. For each crop, the average, effective precipitation for the Alamosa Basin was assumed to be the average of the values calculated for six locations in the basin (Davis Engineering Service, Inc., 1977). The balance of precipitation was assumed to be evapotranspired in addition to consumptive use. For example, the six values for consumptive use by grass average 1.8 feet per year. At the six locations, average total precipitation of 0.64 foot per year was estimated to result in an average effective precipitation on grass (irrigated pasture and other hay) of 0.42 foot per year (Davis Engineering Service, Inc., 1977). The other 0.22 foot per year of precipitation was assumed to be evapotranspired resulting in an estimated evapotranspiration

Table 15.--Crop type, consumptive use, and evapotranspiration  
for irrigated areas in the Alamosa Basin  
[ft/yr, feet per year; ft<sup>3</sup>/s, cubic feet per second]

Crop type	Area (acres)	Consumptive use (ft/yr)	Evapotranspiration	
			(ft/yr)	(ft <sup>3</sup> /s)
Alfalfa	99,000	2.2	2.4	330
Other hay	91,000	1.8	2.0	250
Grain	96,000	1.2	1.6	210
Potatoes	34,000	1.4	1.8	85
Irrigated pasture	180,000	1.8	2.0	500
Nonirrigated pasture	210,000	( <sup>1</sup> )	1.7	490
Total (rounded)	710,000			1,900

<sup>1</sup>Not estimated separately.

from irrigated pasture of 2.0 feet per year (rounded). Total evapotranspiration for nonirrigated pasture was assumed to be 1.7 feet per year, the same as for nonirrigated areas with a depth to water of 4 to 6 feet (table 14). Evapotranspiration from irrigated areas was estimated to be 1,900 cubic feet per second.

Estimated evapotranspiration from the Alamosa Basin (tables 14 and 15) is compared with values reported by Emery and others (1973) in table 16. For only the closed basin, Huntley (1976) estimated evapotranspiration to be 2,600 cubic feet per second for cropland and 1,100 cubic feet per second for irrigated pasture and nonirrigated areas.

Table 16.--Comparison of published estimates of evapotranspiration  
from the Alamosa Basin  
[All estimates are in cubic feet per second]

Source	Estimated evapotranspiration		
	Irrigated areas	Nonirrigated areas	Total
This report	1,900	2,000	3,900
Emery and others (1973)	1,900	1,400	3,300

### Water Budget for the Alamosa Basin

The water budget for the Alamosa Basin (table 17) shows the estimated rates of inflow, outflow, and change in storage for 1950-80. Many of the items in the water budget have been estimated in the sections, "Flow from the San Juan Mountains to the Alamosa Basin", "Flow from the Sangre de Cristo Mountains to the Alamosa Basin and the Costilla Plains", and "Calculated Evapotranspiration for the Alamosa Basin."

Table 17.--*Water budget for the Alamosa Basin (1950-80)*  
[All estimates are in cubic feet per second]

Inflow and outflow	Estimated flow
INFLOW	
Sangre de Cristo Mountains-----	340
San Juan Mountains-----	2,800
Precipitation on the Alamosa Basin-----	1,500
Total inflow-----	4,640
DECREASE OF STORAGE IN THE AQUIFER	
Alamosa Basin-----	87
OUTFLOW	
Evapotranspiration from the Alamosa Basin-----	3,900
(Nonirrigated areas 2,000)	
(Irrigated areas 1,900)	
Rio Grande, near Lobatos, Colo.-----	350
Ground-water flow past the San Luis Hills-----	( <sup>1</sup> )
Total outflow-----	4,250

<sup>1</sup>Not estimated.

Precipitation in the Alamosa Basin was estimated to be 0.64 foot per year, the mean of long-term-precipitation values reported for six sites in the Alamosa Basin (Davis Engineering Service, Inc., 1977). Precipitation on the 1,700,000 acres (rounded) of the Alamosa Basin was calculated to be 1,500 cubic feet per second.

The Rio Grande flows through the Alamosa Basin from Del Norte, Colo., to the gap in the San Luis Hills. Flow in the Rio Grande near Del Norte, Colo., is included in the estimated inflow from the San Juan Mountains. Average streamflow in the Rio Grande near Lobatos, Colo., (08251500) averaged 350 cubic feet per second for 1950-80.

Change in the volume of water stored beneath the Alamosa Basin was estimated for 1950-80. From 1950 through 1969, change in storage was estimated from the analog simulation, which Emery and others (1975, p. 9) describe as "... the same order of magnitude as those observed in the field." Simulated decline in storage for both confined and unconfined aquifers was 730,000 acre-feet; 70 percent was from the unconfined aquifer, and 30 percent was from the confined aquifer (Emery and others, 1975, table 1). From 1970 to 1980, change in storage was estimated from change in hydraulic head in the unconfined aquifer (Crouch, 1983). Assuming a specific yield of 0.20, water in storage in the unconfined aquifer decreased by 860,000 acre-feet during the 10-year period. The decrease in storage in the unconfined aquifer was assumed to be 70 percent of the total decrease in the volume of water stored in the Alamosa Basin. Therefore, the total decrease in storage from 1970 to 1980 was estimated to be 1,200,000 acre-feet. From 1950 to 1980, the storage was estimated to decrease 1,900,000 acre-feet (rounded). The average decrease of 63,000 acre-feet per year is equivalent to an average outflow of 87 cubic feet per second.

Ground-water flow through and around the San Luis Hills, calculated as a residual of the water balance, was 480 cubic feet per second (rounded). The flow calculated as a residual of the water budget for the Costilla Plains was 10 cubic feet per second. Neither estimate is accurate because the flow is small relative to error in other flows estimated in the budget. Therefore, the water budget (table 17) was left unbalanced rather than used to calculate ground-water flow as a residual. Error in estimated rates of evapotranspiration and subsurface recharge could account for the imbalance.

#### Digital Models of Ground-Water Flow

Flow of water in the complex aquifer system of the Alamosa Basin is three dimensional. That is, flow vectors can be resolved into three components--one parallel to each of three orthogonal axes. The equation for three-dimensional flow of ground water in a porous medium (Trescott, 1975) can be written as:

$$\frac{\partial}{\partial x}(K_x \frac{\partial h}{\partial x}) + \frac{\partial}{\partial y}(K_y \frac{\partial h}{\partial y}) + \frac{\partial}{\partial z}(K_z \frac{\partial h}{\partial z}) = S_s \frac{\partial h}{\partial t} + W(x,y,z,t); \quad (10)$$

where

$K_x$ ,  $K_y$ , and  $K_z$  = hydraulic conductivities in the x, y, and z directions (L/T);

$h$  = hydraulic head (L);

$S_s$  = specific storage ( $L^{-1}$ );

$W$  = source-sink term representing the volume of water released from or taken into storage per unit volume of the porous medium per unit time ( $T^{-1}$ ); and

$t$  = time (T).

To simulate a three-dimensional flow system, a large number of brick-shaped cells are used to represent the conceptual model. Continuous hydraulic properties of the porous medium (that is, the ability to store and transmit water) are represented as discrete functions of space by assuming them to be uniform within each cell. Heterogeneity can be simulated because the hydraulic properties are allowed to vary from cell to cell. The hydraulic head associated with each cell is that at the center of the cell. At each cell, a finite-difference approximation for the derivatives in the three-dimensional flow equation yields an algebraic equation in seven unknowns (hydraulic head in the cell and hydraulic head in each of six adjacent cells). For a model with N cells, a set of N simultaneous equations in N unknowns is generated. The simulation program solves this set of simultaneous equations, subject to prescribed initial and boundary conditions. Complex transactions with adjacent systems (pumpage, recharge, evapotranspiration) are simplified to accommodate the format of specified-head, specified-flow, or head-dependent flow boundaries as permitted by the computer program. Refer to Trescott (1975) and Trescott and Larson (1976) for details of the solution algorithm. The computer program used for this study (Hearne, 1982) evolved from that of Trescott. The program was modified to reduce the volume of output and to calculate flow at hydraulic-head-dependent boundaries at each time step rather than at each iteration.

Models of ground-water flow in two dimensions and three dimensions were used to analyze the Alamosa Basin. A three-dimensional model of ground-water flow was used to: (1) Analyze the changes caused by development of ground-water resources from 1950 to 1980; (2) formulate some elementary conclusions regarding system behavior; (3) provide guidelines for establishing priorities for data collection; and (4) predict the changes caused by the Closed Basin Project (U.S. Bureau of Reclamation, 1963). For the three-dimensional model, seven layers were used to represent the upper 3,200 feet of saturated thickness. More detailed two-dimensional vertical-section models were used to demonstrate that this representation caused only moderate errors in simulation results. For the three-dimensional model, it was assumed that although flows and water levels fluctuated prior to 1950, they could be represented as stable by conditions in 1950. Changes from that stable condition were simulated. A two-dimensional vertical-section model was used to demonstrate that 1950 conditions were nearly stable and could be used as initial conditions in the three-dimensional model.

For readers interested in evaluating the three-dimensional model, the following sections discuss the use of two-dimensional models and aquifer characteristics and boundaries in the three-dimensional model. Readers not interested in this detail may skip these sections and resume reading at the section "Analysis of 1950-80 Changes: Calibration."

#### Evaluation of Representation Using a Two-Dimensional Model

A three-dimensional digital model was designed to simulate the response (change in hydraulic head) to stress (change in recharge and discharge) of the complex aquifer system of the Alamosa Basin. Although a uniform grid of small cells would minimize error, storage capacity and computational speed of computers limit the number of cells that reasonably may be used to simulate

hydrologic conditions. Alternatives that would decrease the number of cells include: (1) Using layers of unequal thickness--thin layers near the water table and thicker ones at depth; (2) using larger cells; and (3) modeling less than the total saturated thickness of the aquifer. Application of these alternatives results in a less accurate numerical approximation to the equation of ground-water flow (eq. 10) and a distortion of the geometric representation of flow. Two-dimensional models were used to investigate the error resulting from representation that was introduced by application of these alternatives in the three-dimensional model of the Alamosa Basin.

A vertical section across the closed basin just south of the southern boundary of Saguache County (A-A' on pl. 1) was selected for representation as a section model. A two-dimensional section located along a stream surface (the two-dimensional representation of a stream line) of an aquifer system does not gain or lose water normal to the section. Flow normal to the modeled section (that is, north to south) was negligible in 1950 (Powell, 1958, pl. 8) and in 1970 (Emery and others, 1973, pl. 1) when flow in the closed basin was generally from the mountain front toward the sump area. However, the closed basin may have resulted from irrigation development. The ground-water divide, which forms the southern boundary of the closed basin, may have developed in response to increased recharge from irrigation. Prior to surface-water irrigation, water probably flowed from the Rio Grande near the mountain front, through what is now the closed basin, then returned to the Rio Grande upstream from the San Luis Hills. Therefore, some water probably was flowing normal to the modeled section in 1890 as it did as recently as 1980 (Crouch, 1983). This flow was assumed to be negligible for evaluating the errors resulting from representation and for demonstrating the stability of the 1950 condition. However, further analysis of the prestress or recent conditions using the section model may be questionable because of flow normal to the section.

Within this vertical section, four hydrologic units were represented: the unconfined aquifer, the clay series, the upper confined aquifer, and the lower confined aquifer. Recharge and discharge were calculated from preliminary estimates of evapotranspiration, return flow from irrigation, recharge to the shallow aquifer by surface water flowing from the bounding mountains, and deep recharge through permeable volcanic rocks of the San Juan Mountains. For simplicity, the flow rates were specified, which eliminated any dependence on the depth to water. A reference datum was provided in the model by specifying the hydraulic head in the top layer at a cell near the sump area.

For each model, simulated hydraulic heads resembled measured hydraulic heads in the Alamosa Basin in that: (1) Hydraulic head at the western boundary was about 200 feet higher than hydraulic head near the sump area; (2) hydraulic-head gradients were steeper east of the sump than west; and (3) the simulated vertical hydraulic-head gradient at the sump was about 50 percent greater than the basin average used by Emery and others (1975, p. 9). Because of the generalized nature of the section and the intended use of the model, the authors considered the comparison adequate.

The results of using thicker layers at depth were evaluated by comparing steady-state hydraulic heads simulated by: (1) Models having an uppermost layer 100 feet thick and thicker layers at depth with (2) equivalent models

having many equal layers 100 feet thick. Hydraulic heads simulated at three arbitrarily selected nodes in a three-layer model (fig. 10) differ by as much as 24 percent (table 18) from hydraulic heads simulated by an equivalent model (fig. 11) having equal layers 100 feet thick. Hydraulic heads simulated at three nodes in a seven-layer model (fig. 12) differ by as much as 9 percent (table 18) from hydraulic heads simulated by an equivalent model (fig. 13) having equal layers 100 feet thick. Similarly, hydraulic heads simulated at three nodes in a nine-layer model (fig. 14) differ by as much as 9 percent (table 18) from hydraulic heads simulated by an equivalent model (fig. 15) having equal layers 100 feet thick. These differences (table 18) in simulated hydraulic head result from the less-accurate finite-difference approximation of the flow equation in those models having fewer, thicker layers.

Table 18.--*Sensitivity of simulated hydraulic head to number of layers used to approximate the flow equation*

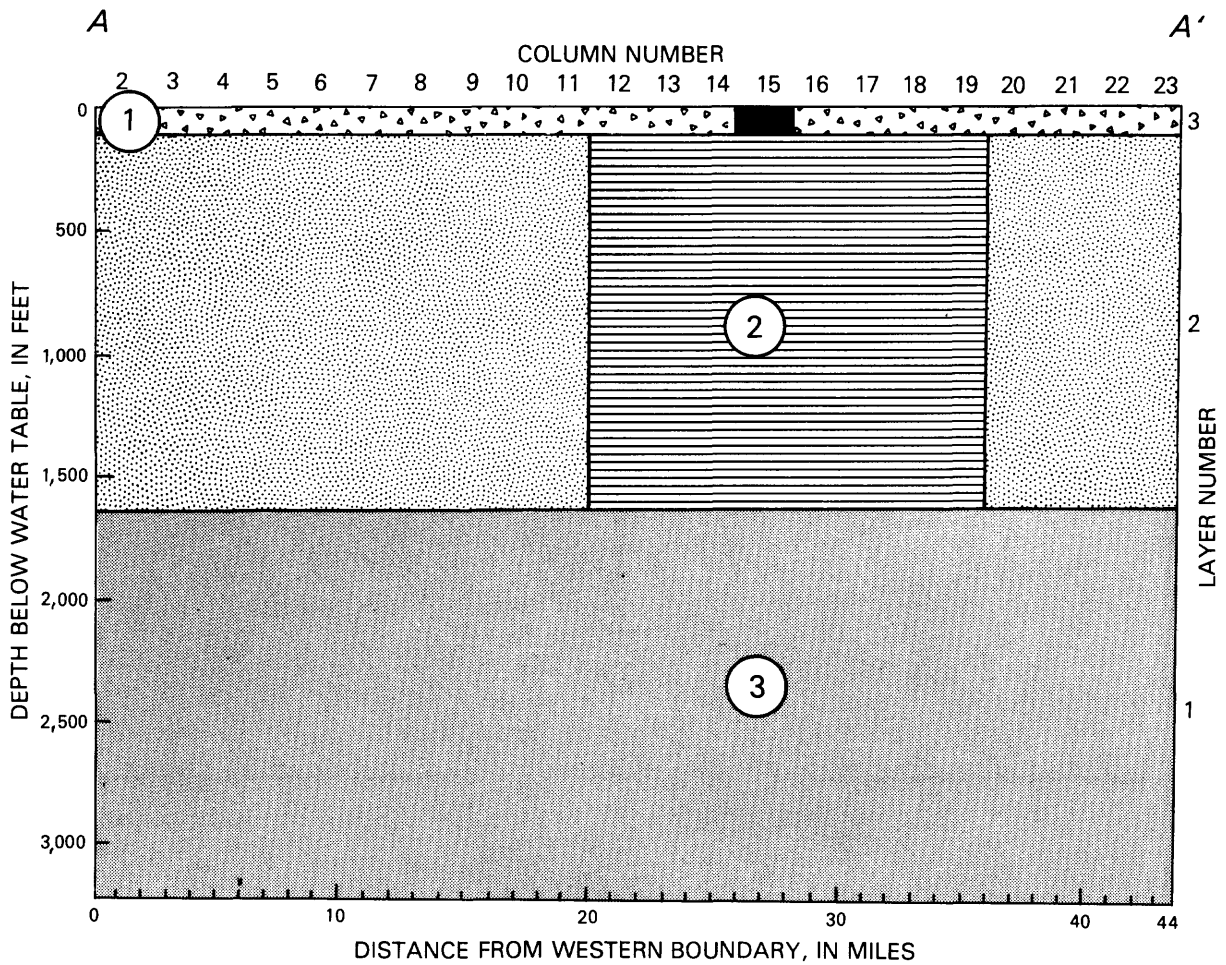
Number of layers in model	Differences from equivalent model (equal layers 100 feet thick), in percent of hydraulic heads simulated at location <sup>1</sup>		
	1	2	3
3	13	10	24
7	3	1	9
9	1	0	9

<sup>1</sup>Location shown on figures 10 to 15.




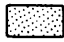

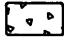
Error introduced by horizontal-grid spacing also was evaluated by comparing alternate models. A model was defined that differed from the model of figure 12 in that a grid spacing of 1 mile rather than 2 miles was used for the central part (mile 6 to mile 36) of the section. Hydraulic head at the three locations differed by less than 1 percent from those for the model represented by figure 12.

The results of not representing the total depth of the basin were evaluated by comparing steady-state hydraulic heads simulated by: (1) A 7-layer (variable thickness) model of the upper 3,200 feet (fig. 12) with (2) an 11-layer model (whose uppermost 7 layers were equivalent to the 7-layer model) of about 17,000 feet of saturated thickness (not illustrated). The complication introduced by horizontal-to-vertical anisotropy was included in the analysis by comparing the results of these simulations for a range of anisotropy ratios (table 19). Representing only the upper 3,200 feet of saturated thickness introduced less than 10 percent error except for anisotropy ratios as low as 300:1. Data are inadequate to determine anisotropy at any depth in the Alamosa Basin. An anisotropy ratio of 2,000:1 was used by Emery and others (1975) for the confined aquifer below 1,600 feet. For Espinola Basin, Hearne (1985a) estimated a ratio of 250:1 in the upper 1,000 feet of Tesuque Formation. Farther south along the Rio Grande, R.R. White (U.S. Geological Survey, written commun., 1984) estimated ratios from 250:1 to 480:1 in aquifer tests on wells in the upper 600 feet of Mesilla Valley. Therefore, it appears likely that the anisotropy ratio in Alamosa Basin is within the range included in table 19.





### EXPLANATION

- |   |                                   |   |   |
|---|-----------------------------------|---|---|
|  | SPECIFIED HYDRAULIC-HEAD BOUNDARY |  | NODE WHERE HYDRAULIC HEADS ARE COMPARED (TABLE 1) |
|  | CLAY SERIES                       |  | UPPER CONFINED AQUIFER                            |
|  | LOWER CONFINED AQUIFER            |  | UNCONFINED AQUIFER                                |

VERTICAL EXAGGERATION X 50

A-A' LOCATION SHOWN ON PLATE 1

Figure 10.--Section model with three layers.

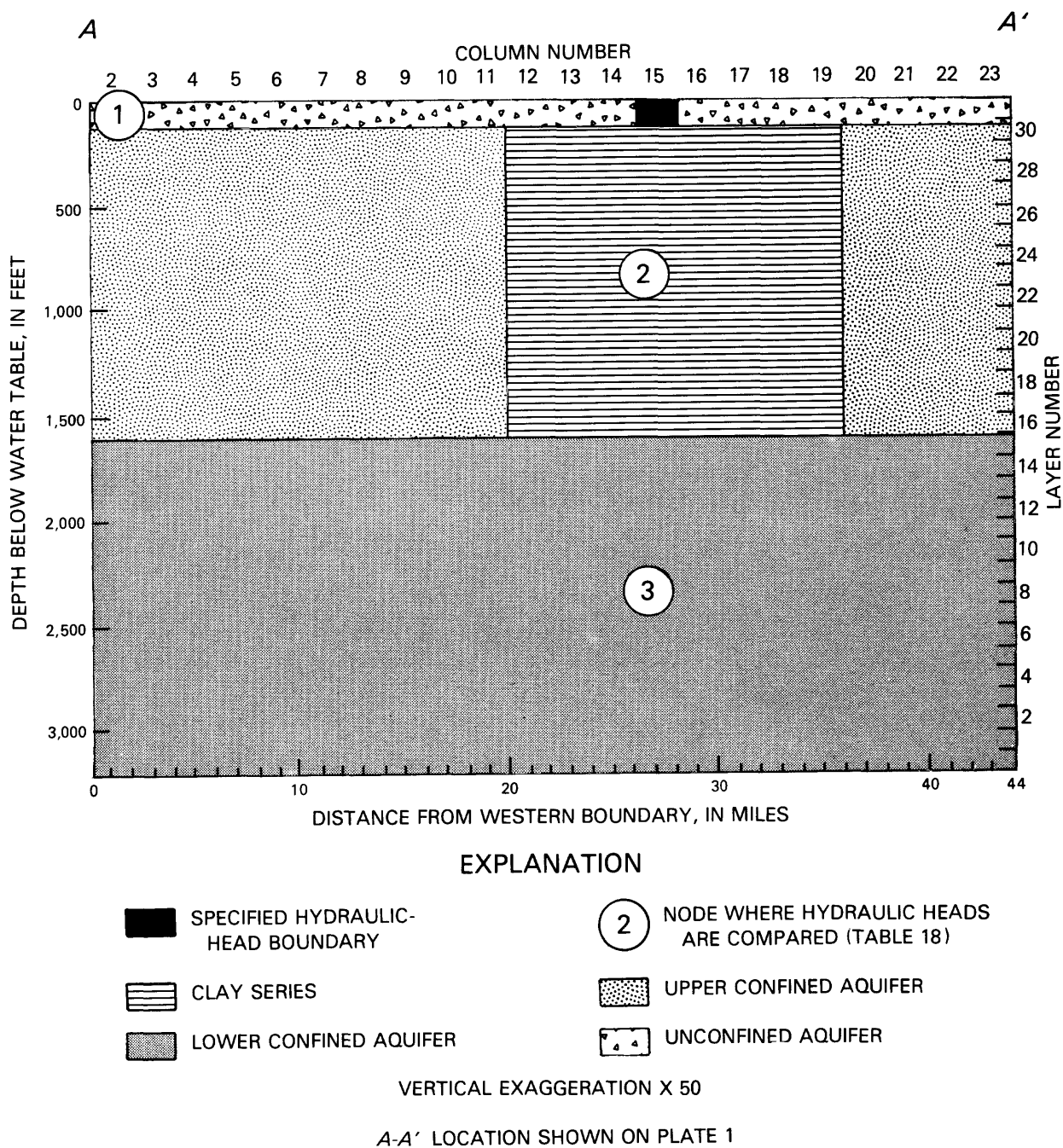
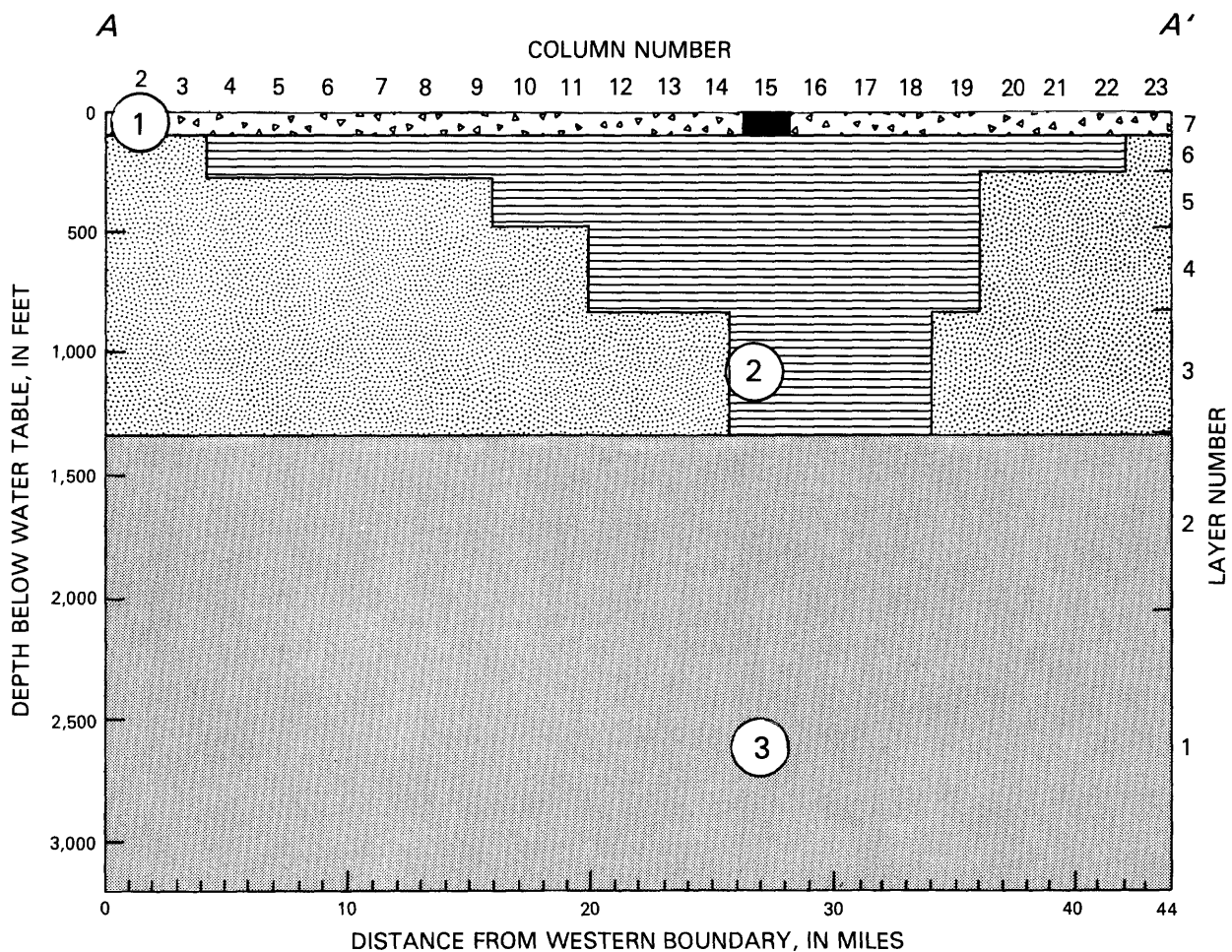


Figure 11.--Section model having equal layers 100 feet thick, equivalent to three-layer model.



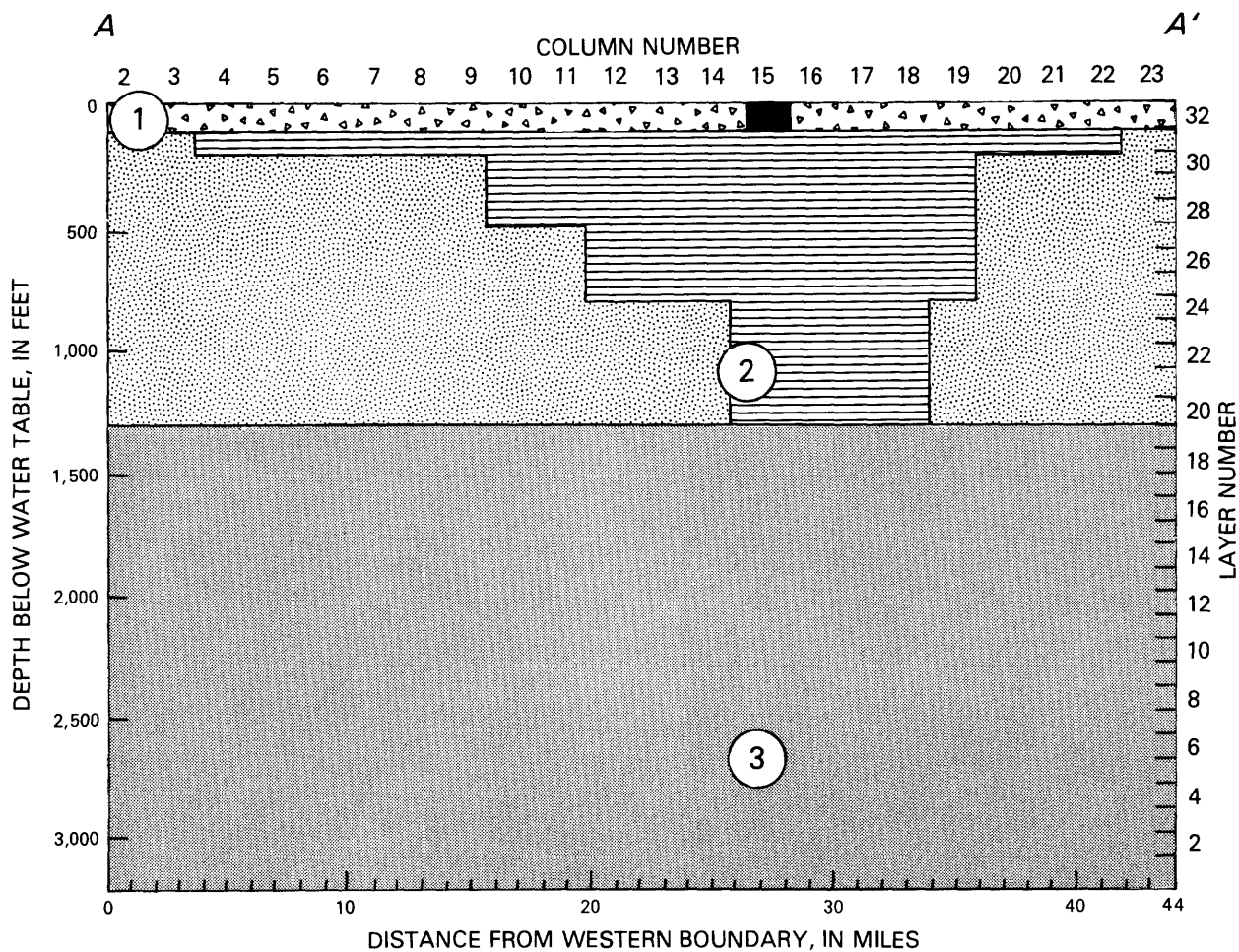
### EXPLANATION

- |                                   |  |
|-----------------------------------|--|
| SPECIFIED HYDRAULIC-HEAD BOUNDARY | NODE WHERE HYDRAULIC HEADS ARE COMPARED (TABLE 18) |
| CLAY SERIES                       | UPPER CONFINED AQUIFER                             |
| LOWER CONFINED AQUIFER            | UNCONFINED AQUIFER                                 |

VERTICAL EXAGGERATION X 50

A-A' LOCATION SHOWN ON PLATE 1

Figure 12.--Section model with seven layers.



### EXPLANATION

SPECIFIED HYDRAULIC-  
HEAD BOUNDARY

CLAY SERIES

LOWER CONFINED AQUIFER

NODE WHERE HYDRAULIC HEADS  
ARE COMPARED (TABLE 18)

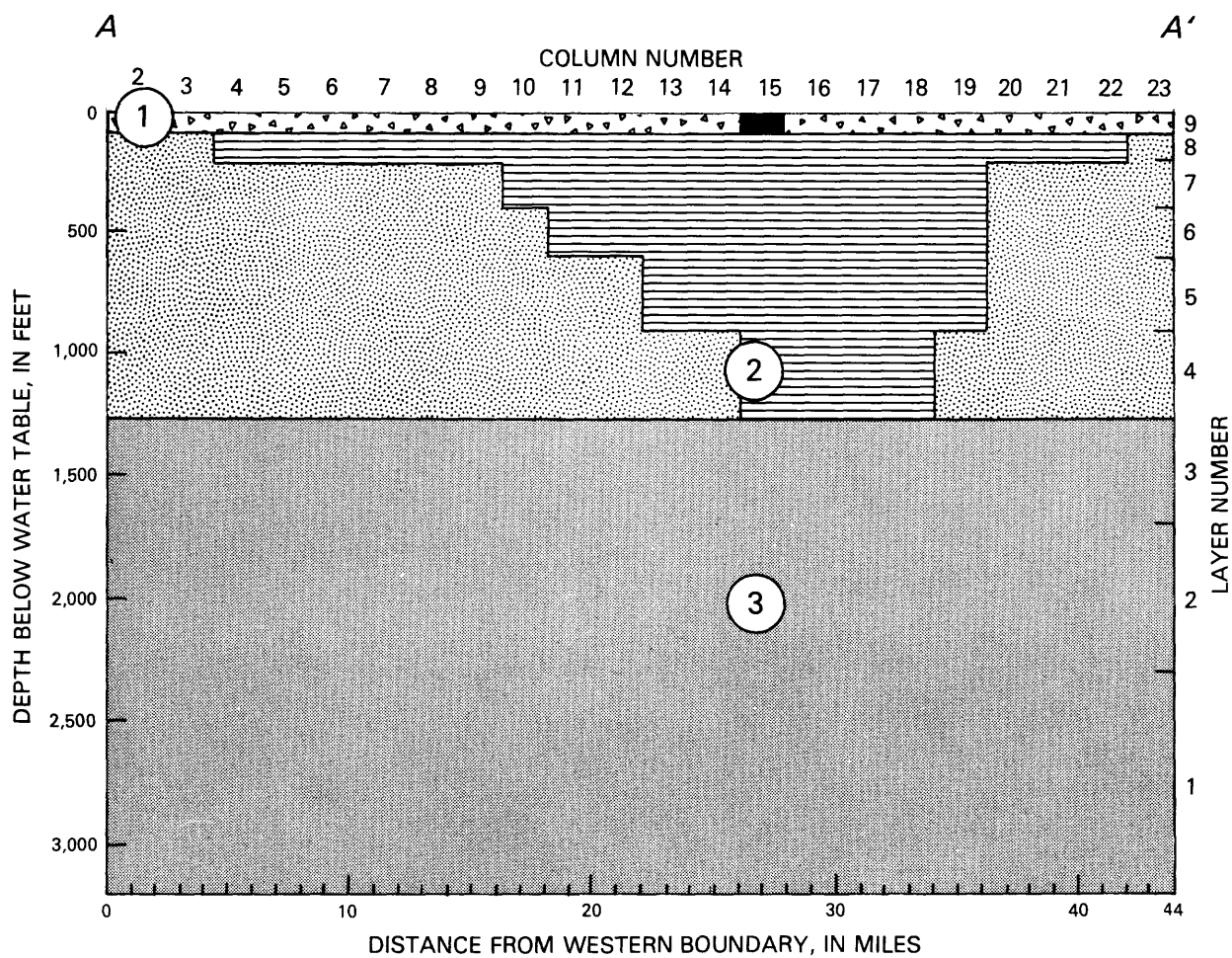
UPPER CONFINED AQUIFER

UNCONFINED AQUIFER

VERTICAL EXAGGERATION X 50

A-A' LOCATION SHOWN ON PLATE 1

Figure 13.--Section model having equal layers 100 feet thick,  
equivalent to seven-layer model.



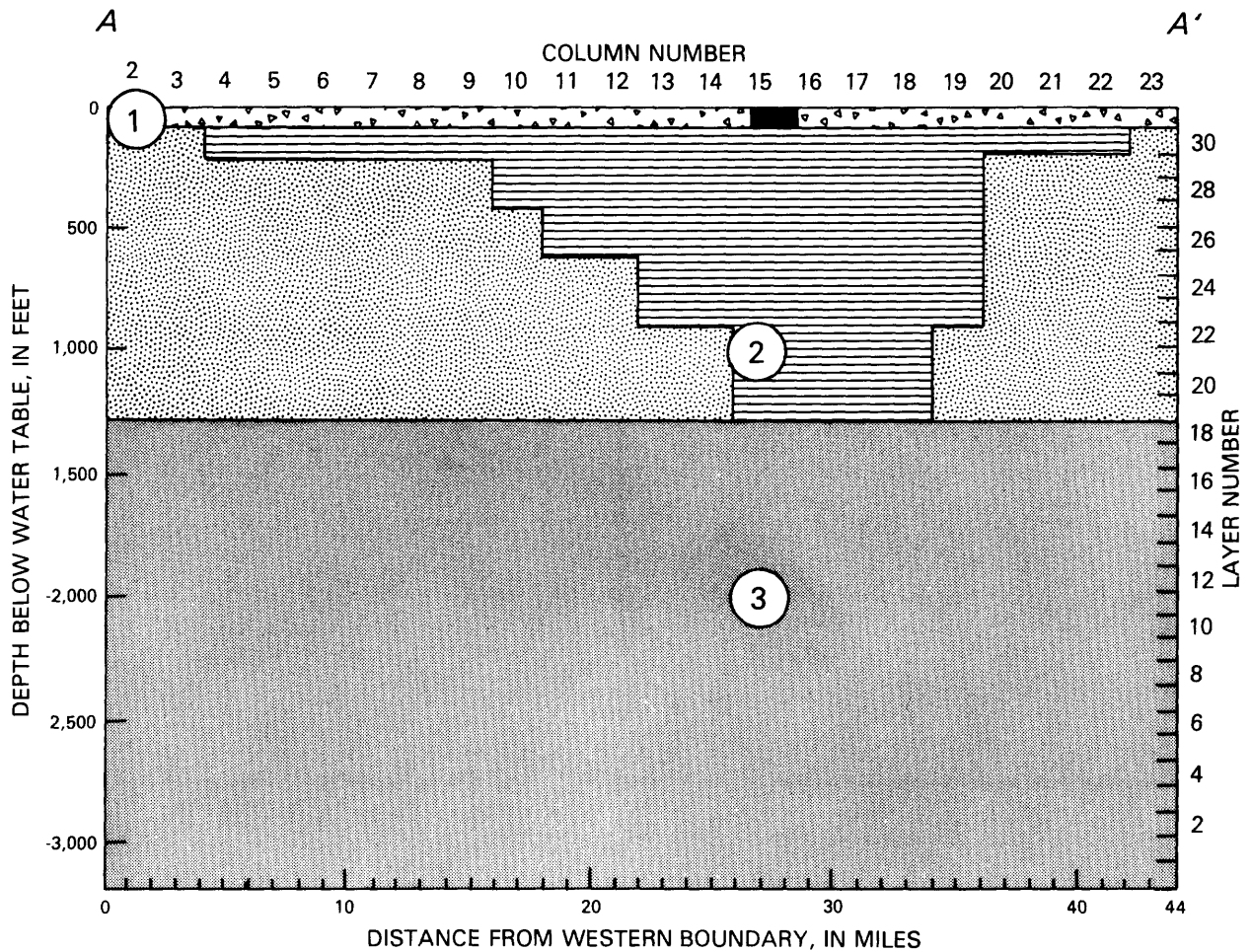
### EXPLANATION

- |                                   |  |
|-----------------------------------|--|
| SPECIFIED HYDRAULIC-HEAD BOUNDARY | NODE WHERE HYDRAULIC HEADS ARE COMPARED (TABLE 13) |
| CLAY SERIES                       | UPPER CONFINED AQUIFER                             |
| LOWER CONFINED AQUIFER            | UNCONFINED AQUIFER                                 |



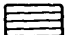



VERTICAL EXAGGERATION X 50

A-A' LOCATION SHOWN ON PLATE 1

Figure 14.--Section model with nine layers.



### EXPLANATION

- |   |  |
|---|--|
|  SPECIFIED HYDRAULIC-HEAD BOUNDARY |  NODE WHERE HYDRAULIC HEADS ARE COMPARED (TABLE 18) |
|  CLAY SERIES                       |  UPPER CONFINED AQUIFER                             |
|  LOWER CONFINED AQUIFER            |  UNCONFINED AQUIFER                                 |

VERTICAL EXAGGERATION X 50

A-A' LOCATION SHOWN ON PLATE 1

Figure 15.--Section model having equal layers 100 feet thick, equivalent to nine-layer model.



Table 19.--Sensitivity of simulated hydraulic head to representing only the upper 3,200 feet of saturated thickness

Ratio of horizontal to vertical hydraulic conductivity	Differences from model representing total saturated thickness in percent of hydraulic heads simulated at location <sup>1</sup>		
	1	2	3
3000:1	1	0	2
1500:1	2	0	6
700:1	6	2	7
300:1	8	9	16

<sup>1</sup>Location shown on figure 12.

Based on the comparisons in tables 18 and 19, the three-dimensional model of the Alamosa Basin was constructed using seven layers varying in thickness from 100 to 1,130 feet to represent the upper 3,200 feet of saturated thickness. The horizontal dimensions of each cell were 2 miles in both directions.

#### Evaluation of Initial Condition Using a Two-Dimensional Model

Anticipating that the three-dimensional digital model of the Alamosa Basin would be constructed with the assumption that hydrologic conditions were stable in 1950 and used to simulate changes from this initial condition, a two-dimensional model of a vertical section was used to evaluate these assumptions to determine if 1950 conditions were nearly stable and could be used as initial conditions in the three-dimensional model. Hydraulic conductivities along this section were the same as those used in the three-dimensional basin model (described in the section entitled "Aquifer Characteristics in the Three-Dimensional Model") for a section across the closed basin just south of the southern boundary of Saguache County (shown as section A-A' on pl. 1.) Three conditions were simulated: (1) Initial steady-state condition (1890); (2) condition in 1950 after 60 years of surface-water irrigation; and (3) condition after an additional 50 years of surface-water irrigation.

#### Initial steady-state condition

During the initial steady-state condition, recharge originated as streamflow and as subsurface flow from the bounding mountains; discharge along the section was through evapotranspiration where the simulated water level was near the land surface. The rates of natural recharge were based on preliminary estimates for the water budget described in the section "Water Budget for the Alamosa Basin." The values represent flow for a 2-mile-wide row of cells. Water from the Sangre de Cristo Mountains reaches the Alamosa Basin as streamflow and shallow ground-water flow. Recharge from the east (10 cubic feet per second) was represented in the top layer only. Measured streamflow accounts for about half the water yield from the San Juan Mountains

to the Alamosa Basin (table 8). Recharge from the west (22 cubic feet per second) was assumed to be evenly divided between surface and subsurface flow. Recharge from surface flow (11 cubic feet per second) was represented in the top layer only. Recharge from subsurface flow (11 cubic feet per second) was arbitrarily represented as uniformly distributed with depth (0.34 cubic foot per second for each 100 feet of saturated thickness).

Natural discharge through evapotranspiration was represented as a broken-line function of depth to water (approximating the curve of fig. 9). Between points indicated in table 20, the rate of evapotranspiration was assumed to vary linearly. Altitude of the land surface was estimated from 1:24,000 scale topographic maps of the U.S. Geological Survey.

Hydraulic heads simulated in response to these recharge and discharge estimates were reasonable. West of U.S. Highway 285 (pl. 1, columns 2-7), simulated water levels were more than 15 feet below land surface. Similarly, near the eastern mountains (pl. 1, columns 22-24) simulated water levels were more than 15 feet below land surface. Simulated water levels in the central part of the valley (pl. 1, columns 8-21) ranged from 5 to 12 feet below land surface. Simulated hydraulic heads were nearest the land surface just east of the present San Luis Lake (pl. 1, column 20).

Table 20.--*Relation between evapotranspiration and depth to water used for nonirrigated areas in the section model*  
[ft, feet; ft/yr, feet per year]

Depth to ground water, (ft)	Rate of evapotranspiration, (ft/yr)
0	5.0
2	2.4
6	1.0
13	.0

#### 1950 Condition

By 1950, irrigated agriculture in the Alamosa Basin had undergone three changes: (1) Extensive surface-water irrigation; (2) development of confined ground water; and (3) a shift in the location of irrigated areas from the center of the Alamosa Basin to the west. Only the first of these changes was represented in the digital model. The latter two were assumed to have a negligible effect on the stability of the 1950 condition. Prior to 1950, discharge from confined aquifers primarily was from small-capacity, nonpumped, flowing wells. Any water not lost to evapotranspiration recharged the unconfined aquifer. Pre-1950 changes in hydraulic head may have resulted in changes in these flow rates. However, these are assumed negligible compared to the larger flows associated with surface-water irrigation. For example, during 1940-49, flowing wells were estimated to discharge about 3 million acre-feet (Emery and others, 1973), whereas surface-water diversions were about 128 million acre-feet. The change in irrigated area from the center of Alamosa Basin to the west was completed by about 1910. The effect on the 1950 condition was assumed negligible.



Prior to 1950, the principal source of water for irrigation was surface water. A large network of canals was built during 1880-90 to divert water for irrigation. By 1904, all streams entering the basin were appropriated for irrigation. The initial steady-state condition described in the previous section was used as the initial condition on which 60 years (1890 through 1950) of surface-water irrigation was imposed to simulate the 1950 condition. Irrigation during this period caused two changes in recharge and discharge that were represented in the section model: percolation of excess irrigation water began and evapotranspiration was modified. Both changes were represented as constant; fluctuations due to changes in surface-water availability and changes in location of land actually irrigated were not represented.

Estimates of the flow rates were based on whether the area represented by the cell was irrigated or nonirrigated (U.S. Soil Conservation Service and Colorado State University Experiment Station, 1979a, b, and c; 1980a and b). In nonirrigated areas, evapotranspiration was related to depth to water (table 20), and no percolation of irrigation water was represented. Percolation to ground water was represented as specified flow, proportional to irrigated area within a cell. In irrigated areas, evapotranspiration was assumed to consume shallow ground water as well as applied surface water. Evapotranspiration from ground water was represented in the model as a function of depth to water. For a given depth to water, evapotranspiration from an irrigated area was arbitrarily assumed to be about a fourth that from a nonirrigated area (table 20). For example, a simulated head 6 feet below the land surface resulted in evapotranspiration simulated at the rate of 1.0 foot per year in nonirrigated areas and 0.25 foot per year in irrigated areas.

The simulated response resulting from these changes in percolation of irrigation water and modified evapotranspiration was an increase in hydraulic head throughout the section. Application of surface water in excess of crop use resulted in increased recharge to the aquifer system. Increased recharge elevated the hydraulic head in the aquifer until evapotranspiration increased to balance the increased recharge. The greatest increase in simulated hydraulic head (as much as 32 feet) occurred west of U.S. Highway 285. In Range 6 east (pl. 1, columns 2-4), the simulated depth to water was greater than 13 feet, and no evapotranspiration was simulated. In Range 7 east (pl. 1, columns 5-7), the depth to water was less than 13 feet, and evapotranspiration was simulated for 1950, where there had been none in 1890. From U.S. Highway 285 east through the sump area (pl. 1, columns 8-21), the increase in water level resulted in greater simulated evapotranspiration for 1950 than that for 1890.

To verify that the 1950 condition was nearly stable, an additional 50 years was simulated with no change in boundary conditions. Additional simulated change in hydraulic head was less than 0.2 foot throughout the top layer. The 1950 condition was accepted as a stable initial condition on which to superimpose the transient response to changes in the 1950 boundary conditions.

## Aquifer Characteristics in the Three-Dimensional Model

The transient response to changes in rates of recharge and discharge since 1950 was simulated with a three-dimensional, ground-water flow model of the Alamosa Basin. Seven layers were used to represent the complex aquifer system to a depth of about 3,200 feet below land surface. This section describes the ability of the ground-water system to store and transmit water as represented by the model. The input file to define these aquifer characteristics is in attachment 1 in the "Supplemental Data" section at the back of the report.

The area represented in the model (fig. 16) was divided into cells by a uniform 2-mile grid of 50 rows and 29 columns (1,450 cells) and 633 active cells in each layer. The irregular boundary to the east of the modeled area approximated the contact between sedimentary rocks of the Alamosa Basin and crystalline rocks of the Sangre de Cristo Mountains. The irregular boundary to the west approximated the contact between sedimentary rocks and volcanic rocks of the San Juan Mountains. To the south, the irregular boundary represented the contact between sedimentary rocks and volcanic rocks of either the Taos Plateau or the San Luis Hills. To the southeast, where sedimentary rocks are continuous between the Alamosa Basin and the Costilla Plains, the boundary represented a flow line orthogonal to water-level contours (Emery and others, 1973).

Within the modeled volume, the aquifer system was represented with five distinct units, listed from top to bottom: (1) The unconfined aquifer in sedimentary rocks of the Alamosa Formation, not including the clay series; (2) the clay series of the Alamosa Formation; (3) the upper confined aquifer in sedimentary rocks of the Santa Fe Formation above 1,300 feet; (4) the upper confined aquifer in sedimentary rocks of the Santa Fe Formation with intercalated volcanic rocks; and (5) the lower confined aquifer in rocks of the Santa Fe Formation below 1,300 feet. The ability of each unit to transmit and store water was estimated using results from previous investigations.

The ability of an aquifer to transmit water is described by transmissivity or hydraulic conductivity. Transmissivity is the rate at which water is transmitted through a unit width of the aquifer under a unit hydraulic gradient. Hydraulic conductivity is the rate at which water is transmitted through a unit area of the aquifer under a unit hydraulic gradient. Therefore, transmissivity is the product of hydraulic conductivity and saturated thickness.

The ability to store water is described by either specific storage or specific yield. In confined conditions, the water derived from storage comes from expansion of water and compression of the aquifer in response to a decline in hydraulic head. Specific storage is the volume of water derived from storage in a unit volume of aquifer in response to a unit decline in hydraulic head. In unconfined conditions, the water derived from storage results from drainage rather than expansion and compression. Specific yield is the volume of water that a unit volume of saturated aquifer will yield by gravity drainage and is commonly hundreds to thousands of times greater than that yielded by confined storage.

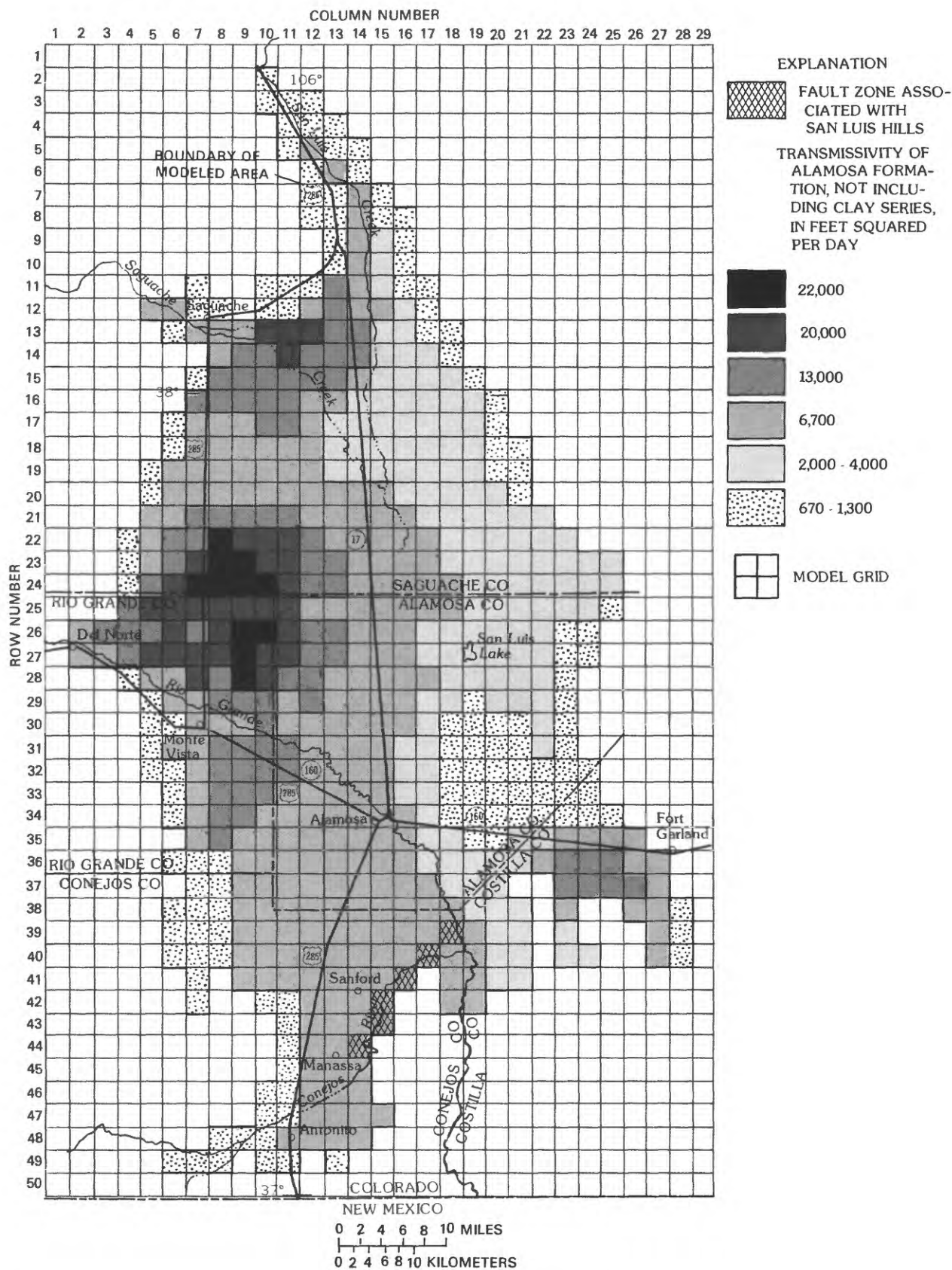


Figure 16.--Transmissivity representing the unconfined aquifer, layer seven (top layer) of the three-dimensional model.

### Alamosa Formation, not including clay series

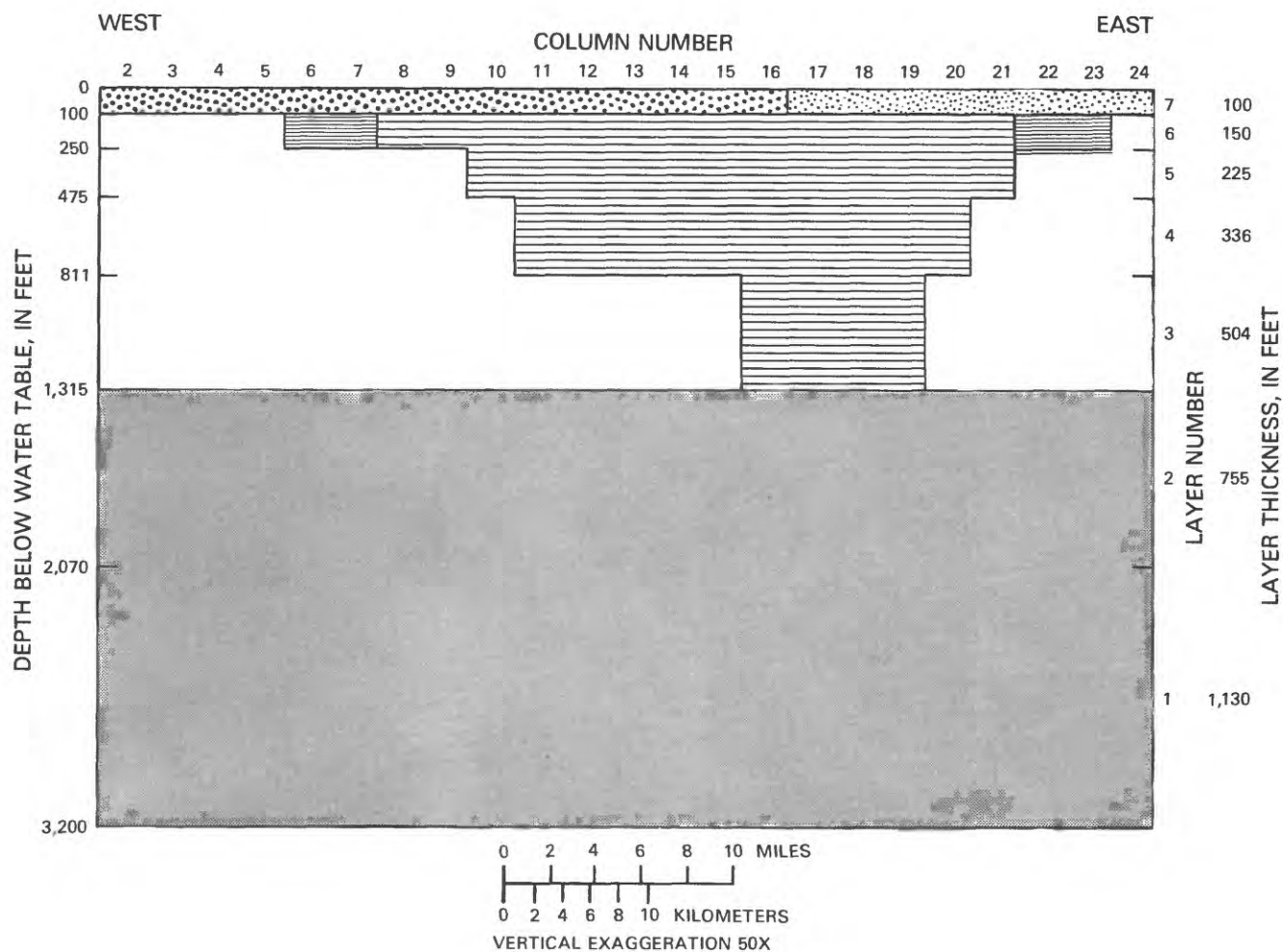
The unconfined aquifer of interbedded gravel, sand, silt, and clay is represented as layer seven of the model. Transmissivity represented in layer seven of the model (fig. 16) approximates that reported by Emery and others (1975, pl. 1) for the unconfined aquifer as estimated from 35 aquifer tests and about 250 specific capacity tests (Emery and others, 1973, pl. 3) and using modifications in the sump area from more recent aquifer tests (G.J. Leonard, U.S. Geological Survey, written commun., 1984). In simulations with the model, transmissivity at each cell was modified as saturated thickness changed. Initial saturated thickness was estimated from depth to water (Emery and others, 1973, pl. 1) and depth to uppermost confining unit (Emery and others, 1973, pl. 2). Hydraulic conductivity, calculated by dividing transmissivity by saturated thickness, ranged from 10 to 450 feet per day. In the absence of measured data, the specific yield of the unconfined aquifer was assumed to be 0.20 (Emery and others, 1975, fig. 4). Average values compiled from several selected reports range from 0.02 for clay to 0.27 for coarse sand (Johnson, 1967). Although 0.20 is a reasonable average, the value probably varies throughout the valley.

### Clay series of Alamosa Formation

The clay series, consisting of clays interbedded with sands, was represented as varying from about 100 to 1,200 feet thick based on a map prepared for Colorado Water Court, (1979, exhibit 95). The general wedged shape and areal distribution of this clay series is shown in vertical sections (figs. 17 and 18) and in horizontal slices (figs. 19-22) through the modeled volume. Because the clay series retards the transmission of water vertically, it is considered the principal confining bed for most of the Alamosa Basin (Emery and others, 1973, pl. 2). Horizontal hydraulic conductivity of the clay series (figs. 17-22) was assumed to be 10 feet per day. This is approximately the lowest value used by Emery and others (1973, pl. 7) for the upper 1,500 feet of confined aquifer where the clay series was mapped as 1,200 feet thick. Vertical hydraulic conductivity was assumed (Emery and others, 1975, pl. 3) to be 0.06 foot per day. The horizontal-to-vertical anisotropy ratio represented by these values was about 170:1. Specific storage was assumed to be  $5 \times 10^{-6}$  per day (Emery and others, 1975, fig. 4).

### Santa Fe Formation, above 1,300 feet

The upper confined aquifer includes gravel, sand, silt, and clay not identified as part of the clay series. Although intercalated volcanic rocks from the San Juan Mountains may transmit a significant source of recharge to the Alamosa Basin, they were included with sedimentary rocks of the Santa Fe Formation when estimating aquifer characteristics. Data are both sparse and of questionable interpretation. Although reliance was given to previous investigations, many assumptions and generalizations were used to estimate the aquifer characteristics. Horizontal hydraulic conductivity (figs. 17-22) was assumed to be 40 feet per day. Measured transmissivities were sparse and only some intervals were reported to contribute flow to wells (Emery and others, 1973). Results from 36 aquifer tests were grouped into four classes (Emery



DESCRIPTION		EXPLANATION	
		HYDRAULIC CONDUCTIVITY (FEET PER DAY)	
		HORIZONTAL	VERTICAL
ALAMOSA FORMATION NOT INCLUDING CLAY SERIES		40 TO 450	0.06
		25 TO 40	0.06
CLAY SERIES OF ALAMOSA FORMATION		10	0.06
CLAY SERIES OF ALAMOSA FORMATION OVERLYING SANTA FE FORMATION		30	0.06
SANTA FE FORMATION ABOVE APPROXIMATELY 1300 FEET		40	0.06
SANTA FE FORMATION BELOW APPROXIMATELY 1300 FEET		30	0.013

Figure 17.--Hydraulic conductivity represented in row 26 of the three-dimensional model.



and others, 1975). Freeze (1972, p. 189) concludes that for simulating a formation that is homogeneous on a large scale, although heterogeneous on a small scale, the appropriate homogeneous hydraulic conductivity is the geometric mean of the measured values. The geometric mean of the values reported by Emery and others (1975, pl. 2) is about 40 feet per day. Vertical hydraulic conductivity was assumed (Emery and others, 1975, pl. 3) to be 0.06 foot per day. The anisotropy ratio represented by these values was 670:1, larger than values of 250:1 (Hearne, 1985a) and 270:1 to 480:1 (R.R. White, U.S. Geological Survey, written commun., 1984) reported for other basins along the Rio Grande. Specific storage was assumed to be  $5 \times 10^{-6}$  per foot (Emery and others, 1975, fig. 4).

#### Santa Fe Formation, with intercalated volcanic rocks

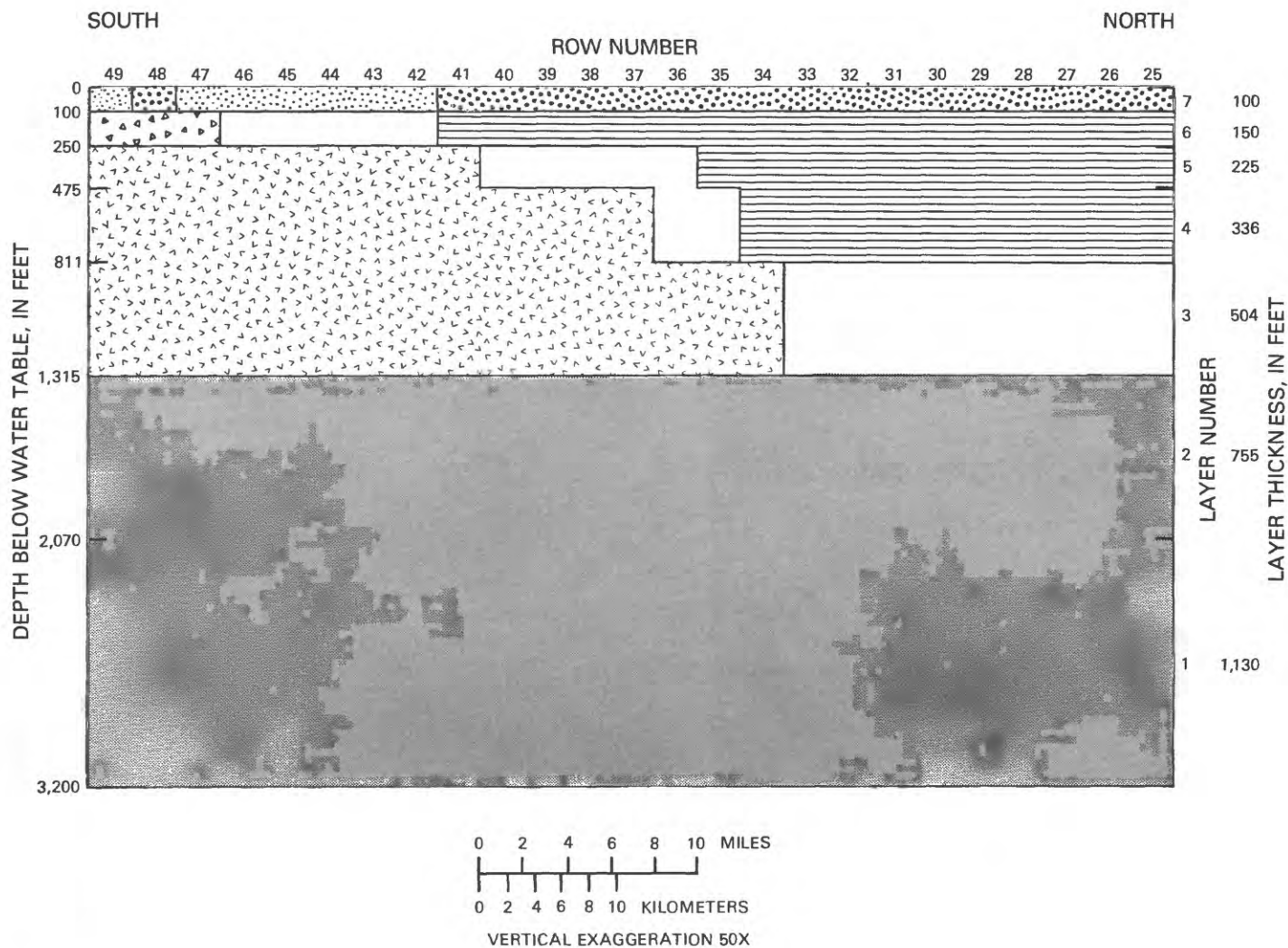
To the southwest, volcanic rocks intercalated with rocks of the Santa Fe Formation were represented as about 1,100 feet thick and as wedging out to the northwest, based on contours of depth to the uppermost volcanic rocks (Emery and others, 1973). The general wedge shape and areal distribution is shown in the north-south section (fig. 18) and the horizontal slices (figs. 19-22). The horizontal hydraulic conductivity was assumed to be 40 feet per day, unchanged by the volcanic rocks. Vertical hydraulic conductivity was assumed (Emery and others, 1975, pl. 3) to be 0.0006 foot per day, a result of assuming that the volcanic rocks are unfractured. The anisotropy ratio represented by these values was 67,000:1, one hundred times that in the Santa Fe Formation without intercalated unfractured volcanic rocks. Specific storage was assumed (Emery and others, 1975, fig. 4) to be  $5 \times 10^{-6}$  per foot.

#### Santa Fe Formation, below 1,300 feet

The lower confined aquifer, approximately 1,300 to 3,200 feet below land surface, includes sedimentary rocks and volcanic rocks similar to those above 1,300 feet except that they are older and have a greater overburden. Hydraulic conductivity was assumed (Emery and others, 1975 fig. 4) to be about 30 feet per day in the horizontal and 0.013 foot per day in the vertical. The anisotropy ratio represented by these values was 2,300:1. Specific storage was assumed to be  $5 \times 10^{-6}$  per foot (Emery and others, 1975, fig. 4).

#### Fault zone

North of the San Luis Hills, a fault zone was represented by increasing the vertical hydraulic conductivity of the upper confined aquifer to about 60 feet per day (figs. 16 and 19-22), about 1,000 times that of sedimentary rocks and 100,000 times that of unfractured volcanic rocks in the upper confined aquifer. This value was used for the analog model (Emery and others, 1975). However, the value has not been verified by either measurement or calibration.



EXPLANATION		HYDRAULIC CONDUCTIVITY (FEET PER DAY)	
DESCRIPTION		HORIZONTAL	VERTICAL
ALAMOSA FORMATION NOT INCLUDING CLAY SERIES		40 TO 450	0.06
		25 TO 40	0.06
CLAY SERIES OF ALAMOSA FORMATION		10	0.06
SANTA FE FORMATION ABOVE APPROXIMATELY 1300 FEET		40	0.06
VOLCANIC ROCKS INTERCALATED WITH SANTA FE FORMATION	UNCONFINED AQUIFER NOT PERCHED	40	0.0006
	UNCONFINED AQUIFER PERCHED	40	0.0
SANTA FE FORMATION BELOW APPROXIMATELY 1300 FEET		30	0.013

Figure 18.--Hydraulic conductivity represented in column 11 from row 25 to row 49 of the three-dimensional model.

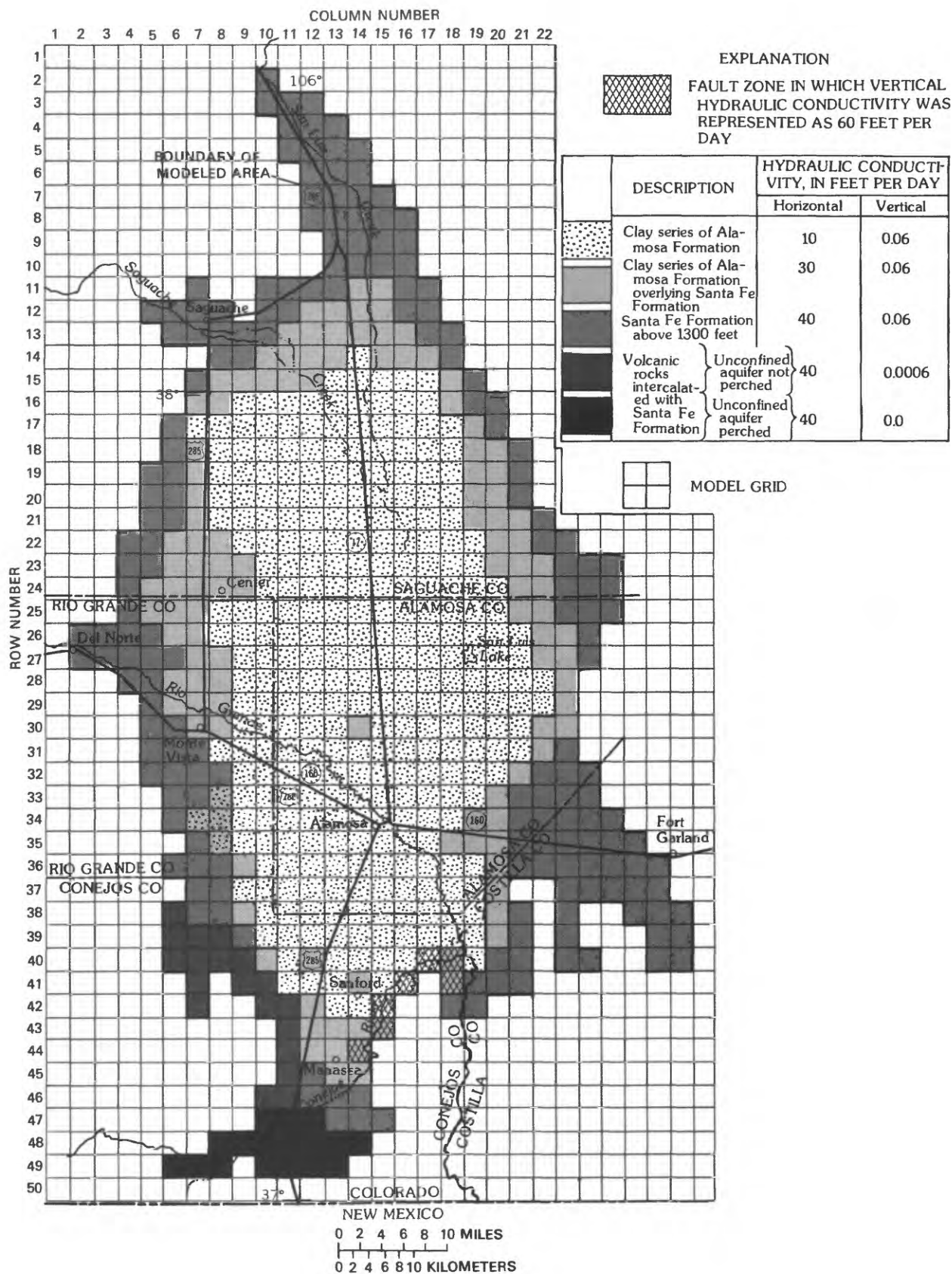


Figure 19.--Hydraulic conductivity of the upper confined aquifer, represented in the three-dimensional model as layer six.



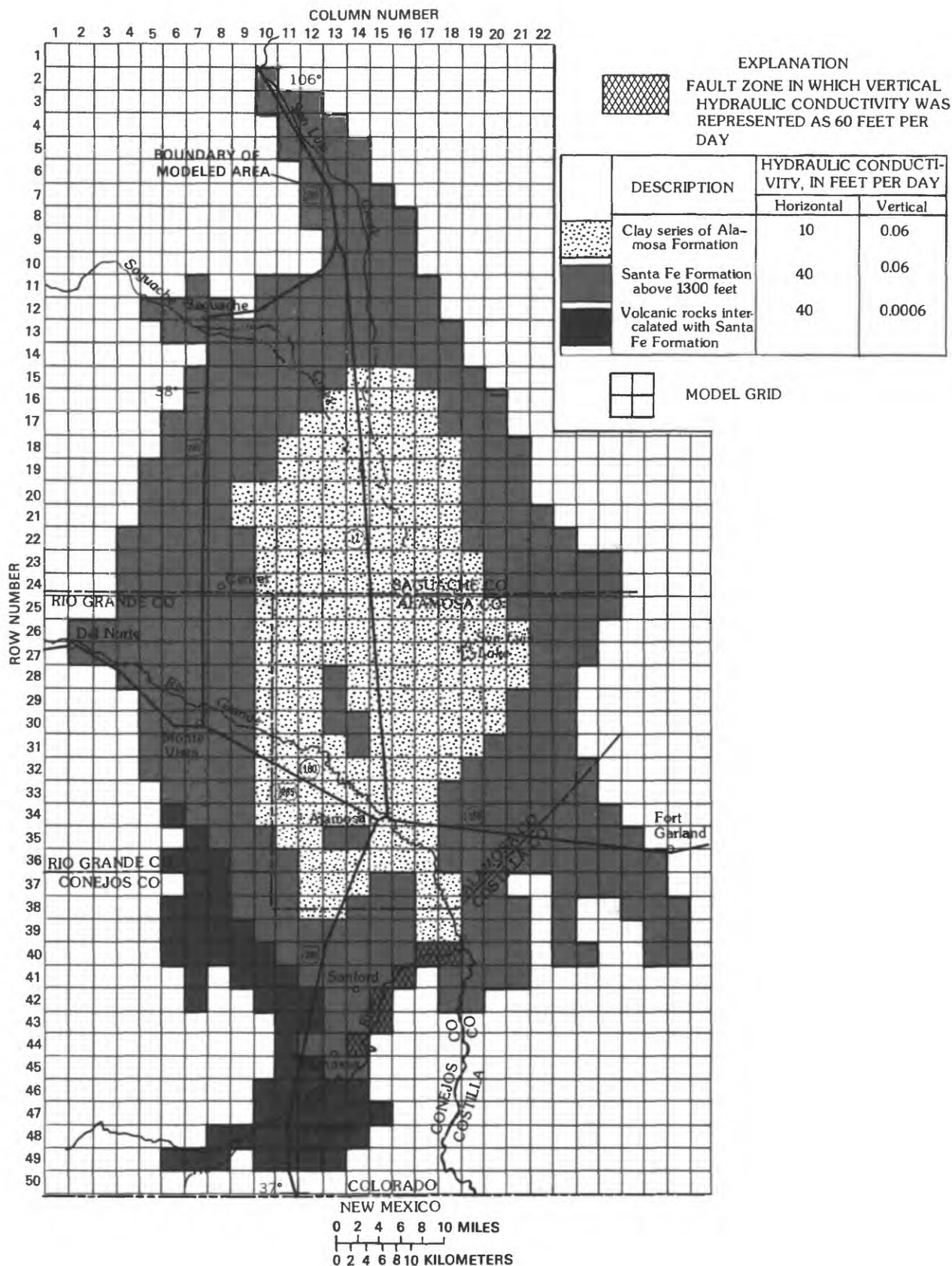


Figure 20.--Hydraulic conductivity of the upper confined aquifer, represented in the three-dimensional model as layer five.

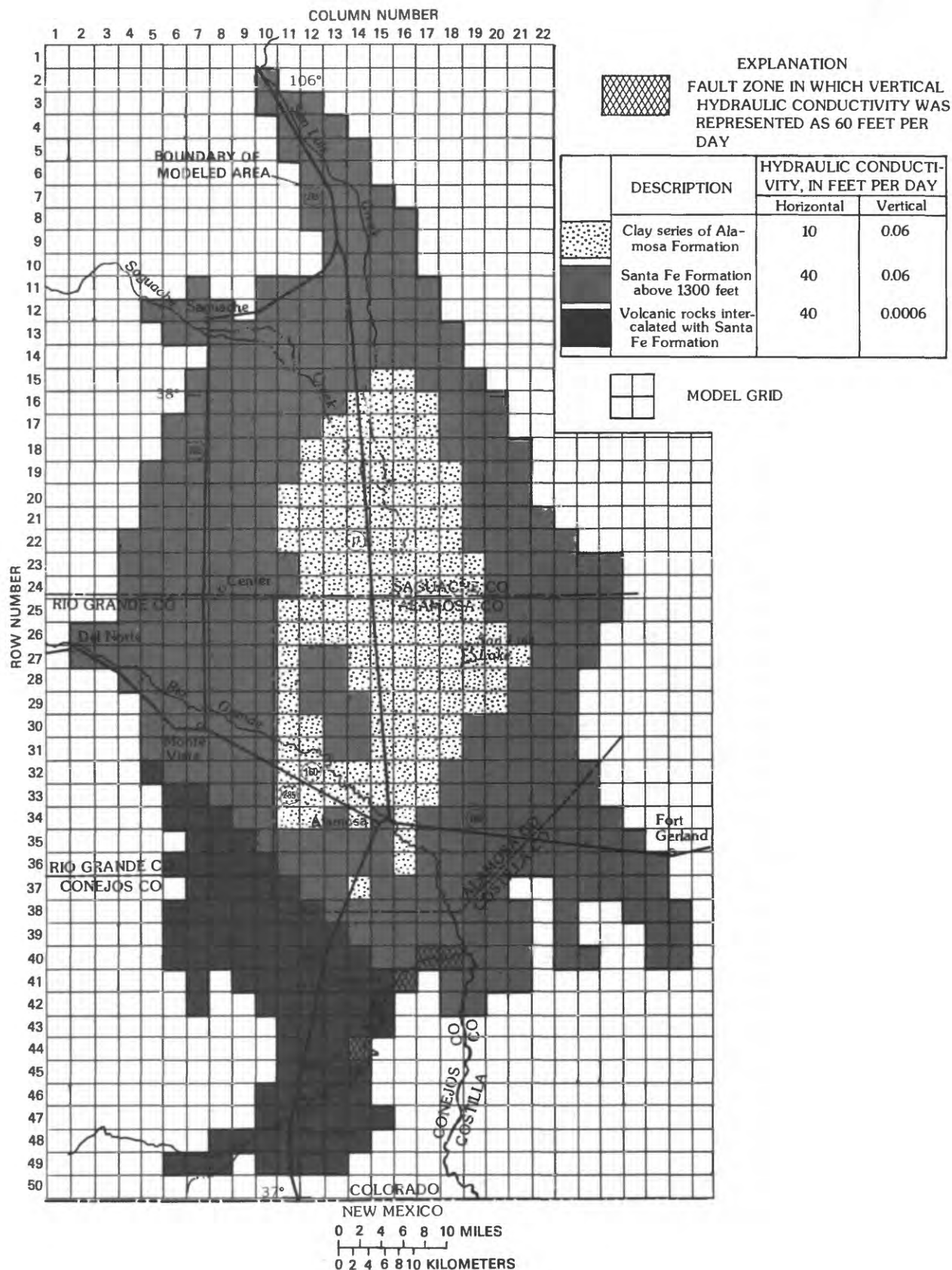


Figure 21.--Hydraulic conductivity of the upper confined aquifer, represented in the three-dimensional model as layer four.

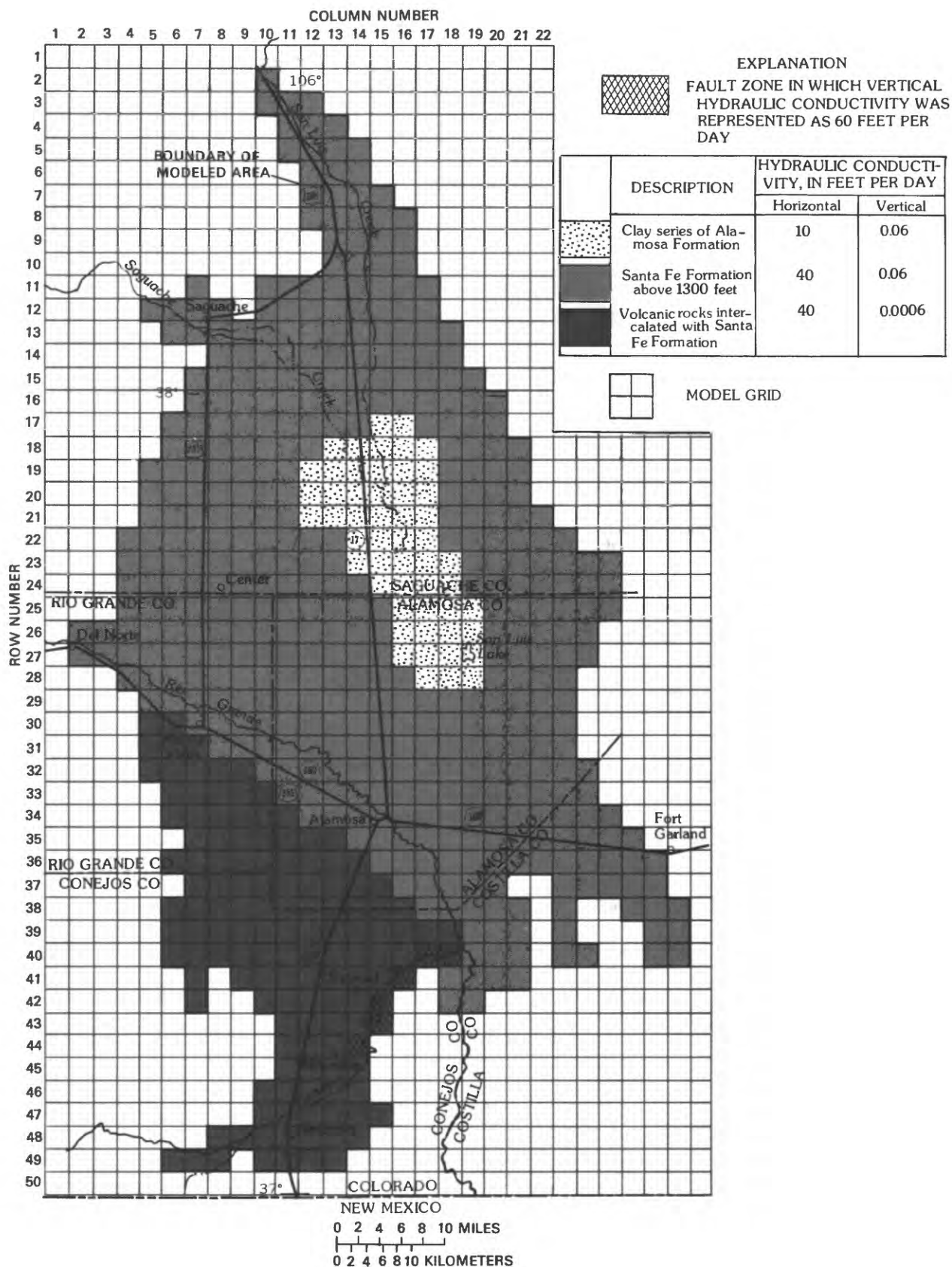


Figure 22.--Hydraulic conductivity of the upper confined aquifer, represented in the three-dimensional model as layer three.

## Representation of Change in Recharge and Discharge

Because the hydrologic system was assumed to be in a stable condition in 1950, recharge and discharge are represented in the model relative to the pre-1950 condition. The simulated flow was either: (1) Constant at the pre-1950 rate; (2) variable as a specified function of time; or (3) variable as a specified function of change in hydraulic head. In terms of change since 1950, these alternatives become: (1) No flow; (2) specified flow; and (3) hydraulic-head-dependent flow boundaries (Hearne, 1982). No specified hydraulic-head boundaries were defined in the model. This section describes how recharge and discharge flows were varied as functions of time and the assumptions and generalizations made to specify them as functions of space.

The model represented no change in the pre-1950 rates of recharge from infiltrating streamflow along the mountain front, subsurface recharge through permeable volcanic rocks of the San Juan Mountains, subsurface flow through and around the San Luis Hills, and irrigation return flow in areas where surface-water irrigation is not supplemented by ground-water withdrawals. Neither the fluctuations in these flows nor the hydraulic-head changes that result from fluctuations in these flows were simulated.

In many areas, recharge and discharge have changed since 1950 because of changes in irrigation practice. The primary changes are: (1) Withdrawal of ground water by large capacity (greater than 300 gallons per minute) wells to supplement irrigation with surface water; and (2) conversion from open (gravity) to closed (sprinkler) irrigation systems. The use of ground water for irrigation has resulted in a larger, more dependable water supply for irrigation. More water has been used for irrigation, and presumably more land has been irrigated; either previously nonirrigated land has been irrigated, or irrigated land that previously had not been irrigated during years of minimal availability of surface water has been more consistently irrigated, or both. The conversion to sprinkler irrigation was represented in the model as a decrease in the rate of ground-water withdrawal and a decrease in the rate of recharge to ground water by infiltration of irrigation water.

These changes in flow were represented in the model by assuming that changes in each cell were proportional to average changes. The average change for the entire Alamosa Basin was calculated from estimates of ground-water withdrawals and surface-water diversions (table 21, fig. 23).

Annual ground-water withdrawals (table 21, fig. 23) were estimated for 1940-79 from power consumption data. Withdrawals for 1940-69 (Emery and others, 1972) were estimated by assuming that withdrawal of an acre-foot of water consumed 100 kilowatt hours of electricity. This conversion factor is about the average of the values of 71 kilowatt hours per acre-foot reported by Powell (1958, p. 87) and 127 kilowatt hours per acre-foot reported by J.M. Dumeyer (U.S. Geological Survey, written commun., 1970). Estimates of the total number of wells, the number of pumps powered by electricity, and the power consumption by electric pumps were used to estimate total withdrawals from ground water for irrigation. Withdrawals for 1970-79 were estimated from number of systems served and power-consumption data (R.F. Pile, Public Service Company of Colorado, written commun., 1982; J.J. Lewis, San Luis Valley Rural Electric Cooperative, Inc., written commun., 1982), and by a similar technique

Table 21.--Ground-water withdrawals and surface-water diversions  
for irrigation

[All estimates are in thousand acre-feet per year]

Year	Ground-water withdrawals			Surface-water diversions	Total irrigation water used
	Gravity systems	Sprinkler systems	Total		
1940	104.0		104.0	769.1	873.1
1941	3		3	1,635.8	1,638.8
1942	5		5	1,398.2	1,403.2
1943	56		56	1,123.2	1,179.2
1944	41		41	1,557.6	1,598.6
1945	37		37	1,318.2	1,355.2
1946	125		125	912.4	1,037.4
1947	65		65	1,351.2	1,416.2
1948	35		35	1,320.5	1,355.5
1949	26		26	1,444.4	1,470.4
Mean (1940-49)	49.7		49.7	1,283.1	1,332.8
1950	128		128	964.5	1,092.5
1951	274		274	631.1	905.1
1952	46		46	1,626.4	1,672.4
1953	156		156	880.4	1,036.4
1954	401		401	772.3	1,173.3
1955	440		440	818.0	1,258.0
1956	542		542	752.5	1,294.5
1957	74		74	1,655.4	1,729.4
1958	142		142	1,181.4	1,323.4
1959	446		446	759.2	1,205.2
Mean (1950-59)	264.9		264.9	1,004.1	1,269.0
1960	299.0		299.0	1,153.2	1,452.2
1961	353		353	1,061.3	1,414.3
1962	177		177	1,352.7	1,529.7
1963	662		662	619.9	1,281.9
1964	733		733	795.4	1,528.4
1965	192		192	1,633.2	1,825.2
1966	314		314	1,132.2	1,446.2
1967	593		593	912.1	1,505.1
1968	407		407	1,263.9	1,670.9
1969	381		381	1,254.0	1,635.0
Mean (1960-69)	411.1		411.1	1,117.8	1,528.9



Table 21.--Ground-water withdrawals and surface-water diversions  
for irrigation--Continued

[All estimates are in thousand acre-feet per year]

Year	Ground-water withdrawals			Surface-water diversions	Total irrigation water used
	Gravity systems	Sprinkler systems	Total		
1970	337	10	347	1,263.0	1,610.0
1971	551	21	572	990.0	1,562.0
1972	727	33	760	807.0	1,567.0
1973	290	60	350	1,436.0	1,786.0
1974	670	107	777	706.0	1,483.0
1975	386	132	518	1,294.0	1,812.0
1976	497	201	698	1,033.0	1,731.0
1977	720	261	981	497.0	1,478.0
1978	637	284	921	788.0	1,709.0
1979	464	282	746	1,371.0	2,117.0
Mean (1970-79)	527.9	139.1	667.0	1,018.5	1,685.5

which differentiated between sprinkler-irrigation systems and gravity-irrigation systems. Conversion factors averaging 299 kilowatt hours per acre-foot for sprinkler systems and 122 kilowatt hours per acre-foot for gravity systems were reported by Ryan and Lutji (1979, p. 12). Withdrawals were calculated by assuming conversion factors of 300 kilowatt hours per acre-foot for sprinkler systems and 100 kilowatt hours per acre-foot for gravity systems. Power consumption data include areas in Costilla County, Colorado, which are in the Costilla Plains rather than the Alamosa Basin. However, these areas represent only about 6 percent of the irrigated acreage in the Alamosa Basin, and no correction was applied.

Surface-water diversions (table 21, fig. 23) for 1940-69 were reported by Emery and others (1972); those for 1970-79 were compiled from the Colorado State Department of Water Resources (T.M. Crouch, U.S. Geological Survey, written commun., 1981).

#### Ground-water withdrawals

Ground-water withdrawals were represented in the model as a specified flow. For each decade, withdrawal at each individual cell was specified as the product of: (1) The change in ground-water withdrawals from the 1940-49 average (table 22); and (2) the fraction of withdrawals for the cell. Estimated annual withdrawals from ground water were assigned to individual cells of the model based on irrigated acreage and the depths of large-capacity irrigation wells (greater than 300 gallons per minute). The input file for the 1950-79 transient simulation is in attachment 2 in the "Supplemental Data" section at the back of the report.

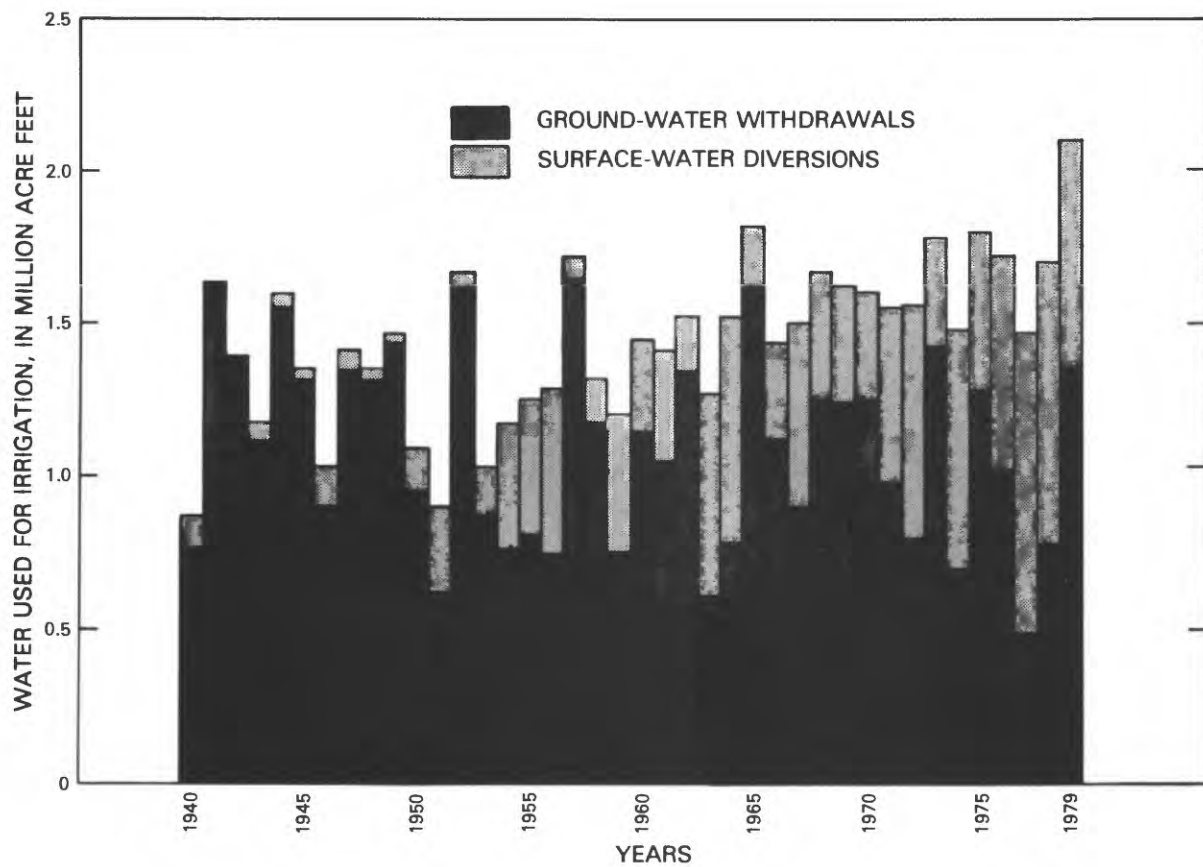


Figure 23.--Ground-water withdrawals and surface-water diversions for irrigation.

Table 22.--Indexes of ground-water withdrawals, return flow, and evapotranspiration  
[acre-ft/yr, acre-feet per year; ft/yr, feet per year; dashes indicate information not available]

Index or intermediate value	Decade			
	1940-49	1950-59	1960-69	1970-79
Ground-water withdrawals (acre-ft/yr)-----	50,000	265,000	411,000	667,000
Change in ground-water withdrawals, from the 1940-49 average (acre-ft/yr)-----	--	215,000	361,000	617,000
Total irrigation water used (acre-ft/yr)-----	1,333,000	1,269,000	1,529,000	1,686,000
Active irrigated area <sup>1</sup> (percent of irrigated area fig. 24)-----	63	60	72	80
Inactive irrigated area <sup>2</sup> (percent of irrigated area, fig. 24)-----	37	40	28	20
Return flow (ft/yr)-----	<sup>3</sup> 0.94	<sup>3</sup> 0.90	<sup>3</sup> 1.08	<sup>3</sup> 1.20 <sup>4</sup> 0.60
Change in return flow, from the 1940-49 average (ft/yr)-----	--	<sup>3</sup> -0.04	<sup>3</sup> 0.14	<sup>3</sup> 0.26 <sup>4</sup> -0.34
Index of evapotranspiration from ground water in irrigated areas (percent)----	--	58	50	44

<sup>1</sup>Calculated as the total irrigation water used as a percent of the 1979 use.

<sup>2</sup>Calculated as 100 minus the active irrigated area.

<sup>3</sup>For gravity irrigation.

<sup>4</sup>For sprinkler irrigation.

Irrigated acreage within each cell was estimated from land use maps prepared by the U.S. Soil Conservation Service and Colorado State University Experiment Station (1979a, b, and c; 1980a and b) that indicate about 750,000 irrigated acres within Alamosa, Conejos, Costilla, Rio Grande, and Saguache Counties of Colorado. Of the 710,000 irrigated acres (fig. 24) within the Alamosa Basin, about 20 percent were in areas with few or no large-capacity irrigation wells. The remaining 80 percent (about 560,000 acres) of irrigated areas had an adequate density of large-capacity irrigation wells to supplement the available surface-water supply with ground-water withdrawals. Each fully irrigated cell of the model (4 square miles or 2,560 acres) constitutes 0.458 percent of the estimated 560,000 acres in the Alamosa Basin that supplemented surface irrigation with ground-water withdrawals. Total withdrawals represented in each cell underlying a row-and-column location were proportional to the fraction of ground-water-supplemented irrigated acreage at the row-and-column location. Therefore, withdrawals from beneath a fully irrigated cell were 0.458 percent of the change in ground-water withdrawals, from the 1940-49 average (table 22).





Withdrawals for individual model cells in the stack of brick-shaped cells at each row-and-column location were based on the depths of large-capacity irrigation wells in the area represented. For ease of computation, the area of ground-water-supplemented irrigation was divided into 29 subareas (fig. 25). In each subarea, the range in depth of large-capacity irrigation wells was similar. For each subarea, the number of large-capacity irrigation wells in each of five depth intervals was estimated from the 1980 data base of the Colorado State Department of Water Resources, Ground Water Section (table 23). These depth intervals approximately correspond with the layers of the digital model. The top layer (layer seven), representing the unconfined aquifer, was typically less than 100 feet thick. Considering layer seven as 100 feet thick, then layer six extended from about 100 to 250 feet below the water table; layer five extended from about 250 to 500 feet below the water table; layer four extended from about 500 to 800 feet below the water table; and layer three extended from about 800 to 1,300 feet below the water table. Wells 0 to 100 feet deep were assumed to withdraw water from layer seven. Wells 101 to 250 feet deep were assumed to withdraw water from layers six and seven. Wells 251 to 500 feet deep were assumed to withdraw water from layers five and six. Wells 501 to 800 feet deep were assumed to withdraw water from layer four and five. Wells greater than 800 feet deep were assumed to withdraw water from layers three and four. Therefore, withdrawals represented in layer seven (fig. 26) were proportional to the sum of: (1) The percentage of wells in the subarea (table 23) that are 0 to 100 feet deep; and (2) half the percentage of wells in the subarea that are 101 to 250 feet deep. Withdrawals represented in layer six (fig. 27) are proportional to half the percentage of wells in the subarea that are 101 to 500 feet deep; withdrawals represented in layer five (fig. 28) are proportional to half the percentage of wells that are 251 to 800 feet deep; withdrawals represented in layer four (fig. 29) are proportional to half the percentage of wells that are greater than 500 feet deep; and withdrawals represented in layer three (fig. 30) are proportional to half the percentage of wells that are greater than 800 feet deep.

For example, in subarea 11 (fig. 25), 91.2 percent of the wells were less than 100 feet deep, 8.8 percent of the wells were 101 to 250 feet deep, and none of the wells were deeper than 250 feet (table 23). Withdrawals represented for each row-and-column location consisted of 95.6 percent ( $91.2 + \frac{1}{2} \times 8.8$ ) from layer seven, 4.4 percent ( $\frac{1}{2} \times 8.8 + 0$ ) from layer six, and none from layers five, four, and three. Because subarea 11 (fig. 25) was fully irrigated (fig. 24), withdrawals were calculated as 0.458 percent of the change in ground-water withdrawals from the 1940-49 average (table 22). Therefore, 0.438 percent (0.458 percent of 95.6 percent) of the annual withdrawals were represented for layer 7 at each row-and-column location in subarea 11. For 1960-69, the change in ground-water withdrawals (table 22) was 361,000 acre-feet per year. About 2.18 cubic feet per second (1,580 acre-feet per year) were represented as withdrawals from layer 7 of each row-and-column location of subarea 11.

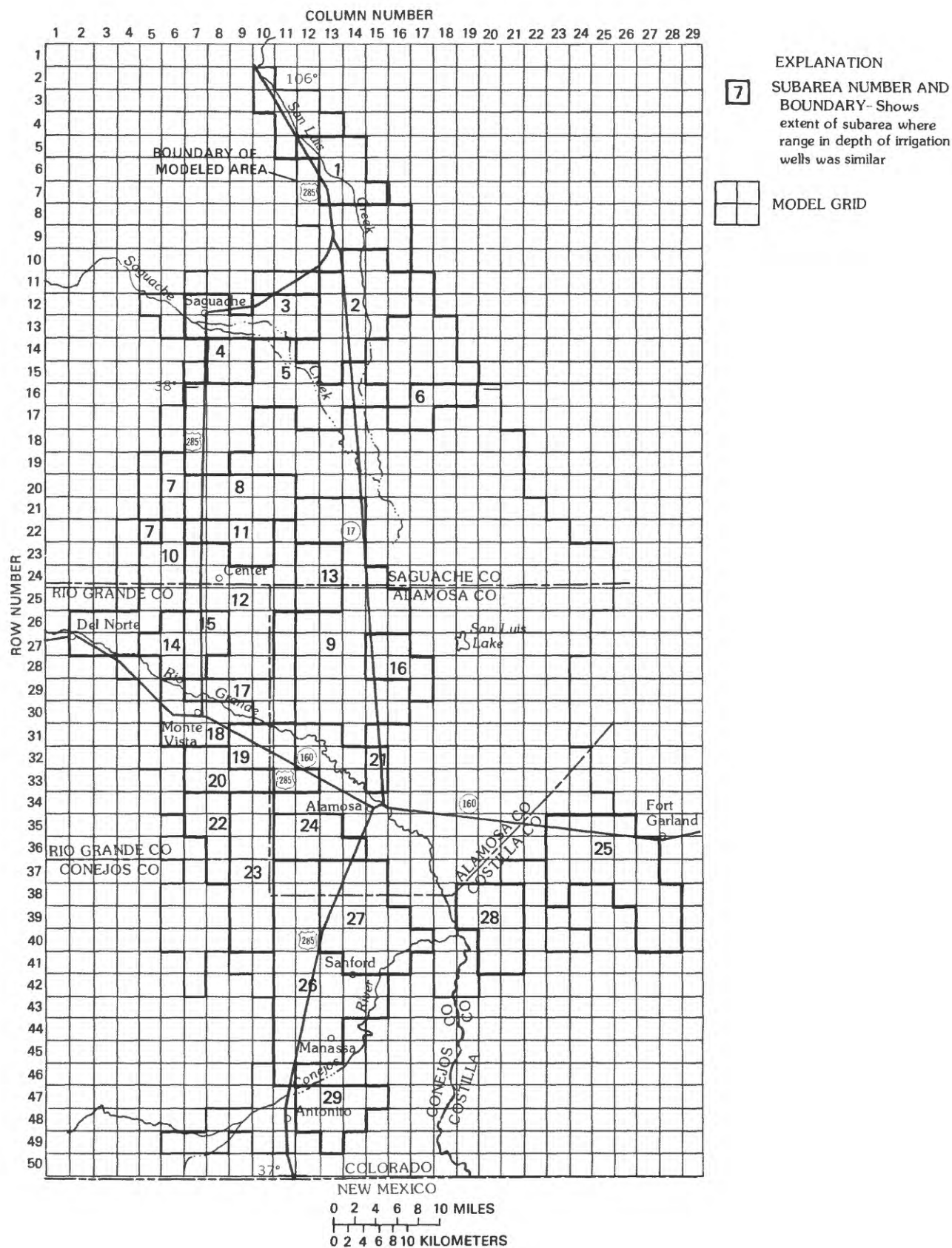


Figure 25.--Subareas where irrigation was supplemented by ground-water withdrawals.

Table 23.--Large-capacity irrigation wells

Subarea (location shown on fig. 25)	Number of large-capacity irrigation wells with a depth in feet of:					
	0-100	101-250	251-500	501-800	Greater than 800	Total
1	0	10	2	3	0	15
2	12	47	10	2	1	72
3	4	16	2	1	0	23
4	2	32	5	2	1	42
5	1	29	4	25	18	77
6	2	5	0	0	0	7
7	0	15	27	0	0	42
8	2	4	1	15	13	35
9	218	156	4	1	8	387
10	82	138	10	1	0	231
11	156	15	0	0	0	171
12	590	232	1	3	3	829
13	54	26	0	0	9	89
14	29	91	2	1	1	124
15	163	97	6	0	0	266
16	27	21	0	0	7	55
17	281	19	1	0	3	304
18	76	17	2	0	0	95
19	91	2	1	4	14	112
20	2	1	0	4	4	11
21	2	1	1	0	9	13
22	5	25	18	2	3	53
23	36	17	43	43	22	161
24	0	0	14	27	25	66
25	8	51	32	12	5	108
26	6	30	62	65	7	170
27	0	0	0	22	30	52
28	0	9	25	3	2	39
29	0	10	12	0	1	23
Totals	1,849	1,116	285	236	186	3,672
Withdrawals represented in layers						
	7	6 and 7	5 and 6	4 and 5	3 and 4	

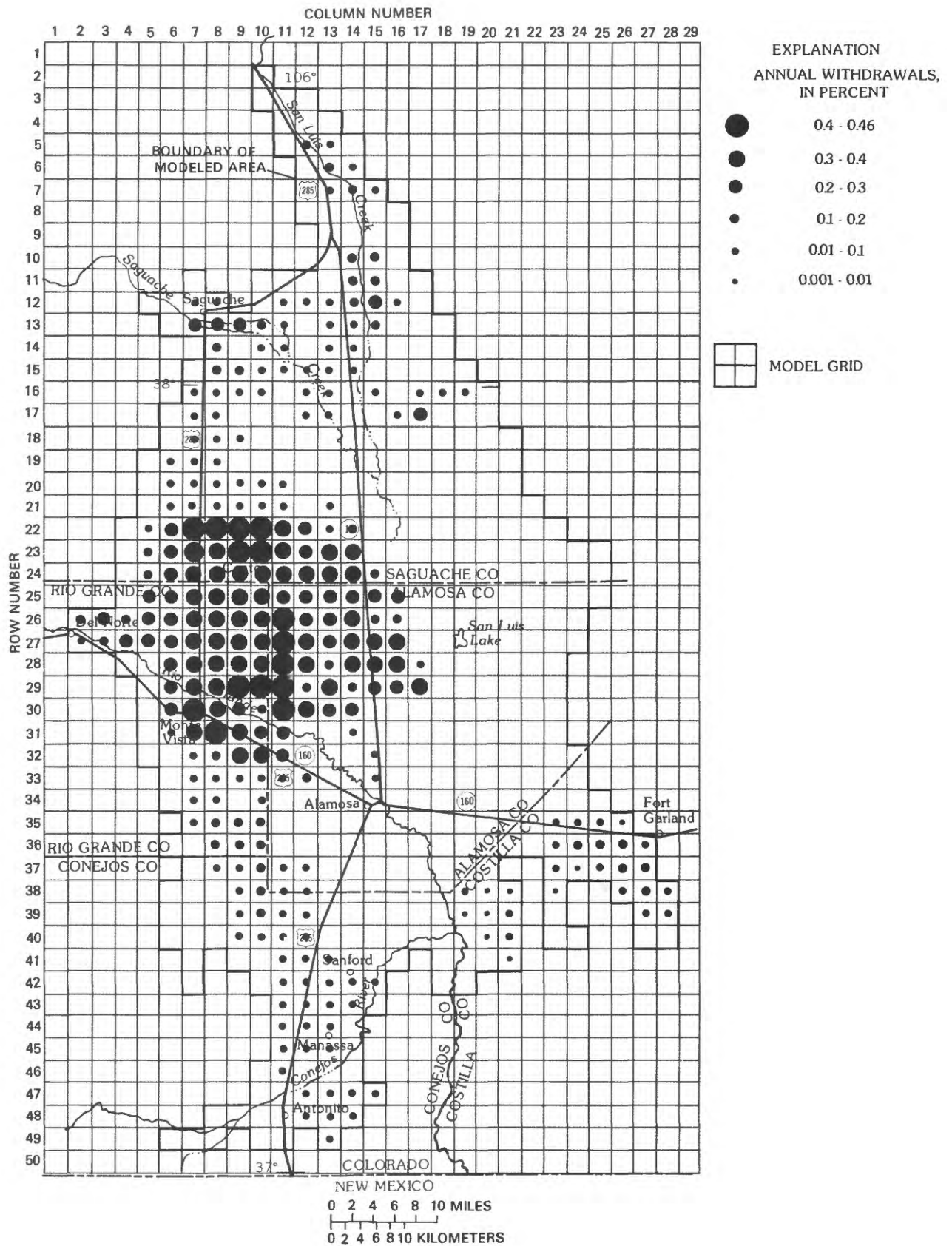


Figure 26.--Ground-water withdrawals represented in the three-dimensional model in layer seven.



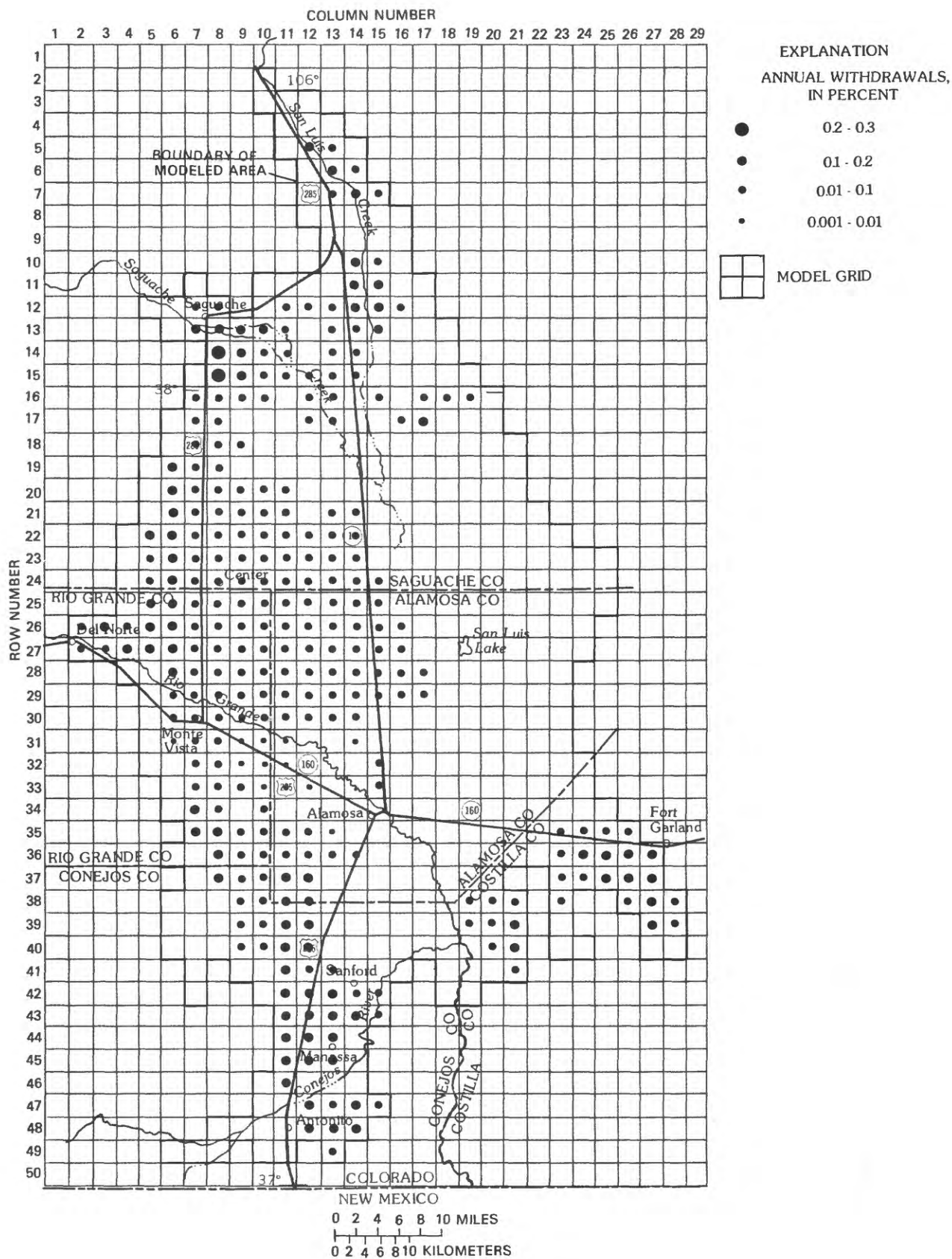


Figure 27.--Ground-water withdrawals represented in the three-dimensional model in layer six.

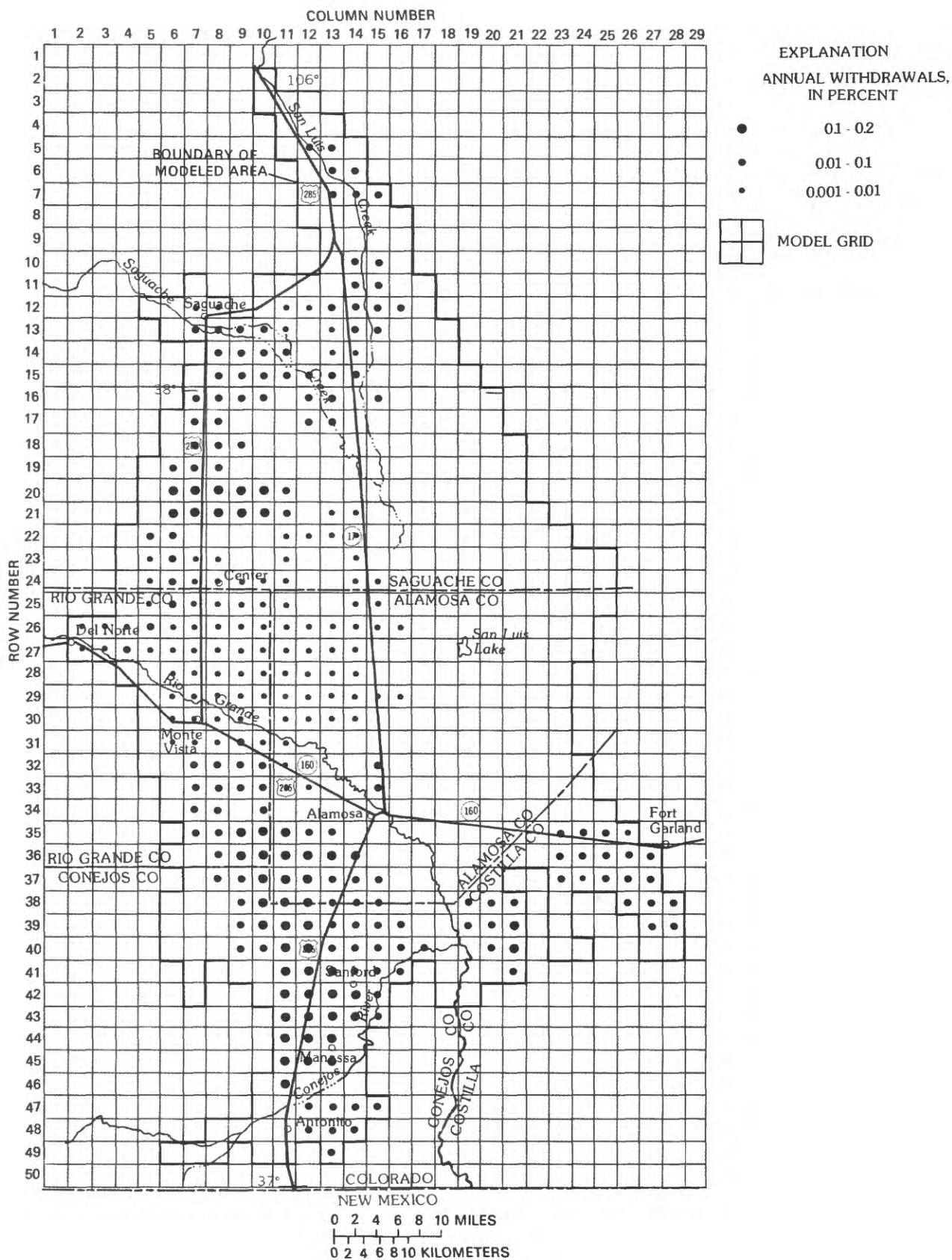


Figure 28.--Ground-water withdrawals represented in the three-dimensional model in layer five.

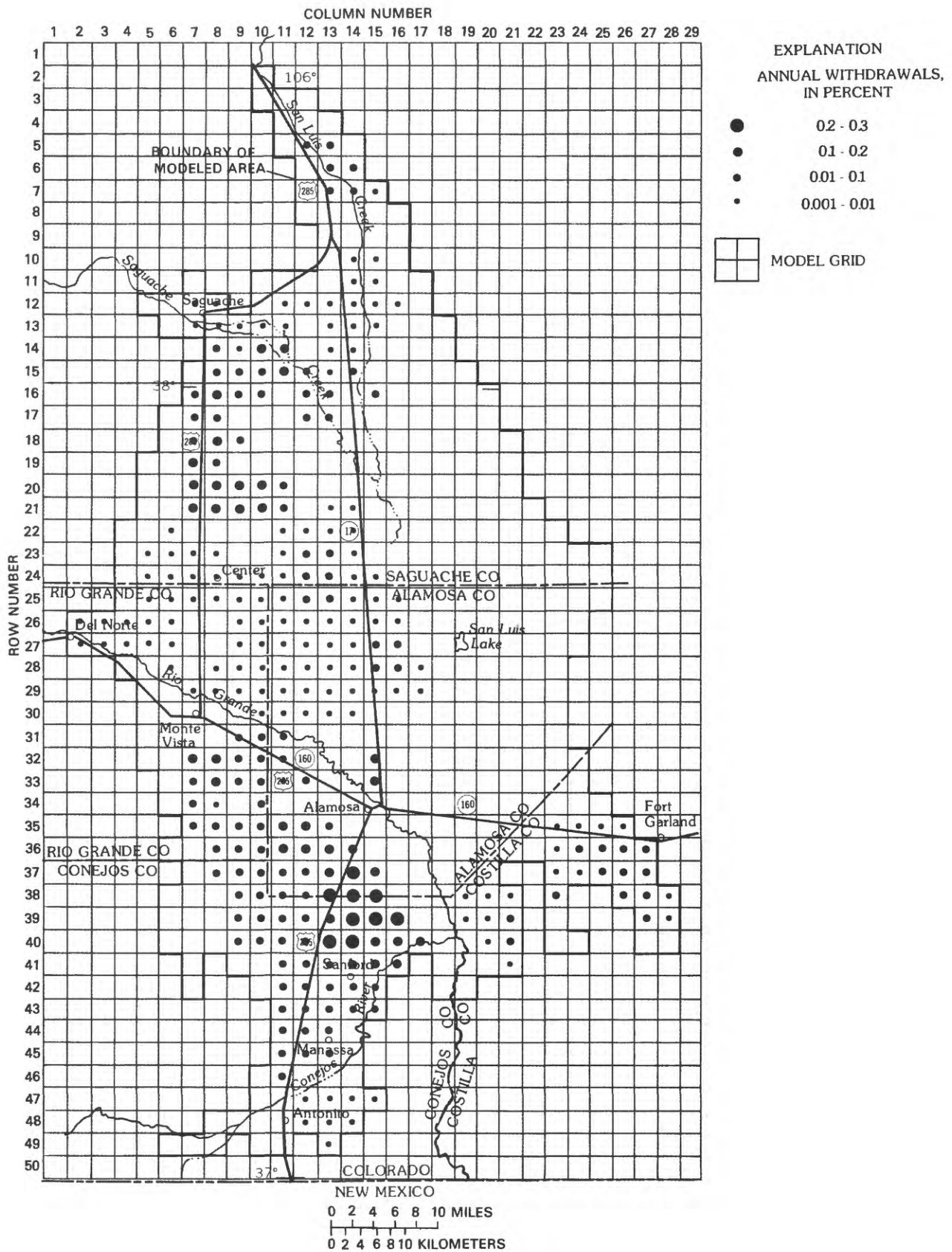


Figure 29.--Ground-water withdrawals represented in the three-dimensional model in layer four.



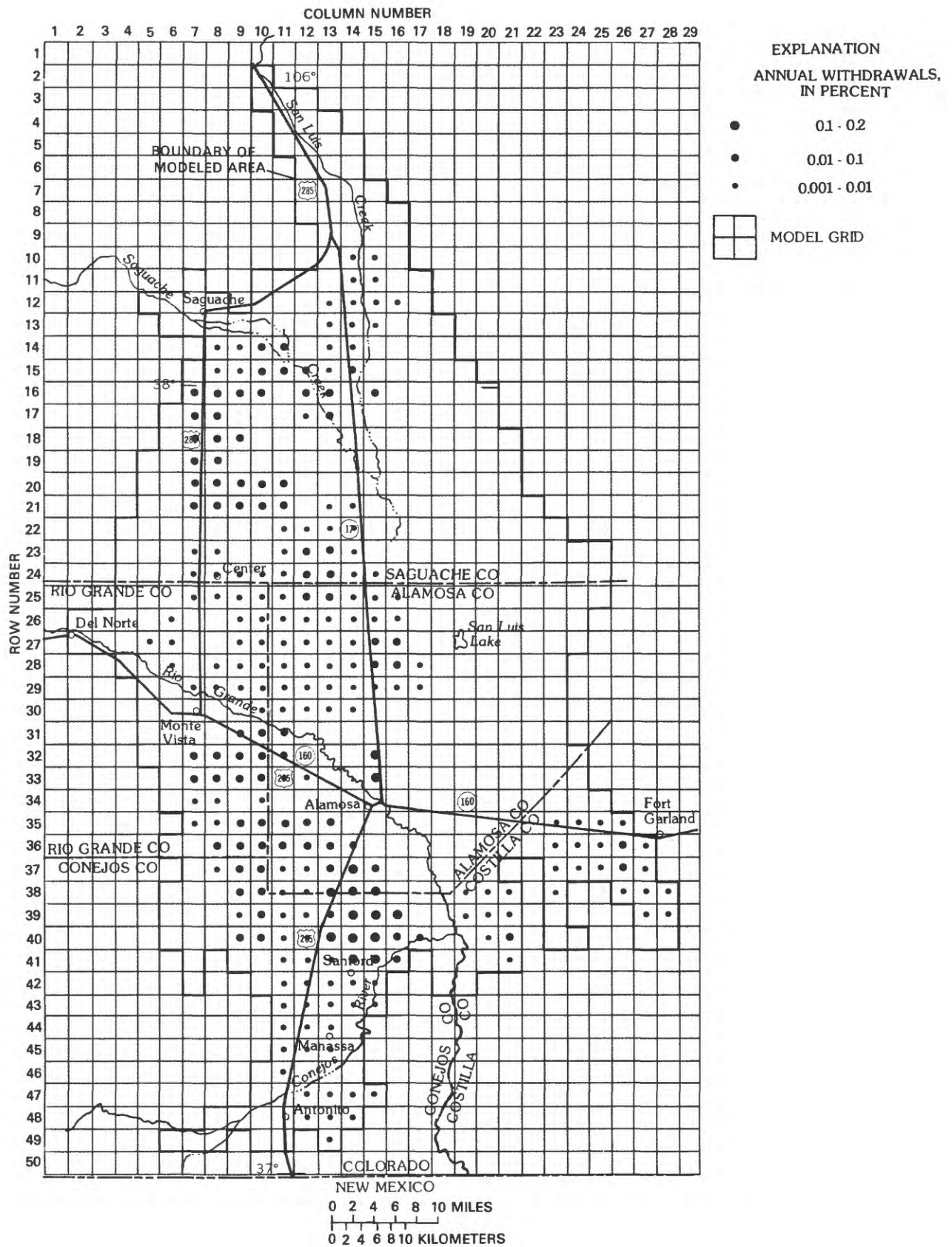


Figure 30.--Ground-water withdrawals represented in the three-dimensional model in layer three.

## Return flow from irrigation

Return flow from irrigation resulted from excess water applied to irrigated areas. Some of the applied irrigation water percolated below the root zone and recharged the ground-water system as irrigation return flow. As the total irrigation water use increased (table 21), return flow was presumed to increase. Return flow from gravity irrigation was calculated (table 22) from the active irrigated area. For each decade, the total irrigation water used was expressed as a percentage of the water used for the year of greatest use (1979). This percentage was accepted as an indicator of active irrigated area, that is, the average area that actually was irrigated during each decade. The percentage of inactive-irrigated area was calculated as the complement of the percentage of active-irrigated area.

Return flow was assumed to be 1.5 feet per year times the active irrigated area. The change in return flow from the 1940-49 average was calculated at each cell. For example, for 1970-79, about 80 percent of the irrigable land was actively irrigated (table 22). Return flow of 1.5 feet per year from the actively irrigated area would be equivalent to 1.2 feet per year from the total irrigated area. This represents 0.26 foot per year return flow more than was calculated for 1940-49 for gravity-irrigation areas. Therefore, at a cell representing 4 square miles (2,560 acres) of gravity irrigation, the model represented a recharge of 0.92 cubic feet per second. The input file for the 1950-79 transient simulation is in attachment 2 in the "Supplemental Data" section at the back of the report.

Less of the applied-irrigation water was assumed to recharge the ground-water system for sprinkler irrigation than for gravity irrigation. Because the transition to sprinkler irrigation started about 1970, the change in return flow (table 22) was calculated only for 1970-79. Average return flow from sprinkler irrigation during the 1970's (while the conversion was being made) was assumed to be 0.75 foot per year. Return flow of 0.75 foot per year from the actively irrigated area was equivalent to 0.60 foot per year from the total irrigated area, which represented a decrease of 0.34 foot per year from the return flow calculated for 1940-49. Therefore, at a cell representing 4 square miles (2,560 acres) of sprinkler irrigation, the model represented a discharge of 1.2 cubic feet per second.

Change in return flow since 1950 was represented at each cell of the model as the product of the change in return flow from the 1940-49 average (table 22) and the area in which large-capacity wells were available to supplement irrigation (fig. 31). For example, in row 22, column 9, there were 2,560 acres (4 square miles) of irrigated land (fig. 31). The change in return flow for 1960-69 was 0.14 feet per year (table 22). Therefore, return flow was represented as about 0.50 cubic feet per second greater during 1960 to 1969 than during 1940 to 1949.

During 1970 to 1979, the irrigated area was divided into areas using sprinkler irrigation (Davis Engineering Service, 1981) and areas using gravity irrigation. Return flow from sprinkler irrigation was calculated from the area of sprinkler irrigation (fig. 32) and the change in return flow from sprinkler irrigation (table 22). Return flow from gravity irrigation was calculated from the area of gravity irrigation (fig. 33) and the change in

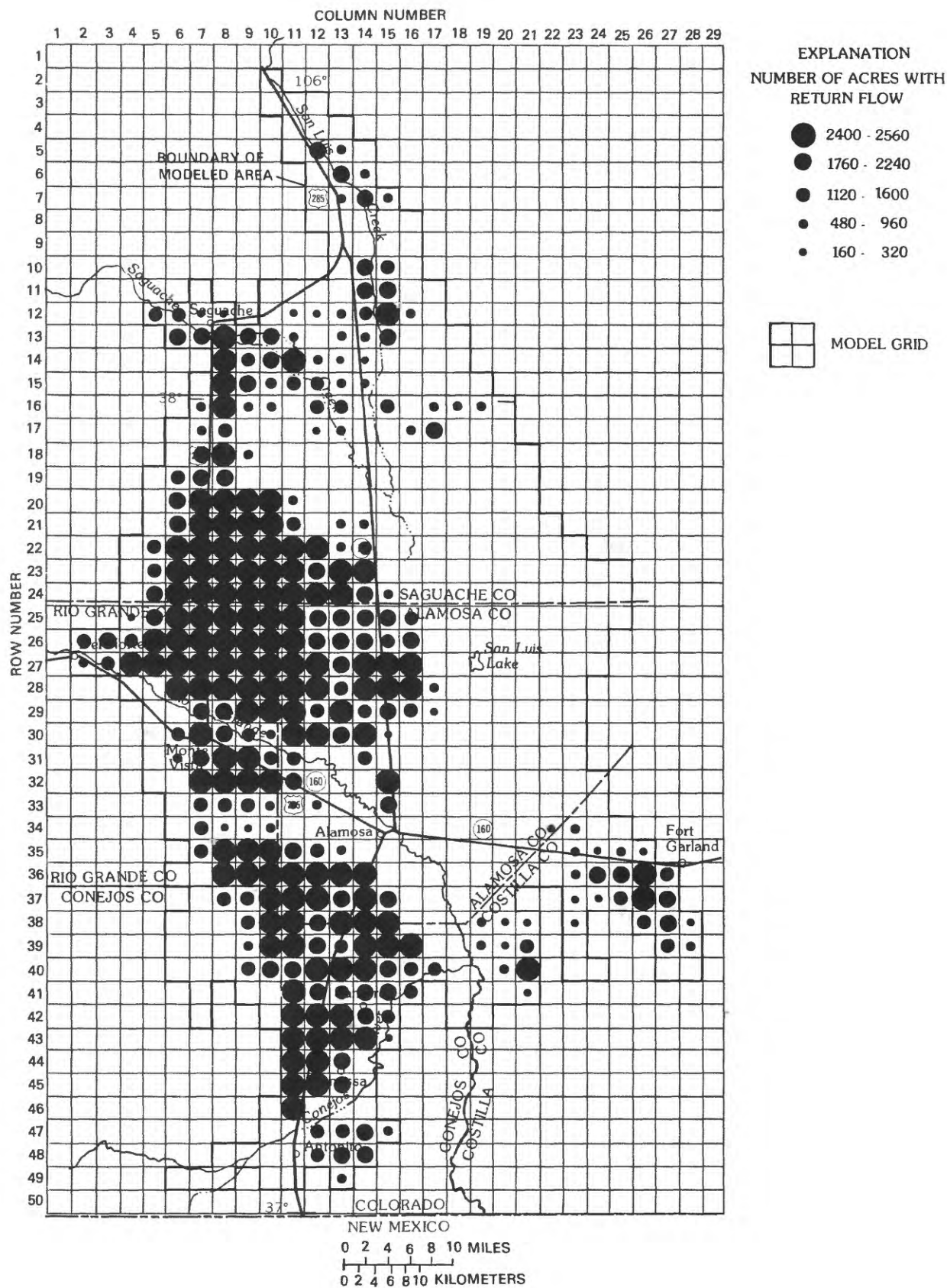


Figure 31.--Recharge to layer seven of the three-dimensional model representing return flow from irrigation.





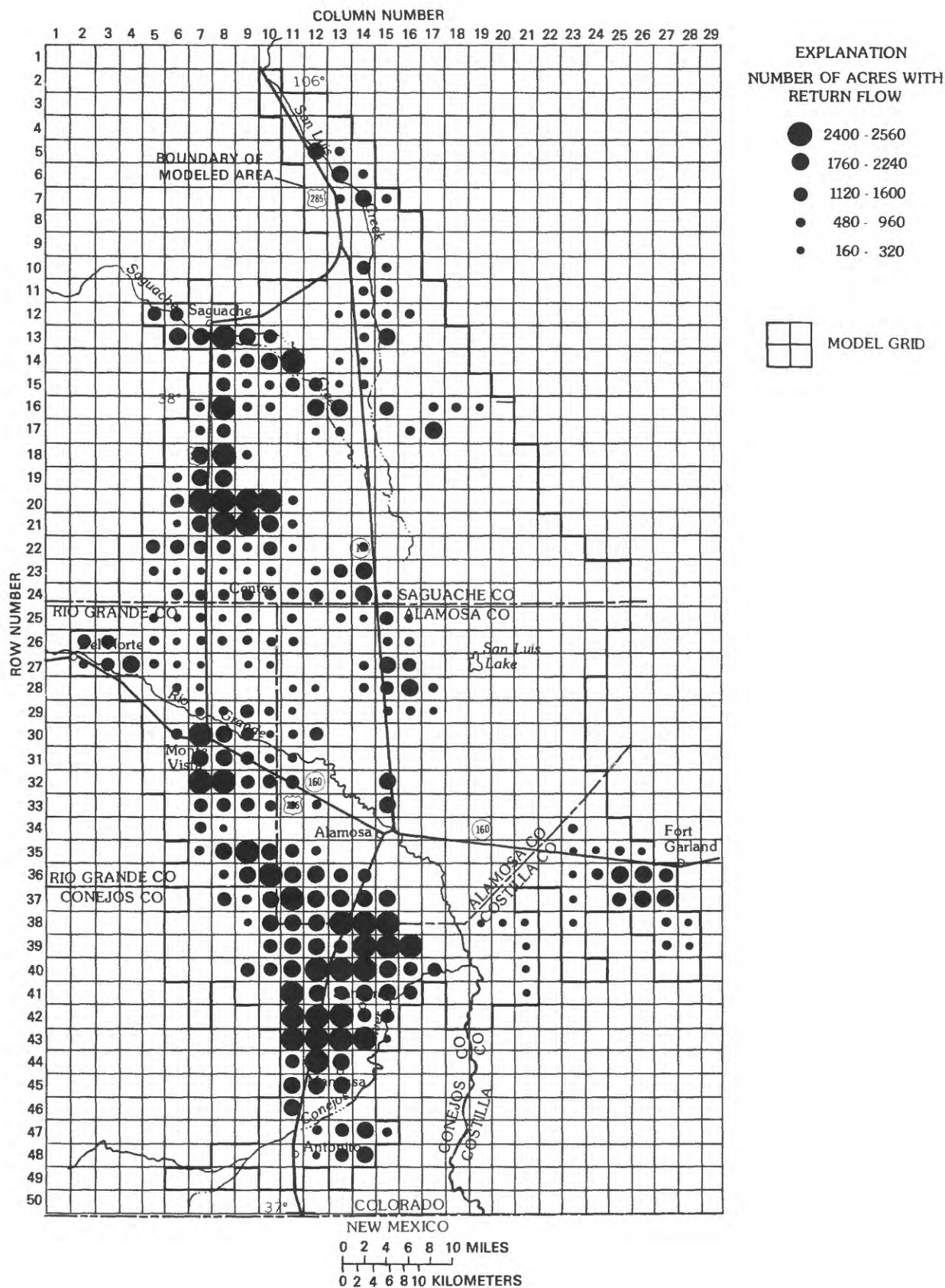


Figure 33.--Recharge to layer seven of the three-dimensional model representing return flow from gravity irrigation.

return flow from gravity irrigation (table 22). For example, in row 22, column 9, of the 2,560 acres of irrigated land, 1,920 acres were mapped as irrigated by sprinkler (fig. 32); the remaining 640 acres were assumed to be irrigated by gravity irrigation (fig. 33). During the 1970's, change in return flow from the 1940-49 average was 0.26 foot for gravity irrigation and negative 0.34 foot for sprinkler irrigation (table 22); that is, return flow from areas of gravity irrigation increased by 0.26 foot per year, and return flow from areas of sprinkler irrigation decreased by 0.34 foot per year. For the 640 acres (1 square mile) of gravity irrigation, return flow was calculated to increase by 0.23 cubic foot per second. For the 1,920 acres (3 square miles) of sprinkler irrigation, return flow was calculated to decrease by 0.90 cubic foot per second. Therefore, return flow at this cell was represented as 0.67 cubic foot per second less during 1970 to 1979 than during 1940 to 1949.

### Evapotranspiration salvage

Evapotranspiration salvage is the decrease in evapotranspiration from ground water that is represented in the model as resulting from an increased depth to water. Because the rate of evapotranspiration (fig. 9) was assumed to be a nonlinear function of depth to water (Emery, 1971), the rate of salvage because of a decline in hydraulic head was also a function of depth to water. Evapotranspiration salvage was represented in the model as a function of both land use (nonirrigated or irrigated, fig. 24) and depth to water. Depth to water was approximated in the model by dividing the Alamosa Basin into three depth-to-water zones based on the depth to water in 1969: (1) Greater than 12 feet; (2) between 6 and 12 feet; and (3) less than 6 feet (Emery and others, 1973). The input file for this hydraulic-head-dependent boundary is in attachment 1. The input file for the 1950-79 transient simulation is in attachment 2. Both attachments are in the "Supplemental Data" section at the back of the report.

For nonirrigated areas, evapotranspiration salvage was represented in the model as a different function of change in hydraulic head for each of the depth-to-water zones. In the greater-than-12-foot depth-to-water zone, the model assumed no salvage of evapotranspiration.

In the 6- to 12-foot depth-to-water zone of nonirrigated areas, the rate of evapotranspiration salvage was represented as a linear function of change in hydraulic head simulated by the model. Average initial depth to water in this zone was assumed to be 8 feet (table 24). A straight-line segment approximated the assumed relation between evapotranspiration and depth to water (fig. 9). For each square mile, the first 5 feet of water-level decline (from 8 to 13 feet below land surface) simulated salvage of 0.101 cubic foot per second for each foot of decline; further declines in water level produced no additional salvage. Therefore, for the 6- to 12-foot depth-to-water zone, the maximum salvage of 0.50 cubic foot per second (0.57 foot per year) was represented for a 5-foot decline in simulated hydraulic head.

Table 24.--Evapotranspiration salvage represented for nonirrigated areas  
[ft, feet; ft/yr, feet per year; ft<sup>3</sup>/s, cubic feet per second]

Simulated decline in hydraulic head (ft)	Depth to water zone					
	0- to 6-foot zone			6- to 12-foot zone		
	Assumed average depth to water (ft)	Evapotrans- piration salvage		Assumed average depth to water (ft)	Evapotrans- piration salvage	
		(ft/yr)	(ft <sup>3</sup> /s) <sup>1</sup>		(ft/yr)	(ft <sup>3</sup> /s) <sup>1</sup>
0	3	0.0	0.0	8	0.0	0.0
1	4	.37	.32	9	.11	.10
2	5	.73	.65	10	.23	.20
3	6	1.10	.97	11	.34	.30
4	7	1.21	1.07	12	.46	.40
5	8	1.33	1.17	13	.57	.50
6	9	1.44	1.28	14	.57	.50
7	10	1.56	1.38	15	.57	.50
8	11	1.67	1.48	16	.57	.50
9	12	1.78	1.58	17	.57	.50
>10	>13	1.90	1.68	>18	.57	.50

<sup>1</sup>Rate of salvage from each square mile (rounded).

In the 0- to 6-foot depth-to-water zone of nonirrigated areas, the rate of evapotranspiration salvage was represented by two linear functions of change in hydraulic head simulated by the model. Average initial depth to water in this zone was assumed to be 3 feet (table 24). Straight-line segments approximated the assumed relation between evapotranspiration and depth to water (fig. 9). For each square mile, the first 3 feet of water-level decline (from 3 to 6 feet below land surface) simulated salvage of 0.324 cubic foot per second for each foot of decline; the next 7 feet of water-level decline (from 6 to 13 feet below land surface) simulated salvage of 0.101 cubic foot per second for each foot of decline; further declines in water level produced no additional salvage. For the 0- to 6-foot depth-to-water zone, the maximum salvage of 1.68 cubic feet per second (1.9 feet per year) was represented for a 10-foot decline in simulated hydraulic head.

Each cell (4 square miles) was described according to the number of square miles that were nonirrigated for each of the depth-to-water zones. For example, the 4 square miles of row 34, column 11 were nonirrigated (fig. 24) and in the 0- to 6-foot depth-to-water zone. The first 1-foot decline in hydraulic head simulated evapotranspiration salvage of 1.30 cubic feet per second (0.324 cubic foot per second for each square mile). For a 10-foot decline in hydraulic head, the maximum simulated evapotranspiration salvage was 6.72 cubic feet per second (1.68 cubic feet per second for each square mile).

Within the irrigated area, evapotranspiration was assumed to change because either previously nonirrigated land was irrigated or marginal land was more consistently irrigated. The increase in total water used for irrigation was assumed to be associated with an increase in evapotranspiration and a corresponding decrease in evapotranspiration from ground water. The change in evapotranspiration from ground water was calculated (table 22) from the total irrigation water used. Water used by growing crops was assumed to be supplied by irrigation and was not represented in the model. However, irrigation was assumed to not supply water for: (1) Evapotranspiration from inactive irrigated areas, or (2) evapotranspiration from active irrigated areas during the nongrowing season. For inactive irrigated areas, evapotranspiration from ground water was assumed to be equal to that for nonirrigated areas. In the Alamosa Basin, about 72 percent (Kohler and others, 1959) of the annual evaporation occurs during the summer (May to October) and 28 percent during the winter. These percentages were assumed to apply to the seasonal differences in evapotranspiration. For actively irrigated areas, evapotranspiration from ground water was assumed to be 30 percent of evapotranspiration from nonirrigated areas. Therefore, for each cell of the model, the change in evapotranspiration from ground water was calculated as the sum of: (1) 30 percent of the active-irrigated area; and (2) 100 percent of the inactive-irrigated area. For example, during 1970-79, for the 80 percent of irrigated area that was active, evapotranspiration was assumed to be 30 percent of that for nonirrigated areas. For the 20 percent of irrigated area that was inactive, evapotranspiration was assumed equal to that for nonirrigated areas. Therefore, in irrigated areas, evapotranspiration of ground water for 1970-79 was 44 percent (table 22) of that for nonirrigated areas (table 24). This value is called the index of evapotranspiration from ground water in irrigated areas.

Within the irrigated area (fig. 24), evapotranspiration salvage was calculated as the product of salvage had the area been nonirrigated and the index of evapotranspiration from ground water in irrigated areas (table 22). For example, the 4 square miles of row 22, column 9 were in the 0- to 6-foot depth-to-water zone. If the area was nonirrigated, evapotranspiration salvage would be 1.30 cubic feet per second for the first 1-foot decline in hydraulic head and a maximum salvage of 6.72 cubic feet per second for a 10-foot decline in hydraulic head. However, the area was totally within the irrigated area. During the 1960's, the index of evapotranspiration from ground water in irrigated areas was 50 percent (table 22). Therefore, evapotranspiration salvage was 0.65 cubic feet per second for the first 1-foot decline in hydraulic head and a maximum salvage of 3.36 cubic feet per second for a 10-foot decline in hydraulic head.

### Streamflow capture

Ground-water flow to and from the Rio Grande and the Conejos River was assumed to vary as a function of hydraulic head in the aquifer. Streamflow capture is the decrease in ground-water flow to the stream plus the increase in ground-water flow from the stream. In the model, the rivers were represented as hydraulic-head-dependent flow boundaries. Streamflow capture for a cell of the model was calculated as the product of simulated change in hydraulic head times the leakance coefficient represented in the cell. The



leakance coefficient was calculated as the ratio of vertical hydraulic conductivity to distance separating the river from the hydraulic head in the aquifer. Vertical hydraulic conductivity was assumed to equal that of the clay series, 0.06 foot per day. Hydraulic head represented in the river was assumed to be separated from hydraulic head simulated in the top layer by 50 feet of aquifer material, half the nominal thickness of the top layer. The resultant leakance coefficient, 0.0012 per day, was applied to the area of each cell assumed to be occupied by the river, which was 10 percent. The resulting constant of proportionality, 0.00012 per day, was applied along the Rio Grande and the reach of the Conejos River upstream of Manassa, Colo. Downstream from Manassa, a value of 0.0012 per day was used for the constant of proportionality. By comparison, the digital model (S.G. Robson, U.S. Geological Survey, written commun., 1980), equivalent to the analog model of Emery and others (1975), used a value of the constant of proportionality of 0.00071 per day. The input file for this hydraulic-head-dependent boundary is in attachment 1. The input file for the 1950-79 transient simulation is in attachment 2. Both attachments are in the "Supplemental Data" section at the back of the report.

#### Analysis of 1950-80 Changes: Calibration

The stress simulated by the digital model included changes in both ground-water withdrawals and return flow from irrigation. The model was used to simulate the response to these changes from 1950 to 1979. To ensure that the assumptions made in developing the model were consistent with each other and with available data, the simulated response was compared with the measured response, and the assumptions were modified to improve the comparison--a process called "calibration." Commonly, the stress is assumed to be known, and calibration results in revised estimates of aquifer and boundary characteristics. Although the results of calibration may not be unique, the calibrated model commonly is assumed to better represent the prototype. However, for the three-dimensional model of the Alamosa Basin, stresses (withdrawals for irrigation and return flows from irrigation) were assumed to be less well-known than the aquifer characteristics. Therefore, calibration resulted in revised estimates of stress rather than revised estimates of aquifer characteristics.

Two criteria were established for comparing simulated and measured response: (1) Simulated changes in hydraulic head in the unconfined aquifer would be less than 6 feet from 1950 to 1969 (Emery and others, 1975), and (2) simulated changes in hydraulic head in the unconfined aquifer from 1970 to 1979 would resemble measured changes (Crouch, 1983) in magnitude and areal distribution. The calibration criteria were met by modifying simulated ground-water withdrawals within reasonable bounds.

Initial estimates of withdrawals resulted in excessive simulated declines in hydraulic head. Decreasing ground-water withdrawals to 70 percent of initial estimates for 1950-69 resulted in less than 4 feet of hydraulic-head change in layer seven throughout most of the modeled area, which was considered adequate to meet the first criterion. This is the approximate decrease in pumpage that would result from using a conversion factor of about 143 kilowatt hours per acre-foot, 12 percent higher than the 127 kilowatt hours

per acre-foot reported by J.M. Dumeyer (U.S. Geological Survey, written commun., 1970) and 17 percent higher than the 122 kilowatt hours per acre-foot reported by Ryan and Lutji (1979).

Areal distribution of withdrawals for 1970-79 was modified by subarea to improve the comparison with measured hydraulic-head changes. For most subareas, withdrawals were decreased to 70 percent. For some subareas in the central valley (fig. 25, subareas 9, 11, 12, 13, 16, and 17), two subareas in northern Conejos County (fig. 25, subareas 22 and 23), and one subarea in eastern Costilla County (fig. 25, subarea 25), withdrawals were decreased to 50 percent. Withdrawals were increased to 130 percent for subareas on the Rio Grande fan (fig. 25, subareas 7, 10, 14, and 15) and retained as 100 percent for parts of subareas adjacent to the Rio Grande fan (fig. 25, parts of subareas 8, 11, and 12). Withdrawals were increased to 300 percent for one subarea in western Costilla County (fig. 25, subarea 28). Average withdrawals for 1970-79 were decreased from 921 to 616 cubic feet per second. These modifications were considered reasonable because of the lack of data describing areal variation of the withdrawals imposed on the aquifer system. Subareas that rely on surface-water diversions may have no ground-water withdrawals. Subareas that rely only on ground-water may have large ground-water withdrawals. The withdrawals resulting from adjustments made during model calibration are given in table 25 and in attachment 2 in the "Supplemental Data" section at the back of the report.

Simulated decline in hydraulic head was within 5 feet of measured changes for 1970-79 (fig. 34) at all but four of the wells used as control points by Crouch (1985) to contour water-level changes. Two of these wells were in the same cell as wells for which change in hydraulic head was within 5 feet. The third well was adjacent to a cell for which the simulated change in hydraulic head was within 5 feet of the change in the well. The fourth well was an isolated well at row 12, column 16 of the model. Areal distribution of simulated water-level declines produced contours (fig. 35) similar to those (Crouch, 1985) from measured water levels (fig. 36). Changes in ground-water withdrawals and irrigation return flows that produced this result are shown in table 25.

Under the assumed, stable, initial condition of 1950, discharge from the aquifer system was equal to recharge; water level in the unconfined aquifer and hydraulic head in confined beds were not changing with time. Changes in irrigation practice since 1950 superimposed additional discharges and recharges on this stable condition (table 25). Because of the net withdrawal of ground water resulting from irrigation, the water level in the unconfined aquifer and hydraulic head in confined beds were decreased. As the hydraulic head decreased in areas of recharge and discharge, the rates of recharge were increased and the rates of discharge were decreased. Given sufficient time, the increase in withdrawals would be balanced by decreases in discharge or increases in recharge. A more general discussion of these principles is offered by Theis (1938 and 1940). Simulation using a digital model provides a quantitative description of this process, and individual components can be isolated for specific study.

Table 25.--Changes in ground-water withdrawals and irrigation return flows as adjusted during model calibration  
[All values are in cubic feet per second]

Type of stress represented by flow	Flow to (+) or from (-) the aquifer				Change in flow relative to 1940-49		
	1940 -49	1950 -59	1960 -69	1970 -79	1950 -59	1960 -69	1970 -79
Ground-water withdrawals.	-69	-277	-419	-616	-208	-350	-547
Return flow from sprinkler-irrigation areas.	+299	+286	+344	+189	-13	+45	-110
Return flow from gravity-irrigation areas.	+429	+410	+494	+551	-19	+65	+122
Totals	+659	+419	+419	+124	-240	-240	-535

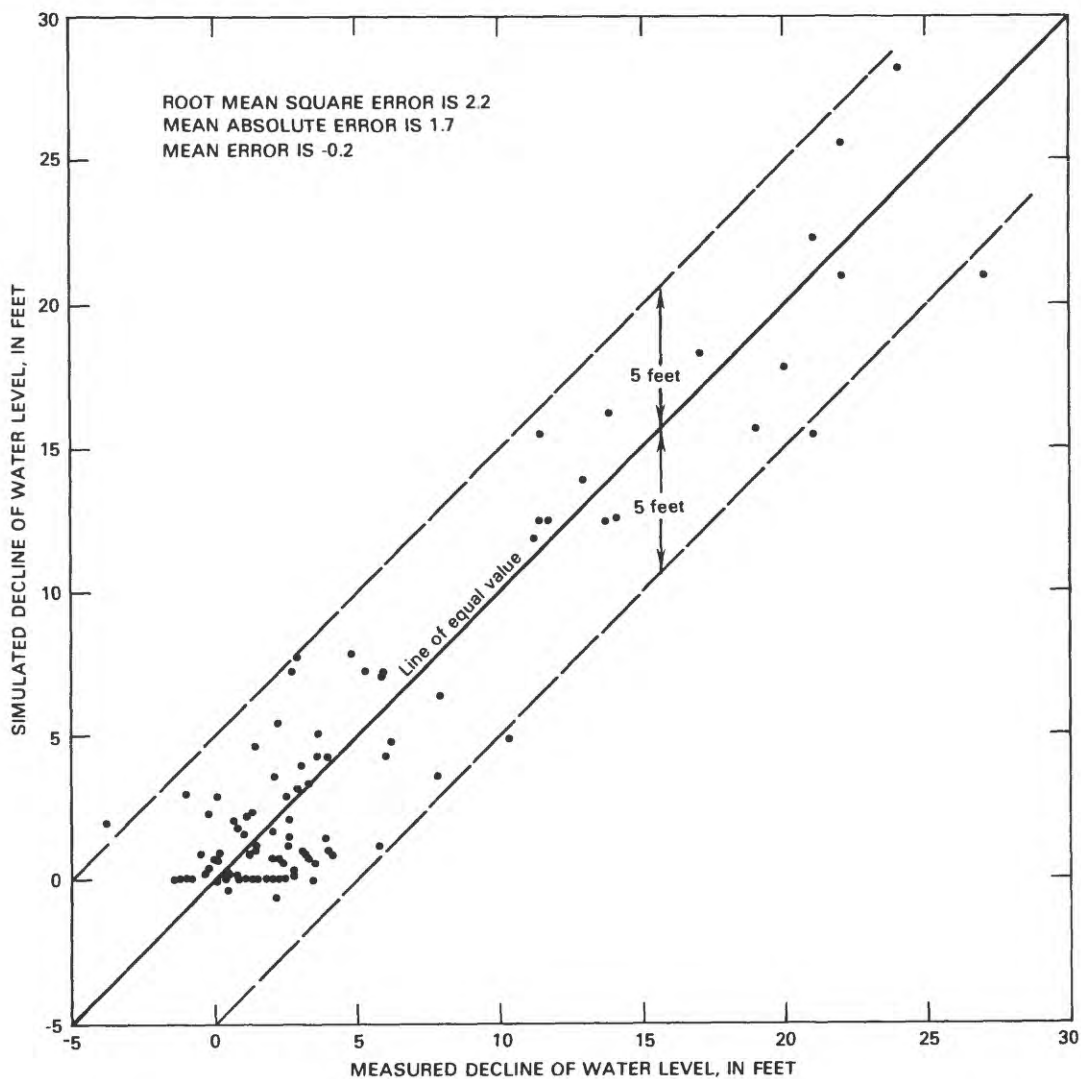


Figure 34.--Comparison between simulated and measured decline of water level in the shallow aquifer for 1970-79.

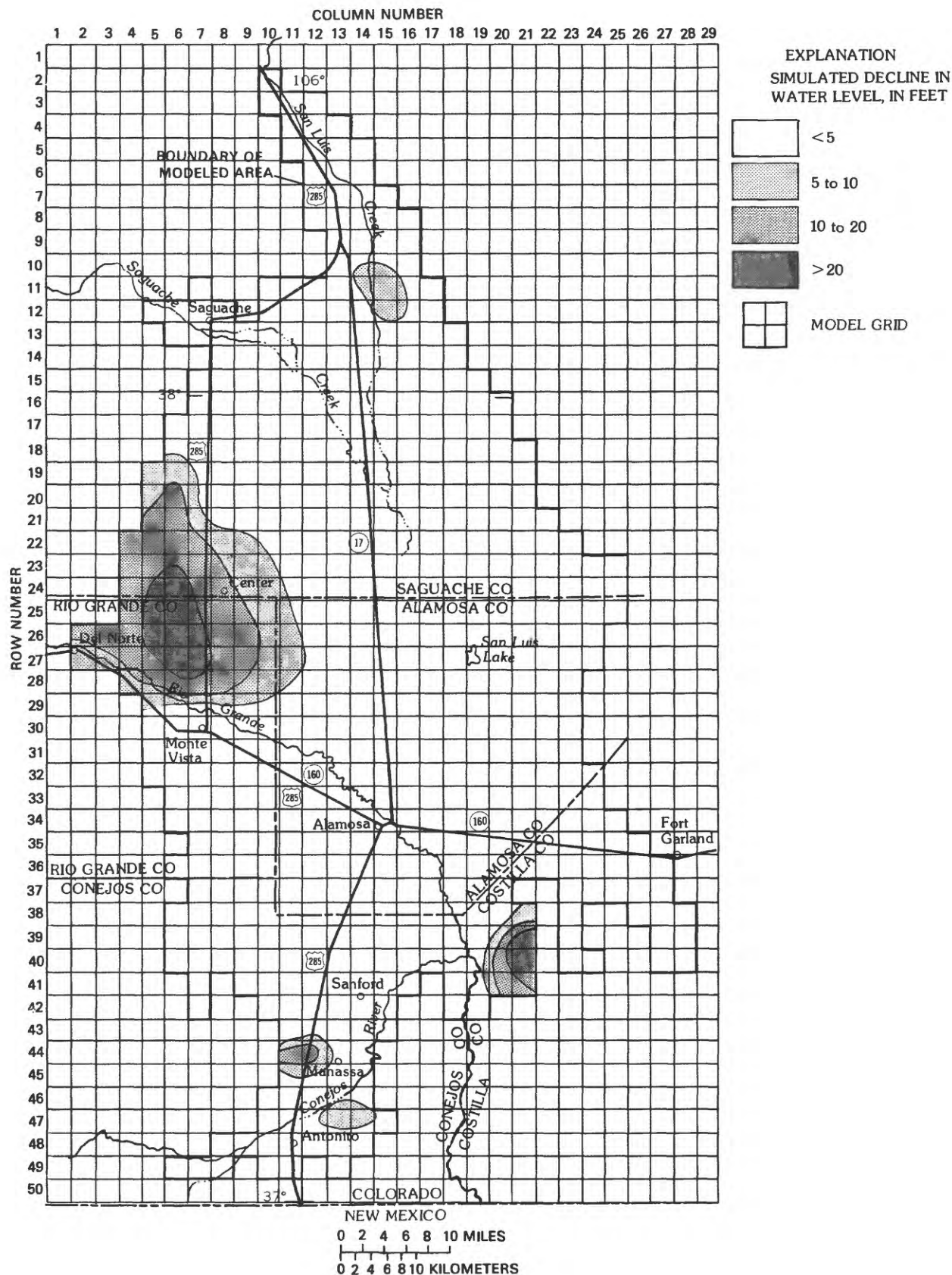


Figure 35.--Simulated decline in water level in the shallow aquifer for 1970-79.



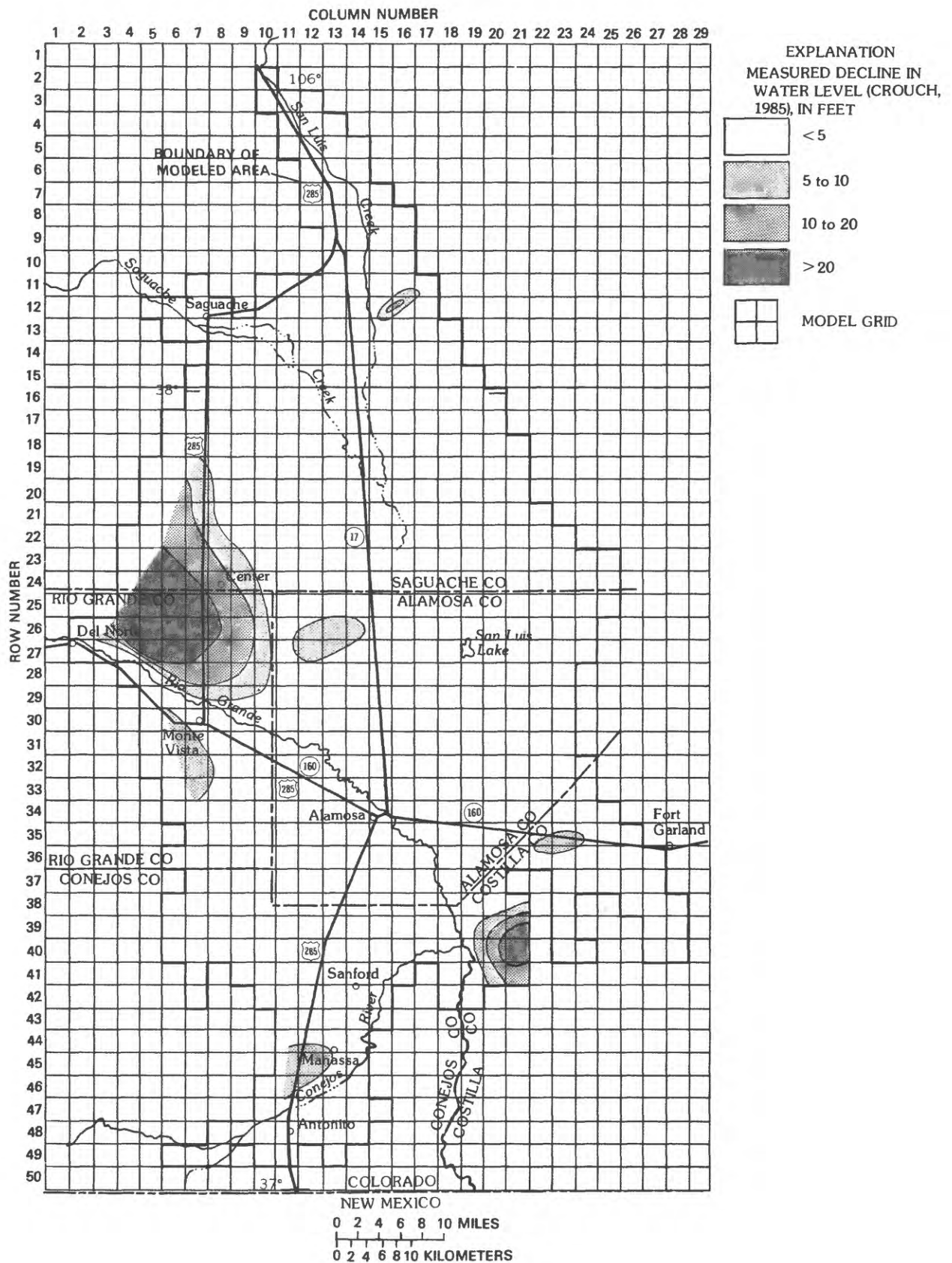


Figure 36.--Measured decline in water level in the shallow aquifer for 1970-79.

Sources of water available in the model of the Alamosa Basin are storage in the aquifer system, evapotranspiration salvage, and streamflow capture as represented in the model by a hydraulic-head-dependent boundary. The uppermost line in figure 37 represents the total change in flow relative to 1940-49 shown on the right side of table 25. The three areas below this line represent simulated flow from each of the available sources. For example, in 1980 (10 years after the step change imposed in 1970), net withdrawals were 535 cubic feet per second. Of these, 75 cubic feet per second (14 percent) were being drawn from storage in the aquifer system. Therefore, water levels were still declining. Streamflow capture was the source for 31 cubic feet per second (6 percent). Evapotranspiration salvage was the source for 429 cubic feet per second (80 percent); of this 429 cubic feet per second, 383 cubic feet per second (89 percent) was from areas with assumed average depth to water of 3 feet, and 46 cubic feet per second (11 percent) was from areas with assumed average depth to water of 8 feet. Expressed another way, of the total of 429 cubic feet per second of evapotranspiration salvage, 294 cubic feet per second (69 percent) was from irrigated areas, and 135 cubic feet per second (31 percent) was from nonirrigated areas.

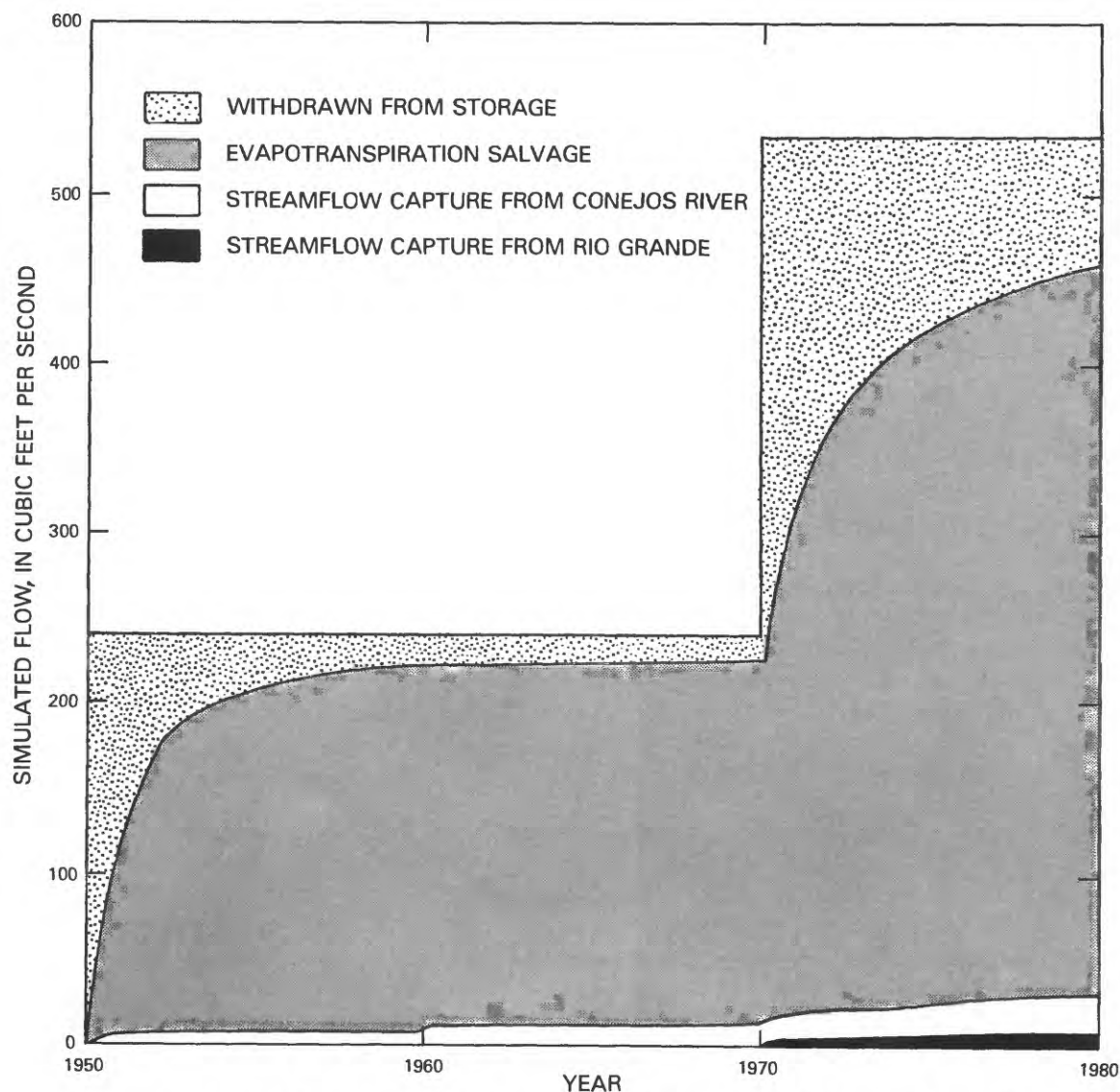


Figure 37.--Simulated source of water withdrawn from the Alamosa Basin.

The solution simulated by the model is not the result of a unique combination of boundary conditions and aquifer characteristics. For example, greater decreases in hydraulic head could have been simulated by increasing the ground-water withdrawals for subareas on the Rio Grande fan, decreasing the change in return flow, or decreasing the evapotranspiration of ground water from irrigated areas. Although ground-water withdrawals were changed to improve the comparison between simulated and measured water-level declines, equally satisfactory results might have been obtained from other changes. Therefore, the increase in ground-water withdrawals to 130 percent for subareas on the Rio Grande fan (fig. 25, subareas 7, 10, 14, and 15) does not necessarily indicate that ground-water withdrawals, in fact, were 30 percent greater than original estimates. Although this assumption is reasonable, equally reasonable solutions might have been obtained by assuming either greater decrease in return flow associated with sprinkler irrigation, smaller salvage of evapotranspiration associated with water-level declines, or some combination of all three. No claim is made to a unique estimate of withdrawals.

The apportionment of captured streamflow is the result of the distribution of withdrawals and the arbitrary designation of a higher constant of proportionality along the Conejos River downstream from Manassa, Colo., (0.0012 per day) than along the Rio Grande (0.00012 per day). For these designated values in 1980, of the simulated 31 cubic feet per second of captured streamflow, 21 cubic feet per second was from the Conejos River and 10 cubic feet per second was from the Rio Grande. Neither the constants of proportionality nor the values of captured streamflow are supported by independent measurements.

#### Analysis of 1950-80 Changes: Sensitivity

The result simulated by the model of ground-water flow was affected only slightly by stresses imposed before 1970. This was demonstrated by comparing alternate simulations. In the first simulation, the 1950-69 withdrawals were included in the simulation followed by the 1970-79 withdrawals (table 25). In the alternate simulation, the 1970-79 withdrawals were imposed on the stable 1950 condition. Ignoring withdrawals prior to 1970 resulted in slightly less evapotranspiration being salvaged, no significant change in streamflow being captured, and more water being withdrawn from storage in the aquifer in 1980. Larger declines in hydraulic head resulted from less of the withdrawals being derived from salvaged evapotranspiration and more from storage in the aquifer. Differences in the simulated 1980 condition (table 26) were considered negligible; analysis proceeded by excluding withdrawals prior to 1970 and comparing the simulated 1980 condition.

Sensitivity of the model to system characteristics was tested by varying the value of system characteristics. That is, the model was varied by changing the value assumed for an individual characteristic; the value for all other characteristics remained the same as in the standard simulation. Except for river leakance, the variation was applied uniformly throughout the model. For example, all storage coefficients were multiplied by a factor of 1.5. River leakance was varied only along the Rio Grande. The simulated change in hydraulic head in the southwestern corner of T. 40 N., R. 8 E. (row 27,

Table 26.--Sensitivity of simulated 1980 condition to rates of withdrawal represented prior to 1970  
[ft<sup>3</sup>/s, cubic feet per second; ft, feet]

Represented withdrawals (ft <sup>3</sup> /s)		Simulated condition			Hydraulic-head decline, 1970-79 at row 27, column 8, layer 7 (ft)
		Percent of withdrawals derived in 1980 from:			
1950-69	1970-79	Aquifer storage	Evapotrans- piration salvage	Stream- flow capture	
240	535	14	80	6	17.0
0	535	17	78	6	18.2



column 8, layer 7) arbitrarily was selected to represent the change in hydraulic head in the shallow aquifer on the Rio Grande fan (where the greatest response was expected). Results of these simulations are summarized in table 27. The simulation indicated as "standard" describes the condition simulated with the system characteristics described in the sections "Aquifer Characteristics in the Three-Dimensional Model" and "Representation of Change in Recharge and Discharge." Other simulations were compared to this standard. For example, multiplying horizontal hydraulic conductivity by a factor of 0.7 decreased 1980 streamflow capture from 6 to 5 percent of the total withdrawals.

The effect of changing a characteristic depends on the amount of change; increasing a characteristic by a factor of 1.5 would have a greater effect than increasing a characteristic by a factor of 1.3. The selection of these limits was arbitrary. Most aquifer characteristics (horizontal and vertical hydraulic conductivity and storage coefficients) were varied by 50 percent (factors of 1.5 and 0.5). Anticipating that the effect of the storage coefficient would be small, only the upper limit was simulated. Horizontal hydraulic conductivity decreased to 50 percent produced conditions that caused the computer program to terminate prior to simulating 10 years. Although other remedies for this problem were possible, the one selected was to simulate a decrease to 70 percent. Vertical hydraulic conductivity was decreased to 10 percent, because some investigators (Zorich-Erker Engineering, Inc., 1980b) have estimated upward leakage in the closed basin at a tenth of the estimate by Emery and others (1975). Similarly, river leakance was increased by a factor of 10. Characteristics defining stress (ground-water withdrawals and return flow) were varied by 30 percent (factors of 1.3 and 0.7). Ground-water withdrawals increased by 30 percent produced conditions that caused the computer program to terminate prior to simulating 10 years. Although other remedies for this problem were possible, the one selected was to simulate a 20-percent increase. Because evapotranspiration salvage from irrigated areas was the largest source of water, simulations were made that decreased evapotranspiration salvage by 60 percent (factor of 0.4) and that eliminated this source (multiplied by a factor of 0.0).

Differences between decline in hydraulic head simulated by the various alternatives and decline in hydraulic head of the standard simulation indicate the sensitivity of the simulated 1980 condition to the individual aquifer characteristic. Decline in hydraulic head was most sensitive to ground-water withdrawals. A 20-percent increase in withdrawals produced a 33-percent increase in hydraulic-head decline (table 27). By comparison, a 30-percent decrease in evapotranspiration salvage produced a 22-percent increase in hydraulic-head decline; a 30-percent increase in return flow from sprinkler irrigation produced a 17-percent increase in hydraulic-head decline; and a 30-percent decrease in horizontal hydraulic conductivity produced an 11-percent increase in hydraulic-head decline.

Table 27.--Sensitivity of simulated 1980 condition to the value assumed for individual system characteristics [ft, feet]

Model characteristic	Multiplied by a factor of:	Percent of withdrawals derived in 1980 from:			Simulated 1970-79 decline in hydraulic head at row 27 column 8, layer 7 (ft)
		Aquifer storage	Evapo-transpiration salvage	Stream-flow capture	
Standard.		17	78	6	18
Horizontal hydraulic conductivity.	1.5	15	79	6	16
	.7	22	74	5	20
Vertical hydraulic conductivity.	1.5	16	79	5	17
	.5	19	75	6	20
	.1	22	69	9	22
Storage coefficients.	1.5	22	73	5	15
Rio Grande leakance.	10.0	15	75	10	18
Ground-water withdrawal.	1.2	19	75	6	24
	.7	13	82	5	11
Sprinkler return flow.	1.3	18	77	5	21
	.7	16	78	6	16
Gravity return flow.	1.3	17	78	6	18
	.7	17	78	6	19
Evapotranspiration salvage (non-irrigated areas).	1.3	16	78	5	18
	.7	17	77	6	18
Evapotranspiration salvage (irrigated areas).	1.3	14	80	5	15
	.7	20	74	6	22
	.4	24	69	7	26
	.0	51	40	9	42

The extent to which each variation alters the simulated response provides insight into the functioning of the system. The 20 simulations shown in table 27 (a small sample of the unlimited number of variations that could be postulated) demonstrate that evapotranspiration salvage from irrigated areas is an important characteristic of the system. The source of water was fairly insensitive to the range of alternatives shown in table 27. In all instances representing salvage from irrigated areas, evapotranspiration salvage was 69 to 82 percent of withdrawals, aquifer storage was 13 to 24 percent of withdrawals, and streamflow capture was 5 to 10 percent of withdrawals. Therefore, regardless of the values of model characteristics, evapotranspiration salvage was the main source for withdrawals.

When evapotranspiration salvage is eliminated from irrigated areas (multiplied by a factor of 0.0), the simulated hydraulic-head decline on the Rio Grande fan (at row 27, column 8, layer 7) is more than twice that for the standard simulation (table 27). The extensive nature of these declines is indicated by the increase in the percent of withdrawals derived from storage. Without evapotranspiration salvage from irrigated areas, achieving a reasonable agreement between simulated and measured declines probably would require unreasonable decreases in estimated stress. Therefore, evapotranspiration from ground water does occur in irrigated areas, and it has decreased as hydraulic head declined.

#### Priorities for Data Collection

A program of data collection and model calibration would improve the understanding of the hydrologic system and produce a model capable of more reliable predictions. However, all models will be limited by the accuracy, reliability, and areal distribution of available data; data collection may be expensive and time consuming. Therefore, an important step in data collection and model development is to formulate the specific problem to be addressed. For example, if the problem is to determine the effect of withdrawals on streamflow, then data collection needs to be concentrated near the streams.

Because calibration is more likely to be unique if fewer variables are unknown, only those variables for which accurate independent estimates are not available should be estimated by calibration. Vertical hydraulic conductivity and river leakance are not reliably measured on site. A properly designed aquifer test can be analyzed to estimate vertical hydraulic conductivity. However, the discontinuity of less permeable beds may improve vertical hydraulic communication by providing a tortuous path around rather than through these beds. If so, then on the large scale of a basin model, the effective vertical hydraulic conductivity would be greater than that determined from the aquifer test. Seepage runs on streams may provide estimates of ground-water flow to or from a river. However, the model characteristic of leakance is not amenable to onsite measurement. These two parameters would be determined best by model calibration.

Details of a data-collection program for the Alamosa Basin would require additional testing with the model; however, the comparisons of table 27 are adequate to describe the general priorities for such a program. For those

characteristics to which the model is more sensitive, more accurate estimates are required. For those characteristics to which the model is less sensitive, less accurate estimates are acceptable. The model response (table 27) was less sensitive to aquifer characteristics (hydraulic conductivity and storage) than to boundary conditions (withdrawals and return flow). However, to define hydrology at sites of particular interest, additional measurements of both would be needed. Horizontal hydraulic conductivity, specific yield, and specific storage can be estimated independently of the model. Present estimates are more reliable for unconfined than for confined beds of the aquifer system. However, carefully designed and executed aquifer tests could obtain reliable estimates for the confined aquifer system.

Some characteristics of a data-collection program for the Alamosa Basin are the consequence of requirements and limitations of the calibration process. Calibration requires a known response to a known stress. In the Alamosa Basin, the response includes changes in hydraulic head, evapotranspiration from ground water, and ground-water flow to and from streams; the stress includes ground-water withdrawals and irrigation return flow. Therefore, data collection needs to include at least the following:

1. Hydraulic head needs to be monitored in confined and unconfined beds of the aquifer system. Observation wells need to be constructed to represent hydraulic head at a selected depth. In areas of particular interest (near streams, for example), hydraulic heads might be monitored at more than one depth to define more accurately vertical gradients near the stream and ground-water flow to and from the stream.

2. Evapotranspiration salvage needs to be estimated independently from the model. This would require estimating evapotranspiration of ground water as a function of land use and the change in this evapotranspiration resulting from changes in depth to water. Areal distribution of land use needs to be monitored to enable the areal apportionment of evapotranspiration salvage. The dominance of evapotranspiration salvage as a source for withdrawals has several implications. Perhaps the most obvious implication is that reliability of the model depends on the accuracy with which salvage is simulated. Therefore, salvage needs to be estimated independently of the model; such estimates need to identify salvage rather than evapotranspiration only; in addition, such estimates need to identify salvage from irrigated areas as well as from nonirrigated areas. Without independent measurements of salvage, the ability of the model to accurately predict the response to a specific stress will be uncertain.

3. Changes in ground-water flow to and from streams and springs need to be estimated independently of the model. Commonly, ground-water flow is calculated as a residual from a water balance of surface-water flows. Because ground-water flow commonly is small relative to surface-water flows, the measurements need to be accurate. To identify the source of the flow may require measurements of hydraulic head and water quality from suspected sources.

4. Ground-water withdrawals need to be estimated independently from the model. Not only the total withdrawals, but their distribution in both space and time need to be measured independently from the model. Because the model



is sensitive to withdrawals, the accuracy with which other characteristics can be estimated through calibration will be limited by the accuracy of these measurements.

5. Return flow associated with various irrigation methods needs to be estimated independently from the model. The estimate does not need to be as accurate as the estimate of withdrawals. However, the model appears to be more sensitive to the change in return flow resulting from the change of irrigation method from gravity to sprinkler than it is to vertical hydraulic conductivity. Areal distribution of land use and irrigation method needs to be monitored to enable the areal apportionment of irrigation return flow.

#### Projected Response to Withdrawals in Nonirrigated Areas

Because salvage is such a dominant source, the model of ground-water flow in the Alamosa Basin is not linear. Superposition, if used at all, needs to be used with caution. The effect of one water user on the system cannot be accurately simulated independently of other stresses. However, if the stresses are in widely separated areas, the error introduced by superposition should be negligible.

The reliability with which the model of the Alamosa Basin can project the response to withdrawals in nonirrigated areas is limited by the lack of calibration data in these areas. Any reliability gained for the three-dimensional model by comparing simulated and measured hydraulic-head changes is restricted to the area of effect of the stress and response used for the comparison. The model of the Alamosa Basin is most reliable in projecting the response to withdrawals from the Rio Grande fan and least reliable in projecting the response to withdrawals from nonirrigated areas. Although the model has demonstrated that evapotranspiration salvage from irrigated areas is a significant source, this has not been demonstrated for salvage from nonirrigated areas.

To demonstrate the nature of the response and the consequences of specific assumptions, withdrawals were defined (table 28) that approximate those for the Closed Basin Project (U.S. Bureau of Reclamation, 1963). The Closed Basin Project entails a well field on the east side of the Alamosa Basin (located approximately from T.42N.R.9E to T.37N.R.11E) to pump water from the unconfined aquifer into a channel extending to the Rio Grande. Most of the water withdrawn is expected to come from salvaged ground water that would otherwise have been lost to evapotranspiration from nonirrigated areas (Emery, 1970). The Reclamation Project Authorization Act of 1972 (Public Law 92-514) authorized operation of the project ". . . in a manner that will not cause the water table available for any irrigation or domestic wells in existence prior to the construction of the project to drop more than two feet and in a manner that will not cause reduction of artesian flows in existence prior to the construction of the project." Although more recent estimates of withdrawals are available (Lindell Elfrink, U.S. Bureau of Reclamation, written commun., 1984), the initial estimates were used for this demonstration. The principle of superposition was assumed to be approximately valid, and the withdrawals shown in table 28 were simulated without withdrawals in irrigated areas.

Table 28.--*Withdrawals represented in the model to demonstrate response in nonirrigated areas*  
[All values are in cubic feet per second]

Location			Withdrawal
Row	Column	Layer	
18	23	7	2.6
19	13	7	2.6
19	14	7	2.6
20	13	7	2.6
20	14	7	2.6
19	15	7	5.4
20	15	7	5.4
20	16	7	5.4
21	15	7	5.4
21	16	7	5.4
22	16	7	5.4
22	17	7	5.4
23	16	7	5.4
23	17	7	5.4
24	16	7	5.4
24	17	7	6.5
25	16	7	6.5
25	17	7	6.5
25	18	7	6.5
26	17	7	6.5
26	18	7	6.5
27	18	7	6.5
27	20	7	3.3
28	20	7	3.3
28	21	7	3.3
29	21	7	3.3
29	22	7	3.3
31	21	7	3.3
32	20	7	3.3

The model was approaching a new equilibrium by the end of 10 years. Evapotranspiration salvage was the source for more than 98 percent of the withdrawals. Simulated declines in the water table (fig. 38) were generally less than 2 feet and exceeded 10 feet in only one cell. Simulated hydraulic-head declines in confined beds of the aquifer system were in excess of 2 feet throughout much the same area as in the unconfined beds. In the section (A-A') across the model (fig. 38), contours of the 2-foot hydraulic-head decline are nearly vertical; beyond this contour, simulated changes in vertical gradient were small. The maximum decline of 11.9 feet was simulated at row 25, column 16, layer 7. Less decline was simulated in lower layers at this row-and-column location: 9.2 feet in layer six; 7.0 feet in layer five; 5.0 feet in layer four; and 3.3 feet in layer three.

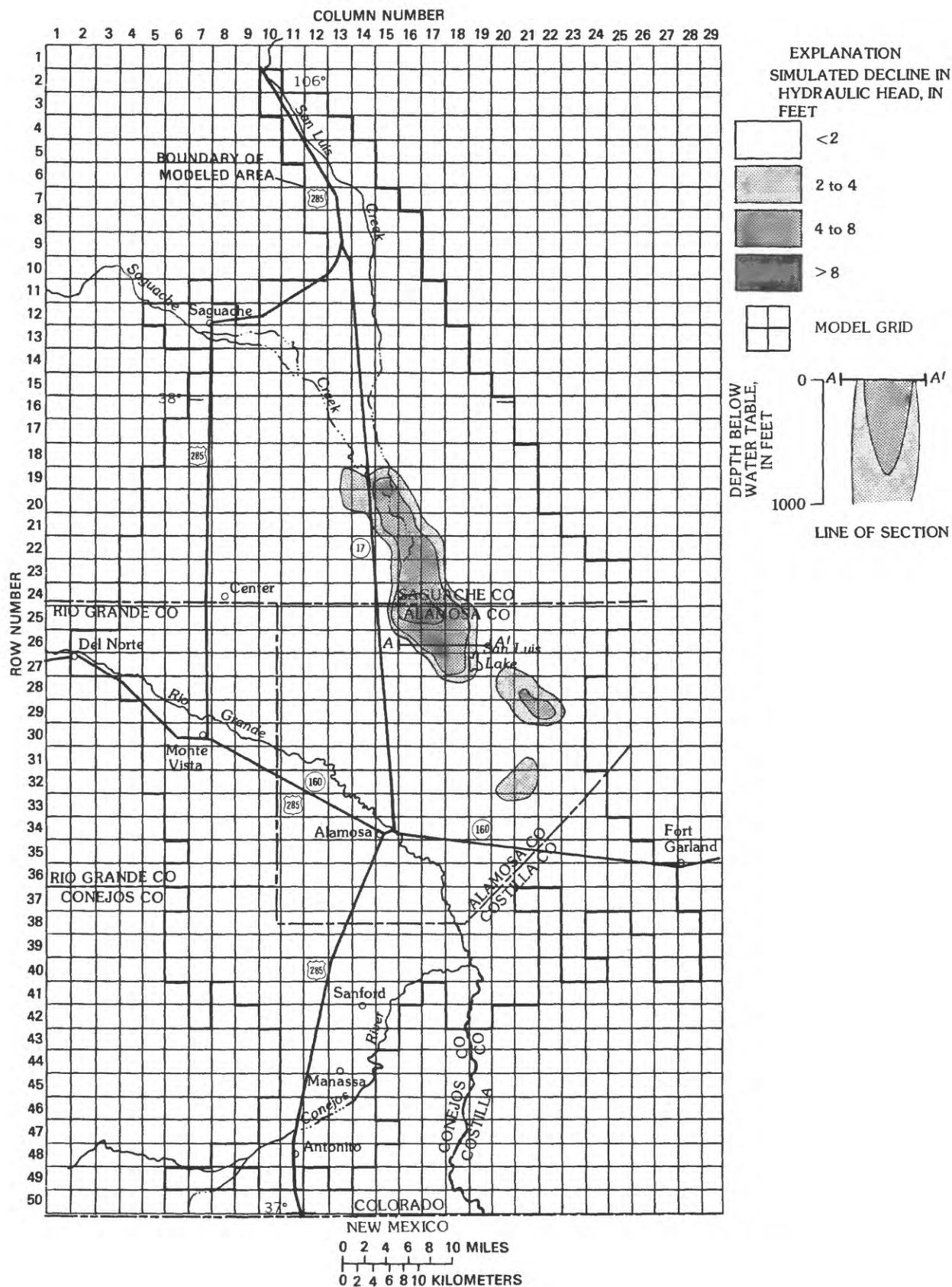


Figure 38.--Simulated decline in hydraulic head after 10 years of withdrawals shown in table 28.

The effect of varying system characteristics was similar to that for the simulation of 1970-79 changes. However, withdrawals were known, pumpage was specified, and no return flow was assumed. Because of the distance of the withdrawals from irrigated areas and streams, the response was assumed to be insensitive to evapotranspiration salvage in irrigated areas and river leakage. Horizontal hydraulic conductivity, specific yield, and specific storage were assumed to be estimated accurately, independent of the model. Therefore, the only system characteristics varied were evapotranspiration salvage from nonirrigated areas and vertical hydraulic conductivity. Evapotranspiration salvage was multiplied by factors of 1.0, 0.7, and 0.5. Vertical hydraulic conductivity was multiplied by 1.0 and 0.1. Within this range, some simulated results were sufficiently persistent that the predictions were reliable. For all alternatives, evapotranspiration salvage was the source for most of the withdrawals (at least 86 percent by the 10th year), and hydraulic-head declines were simulated in confined beds (declines of 2 feet, at least as deep as layer four, which is more than 400 feet below the water table). The major differences in simulated response were in simulated hydraulic-head declines (table 29). If the difference between 11 and 27 feet of water-level declines at this location is considered to be critical, then estimates of vertical hydraulic conductivity and evapotranspiration salvage need to be more accurate than the ranges shown in table 29.

Table 29.--Declines in hydraulic head simulated after 10 years of withdrawals in nonirrigated areas

Vertical hydraulic conductivity multiplied by a factor of:	Water-level decline is at row 25, column 16, layer 7 (feet)		
	Evapotranspiration salvage multiplied by a factor of:		
	1.0	0.7	0.5
1.0	11	15	20
0.1	15	22	27

## SUMMARY

The major hydrologic regimes in the 10,400 square miles of Rio Grande Basin above Embudo, N. Mex., (pl. 1) were analyzed. The purposes of the analyses were to provide estimates of water flow rates between components of the flow system and to improve the ability to estimate the hydrologic changes in the ground-water flow system in response to management alternatives in the Alamosa Basin. Boundaries of the study area were the drainage divides in the Sangre de Cristo Mountains on the east and the San Juan Mountains on the west. The intermontane area is divided by the San Luis Hills into the Alamosa Basin to the north and the Costilla Plains and the Taos Plateau to the south (fig. 2). The Alamosa Basin is dissected by a low topographic divide, forming a closed basin north of the Rio Grande drainage basin.



The San Juan Mountains and the Sangre de Cristo Mountains are the source of most water for the Alamosa Basin, the Costilla Plains, and the Rio Grande downstream from the study area. In the mountains, precipitation exceeds evapotranspiration, and excess water flows to the intermontane area. Water yield (surface flow and ground-water flow) from the San Juan Mountains was estimated to be about 2,800 cubic feet per second. Water yield from the Sangre de Cristo Mountains was estimated to be about 780 cubic feet per second.

The intermontane area contains several thousand feet of interbedded sedimentary and volcanic rocks that form complex aquifer systems. The San Luis Hills are a barrier to ground-water flow between the Alamosa Basin and the Taos Plateau or the Costilla Plains. On the Taos Plateau, precipitation was estimated to exceed evapotranspiration. About 28 cubic feet per second was estimated to flow through the fractured volcanic rocks to discharge as spring flow or seepage flow to the Rio Grande. On the Costilla Plains, evapotranspiration was estimated to exceed precipitation by about 150 cubic feet per second (table 13). Irrigation development is extensive only in the Alamosa Basin. Surface-water irrigation has been extensive since about 1890. Significant ground-water irrigation began about 1950. On the Alamosa Basin, evapotranspiration was estimated to be 3,900 cubic feet per second (table 17) --about 1,900 cubic feet per second (rounded) from irrigated areas (table 15), and about 2,000 cubic feet per second (rounded) from nonirrigated areas (table 14). Evapotranspiration exceeded estimated precipitation by 2,400 cubic feet per second (table 17). These flows are summarized in table 30.

Table 30.--*Estimated contribution to flow in the Rio Grande at Embudo, N. Mex., for each hydrologic regime, showing methods of estimation*  
[All estimates are in cubic feet per second]

Hydrologic regime	Method of estimation	Precipitation minus evapotranspiration for 1950-80
San Juan Mountains	Mountain water balance	2,800
Sangre de Cristo Mountains	Regression model of mountain water yield	780
Taos Plateau	Regression model of plateau water yield	28
Costilla Plains	Evapotranspiration calculation for the Costilla Plains	-150
Alamosa Basin	Evapotranspiration calculation for the Alamosa Basin	-2,400

The sum of the estimated flows in table 30 and the decrease in storage in the Alamosa Basin (87 cubic feet per second, table 17) indicate that the calculated discharge from the study area (1,145 cubic feet per second) was 69 percent greater than the average 1950-80 streamflow (680 cubic feet per second) in the Rio Grande at Embudo, N. Mex. This difference probably results from inaccuracies in estimating individual flow rates. Although each of the models described in this report could be improved, they are adequate to demonstrate that: (1) Flow from the San Juan Mountains is the largest source of water to the Rio Grande; (2) evapotranspiration from the Alamosa Basin is the largest consumer of water in the study area; and (3) large flows past the San Luis Hills are not needed to account for measured gains in flow of the Rio Grande between Lobatos, Colo., (350 cubic feet per second) and Embudo, N. Mex., (680 cubic feet per second). Calculating flow past the San Luis Hills as a residual in a water budget is inappropriate because of the error in estimating the large flows.

A three-dimensional model was constructed to represent the aquifer system in the Alamosa Basin. A preliminary analysis using a two-dimensional section model concluded that: (1) A seven-layer model, representing 3,200 feet of saturated thickness, could accurately (table 18) simulate the behavior of the flow system, and (2) the 1950 condition was approximately stable and would be a satisfactory initial condition. Values of aquifer characteristics were assumed or estimated from the work of previous investigators. Recharge and discharge were defined to represent the changes since 1950--ground-water withdrawals, change in return flow, evapotranspiration salvage, and streamflow capture. Reasonable modifications to ground-water withdrawals resulted in simulated changes approximating the measured data--small declines in water level for 1950-69 and water-level declines for 1970-79 within about 5 feet of measured water-level decline. In 1980, the sources of water withdrawn from the aquifer were 80 percent from evapotranspiration salvage, 14 percent from storage in the aquifer, and 6 percent from streamflow capture.

Analysis included sensitivity tests on the three-dimensional model that indicated that simulated 1970-79 hydraulic-head declines were most sensitive to ground-water withdrawals. However, for most of the simulations (table 27), evapotranspiration salvage was the major source (69 to 82 percent) of ground-water withdrawals. The simulations implied that evapotranspiration of ground water does occur in irrigated areas and that it has decreased as hydraulic head declined.

Calibration of the three-dimensional model of ground-water flow did not result in a unique combination of aquifer characteristics and boundary conditions. Calibration to improve estimates of system characteristics would require data that have not been collected. Specific problems need to be formulated before data-collection programs are designed. Because calibration requires a known response to a known stress, independent estimates of hydraulic head, evapotranspiration salvage, changes in ground-water flow to and from streams and springs, ground-water withdrawals, and return flow from irrigation need to be more accurate than estimates of aquifer characteristics. With these, vertical hydraulic conductivity and river leakance could be estimated by model calibration. Because data collection is expensive, a site-specific model designed to address a specific problem may be appropriate.

The three-dimensional model of ground-water flow was used to project the water-level declines in response to withdrawals from the Closed Basin Project (U.S. Bureau of Reclamation, 1963) in the Alamosa Basin. Although evapotranspiration salvage is nonlinear, superposition was assumed. The reliability of projected water-level declines is limited by the lack of calibration data in nonirrigated areas. However, for a range of alternatives, evapotranspiration salvage was the source of most water withdrawals.

## SELECTED REFERENCES

- Allison, Web, and Sheppard, John, 1980, Irrigation power study: Monte Vista, Colo., San Luis Valley Rural Electric Cooperative, Inc., 128 p.
- Baltz, E.H., 1978, Résumé of Rio Grande depression in north-central New Mexico, in Hawley, J.W., ed., Guidebook to Rio Grande Rift in New Mexico and Colorado: Socorro, N. Mex., New Mexico Bureau of Mines and Mineral Resources Circular 163, p. 210-228.
- Bingler, E.C., 1968, Geology and mineral resources of Rio Arriba County, New Mexico: Socorro, N. Mex., New Mexico Bureau of Mines and Mineral Resources Bulletin 91, 158 p.
- Blaney, H.F., and Hanson, E.G., 1965, Consumptive use and water requirements in New Mexico: Santa Fe, N. Mex., New Mexico State Engineer Technical Report 32, 82 p.
- Borland, J.P., 1970, A proposed streamflow data program for New Mexico: U.S. Geological Survey Open-File Report 70-35, 71 p.
- Brown, H.E., and Thompson, J.R., 1965, Summer water use by aspen, spruce, and grassland in western Colorado: Journal of Forestry, v. 63, p. 756-760.
- Bryan, Kirk, 1928, Preliminary report on the geology of the Rio Grande Canyon as affecting the increase in flow of the Rio Grande south of the New Mexico-Colorado boundary: Santa Fe, N. Mex., New Mexico State Engineer Ninth Biennial Report, 1928-30, p. 107-120.
- Burroughs, R.L., 1971, Geology of the San Luis Hills, south-central Colorado, in James, H.L., ed., Guidebook of the San Luis basin, Colorado: Socorro, N. Mex., New Mexico Geological Society, 22nd Field Conference, 1971, p. 277-287.
- \_\_\_\_\_, 1978, Northern rift, Guide 2, Alamosa, Colorado-Santa Fe, New Mexico--Alamosa to Antonito, Colorado, in Hawley, J.W., ed., Guidebook to Rio Grande Rift in New Mexico and Colorado: Socorro, N. Mex., New Mexico Bureau of Mines and Mineral Resources Circular 163, p. 33-36.
- \_\_\_\_\_, 1981, A summary of the geology of the San Luis basin, Colorado-New Mexico with emphasis on the geothermal potential for the Monte Vista Graben: Denver, Colo., Colorado Geological Survey Special Publication 17, 30 p.
- Burroughs, R.L., and McFadden, D.H., 1976, Some hydrogeologic problems in the San Luis basin, Colorado-New Mexico, in Epis, R.C., and Weimer, R.J., eds., Studies in Colorado field geology: Golden, Colo., Colorado School of Mines Professional Contribution No. 8, p. 544-550.
- Carpenter, L.G., 1891, Artesian wells of Colorado and their relation to irrigation: Fort Collins, Colo., Colorado Agricultural College Experimental Station Bulletin 16, p. 17-27.
- Chapin, C.E., 1971, The Rio Grande Rift, Part I--Modifications and additions, in James, H.L. ed., Guidebook of the San Luis basin, Colorado: Socorro, N. Mex., New Mexico Geological Society, 22nd Field Conference, 1971, p. 191-201.
- \_\_\_\_\_, 1979, Evolution of the Rio Grande Rift--A summary, in Riecker, R.E., ed., Rio Grande Rift--Tectonics and magmatism: Washington, D.C., American Geophysical Union, p. 1-5.
- Colorado Department of Agriculture, 1979, Colorado agricultural statistics, 1978 preliminary [1971-77 revised]--Bulletin 1-79: Denver, Colo., 182 p.
- \_\_\_\_\_, 1980, Colorado agricultural statistics, 1979 preliminary [1978 revised], Bulletin 1-80: Denver, Colo., 100 p.
- \_\_\_\_\_, 1981, Colorado agricultural statistics, 1980 preliminary, [1975-79 revised], Bulletin 1-81: Denver, Colo., 162 p.

- Colorado Water Court, Division 3, 1979, Case W3466, In the matter of rules and regulations governing the uses, control, and protection of water rights for both surface and underground water located in the Rio Grande and Conejos River basins and their tributaries: Alamosa, Colo.
- Croft, A.R., 1944, Evaporation from snow: American Meteorological Society Bulletin, v. 25, p. 334-337.
- Croft, A.R., and Monninger, L.V., 1953, Evapotranspiration and other water losses on some aspen forest types in relation to water available for stream flow: American Geophysical Union Transactions, v. 34, no. 4, p. 563-574.
- Crouch, T.M., 1985, Potentiometric surface, 1980, and water-level changes, 1969-80, in the unconfined valley-fill aquifers of the San Luis basin, Colorado and New Mexico: U.S. Geological Survey Hydrologic Investigations Atlas HA-683, scale 1:250,000, 2 sheets.
- Davis Engineering Service, Inc., 1977, Estimated consumptive use of water and irrigation demand for commonly grown crops in the San Luis Valley, Colorado, prepared for Rio Grande Water Conservation District: Del Norte, Colo., 13 p.
- \_\_\_\_\_, 1981, Map of the San Luis Valley, Colorado, showing sprinkler locations, approximate limit of alluvial fill and approximate location of the hydraulic divide, prepared for Rio Grande Water Conservation District: Del Norte, Colo., scale 1:125,000.
- Davis, G.H., 1979, A gravity study of the San Luis basin, Colorado: El Paso, Tex., University of Texas, Masters Thesis, 101 p.
- Davis, G.H., and Keller, G.R., 1978, Subsurface structure of San Luis Valley, in Hawley, J.W., ed., Guidebook to Rio Grande Rift in New Mexico and Colorado: Socorro, N. Mex., New Mexico Bureau of Mines and Mineral Resources Circular 163, p. 28.
- Emery, P.A., 1970, Electric analog model evaluation of a water-salvage plan, San Luis Valley, south-central Colorado: Denver, Colo., Colorado Water Conservation Board Ground-Water Circular 14, 11 p.
- \_\_\_\_\_, 1971, Water resources of the San Luis Valley, Colorado, in James, H.L., ed., Guidebook of the San Luis basin, Colorado: Socorro, N. Mex., New Mexico Geological Society, 22nd Field Conference, 1971, p. 129-132.
- \_\_\_\_\_, 1979, Geohydrology of the San Luis Valley, Colorado, USA, in The hydrology of areas of low precipitation, Symposium, Canberra, Australia, 1979, Proceedings: Paris, IAHS-AISH Publication No. 128, p. 297-305.
- Emery, P.A., Boettcher, A.J., Snipes, R.J., and McIntyre, H.J., Jr., 1971, Hydrology of the San Luis Valley, south-central Colorado: U.S. Geological Survey Hydrologic Investigations Atlas HA-381, scale 1:250,000, 2 sheets.
- Emery, P.A., Dumeyer, J.M., and McIntyre, H.J., Jr., 1969, Irrigation and municipal wells in the San Luis Valley, Colorado: U.S. Geological Survey open-file report, 7 p.
- Emery, P.A., Patten, E.P., Jr., and Moore, J.E., 1975, Analog model study of the hydrology of the San Luis Valley, south-central Colorado: Denver, Colo., Colorado Water Conservation Board Ground-Water Circular 29, 21 p.
- Emery, P.A., Snipes, R.J., and Dumeyer, J.M., 1972, Hydrologic data for the San Luis Valley, Colorado: Denver, Colo., Colorado Water Conservation Board Basic-Data Release 22, 146 p.
- Emery, P.A., Snipes, R.J., Dumeyer, J.M., and Klein, J.M., 1973, Water in the San Luis Valley, south-central Colorado: Denver, Colo., Colorado Water Conservation Board Water-Resources Circular 18, 26 p.

- Frazier, A.H., and Heckler, Wilbur, 1972, Embudo, New Mexico, birthplace of systematic stream gaging: U.S. Geological Survey Professional Paper 778, 23 p.
- Freeze, R.A., 1972, Regionalization of hydrogeologic parameters for use in mathematical models of ground-water flow, in 24th International Geological Congress, Montreal, Canada, section 11, Hydrogeology: Utrecht, The Netherlands, VNU Science Press, p. 177-190.
- Gaca, J.R., and Karig, D.E., 1966, Gravity survey in the San Luis Valley area, Colorado: U.S. Geological Survey open-file report, 21 p.
- Halverson, H.G., 1972, Seasonal snow-surface-energy balance in a forest opening: Pacific Southwest Forest and Range Experiment Station Report, 49 p.
- Hawley, J.W., ed., 1978, Guidebook to Rio Grande Rift in New Mexico and Colorado: Socorro, N. Mex., New Mexico Bureau of Mines and Mineral Resources Circular 163, 241 p.
- Hearne, G.A., 1982, Supplement to the New Mexico three-dimensional model: U.S. Geological Survey Open-File Report 82-857, 90 p.
- \_\_\_\_\_, 1985a, Mathematical model of the Tesuque aquifer system, north-central New Mexico: U.S. Geological Survey Water-Supply Paper 2205, 75 p.
- \_\_\_\_\_, 1985b, Simulation of an aquifer test on the Tesuque Pueblo Grant, New Mexico: U.S. Geological Survey Water-Supply Paper 2206, 24 p.
- Huntley, David, 1976, Ground-water recharge to the aquifers of northern San Luis Valley, Colorado: Golden, Colo., Colorado School of Mines, Remote Sensing Report 76-3, 247 p.
- \_\_\_\_\_, 1979a, Ground-water recharge to the aquifers of northern San Luis Valley, Colorado--Summary: Geological Society of America Bulletin, v. 90, no. 8, Part I, p. 707-709.
- \_\_\_\_\_, 1979b, Ground-water recharge to the aquifers of northern San Luis Valley, Colorado: Geological Society of America Bulletin, v. 90, no. 8, Part II, p. 1196-1281.
- Jensen, M.E., and Haise, H.R., 1963, Estimating evapotranspiration from solar radiation: American Society of Civil Engineers, Journal of the Irrigation and Drainage Division, v. 89, no. 4, December 1963, p. 15-41.
- Johnson, A.I., 1967, Hydrologic properties of earth materials, specific yield--Compilation of specific yields for various materials: U.S. Geological Survey Water-Supply Paper 1662-D, 74 p.
- Johnson, R.B., 1969, Geologic map of the Trinidad quadrangle, south-central Colorado: U.S. Geological Survey Miscellaneous Geological Investigations Map I-558.
- \_\_\_\_\_, 1971, The Great Sand Dunes of southern Colorado, in James, H.L. ed., Guidebook of the San Luis basin, Colorado: Socorro, N. Mex., New Mexico Geological Society, 22nd Field Conference, 1971, p.123-128.
- Kelley, V.C., 1978, Geology of Española Basin, New Mexico: Socorro, N. Mex., New Mexico Bureau of Mines and Mineral Resources Geologic Map 48, scale 1:225,000.
- \_\_\_\_\_, 1979, Tectonics, Middle Rio Grande Rift, New Mexico, in Riecker, R.E., ed., Rio Grande Rift--Tectonics and magmatism: Washington, D.C., American Geophysical Union, p. 57-70.
- Kohler, M.A., Nordenson, T.J., and Baker, D.R., 1959, Evaporation maps for the United States: Washington, D.C., U.S. Weather Bureau, Technical Paper 37, 13 p.

- Kruse, E.G., and Haise, H.R., 1974, Water use by native grasses in high altitude Colorado meadows: Berkeley, Calif., Agricultural Research Service, Western Region, U.S. Department of Agriculture, ARS-W-6, 60 p.
- Lansford, R.R., and Sorensen, E.F., 1971, Planted cropland acreage in New Mexico in 1969 and 1970, New Mexico agriculture--1970: Las Cruces, N. Mex., New Mexico State University Agricultural Experiment Station Research Report 195, p. 6-12.
- \_\_\_\_\_, 1972, Trends in irrigated agriculture, 1970 and 1971, New Mexico agriculture--1971: Las Cruces, N. Mex., New Mexico State University Agricultural Experiment Station Research Report 235, p. 42-43.
- \_\_\_\_\_, 1973, Trends in irrigated agriculture 1940-1972, New Mexico agriculture--1972: Las Cruces, N. Mex., New Mexico State University Agricultural Experiment Station Research Report 260, p. 16-17.
- Lansford, R.R., Sorensen, E.F., Creel, B.J., and Wile, W.W., 1975, Irrigated cropland acreage and source of water used for irrigation in New Mexico, by county: Las Cruces, N. Mex., New Mexico State University Agricultural Experiment Station Research Report 305, 39 p.
- Lansford, R.R., Sorensen, E.F., Creel, B.J., Latham, R.D., and Wile, W.W., 1976, Sources of irrigation water and irrigated and dry cropland acreages in New Mexico, by county: Las Cruces, N. Mex., New Mexico State University Agricultural Experiment Station Research Report 324, p. 1-5 and 34.
- Lansford, R.R., Sorensen, E.F., Creel, B.J., Wile, W.W., and Stacks, H.M., 1977, Sources of irrigation water and irrigated and dry cropland acreages in New Mexico, by county, 1971-1976: Las Cruces, N. Mex., New Mexico State University Agricultural Experiment Station Research Report 348, p. 1-5 and 34.
- Lansford, R.R., Sorensen, E.F., Creel, B.J., Wile, W.W., and Stacks, H.M., 1978a, Sources of irrigation water and irrigated and dry cropland acreages in New Mexico, by county, 1972-1977: Las Cruces, N. Mex., New Mexico State University Agricultural Experiment Station Research Report 377, p. 1-5 and 34.
- Lansford, R.R., Sorensen, E.F., Creel, B.J., Wile, W.W., and Thompson, Aubrey, 1978b, Sources of irrigation water and irrigated and dry cropland acreages in New Mexico, by county, 1973-1978: Las Cruces, N. Mex., New Mexico State University Agricultural Experiment Station Research Report 405, p. 1-5 and 34.
- Lansford, R.R., Sorensen, E.F., Gollehon, N.R., Fishburn, M., Loslebon, L., Creel, B.J., West, F.G., 1980, Sources of irrigation water and irrigated and dry cropland acreages in New Mexico, by county, 1974-1979: Las Cruces, N. Mex., New Mexico State University Agricultural Experiment Station Research Report 422, p. 1-5 and 34.
- Lansford, R.R., Sorensen, E.F., Creel, B.J., Gollehon, N.R., Fishburn, M., Loslebon, L., Wilson, B.C., and Roark, R., 1981, Sources of irrigation water and irrigated and dry cropland acreages in New Mexico, by county, 1975-1980: Las Cruces, N. Mex., New Mexico State University Agricultural Experiment Station Research Report 454, p. 1-5 and 34.
- Larsen, E.S., Jr., and Cross, Whitman, 1956, Geology and petrology of the San Juan region, southwestern Colorado: U.S. Geological Survey Professional Paper 258, 303 p.

- Lipman, P.W., 1978, Northern Rift, Guide 2, Alamosa, Colorado-Santa Fe, New Mexico--Antonito, Colorado, to Rio Grande Gorge, New Mexico, in Hawley, J.W., ed., Guidebook to Rio Grande Rift in New Mexico and Colorado: Socorro, N. Mex., New Mexico Bureau of Mines and Mineral Resources Circular 163, p. 36-42.
- Lipman, P.W., and Mehnert, H.H., 1979, The Taos Plateau volcanic field, northern Rio Grande rift, New Mexico, in Riecker, R.E., ed., Rio Grande Rift--Tectonics and magmatism: Washington, D.C., American Geophysical Union, p. 289-311.
- Lipman, P.W., Steven, T.A., and Mehnert, H.H., 1970, Volcanic history of the San Juan Mountains, Colorado, as indicated by potassium-argon dating: Geological Society of America Bulletin, v. 18, p. 2329-2352.
- Lohman, S.W., and others, 1972, Definitions of selected ground-water terms--Revisions and conceptual refinements: U.S. Geological Survey Water-Supply Paper 1988, 21 p.
- Manley, Kim, and Scott, G.R., 1978, Preliminary geologic map of the Aztec 1° × 2° quadrangle, northwestern New Mexico and southern Colorado: U.S. Geological Survey Open-File Report 78-466.
- McKinlay, P.F., 1956, Geology of Costilla and Latin Peak quadrangles, Taos County, New Mexico: Socorro, N. Mex., New Mexico Bureau of Mines and Mineral Resources Bulletin 42.
- \_\_\_\_\_, 1957, Geology of Questa quadrangle, Taos County, New Mexico: Socorro, N. Mex., New Mexico Bureau of Mines and Mineral Resources Bulletin 53.
- Muehlberger, W.R., 1978, Northern Rift, Guide 2, Alamosa, Colorado-Santa Fe, New Mexico--Frontal fault zone of northern Picuris Range, in Hawley, J.W., ed., Guidebook to Rio Grande Rift in New Mexico and Colorado: Socorro, N. Mex., New Mexico Bureau of Mines and Mineral Resources Circular 163, p. 44-46.
- Muehlberger, W.R., and Hawley, J.W., 1978, Northern Rift, Guide 2, Alamosa, Colorado-Santa Fe, New Mexico--Rio Grande Gorge to Rio Embudo, New Mexico, in Hawley, J.W., ed., Guidebook to Rio Grande Rift in New Mexico and Colorado: Socorro, N. Mex., New Mexico Bureau of Mines and Mineral Resources Circular 163, p. 42-44.
- National Oceanic and Atmospheric Administration, 1980, Climates of the States: Detroit, Mich., Gale Research Company, v. 2.
- New Mexico State Engineer, 1980, Irrigation maps and tabulation for Rio Arriba and Taos Counties, New Mexico: Santa Fe, N. Mex., scale 1:250,000, 2 sheets.
- Posson, D.R., Hearne, G.A., Tracy, J.V., and Frenzel, P.F., 1980, A computer program for simulating geohydrologic systems in three dimensions: U.S. Geological Survey Open-File Report 80-421, 806 p.
- Powell, W.J., 1958, Ground-water resources of the San Luis Valley, Colorado: U.S. Geological Survey Water-Supply Paper 1379, 284 p.
- Radosevich, G.E., and Rutz, R.W., 1979, San Luis Valley water problems--A legal perspective: Fort Collins, Colo., Colorado Water Resources Research Institute Information Series No. 34, 44 p.
- Rio Grande Compact Commission, 1981, Report to the Governors of Colorado, New Mexico, and Texas: 55 p.
- Robinson, T.W., 1970, Evapotranspiration by woody phreatophytes in the Humboldt River Valley near Winnemucca, Nevada: U.S. Geological Survey Survey Professional Paper 491-D, 41 p.



- Robinson, T.W., Jr., and Waite, H.A., 1938, Ground water in the San Luis Valley, Colorado, in Part 6, The Rio Grande joint investigation in the upper Rio Grande basin: Washington, D.C., U.S. National Resources Commission, p. 226-227.
- Ryan, Mark, and Lutji, Joe, 1979, Pump test program report: Monte Vista, Colo., San Luis Valley Rural Electric Cooperative, Inc., 13 p.
- San Luis Valley Rural Electric Cooperative, Inc., 1980, Irrigation power study: Monte Vista, Colo., 128 p.
- Scott, G.R., Taylor, R.B., Epis, R.C., and Wobus, R.A., 1978, Geologic map of the Pueblo 1° × 2° quadrangle, south-central Colorado: U.S. Geological Survey Miscellaneous Investigations Series Map I-1022.
- Siebenthal, C.E., 1910, Geology and water resources of the San Luis Valley, Colorado: U.S. Geological Survey Water-Supply Paper 240, 128 p.
- Smith, R.P., 1979, Early rift magmatism at Spanish Peaks, Colorado, in Riecker, R.E., ed., Rio Grande Rift--Tectonics and magmatism: Washington, D.C., American Geophysical Union, p. 313-321.
- Sorensen, E.F., 1977, Water use by categories in New Mexico counties, river basins, and irrigated and dry cropland acreage in 1975: Santa Fe, N. Mex., New Mexico State Engineer Technical Report 41, 34 p.
- \_\_\_\_\_, 1982, Water use by categories in New Mexico counties, river basins, and irrigated acreage in 1980: Santa Fe, N. Mex., New Mexico State Engineer Technical Report 44, 51 p.
- Spiegel, Zane, 1962, Hydraulics of certain stream-connected aquifer systems: Santa Fe, N. Mex., New Mexico State Engineer special report, 105 p.
- Steven, T.A., Lipman, P.W., Hail, W.J., Jr., Barker, Fred, and Luedke, R.G., 1974, Geologic map of the Durango quadrangle, southwestern Colorado: U.S. Geological Survey Miscellaneous Investigations Series Map I-764, scale 1:250,000.
- Stone, W.J., Mizell, N.H., and Hawley, J.W., 1979, Availability of geological and geophysical data for the eastern half of the U.S. Geological Survey's southwestern alluvial basins regional aquifer study: Socorro, N. Mex., New Mexico Bureau of Mines and Mineral Resources Open-File Report 109, 80 p.
- Theis, C.V., 1938, The significance and nature of the cone of depression in ground-water bodies: Economic Geology, v. 33, no. 8, p. 889-902.
- \_\_\_\_\_, 1940, The source of water derived from wells: Civil Engineering, v. 10, no. 5, p. 277-280.
- Trescott, P.C., 1975, Documentation of finite-difference model for simulation of three-dimensional ground-water flow: U.S. Geological Survey Open-File Report 75-438, 103 p.
- Trescott, P.C., and Larson, S.P., 1976, Supplement to Open-File Report 75-438, Documentation of a finite-difference model for simulation of three-dimensional ground-water flow: U.S. Geological Survey Open-File Report 76-591, 21 p.
- Tweto, Ogden, 1978, Northern Rift, Guide 1, Denver-Alamosa, Colorado, in Hawley, J.W., ed., Guidebook to Rio Grande Rift in New Mexico and Colorado: Socorro, N. Mex., New Mexico Bureau of Mines and Mineral Resources Circular 163, p. 13-27.
- \_\_\_\_\_, 1979, The Rio Grande Rift system in Colorado, in Riecker, R.E., ed., Rio Grande Rift--Tectonics and magmatism, Washington, D.C., American Geophysical Union, p. 33-56.

- Tweto, Ogden, Steven, T.A., Hail, W.J., Jr., and Moench, R.H., 1976, Preliminary geologic map of the Montrose 1° × 2° quadrangle, southwestern Colorado: U.S. Geological Survey Miscellaneous Field Studies Map MF-761, scale 1:250,000.
- Uitti, P.B., 1980, Interpretation of seismic reflection data from the southern San Luis Valley, south-central Colorado: Golden, Colo., Colorado School of Mines, Masters Thesis, 49 p.
- Upson, J.E., 1939, Physiographic subdivisions of the San Luis Valley, southern Colorado: Journal of Geology, v. 47, no. 7, p. 721-736.
- U.S. Bureau of Agricultural Engineering, 1938, Water utilization, in The Rio Grande joint investigation in the Upper Rio Grande Basin, Part III: Washington, D.C., U.S. National Resources Committee, p. 293-427.
- U.S. Bureau of Reclamation, Region 5, 1963, Plan for development of closed basin division, San Luis Valley project, Colorado: Amarillo, Tex., Project Planning Report, 87 p.
- U.S. Geological Survey, 1960, Compilation of records of surface waters of the United States through September 1950--Part 8, Western Gulf of Mexico basins: U.S. Geological Survey Water-Supply Paper 1312, 633 p.
- \_\_\_\_\_, 1964, Compilation of records of surface waters of the United States, October 1950 to September 1960--Part 8, Western Gulf of Mexico basins: U.S. Geological Survey Water-Supply Paper 1732, 574 p.
- \_\_\_\_\_, 1965-70, Surface water supply of the United States 1966-70--Part 8, Western Gulf of Mexico basins--Volume 2, Basins from Lavaca River to Rio Grande: U.S. Geological Survey Water-Supply Paper 2123, 861 p.
- \_\_\_\_\_, 1969, Surface water supply of the United States 1961-65--Part 7, Lower Mississippi River basin--Volume 2, Arkansas River basin: U.S. Geological Survey Water-Supply Paper 1921, 878 p.
- \_\_\_\_\_, 1970, Surface-water supply of the United States 1961-65--Part 8, Western Gulf of Mexico basins: U.S. Geological Survey Water-Supply Paper 1923, 786 p.
- \_\_\_\_\_, 1971-1975a, Water resources data for Colorado, water years 1970-1974--Part 1, Surface Water Records: Water-Data Reports CO-71-1 to CO-74-1 (published annually); available from U.S. Department of Commerce, National Technical Information Service, Springfield, Va.
- \_\_\_\_\_, 1971-1975b, Water resources data for New Mexico, water years 1970-1974--Part 1, Surface Water Records: Water-Data Reports NM-71-1 to NM-74-1 (published annually); available from U.S. Department of Commerce, National Technical Information Service, Springfield, Va.
- \_\_\_\_\_, 1976-1982a, Water resources data for New Mexico, water years 1975-1981: Water-Data Reports NM-75-1 to NM-81 (published annually); available from U.S. Department of Commerce, National Technical Information Service, Springfield, Va.
- \_\_\_\_\_, 1976-1982b, Water resources data for Colorado, water years 1975-1981--Volume 1, Missouri River basin, Arkansas River basin, and Rio Grande basin: Water-Data Reports CO-76-1 to CO-81-1 (published annually); available from U.S. Department of Commerce, National Technical Information Service, Springfield, Va.
- U.S. Soil Conservation Service, 1969, Irrigation water management study of the San Luis Valley, Colorado, prepared for Four Corners Regional Commission: Washington, D.C., 65 p.
- \_\_\_\_\_, 1978, Water and related land resources, Rio Grande basin, Colorado: Washington, D.C., various pagination.

- U.S. Soil Conservation Service and Colorado State University Experiment Station, 1979a, Important farmlands of Alamosa County, Colorado: Fort Collins, Colo., scale 1:100,000.
- \_\_\_\_\_, 1979b, Important farmlands of Conejos County, Colorado: Fort Collins, Colo., scale 1:100,000, 2 sheets.
- \_\_\_\_\_, 1979c, Important farmlands of Rio Grande County, Colorado: Fort Collins, Colo., scale 1:100,000.
- U.S. Soil Conservation Service and Colorado State University Experiment Station, 1980a, Important farmlands of Costilla County, Colorado: Fort Collins, Colo., scale 1:100,000, 2 sheets.
- \_\_\_\_\_, 1980b, Important farmlands of Saguache County, Colorado: Fort Collins, Colo., scale 1:100,000, 2 sheets.
- U.S. Weather Bureau, undated, a, Isohyetal map of normal October-April precipitation (1931-1960), Colorado: scale 1:500,000.
- \_\_\_\_\_, undated, b, Isohyetal map of normal October-April precipitation (1931-1960), New Mexico: scale 1:500,000.
- West, S.W., and Broadhurst, W.L., 1973, Summary appraisals of the nation's ground-water resources--Rio Grande region: U.S. Geological Survey, open-file report, 131 p.
- Wheeler, W.W., and Associates, Inc., 1981, Water-resources investigations ground water in the closed basin San Luis Valley, Colorado, report to Rio Grande Water Users Association and Rio Grande Canal Water Users Association: Denver, Colo., 22 p.
- White, W.N., 1932, A method of estimating ground-water supplies based on discharge by plants and evaporation from soil: U.S. Geological Survey Water-Supply Paper 659-A, 105 p.
- Wilkins, D.W., Scott, W.B., and Kaehler, C.A., 1980, Planning report for the southwest alluvial basins (east) regional aquifer-system analysis, parts of Colorado, New Mexico, and Texas: U.S. Geological Survey Open-File Report 80-564, 39 p.
- Wilm, H.G., and Dunnford, E.G., 1948, Effect of timber cutting on water available for stream flow from a lodgepole pine forest: U.S. Department of Agriculture Technical Bulletin 978, 34 p.
- Wilson, C.A., and White, R.R., 1984, Geohydrology of the central Mesilla Valley, Doña Ana County, New Mexico: U.S. Geological Survey Water-Resources Investigations Report 82-555, 144 p.
- Winograd, I.J., 1959, Ground-water conditions and geology of Sunshine Valley and western Taos County, New Mexico: Santa Fe, N. Mex., New Mexico State Engineer Technical Report No. 12, 70 p.
- Wymore, I.F., 1974, Estimated average water balance for Piceance and Yellow Creek watersheds: Fort Collins, Colo., Colorado State University Environmental Resources Technical Report Series, no. 2, 60 p.
- Zahner, Robert, 1967, Refinement in empirical functions for realistic soil-moisture regimes under forest cover, in Sopper, W.E., and Lull, H.W., eds., International symposium of forest hydrology: New York, Pergamon Press, p. 261-274.
- Zorich-Erker Engineering, Inc., 1980a, Ground water availability on the San Marco property near Mesita in Costilla County, Colorado, prepared for San Marco Pipeline Company: Denver, Colo., 111 p.
- \_\_\_\_\_, 1980b, Leakage from confined aquifer to unconfined aquifer--Closed basin, San Luis Valley, Colorado, prepared for Rio Grande Water Users Association: Denver, Colo., 9 p.

## **SUPPLEMENTAL DATA**

Attachment 1.--Input file to define aquifer characteristics and  
hydraulic-head-dependent boundaries

```
GAHMG,STCRA.
*/JOB
*FILE NAME=INPUT
$CONTROL
    SELRES=.TRUE.,
    PHISET=.TRUE.,
$END
DUMMY
$INLIST
    EQN4=.TRUE.,    WTABLE=.TRUE.,    NVPN=13,
    CLSURE=0.1,
    ITMAX=1,
    WMAX=0.999,
    NRHOP=5,
    FACTX= 7.6,    5.1,    5.04,    3.36,    2.25,    1.50,    1.0,
    FACTY= 7.6,    5.1,    5.04,    3.36,    2.25,    1.50,    1.0,
    FACTZ= 2*3.35E-6,    5*1.5E-5,
    NROW=50,    NCOL=30,    NLAYER=7,
    DELX=30*10560,    DELY=50*10560,
    DELZ=1130,755,504,336,225,150,100,
    NPER=1,
    MODPR=20,
    DAMP=0.0,
$END
HEADER
- - - GROUND-WATER FLOW MODEL OF SAN LUIS VALLEY NORTH OF SAN LUIS HILLS - - -
    AUGUST 1983    * * *    DEFINE T,TK FOR ALL LAYERS
END
SYMBOLS
H            100.
TA            .00775
TB            .0155
TC            .0233
TD            .0310
TE            .0465
TF            .0775
TG            .155
TH            .233
TI            .310
TS            0.0463
TS6           0.0463
TC6           0.0116
T50           0.0347
TB6           0.0463
VS6           5.46E-09
VC6           5.46E-09
V50           5.46E-09
VB6           5.46E-11
VF6           5.46E-06
```

Attachment 1.--Input file to define aquifer characteristics and  
hydraulics-head-dependent boundaries--Continued

TC5 0.0116  
TB5 0.0463  
VS5 3.64E-09  
VC5 3.64E-09  
VB5 3.64E-11  
VF5 3.64E-06  
TC4 0.0116  
TB4 0.0463  
VS4 2.43E-09  
VC4 2.43E-09  
VB4 2.43E-11  
VF4 2.43E-06  
TC3 0.0116  
TB3 0.0463  
VS3 1.63E-09  
VC3 1.63E-09  
VB3 1.63E-11  
VF3 1.63E-06  
VS2 2.46E-10  
VS1 1.64E-10  
M20 1.0E-20  
ZIP 0  
ONE 1  
THR 3  
SVN 7  
END  
3D INPUT

H

ONE

2	10	7	TB	
3	10	12	7	TB
4	11	13	7	TB
5	11	7	TB	
5	12	7	TF	
5	13	14	7	TB
6	12	7	TB	
6	13	7	TF	
6	14	7	TB	
7	12	13	7	TB
7	14	7	TF	
7	15	7	TB	
8	12	13	7	TB
8	14	7	TF	
8	15	16	7	TB
9	13	7	TB	
9	14	7	TF	
9	15	7	TD	
9	16	7	TB	
10	13	7	TB	

Attachment 1.--Input file to define aquifer characteristics and  
hydraulic-head-dependent boundaries--Continued

10	14	7	TF
10	15	7	TD
10	16	7	TB
11	7	7	TB
11	10 12	7	TB
11	13	7	TG
11	14	7	TF
11	15	7	TD
11	16 17	7	TB
12	5 6	7	TF
12	7 8	7	TB
12	10 11	7	TB
12	12	7	TF
12	13	7	TG
12	14 15	7	TF
12	16	7	TD
12	17	7	TB
13	6	7	TB
13	7 9	7	TF
13	10 12	7	TH
13	13 14	7	TG
13	15 16	7	TD
13	17 18	7	TB
14	8	7	TF
14	9 10	7	TG
14	11	7	TH
14	12 14	7	TG
14	15 17	7	TD
14	18	7	TB
15	7	7	TB
15	8 13	7	TG
15	14	7	TF
15	15 18	7	TD
15	19	7	TB
16	7 11	7	TG
16	12 13	7	TF
16	14 19	7	TD
16	20	7	TB
17	6	7	TB
17	7 9	7	TF
17	10 11	7	TG
17	12	7	TF
17	13 19	7	TD
17	20	7	TB
18	6	7	TB
18	7 12	7	TF
18	13 19	7	TD
18	20 21	7	TB
19	5	7	TB

Attachment 1.--Input file to define aquifer characteristics and  
hydraulic-head-dependent boundaries--Continued

19	6	12	7	TF
19	13	19	7	TD
19	20	21	7	TB
20		5	7	TB
20	6	15	7	TF
20	16	20	7	TD
20		21	7	TB
21	5	6	7	TF
21	7	11	7	TG
21	12	16	7	TF
21	17	22	7	TD
22		4	7	TB
22		5	7	TF
22	6	7	7	TG
22		8	7	TI
22	9	11	7	TH
22		12	7	TG
22	13	17	7	TF
22	18	22	7	TD
23		4	7	TB
23		5	7	TD
23		6	7	TG
23		7	7	TH
23	8	9	7	TI
23	10	11	7	TH
23	12	13	7	TG
23	14	17	7	TF
23	18	25	7	TD
24		4	7	TB
24		5	7	TG
24		6	7	TH
24	7	10	7	TI
24		11	7	TH
24	12	13	7	TG
24	14	18	7	TF
24	19	25	7	TD
25		4	7	TG
25	5	11	7	TH
25	12	18	7	TF
25	19	24	7	TD
25		25	7	TB
26		2	7	TF
26	3	5	7	TG
26		6	7	TH
26		7	7	TG
26		8	7	TH
26	9	10	7	TI
26		11	7	TH
26	12	13	7	TG



Attachment 1:--Input file to define aquifer characteristics and  
hydraulic-head-dependent boundaries--Continued

26	14	16	7	TF
26	17	22	7	TD
26	23	24	7	TB
27	2	3	7	TF
27		4	7	TG
27	5	8	7	TH
27		9	7	TI
27	10	11	7	TH
27	12	13	7	TG
27	14	16	7	TF
27	17	19	7	TD
27	20	22	7	TE
27	23	24	7	TB
28		4	7	TB
28	5	6	7	TF
28		7	7	TH
28		8	7	TG
28		9	7	TI
28		10	7	TH
28	11	12	7	TG
28	13	17	7	TF
28		18	7	TD
28	19	20	7	TC
28		21	7	TD
28		22	7	TE
28		23	7	TB
29		5	7	TB
29	6	7	7	TF
29	8	10	7	TG
29		11	7	TF
29		12	7	TG
29	13	16	7	TF
29		17	7	TD
29		18	7	TC
29		19	7	TB
29	20	22	7	TC
29		23	7	TB
30	5	6	7	TB
30	7	9	7	TF
30		10	7	TG
30	11	16	7	TF
30		17	7	TC
30	18	22	7	TB
30		23	7	TC
30		24	7	TB
31		5	7	TB
31	6	7	7	TF
31	8	11	7	TG
31	12	15	7	TF

Attachment 1.--Input file to define aquifer characteristics and  
hydraulic-head-dependent boundaries--Continued

31	16	7	TD
31	17	7	TC
31	18	7	TB
31	19 20	7	TA
31	21	7	TB
31	22	7	TC
31	23	7	TB
32	5 6	7	TB
32	7	7	TF
32	8 11	7	TG
32	12 15	7	TF
32	16	7	TD
32	17	7	TC
32	18 20	7	TA
32	21 24	7	TB
33	6	7	TB
33	7	7	TF
33	8 10	7	TG
33	11 15	7	TF
33	16	7	TD
33	17	7	TC
33	18 19	7	TA
33	20 24	7	TB
34	6	7	TB
34	7	7	TF
34	8 9	7	TG
34	10 16	7	TF
34	17	7	TC
34	18	7	TA
34	19 25	7	TB
35	7	7	TF
35	8	7	TG
35	9 16	7	TF
35	17 18	7	TC
35	19 20	7	TB
35	21	7	TC
35	22	7	TD
35	23 26	7	TF
36	6 8	7	TB
36	9 16	7	TF
36	17	7	TD
36	18 20	7	TC
36	21	7	TD
36	22	7	TF
36	23 25	7	TG
36	26 27	7	TF
37	7 8	7	TB
37	9 17	7	TF
37	18 20	7	TD

Attachment 1.--Input file to define aquifer characteristics and  
hydraulic-head-dependent boundaries--Continued

37	22	7	TF		
37	23	26	7	TG	
37	27	7	TF		
38	6	8	7	TB	
38	9	18	7	TF	
38	19	21	7	TD	
38	23	7	TF		
38	26	27	7	TF	
38	28	7	TB		
39	6	8	7	TB	
39	9	19	7	TF	
39	20	21	7	TD	
39	23	7	TD		
39	27	7	TF		
39	28	7	TB		
40	6	8	7	TB	
40	9	19	7	TF	
40	20	21	7	TD	
40	23	24	7	TD	
40	27	7	TF		
40	28	7	TB		
41	7	7	TB		
41	9	16	7	TF	
41	18	19	7	TF	
41	20	21	7	TD	
42	7	7	TB		
42	10	11	7	TB	
42	12	15	7	TF	
42	18	19	7	TF	
43	11	7	TB		
43	12	15	7	TF	
44	11	7	TB		
44	12	14	7	TF	
45	11	7	TB		
45	12	14	7	TF	
46	10	11	7	TB	
46	12	14	7	TF	
47	10	11	7	TB	
47	12	15	7	TF	
48	8	10	7	TB	
48	11	14	7	TF	
49	6	8	7	TB	
49	10	11	7	TB	
49	13	7	TB		
2	10	6	TS6	VS6	
3	10	12	6	TS6	VS6
4	11	13	6	TS6	VS6
5	11	14	6	TS6	VS6
6	12	14	6	TS6	VS6

Attachment 1.--Input file to define aquifer characteristics and  
hydraulic-head-dependent boundaries--Continued

7	12	15	6	TS6	VS6
8	12	16	6	TS6	VS6
9	13	16	6	TS6	VS6
10	13	16	6	TS6	VS6
11		7	6	TS6	VS6
11	10	17	6	TS6	VS6
12	5	8	6	TS6	VS6
12	10	17	6	TS6	VS6
13	6	18	6	TS6	VS6
14	8	18	6	TS6	VS6
15	7	19	6	TS6	VS6
16	7	20	6	TS6	VS6
17	6	20	6	TS6	VS6
18	6	21	6	TS6	VS6
19	5	21	6	TS6	VS6
20	5	21	6	TS6	VS6
21	5	22	6	TS6	VS6
22	4	23	6	TS6	VS6
23	4	25	6	TS6	VS6
24	4	25	6	TS6	VS6
25	4	25	6	TS6	VS6
26	2	24	6	TS6	VS6
27	2	24	6	TS6	VS6
28	4	23	6	TS6	VS6
29	5	23	6	TS6	VS6
30	5	23	6	TS6	VS6
31	5	23	6	TS6	VS6
32	5	24	6	TS6	VS6
33	6	24	6	TS6	VS6
34	6	25	6	TS6	VS6
35	7	26	6	TS6	VS6
36	6	27	6	TS6	VS6
37	7	20	6	TS6	VS6
37	22	27	6	TS6	VS6
38	6	21	6	TS6	VS6
38		23	6	TS6	VS6
38	26	28	6	TS6	VS6
39	6	21	6	TS6	VS6
39		23	6	TS6	VS6
39	27	28	6	TS6	VS6
40	6	21	6	TS6	VS6
40	23	24	6	TS6	VS6
40	27	28	6	TS6	VS6
41		7	6	TS6	VS6
41	9	16	6	TS6	VS6
41	18	21	6	TS6	VS6
42		7	6	TS6	VS6
42	10	15	6	TS6	VS6
42	18	19	6	TS6	VS6

**Attachment 1.--Input file to define aquifer characteristics and  
hydraulic-head-dependent boundaries--Continued**

43	11	15	6	TS6	VS6
44	11	14	6	TS6	VS6
45	11	14	6	TS6	VS6
46	10	14	6	TS6	VS6
47	10	15	6	TS6	VS6
48	8	14	6	TS6	VS6
49	6	8	6	TS6	VS6
49	10	11	6	TS6	VS6
49		13	6	TS6	VS6
11	14	15	6	T50	V50
12	12	15	6	T50	V50
13	11	16	6	T50	V50
14	10	17	6	T50	V50
15	8	18	6	T50	V50
16	7	18	6	T50	V50
17	7	19	6	T50	V50
18	7	20	6	T50	V50
19	7	20	6	T50	V50
20	7	20	6	T50	V50
21	7	21	6	T50	V50
22	6	21	6	T50	V50
23	6	22	6	T50	V50
24	5	22	6	T50	V50
25	5	22	6	T50	V50
26	6	23	6	T50	V50
27	7	23	6	T50	V50
28	6	23	6	T50	V50
29	6	23	6	T50	V50
30	7	23	6	T50	V50
31	8	22	6	T50	V50
32	9	21	6	T50	V50
33	8	20	6	T50	V50
34	7	20	6	T50	V50
35	8	20	6	T50	V50
36	9	20	6	T50	V50
37	9	20	6	T50	V50
38	9	20	6	T50	V50
39	10	20	6	T50	V50
40	10	19	6	T50	V50
41	10	16	6	T50	V50
41		18	6	T50	V50
42	11	15	6	T50	V50
43	11	14	6	T50	V50
44	11	14	6	T50	V50
45	13	14	6	T50	V50
14		14	6	TC6	VC6
15	13	17	6	TC6	VC6
16	9	17	6	TC6	VC6
17	7	18	6	TC6	VC6

Attachment 1.--Input file to define aquifer characteristics and  
hydraulic-head-dependent boundaries--Continued

18	8	18	6	TC6	VC6
19	8	18	6	TC6	VC6
20	8	18	6	TC6	VC6
21	8	18	6	TC6	VC6
22	9	19	6	TC6	VC6
23	10	19	6	TC6	VC6
24	10	20	6	TC6	VC6
25	8	20	6	TC6	VC6
26	8	21	6	TC6	VC6
27	9	21	6	TC6	VC6
28	9	22	6	TC6	VC6
29	9	22	6	TC6	VC6
30	9	13	6	TC6	VC6
30	15	21	6	TC6	VC6
31	8	21	6	TC6	VC6
32	9	20	6	TC6	VC6
33	9	19	6	TC6	VC6
34	9	18	6	TC6	VC6
35	9	17	6	TC6	VC6
36	10	19	6	TC6	VC6
37	9	19	6	TC6	VC6
38	10	19	6	TC6	VC6
39	10	19	6	TC6	VC6
40		11	6	TC6	VC6
40	13	17	6	TC6	VC6
40		19	6	TC6	VC6
41	11	13	6	TC6	VC6
41	15	16	6	TC6	VC6
42	13	15	6	TC6	VC6
38		6	6	TB6	VB6
39	6	8	6	TB6	VB6
40	6	9	6	TB6	VB6
41		7	6	TB6	VB6
41	9	10	6	TB6	VB6
42		7	6	TB6	VB6
42	10	11	6	TB6	VB6
43		11	6	TB6	VB6
44		11	6	TB6	VB6
45		11	6	TB6	VB6
46	10	11	6	TB6	VB6
47	10	11	6	TB6	VB6
48	8	14	6	TB6	VB6
49	6	8	6	TB6	VB6
49	10	11	6	TB6	VB6
49		13	6	TB6	VB6
49		12	6	TB6	
47	10	12	6		M20
48	8	14	6		M20
49	6	8	6		M20
49	10	11	6		M20

**Attachment 1.--Input file to define aquifer characteristics and  
hydraulic-head-dependent boundaries--Continued**

49	12	6		ZIP
49	13	6		M20
37	22	6	ZIP	ZIP
40	18	6	T50	VF6
40	17	6	TC6	VF6
41	16	6	TC6	VF6
42	15	6	TC6	VF6
43	15	6	T50	VF6
44	14	6	T50	VF6
2	10	5	TS	VS5
3	10	12	5	TS
4	11	13	5	TS
5	11	14	5	TS
6	12	14	5	TS
7	12	15	5	TS
8	12	16	5	TS
9	13	16	5	TS
10	13	16	5	TS
11	7	5	TS	VS5
11	10	17	5	TS
12	5	8	5	TS
12	10	17	5	TS
13	6	18	5	TS
14	8	18	5	TS
15	7	19	5	TS
16	7	20	5	TS
17	6	20	5	TS
18	6	21	5	TS
19	5	21	5	TS
20	5	21	5	TS
21	5	22	5	TS
22	4	23	5	TS
23	4	25	5	TS
24	4	25	5	TS
25	4	25	5	TS
26	2	24	5	TS
27	2	24	5	TS
28	4	23	5	TS
29	5	23	5	TS
30	5	23	5	TS
31	5	22	5	TS
32	5	22	5	TS
33	6	21	5	TS
34	6	21	5	TS
35	7	20	5	TS
36	6	20	5	TS
37	7	19	5	TS
38	6	18	5	TS
39	6	17	5	TS

Attachment 1.--Input file to define aquifer characteristics and  
hydraulic-head-dependent boundaries--Continued

40	6	16	5	TS	VS5
41		7	5	TS	VS5
41	9	15	5	TS	VS5
42		7	5	TS	VS5
42	10	15	5	TS	VS5
43	11	14	5	TS	VS5
44	11	13	5	TS	VS5
45	11	13	5	TS	VS5
46	10	13	5	TS	VS5
47	10	14	5	TS	VS5
48	8	14	5	TS	VS5
49	6	8	5	TS	VS5
49	10	11	5	TS	VS5
49		13	5	TS	VS5
15	14	16	5	TC5	VC5
16	13	17	5	TC5	VC5
17	12	17	5	TC5	VC5
18	11	18	5	TC5	VC5
19	11	18	5	TC5	VC5
20	9	18	5	TC5	VC5
21	9	18	5	TC5	VC5
22	10	18	5	TC5	VC5
23	10	19	5	TC5	VC5
24	10	19	5	TC5	VC5
25	10	20	5	TC5	VC5
26	10	21	5	TC5	VC5
27	10	21	5	TC5	VC5
28	10	12	5	TC5	VC5
28	14	21	5	TC5	VC5
29	10	12	5	TC5	VC5
29	14	20	5	TC5	VC5
30	10	12	5	TC5	VC5
30	15	20	5	TC5	VC5
31	10	13	5	TC5	VC5
31	15	19	5	TC5	VC5
32	10	18	5	TC5	VC5
33	10	17	5	TC5	VC5
34	10	17	5	TC5	VC5
35	11	12	5	TC5	VC5
35	15	17	5	TC5	VC5
36	12	17	5	TC5	VC5
37	12	14	5	TC5	VC5
37	17	18	5	TC5	VC5
38	12	13	5	TC5	VC5
38	17	18	5	TC5	VC5
39	17	18	5	TC5	VC5
34		6	5	TB5	VB5
35		7	5	TB5	VB5
36	6	8	5	TB5	VB5
37	7	8	5	TB5	VB5



Attachment 1.--Input file to define aquifer characteristics and  
hydraulic-head-dependent boundaries--Continued

38	6	8	5	TB5	VB5
39	6	9	5	TB5	VB5
40	6	10	5	TB5	VB5
41		7	5	TB5	VB5
41	9	11	5	TB5	VB5
42		7	5	TB5	VB5
42	10	12	5	TB5	VB5
43	11	12	5	TB5	VB5
44		11	5	TB5	VB5
45	11	12	5	TB5	VB5
46	10	14	5	TB5	VB5
47	10	15	5	TB5	VB5
48	8	14	5	TB5	VB5
49	6	8	5	TB5	VB5
49	10	11	5	TB5	VB5
49		13	5	TB5	VB5
49		12	5	TB5	VB5
40		17	5	TB5	VB5
41		16	5	TB5	VB5
43		15	5	TB5	VB5
44		14	5	TB5	VB5
40		18	5	TS	VF5
40		17	5	TS	VF5
41		16	5	TS	VF5
42 43		15	5	TS	VF5
44		14	5	TS	VF5
2		10	4	TS	VS4
3	10	12	4	TS	VS4
4	11	13	4	TS	VS4
5	11	14	4	TS	VS4
6	12	14	4	TS	VS4
7	12	15	4	TS	VS4
8	12	16	4	TS	VS4
9	13	16	4	TS	VS4
10	13	16	4	TS	VS4
11		7	4	TS	VS4
11	10	17	4	TS	VS4
12	5	8	4	TS	VS4
12	10	17	4	TS	VS4
13	6	18	4	TS	VS4
14	8	18	4	TS	VS4
15	7	19	4	TS	VS4
16	7	20	4	TS	VS4
17	6	20	4	TS	VS4
18	6	21	4	TS	VS4
19	5	21	4	TS	VS4
20	5	21	4	TS	VS4
21	5	22	4	TS	VS4
22	4	23	4	TS	VS4
23	4	25	4	TS	VS4

Attachment 1.--Input file to define aquifer characteristics and  
hydraulic-head-dependent boundaries--Continued

24	4	25	4	TS	VS4
25	4	25	4	TS	VS4
26	2	24	4	TS	VS4
27	2	24	4	TS	VS4
28	4	23	4	TS	VS4
29	5	23	4	TS	VS4
30	5	23	4	TS	VS4
31	5	22	4	TS	VS4
32	5	22	4	TS	VS4
33	6	21	4	TS	VS4
34	6	21	4	TS	VS4
35	7	20	4	TS	VS4
36	6	20	4	TS	VS4
37	7	19	4	TS	VS4
38	6	18	4	TS	VS4
39	6	17	4	TS	VS4
40	6	16	4	TS	VS4
41		7	4	TS	VS4
41	9	15	4	TS	VS4
42		7	4	TS	VS4
42	10	15	4	TS	VS4
43	11	14	4	TS	VS4
44	11	13	4	TS	VS4
45	11	13	4	TS	VS4
46	10	13	4	TS	VS4
47	10	14	4	TS	VS4
48	8	14	4	TS	VS4
49	6	8	4	TS	VS4
49	10	11	4	TS	VS4
49		13	4	TS	VS4
15	15	16	4	TC4	VC4
16	14	17	4	TC4	VC4
17	13	17	4	TC4	VC4
18	12	17	4	TC4	VC4
19	12	18	4	TC4	VC4
20	11	18	4	TC4	VC4
21	11	18	4	TC4	VC4
22	11	18	4	TC4	VC4
23	12	19	4	TC4	VC4
24	12	19	4	TC4	VC4
25	11	19	4	TC4	VC4
26	11	20	4	TC4	VC4
27		11	4	TC4	VC4
27	14	21	4	TC4	VC4
28		11	4	TC4	VC4
28	14	20	4	TC4	VC4
29		11	4	TC4	VC4
29	15	20	4	TC4	VC4
30	11	12	4	TC4	VC4
30	15	18	4	TC4	VC4

Attachment 1.--Input file to define aquifer characteristics and  
hydraulic-head-dependent boundaries--Continued

31	11	12	4	TC4	VC4
31	15	18	4	TC4	VC4
32	11	17	4	TC4	VC4
33	11	17	4	TC4	VC4
34	11	12	4	TC4	VC4
34		14	4	TC4	VC4
34		16	4	TC4	VC4
35		16	4	TC4	VC4
36		16	4	TC4	VC4
37		14	4	TC4	VC4
32		5	4	TB4	VB4
33	6	7	4	TB4	VB4
34	6	8	4	TB4	VB4
35	7	9	4	TB4	VB4
36	6	10	4	TB4	VB4
37	7	11	4	TB4	VB4
38	6	12	4	TB4	VB4
39	6	13	4	TB4	VB4
40	6	14	4	TB4	VB4
41		7	4	TB4	VB4
41	9	16	4	TB4	VB4
42		7	4	TB4	VB4
42	10	15	4	TB4	VB4
43	11	15	4	TB4	VB4
44	11	14	4	TB4	VB4
45	11	14	4	TB4	VB4
46	10	14	4	TB4	VB4
47	10	15	4	TB4	VB4
48	8	14	4	TB4	VB4
49	6	8	4	TB4	VB4
49	10	11	4	TB4	VB4
49		13	4	TB4	VB4
49		12	4	TB4	VB4
39		18	4	TB4	VB4
40		17	4	TB4	VB4
40		18	4	TS	VF4
40		17	4	TS	VF4
41		16	4	TB4	VF4
42	43	15	4	TB4	VF4
44		14	4	TB4	VF4
2		10	3	TS	VS3
3	10	12	3	TS	VS3
4	11	13	3	TS	VS3
5	11	14	3	TS	VS3
6	12	14	3	TS	VS3
7	12	15	3	TS	VS3
8	12	16	3	TS	VS3
9	13	16	3	TS	VS3
10	13	16	3	TS	VS3
11		7	3	TS	VS3

Attachment 1.--Input file to define aquifer characteristics and  
hydraulic-head-dependent boundaries--Continued

11	10	17	3	TS	VS3
12	5	8	3	TS	VS3
12	10	17	3	TS	VS3
13	6	18	3	TS	VS3
14	8	18	3	TS	VS3
15	7	19	3	TS	VS3
16	7	20	3	TS	VS3
17	6	20	3	TS	VS3
18	6	21	3	TS	VS3
19	5	21	3	TS	VS3
20	5	21	3	TS	VS3
21	5	22	3	TS	VS3
22	4	23	3	TS	VS3
23	4	25	3	TS	VS3
24	4	25	3	TS	VS3
25	4	25	3	TS	VS3
26	2	24	3	TS	VS3
27	2	24	3	TS	VS3
28	4	23	3	TS	VS3
29	5	23	3	TS	VS3
30	5	23	3	TS	VS3
31	5	22	3	TS	VS3
32	5	22	3	TS	VS3
33	6	21	3	TS	VS3
34	6	21	3	TS	VS3
35	7	20	3	TS	VS3
36	6	20	3	TS	VS3
37	7	19	3	TS	VS3
38	6	18	3	TS	VS3
39	6	17	3	TS	VS3
40	6	16	3	TS	VS3
41		7	3	TS	VS3
41	9	15	3	TS	VS3
42		7	3	TS	VS3
42	10	15	3	TS	VS3
43	11	14	3	TS	VS3
44	11	13	3	TS	VS3
45	11	13	3	TS	VS3
46	10	13	3	TS	VS3
47	10	14	3	TS	VS3
48	8	14	3	TS	VS3
49	6	8	3	TS	VS3
49	10	11	3	TS	VS3
49		13	3	TS	VS3
18	13	17	3	TC3	VC3
19	12	17	3	TC3	VC3
20	12	17	3	TC3	VC3
21	12	17	3	TC3	VC3
22	14	17	3	TC3	VC3
23	14	18	3	TC3	VC3

Attachment 1.--Input file to define aquifer characteristics and  
hydraulic-head-dependent boundaries--Continued

24	15	18	3	TC3	VC3
25	16	19	3	TC3	VC3
26	16	19	3	TC3	VC3
27	16	19	3	TC3	VC3
28	17	19	3	TC3	VC3
17	15	16	3	TC3	VC3
30	5	6	3	TB3	VB3
31	5	7	3	TB3	VB3
32	5	9	3	TB3	VB3
33	6	10	3	TB3	VB3
34	6	11	3	TB3	VB3
35	7	13	3	TB3	VB3
36	6	14	3	TB3	VB3
37	7	15	3	TB3	VB3
38	6	16	3	TB3	VB3
39	6	17	3	TB3	VB3
40	6	18	3	TB3	VB3
41		7	3	TB3	VB3
41	9	16	3	TB3	VB3
42		7	3	TB3	VB3
42	10	15	3	TB3	VB3
43	11	15	3	TB3	VB3
44	11	14	3	TB3	VB3
45	11	14	3	TB3	VB3
46	10	14	3	TB3	VB3
47	10	15	3	TB3	VB3
48	8	14	3	TB3	VB3
49	6	8	3	TB3	VB3
49	10	11	3	TB3	VB3
49		13	3	TB3	VB3
49		12	3	TB3	VB3
39		18	3	TB3	VB3
40		18	3	TS	VF3
40		17	3	TB3	VF3
41		16	3	TB3	VF3
42	43	15	3	TB3	VF3
	44	14	3	TB3	VF3
	2	10	2	TS	VS2
	3	10	2	TS	VS2
	4	11	2	TS	VS2
	5	11	2	TS	VS2
	6	12	2	TS	VS2
	7	12	2	TS	VS2
	8	12	2	TS	VS2
	9	13	2	TS	VS2
	10	13	2	TS	VS2
	11		2	TS	VS2
	11	10	2	TS	VS2
	12	5	2	TS	VS2
	12	10	2	TS	VS2

Attachment 1.--Input file to define aquifer characteristics and  
hydraulic-head-dependent boundaries--Continued

13	6	18	2	TS	VS2
14	8	18	2	TS	VS2
15	7	19	2	TS	VS2
16	7	20	2	TS	VS2
17	6	20	2	TS	VS2
18	6	21	2	TS	VS2
19	5	21	2	TS	VS2
20	5	21	2	TS	VS2
21	5	22	2	TS	VS2
22	4	23	2	TS	VS2
23	4	25	2	TS	VS2
24	4	25	2	TS	VS2
25	4	25	2	TS	VS2
26	2	24	2	TS	VS2
27	2	24	2	TS	VS2
28	4	23	2	TS	VS2
29	5	23	2	TS	VS2
30	5	23	2	TS	VS2
31	5	22	2	TS	VS2
32	5	22	2	TS	VS2
33	6	21	2	TS	VS2
34	6	21	2	TS	VS2
35	7	20	2	TS	VS2
36	6	20	2	TS	VS2
37	7	19	2	TS	VS2
38	6	18	2	TS	VS2
39	6	17	2	TS	VS2
40	6	16	2	TS	VS2
41		7	2	TS	VS2
41	9	15	2	TS	VS2
42		7	2	TS	VS2
42	10	15	2	TS	VS2
43	11	14	2	TS	VS2
44	11	13	2	TS	VS2
45	11	13	2	TS	VS2
46	10	13	2	TS	VS2
47	10	14	2	TS	VS2
48	8	14	2	TS	VS2
49	6	8	2	TS	VS2
49	10	11	2	TS	VS2
49		13	2	TS	VS2
49		12	2	TS	VS2
39		18	2	TS	VS2
40		17	2	TS	VS2
41		16	2	TS	VS2
43		15	2	TS	VS2
44		14	2	TS	VS2
46		14	2	TS	VS2
2		10	1	TS	VS1

Attachment 1.--Input file to define aquifer characteristics and  
hydraulic-head-dependent boundaries--Continued

3	10	12	1	TS	VS1
4	11	13	1	TS	VS1
5	11	14	1	TS	VS1
6	12	14	1	TS	VS1
7	12	15	1	TS	VS1
8	12	16	1	TS	VS1
9	13	16	1	TS	VS1
10	13	16	1	TS	VS1
11		7	1	TS	VS1
11	10	17	1	TS	VS1
12	5	8	1	TS	VS1
12	10	17	1	TS	VS1
13	6	18	1	TS	VS1
14	8	18	1	TS	VS1
15	7	19	1	TS	VS1
16	7	20	1	TS	VS1
17	6	20	1	TS	VS1
18	6	21	1	TS	VS1
19	5	21	1	TS	VS1
20	5	21	1	TS	VS1
21	5	22	1	TS	VS1
22	4	23	1	TS	VS1
23	4	25	1	TS	VS1
24	4	25	1	TS	VS1
25	4	25	1	TS	VS1
26	2	24	1	TS	VS1
27	2	24	1	TS	VS1
28	4	23	1	TS	VS1
29	5	23	1	TS	VS1
30	5	23	1	TS	VS1
31	5	22	1	TS	VS1
32	5	22	1	TS	VS1
33	6	21	1	TS	VS1
34	6	21	1	TS	VS1
35	7	20	1	TS	VS1
36	6	20	1	TS	VS1
37	7	19	1	TS	VS1
38	6	18	1	TS	VS1
39	6	17	1	TS	VS1
40	6	16	1	TS	VS1
41		7	1	TS	VS1
41	9	15	1	TS	VS1
42		7	1	TS	VS1
42	10	15	1	TS	VS1
43	11	14	1	TS	VS1
44	11	13	1	TS	VS1
45	11	13	1	TS	VS1
46	10	13	1	TS	VS1
47	10	14	1	TS	VS1
48	8	14	1	TS	VS1
49	6	8	1	TS	VS1
49	10	11	1	TS	VS1

Attachment 1.--Input file to define aquifer characteristics and  
hydraulic-head-dependent boundaries--Continued

49	13	1	TS	VS1
49	12	1	TS	VS1
39	18	1	TS	VS1
40	17	1	TS	VS1
41	16	1	TS	VS1
43	15	1	TS	VS1
44	14	1	TS	VS1
46	14	1	TS	VS1
31	23	5	TS	VS5
32 33	22 24	5	TS	VS5
34	22 25	5	TS	VS5
35	21 26	5	TS	VS5
36	21 27	5	TS	VS5
37	20	5	TS	VS5
37	23 27	5	TS	VS5
38	19 21	5	TS	VS5
38	23	5	TS	VS5
38	26 28	5	TS	VS5
39	19 21	5	TS	VS5
39	23	5	TS	VS5
39	27 28	5	TS	VS5
40	18 21	5	TS	VS5
40	23 24	5	TS	VS5
40	27 28	5	TS	VS5
41	18 21	5	TS	VS5
42	18 19	5	TS	VS5
45	14	5	TS	VS5
31	23	4	TS	VS4
32 33	22 24	4	TS	VS4
34	22 25	4	TS	VS4
35	21 26	4	TS	VS4
36	21 27	4	TS	VS4
37	20	4	TS	VS4
37	23 27	4	TS	VS4
38	19 21	4	TS	VS4
38	23	4	TS	VS4
38	26 28	4	TS	VS4
39	19 21	4	TS	VS4
39	23	4	TS	VS4
39	27 28	4	TS	VS4
40	18 21	4	TS	VS4
40	23 24	4	TS	VS4
40	27 28	4	TS	VS4
41	18 21	4	TS	VS4
42	18 19	4	TS	VS4
36	6	4	TB4	VB4
31	23	3	TS	VS3
32 33	22 24	3	TS	VS3
34	22 25	3	TS	VS3



Attachment 1.--Input file to define aquifer characteristics and  
hydraulic-head-dependent boundaries--Continued

35	21	26	3	TS	VS3
36	21	27	3	TS	VS3
37		20	3	TS	VS3
37	23	27	3	TS	VS3
38	19	21	3	TS	VS3
38		23	3	TS	VS3
38	26	28	3	TS	VS3
39	19	21	3	TS	VS3
39		23	3	TS	VS3
39	27	28	3	TS	VS3
40	18	21	3	TS	VS3
40	23	24	3	TS	VS3
40	27	28	3	TS	VS3
41	18	21	3	TS	VS3
42	18	19	3	TS	VS3
31		23	2	TS	VS2
32	33	22	2	TS	VS2
	34	22	2	TS	VS2
	35	21	2	TS	VS2
	36	21	2	TS	VS2
	37		2	TS	VS2
	37	23	2	TS	VS2
	38	19	2	TS	VS2
	38		2	TS	VS2
	38	26	2	TS	VS2
	39	19	2	TS	VS2
	39		2	TS	VS2
	39	27	2	TS	VS2
	40	18	2	TS	VS2
	40	23	2	TS	VS2
	40	27	2	TS	VS2
	41	18	2	TS	VS2
	42	18	2	TS	VS2
	45		2	TS	VS2
	47		2	TS	VS2
	31		1	TS	VS1
32	33	22	1	TS	VS1
	34	22	1	TS	VS1
	35	21	1	TS	VS1
	36	21	1	TS	VS1
	37		1	TS	VS1
	37	23	1	TS	VS1
	38	19	1	TS	VS1
	38		1	TS	VS1
	38	26	1	TS	VS1
	39	19	1	TS	VS1
	39		1	TS	VS1
	39	27	1	TS	VS1
	40	18	1	TS	VS1

Attachment 1.--Input file to define aquifer characteristics and  
hydraulic-head-dependent boundaries--Continued

40	23	24	1	TS	VS1
40	27	28	1	TS	VS1
41	18	21	1	TS	VS1
42	18	19	1	TS	VS1
45	14	1	1	TS	VS1
47	15	1	1	TS	VS1
37	22	7		ZIP	ZIP
30	24	7		ZIP	ZIP

END  
OUTPUT CUBES  
END  
ENDOF CUBES  
\$NEWPP KP=1, TMAX=1, NUMT=1, CDLT=1.0, DELT=24, \$END  
\$NEWELL ROW=0, \$END  
\$NEWIRIV \$END  
\*MASS GET WAIT=ON WAITIME=60 CODE:/SLV/CTSS/CODE/B3KWMT  
\*& REDEND2:/GLENN/UTILITY/REDDEND2  
\*LDR BIN=CODE, LIB=METALIB \*/LOAD BINARIES  
\*XCORE \*/EXECUTE  
\*COPY BAKOUT BAKIN  
\*TRIXGL \*/EDIT TO TRIM EXCESS  
A  
REDDEND2  
\*DISPOSE DN=NEWOUT,TID=MFARV,FID=GAHMG,SF="CC",WAIT  
\*DESTROY BAKOUT INPUT OUTPUT NEWOUT  
\*FILE NAME=INPUT  
\$CONTROL  
SELRES=.TRUE.,  
RESTRT=.TRUE.,  
ZRMBA=.TRUE.,  
\$END  
DUMMY  
\$INLIST  
NR=33,  
NRC=50, 21, 16, 10, 64, 24, 11, 5, 73, 73,  
59, 59, 35, 35, 56, 56, 76, 76, 75, 75,  
43, 43, 97, 97, 3, 3, 3, 1, 1, 1,  
19, 16, 3,  
RQ=1000,3\*0,  
1000,3\*0,  
1000,7\*0,  
1000,7\*0,  
1000,5\*0,  
500, 300, 0,

Attachment 1.--Input file to define aquifer characteristics and  
hydraulic-head-dependent boundaries--Continued

```

NADD=  2,  3,  4,  0,
      6,  7,  8,  0,
      10, 11, 12, 13, 14, 15, 16, 0,
      18, 19, 20, 21, 22, 23, 24, 0,
      26, 27, 28, 29, 30, 0,
      33, 33, 0,
INDX=12,13, 13, 9, 13,11, 14, 9, 14,13, 17, 7, 17,16, 18,16,
      18,17, 18,18, 18,20, 19,19, 20,17, 21,19, 22,19, 23,18,
      24,19, 24,21, 25, 5, 25,22, 26, 4, 26,13, 27,13, 27,19,
      27,20, 28,20,      29,14, 29,15, 29,16, 30,14, 30,23,
      31,13, 31,14, 31,21, 31,23, 32,22, 33, 7, 34, 7, 34,21,
      35,20, 35,24, 35,25, 36,24, 36,25, 38,19, 45,12,
      28,22, 29,22, 31, 8, 30, 8,
      16,17, 18,19, 19,18, 20,18, 25, 4, 25,21, 26,21, 27,21,
      29,21,      30,22, 31,22, 32,17, 32,18, 32,21,
      33,19, 33,20, 33,21, 35,19, 36,19, 37,19, 38,20,
      13,12, 13,13, 14,12, 16,16, 21,18, 23,19, 24,20, 28,21,
      30,15, 30,16, 30,20, 31,17, 31,20, 32,19, 34,19, 31,18,
      28,19, 29,17, 29,18, 29,19, 29,20, 30,17, 30,18, 30,19,
      31,19, 34,20,
      10,14, 10,15, 11,14, 11,15, 12,13, 12,15, 13, 7, 13, 9,
      13,10, 13,11, 13,13, 13,15, 14, 9, 14,15, 15, 9, 15,16,
      16, 8, 16,15, 16,18, 17,17, 17,18, 18, 7, 18,16, 18,17,
      20,18, 24,13, 25, 5, 25,14, 26, 2, 27, 3, 27, 4, 27, 5,
      27, 7, 27,13, 28, 4, 28, 5, 28,13, 28,15, 28,17,
      30, 7,      30,13, 32, 7, 35, 7, 35, 8, 36, 8, 36, 9,
      37, 9, 38,19, 40, 9, 40,11, 41,10, 42,10, 43,12, 45,12,
      46,11, 47,11, 47,12, 47,14, 48,13, 31, 8,
      16, 7, 28,22, 28,23, 31,18,
      12,14, 13, 8, 15,15, 19, 7, 20, 7, 21, 6, 22, 6, 23, 6,
      24, 6, 26,13, 26,14, 27, 6, 28,16, 29,14, 31, 7,
      31, 9, 36,25, 37,10, 38,10, 39,10, 40,10, 43,11, 47,13,
      29,22,
      25, 6, 25,13, 26, 3, 26, 4, 27,14, 28, 7, 28,14, 29,15,
      29,16, 30,14, 38,11,
      26, 5, 26, 6, 28, 6, 39,11, 44,12,
      13,10, 13,11, 14, 9, 14,10, 14,12, 15, 9, 15,12, 16,12,
      18,16, 19, 8, 20,17, 21,18, 22,19, 23,12, 24,21,
      24,22, 25,12, 25,14, 25,15, 25,16, 26,12, 26,16, 26,19,
      27, 2, 27, 3, 28,21, 28,22, 29, 7, 29, 8, 29,14, 30, 8,
      30,13, 30,15, 30,16, 30,20, 31,10, 31,12, 31,17, 31,20,
      32,11, 32,19, 33, 7, 33, 8, 34,17, 34,19, 35,11, 35,12,
      35,16, 36,18, 37,13, 37,15, 37,16, 38,12, 38,18, 38,20,
      39,12, 40,11, 40,17, 41,15, 41,16, 42,14, 42,15, 44,13,

```

Attachment 1.--Input file to define aquifer characteristics and  
hydraulic-head-dependent boundaries--Continued

44,14,	45,14,	46,13,	46,14,	47,11,	47,12,	48, 9,	
25,19,	29,22,	29, 6,					
13,10,	13,11,	14, 9,	14,10,	14,12,	15, 9,	15,12,	16,12,
	18,16,	19, 8,	20,17,	21,18,	22,19,	23,12,	24,21,
24,22,	25,12,	25,14,	25,15,	25,16,	26,12,	26,16,	26,19,
27, 2,	27, 3,	28,21,	28,22,	29, 7,	29, 8,	29,14,	30, 8,
30,13,	30,15,	30,16,	30,20,	31,10,	31,12,	31,17,	31,20,
32,11,	32,19,	33, 7,	33, 8,	34,17,	34,19,	35,11,	35,12,
35,16,	36,18,	37,13,	37,15,	37,16,	38,12,	38,18,	38,20,
39,12,	40,11,	40,17,	41,15,	41,16,	42,14,	42,15,	44,13,
44,14,	45,14,	46,13,	46,14,	47,11,	47,12,	48, 9,	
25,19,	29,22,	29, 6,					
15,10,	15,11,	16,13,	16,15,	17, 8,	17,13,	17,16,	20,11,
21,11,	21,17,	22,14,	25,21,	26,21,	27,19,	27,20,	27,21,
28,13,	29,12,	29,21,		30, 9,	30,22,	31,11,	31,13,
31,16,	31,22,	32,13,	32,17,	32,18,	32,21,	33, 9,	33,10,
33,12,	33,14,	33,19,	33,20,	34,16,	34,18,	35,17,	35,19,
36,15,	36,19,	37,18,	37,19,	37,24,	38,19,	38,21,	39,13,
39,17,	39,20,	40,16,	40,18,	40,19,	41,12,	41,13,	43,15,
12,14,	25,20,	26,15,	26,20,				
15,10,	15,11,	16,13,	16,15,	17, 8,	17,13,	17,16,	20,11,
21,11,	21,17,	22,14,	25,21,	26,21,	27,19,	27,20,	27,21,
28,13,	29,12,	29,21,		30, 9,	30,22,	31,11,	31,13,
31,16,	31,22,	32,13,	32,17,	32,18,	32,21,	33, 9,	33,10,
33,12,	33,14,	33,19,	33,20,	34,16,	34,18,	35,17,	35,19,
36,15,	36,19,	37,18,	37,19,	37,24,	38,19,	38,21,	39,13,
39,17,	39,20,	40,16,	40,18,	40,19,	41,12,	41,13,	43,15,
12,14,	25,20,	26,15,	26,20,				
13,14,	14,13,	15,13,	15,14,	16, 9,	16,10,	18, 9,	19,17,
21,13,	21,14,	22,17,	23,16,	23,18,	24,15,	24,16,	24,19,
	26,18,	28,17,	28,20,	30,10,	31,14,	31,21,	32,16,
33,13,	33,16,	33,17,	33,18,	34, 8,	34,10,	34,15,	35,13,
35,14,	35,18,	36,16,	39,19,				
13,14,	14,13,	15,13,	15,14,	16, 9,	16,10,	18, 9,	19,17,
21,13,	21,14,	22,17,	23,16,	23,18,	24,15,	24,16,	24,19,
	26,18,	28,17,	28,20,	30,10,	31,14,	31,21,	32,16,
33,13,	33,16,	33,17,	33,18,	34, 8,	34,10,	34,15,	35,13,
35,14,	35,18,	36,16,	39,19,				
14,14,	16,11,	16,14,	17, 9,	17,10,	17,11,	17,12,	17,14,
17,15,	18,10,	18,11,	18,12,	18,13,	18,14,	18,15,	19, 9,
19,10,	19,11,	19,12,	19,13,	19,14,	19,15,	19,16,	20,12,
20,13,	20,14,	20,15,	20,16,	21,12,	21,15,	21,16,	22,13,
22,15,	22,16,	22,18,	23,15,	23,17,	24,17,	24,18,	25,17,

Attachment 1.--Input file to define aquifer characteristics and  
hydraulic-head-dependent boundaries--Continued

25,18,			26,17,		27,17,	27,18,	28,18,
30,21,	31,15,	32,20,	33,11,	34, 9,	34,11,	34,12,	34,13,
34,14,	35,15,	39,18,					
14,14,	16,11,	16,14,	17, 9,	17,10,	17,11,	17,12,	17,14,
17,15,	18,10,	18,11,	18,12,	18,13,	18,14,	18,15,	19, 9,
19,10,	19,11,	19,12,	19,13,	19,14,	19,15,	19,16,	20,12,
20,13,	20,14,	20,15,	20,16,	21,12,	21,15,	21,16,	22,13,
22,15,	22,16,	22,18,	23,15,	23,17,	24,17,	24,18,	25,17,
25,18,			26,17,		27,17,	27,18,	28,18,
30,21,	31,15,	32,20,	33,11,	34, 9,	34,11,	34,12,	34,13,
34,14,	35,15,	39,18,					
5,12,	7,14,	8,14,	9,14,	10,14,	12, 5,	12,15,	13, 7,
13, 8,	13,14,	13,15,	15, 8,	15,13,	15,14,	16, 9,	16,10,
17,16,	17,17,	18, 9,	18,16,	18,18,	18,19,	19, 7,	19,17,
19,19,	21,13,	21,14,	22,17,	23, 6,	23,16,	24, 6,	24,15,
24,16,	25,13,	26, 2,	26,13,		27, 3,	27,14,	28, 4,
28, 7,	28,13,	28,14,	29, 5,	30, 6,	30,10,	31,13,	32,16,
33,13,	33,16,	33,17,	33,18,	34, 8,	34,10,	34,15,	35,13,
35,14,	35,18,	36,16,	36,25,	36,26,	37,26,	38,11,	38,23,
39,19,	40,10,	40,19,	43,11,	43,15,	46,11,	47,10,	47,11,
47,12,	47,15,	48,10,	48,12,	16,15,			
5,12,	7,14,	8,14,	9,14,	10,14,	12, 5,	12,15,	13, 7,
13, 8,	13,14,	13,15,	15, 8,	15,13,	15,14,	16, 9,	16,10,
17,16,	17,17,	18, 9,	18,16,	18,18,	18,19,	19, 7,	19,17,
19,19,	21,13,	21,14,	22,17,	23, 6,	23,16,	24, 6,	24,15,
24,16,	25,13,	26, 2,	26,13,		27, 3,	27,14,	28, 4,
28, 7,	28,13,	28,14,	29, 5,	30, 6,	30,10,	31,13,	32,16,
33,13,	33,16,	33,17,	33,18,	34, 8,	34,10,	34,15,	35,13,
35,14,	35,18,	36,16,	36,25,	36,26,	37,26,	38,11,	38,23,
39,19,	40,10,	40,19,	43,11,	43,15,	46,11,	47,10,	47,11,
47,12,	47,15,	48,10,	48,12,	16,15,			
6,13,	11,14,	12, 6,	13, 9,	13,10,	14,15,	15, 9,	15,10,
15,11,	15,15,	16,13,	17, 7,	17, 8,	17,13,		18, 7,
19,18,	20, 7,	20,11,	20,17,	21,11,	21,17,	22, 6,	22,14,
25,14,	26,14,	27, 4,	27, 6,	27,13,	28, 5,	28,16,	29,12,
30, 7,	30, 8,	30, 9,	30,13,	31, 8,	31, 9,	31,11,	31,16,
32, 7,	32,13,	33, 7,	33, 9,	33,10,	33,12,	33,14,	34, 7,
34,16,	34,18,	35,17,	36,15,	37,10,	37,18,	39,13,	39,17,
40,11,	40,16,	40,18,	41, 9,	41,10,	41,12,	41,13,	41,16,
41,18,	41,19,	42,15,	42,18,	45,12,	46,14,	47,14,	48,13,
48,14,	25,20,	26,15,	26,20,				
6,13,	11,14,	12, 6,	13, 9,	13,10,	14,15,	15, 9,	15,10,
15,11,	15,15,	16,13,	17, 7,	17, 8,	17,13,		18, 7,

Attachment 1.--Input file to define aquifer characteristics and  
hydraulic-head-dependent boundaries--Continued

19,18,	20, 7,	20,11,	20,17,	21,11,	21,17,	22, 6,	22,14,
25,14,	26,14,	27, 4,	27, 6,	27,13,	28, 5,	28,16,	29,12,
30, 7,	30, 8,	30, 9,	30,13,	31, 8,	31, 9,	31,11,	31,16,
32, 7,	32,13,	33, 7,	33, 9,	33,10,	33,12,	33,14,	34, 7,
34,16,	34,18,	35,17,	36,15,	37,10,	37,18,	39,13,	39,17,
40,11,	40,16,	40,18,	41, 9,	41,10,	41,12,	41,13,	41,16,
41,18,	41,19,	42,15,	42,18,	45,12,	46,14,	47,14,	48,13,
48,14,	25,20,	26,15,	26,20,				
14,10,	15,12,	16, 8,	16,12,	19, 8,	23,12,	24,13,	25,12,
25,15,	25,16,	26,12,	26,16,	27, 7,	28,15,	29, 6,	29, 7,
29, 8,	31,10,	31,12,	32,11,	33, 8,	34,17,	35,11,	35,12,
35,16,	36, 9,	36,18,	37,13,	37,15,	37,16,	37,25,	38,12,
38,18,	39,12,	40,17,	41,15,	42,14,	43,12,	44,13,	44,14,
45,14,	46,13,	25,19,					
14,10,	15,12,	16, 8,	16,12,	19, 8,	23,12,	24,13,	25,12,
25,15,	25,16,	26,12,	26,16,	27, 7,	28,15,	29, 6,	29, 7,
29, 8,	31,10,	31,12,	32,11,	33, 8,	34,17,	35,11,	35,12,
35,16,	36, 9,	36,18,	37,13,	37,15,	37,16,	37,25,	38,12,
38,18,	39,12,	40,17,	41,15,	42,14,	43,12,	44,13,	44,14,
45,14,	46,13,	25,19,					
14,11,	18, 8,	20, 8,	20, 9,	20,10,	21, 7,	21, 8,	21, 9,
21,10,	22, 7,	22, 8,	22, 9,	22,10,	22,11,	22,12,	23, 7,
23, 8,	23, 9,	23,10,	23,11,	23,13,	23,14,	24, 7,	24, 8,
24, 9,	24,10,	24,11,	24,12,	24,14,	25, 7,	25, 8,	25, 9,
25,10,	25,11,	26, 7,	26, 8,	26, 9,	26,10,	26,11,	27, 8,
27, 9,	27,10,	27,11,	27,12,	27,15,	27,16,	28, 8,	28, 9,
28,10,	28,11,	28,12,	29, 9,	29,10,	29,11,	29,13,	30,11,
30,12,	32, 8,	32, 9,	32,10,	32,12,	32,14,	32,15,	33,15,
35, 9,	35,10,	36,10,	36,11,	36,12,	36,13,	36,14,	36,17,
37,11,	37,12,	37,14,	37,17,	38,13,	38,14,	38,15,	38,16,
38,17,	39,14,	39,15,	39,16,	40,12,	40,13,	40,14,	40,15,
41,11,	41,14,	42,11,	42,12,	42,13,	43,13,	43,14,	45,13,
46,12,							
14,11,	18, 8,	20, 8,	20, 9,	20,10,	21, 7,	21, 8,	21, 9,
21,10,	22, 7,	22, 8,	22, 9,	22,10,	22,11,	22,12,	23, 7,
23, 8,	23, 9,	23,10,	23,11,	23,13,	23,14,	24, 7,	24, 8,
24, 9,	24,10,	24,11,	24,12,	24,14,	25, 7,	25, 8,	25, 9,
25,10,	25,11,	26, 7,	26, 8,	26, 9,	26,10,	26,11,	27, 8,
27, 9,	27,10,	27,11,	27,12,	27,15,	27,16,	28, 8,	28, 9,
28,10,	28,11,	28,12,	29, 9,	29,10,	29,11,	29,13,	30,11,
30,12,	32, 8,	32, 9,	32,10,	32,12,	32,14,	32,15,	33,15,
35, 9,	35,10,	36,10,	36,11,	36,12,	36,13,	36,14,	36,17,
37,11,	37,12,	37,14,	37,17,	38,13,	38,14,	38,15,	38,16,
38,17,	39,14,	39,15,	39,16,	40,12,	40,13,	40,14,	40,15,
41,11,	41,14,	42,11,	42,12,	42,13,	43,13,	43,14,	45,13,
46,12,							
26,18,	27,19,	27,20,					
26,18,	27,19,	27,20,					
26,18,	27,19,	27,20,					
26,19,							

Attachment 1.--Input file to define aquifer characteristics and  
hydraulic-head-dependent boundaries--Continued

26,19,  
26,19,  
27, 2, 27, 3, 27, 4, 28, 5, 29, 6, 29, 7, 30, 8, 30, 9,  
31,10, 31,11, 31,12, 32,13, 33,14, 34,15, 35,16, 36,17,  
37,18, 38,18, 39,19,  
49, 6, 49, 7, 49, 8, 48, 9, 48,10, 47,11, 47,12, 46,13,  
46,14, 45,14, 44,14, 43,15, 42,15, 41,16, 40,17, 40,18,  
40,19, 41,19, 42,19,  
RIVER= 50\*100, 21\*100, 16\*100, 10\*100, 64\*100,  
24\*100, 11\*100, 5\*100, 73\*100, 73\*97,  
59\*100, 59\* 97, 35\*100, 35\* 97, 56\*100,  
56\* 97, 76\*100, 76\* 97, 75\*100, 75\* 97,  
43\*100, 43\* 97, 97\*100, 97\* 97, 3\*100,  
3\* 97, 3\* 94, 1\*100, 1\* 97, 1\* 94,  
38\*100,

\$END

HEADER

- - - GROUND-WATER FLOW MODEL OF SAN LUIS VALLEY NORTH OF SAN LUIS HILLS - - -  
AUGUST 1983 \* DEFINE PRM,BOT,AND RIVERS

END

SYMBOLS

TH	0.233
TG	0.155
TF	0.0775
TD	0.0310
TB	0.0155
A4	1.94E-4
A5	1.55E-4
A7	1.11E-4
B2	7.75E-4
B3	5.17E-4
B5	3.10E-4
B7	2.21E-4
B8	1.94E-4
B9	1.72E-4
B11	1.41E-4
B13	1.19E-4
C5	4.66E-4
C7	3.33E-4
C9	2.59E-4
D2	15.50E-4
D3	10.33E-4
D5	6.20E-4
D7	4.43E-4
D8	3.88E-4
D9	3.44E-4
D11	2.82E-4
D13	2.38E-4
E9	5.17E-4

Attachment 1.--Input file to define aquifer characteristics and  
hydraulic-head-dependent boundaries--Continued

E11	4.23E-4
F2	38.75E-4
F3	25.83E-4
F5	15.50E-4
F7	11.07E-4
F8	9.69E-4
F9	8.61E-4
F10	7.75E-4
F11	7.04E-4
G3	51.67E-4
G5	31.00E-4
G7	22.14E-4
G9	17.22E-4
G10	15.50E-4
G11	14.09E-4
H7	33.29E-4
H9	25.89E-4
H10	23.30E-4
I9	34.44E-4
I10	31.00E-4
M2	80.
M3	70.
M4	60.
M5	50.
M7	30.
M8	20.
M9	10.
M10	0.
M11	-10.
M13	-30.
ZIP	0
ONE	1
THR	3
SVN	7
VF5	0.364E-5
VF4	0.243E-5
VF3	0.163E-5
VS4	0.243E-8

END

3D INPUT

26	7	7	TH
28	5	7	TH
28	11	7	TH
14	11	7	TG
22	11	7	TG
24	11	7	TG
25	11	7	TG
25	6	7	TG
26	6	7	TG
28	7	7	TG
29	11	7	TG



Attachment 1.--Input file to define aquifer characteristics and  
hydraulic-head-dependent boundaries--Continued

36	26	7	TG	
12	7	7	TF	
15	7	7	TF	
18	13	7	TF	
19	14	7	TF	
19	16	7	TF	
19	17	7	TF	
20	16	7	TF	
20	17	7	TF	
21	17	18	7	TF
22	23	18	7	TF
24	4	7	TF	
25	19	7	TF	
26	17	21	7	TF
27	6	7	TF	
27	18	22	7	TF
28	21	22	7	TF
36	8	7	TF	
40	19	7	TF	
36	23	7	TF	
37	24	25	7	TF
39	27	7	TF	
12	15	7	TD	
20	23	14	7	TD
24	25	15	7	TD
26	16	7	TD	
28	17	7	TD	
30	16	7	TD	
34	16	7	TD	
33	34	22	7	TD
34	35	23	7	TD
36	22	7	TD	
38	23	7	TD	
39	21	7	TD	
40	20	21	7	TD
40	27	7	TD	
41	20	21	7	TD
18	14	7	TB	
19	15	7	TB	
20	21	13	7	TB
27	17	7	TB	
28	18	20	7	TB
29	18	7	TB	
29	20	22	7	TB
30	35	17	7	TB
30	31	22	7	TB
34	35	18	7	TB
35	21	7	TB	
36	18	20	7	TB

Attachment 1.--Input file to define aquifer characteristics and  
hydraulic-head-dependent boundaries--Continued

40	28	7	TB	
40	18	3		VF3
39	18	4		VS4
40	18	4		VF4
40	18	5		VF5
END				
2D INPUT				
31	19	7	PRMA5	
31	20	7	PRMA7	
32	18	7	PRMA4	
32	19	7	PRMA5	
32	20	7	PRMA7	
33	18	19	7	PRMA5
34	18	7	PRMA5	
2	10	7	PRMB7	
3	10	12	7	PRMB7
4	11	13	7	PRMB7
5	11	7	PRMB5	
5	13	14	7	PRMB7
6	12	7	PRMB5	
6	14	7	PRMB7	
7	12	13	7	PRMB5
7	15	7	PRMB7	
8	12	13	7	PRMB5
8	15	16	7	PRMB7
9	13	7	PRMB5	
9	16	7	PRMB7	
10	13	7	PRMB5	
10	16	7	PRMB9	
11	7	7	PRMB5	
11	10	12	7	PRMB5
11	16	7	PRMB9	
11	17	7	PRMB11	
12	7	8	7	PRMB5
12	10	11	7	PRMB5
12	17	7	PRMB11	
13	6	7	PRMB5	
13	17	18	7	PRMB11
14	18	7	PRMB11	
15	7	7	PRMB5	
15	19	7	PRMB11	
16	20	7	PRMB13	
17	6	7	PRMB3	
17	20	7	PRMB13	
18	6	7	PRMB3	
18	20	21	7	PRMB13
19	5	7	PRMB3	
19	20	21	7	PRMB13
20	5	7	PRMB3	

Attachment 1.--Input file to define aquifer characteristics and  
hydraulic-head-dependent boundaries--Continued

20	21	7	PRMB13
22	4	7	PRMB3
23	4	7	PRMB3
24	4	7	PRMB5
25	25	7	PRMB13
26	23 24	7	PRMB13
27	23 24	7	PRMB13
28	4	7	PRMB7
28	23	7	PRMB11
29	5	7	PRMB7
29	19	7	PRMB7
29	23	7	PRMB11
30	5 6	7	PRMB5
30	18 19	7	PRMB5
30	20 21	7	PRMB7
30	23	7	PRMB9
31	5	7	PRMB5
31	18	7	PRMB5
31	21	7	PRMB7
31	23	7	PRMB9
32	5 6	7	PRMB3
32	21	7	PRMB7
32	22 24	7	PRMB9
33	6	7	PRMB3
33	20 21	7	PRMB7
33	22 24	7	PRMB9
34	6	7	PRMB5
34	19	7	PRMB5
34	20 22	7	PRMB7
34	23 25	7	PRMB9
35	19 20	7	PRMB7
36	6 7	7	PRMB7
36	8	7	PRMB5
37	7 8	7	PRMB7
38	6	7	PRMB7
38	7 8	7	PRMB5
38	28	7	PRMB3
39	6 8	7	PRMB5
39	28	7	PRMB3
40	6 8	7	PRMB5
40	28	7	PRMB2
41	7	7	PRMB5
42	7	7	PRMB5
42	10 11	7	PRMB5
43	11	7	PRMB5
44	11	7	PRMB5
45	11	7	PRMB5
46	10 11	7	PRMB5

Attachment 1.--Input file to define aquifer characteristics and  
hydraulic-head-dependent boundaries--Continued

47	10	11	7	PRMB5
48	8	10	7	PRMB5
49	6	8	7	PRMB5
49	10	11	7	PRMB5
49		13	7	PRMB3
28	19	20	7	PRMC9
29		18	7	PRMC7
29		20	7	PRMC7
29	21	22	7	PRMC9
30		17	7	PRMC5
30		22	7	PRMC9
31		17	7	PRMC5
31		22	7	PRMC9
32		17	7	PRMC5
33		17	7	PRMC5
34		17	7	PRMC7
35		17	7	PRMC7
35		18	7	PRMC5
35		21	7	PRMC7
36	18	20	7	PRMC5
9		15	7	PRMD7
10		15	7	PRMD7
11		15	7	PRMD9
12		16	7	PRMD9
13	15	16	7	PRMD11
14	15	17	7	PRMD11
15		15	7	PRMD11
15	16	17	7	PRMD9
15		18	7	PRMD11
16	14	17	7	PRMD9
16		18	7	PRMD11
16		19	7	PRMD13
17	13	17	7	PRMD9
17		18	7	PRMD11
17		19	7	PRMD13
18	13	17	7	PRMD9
18		18	7	PRMD11
18		19	7	PRMD13
19	13	14	7	PRMD9
19		15	7	PRMD8
19	16	18	7	PRMD9
19		19	7	PRMD11
20		16	7	PRMD8
20	17	18	7	PRMD9
20		19	7	PRMD11
20		20	7	PRMD13
21	17	18	7	PRMD9
21		19	7	PRMD11

Attachment 1.--Input file to define aquifer characteristics and  
hydraulic-head-dependent boundaries--Continued

21	20	22	7	PRMD13
22		18	7	PRMD9
22		19	7	PRMD11
22	20	23	7	PRMD13
23		18	7	PRMD9
23		19	7	PRMD11
23	20	25	7	PRMD13
24		19	7	PRMD11
24	20	25	7	PRMD13
25	19	20	7	PRMD9
25		21	7	PRMD11
25	22	24	7	PRMD13
26		17	7	PRMD7
26	18	21	7	PRMD9
26		22	7	PRMD13
27		17	7	PRMD7
27	18	19	7	PRMD9
28		18	7	PRMD9
28		21	7	PRMD9
29		17	7	PRMD5
31		16	7	PRMD5
32		16	7	PRMD5
33		16	7	PRMD7
35		22	7	PRMD7
36		17	7	PRMD5
36		21	7	PRMD5
37		18	7	PRMD3
37	19	20	7	PRMD5
38		19	7	PRMD3
38		20	7	PRMD5
38		21	7	PRMD3
39	20	21	7	PRMD3
39		23	7	PRMD3
40	20	21	7	PRMD2
40	23	24	7	PRMD2
41	20	21	7	PRMD2
27	20	21	7	PRME9
27		22	7	PRME11
28		22	7	PRME9
5		12	7	PRMF7
6		13	7	PRMF7
7		14	7	PRMF7
8		14	7	PRMF5
9		14	7	PRMF5
10		14	7	PRMF7
11		14	7	PRMF9
12	5	6	7	PRMF5
12		12	7	PRMF5
12	14	15	7	PRMF9

Attachment 1.--Input file to define aquifer characteristics and  
hydraulic-head-dependent boundaries--Continued

13	7	9	7	PRMF5
14		8	7	PRMF5
15		14	7	PRMF11
16		12	7	PRMF11
16		13	7	PRMF9
17	7	8	7	PRMF5
17		9	7	PRMF7
17		12	7	PRMF9
18	7	8	7	PRMF5
18		9	7	PRMF7
18	10	12	7	PRMF9
19		6	7	PRMF3
19		7	7	PRMF5
19		8	7	PRMF7
19	9	12	7	PRMF9
20		6	7	PRMF3
20		7	7	PRMF5
20		8	7	PRMF9
20	9	10	7	PRMF10
20	11	13	7	PRMF9
20	14	15	7	PRMF8
21		5	7	PRMF3
21		6	7	PRMF5
21	12	13	7	PRMF9
21	14	16	7	PRMF8
22		5	7	PRMF3
22		13	7	PRMF9
22	14	16	7	PRMF8
22		17	7	PRMF9
23		5	7	PRMF5
23	14	17	7	PRMF9
24	14	18	7	PRMF9
25		12	7	PRMF9
25	13	17	7	PRMF7
25		18	7	PRMF9
26		2	7	PRMF5
26	14	16	7	PRMF7
27	2	3	7	PRMF7
27	14	16	7	PRMF7
28	5	6	7	PRMF7
28	13	14	7	PRMF7
28	15	16	7	PRMF5
28		17	7	PRMF7
29	6	7	7	PRMF7
29		11	7	PRMF7
29	13	14	7	PRMF7
29	15	16	7	PRMF5
30		7	7	PRMF5
30		8	7	PRMF3
30		9	7	PRMF5

Attachment 1.--Input file to define aquifer characteristics and  
hydraulic-head-dependent boundaries--Continued

30	11	13	7	PRMF7
30	14	16	7	PRMF5
31	6	7	7	PRMF3
31	12	15	7	PRMF5
32		7	7	PRMF3
32	12	13	7	PRMF5
32	14	15	7	PRMF7
33		7	7	PRMF3
33		11	7	PRMF5
33	12	15	7	PRMF7
34		7	7	PRMF3
34		10	7	PRMF5
34	11	14	7	PRMF7
34		15	7	PRMF8
34		16	7	PRMF7
35		7	7	PRMF5
35	9	10	7	PRMF5
35	11	14	7	PRMF7
35		15	7	PRMF8
35		16	7	PRMF7
35	23	26	7	PRMF7
36		9	7	PRMF5
36	10	13	7	PRMF7
36	14	15	7	PRMF8
36		16	7	PRMF7
36		22	7	PRMF5
36	26	27	7	PRMF5
37	9	12	7	PRMF7
37	13	14	7	PRMF8
37	15	16	7	PRMF7
37		17	7	PRMF5
37		22	7	PRMF3
37		27	7	PRMF5
38	9	12	7	PRMF5
38	13	15	7	PRMF7
38		16	7	PRMF5
38	17	18	7	PRMF3
38		23	7	PRMF3
38	26	27	7	PRMF3
39	9	10	7	PRMF5
39	11	12	7	PRMF3
39	13	14	7	PRMF5
39		15	7	PRMF7
39		16	7	PRMF5
39		17	7	PRMF3
39	18	19	7	PRMF2
39		27	7	PRMF2
40	9	11	7	PRMF5
40	12	13	7	PRMF3
40	14	15	7	PRMF5

Attachment 1.--Input file to define aquifer characteristics and  
hydraulic-head-dependent boundaries--Continued

40	16	17	7	PRMF3
40	18	19	7	PRMF2
40		27	7	PRMF2
41	9	11	7	PRMF5
41	12	15	7	PRMF3
41		16	7	PRMF2
41	18	19	7	PRMF2
42	12	15	7	PRMF3
42	18	19	7	PRMF2
43		12	7	PRMF5
43	13	14	7	PRMF3
43		15	7	PRMF2
44	12	13	7	PRMF5
44		14	7	PRMF2
45		12	7	PRMF5
45		13	7	PRMF3
45		14	7	PRMF2
46		12	7	PRMF5
46		13	7	PRMF3
46		14	7	PRMF2
47	12	13	7	PRMF3
47	14	15	7	PRMF2
48		11	7	PRMF5
48	12	13	7	PRMF3
48		14	7	PRMF2
11		13	7	PRMG5
12		13	7	PRMG9
13	13	14	7	PRMG9
14		9	7	PRMG7
14		10	7	PRMG9
14	12	14	7	PRMG11
15	8	9	7	PRMG7
15	10	11	7	PRMG9
15	12	13	7	PRMG11
16	7	8	7	PRMG5
16		9	7	PRMG7
16	10	11	7	PRMG9
17	10	11	7	PRMG9
21		7	7	PRMG5
21		8	7	PRMG9
21	9	10	7	PRMG10
21		11	7	PRMG9
22		6	7	PRMG5
22		7	7	PRMG7
22		12	7	PRMG9
23		6	7	PRMG7
23	12	13	7	PRMG9
24		5	7	PRMG7
24	12	13	7	PRMG9
25		4	7	PRMG5



Attachment 1.--Input file to define aquifer characteristics and  
hydraulic-head-dependent boundaries--Continued

26	3	5	7	PRMG7
26		7	7	PRMG9
26	12	13	7	PRMG7
27		4	7	PRMG7
27	12	13	7	PRMG7
28		8	7	PRMG9
28	11	12	7	PRMG7
29	8	10	7	PRMG7
29		12	7	PRMG7
30		10	7	PRMG5
31		8	7	PRMG3
31	9	11	7	PRMG5
32		8	7	PRMG3
32		9	7	PRMG5
32	10	11	7	PRMG7
33		8	7	PRMG3
33	9	10	7	PRMG5
34		8	7	PRMG3
34		9	7	PRMG5
35		8	7	PRMG3
36	23	25	7	PRMG5
37	23	24	7	PRMG3
37	25	26	7	PRMG5
13	10	11	7	PRMH7
13		12	7	PRMH9
14		11	7	PRMH9
22	9	10	7	PRMH10
22		11	7	PRMH9
23		7	7	PRMH7
23		10	7	PRMH10
23		11	7	PRMH9
24		6	7	PRMH9
24		11	7	PRMH9
25		5	7	PRMH7
25	6	7	7	PRMH9
25	8	9	7	PRMH10
25	10	11	7	PRMH9
26		6	7	PRMH9
26		8	7	PRMH9
26		11	7	PRMH9
27	5	6	7	PRMH7
27	7	8	7	PRMH9
27		10	7	PRMH9
27		11	7	PRMH7
28		7	7	PRMH7
28		10	7	PRMH9
22		8	7	PRMI9
23		8	7	PRMI9
23		9	7	PRMI10
24		7	7	PRMI9

Attachment 1.--Input file to define aquifer characteristics and  
hydraulic-head-dependent boundaries--Continued

24	8	9	7	PRMI10
24		10	7	PRMI9
26	9	10	7	PRMI9
27		9	7	PRMI9
28		9	7	PRMI9
2		10	7	BOTM7
3	10	12	7	BOTM7
4	11	13	7	BOTM7
5		11	7	BOTM5
5	12	14	7	BOTM7
6		12	7	BOTM5
6	13	14	7	BOTM7
7	12	13	7	BOTM5
7	14	15	7	BOTM7
8	12	14	7	BOTM5
8	15	16	7	BOTM7
9	13	14	7	BOTM5
9	15	16	7	BOTM7
10		13	7	BOTM5
10	14	15	7	BOTM7
10		16	7	BOTM9
11		7	7	BOTM5
11	10	13	7	BOTM5
11	14	16	7	BOTM9
11		17	7	BOTM11
12	5	8	7	BOTM5
12	10	12	7	BOTM5
12	13	16	7	BOTM9
12		17	7	BOTM11
13	6	9	7	BOTM5
13	10	11	7	BOTM7
13	12	14	7	BOTM9
13	15	18	7	BOTM11
14		8	7	BOTM5
14		9	7	BOTM7
14	10	11	7	BOTM9
14	12	18	7	BOTM11
15		7	7	BOTM5
15	8	9	7	BOTM7
15	10	11	7	BOTM9
15	12	15	7	BOTM11
15	16	17	7	BOTM9
15	18	19	7	BOTM11
16	7	8	7	BOTM5
16		9	7	BOTM7
16	10	11	7	BOTM9
16		12	7	BOTM11
16	13	17	7	BOTM9
16		18	7	BOTM11
16	19	20	7	BOTM13

Attachment 1.--Input file to define aquifer characteristics and  
hydraulic-head-dependent boundaries--Continued

17	6	7	BOTM3
17	7 8	7	BOTM5
17	9	7	BOTM7
17	10 17	7	BOTM9
17	18	7	BOTM11
17	19 20	7	BOTM13
18	6	7	BOTM3
18	7 8	7	BOTM5
18	9	7	BOTM7
18	10 17	7	BOTM9
18	18	7	BOTM11
18	19 21	7	BOTM13
19	5 6	7	BOTM3
19	7	7	BOTM5
19	8	7	BOTM7
19	9 14	7	BOTM9
19	15	7	BOTM8
19	16 18	7	BOTM9
19	19	7	BOTM11
19	20 21	7	BOTM13
20	5 6	7	BOTM3
20	7	7	BOTM5
20	8	7	BOTM9
20	9 10	7	BOTM10
20	11 13	7	BOTM9
20	14 16	7	BOTM8
20	17 18	7	BOTM9
20	19	7	BOTM11
20	20 21	7	BOTM13
21	5	7	BOTM3
21	6 7	7	BOTM5
21	8	7	BOTM9
21	9 10	7	BOTM10
21	11 13	7	BOTM9
21	14 16	7	BOTM8
21	17 18	7	BOTM9
21	19	7	BOTM11
21	20 22	7	BOTM13
22	4 5	7	BOTM3
22	6	7	BOTM5
22	7	7	BOTM7
22	8	7	BOTM9
22	9 10	7	BOTM10
22	11 13	7	BOTM9
22	14 16	7	BOTM8
22	17 18	7	BOTM9
22	19	7	BOTM11
22	20 23	7	BOTM13
23	4	7	BOTM3
23	5	7	BOTM5

Attachment 1.--Input file to define aquifer characteristics and  
hydraulic-head-dependent boundaries--Continued

23	6	7	7	BOTM7
23		8	7	BOTM9
23	9	10	7	BOTM10
23	11	18	7	BOTM9
23		19	7	BOTM11
23	20	25	7	BOTM13
24		4	7	BOTM5
24		5	7	BOTM7
24	6	7	7	BOTM9
24	8	9	7	BOTM10
24	10	18	7	BOTM9
24		19	7	BOTM11
24	20	25	7	BOTM13
25		4	7	BOTM5
25		5	7	BOTM7
25	6	7	7	BOTM9
25	8	9	7	BOTM10
25	10	12	7	BOTM9
25	13	17	7	BOTM7
25	18	20	7	BOTM9
25		21	7	BOTM11
25	22	25	7	BOTM13
26		2	7	BOTM5
26	3	5	7	BOTM7
26	6	11	7	BOTM9
26	12	17	7	BOTM7
26	18	21	7	BOTM9
26	22	24	7	BOTM13
27	2	6	7	BOTM7
27	7	10	7	BOTM9
27	11	17	7	BOTM7
27	18	21	7	BOTM9
27		22	7	BOTM11
27	23	24	7	BOTM13
28	4	7	7	BOTM7
28	8	10	7	BOTM9
28	11	14	7	BOTM7
28	15	16	7	BOTM5
28		17	7	BOTM7
28	18	22	7	BOTM9
28		23	7	BOTM11
29	5	14	7	BOTM7
29	15	17	7	BOTM5
29	18	20	7	BOTM7
29	21	22	7	BOTM9
29		23	7	BOTM11
30	5	7	7	BOTM5
30		8	7	BOTM3
30	9	10	7	BOTM5
30	11	13	7	BOTM7

Attachment 1.--Input file to define aquifer characteristics and  
hydraulic-head-dependent boundaries--Continued

30	14	19	7	BOTM5
30	20	21	7	BOTM7
30	22	23	7	BOTM9
31		5	7	BOTM5
31	6	8	7	BOTM3
31	9	19	7	BOTM5
31	20	21	7	BOTM7
31	22	23	7	BOTM9
32	5	8	7	BOTM3
32		9	7	BOTM5
32	10	11	7	BOTM7
32	12	13	7	BOTM5
32	14	15	7	BOTM7
32	16	17	7	BOTM5
32		18	7	BOTM4
32		19	7	BOTM5
32	20	21	7	BOTM7
32	22	24	7	BOTM9
33	6	8	7	BOTM3
33	9	11	7	BOTM5
33	12	16	7	BOTM7
33	17	19	7	BOTM5
33	20	21	7	BOTM7
33	22	24	7	BOTM9
34		6	7	BOTM5
34	7	8	7	BOTM3
34	9	10	7	BOTM5
34	11	14	7	BOTM7
34		15	7	BOTM8
34	16	17	7	BOTM7
34	18	19	7	BOTM5
34	20	22	7	BOTM7
34	23	25	7	BOTM9
35		7	7	BOTM5
35		8	7	BOTM3
35	9	10	7	BOTM5
35	11	14	7	BOTM7
35		15	7	BOTM8
35	16	17	7	BOTM7
35		18	7	BOTM5
35	19	26	7	BOTM7
36	6	7	7	BOTM7
36	8	9	7	BOTM5
36	10	13	7	BOTM7
36	14	15	7	BOTM8
36		16	7	BOTM7
36	17	27	7	BOTM5
37	7	12	7	BOTM7
37	13	14	7	BOTM8
37	15	16	7	BOTM7

Attachment 1.--Input file to define aquifer characteristics and  
hydraulic-head-dependent boundaries--Continued

37	17	7	BOTM5
37	18	7	BOTM3
37	19 20	7	BOTM5
37	22 24	7	BOTM3
37	25 27	7	BOTM5
38	6	7	BOTM7
38	7 12	7	BOTM5
38	13 15	7	BOTM7
38	16	7	BOTM5
38	17 19	7	BOTM3
38	20	7	BOTM5
38	21	7	BOTM3
38	23	7	BOTM3
38	26 28	7	BOTM3
39	6 10	7	BOTM5
39	11 12	7	BOTM3
39	13 14	7	BOTM5
39	15	7	BOTM7
39	16	7	BOTM5
39	17	7	BOTM3
39	18 19	7	BOTM2
39	20 21	7	BOTM3
39	23	7	BOTM3
39	27	7	BOTM2
39	28	7	BOTM3
40	6 11	7	BOTM5
40	12 13	7	BOTM3
40	14 15	7	BOTM5
40	16 17	7	BOTM3
40	18 21	7	BOTM2
40	23 24	7	BOTM2
40	27 28	7	BOTM2
41	7	7	BOTM5
41	9 11	7	BOTM5
41	12 15	7	BOTM3
41	16	7	BOTM2
41	18 21	7	BOTM2
42	7	7	BOTM5
42	10 11	7	BOTM5
42	12 15	7	BOTM3
42	18 19	7	BOTM2
43	11 12	7	BOTM5
43	13 14	7	BOTM3
43	15	7	BOTM2
44	11 13	7	BOTM5
44	14	7	BOTM2
45	11 12	7	BOTM5
45	13	7	BOTM3
45	14	7	BOTM2
46	10 12	7	BOTM5

Attachment 1.--Input file to define aquifer characteristics and  
hydraulic-head-dependent boundaries--Continued

46	13	7	BOTM3
46	14	7	BOTM2
47	10 11	7	BOTM5
47	12 13	7	BOTM3
47	14 15	7	BOTM2
48	8 11	7	BOTM5
48	12 13	7	BOTM3
48	14	7	BOTM2
49	6 8	7	BOTM5
49	10 11	7	BOTM5
49	13	7	BOTM3
37	22	7	PRMZIP
37	22	7	BOTZIP
39	27	7	BOTM3
40	27 28	7	BOTM3
39	21	7	BOTM5
40	20 21	7	BOTM5
41	21	7	BOTM5
40	19	7	BOTM3
41	20	7	BOTM3
26	7	7	PRMH9
28	5	7	PRMH7
28	11	7	PRMH7
14	11	7	PRMG9
22	11	7	PRMG9
24	25 11	7	PRMG9
25	26 6	7	PRMG9
28	7	7	PRMG7
29	11	7	PRMG7
36	26	7	PRMG5
12	7	7	PRMF5
15	7	7	PRMF5
18	13	7	PRMF9
19	14	7	PRMF9
19	16 17	7	PRMF9
20	16	7	PRMF8
20	17	7	PRMF9
21	17 18	7	PRMF9
22	23 18	7	PRMF9
24	4	7	PRMF5
25	19	7	PRMF9
26	17	7	PRMF7
26	18 21	7	PRMF9
27	6	7	PRMF7
27	18 21	7	PRMF9
27	22	7	PRMF11
28	21 22	7	PRMF9
36	8	7	PRMF5
40	19	7	PRMF3
36	23	7	PRMF5

Attachment 1.--Input file to define aquifer characteristics and  
hydraulic-head-dependent boundaries--Continued

37	24	7	PRMF3
37	25	7	PRMF5
39	27	7	PRMF3
12	15	7	PRMD9
20 22	14	7	PRMD8
23	14	7	PRMD9
24	15	7	PRMD9
25	15	7	PRMD7
26	16	7	PRMD7
28	17	7	PRMD7
30	16	7	PRMD5
34	16	7	PRMD7
33	22	7	PRMD9
34	22	7	PRMD7
34	23	7	PRMD9
35	23	7	PRMD7
36	22	7	PRMD5
38	23	7	PRMD3
39	21	7	PRMD5
40 20	21	7	PRMD5
40	27	7	PRMD3
41	20	7	PRMD3
41	21	7	PRMD5
18	14	7	PRMB9
19	15	7	PRMB8
20 21	13	7	PRMB9
27	17	7	PRMB7
28 18	20	7	PRMB9
29	18	7	PRMB7
29	20	7	PRMB7
29 21	22	7	PRMB9
30 33	17	7	PRMB5
30 31	22	7	PRMB9
34 35	17	7	PRMB7
34 35	18	7	PRMB5
35	21	7	PRMB7
36 18	20	7	PRMB5
40	28	7	PRMB3

END  
 ENDOFCUBES  
 \$NEWPP KP=1, TMAX=1, NUMT=1, CDLT=1.0, DELT=24, \$END  
 \$NEWELL ROW=0, \$END  
 \$NEWRIV \$END  
 \*XCODE  
 \*MASS STORE WAIT=ON WAITIME=60 BAKOUT:/SLV/OCT/BAKMG0  
 \*TRIXGL  
 A  
 REDEND2  
 \*DISPOSE DN=NEWOUT,TID=MFARV,FID=GAHMG,SF="CC",WAIT  
 \*DESTROY BAKIN  
 \*COPY BAKOUT BAKIN



Attachment 1.--Input file to define aquifer characteristics and  
hydraulic-head-dependent boundaries--Continued

```

*DESTROY BAKOUT INPUT OUTPUT NEWOUT
*FILE NAME=INPUT
$CONTROL    SELRES=.TRUE.,
             RESTRT=.TRUE.,
             ZRMBAL=.TRUE.,
$END
DUMMY
$INLIST
             ITMAX=5,          DAMP=0.0,
$END
SYMBOLS
THR          3
SVN          7
END
OUTPUT CUBES
             7 CUB   LSTBOT
             7 CUB   LSTPRM
             CUBTHRLST
             1 6 CUBSVNLST
END
ENDOFCUBES
$NEWPP      KP=1,   TMAX=1,   NUMT=1,   CDLT=1.0,   DELT=24,   $END
$NEWELL     ROW=0,   $END
$NEWRIV     $END
*XCORE                      */EXECUTE
*MASS STORE WAIT=ON WAITIME=60 BAKOUT:/SLV/OCT/BAKMG
*&                          OUTPUT:/SLV/OCT/OUTMG
*TRIXGL                      */EDIT TO  TRIM EXCESS
A
REDEND2
*DISPOSE DN=NEWOUT,TID=MFARV,FID=GAHMG,SF="CC",WAIT
*ENDJOB:

```

Attachment 2.--Input file for the 1950-79 transient simulation

```

GAHMK,STCRA.
*/JOB
*FILE NAME=INPUT
$CONTROL
    RESTRT=TRUE.,
    SELRES=.TRUE.,
    ZRMBAL=.TRUE.,
$END
DUMMY
$INLIST
    SY=7*0.20,
    NCUBES=0,
    CLSURE=0.05,
    ITMAX=25,
    NPER=2,
    MODPR=16,
    DAMP=1.0,
$END
HEADER
- - - GROUND-WATER FLOW MODEL OF SAN LUIS VALLEY NORTH OF SAN LUIS HILLS - - -
OCTOBER 1983 *** TRANSIENT 1950-69
END
SYMBOLS
S7      0.20
S6      0.00075
S5      0.001124
S4      0.00168
S3      0.00252
S2      0.003775
S1      0.00565
H       100
ZIP     0
ONE     1
END
3D INPUT
          H          ZIPZIP
          7          S7
          6          S6
          5          S5
          4          S4
          3          S3
          2          S2
          1          S1
END
OUTPUT CUBES
          1  7  DDN  LST
END
ENDOF CUBES
$NEWPP   KP=1,   TMAX=3650,   NUMT=100,   CDLT=1.0,   DELT=2190,
          QFAC=29*-150600,

```

Attachment 2.--Input file for the 1950-79 transient simulation---Continued

```

QFAC(30)=-0.04,
QFAC(40)=-0.04,
QFAC(58)=-150600,
QFAC(61)=-150600,
QFAC(62)=-150600,
$END
$NEWELL ROW= 5, COL=12, Q=.00000159, LAYER=7, QTYPE=1, $END A= 1
$NEWELL ROW= 5, COL=13, Q=.00000079, LAYER=7, QTYPE=1, $END A= 1
$NEWELL ROW= 6, COL=13, Q=.00000159, LAYER=7, QTYPE=1, $END A= 1
$NEWELL ROW= 6, COL=14, Q=.00000079, LAYER=7, QTYPE=1, $END A= 1
$NEWELL ROW= 7, COL=13, Q=.00000079, LAYER=7, QTYPE=1, $END A= 1
$NEWELL ROW= 7, COL=14, Q=.00000171, LAYER=7, QTYPE=1, $END A= 1
$NEWELL ROW= 7, COL=15, Q=.00000040, LAYER=7, QTYPE=1, $END A= 1
$NEWELL ROW= 5, COL=12, Q=.00000189, LAYER=6, QTYPE=1, $END A= 1
$NEWELL ROW= 5, COL=13, Q=.00000095, LAYER=6, QTYPE=1, $END A= 1
$NEWELL ROW= 6, COL=13, Q=.00000189, LAYER=6, QTYPE=1, $END A= 1
$NEWELL ROW= 6, COL=14, Q=.00000095, LAYER=6, QTYPE=1, $END A= 1
$NEWELL ROW= 7, COL=13, Q=.00000095, LAYER=6, QTYPE=1, $END A= 1
$NEWELL ROW= 7, COL=14, Q=.00000206, LAYER=6, QTYPE=1, $END A= 1
$NEWELL ROW= 7, COL=15, Q=.00000047, LAYER=6, QTYPE=1, $END A= 1
$NEWELL ROW= 5, COL=12, Q=.00000079, LAYER=5, QTYPE=1, $END A= 1
$NEWELL ROW= 5, COL=13, Q=.00000040, LAYER=5, QTYPE=1, $END A= 1
$NEWELL ROW= 6, COL=13, Q=.00000079, LAYER=5, QTYPE=1, $END A= 1
$NEWELL ROW= 6, COL=14, Q=.00000040, LAYER=5, QTYPE=1, $END A= 1
$NEWELL ROW= 7, COL=13, Q=.00000040, LAYER=5, QTYPE=1, $END A= 1
$NEWELL ROW= 7, COL=14, Q=.00000086, LAYER=5, QTYPE=1, $END A= 1
$NEWELL ROW= 7, COL=15, Q=.00000019, LAYER=5, QTYPE=1, $END A= 1
$NEWELL ROW= 5, COL=12, Q=.00000047, LAYER=4, QTYPE=1, $END A= 1
$NEWELL ROW= 5, COL=13, Q=.00000023, LAYER=4, QTYPE=1, $END A= 1
$NEWELL ROW= 6, COL=13, Q=.00000047, LAYER=4, QTYPE=1, $END A= 1
$NEWELL ROW= 6, COL=14, Q=.00000023, LAYER=4, QTYPE=1, $END A= 1
$NEWELL ROW= 7, COL=13, Q=.00000023, LAYER=4, QTYPE=1, $END A= 1
$NEWELL ROW= 7, COL=14, Q=.00000051, LAYER=4, QTYPE=1, $END A= 1
$NEWELL ROW= 7, COL=15, Q=.00000012, LAYER=4, QTYPE=1, $END A= 1
$NEWELL ROW=10, COL=14, Q=.00000235, LAYER=7, QTYPE=2, $END A= 2
$NEWELL ROW=10, COL=15, Q=.00000156, LAYER=7, QTYPE=2, $END A= 2
$NEWELL ROW=11, COL=14, Q=.00000235, LAYER=7, QTYPE=2, $END A= 2
$NEWELL ROW=11, COL=15, Q=.00000254, LAYER=7, QTYPE=2, $END A= 2
$NEWELL ROW=12, COL=13, Q=.00000079, LAYER=7, QTYPE=2, $END A= 2
$NEWELL ROW=12, COL=14, Q=.00000175, LAYER=7, QTYPE=2, $END A= 2
$NEWELL ROW=12, COL=15, Q=.00000293, LAYER=7, QTYPE=2, $END A= 2
$NEWELL ROW=12, COL=16, Q=.00000117, LAYER=7, QTYPE=2, $END A= 2
$NEWELL ROW=13, COL=13, Q=.00000039, LAYER=7, QTYPE=2, $END A= 2
$NEWELL ROW=13, COL=14, Q=.00000079, LAYER=7, QTYPE=2, $END A= 2
$NEWELL ROW=13, COL=15, Q=.00000235, LAYER=7, QTYPE=2, $END A= 2
$NEWELL ROW=14, COL=13, Q=.00000039, LAYER=7, QTYPE=2, $END A= 2
$NEWELL ROW=14, COL=14, Q=.00000039, LAYER=7, QTYPE=2, $END A= 2
$NEWELL ROW=15, COL=13, Q=.00000079, LAYER=7, QTYPE=2, $END A= 2
$NEWELL ROW=10, COL=14, Q=.00000188, LAYER=6, QTYPE=2, $END A= 2
$NEWELL ROW=10, COL=15, Q=.00000126, LAYER=6, QTYPE=2, $END A= 2
$NEWELL ROW=11, COL=14, Q=.00000188, LAYER=6, QTYPE=2, $END A= 2
$NEWELL ROW=11, COL=15, Q=.00000203, LAYER=6, QTYPE=2, $END A= 2

```

Attachment 2.--Input file for the 1950-79 transient simulation--Continued

\$NEWELL	ROW=12,	COL=13,	Q=.00000062,	LAYER=6,	QTYPE=2,	\$END	A= 2
\$NEWELL	ROW=12,	COL=14,	Q=.00000141,	LAYER=6,	QTYPE=2,	\$END	A= 2
\$NEWELL	ROW=12,	COL=15,	Q=.00000235,	LAYER=6,	QTYPE=2,	\$END	A= 2
\$NEWELL	ROW=12,	COL=16,	Q=.00000094,	LAYER=6,	QTYPE=2,	\$END	A= 2
\$NEWELL	ROW=13,	COL=13,	Q=.00000032,	LAYER=6,	QTYPE=2,	\$END	A= 2
\$NEWELL	ROW=13,	COL=14,	Q=.00000062,	LAYER=6,	QTYPE=2,	\$END	A= 2
\$NEWELL	ROW=13,	COL=15,	Q=.00000188,	LAYER=6,	QTYPE=2,	\$END	A= 2
\$NEWELL	ROW=14,	COL=13,	Q=.00000032,	LAYER=6,	QTYPE=2,	\$END	A= 2
\$NEWELL	ROW=14,	COL=14,	Q=.00000032,	LAYER=6,	QTYPE=2,	\$END	A= 2
\$NEWELL	ROW=15,	COL=13,	Q=.00000062,	LAYER=6,	QTYPE=2,	\$END	A= 2
\$NEWELL	ROW=10,	COL=14,	Q=.00000040,	LAYER=5,	QTYPE=2,	\$END	A= 2
\$NEWELL	ROW=10,	COL=15,	Q=.00000026,	LAYER=5,	QTYPE=2,	\$END	A= 2
\$NEWELL	ROW=11,	COL=14,	Q=.00000040,	LAYER=5,	QTYPE=2,	\$END	A= 2
\$NEWELL	ROW=11,	COL=15,	Q=.00000043,	LAYER=5,	QTYPE=2,	\$END	A= 2
\$NEWELL	ROW=12,	COL=13,	Q=.00000014,	LAYER=5,	QTYPE=2,	\$END	A= 2
\$NEWELL	ROW=12,	COL=14,	Q=.00000030,	LAYER=5,	QTYPE=2,	\$END	A= 2
\$NEWELL	ROW=12,	COL=15,	Q=.00000050,	LAYER=5,	QTYPE=2,	\$END	A= 2
\$NEWELL	ROW=12,	COL=16,	Q=.00000019,	LAYER=5,	QTYPE=2,	\$END	A= 2
\$NEWELL	ROW=13,	COL=13,	Q=.00000007,	LAYER=5,	QTYPE=2,	\$END	A= 2
\$NEWELL	ROW=13,	COL=14,	Q=.00000014,	LAYER=5,	QTYPE=2,	\$END	A= 2
\$NEWELL	ROW=13,	COL=15,	Q=.00000040,	LAYER=5,	QTYPE=2,	\$END	A= 2
\$NEWELL	ROW=14,	COL=13,	Q=.00000007,	LAYER=5,	QTYPE=2,	\$END	A= 2
\$NEWELL	ROW=14,	COL=14,	Q=.00000007,	LAYER=5,	QTYPE=2,	\$END	A= 2
\$NEWELL	ROW=15,	COL=13,	Q=.00000014,	LAYER=5,	QTYPE=2,	\$END	A= 2
\$NEWELL	ROW=10,	COL=14,	Q=.00000010,	LAYER=4,	QTYPE=2,	\$END	A= 2
\$NEWELL	ROW=10,	COL=15,	Q=.00000007,	LAYER=4,	QTYPE=2,	\$END	A= 2
\$NEWELL	ROW=11,	COL=14,	Q=.00000010,	LAYER=4,	QTYPE=2,	\$END	A= 2
\$NEWELL	ROW=11,	COL=15,	Q=.00000011,	LAYER=4,	QTYPE=2,	\$END	A= 2
\$NEWELL	ROW=12,	COL=13,	Q=.00000003,	LAYER=4,	QTYPE=2,	\$END	A= 2
\$NEWELL	ROW=12,	COL=14,	Q=.00000007,	LAYER=4,	QTYPE=2,	\$END	A= 2
\$NEWELL	ROW=12,	COL=15,	Q=.00000012,	LAYER=4,	QTYPE=2,	\$END	A= 2
\$NEWELL	ROW=12,	COL=16,	Q=.00000006,	LAYER=4,	QTYPE=2,	\$END	A= 2
\$NEWELL	ROW=13,	COL=13,	Q=.00000001,	LAYER=4,	QTYPE=2,	\$END	A= 2
\$NEWELL	ROW=13,	COL=14,	Q=.00000003,	LAYER=4,	QTYPE=2,	\$END	A= 2
\$NEWELL	ROW=13,	COL=15,	Q=.00000010,	LAYER=4,	QTYPE=2,	\$END	A= 2
\$NEWELL	ROW=14,	COL=13,	Q=.00000001,	LAYER=4,	QTYPE=2,	\$END	A= 2
\$NEWELL	ROW=14,	COL=14,	Q=.00000001,	LAYER=4,	QTYPE=2,	\$END	A= 2
\$NEWELL	ROW=15,	COL=13,	Q=.00000003,	LAYER=4,	QTYPE=2,	\$END	A= 2
\$NEWELL	ROW=10,	COL=14,	Q=.00000003,	LAYER=3,	QTYPE=2,	\$END	A= 2
\$NEWELL	ROW=10,	COL=15,	Q=.00000003,	LAYER=3,	QTYPE=2,	\$END	A= 2
\$NEWELL	ROW=11,	COL=14,	Q=.00000003,	LAYER=3,	QTYPE=2,	\$END	A= 2
\$NEWELL	ROW=11,	COL=15,	Q=.00000004,	LAYER=3,	QTYPE=2,	\$END	A= 2
\$NEWELL	ROW=12,	COL=13,	Q=.00000001,	LAYER=3,	QTYPE=2,	\$END	A= 2
\$NEWELL	ROW=12,	COL=14,	Q=.00000003,	LAYER=3,	QTYPE=2,	\$END	A= 2
\$NEWELL	ROW=12,	COL=15,	Q=.00000004,	LAYER=3,	QTYPE=2,	\$END	A= 2
\$NEWELL	ROW=12,	COL=16,	Q=.00000001,	LAYER=3,	QTYPE=2,	\$END	A= 2
\$NEWELL	ROW=13,	COL=13,	Q=.00000001,	LAYER=3,	QTYPE=2,	\$END	A= 2
\$NEWELL	ROW=13,	COL=14,	Q=.00000001,	LAYER=3,	QTYPE=2,	\$END	A= 2
\$NEWELL	ROW=13,	COL=15,	Q=.00000003,	LAYER=3,	QTYPE=2,	\$END	A= 2
\$NEWELL	ROW=14,	COL=13,	Q=.00000001,	LAYER=3,	QTYPE=2,	\$END	A= 2
\$NEWELL	ROW=14,	COL=14,	Q=.00000001,	LAYER=3,	QTYPE=2,	\$END	A= 2
\$NEWELL	ROW=15,	COL=13,	Q=.00000001,	LAYER=3,	QTYPE=2,	\$END	A= 2

## Attachment 2.--Input file for the 1950-79 transient simulation--Continued

\$NEWELL	ROW=12,	COL= 7,	Q=.000000021,	LAYER=7,	QTYPE=3,	\$END	A= 3
\$NEWELL	ROW=12,	COL= 8,	Q=.000000021,	LAYER=7,	QTYPE=3,	\$END	A= 3
\$NEWELL	ROW=12,	COL=11,	Q=.000000021,	LAYER=7,	QTYPE=3,	\$END	A= 3
\$NEWELL	ROW=12,	COL=12,	Q=.000000021,	LAYER=7,	QTYPE=3,	\$END	A= 3
\$NEWELL	ROW=13,	COL= 7,	Q=.000000288,	LAYER=7,	QTYPE=3,	\$END	A= 3
\$NEWELL	ROW=13,	COL= 8,	Q=.000000309,	LAYER=7,	QTYPE=3,	\$END	A= 3
\$NEWELL	ROW=13,	COL= 9,	Q=.000000288,	LAYER=7,	QTYPE=3,	\$END	A= 3
\$NEWELL	ROW=13,	COL=10,	Q=.000000268,	LAYER=7,	QTYPE=3,	\$END	A= 3
\$NEWELL	ROW=13,	COL=11,	Q=.000000083,	LAYER=7,	QTYPE=3,	\$END	A= 3
\$NEWELL	ROW=12,	COL= 7,	Q=.000000015,	LAYER=6,	QTYPE=3,	\$END	A= 3
\$NEWELL	ROW=12,	COL= 8,	Q=.000000015,	LAYER=6,	QTYPE=3,	\$END	A= 3
\$NEWELL	ROW=12,	COL=11,	Q=.000000015,	LAYER=6,	QTYPE=3,	\$END	A= 3
\$NEWELL	ROW=12,	COL=12,	Q=.000000015,	LAYER=6,	QTYPE=3,	\$END	A= 3
\$NEWELL	ROW=13,	COL= 7,	Q=.000000217,	LAYER=6,	QTYPE=3,	\$END	A= 3
\$NEWELL	ROW=13,	COL= 8,	Q=.000000232,	LAYER=6,	QTYPE=3,	\$END	A= 3
\$NEWELL	ROW=13,	COL= 9,	Q=.000000217,	LAYER=6,	QTYPE=3,	\$END	A= 3
\$NEWELL	ROW=13,	COL=10,	Q=.000000201,	LAYER=6,	QTYPE=3,	\$END	A= 3
\$NEWELL	ROW=13,	COL=11,	Q=.000000062,	LAYER=6,	QTYPE=3,	\$END	A= 3
\$NEWELL	ROW=12,	COL= 7,	Q=.000000003,	LAYER=5,	QTYPE=3,	\$END	A= 3
\$NEWELL	ROW=12,	COL= 8,	Q=.000000003,	LAYER=5,	QTYPE=3,	\$END	A= 3
\$NEWELL	ROW=12,	COL=11,	Q=.000000003,	LAYER=5,	QTYPE=3,	\$END	A= 3
\$NEWELL	ROW=12,	COL=12,	Q=.000000003,	LAYER=5,	QTYPE=3,	\$END	A= 3
\$NEWELL	ROW=13,	COL= 7,	Q=.000000036,	LAYER=5,	QTYPE=3,	\$END	A= 3
\$NEWELL	ROW=13,	COL= 8,	Q=.000000039,	LAYER=5,	QTYPE=3,	\$END	A= 3
\$NEWELL	ROW=13,	COL= 9,	Q=.000000036,	LAYER=5,	QTYPE=3,	\$END	A= 3
\$NEWELL	ROW=13,	COL=10,	Q=.000000035,	LAYER=5,	QTYPE=3,	\$END	A= 3
\$NEWELL	ROW=13,	COL=11,	Q=.000000011,	LAYER=5,	QTYPE=3,	\$END	A= 3
\$NEWELL	ROW=12,	COL= 7,	Q=.000000001,	LAYER=4,	QTYPE=3,	\$END	A= 3
\$NEWELL	ROW=12,	COL= 8,	Q=.000000001,	LAYER=4,	QTYPE=3,	\$END	A= 3
\$NEWELL	ROW=12,	COL=11,	Q=.000000001,	LAYER=4,	QTYPE=3,	\$END	A= 3
\$NEWELL	ROW=12,	COL=12,	Q=.000000001,	LAYER=4,	QTYPE=3,	\$END	A= 3
\$NEWELL	ROW=13,	COL= 7,	Q=.000000012,	LAYER=4,	QTYPE=3,	\$END	A= 3
\$NEWELL	ROW=13,	COL= 8,	Q=.000000012,	LAYER=4,	QTYPE=3,	\$END	A= 3
\$NEWELL	ROW=13,	COL= 9,	Q=.000000012,	LAYER=4,	QTYPE=3,	\$END	A= 3
\$NEWELL	ROW=13,	COL=10,	Q=.000000011,	LAYER=4,	QTYPE=3,	\$END	A= 3
\$NEWELL	ROW=13,	COL=11,	Q=.000000004,	LAYER=4,	QTYPE=3,	\$END	A= 3
\$NEWELL	ROW=14,	COL= 8,	Q=.000000270,	LAYER=7,	QTYPE=4,	\$END	A= 4
\$NEWELL	ROW=14,	COL= 9,	Q=.000000135,	LAYER=7,	QTYPE=4,	\$END	A= 4
\$NEWELL	ROW=15,	COL= 8,	Q=.000000270,	LAYER=7,	QTYPE=4,	\$END	A= 4
\$NEWELL	ROW=15,	COL= 9,	Q=.000000203,	LAYER=7,	QTYPE=4,	\$END	A= 4
\$NEWELL	ROW=14,	COL= 8,	Q=.000000277,	LAYER=6,	QTYPE=4,	\$END	A= 4
\$NEWELL	ROW=14,	COL= 9,	Q=.000000139,	LAYER=6,	QTYPE=4,	\$END	A= 4
\$NEWELL	ROW=15,	COL= 8,	Q=.000000277,	LAYER=6,	QTYPE=4,	\$END	A= 4
\$NEWELL	ROW=15,	COL= 9,	Q=.000000208,	LAYER=6,	QTYPE=4,	\$END	A= 4
\$NEWELL	ROW=14,	COL= 8,	Q=.000000052,	LAYER=5,	QTYPE=4,	\$END	A= 4
\$NEWELL	ROW=14,	COL= 9,	Q=.000000026,	LAYER=5,	QTYPE=4,	\$END	A= 4
\$NEWELL	ROW=15,	COL= 8,	Q=.000000052,	LAYER=5,	QTYPE=4,	\$END	A= 4
\$NEWELL	ROW=15,	COL= 9,	Q=.000000040,	LAYER=5,	QTYPE=4,	\$END	A= 4
\$NEWELL	ROW=14,	COL= 8,	Q=.000000022,	LAYER=4,	QTYPE=4,	\$END	A= 4
\$NEWELL	ROW=14,	COL= 9,	Q=.000000011,	LAYER=4,	QTYPE=4,	\$END	A= 4
\$NEWELL	ROW=15,	COL= 8,	Q=.000000022,	LAYER=4,	QTYPE=4,	\$END	A= 4
\$NEWELL	ROW=15,	COL= 9,	Q=.000000017,	LAYER=4,	QTYPE=4,	\$END	A= 4

Attachment 2.--Input file for the 1950-79 transient simulation--Continued

\$NEWELL	ROW=14,	COL= 8,	Q=.00000007,	LAYER=3,	QTYPE=4,	\$END	A= 4
\$NEWELL	ROW=14,	COL= 9,	Q=.00000004,	LAYER=3,	QTYPE=4,	\$END	A= 4
\$NEWELL	ROW=15,	COL= 8,	Q=.00000007,	LAYER=3,	QTYPE=4,	\$END	A= 4
\$NEWELL	ROW=15,	COL= 9,	Q=.00000006,	LAYER=3,	QTYPE=4,	\$END	A= 4
\$NEWELL	ROW=14,	COL=10,	Q=.00000112,	LAYER=7,	QTYPE=5,	\$END	A= 5
\$NEWELL	ROW=14,	COL=11,	Q=.00000120,	LAYER=7,	QTYPE=5,	\$END	A= 5
\$NEWELL	ROW=15,	COL=10,	Q=.00000048,	LAYER=7,	QTYPE=5,	\$END	A= 5
\$NEWELL	ROW=15,	COL=11,	Q=.00000055,	LAYER=7,	QTYPE=5,	\$END	A= 5
\$NEWELL	ROW=15,	COL=12,	Q=.00000080,	LAYER=7,	QTYPE=5,	\$END	A= 5
\$NEWELL	ROW=15,	COL=14,	Q=.00000032,	LAYER=7,	QTYPE=5,	\$END	A= 5
\$NEWELL	ROW=16,	COL= 7,	Q=.00000023,	LAYER=7,	QTYPE=5,	\$END	A= 5
\$NEWELL	ROW=16,	COL= 8,	Q=.00000127,	LAYER=7,	QTYPE=5,	\$END	A= 5
\$NEWELL	ROW=16,	COL= 9,	Q=.00000032,	LAYER=7,	QTYPE=5,	\$END	A= 5
\$NEWELL	ROW=16,	COL=10,	Q=.00000048,	LAYER=7,	QTYPE=5,	\$END	A= 5
\$NEWELL	ROW=16,	COL=12,	Q=.00000080,	LAYER=7,	QTYPE=5,	\$END	A= 5
\$NEWELL	ROW=16,	COL=13,	Q=.00000063,	LAYER=7,	QTYPE=5,	\$END	A= 5
\$NEWELL	ROW=16,	COL=15,	Q=.00000063,	LAYER=7,	QTYPE=5,	\$END	A= 5
\$NEWELL	ROW=17,	COL= 7,	Q=.00000048,	LAYER=7,	QTYPE=5,	\$END	A= 5
\$NEWELL	ROW=17,	COL= 8,	Q=.00000080,	LAYER=7,	QTYPE=5,	\$END	A= 5
\$NEWELL	ROW=17,	COL=12,	Q=.00000017,	LAYER=7,	QTYPE=5,	\$END	A= 5
\$NEWELL	ROW=17,	COL=13,	Q=.00000048,	LAYER=7,	QTYPE=5,	\$END	A= 5
\$NEWELL	ROW=18,	COL= 7,	Q=.00000095,	LAYER=7,	QTYPE=5,	\$END	A= 5
\$NEWELL	ROW=18,	COL= 8,	Q=.00000127,	LAYER=7,	QTYPE=5,	\$END	A= 5
\$NEWELL	ROW=18,	COL= 9,	Q=.00000048,	LAYER=7,	QTYPE=5,	\$END	A= 5
\$NEWELL	ROW=19,	COL= 7,	Q=.00000104,	LAYER=7,	QTYPE=5,	\$END	A= 5
\$NEWELL	ROW=19,	COL= 8,	Q=.00000095,	LAYER=7,	QTYPE=5,	\$END	A= 5
\$NEWELL	ROW=14,	COL=10,	Q=.00000119,	LAYER=6,	QTYPE=5,	\$END	A= 5
\$NEWELL	ROW=14,	COL=11,	Q=.00000127,	LAYER=6,	QTYPE=5,	\$END	A= 5
\$NEWELL	ROW=15,	COL=10,	Q=.00000051,	LAYER=6,	QTYPE=5,	\$END	A= 5
\$NEWELL	ROW=15,	COL=11,	Q=.00000059,	LAYER=6,	QTYPE=5,	\$END	A= 5
\$NEWELL	ROW=15,	COL=12,	Q=.00000084,	LAYER=6,	QTYPE=5,	\$END	A= 5
\$NEWELL	ROW=15,	COL=14,	Q=.00000035,	LAYER=6,	QTYPE=5,	\$END	A= 5
\$NEWELL	ROW=16,	COL= 7,	Q=.00000025,	LAYER=6,	QTYPE=5,	\$END	A= 5
\$NEWELL	ROW=16,	COL= 8,	Q=.00000135,	LAYER=6,	QTYPE=5,	\$END	A= 5
\$NEWELL	ROW=16,	COL= 9,	Q=.00000035,	LAYER=6,	QTYPE=5,	\$END	A= 5
\$NEWELL	ROW=16,	COL=10,	Q=.00000051,	LAYER=6,	QTYPE=5,	\$END	A= 5
\$NEWELL	ROW=16,	COL=12,	Q=.00000084,	LAYER=6,	QTYPE=5,	\$END	A= 5
\$NEWELL	ROW=16,	COL=13,	Q=.00000068,	LAYER=6,	QTYPE=5,	\$END	A= 5
\$NEWELL	ROW=16,	COL=15,	Q=.00000068,	LAYER=6,	QTYPE=5,	\$END	A= 5
\$NEWELL	ROW=17,	COL= 7,	Q=.00000051,	LAYER=6,	QTYPE=5,	\$END	A= 5
\$NEWELL	ROW=17,	COL= 8,	Q=.00000084,	LAYER=6,	QTYPE=5,	\$END	A= 5
\$NEWELL	ROW=17,	COL=12,	Q=.00000017,	LAYER=6,	QTYPE=5,	\$END	A= 5
\$NEWELL	ROW=17,	COL=13,	Q=.00000051,	LAYER=6,	QTYPE=5,	\$END	A= 5
\$NEWELL	ROW=18,	COL= 7,	Q=.00000102,	LAYER=6,	QTYPE=5,	\$END	A= 5
\$NEWELL	ROW=18,	COL= 8,	Q=.00000135,	LAYER=6,	QTYPE=5,	\$END	A= 5
\$NEWELL	ROW=18,	COL= 9,	Q=.00000051,	LAYER=6,	QTYPE=5,	\$END	A= 5
\$NEWELL	ROW=19,	COL= 7,	Q=.00000110,	LAYER=6,	QTYPE=5,	\$END	A= 5
\$NEWELL	ROW=19,	COL= 8,	Q=.00000102,	LAYER=6,	QTYPE=5,	\$END	A= 5
\$NEWELL	ROW=14,	COL=10,	Q=.00000105,	LAYER=5,	QTYPE=5,	\$END	A= 5
\$NEWELL	ROW=14,	COL=11,	Q=.00000112,	LAYER=5,	QTYPE=5,	\$END	A= 5
\$NEWELL	ROW=15,	COL=10,	Q=.00000044,	LAYER=5,	QTYPE=5,	\$END	A= 5
\$NEWELL	ROW=15,	COL=11,	Q=.00000052,	LAYER=5,	QTYPE=5,	\$END	A= 5

## Attachment 2.--Input file for the 1950-79 transient simulation--Continued

\$NEWELL	ROW=15,	COL=12,	Q=.00000090,	LAYER=5,	QTYPE=5,	\$END	A= 5
\$NEWELL	ROW=15,	COL=14,	Q=.00000030,	LAYER=5,	QTYPE=5,	\$END	A= 5
\$NEWELL	ROW=16,	COL= 7,	Q=.00000022,	LAYER=5,	QTYPE=5,	\$END	A= 5
\$NEWELL	ROW=16,	COL= 8,	Q=.00000119,	LAYER=5,	QTYPE=5,	\$END	A= 5
\$NEWELL	ROW=16,	COL= 9,	Q=.00000030,	LAYER=5,	QTYPE=5,	\$END	A= 5
\$NEWELL	ROW=16,	COL=10,	Q=.00000044,	LAYER=5,	QTYPE=5,	\$END	A= 5
\$NEWELL	ROW=16,	COL=12,	Q=.00000075,	LAYER=5,	QTYPE=5,	\$END	A= 5
\$NEWELL	ROW=16,	COL=13,	Q=.00000059,	LAYER=5,	QTYPE=5,	\$END	A= 5
\$NEWELL	ROW=16,	COL=15,	Q=.00000059,	LAYER=5,	QTYPE=5,	\$END	A= 5
\$NEWELL	ROW=17,	COL= 7,	Q=.00000044,	LAYER=5,	QTYPE=5,	\$END	A= 5
\$NEWELL	ROW=17,	COL= 8,	Q=.00000075,	LAYER=5,	QTYPE=5,	\$END	A= 5
\$NEWELL	ROW=17,	COL=12,	Q=.00000015,	LAYER=5,	QTYPE=5,	\$END	A= 5
\$NEWELL	ROW=17,	COL=13,	Q=.00000044,	LAYER=5,	QTYPE=5,	\$END	A= 5
\$NEWELL	ROW=18,	COL= 7,	Q=.00000090,	LAYER=5,	QTYPE=5,	\$END	A= 5
\$NEWELL	ROW=18,	COL= 8,	Q=.00000119,	LAYER=5,	QTYPE=5,	\$END	A= 5
\$NEWELL	ROW=18,	COL= 9,	Q=.00000044,	LAYER=5,	QTYPE=5,	\$END	A= 5
\$NEWELL	ROW=19,	COL= 7,	Q=.00000097,	LAYER=5,	QTYPE=5,	\$END	A= 5
\$NEWELL	ROW=19,	COL= 8,	Q=.00000090,	LAYER=5,	QTYPE=5,	\$END	A= 5
\$NEWELL	ROW=14,	COL=10,	Q=.00000155,	LAYER=4,	QTYPE=5,	\$END	A= 5
\$NEWELL	ROW=14,	COL=11,	Q=.00000166,	LAYER=4,	QTYPE=5,	\$END	A= 5
\$NEWELL	ROW=15,	COL=10,	Q=.00000066,	LAYER=4,	QTYPE=5,	\$END	A= 5
\$NEWELL	ROW=15,	COL=11,	Q=.00000177,	LAYER=4,	QTYPE=5,	\$END	A= 5
\$NEWELL	ROW=15,	COL=12,	Q=.00000132,	LAYER=4,	QTYPE=5,	\$END	A= 5
\$NEWELL	ROW=15,	COL=14,	Q=.00000044,	LAYER=4,	QTYPE=5,	\$END	A= 5
\$NEWELL	ROW=16,	COL= 7,	Q=.00000033,	LAYER=4,	QTYPE=5,	\$END	A= 5
\$NEWELL	ROW=16,	COL= 8,	Q=.00000177,	LAYER=4,	QTYPE=5,	\$END	A= 5
\$NEWELL	ROW=16,	COL= 9,	Q=.00000044,	LAYER=4,	QTYPE=5,	\$END	A= 5
\$NEWELL	ROW=16,	COL=10,	Q=.00000066,	LAYER=4,	QTYPE=5,	\$END	A= 5
\$NEWELL	ROW=16,	COL=12,	Q=.00000110,	LAYER=4,	QTYPE=5,	\$END	A= 5
\$NEWELL	ROW=16,	COL=13,	Q=.00000088,	LAYER=4,	QTYPE=5,	\$END	A= 5
\$NEWELL	ROW=16,	COL=15,	Q=.00000088,	LAYER=4,	QTYPE=5,	\$END	A= 5
\$NEWELL	ROW=17,	COL= 7,	Q=.00000066,	LAYER=4,	QTYPE=5,	\$END	A= 5
\$NEWELL	ROW=17,	COL= 8,	Q=.00000110,	LAYER=4,	QTYPE=5,	\$END	A= 5
\$NEWELL	ROW=17,	COL=12,	Q=.00000022,	LAYER=4,	QTYPE=5,	\$END	A= 5
\$NEWELL	ROW=17,	COL=13,	Q=.00000066,	LAYER=4,	QTYPE=5,	\$END	A= 5
\$NEWELL	ROW=18,	COL= 7,	Q=.00000132,	LAYER=4,	QTYPE=5,	\$END	A= 5
\$NEWELL	ROW=18,	COL= 8,	Q=.00000177,	LAYER=4,	QTYPE=5,	\$END	A= 5
\$NEWELL	ROW=18,	COL= 9,	Q=.00000066,	LAYER=4,	QTYPE=5,	\$END	A= 5
\$NEWELL	ROW=19,	COL= 7,	Q=.00000144,	LAYER=4,	QTYPE=5,	\$END	A= 5
\$NEWELL	ROW=19,	COL= 8,	Q=.00000132,	LAYER=4,	QTYPE=5,	\$END	A= 5
\$NEWELL	ROW=14,	COL=10,	Q=.00000065,	LAYER=3,	QTYPE=5,	\$END	A= 5
\$NEWELL	ROW=14,	COL=11,	Q=.00000069,	LAYER=3,	QTYPE=5,	\$END	A= 5
\$NEWELL	ROW=15,	COL=10,	Q=.00000028,	LAYER=3,	QTYPE=5,	\$END	A= 5
\$NEWELL	ROW=15,	COL=11,	Q=.00000032,	LAYER=3,	QTYPE=5,	\$END	A= 5
\$NEWELL	ROW=15,	COL=12,	Q=.00000046,	LAYER=3,	QTYPE=5,	\$END	A= 5
\$NEWELL	ROW=15,	COL=14,	Q=.00000018,	LAYER=3,	QTYPE=5,	\$END	A= 5
\$NEWELL	ROW=16,	COL= 7,	Q=.00000014,	LAYER=3,	QTYPE=5,	\$END	A= 5
\$NEWELL	ROW=16,	COL= 8,	Q=.00000075,	LAYER=3,	QTYPE=5,	\$END	A= 5
\$NEWELL	ROW=16,	COL= 9,	Q=.00000018,	LAYER=3,	QTYPE=5,	\$END	A= 5
\$NEWELL	ROW=16,	COL=10,	Q=.00000028,	LAYER=3,	QTYPE=5,	\$END	A= 5
\$NEWELL	ROW=16,	COL=12,	Q=.00000046,	LAYER=3,	QTYPE=5,	\$END	A= 5
\$NEWELL	ROW=16,	COL=13,	Q=.00000037,	LAYER=3,	QTYPE=5,	\$END	A= 5

## Attachment 2.--Input file for the 1950-79 transient simulation--Continued

\$NEWELL	ROW=16,	COL=15,	Q=.00000037,	LAYER=3,	QTYPE=5,	\$END	A= 5
\$NEWELL	ROW=17,	COL= 7,	Q=.00000028,	LAYER=3,	QTYPE=5,	\$END	A= 5
\$NEWELL	ROW=17,	COL= 8,	Q=.00000046,	LAYER=3,	QTYPE=5,	\$END	A= 5
\$NEWELL	ROW=17,	COL=12,	Q=.00000010,	LAYER=3,	QTYPE=5,	\$END	A= 5
\$NEWELL	ROW=17,	COL=13,	Q=.00000028,	LAYER=3,	QTYPE=5,	\$END	A= 5
\$NEWELL	ROW=18,	COL= 7,	Q=.00000055,	LAYER=3,	QTYPE=5,	\$END	A= 5
\$NEWELL	ROW=18,	COL= 8,	Q=.00000075,	LAYER=3,	QTYPE=5,	\$END	A= 5
\$NEWELL	ROW=18,	COL= 9,	Q=.00000028,	LAYER=3,	QTYPE=5,	\$END	A= 5
\$NEWELL	ROW=19,	COL= 7,	Q=.00000061,	LAYER=3,	QTYPE=5,	\$END	A= 5
\$NEWELL	ROW=19,	COL= 8,	Q=.00000055,	LAYER=3,	QTYPE=5,	\$END	A= 5
\$NEWELL	ROW=16,	COL=17,	Q=.00000102,	LAYER=7,	QTYPE=6,	\$END	A= 6
\$NEWELL	ROW=16,	COL=18,	Q=.00000102,	LAYER=7,	QTYPE=6,	\$END	A= 6
\$NEWELL	ROW=16,	COL=19,	Q=.00000102,	LAYER=7,	QTYPE=6,	\$END	A= 6
\$NEWELL	ROW=17,	COL=16,	Q=.00000102,	LAYER=7,	QTYPE=6,	\$END	A= 6
\$NEWELL	ROW=17,	COL=17,	Q=.00000315,	LAYER=7,	QTYPE=6,	\$END	A= 6
\$NEWELL	ROW=16,	COL=17,	Q=.00000057,	LAYER=6,	QTYPE=6,	\$END	A= 6
\$NEWELL	ROW=16,	COL=18,	Q=.00000057,	LAYER=6,	QTYPE=6,	\$END	A= 6
\$NEWELL	ROW=16,	COL=19,	Q=.00000057,	LAYER=6,	QTYPE=6,	\$END	A= 6
\$NEWELL	ROW=17,	COL=16,	Q=.00000057,	LAYER=6,	QTYPE=6,	\$END	A= 6
\$NEWELL	ROW=17,	COL=17,	Q=.00000155,	LAYER=6,	QTYPE=6,	\$END	A= 6
\$NEWELL	ROW=19,	COL= 6,	Q=.00000063,	LAYER=7,	QTYPE=7,	\$END	A= 7
\$NEWELL	ROW=20,	COL= 6,	Q=.00000084,	LAYER=7,	QTYPE=7,	\$END	A= 7
\$NEWELL	ROW=21,	COL= 6,	Q=.00000092,	LAYER=7,	QTYPE=7,	\$END	A= 7
\$NEWELL	ROW=22,	COL= 5,	Q=.00000070,	LAYER=7,	QTYPE=7,	\$END	A= 7
\$NEWELL	ROW=19,	COL= 6,	Q=.00000178,	LAYER=6,	QTYPE=7,	\$END	A= 7
\$NEWELL	ROW=20,	COL= 6,	Q=.00000237,	LAYER=6,	QTYPE=7,	\$END	A= 7
\$NEWELL	ROW=21,	COL= 6,	Q=.00000257,	LAYER=6,	QTYPE=7,	\$END	A= 7
\$NEWELL	ROW=22,	COL= 5,	Q=.00000197,	LAYER=6,	QTYPE=7,	\$END	A= 7
\$NEWELL	ROW=19,	COL= 6,	Q=.00000115,	LAYER=5,	QTYPE=7,	\$END	A= 7
\$NEWELL	ROW=20,	COL= 6,	Q=.00000153,	LAYER=5,	QTYPE=7,	\$END	A= 7
\$NEWELL	ROW=21,	COL= 6,	Q=.00000166,	LAYER=5,	QTYPE=7,	\$END	A= 7
\$NEWELL	ROW=22,	COL= 5,	Q=.00000127,	LAYER=5,	QTYPE=7,	\$END	A= 7
\$NEWELL	ROW=20,	COL= 7,	Q=.00000072,	LAYER=7,	QTYPE=58,	\$END	A= 8
\$NEWELL	ROW=20,	COL= 8,	Q=.00000072,	LAYER=7,	QTYPE=8,	\$END	A= 8
\$NEWELL	ROW=20,	COL= 9,	Q=.00000072,	LAYER=7,	QTYPE=8,	\$END	A= 8
\$NEWELL	ROW=20,	COL=10,	Q=.00000072,	LAYER=7,	QTYPE=8,	\$END	A= 8
\$NEWELL	ROW=20,	COL=11,	Q=.00000028,	LAYER=7,	QTYPE=8,	\$END	A= 8
\$NEWELL	ROW=21,	COL= 7,	Q=.00000072,	LAYER=7,	QTYPE=58,	\$END	A= 8
\$NEWELL	ROW=21,	COL= 8,	Q=.00000072,	LAYER=7,	QTYPE=8,	\$END	A= 8
\$NEWELL	ROW=21,	COL= 9,	Q=.00000072,	LAYER=7,	QTYPE=8,	\$END	A= 8
\$NEWELL	ROW=21,	COL=10,	Q=.00000072,	LAYER=7,	QTYPE=8,	\$END	A= 8
\$NEWELL	ROW=21,	COL=11,	Q=.00000036,	LAYER=7,	QTYPE=8,	\$END	A= 8
\$NEWELL	ROW=20,	COL= 7,	Q=.00000046,	LAYER=6,	QTYPE=58,	\$END	A= 8
\$NEWELL	ROW=20,	COL= 8,	Q=.00000046,	LAYER=6,	QTYPE=8,	\$END	A= 8
\$NEWELL	ROW=20,	COL= 9,	Q=.00000046,	LAYER=6,	QTYPE=8,	\$END	A= 8
\$NEWELL	ROW=20,	COL=10,	Q=.00000046,	LAYER=6,	QTYPE=8,	\$END	A= 8
\$NEWELL	ROW=20,	COL=11,	Q=.00000017,	LAYER=6,	QTYPE=8,	\$END	A= 8
\$NEWELL	ROW=21,	COL= 7,	Q=.00000046,	LAYER=6,	QTYPE=58,	\$END	A= 8
\$NEWELL	ROW=21,	COL= 8,	Q=.00000046,	LAYER=6,	QTYPE=8,	\$END	A= 8
\$NEWELL	ROW=21,	COL= 9,	Q=.00000046,	LAYER=6,	QTYPE=8,	\$END	A= 8
\$NEWELL	ROW=21,	COL=10,	Q=.00000046,	LAYER=6,	QTYPE=8,	\$END	A= 8
\$NEWELL	ROW=21,	COL=11,	Q=.00000022,	LAYER=6,	QTYPE=8,	\$END	A= 8



Attachment 2.--Input file for the 1950-79 transient simulation--Continued

\$NEWELL	ROW=20,	COL= 7,	Q=.00000145,	LAYER=5,	QTYPE=58,	\$END	A= 8
\$NEWELL	ROW=20,	COL= 8,	Q=.00000145,	LAYER=5,	QTYPE=8,	\$END	A= 8
\$NEWELL	ROW=20,	COL= 9,	Q=.00000145,	LAYER=5,	QTYPE=8,	\$END	A= 8
\$NEWELL	ROW=20,	COL=10,	Q=.00000145,	LAYER=5,	QTYPE=8,	\$END	A= 8
\$NEWELL	ROW=20,	COL=11,	Q=.00000054,	LAYER=5,	QTYPE=8,	\$END	A= 8
\$NEWELL	ROW=21,	COL= 7,	Q=.00000145,	LAYER=5,	QTYPE=58,	\$END	A= 8
\$NEWELL	ROW=21,	COL= 8,	Q=.00000145,	LAYER=5,	QTYPE=8,	\$END	A= 8
\$NEWELL	ROW=21,	COL= 9,	Q=.00000145,	LAYER=5,	QTYPE=8,	\$END	A= 8
\$NEWELL	ROW=21,	COL=10,	Q=.00000145,	LAYER=5,	QTYPE=8,	\$END	A= 8
\$NEWELL	ROW=21,	COL=11,	Q=.00000072,	LAYER=5,	QTYPE=8,	\$END	A= 8
\$NEWELL	ROW=20,	COL= 7,	Q=.00000253,	LAYER=4,	QTYPE=58,	\$END	A= 8
\$NEWELL	ROW=20,	COL= 8,	Q=.00000253,	LAYER=4,	QTYPE=8,	\$END	A= 8
\$NEWELL	ROW=20,	COL= 9,	Q=.00000253,	LAYER=4,	QTYPE=8,	\$END	A= 8
\$NEWELL	ROW=20,	COL=10,	Q=.00000253,	LAYER=4,	QTYPE=8,	\$END	A= 8
\$NEWELL	ROW=20,	COL=11,	Q=.00000095,	LAYER=4,	QTYPE=8,	\$END	A= 8
\$NEWELL	ROW=21,	COL= 7,	Q=.00000253,	LAYER=4,	QTYPE=58,	\$END	A= 8
\$NEWELL	ROW=21,	COL= 8,	Q=.00000253,	LAYER=4,	QTYPE=8,	\$END	A= 8
\$NEWELL	ROW=21,	COL= 9,	Q=.00000253,	LAYER=4,	QTYPE=8,	\$END	A= 8
\$NEWELL	ROW=21,	COL=10,	Q=.00000253,	LAYER=4,	QTYPE=8,	\$END	A= 8
\$NEWELL	ROW=21,	COL=11,	Q=.00000127,	LAYER=4,	QTYPE=8,	\$END	A= 8
\$NEWELL	ROW=20,	COL= 7,	Q=.00000117,	LAYER=3,	QTYPE=58,	\$END	A= 8
\$NEWELL	ROW=20,	COL= 8,	Q=.00000117,	LAYER=3,	QTYPE=8,	\$END	A= 8
\$NEWELL	ROW=20,	COL= 9,	Q=.00000117,	LAYER=3,	QTYPE=8,	\$END	A= 8
\$NEWELL	ROW=20,	COL=10,	Q=.00000117,	LAYER=3,	QTYPE=8,	\$END	A= 8
\$NEWELL	ROW=20,	COL=11,	Q=.00000044,	LAYER=3,	QTYPE=8,	\$END	A= 8
\$NEWELL	ROW=21,	COL= 7,	Q=.00000117,	LAYER=3,	QTYPE=58,	\$END	A= 8
\$NEWELL	ROW=21,	COL= 8,	Q=.00000117,	LAYER=3,	QTYPE=8,	\$END	A= 8
\$NEWELL	ROW=21,	COL= 9,	Q=.00000117,	LAYER=3,	QTYPE=8,	\$END	A= 8
\$NEWELL	ROW=21,	COL=10,	Q=.00000117,	LAYER=3,	QTYPE=8,	\$END	A= 8
\$NEWELL	ROW=21,	COL=11,	Q=.00000059,	LAYER=3,	QTYPE=8,	\$END	A= 8
\$NEWELL	ROW=21,	COL=13,	Q=.00000121,	LAYER=7,	QTYPE=9,	\$END	A= 9
\$NEWELL	ROW=21,	COL=14,	Q=.00000091,	LAYER=7,	QTYPE=9,	\$END	A= 9
\$NEWELL	ROW=22,	COL=12,	Q=.00000363,	LAYER=7,	QTYPE=9,	\$END	A= 9
\$NEWELL	ROW=22,	COL=13,	Q=.00000061,	LAYER=7,	QTYPE=9,	\$END	A= 9
\$NEWELL	ROW=22,	COL=14,	Q=.00000211,	LAYER=7,	QTYPE=9,	\$END	A= 9
\$NEWELL	ROW=23,	COL=14,	Q=.00000483,	LAYER=7,	QTYPE=9,	\$END	A= 9
\$NEWELL	ROW=24,	COL=14,	Q=.00000483,	LAYER=7,	QTYPE=9,	\$END	A= 9
\$NEWELL	ROW=24,	COL=15,	Q=.00000150,	LAYER=7,	QTYPE=9,	\$END	A= 9
\$NEWELL	ROW=25,	COL=14,	Q=.00000333,	LAYER=7,	QTYPE=9,	\$END	A= 9
\$NEWELL	ROW=25,	COL=15,	Q=.00000363,	LAYER=7,	QTYPE=9,	\$END	A= 9
\$NEWELL	ROW=25,	COL=16,	Q=.00000302,	LAYER=7,	QTYPE=9,	\$END	A= 9
\$NEWELL	ROW=26,	COL=12,	Q=.00000302,	LAYER=7,	QTYPE=9,	\$END	A= 9
\$NEWELL	ROW=26,	COL=13,	Q=.00000363,	LAYER=7,	QTYPE=9,	\$END	A= 9
\$NEWELL	ROW=26,	COL=14,	Q=.00000422,	LAYER=7,	QTYPE=9,	\$END	A= 9
\$NEWELL	ROW=26,	COL=15,	Q=.00000181,	LAYER=7,	QTYPE=9,	\$END	A= 9
\$NEWELL	ROW=26,	COL=16,	Q=.00000272,	LAYER=7,	QTYPE=9,	\$END	A= 9
\$NEWELL	ROW=27,	COL=12,	Q=.00000483,	LAYER=7,	QTYPE=9,	\$END	A= 9
\$NEWELL	ROW=27,	COL=13,	Q=.00000302,	LAYER=7,	QTYPE=9,	\$END	A= 9
\$NEWELL	ROW=27,	COL=14,	Q=.00000483,	LAYER=7,	QTYPE=9,	\$END	A= 9
\$NEWELL	ROW=28,	COL=12,	Q=.00000453,	LAYER=7,	QTYPE=9,	\$END	A= 9
\$NEWELL	ROW=28,	COL=13,	Q=.00000211,	LAYER=7,	QTYPE=9,	\$END	A= 9
\$NEWELL	ROW=28,	COL=14,	Q=.00000483,	LAYER=7,	QTYPE=9,	\$END	A= 9

## Attachment 2.--Input file for the 1950-79 transient simulation--Continued

\$NEWELL	ROW=29,	COL=12,	Q=.00000242,	LAYER=7,	QTYPE=9,	\$END	A= 9
\$NEWELL	ROW=29,	COL=13,	Q=.00000483,	LAYER=7,	QTYPE=9,	\$END	A= 9
\$NEWELL	ROW=29,	COL=14,	Q=.00000242,	LAYER=7,	QTYPE=9,	\$END	A= 9
\$NEWELL	ROW=29,	COL=15,	Q=.00000363,	LAYER=7,	QTYPE=9,	\$END	A= 9
\$NEWELL	ROW=29,	COL=16,	Q=.00000302,	LAYER=7,	QTYPE=9,	\$END	A= 9
\$NEWELL	ROW=30,	COL=12,	Q=.00000483,	LAYER=7,	QTYPE=9,	\$END	A= 9
\$NEWELL	ROW=30,	COL=13,	Q=.00000302,	LAYER=7,	QTYPE=9,	\$END	A= 9
\$NEWELL	ROW=30,	COL=14,	Q=.00000363,	LAYER=7,	QTYPE=9,	\$END	A= 9
\$NEWELL	ROW=31,	COL=14,	Q=.00000030,	LAYER=7,	QTYPE=9,	\$END	A= 9
\$NEWELL	ROW=21,	COL=13,	Q=.00000033,	LAYER=6,	QTYPE=9,	\$END	A= 9
\$NEWELL	ROW=21,	COL=14,	Q=.00000025,	LAYER=6,	QTYPE=9,	\$END	A= 9
\$NEWELL	ROW=22,	COL=12,	Q=.00000131,	LAYER=6,	QTYPE=9,	\$END	A= 9
\$NEWELL	ROW=22,	COL=13,	Q=.00000017,	LAYER=6,	QTYPE=9,	\$END	A= 9
\$NEWELL	ROW=22,	COL=14,	Q=.00000057,	LAYER=6,	QTYPE=9,	\$END	A= 9
\$NEWELL	ROW=23,	COL=14,	Q=.00000131,	LAYER=6,	QTYPE=9,	\$END	A= 9
\$NEWELL	ROW=24,	COL=14,	Q=.00000131,	LAYER=6,	QTYPE=9,	\$END	A= 9
\$NEWELL	ROW=24,	COL=15,	Q=.00000041,	LAYER=6,	QTYPE=9,	\$END	A= 9
\$NEWELL	ROW=25,	COL=14,	Q=.00000090,	LAYER=6,	QTYPE=9,	\$END	A= 9
\$NEWELL	ROW=25,	COL=15,	Q=.00000098,	LAYER=6,	QTYPE=9,	\$END	A= 9
\$NEWELL	ROW=25,	COL=16,	Q=.00000081,	LAYER=6,	QTYPE=9,	\$END	A= 9
\$NEWELL	ROW=26,	COL=12,	Q=.00000081,	LAYER=6,	QTYPE=9,	\$END	A= 9
\$NEWELL	ROW=26,	COL=13,	Q=.00000098,	LAYER=6,	QTYPE=9,	\$END	A= 9
\$NEWELL	ROW=26,	COL=14,	Q=.00000115,	LAYER=6,	QTYPE=9,	\$END	A= 9
\$NEWELL	ROW=26,	COL=15,	Q=.00000050,	LAYER=6,	QTYPE=9,	\$END	A= 9
\$NEWELL	ROW=26,	COL=16,	Q=.00000073,	LAYER=6,	QTYPE=9,	\$END	A= 9
\$NEWELL	ROW=27,	COL=12,	Q=.00000131,	LAYER=6,	QTYPE=9,	\$END	A= 9
\$NEWELL	ROW=27,	COL=13,	Q=.00000081,	LAYER=6,	QTYPE=9,	\$END	A= 9
\$NEWELL	ROW=27,	COL=14,	Q=.00000131,	LAYER=6,	QTYPE=9,	\$END	A= 9
\$NEWELL	ROW=28,	COL=12,	Q=.00000123,	LAYER=6,	QTYPE=9,	\$END	A= 9
\$NEWELL	ROW=28,	COL=13,	Q=.00000057,	LAYER=6,	QTYPE=9,	\$END	A= 9
\$NEWELL	ROW=28,	COL=14,	Q=.00000131,	LAYER=6,	QTYPE=9,	\$END	A= 9
\$NEWELL	ROW=29,	COL=12,	Q=.00000065,	LAYER=6,	QTYPE=9,	\$END	A= 9
\$NEWELL	ROW=29,	COL=13,	Q=.00000131,	LAYER=6,	QTYPE=9,	\$END	A= 9
\$NEWELL	ROW=29,	COL=14,	Q=.00000065,	LAYER=6,	QTYPE=9,	\$END	A= 9
\$NEWELL	ROW=29,	COL=15,	Q=.00000098,	LAYER=6,	QTYPE=9,	\$END	A= 9
\$NEWELL	ROW=29,	COL=16,	Q=.00000081,	LAYER=6,	QTYPE=9,	\$END	A= 9
\$NEWELL	ROW=30,	COL=12,	Q=.00000131,	LAYER=6,	QTYPE=9,	\$END	A= 9
\$NEWELL	ROW=30,	COL=13,	Q=.00000081,	LAYER=6,	QTYPE=9,	\$END	A= 9
\$NEWELL	ROW=30,	COL=14,	Q=.00000098,	LAYER=6,	QTYPE=9,	\$END	A= 9
\$NEWELL	ROW=31,	COL=14,	Q=.00000008,	LAYER=6,	QTYPE=9,	\$END	A= 9
\$NEWELL	ROW=21,	COL=13,	Q=.00000001,	LAYER=5,	QTYPE=9,	\$END	A= 9
\$NEWELL	ROW=21,	COL=14,	Q=.00000001,	LAYER=5,	QTYPE=9,	\$END	A= 9
\$NEWELL	ROW=22,	COL=12,	Q=.00000004,	LAYER=5,	QTYPE=9,	\$END	A= 9
\$NEWELL	ROW=22,	COL=13,	Q=.00000001,	LAYER=5,	QTYPE=9,	\$END	A= 9
\$NEWELL	ROW=22,	COL=14,	Q=.00000001,	LAYER=5,	QTYPE=9,	\$END	A= 9
\$NEWELL	ROW=23,	COL=14,	Q=.00000004,	LAYER=5,	QTYPE=9,	\$END	A= 9
\$NEWELL	ROW=24,	COL=14,	Q=.00000004,	LAYER=5,	QTYPE=9,	\$END	A= 9
\$NEWELL	ROW=24,	COL=15,	Q=.00000001,	LAYER=5,	QTYPE=9,	\$END	A= 9
\$NEWELL	ROW=25,	COL=14,	Q=.00000003,	LAYER=5,	QTYPE=9,	\$END	A= 9
\$NEWELL	ROW=25,	COL=15,	Q=.00000003,	LAYER=5,	QTYPE=9,	\$END	A= 9
\$NEWELL	ROW=25,	COL=16,	Q=.00000003,	LAYER=5,	QTYPE=9,	\$END	A= 9
\$NEWELL	ROW=26,	COL=12,	Q=.00000003,	LAYER=5,	QTYPE=9,	\$END	A= 9

## Attachment 2.--Input file for the 1950-79 transient simulation--Continued

\$NEWELL	ROW=26,	COL=13,	Q=.00000003,	LAYER=5,	QTYPE=9,	\$END	A= 9
\$NEWELL	ROW=26,	COL=14,	Q=.00000004,	LAYER=5,	QTYPE=9,	\$END	A= 9
\$NEWELL	ROW=26,	COL=15,	Q=.00000001,	LAYER=5,	QTYPE=9,	\$END	A= 9
\$NEWELL	ROW=26,	COL=16,	Q=.00000003,	LAYER=5,	QTYPE=9,	\$END	A= 9
\$NEWELL	ROW=27,	COL=12,	Q=.00000004,	LAYER=5,	QTYPE=9,	\$END	A= 9
\$NEWELL	ROW=27,	COL=13,	Q=.00000003,	LAYER=5,	QTYPE=9,	\$END	A= 9
\$NEWELL	ROW=27,	COL=14,	Q=.00000004,	LAYER=5,	QTYPE=9,	\$END	A= 9
\$NEWELL	ROW=28,	COL=12,	Q=.00000004,	LAYER=5,	QTYPE=9,	\$END	A= 9
\$NEWELL	ROW=28,	COL=13,	Q=.00000001,	LAYER=5,	QTYPE=9,	\$END	A= 9
\$NEWELL	ROW=28,	COL=14,	Q=.00000004,	LAYER=5,	QTYPE=9,	\$END	A= 9
\$NEWELL	ROW=29,	COL=12,	Q=.00000003,	LAYER=5,	QTYPE=9,	\$END	A= 9
\$NEWELL	ROW=29,	COL=13,	Q=.00000004,	LAYER=5,	QTYPE=9,	\$END	A= 9
\$NEWELL	ROW=29,	COL=14,	Q=.00000003,	LAYER=5,	QTYPE=9,	\$END	A= 9
\$NEWELL	ROW=29,	COL=15,	Q=.00000003,	LAYER=5,	QTYPE=9,	\$END	A= 9
\$NEWELL	ROW=29,	COL=16,	Q=.00000003,	LAYER=5,	QTYPE=9,	\$END	A= 9
\$NEWELL	ROW=30,	COL=12,	Q=.00000004,	LAYER=5,	QTYPE=9,	\$END	A= 9
\$NEWELL	ROW=30,	COL=13,	Q=.00000003,	LAYER=5,	QTYPE=9,	\$END	A= 9
\$NEWELL	ROW=30,	COL=14,	Q=.00000003,	LAYER=5,	QTYPE=9,	\$END	A= 9
\$NEWELL	ROW=21,	COL=13,	Q=.00000001,	LAYER=4,	QTYPE=9,	\$END	A= 9
\$NEWELL	ROW=21,	COL=14,	Q=.00000001,	LAYER=4,	QTYPE=9,	\$END	A= 9
\$NEWELL	ROW=22,	COL=12,	Q=.00000007,	LAYER=4,	QTYPE=9,	\$END	A= 9
\$NEWELL	ROW=22,	COL=13,	Q=.00000001,	LAYER=4,	QTYPE=9,	\$END	A= 9
\$NEWELL	ROW=22,	COL=14,	Q=.00000003,	LAYER=4,	QTYPE=9,	\$END	A= 9
\$NEWELL	ROW=23,	COL=14,	Q=.00000007,	LAYER=4,	QTYPE=9,	\$END	A= 9
\$NEWELL	ROW=24,	COL=14,	Q=.00000007,	LAYER=4,	QTYPE=9,	\$END	A= 9
\$NEWELL	ROW=24,	COL=15,	Q=.00000003,	LAYER=4,	QTYPE=9,	\$END	A= 9
\$NEWELL	ROW=25,	COL=14,	Q=.00000006,	LAYER=4,	QTYPE=9,	\$END	A= 9
\$NEWELL	ROW=25,	COL=15,	Q=.00000006,	LAYER=4,	QTYPE=9,	\$END	A= 9
\$NEWELL	ROW=25,	COL=16,	Q=.00000004,	LAYER=4,	QTYPE=9,	\$END	A= 9
\$NEWELL	ROW=26,	COL=12,	Q=.00000004,	LAYER=4,	QTYPE=9,	\$END	A= 9
\$NEWELL	ROW=26,	COL=13,	Q=.00000006,	LAYER=4,	QTYPE=9,	\$END	A= 9
\$NEWELL	ROW=26,	COL=14,	Q=.00000007,	LAYER=4,	QTYPE=9,	\$END	A= 9
\$NEWELL	ROW=26,	COL=15,	Q=.00000003,	LAYER=4,	QTYPE=9,	\$END	A= 9
\$NEWELL	ROW=26,	COL=16,	Q=.00000004,	LAYER=4,	QTYPE=9,	\$END	A= 9
\$NEWELL	ROW=27,	COL=12,	Q=.00000007,	LAYER=4,	QTYPE=9,	\$END	A= 9
\$NEWELL	ROW=27,	COL=13,	Q=.00000004,	LAYER=4,	QTYPE=9,	\$END	A= 9
\$NEWELL	ROW=27,	COL=14,	Q=.00000007,	LAYER=4,	QTYPE=9,	\$END	A= 9
\$NEWELL	ROW=28,	COL=12,	Q=.00000007,	LAYER=4,	QTYPE=9,	\$END	A= 9
\$NEWELL	ROW=28,	COL=13,	Q=.00000003,	LAYER=4,	QTYPE=9,	\$END	A= 9
\$NEWELL	ROW=28,	COL=14,	Q=.00000007,	LAYER=4,	QTYPE=9,	\$END	A= 9
\$NEWELL	ROW=29,	COL=12,	Q=.00000004,	LAYER=4,	QTYPE=9,	\$END	A= 9
\$NEWELL	ROW=29,	COL=13,	Q=.00000007,	LAYER=4,	QTYPE=9,	\$END	A= 9
\$NEWELL	ROW=29,	COL=14,	Q=.00000004,	LAYER=4,	QTYPE=9,	\$END	A= 9
\$NEWELL	ROW=29,	COL=15,	Q=.00000006,	LAYER=4,	QTYPE=9,	\$END	A= 9
\$NEWELL	ROW=29,	COL=16,	Q=.00000004,	LAYER=4,	QTYPE=9,	\$END	A= 9
\$NEWELL	ROW=30,	COL=12,	Q=.00000007,	LAYER=4,	QTYPE=9,	\$END	A= 9
\$NEWELL	ROW=30,	COL=13,	Q=.00000004,	LAYER=4,	QTYPE=9,	\$END	A= 9
\$NEWELL	ROW=30,	COL=14,	Q=.00000006,	LAYER=4,	QTYPE=9,	\$END	A= 9
\$NEWELL	ROW=21,	COL=13,	Q=.00000001,	LAYER=3,	QTYPE=9,	\$END	A= 9
\$NEWELL	ROW=21,	COL=14,	Q=.00000001,	LAYER=3,	QTYPE=9,	\$END	A= 9
\$NEWELL	ROW=22,	COL=12,	Q=.00000007,	LAYER=3,	QTYPE=9,	\$END	A= 9
\$NEWELL	ROW=22,	COL=13,	Q=.00000001,	LAYER=3,	QTYPE=9,	\$END	A= 9

Attachment 2.--Input file for the 1950-79 transient simulation--Continued

\$NEWELL	ROW=22,	COL=14,	Q=.00000003,	LAYER=3,	QTYPE=9,	\$END	A= 9
\$NEWELL	ROW=23,	COL=14,	Q=.00000007,	LAYER=3,	QTYPE=9,	\$END	A= 9
\$NEWELL	ROW=24,	COL=14,	Q=.00000007,	LAYER=3,	QTYPE=9,	\$END	A= 9
\$NEWELL	ROW=24,	COL=15,	Q=.00000003,	LAYER=3,	QTYPE=9,	\$END	A= 9
\$NEWELL	ROW=25,	COL=14,	Q=.00000004,	LAYER=3,	QTYPE=9,	\$END	A= 9
\$NEWELL	ROW=25,	COL=15,	Q=.00000006,	LAYER=3,	QTYPE=9,	\$END	A= 9
\$NEWELL	ROW=25,	COL=16,	Q=.00000004,	LAYER=3,	QTYPE=9,	\$END	A= 9
\$NEWELL	ROW=26,	COL=12,	Q=.00000004,	LAYER=3,	QTYPE=9,	\$END	A= 9
\$NEWELL	ROW=26,	COL=13,	Q=.00000006,	LAYER=3,	QTYPE=9,	\$END	A= 9
\$NEWELL	ROW=26,	COL=14,	Q=.00000006,	LAYER=3,	QTYPE=9,	\$END	A= 9
\$NEWELL	ROW=26,	COL=15,	Q=.00000003,	LAYER=3,	QTYPE=9,	\$END	A= 9
\$NEWELL	ROW=26,	COL=16,	Q=.00000004,	LAYER=3,	QTYPE=9,	\$END	A= 9
\$NEWELL	ROW=27,	COL=12,	Q=.00000007,	LAYER=3,	QTYPE=9,	\$END	A= 9
\$NEWELL	ROW=27,	COL=13,	Q=.00000004,	LAYER=3,	QTYPE=9,	\$END	A= 9
\$NEWELL	ROW=27,	COL=14,	Q=.00000007,	LAYER=3,	QTYPE=9,	\$END	A= 9
\$NEWELL	ROW=28,	COL=12,	Q=.00000007,	LAYER=3,	QTYPE=9,	\$END	A= 9
\$NEWELL	ROW=28,	COL=13,	Q=.00000003,	LAYER=3,	QTYPE=9,	\$END	A= 9
\$NEWELL	ROW=28,	COL=14,	Q=.00000007,	LAYER=3,	QTYPE=9,	\$END	A= 9
\$NEWELL	ROW=29,	COL=12,	Q=.00000004,	LAYER=3,	QTYPE=9,	\$END	A= 9
\$NEWELL	ROW=29,	COL=13,	Q=.00000007,	LAYER=3,	QTYPE=9,	\$END	A= 9
\$NEWELL	ROW=29,	COL=14,	Q=.00000004,	LAYER=3,	QTYPE=9,	\$END	A= 9
\$NEWELL	ROW=29,	COL=15,	Q=.00000006,	LAYER=3,	QTYPE=9,	\$END	A= 9
\$NEWELL	ROW=29,	COL=16,	Q=.00000004,	LAYER=3,	QTYPE=9,	\$END	A= 9
\$NEWELL	ROW=30,	COL=12,	Q=.00000007,	LAYER=3,	QTYPE=9,	\$END	A= 9
\$NEWELL	ROW=30,	COL=13,	Q=.00000004,	LAYER=3,	QTYPE=9,	\$END	A= 9
\$NEWELL	ROW=30,	COL=14,	Q=.00000006,	LAYER=3,	QTYPE=9,	\$END	A= 9
\$NEWELL	ROW=22,	COL= 6,	Q=.00000413,	LAYER=7,	QTYPE=10,	\$END	A=10
\$NEWELL	ROW=23,	COL= 5,	Q=.00000206,	LAYER=7,	QTYPE=10,	\$END	A=10
\$NEWELL	ROW=23,	COL= 6,	Q=.00000413,	LAYER=7,	QTYPE=10,	\$END	A=10
\$NEWELL	ROW=24,	COL= 5,	Q=.00000232,	LAYER=7,	QTYPE=10,	\$END	A=10
\$NEWELL	ROW=24,	COL= 6,	Q=.00000413,	LAYER=7,	QTYPE=10,	\$END	A=10
\$NEWELL	ROW=25,	COL= 5,	Q=.00000310,	LAYER=7,	QTYPE=10,	\$END	A=10
\$NEWELL	ROW=25,	COL= 6,	Q=.00000413,	LAYER=7,	QTYPE=10,	\$END	A=10
\$NEWELL	ROW=26,	COL= 2,	Q=.00000232,	LAYER=7,	QTYPE=10,	\$END	A=10
\$NEWELL	ROW=26,	COL= 3,	Q=.00000310,	LAYER=7,	QTYPE=10,	\$END	A=10
\$NEWELL	ROW=26,	COL= 4,	Q=.00000258,	LAYER=7,	QTYPE=10,	\$END	A=10
\$NEWELL	ROW=26,	COL= 5,	Q=.00000413,	LAYER=7,	QTYPE=10,	\$END	A=10
\$NEWELL	ROW=27,	COL= 2,	Q=.00000103,	LAYER=7,	QTYPE=10,	\$END	A=10
\$NEWELL	ROW=27,	COL= 3,	Q=.00000258,	LAYER=7,	QTYPE=10,	\$END	A=10
\$NEWELL	ROW=27,	COL= 4,	Q=.00000413,	LAYER=7,	QTYPE=10,	\$END	A=10
\$NEWELL	ROW=22,	COL= 6,	Q=.00000202,	LAYER=6,	QTYPE=10,	\$END	A=10
\$NEWELL	ROW=23,	COL= 5,	Q=.00000101,	LAYER=6,	QTYPE=10,	\$END	A=10
\$NEWELL	ROW=23,	COL= 6,	Q=.00000202,	LAYER=6,	QTYPE=10,	\$END	A=10
\$NEWELL	ROW=24,	COL= 5,	Q=.00000114,	LAYER=6,	QTYPE=10,	\$END	A=10
\$NEWELL	ROW=24,	COL= 6,	Q=.00000202,	LAYER=6,	QTYPE=10,	\$END	A=10
\$NEWELL	ROW=25,	COL= 5,	Q=.00000152,	LAYER=6,	QTYPE=10,	\$END	A=10
\$NEWELL	ROW=25,	COL= 6,	Q=.00000202,	LAYER=6,	QTYPE=10,	\$END	A=10
\$NEWELL	ROW=26,	COL= 2,	Q=.00000114,	LAYER=6,	QTYPE=10,	\$END	A=10
\$NEWELL	ROW=26,	COL= 3,	Q=.00000152,	LAYER=6,	QTYPE=10,	\$END	A=10
\$NEWELL	ROW=26,	COL= 4,	Q=.00000126,	LAYER=6,	QTYPE=10,	\$END	A=10
\$NEWELL	ROW=26,	COL= 5,	Q=.00000202,	LAYER=6,	QTYPE=10,	\$END	A=10
\$NEWELL	ROW=27,	COL= 2,	Q=.00000051,	LAYER=6,	QTYPE=10,	\$END	A=10

## Attachment 2.--Input file for the 1950-79 transient simulation--Continued

\$NEWELL	ROW=27,	COL= 3,	Q=.00000126,	LAYER=6,	QTYPE=10,	\$END	A=10
\$NEWELL	ROW=27,	COL= 4,	Q=.00000202,	LAYER=6,	QTYPE=10,	\$END	A=10
\$NEWELL	ROW=22,	COL= 6,	Q=.00000015,	LAYER=5,	QTYPE=10,	\$END	A=10
\$NEWELL	ROW=23,	COL= 5,	Q=.00000008,	LAYER=5,	QTYPE=10,	\$END	A=10
\$NEWELL	ROW=23,	COL= 6,	Q=.00000015,	LAYER=5,	QTYPE=10,	\$END	A=10
\$NEWELL	ROW=24,	COL= 5,	Q=.00000009,	LAYER=5,	QTYPE=10,	\$END	A=10
\$NEWELL	ROW=24,	COL= 6,	Q=.00000015,	LAYER=5,	QTYPE=10,	\$END	A=10
\$NEWELL	ROW=25,	COL= 5,	Q=.00000011,	LAYER=5,	QTYPE=10,	\$END	A=10
\$NEWELL	ROW=25,	COL= 6,	Q=.00000015,	LAYER=5,	QTYPE=10,	\$END	A=10
\$NEWELL	ROW=26,	COL= 2,	Q=.00000009,	LAYER=5,	QTYPE=10,	\$END	A=10
\$NEWELL	ROW=26,	COL= 3,	Q=.00000011,	LAYER=5,	QTYPE=10,	\$END	A=10
\$NEWELL	ROW=26,	COL= 4,	Q=.00000009,	LAYER=5,	QTYPE=10,	\$END	A=10
\$NEWELL	ROW=26,	COL= 5,	Q=.00000015,	LAYER=5,	QTYPE=10,	\$END	A=10
\$NEWELL	ROW=27,	COL= 2,	Q=.00000004,	LAYER=5,	QTYPE=10,	\$END	A=10
\$NEWELL	ROW=27,	COL= 3,	Q=.00000009,	LAYER=5,	QTYPE=10,	\$END	A=10
\$NEWELL	ROW=27,	COL= 4,	Q=.00000015,	LAYER=5,	QTYPE=10,	\$END	A=10
\$NEWELL	ROW=22,	COL= 6,	Q=.00000001,	LAYER=4,	QTYPE=10,	\$END	A=10
\$NEWELL	ROW=23,	COL= 5,	Q=.00000001,	LAYER=4,	QTYPE=10,	\$END	A=10
\$NEWELL	ROW=23,	COL= 6,	Q=.00000001,	LAYER=4,	QTYPE=10,	\$END	A=10
\$NEWELL	ROW=24,	COL= 5,	Q=.00000001,	LAYER=4,	QTYPE=10,	\$END	A=10
\$NEWELL	ROW=24,	COL= 6,	Q=.00000001,	LAYER=4,	QTYPE=10,	\$END	A=10
\$NEWELL	ROW=25,	COL= 5,	Q=.00000001,	LAYER=4,	QTYPE=10,	\$END	A=10
\$NEWELL	ROW=25,	COL= 6,	Q=.00000001,	LAYER=4,	QTYPE=10,	\$END	A=10
\$NEWELL	ROW=26,	COL= 2,	Q=.00000001,	LAYER=4,	QTYPE=10,	\$END	A=10
\$NEWELL	ROW=26,	COL= 3,	Q=.00000001,	LAYER=4,	QTYPE=10,	\$END	A=10
\$NEWELL	ROW=26,	COL= 4,	Q=.00000001,	LAYER=4,	QTYPE=10,	\$END	A=10
\$NEWELL	ROW=26,	COL= 5,	Q=.00000001,	LAYER=4,	QTYPE=10,	\$END	A=10
\$NEWELL	ROW=27,	COL= 2,	Q=.00000004,	LAYER=4,	QTYPE=10,	\$END	A=10
\$NEWELL	ROW=27,	COL= 3,	Q=.00000001,	LAYER=4,	QTYPE=10,	\$END	A=10
\$NEWELL	ROW=27,	COL= 4,	Q=.00000001,	LAYER=4,	QTYPE=10,	\$END	A=10
\$NEWELL	ROW=22,	COL= 7,	Q=.00000604,	LAYER=7,	QTYPE=61,	\$END	A=11
\$NEWELL	ROW=22,	COL= 8,	Q=.00000604,	LAYER=7,	QTYPE=11,	\$END	A=11
\$NEWELL	ROW=22,	COL= 9,	Q=.00000604,	LAYER=7,	QTYPE=11,	\$END	A=11
\$NEWELL	ROW=22,	COL=10,	Q=.00000604,	LAYER=7,	QTYPE=11,	\$END	A=11
\$NEWELL	ROW=23,	COL= 9,	Q=.00000604,	LAYER=7,	QTYPE=11,	\$END	A=11
\$NEWELL	ROW=23,	COL=10,	Q=.00000604,	LAYER=7,	QTYPE=11,	\$END	A=11
\$NEWELL	ROW=22,	COL= 7,	Q=.00000028,	LAYER=6,	QTYPE=61,	\$END	A=11
\$NEWELL	ROW=22,	COL= 8,	Q=.00000028,	LAYER=6,	QTYPE=11,	\$END	A=11
\$NEWELL	ROW=22,	COL= 9,	Q=.00000028,	LAYER=6,	QTYPE=11,	\$END	A=11
\$NEWELL	ROW=22,	COL=10,	Q=.00000028,	LAYER=6,	QTYPE=11,	\$END	A=11
\$NEWELL	ROW=23,	COL= 9,	Q=.00000028,	LAYER=6,	QTYPE=11,	\$END	A=11
\$NEWELL	ROW=23,	COL=10,	Q=.00000028,	LAYER=6,	QTYPE=11,	\$END	A=11
\$NEWELL	ROW=22,	COL=11,	Q=.00000538,	LAYER=7,	QTYPE=12,	\$END	A=12
\$NEWELL	ROW=23,	COL= 7,	Q=.00000538,	LAYER=7,	QTYPE=62,	\$END	A=12
\$NEWELL	ROW=23,	COL= 8,	Q=.00000538,	LAYER=7,	QTYPE=12,	\$END	A=12
\$NEWELL	ROW=23,	COL=11,	Q=.00000538,	LAYER=7,	QTYPE=12,	\$END	A=12
\$NEWELL	ROW=24,	COL= 7,	Q=.00000538,	LAYER=7,	QTYPE=62,	\$END	A=12
\$NEWELL	ROW=24,	COL= 8,	Q=.00000504,	LAYER=7,	QTYPE=12,	\$END	A=12
\$NEWELL	ROW=24,	COL= 9,	Q=.00000504,	LAYER=7,	QTYPE=12,	\$END	A=12
\$NEWELL	ROW=24,	COL=10,	Q=.00000538,	LAYER=7,	QTYPE=12,	\$END	A=12
\$NEWELL	ROW=24,	COL=11,	Q=.00000538,	LAYER=7,	QTYPE=12,	\$END	A=12
\$NEWELL	ROW=25,	COL= 7,	Q=.00000538,	LAYER=7,	QTYPE=62,	\$END	A=12

## Attachment 2.--Input file for the 1950-79 transient simulation--Continued

\$NEWELL	ROW=25,	COL= 8,	Q=.00000538,	LAYER=7,	QTYPE=62,	\$END	A=12
\$NEWELL	ROW=25,	COL= 9,	Q=.00000538,	LAYER=7,	QTYPE=12,	\$END	A=12
\$NEWELL	ROW=25,	COL=10,	Q=.00000538,	LAYER=7,	QTYPE=12,	\$END	A=12
\$NEWELL	ROW=25,	COL=11,	Q=.00000538,	LAYER=7,	QTYPE=12,	\$END	A=12
\$NEWELL	ROW=26,	COL= 9,	Q=.00000538,	LAYER=7,	QTYPE=62,	\$END	A=12
\$NEWELL	ROW=26,	COL=10,	Q=.00000538,	LAYER=7,	QTYPE=12,	\$END	A=12
\$NEWELL	ROW=27,	COL= 9,	Q=.00000538,	LAYER=7,	QTYPE=62,	\$END	A=12
\$NEWELL	ROW=27,	COL=10,	Q=.00000538,	LAYER=7,	QTYPE=12,	\$END	A=12
\$NEWELL	ROW=28,	COL= 8,	Q=.00000538,	LAYER=7,	QTYPE=62,	\$END	A=12
\$NEWELL	ROW=28,	COL= 9,	Q=.00000538,	LAYER=7,	QTYPE=12,	\$END	A=12
\$NEWELL	ROW=28,	COL=10,	Q=.00000538,	LAYER=7,	QTYPE=12,	\$END	A=12
\$NEWELL	ROW=22,	COL=11,	Q=.00000089,	LAYER=6,	QTYPE=12,	\$END	A=12
\$NEWELL	ROW=23,	COL= 7,	Q=.00000089,	LAYER=6,	QTYPE=62,	\$END	A=12
\$NEWELL	ROW=23,	COL= 8,	Q=.00000089,	LAYER=6,	QTYPE=12,	\$END	A=12
\$NEWELL	ROW=23,	COL=11,	Q=.00000089,	LAYER=6,	QTYPE=12,	\$END	A=12
\$NEWELL	ROW=24,	COL= 7,	Q=.00000089,	LAYER=6,	QTYPE=62,	\$END	A=12
\$NEWELL	ROW=24,	COL= 8,	Q=.00000083,	LAYER=6,	QTYPE=12,	\$END	A=12
\$NEWELL	ROW=24,	COL= 9,	Q=.00000083,	LAYER=6,	QTYPE=12,	\$END	A=12
\$NEWELL	ROW=24,	COL=10,	Q=.00000089,	LAYER=6,	QTYPE=12,	\$END	A=12
\$NEWELL	ROW=24,	COL=11,	Q=.00000089,	LAYER=6,	QTYPE=12,	\$END	A=12
\$NEWELL	ROW=25,	COL= 7,	Q=.00000089,	LAYER=6,	QTYPE=62,	\$END	A=12
\$NEWELL	ROW=25,	COL= 8,	Q=.00000089,	LAYER=6,	QTYPE=62,	\$END	A=12
\$NEWELL	ROW=25,	COL= 9,	Q=.00000089,	LAYER=6,	QTYPE=12,	\$END	A=12
\$NEWELL	ROW=25,	COL=10,	Q=.00000089,	LAYER=6,	QTYPE=12,	\$END	A=12
\$NEWELL	ROW=25,	COL=11,	Q=.00000089,	LAYER=6,	QTYPE=12,	\$END	A=12
\$NEWELL	ROW=26,	COL= 9,	Q=.00000089,	LAYER=6,	QTYPE=62,	\$END	A=12
\$NEWELL	ROW=26,	COL=10,	Q=.00000089,	LAYER=6,	QTYPE=12,	\$END	A=12
\$NEWELL	ROW=27,	COL= 9,	Q=.00000089,	LAYER=6,	QTYPE=62,	\$END	A=12
\$NEWELL	ROW=27,	COL=10,	Q=.00000089,	LAYER=6,	QTYPE=12,	\$END	A=12
\$NEWELL	ROW=28,	COL= 8,	Q=.00000089,	LAYER=6,	QTYPE=62,	\$END	A=12
\$NEWELL	ROW=28,	COL= 9,	Q=.00000089,	LAYER=6,	QTYPE=12,	\$END	A=12
\$NEWELL	ROW=28,	COL=10,	Q=.00000089,	LAYER=6,	QTYPE=12,	\$END	A=12
\$NEWELL	ROW=22,	COL=11,	Q=.00000002,	LAYER=5,	QTYPE=12,	\$END	A=12
\$NEWELL	ROW=23,	COL= 7,	Q=.00000002,	LAYER=5,	QTYPE=62,	\$END	A=12
\$NEWELL	ROW=23,	COL= 8,	Q=.00000002,	LAYER=5,	QTYPE=12,	\$END	A=12
\$NEWELL	ROW=23,	COL=11,	Q=.00000002,	LAYER=5,	QTYPE=12,	\$END	A=12
\$NEWELL	ROW=24,	COL= 7,	Q=.00000002,	LAYER=5,	QTYPE=62,	\$END	A=12
\$NEWELL	ROW=24,	COL= 8,	Q=.00000002,	LAYER=5,	QTYPE=12,	\$END	A=12
\$NEWELL	ROW=24,	COL= 9,	Q=.00000002,	LAYER=5,	QTYPE=12,	\$END	A=12
\$NEWELL	ROW=24,	COL=10,	Q=.00000002,	LAYER=5,	QTYPE=12,	\$END	A=12
\$NEWELL	ROW=24,	COL=11,	Q=.00000002,	LAYER=5,	QTYPE=12,	\$END	A=12
\$NEWELL	ROW=25,	COL= 7,	Q=.00000002,	LAYER=5,	QTYPE=62,	\$END	A=12
\$NEWELL	ROW=25,	COL= 8,	Q=.00000002,	LAYER=5,	QTYPE=62,	\$END	A=12
\$NEWELL	ROW=25,	COL= 9,	Q=.00000002,	LAYER=5,	QTYPE=12,	\$END	A=12
\$NEWELL	ROW=25,	COL=10,	Q=.00000002,	LAYER=5,	QTYPE=12,	\$END	A=12
\$NEWELL	ROW=25,	COL=11,	Q=.00000002,	LAYER=5,	QTYPE=12,	\$END	A=12
\$NEWELL	ROW=26,	COL= 9,	Q=.00000002,	LAYER=5,	QTYPE=62,	\$END	A=12
\$NEWELL	ROW=26,	COL=10,	Q=.00000002,	LAYER=5,	QTYPE=12,	\$END	A=12
\$NEWELL	ROW=27,	COL= 9,	Q=.00000002,	LAYER=5,	QTYPE=62,	\$END	A=12
\$NEWELL	ROW=27,	COL=10,	Q=.00000002,	LAYER=5,	QTYPE=12,	\$END	A=12
\$NEWELL	ROW=28,	COL= 8,	Q=.00000002,	LAYER=5,	QTYPE=62,	\$END	A=12
\$NEWELL	ROW=28,	COL= 9,	Q=.00000002,	LAYER=5,	QTYPE=12,	\$END	A=12

Attachment 2.--Input file for the 1950-79 transient simulation--Continued

```

$NEWELL ROW=28, COL=10, Q=.00000002, LAYER=5, QTYPE=12, $END A=12
$NEWELL ROW=22, COL=11, Q=.00000003, LAYER=4, QTYPE=12, $END A=12
$NEWELL ROW=23, COL= 7, Q=.00000003, LAYER=4, QTYPE=62, $END A=12
$NEWELL ROW=23, COL= 8, Q=.00000003, LAYER=4, QTYPE=12, $END A=12
$NEWELL ROW=23, COL=11, Q=.00000003, LAYER=4, QTYPE=12, $END A=12
$NEWELL ROW=24, COL= 7, Q=.00000003, LAYER=4, QTYPE=62, $END A=12
$NEWELL ROW=24, COL= 8, Q=.00000002, LAYER=4, QTYPE=12, $END A=12
$NEWELL ROW=24, COL= 9, Q=.00000002, LAYER=4, QTYPE=12, $END A=12
$NEWELL ROW=24, COL=10, Q=.00000003, LAYER=4, QTYPE=12, $END A=12
$NEWELL ROW=24, COL=11, Q=.00000003, LAYER=4, QTYPE=12, $END A=12
$NEWELL ROW=25, COL= 7, Q=.00000003, LAYER=4, QTYPE=62, $END A=12
$NEWELL ROW=25, COL= 8, Q=.00000003, LAYER=4, QTYPE=62, $END A=12
$NEWELL ROW=25, COL= 9, Q=.00000003, LAYER=4, QTYPE=12, $END A=12
$NEWELL ROW=25, COL=10, Q=.00000003, LAYER=4, QTYPE=12, $END A=12
$NEWELL ROW=25, COL=11, Q=.00000003, LAYER=4, QTYPE=12, $END A=12
$NEWELL ROW=26, COL= 9, Q=.00000003, LAYER=4, QTYPE=62, $END A=12
$NEWELL ROW=26, COL=10, Q=.00000003, LAYER=4, QTYPE=12, $END A=12
$NEWELL ROW=27, COL= 9, Q=.00000003, LAYER=4, QTYPE=62, $END A=12
$NEWELL ROW=27, COL=10, Q=.00000003, LAYER=4, QTYPE=12, $END A=12
$NEWELL ROW=28, COL= 8, Q=.00000003, LAYER=4, QTYPE=62, $END A=12
$NEWELL ROW=28, COL= 9, Q=.00000003, LAYER=4, QTYPE=12, $END A=12
$NEWELL ROW=28, COL=10, Q=.00000003, LAYER=4, QTYPE=12, $END A=12
$NEWELL ROW=22, COL=11, Q=.00000001, LAYER=3, QTYPE=12, $END A=12
$NEWELL ROW=23, COL= 7, Q=.00000001, LAYER=3, QTYPE=62, $END A=12
$NEWELL ROW=23, COL= 8, Q=.00000001, LAYER=3, QTYPE=12, $END A=12
$NEWELL ROW=23, COL=11, Q=.00000001, LAYER=3, QTYPE=12, $END A=12
$NEWELL ROW=24, COL= 7, Q=.00000001, LAYER=3, QTYPE=62, $END A=12
$NEWELL ROW=24, COL= 8, Q=.00000001, LAYER=3, QTYPE=12, $END A=12
$NEWELL ROW=24, COL= 9, Q=.00000001, LAYER=3, QTYPE=12, $END A=12
$NEWELL ROW=24, COL=10, Q=.00000001, LAYER=3, QTYPE=12, $END A=12
$NEWELL ROW=24, COL=11, Q=.00000001, LAYER=3, QTYPE=12, $END A=12
$NEWELL ROW=25, COL= 7, Q=.00000001, LAYER=3, QTYPE=62, $END A=12
$NEWELL ROW=25, COL= 8, Q=.00000001, LAYER=3, QTYPE=62, $END A=12
$NEWELL ROW=25, COL= 9, Q=.00000001, LAYER=3, QTYPE=12, $END A=12
$NEWELL ROW=25, COL=10, Q=.00000001, LAYER=3, QTYPE=12, $END A=12
$NEWELL ROW=25, COL=11, Q=.00000001, LAYER=3, QTYPE=12, $END A=12
$NEWELL ROW=26, COL= 9, Q=.00000001, LAYER=3, QTYPE=62, $END A=12
$NEWELL ROW=26, COL=10, Q=.00000001, LAYER=3, QTYPE=12, $END A=12
$NEWELL ROW=27, COL= 9, Q=.00000001, LAYER=3, QTYPE=62, $END A=12
$NEWELL ROW=27, COL=10, Q=.00000001, LAYER=3, QTYPE=12, $END A=12
$NEWELL ROW=28, COL= 8, Q=.00000001, LAYER=3, QTYPE=62, $END A=12
$NEWELL ROW=28, COL= 9, Q=.00000001, LAYER=3, QTYPE=12, $END A=12
$NEWELL ROW=28, COL=10, Q=.00000001, LAYER=3, QTYPE=12, $END A=12
$NEWELL ROW=23, COL=12, Q=.00000357, LAYER=7, QTYPE=13, $END A=13
$NEWELL ROW=23, COL=13, Q=.00000476, LAYER=7, QTYPE=13, $END A=13
$NEWELL ROW=24, COL=12, Q=.00000476, LAYER=7, QTYPE=13, $END A=13
$NEWELL ROW=24, COL=13, Q=.00000476, LAYER=7, QTYPE=13, $END A=13
$NEWELL ROW=25, COL=12, Q=.00000297, LAYER=7, QTYPE=13, $END A=13
$NEWELL ROW=25, COL=13, Q=.00000357, LAYER=7, QTYPE=13, $END A=13
$NEWELL ROW=23, COL=12, Q=.00000069, LAYER=6, QTYPE=13, $END A=13
$NEWELL ROW=23, COL=13, Q=.00000092, LAYER=6, QTYPE=13, $END A=13
$NEWELL ROW=24, COL=12, Q=.00000092, LAYER=6, QTYPE=13, $END A=13

```

Attachment 2.--Input file for the 1950-79 transient simulation--Continued

\$NEWELL	ROW=24,	COL=13,	Q=.00000092,	LAYER=6,	QTYPE=13,	\$END	A=13
\$NEWELL	ROW=25,	COL=12,	Q=.00000058,	LAYER=6,	QTYPE=13,	\$END	A=13
\$NEWELL	ROW=25,	COL=13,	Q=.00000069,	LAYER=6,	QTYPE=13,	\$END	A=13
\$NEWELL	ROW=23,	COL=12,	Q=.00000024,	LAYER=4,	QTYPE=13,	\$END	A=13
\$NEWELL	ROW=23,	COL=13,	Q=.00000032,	LAYER=4,	QTYPE=13,	\$END	A=13
\$NEWELL	ROW=24,	COL=12,	Q=.00000032,	LAYER=4,	QTYPE=13,	\$END	A=13
\$NEWELL	ROW=24,	COL=13,	Q=.00000032,	LAYER=4,	QTYPE=13,	\$END	A=13
\$NEWELL	ROW=25,	COL=12,	Q=.00000020,	LAYER=4,	QTYPE=13,	\$END	A=13
\$NEWELL	ROW=25,	COL=13,	Q=.00000024,	LAYER=4,	QTYPE=13,	\$END	A=13
\$NEWELL	ROW=23,	COL=12,	Q=.00000024,	LAYER=3,	QTYPE=13,	\$END	A=13
\$NEWELL	ROW=23,	COL=13,	Q=.00000032,	LAYER=3,	QTYPE=13,	\$END	A=13
\$NEWELL	ROW=24,	COL=12,	Q=.00000032,	LAYER=3,	QTYPE=13,	\$END	A=13
\$NEWELL	ROW=24,	COL=13,	Q=.00000032,	LAYER=3,	QTYPE=13,	\$END	A=13
\$NEWELL	ROW=25,	COL=12,	Q=.00000020,	LAYER=3,	QTYPE=13,	\$END	A=13
\$NEWELL	ROW=25,	COL=13,	Q=.00000024,	LAYER=3,	QTYPE=13,	\$END	A=13
\$NEWELL	ROW=26,	COL= 6,	Q=.00000380,	LAYER=7,	QTYPE=14,	\$END	A=14
\$NEWELL	ROW=27,	COL= 5,	Q=.00000380,	LAYER=7,	QTYPE=14,	\$END	A=14
\$NEWELL	ROW=27,	COL= 6,	Q=.00000380,	LAYER=7,	QTYPE=14,	\$END	A=14
\$NEWELL	ROW=28,	COL= 6,	Q=.00000380,	LAYER=7,	QTYPE=14,	\$END	A=14
\$NEWELL	ROW=26,	COL= 6,	Q=.00000237,	LAYER=6,	QTYPE=14,	\$END	A=14
\$NEWELL	ROW=27,	COL= 5,	Q=.00000237,	LAYER=6,	QTYPE=14,	\$END	A=14
\$NEWELL	ROW=27,	COL= 6,	Q=.00000237,	LAYER=6,	QTYPE=14,	\$END	A=14
\$NEWELL	ROW=28,	COL= 6,	Q=.00000237,	LAYER=6,	QTYPE=14,	\$END	A=14
\$NEWELL	ROW=26,	COL= 6,	Q=.00000008,	LAYER=5,	QTYPE=14,	\$END	A=14
\$NEWELL	ROW=27,	COL= 5,	Q=.00000008,	LAYER=5,	QTYPE=14,	\$END	A=14
\$NEWELL	ROW=27,	COL= 6,	Q=.00000008,	LAYER=5,	QTYPE=14,	\$END	A=14
\$NEWELL	ROW=28,	COL= 6,	Q=.00000008,	LAYER=5,	QTYPE=14,	\$END	A=14
\$NEWELL	ROW=26,	COL= 6,	Q=.00000005,	LAYER=4,	QTYPE=14,	\$END	A=14
\$NEWELL	ROW=27,	COL= 5,	Q=.00000005,	LAYER=4,	QTYPE=14,	\$END	A=14
\$NEWELL	ROW=27,	COL= 6,	Q=.00000005,	LAYER=4,	QTYPE=14,	\$END	A=14
\$NEWELL	ROW=28,	COL= 6,	Q=.00000005,	LAYER=4,	QTYPE=14,	\$END	A=14
\$NEWELL	ROW=26,	COL= 6,	Q=.00000002,	LAYER=3,	QTYPE=14,	\$END	A=14
\$NEWELL	ROW=27,	COL= 5,	Q=.00000002,	LAYER=3,	QTYPE=14,	\$END	A=14
\$NEWELL	ROW=27,	COL= 6,	Q=.00000002,	LAYER=3,	QTYPE=14,	\$END	A=14
\$NEWELL	ROW=28,	COL= 6,	Q=.00000002,	LAYER=3,	QTYPE=14,	\$END	A=14
\$NEWELL	ROW=26,	COL= 7,	Q=.00000503,	LAYER=7,	QTYPE=15,	\$END	A=15
\$NEWELL	ROW=26,	COL= 8,	Q=.00000503,	LAYER=7,	QTYPE=15,	\$END	A=15
\$NEWELL	ROW=27,	COL= 7,	Q=.00000503,	LAYER=7,	QTYPE=15,	\$END	A=15
\$NEWELL	ROW=27,	COL= 8,	Q=.00000503,	LAYER=7,	QTYPE=15,	\$END	A=15
\$NEWELL	ROW=28,	COL= 7,	Q=.00000503,	LAYER=7,	QTYPE=15,	\$END	A=15
\$NEWELL	ROW=26,	COL= 7,	Q=.00000123,	LAYER=6,	QTYPE=15,	\$END	A=15
\$NEWELL	ROW=26,	COL= 8,	Q=.00000123,	LAYER=6,	QTYPE=15,	\$END	A=15
\$NEWELL	ROW=27,	COL= 7,	Q=.00000123,	LAYER=6,	QTYPE=15,	\$END	A=15
\$NEWELL	ROW=27,	COL= 8,	Q=.00000123,	LAYER=6,	QTYPE=15,	\$END	A=15
\$NEWELL	ROW=28,	COL= 7,	Q=.00000123,	LAYER=6,	QTYPE=15,	\$END	A=15
\$NEWELL	ROW=26,	COL= 7,	Q=.00000008,	LAYER=5,	QTYPE=15,	\$END	A=15
\$NEWELL	ROW=26,	COL= 8,	Q=.00000008,	LAYER=5,	QTYPE=15,	\$END	A=15
\$NEWELL	ROW=27,	COL= 7,	Q=.00000008,	LAYER=5,	QTYPE=15,	\$END	A=15
\$NEWELL	ROW=27,	COL= 8,	Q=.00000008,	LAYER=5,	QTYPE=15,	\$END	A=15
\$NEWELL	ROW=28,	COL= 7,	Q=.00000008,	LAYER=5,	QTYPE=15,	\$END	A=15
\$NEWELL	ROW=27,	COL=15,	Q=.00000431,	LAYER=7,	QTYPE=16,	\$END	A=16
\$NEWELL	ROW=27,	COL=16,	Q=.00000431,	LAYER=7,	QTYPE=16,	\$END	A=16



## Attachment 2.--Input file for the 1950-79 transient simulation--Continued

\$NEWELL	ROW=28,	COL=15,	Q=.00000431,	LAYER=7,	QTYPE=16,	\$END	A=16
\$NEWELL	ROW=28,	COL=16,	Q=.00000431,	LAYER=7,	QTYPE=16,	\$END	A=16
\$NEWELL	ROW=28,	COL=17,	Q=.00000108,	LAYER=7,	QTYPE=16,	\$END	A=16
\$NEWELL	ROW=29,	COL=17,	Q=.00000054,	LAYER=7,	QTYPE=16,	\$END	A=16
\$NEWELL	ROW=27,	COL=15,	Q=.00000121,	LAYER=6,	QTYPE=16,	\$END	A=16
\$NEWELL	ROW=27,	COL=16,	Q=.00000121,	LAYER=6,	QTYPE=16,	\$END	A=16
\$NEWELL	ROW=28,	COL=15,	Q=.00000121,	LAYER=6,	QTYPE=16,	\$END	A=16
\$NEWELL	ROW=28,	COL=16,	Q=.00000121,	LAYER=6,	QTYPE=16,	\$END	A=16
\$NEWELL	ROW=28,	COL=17,	Q=.00000030,	LAYER=6,	QTYPE=16,	\$END	A=16
\$NEWELL	ROW=29,	COL=17,	Q=.00000015,	LAYER=6,	QTYPE=16,	\$END	A=16
\$NEWELL	ROW=27,	COL=15,	Q=.00000040,	LAYER=4,	QTYPE=16,	\$END	A=16
\$NEWELL	ROW=27,	COL=16,	Q=.00000040,	LAYER=4,	QTYPE=16,	\$END	A=16
\$NEWELL	ROW=28,	COL=15,	Q=.00000040,	LAYER=4,	QTYPE=16,	\$END	A=16
\$NEWELL	ROW=28,	COL=16,	Q=.00000040,	LAYER=4,	QTYPE=16,	\$END	A=16
\$NEWELL	ROW=28,	COL=17,	Q=.00000010,	LAYER=4,	QTYPE=16,	\$END	A=16
\$NEWELL	ROW=29,	COL=17,	Q=.00000005,	LAYER=4,	QTYPE=16,	\$END	A=16
\$NEWELL	ROW=27,	COL=15,	Q=.00000040,	LAYER=3,	QTYPE=16,	\$END	A=16
\$NEWELL	ROW=27,	COL=16,	Q=.00000040,	LAYER=3,	QTYPE=16,	\$END	A=16
\$NEWELL	ROW=28,	COL=15,	Q=.00000040,	LAYER=3,	QTYPE=16,	\$END	A=16
\$NEWELL	ROW=28,	COL=16,	Q=.00000040,	LAYER=3,	QTYPE=16,	\$END	A=16
\$NEWELL	ROW=28,	COL=17,	Q=.00000010,	LAYER=3,	QTYPE=16,	\$END	A=16
\$NEWELL	ROW=29,	COL=17,	Q=.00000005,	LAYER=3,	QTYPE=16,	\$END	A=16
\$NEWELL	ROW=26,	COL=11,	Q=.00000566,	LAYER=7,	QTYPE=17,	\$END	A=17
\$NEWELL	ROW=27,	COL=11,	Q=.00000604,	LAYER=7,	QTYPE=17,	\$END	A=17
\$NEWELL	ROW=28,	COL=11,	Q=.00000604,	LAYER=7,	QTYPE=17,	\$END	A=17
\$NEWELL	ROW=29,	COL= 7,	Q=.00000453,	LAYER=7,	QTYPE=17,	\$END	A=17
\$NEWELL	ROW=29,	COL= 8,	Q=.00000528,	LAYER=7,	QTYPE=17,	\$END	A=17
\$NEWELL	ROW=29,	COL= 9,	Q=.00000604,	LAYER=7,	QTYPE=17,	\$END	A=17
\$NEWELL	ROW=29,	COL=10,	Q=.00000604,	LAYER=7,	QTYPE=17,	\$END	A=17
\$NEWELL	ROW=29,	COL=11,	Q=.00000604,	LAYER=7,	QTYPE=17,	\$END	A=17
\$NEWELL	ROW=30,	COL=10,	Q=.00000151,	LAYER=7,	QTYPE=17,	\$END	A=17
\$NEWELL	ROW=30,	COL=11,	Q=.00000566,	LAYER=7,	QTYPE=17,	\$END	A=17
\$NEWELL	ROW=26,	COL=11,	Q=.00000020,	LAYER=6,	QTYPE=17,	\$END	A=17
\$NEWELL	ROW=27,	COL=11,	Q=.00000021,	LAYER=6,	QTYPE=17,	\$END	A=17
\$NEWELL	ROW=28,	COL=11,	Q=.00000021,	LAYER=6,	QTYPE=17,	\$END	A=17
\$NEWELL	ROW=29,	COL= 7,	Q=.00000016,	LAYER=6,	QTYPE=17,	\$END	A=17
\$NEWELL	ROW=29,	COL= 8,	Q=.00000018,	LAYER=6,	QTYPE=17,	\$END	A=17
\$NEWELL	ROW=29,	COL= 9,	Q=.00000021,	LAYER=6,	QTYPE=17,	\$END	A=17
\$NEWELL	ROW=29,	COL=10,	Q=.00000021,	LAYER=6,	QTYPE=17,	\$END	A=17
\$NEWELL	ROW=29,	COL=11,	Q=.00000021,	LAYER=6,	QTYPE=17,	\$END	A=17
\$NEWELL	ROW=30,	COL=10,	Q=.00000005,	LAYER=6,	QTYPE=17,	\$END	A=17
\$NEWELL	ROW=30,	COL=11,	Q=.00000021,	LAYER=6,	QTYPE=17,	\$END	A=17
\$NEWELL	ROW=26,	COL=11,	Q=.00000001,	LAYER=5,	QTYPE=17,	\$END	A=17
\$NEWELL	ROW=27,	COL=11,	Q=.00000001,	LAYER=5,	QTYPE=17,	\$END	A=17
\$NEWELL	ROW=28,	COL=11,	Q=.00000001,	LAYER=5,	QTYPE=17,	\$END	A=17
\$NEWELL	ROW=29,	COL= 7,	Q=.00000001,	LAYER=5,	QTYPE=17,	\$END	A=17
\$NEWELL	ROW=29,	COL= 8,	Q=.00000001,	LAYER=5,	QTYPE=17,	\$END	A=17
\$NEWELL	ROW=29,	COL= 9,	Q=.00000001,	LAYER=5,	QTYPE=17,	\$END	A=17
\$NEWELL	ROW=29,	COL=10,	Q=.00000001,	LAYER=5,	QTYPE=17,	\$END	A=17
\$NEWELL	ROW=29,	COL=11,	Q=.00000001,	LAYER=5,	QTYPE=17,	\$END	A=17
\$NEWELL	ROW=30,	COL=11,	Q=.00000001,	LAYER=5,	QTYPE=17,	\$END	A=17
\$NEWELL	ROW=26,	COL=11,	Q=.00000003,	LAYER=4,	QTYPE=17,	\$END	A=17

## Attachment 2.--Input file for the 1950-79 transient simulation--Continued

\$NEWELL	ROW=27,	COL=11,	Q=.00000003,	LAYER=4,	QTYPE=17,	\$END	A=17
\$NEWELL	ROW=28,	COL=11,	Q=.00000003,	LAYER=4,	QTYPE=17,	\$END	A=17
\$NEWELL	ROW=29,	COL= 7,	Q=.00000002,	LAYER=4,	QTYPE=17,	\$END	A=17
\$NEWELL	ROW=29,	COL= 8,	Q=.00000003,	LAYER=4,	QTYPE=17,	\$END	A=17
\$NEWELL	ROW=29,	COL= 9,	Q=.00000003,	LAYER=4,	QTYPE=17,	\$END	A=17
\$NEWELL	ROW=29,	COL=10,	Q=.00000003,	LAYER=4,	QTYPE=17,	\$END	A=17
\$NEWELL	ROW=29,	COL=11,	Q=.00000003,	LAYER=4,	QTYPE=17,	\$END	A=17
\$NEWELL	ROW=30,	COL=10,	Q=.00000001,	LAYER=4,	QTYPE=17,	\$END	A=17
\$NEWELL	ROW=30,	COL=11,	Q=.00000003,	LAYER=4,	QTYPE=17,	\$END	A=17
\$NEWELL	ROW=26,	COL=11,	Q=.00000003,	LAYER=3,	QTYPE=17,	\$END	A=17
\$NEWELL	ROW=27,	COL=11,	Q=.00000003,	LAYER=3,	QTYPE=17,	\$END	A=17
\$NEWELL	ROW=28,	COL=11,	Q=.00000003,	LAYER=3,	QTYPE=17,	\$END	A=17
\$NEWELL	ROW=29,	COL= 7,	Q=.00000002,	LAYER=3,	QTYPE=17,	\$END	A=17
\$NEWELL	ROW=29,	COL= 8,	Q=.00000003,	LAYER=3,	QTYPE=17,	\$END	A=17
\$NEWELL	ROW=29,	COL= 9,	Q=.00000003,	LAYER=3,	QTYPE=17,	\$END	A=17
\$NEWELL	ROW=29,	COL=10,	Q=.00000003,	LAYER=3,	QTYPE=17,	\$END	A=17
\$NEWELL	ROW=29,	COL=11,	Q=.00000003,	LAYER=3,	QTYPE=17,	\$END	A=17
\$NEWELL	ROW=30,	COL=10,	Q=.00000001,	LAYER=3,	QTYPE=17,	\$END	A=17
\$NEWELL	ROW=30,	COL=11,	Q=.00000003,	LAYER=3,	QTYPE=17,	\$END	A=17
\$NEWELL	ROW=29,	COL= 6,	Q=.00000351,	LAYER=7,	QTYPE=18,	\$END	A=18
\$NEWELL	ROW=30,	COL= 6,	Q=.00000281,	LAYER=7,	QTYPE=18,	\$END	A=18
\$NEWELL	ROW=30,	COL= 7,	Q=.00000562,	LAYER=7,	QTYPE=18,	\$END	A=18
\$NEWELL	ROW=30,	COL= 8,	Q=.00000455,	LAYER=7,	QTYPE=18,	\$END	A=18
\$NEWELL	ROW=30,	COL= 9,	Q=.00000351,	LAYER=7,	QTYPE=18,	\$END	A=18
\$NEWELL	ROW=31,	COL= 6,	Q=.00000105,	LAYER=7,	QTYPE=18,	\$END	A=18
\$NEWELL	ROW=31,	COL= 7,	Q=.00000527,	LAYER=7,	QTYPE=18,	\$END	A=18
\$NEWELL	ROW=31,	COL= 8,	Q=.00000562,	LAYER=7,	QTYPE=18,	\$END	A=18
\$NEWELL	ROW=29,	COL= 6,	Q=.00000039,	LAYER=6,	QTYPE=18,	\$END	A=18
\$NEWELL	ROW=30,	COL= 6,	Q=.00000032,	LAYER=6,	QTYPE=18,	\$END	A=18
\$NEWELL	ROW=30,	COL= 7,	Q=.00000063,	LAYER=6,	QTYPE=18,	\$END	A=18
\$NEWELL	ROW=30,	COL= 8,	Q=.00000051,	LAYER=6,	QTYPE=18,	\$END	A=18
\$NEWELL	ROW=30,	COL= 9,	Q=.00000039,	LAYER=6,	QTYPE=18,	\$END	A=18
\$NEWELL	ROW=31,	COL= 6,	Q=.00000012,	LAYER=6,	QTYPE=18,	\$END	A=18
\$NEWELL	ROW=31,	COL= 7,	Q=.00000059,	LAYER=6,	QTYPE=18,	\$END	A=18
\$NEWELL	ROW=31,	COL= 8,	Q=.00000063,	LAYER=6,	QTYPE=18,	\$END	A=18
\$NEWELL	ROW=29,	COL= 6,	Q=.00000004,	LAYER=5,	QTYPE=18,	\$END	A=18
\$NEWELL	ROW=30,	COL= 6,	Q=.00000003,	LAYER=5,	QTYPE=18,	\$END	A=18
\$NEWELL	ROW=30,	COL= 7,	Q=.00000007,	LAYER=5,	QTYPE=18,	\$END	A=18
\$NEWELL	ROW=30,	COL= 8,	Q=.00000006,	LAYER=5,	QTYPE=18,	\$END	A=18
\$NEWELL	ROW=30,	COL= 9,	Q=.00000004,	LAYER=5,	QTYPE=18,	\$END	A=18
\$NEWELL	ROW=31,	COL= 6,	Q=.00000001,	LAYER=5,	QTYPE=18,	\$END	A=18
\$NEWELL	ROW=31,	COL= 7,	Q=.00000007,	LAYER=5,	QTYPE=18,	\$END	A=18
\$NEWELL	ROW=31,	COL= 8,	Q=.00000007,	LAYER=5,	QTYPE=18,	\$END	A=18
\$NEWELL	ROW=31,	COL= 9,	Q=.00000519,	LAYER=7,	QTYPE=19,	\$END	A=19
\$NEWELL	ROW=31,	COL=10,	Q=.00000292,	LAYER=7,	QTYPE=19,	\$END	A=19
\$NEWELL	ROW=31,	COL=11,	Q=.00000292,	LAYER=7,	QTYPE=19,	\$END	A=19
\$NEWELL	ROW=32,	COL= 9,	Q=.00000519,	LAYER=7,	QTYPE=19,	\$END	A=19
\$NEWELL	ROW=32,	COL=10,	Q=.00000519,	LAYER=7,	QTYPE=19,	\$END	A=19
\$NEWELL	ROW=32,	COL=11,	Q=.00000389,	LAYER=7,	QTYPE=19,	\$END	A=19
\$NEWELL	ROW=33,	COL=11,	Q=.00000032,	LAYER=7,	QTYPE=19,	\$END	A=19
\$NEWELL	ROW=33,	COL=12,	Q=.00000162,	LAYER=7,	QTYPE=19,	\$END	A=19
\$NEWELL	ROW=31,	COL= 9,	Q=.00000009,	LAYER=6,	QTYPE=19,	\$END	A=19

## Attachment 2.--Input file for the 1950-79 transient simulation--Continued

\$NEWELL	ROW=31,	COL=10,	Q=.00000005,	LAYER=6,	QTYPE=19,	\$END	A=19
\$NEWELL	ROW=31,	COL=11,	Q=.00000005,	LAYER=6,	QTYPE=19,	\$END	A=19
\$NEWELL	ROW=32,	COL= 9,	Q=.00000009,	LAYER=6,	QTYPE=19,	\$END	A=19
\$NEWELL	ROW=32,	COL=10,	Q=.00000009,	LAYER=6,	QTYPE=19,	\$END	A=19
\$NEWELL	ROW=32,	COL=11,	Q=.00000007,	LAYER=6,	QTYPE=19,	\$END	A=19
\$NEWELL	ROW=33,	COL=11,	Q=.00000001,	LAYER=6,	QTYPE=19,	\$END	A=19
\$NEWELL	ROW=33,	COL=12,	Q=.00000003,	LAYER=6,	QTYPE=19,	\$END	A=19
\$NEWELL	ROW=31,	COL= 9,	Q=.00000015,	LAYER=5,	QTYPE=19,	\$END	A=19
\$NEWELL	ROW=31,	COL=10,	Q=.00000008,	LAYER=5,	QTYPE=19,	\$END	A=19
\$NEWELL	ROW=31,	COL=11,	Q=.00000008,	LAYER=5,	QTYPE=19,	\$END	A=19
\$NEWELL	ROW=32,	COL= 9,	Q=.00000015,	LAYER=5,	QTYPE=19,	\$END	A=19
\$NEWELL	ROW=32,	COL=10,	Q=.00000015,	LAYER=5,	QTYPE=19,	\$END	A=19
\$NEWELL	ROW=32,	COL=11,	Q=.00000011,	LAYER=5,	QTYPE=19,	\$END	A=19
\$NEWELL	ROW=33,	COL=11,	Q=.00000001,	LAYER=5,	QTYPE=19,	\$END	A=19
\$NEWELL	ROW=33,	COL=12,	Q=.00000005,	LAYER=5,	QTYPE=19,	\$END	A=19
\$NEWELL	ROW=31,	COL= 9,	Q=.00000051,	LAYER=4,	QTYPE=19,	\$END	A=19
\$NEWELL	ROW=31,	COL=10,	Q=.00000029,	LAYER=4,	QTYPE=19,	\$END	A=19
\$NEWELL	ROW=31,	COL=11,	Q=.00000029,	LAYER=4,	QTYPE=19,	\$END	A=19
\$NEWELL	ROW=32,	COL= 9,	Q=.00000051,	LAYER=4,	QTYPE=19,	\$END	A=19
\$NEWELL	ROW=32,	COL=10,	Q=.00000051,	LAYER=4,	QTYPE=19,	\$END	A=19
\$NEWELL	ROW=32,	COL=11,	Q=.00000038,	LAYER=4,	QTYPE=19,	\$END	A=19
\$NEWELL	ROW=33,	COL=11,	Q=.00000003,	LAYER=4,	QTYPE=19,	\$END	A=19
\$NEWELL	ROW=33,	COL=12,	Q=.00000016,	LAYER=4,	QTYPE=19,	\$END	A=19
\$NEWELL	ROW=31,	COL= 9,	Q=.00000040,	LAYER=3,	QTYPE=19,	\$END	A=19
\$NEWELL	ROW=31,	COL=10,	Q=.00000022,	LAYER=3,	QTYPE=19,	\$END	A=19
\$NEWELL	ROW=31,	COL=11,	Q=.00000022,	LAYER=3,	QTYPE=19,	\$END	A=19
\$NEWELL	ROW=32,	COL= 9,	Q=.00000040,	LAYER=3,	QTYPE=19,	\$END	A=19
\$NEWELL	ROW=32,	COL=10,	Q=.00000040,	LAYER=3,	QTYPE=19,	\$END	A=19
\$NEWELL	ROW=32,	COL=11,	Q=.00000030,	LAYER=3,	QTYPE=19,	\$END	A=19
\$NEWELL	ROW=33,	COL=11,	Q=.00000002,	LAYER=3,	QTYPE=19,	\$END	A=19
\$NEWELL	ROW=33,	COL=12,	Q=.00000012,	LAYER=3,	QTYPE=19,	\$END	A=19
\$NEWELL	ROW=32,	COL= 7,	Q=.00000135,	LAYER=7,	QTYPE=20,	\$END	A=20
\$NEWELL	ROW=32,	COL= 8,	Q=.00000144,	LAYER=7,	QTYPE=20,	\$END	A=20
\$NEWELL	ROW=33,	COL= 7,	Q=.00000072,	LAYER=7,	QTYPE=20,	\$END	A=20
\$NEWELL	ROW=33,	COL= 8,	Q=.00000090,	LAYER=7,	QTYPE=20,	\$END	A=20
\$NEWELL	ROW=33,	COL= 9,	Q=.00000072,	LAYER=7,	QTYPE=20,	\$END	A=20
\$NEWELL	ROW=33,	COL=10,	Q=.00000054,	LAYER=7,	QTYPE=20,	\$END	A=20
\$NEWELL	ROW=32,	COL= 7,	Q=.00000027,	LAYER=6,	QTYPE=20,	\$END	A=20
\$NEWELL	ROW=32,	COL= 8,	Q=.00000029,	LAYER=6,	QTYPE=20,	\$END	A=20
\$NEWELL	ROW=33,	COL= 7,	Q=.00000015,	LAYER=6,	QTYPE=20,	\$END	A=20
\$NEWELL	ROW=33,	COL= 8,	Q=.00000018,	LAYER=6,	QTYPE=20,	\$END	A=20
\$NEWELL	ROW=33,	COL= 9,	Q=.00000015,	LAYER=6,	QTYPE=20,	\$END	A=20
\$NEWELL	ROW=33,	COL=10,	Q=.00000011,	LAYER=6,	QTYPE=20,	\$END	A=20
\$NEWELL	ROW=32,	COL= 7,	Q=.00000108,	LAYER=5,	QTYPE=20,	\$END	A=20
\$NEWELL	ROW=32,	COL= 8,	Q=.00000115,	LAYER=5,	QTYPE=20,	\$END	A=20
\$NEWELL	ROW=33,	COL= 7,	Q=.00000057,	LAYER=5,	QTYPE=20,	\$END	A=20
\$NEWELL	ROW=33,	COL= 8,	Q=.00000072,	LAYER=5,	QTYPE=20,	\$END	A=20
\$NEWELL	ROW=33,	COL= 9,	Q=.00000057,	LAYER=5,	QTYPE=20,	\$END	A=20
\$NEWELL	ROW=33,	COL=10,	Q=.00000043,	LAYER=5,	QTYPE=20,	\$END	A=20
\$NEWELL	ROW=32,	COL= 7,	Q=.00000215,	LAYER=4,	QTYPE=20,	\$END	A=20
\$NEWELL	ROW=32,	COL= 8,	Q=.00000230,	LAYER=4,	QTYPE=20,	\$END	A=20
\$NEWELL	ROW=33,	COL= 7,	Q=.00000115,	LAYER=4,	QTYPE=20,	\$END	A=20

Attachment 2.--Input file for the 1950-79 transient simulation--Continued

\$NEWELL	ROW=33,	COL= 8,	Q=.00000144,	LAYER=4,	QTYPE=20,	\$END	A=20
\$NEWELL	ROW=33,	COL= 9,	Q=.00000115,	LAYER=4,	QTYPE=20,	\$END	A=20
\$NEWELL	ROW=33,	COL=10,	Q=.00000086,	LAYER=4,	QTYPE=20,	\$END	A=20
\$NEWELL	ROW=32,	COL= 7,	Q=.00000108,	LAYER=3,	QTYPE=20,	\$END	A=20
\$NEWELL	ROW=32,	COL= 8,	Q=.00000115,	LAYER=3,	QTYPE=20,	\$END	A=20
\$NEWELL	ROW=33,	COL= 7,	Q=.00000057,	LAYER=3,	QTYPE=20,	\$END	A=20
\$NEWELL	ROW=33,	COL= 8,	Q=.00000072,	LAYER=3,	QTYPE=20,	\$END	A=20
\$NEWELL	ROW=33,	COL= 9,	Q=.00000057,	LAYER=3,	QTYPE=20,	\$END	A=20
\$NEWELL	ROW=33,	COL=10,	Q=.00000043,	LAYER=3,	QTYPE=20,	\$END	A=20
\$NEWELL	ROW=32,	COL=15,	Q=.00000114,	LAYER=7,	QTYPE=21,	\$END	A=21
\$NEWELL	ROW=33,	COL=15,	Q=.00000107,	LAYER=7,	QTYPE=21,	\$END	A=21
\$NEWELL	ROW=32,	COL=15,	Q=.00000046,	LAYER=6,	QTYPE=21,	\$END	A=21
\$NEWELL	ROW=33,	COL=15,	Q=.00000043,	LAYER=6,	QTYPE=21,	\$END	A=21
\$NEWELL	ROW=32,	COL=15,	Q=.00000023,	LAYER=5,	QTYPE=21,	\$END	A=21
\$NEWELL	ROW=33,	COL=15,	Q=.00000022,	LAYER=5,	QTYPE=21,	\$END	A=21
\$NEWELL	ROW=32,	COL=15,	Q=.00000205,	LAYER=4,	QTYPE=21,	\$END	A=21
\$NEWELL	ROW=33,	COL=15,	Q=.00000191,	LAYER=4,	QTYPE=21,	\$END	A=21
\$NEWELL	ROW=32,	COL=15,	Q=.00000205,	LAYER=3,	QTYPE=21,	\$END	A=21
\$NEWELL	ROW=33,	COL=15,	Q=.00000191,	LAYER=3,	QTYPE=21,	\$END	A=21
\$NEWELL	ROW=34,	COL= 7,	Q=.00000130,	LAYER=7,	QTYPE=22,	\$END	A=22
\$NEWELL	ROW=34,	COL= 8,	Q=.00000026,	LAYER=7,	QTYPE=22,	\$END	A=22
\$NEWELL	ROW=35,	COL= 7,	Q=.00000130,	LAYER=7,	QTYPE=22,	\$END	A=22
\$NEWELL	ROW=35,	COL= 8,	Q=.00000208,	LAYER=7,	QTYPE=22,	\$END	A=22
\$NEWELL	ROW=36,	COL= 8,	Q=.00000208,	LAYER=7,	QTYPE=22,	\$END	A=22
\$NEWELL	ROW=37,	COL= 8,	Q=.00000117,	LAYER=7,	QTYPE=22,	\$END	A=22
\$NEWELL	ROW=34,	COL= 7,	Q=.00000160,	LAYER=6,	QTYPE=22,	\$END	A=22
\$NEWELL	ROW=34,	COL= 8,	Q=.00000032,	LAYER=6,	QTYPE=22,	\$END	A=22
\$NEWELL	ROW=35,	COL= 7,	Q=.00000160,	LAYER=6,	QTYPE=22,	\$END	A=22
\$NEWELL	ROW=35,	COL= 8,	Q=.00000256,	LAYER=6,	QTYPE=22,	\$END	A=22
\$NEWELL	ROW=36,	COL= 8,	Q=.00000256,	LAYER=6,	QTYPE=22,	\$END	A=22
\$NEWELL	ROW=37,	COL= 8,	Q=.00000144,	LAYER=6,	QTYPE=22,	\$END	A=22
\$NEWELL	ROW=34,	COL= 7,	Q=.00000075,	LAYER=5,	QTYPE=22,	\$END	A=22
\$NEWELL	ROW=34,	COL= 8,	Q=.00000015,	LAYER=5,	QTYPE=22,	\$END	A=22
\$NEWELL	ROW=35,	COL= 7,	Q=.00000075,	LAYER=5,	QTYPE=22,	\$END	A=22
\$NEWELL	ROW=35,	COL= 8,	Q=.00000119,	LAYER=5,	QTYPE=22,	\$END	A=22
\$NEWELL	ROW=36,	COL= 8,	Q=.00000119,	LAYER=5,	QTYPE=22,	\$END	A=22
\$NEWELL	ROW=37,	COL= 8,	Q=.00000067,	LAYER=5,	QTYPE=22,	\$END	A=22
\$NEWELL	ROW=34,	COL= 7,	Q=.00000019,	LAYER=4,	QTYPE=22,	\$END	A=22
\$NEWELL	ROW=34,	COL= 8,	Q=.00000004,	LAYER=4,	QTYPE=22,	\$END	A=22
\$NEWELL	ROW=35,	COL= 7,	Q=.00000019,	LAYER=4,	QTYPE=22,	\$END	A=22
\$NEWELL	ROW=35,	COL= 8,	Q=.00000030,	LAYER=4,	QTYPE=22,	\$END	A=22
\$NEWELL	ROW=36,	COL= 8,	Q=.00000030,	LAYER=4,	QTYPE=22,	\$END	A=22
\$NEWELL	ROW=37,	COL= 8,	Q=.00000017,	LAYER=4,	QTYPE=22,	\$END	A=22
\$NEWELL	ROW=34,	COL= 7,	Q=.00000011,	LAYER=3,	QTYPE=22,	\$END	A=22
\$NEWELL	ROW=34,	COL= 8,	Q=.00000002,	LAYER=3,	QTYPE=22,	\$END	A=22
\$NEWELL	ROW=35,	COL= 7,	Q=.00000011,	LAYER=3,	QTYPE=22,	\$END	A=22
\$NEWELL	ROW=35,	COL= 8,	Q=.00000013,	LAYER=3,	QTYPE=22,	\$END	A=22
\$NEWELL	ROW=36,	COL= 8,	Q=.00000018,	LAYER=3,	QTYPE=22,	\$END	A=22
\$NEWELL	ROW=37,	COL= 8,	Q=.00000010,	LAYER=3,	QTYPE=22,	\$END	A=22
\$NEWELL	ROW=34,	COL=10,	Q=.00000022,	LAYER=7,	QTYPE=23,	\$END	A=23
\$NEWELL	ROW=35,	COL= 9,	Q=.00000175,	LAYER=7,	QTYPE=23,	\$END	A=23
\$NEWELL	ROW=35,	COL=10,	Q=.00000164,	LAYER=7,	QTYPE=23,	\$END	A=23

Attachment 2.--Input file for the 1950-79 transient simulation--Continued

\$NEWELL	ROW=36,	COL= 9,	Q=.00000175,	LAYER=7,	QTYPE=23,	\$END	A=23
\$NEWELL	ROW=36,	COL=10,	Q=.00000175,	LAYER=7,	QTYPE=23,	\$END	A=23
\$NEWELL	ROW=37,	COL= 9,	Q=.00000077,	LAYER=7,	QTYPE=23,	\$END	A=23
\$NEWELL	ROW=37,	COL=10,	Q=.00000175,	LAYER=7,	QTYPE=23,	\$END	A=23
\$NEWELL	ROW=38,	COL= 9,	Q=.00000066,	LAYER=7,	QTYPE=23,	\$END	A=23
\$NEWELL	ROW=38,	COL=10,	Q=.00000175,	LAYER=7,	QTYPE=23,	\$END	A=23
\$NEWELL	ROW=39,	COL= 9,	Q=.00000022,	LAYER=7,	QTYPE=23,	\$END	A=23
\$NEWELL	ROW=39,	COL=10,	Q=.00000175,	LAYER=7,	QTYPE=23,	\$END	A=23
\$NEWELL	ROW=40,	COL= 9,	Q=.00000098,	LAYER=7,	QTYPE=23,	\$END	A=23
\$NEWELL	ROW=40,	COL=10,	Q=.00000131,	LAYER=7,	QTYPE=23,	\$END	A=23
\$NEWELL	ROW=34,	COL=10,	Q=.00000015,	LAYER=6,	QTYPE=23,	\$END	A=23
\$NEWELL	ROW=35,	COL= 9,	Q=.00000118,	LAYER=6,	QTYPE=23,	\$END	A=23
\$NEWELL	ROW=35,	COL=10,	Q=.00000111,	LAYER=6,	QTYPE=23,	\$END	A=23
\$NEWELL	ROW=36,	COL= 9,	Q=.00000118,	LAYER=6,	QTYPE=23,	\$END	A=23
\$NEWELL	ROW=36,	COL=10,	Q=.00000118,	LAYER=6,	QTYPE=23,	\$END	A=23
\$NEWELL	ROW=37,	COL= 9,	Q=.00000052,	LAYER=6,	QTYPE=23,	\$END	A=23
\$NEWELL	ROW=37,	COL=10,	Q=.00000118,	LAYER=6,	QTYPE=23,	\$END	A=23
\$NEWELL	ROW=38,	COL= 9,	Q=.00000044,	LAYER=6,	QTYPE=23,	\$END	A=23
\$NEWELL	ROW=38,	COL=10,	Q=.00000118,	LAYER=6,	QTYPE=23,	\$END	A=23
\$NEWELL	ROW=39,	COL= 9,	Q=.00000015,	LAYER=6,	QTYPE=23,	\$END	A=23
\$NEWELL	ROW=39,	COL=10,	Q=.00000118,	LAYER=6,	QTYPE=23,	\$END	A=23
\$NEWELL	ROW=40,	COL= 9,	Q=.00000066,	LAYER=6,	QTYPE=23,	\$END	A=23
\$NEWELL	ROW=40,	COL=10,	Q=.00000089,	LAYER=6,	QTYPE=23,	\$END	A=23
\$NEWELL	ROW=34,	COL=10,	Q=.00000021,	LAYER=5,	QTYPE=23,	\$END	A=23
\$NEWELL	ROW=35,	COL= 9,	Q=.00000169,	LAYER=5,	QTYPE=23,	\$END	A=23
\$NEWELL	ROW=35,	COL=10,	Q=.00000158,	LAYER=5,	QTYPE=23,	\$END	A=23
\$NEWELL	ROW=36,	COL= 9,	Q=.00000169,	LAYER=5,	QTYPE=23,	\$END	A=23
\$NEWELL	ROW=36,	COL=10,	Q=.00000169,	LAYER=5,	QTYPE=23,	\$END	A=23
\$NEWELL	ROW=37,	COL= 9,	Q=.00000074,	LAYER=5,	QTYPE=23,	\$END	A=23
\$NEWELL	ROW=37,	COL=10,	Q=.00000169,	LAYER=5,	QTYPE=23,	\$END	A=23
\$NEWELL	ROW=38,	COL= 9,	Q=.00000063,	LAYER=5,	QTYPE=23,	\$END	A=23
\$NEWELL	ROW=38,	COL=10,	Q=.00000169,	LAYER=5,	QTYPE=23,	\$END	A=23
\$NEWELL	ROW=39,	COL= 9,	Q=.00000021,	LAYER=5,	QTYPE=23,	\$END	A=23
\$NEWELL	ROW=39,	COL=10,	Q=.00000169,	LAYER=5,	QTYPE=23,	\$END	A=23
\$NEWELL	ROW=40,	COL= 9,	Q=.00000095,	LAYER=5,	QTYPE=23,	\$END	A=23
\$NEWELL	ROW=40,	COL=10,	Q=.00000126,	LAYER=5,	QTYPE=23,	\$END	A=23
\$NEWELL	ROW=34,	COL=10,	Q=.00000016,	LAYER=4,	QTYPE=23,	\$END	A=23
\$NEWELL	ROW=35,	COL= 9,	Q=.00000128,	LAYER=4,	QTYPE=23,	\$END	A=23
\$NEWELL	ROW=35,	COL=10,	Q=.00000120,	LAYER=4,	QTYPE=23,	\$END	A=23
\$NEWELL	ROW=36,	COL= 9,	Q=.00000128,	LAYER=4,	QTYPE=23,	\$END	A=23
\$NEWELL	ROW=36,	COL=10,	Q=.00000128,	LAYER=4,	QTYPE=23,	\$END	A=23
\$NEWELL	ROW=37,	COL= 9,	Q=.00000056,	LAYER=4,	QTYPE=23,	\$END	A=23
\$NEWELL	ROW=37,	COL=10,	Q=.00000128,	LAYER=4,	QTYPE=23,	\$END	A=23
\$NEWELL	ROW=38,	COL= 9,	Q=.00000048,	LAYER=4,	QTYPE=23,	\$END	A=23
\$NEWELL	ROW=38,	COL=10,	Q=.00000128,	LAYER=4,	QTYPE=23,	\$END	A=23
\$NEWELL	ROW=39,	COL= 9,	Q=.00000016,	LAYER=4,	QTYPE=23,	\$END	A=23
\$NEWELL	ROW=39,	COL=10,	Q=.00000128,	LAYER=4,	QTYPE=23,	\$END	A=23
\$NEWELL	ROW=40,	COL= 9,	Q=.00000072,	LAYER=4,	QTYPE=23,	\$END	A=23
\$NEWELL	ROW=40,	COL=10,	Q=.00000096,	LAYER=4,	QTYPE=23,	\$END	A=23
\$NEWELL	ROW=34,	COL=10,	Q=.00000005,	LAYER=3,	QTYPE=23,	\$END	A=23
\$NEWELL	ROW=35,	COL= 9,	Q=.00000044,	LAYER=3,	QTYPE=23,	\$END	A=23
\$NEWELL	ROW=35,	COL=10,	Q=.00000041,	LAYER=3,	QTYPE=23,	\$END	A=23

Attachment 2.--Input file for the 1950-79 transient simulation--Continued

\$NEWELL	ROW=36,	COL= 9,	Q=.00000044,	LAYER=3,	QTYPE=23,	\$END	A=23
\$NEWELL	ROW=36,	COL=10,	Q=.00000044,	LAYER=3,	QTYPE=23,	\$END	A=23
\$NEWELL	ROW=37,	COL= 9,	Q=.00000019,	LAYER=3,	QTYPE=23,	\$END	A=23
\$NEWELL	ROW=37,	COL=10,	Q=.00000044,	LAYER=3,	QTYPE=23,	\$END	A=23
\$NEWELL	ROW=38,	COL= 9,	Q=.00000016,	LAYER=3,	QTYPE=23,	\$END	A=23
\$NEWELL	ROW=38,	COL=10,	Q=.00000044,	LAYER=3,	QTYPE=23,	\$END	A=23
\$NEWELL	ROW=39,	COL= 9,	Q=.00000005,	LAYER=3,	QTYPE=23,	\$END	A=23
\$NEWELL	ROW=39,	COL=10,	Q=.00000044,	LAYER=3,	QTYPE=23,	\$END	A=23
\$NEWELL	ROW=40,	COL= 9,	Q=.00000025,	LAYER=3,	QTYPE=23,	\$END	A=23
\$NEWELL	ROW=40,	COL=10,	Q=.00000033,	LAYER=3,	QTYPE=23,	\$END	A=23
\$NEWELL	ROW=35,	COL=11,	Q=.00000050,	LAYER=6,	QTYPE=24,	\$END	A=24
\$NEWELL	ROW=35,	COL=12,	Q=.00000042,	LAYER=6,	QTYPE=24,	\$END	A=24
\$NEWELL	ROW=35,	COL=13,	Q=.00000013,	LAYER=6,	QTYPE=24,	\$END	A=24
\$NEWELL	ROW=36,	COL=11,	Q=.00000067,	LAYER=6,	QTYPE=24,	\$END	A=24
\$NEWELL	ROW=36,	COL=12,	Q=.00000067,	LAYER=6,	QTYPE=24,	\$END	A=24
\$NEWELL	ROW=36,	COL=13,	Q=.00000067,	LAYER=6,	QTYPE=24,	\$END	A=24
\$NEWELL	ROW=36,	COL=14,	Q=.00000063,	LAYER=6,	QTYPE=24,	\$END	A=24
\$NEWELL	ROW=35,	COL=11,	Q=.00000147,	LAYER=5,	QTYPE=24,	\$END	A=24
\$NEWELL	ROW=35,	COL=12,	Q=.00000123,	LAYER=5,	QTYPE=24,	\$END	A=24
\$NEWELL	ROW=35,	COL=13,	Q=.00000037,	LAYER=5,	QTYPE=24,	\$END	A=24
\$NEWELL	ROW=36,	COL=11,	Q=.00000196,	LAYER=5,	QTYPE=24,	\$END	A=24
\$NEWELL	ROW=36,	COL=12,	Q=.00000196,	LAYER=5,	QTYPE=24,	\$END	A=24
\$NEWELL	ROW=36,	COL=13,	Q=.00000196,	LAYER=5,	QTYPE=24,	\$END	A=24
\$NEWELL	ROW=36,	COL=14,	Q=.00000184,	LAYER=5,	QTYPE=24,	\$END	A=24
\$NEWELL	ROW=35,	COL=11,	Q=.00000187,	LAYER=4,	QTYPE=24,	\$END	A=24
\$NEWELL	ROW=35,	COL=12,	Q=.00000156,	LAYER=4,	QTYPE=24,	\$END	A=24
\$NEWELL	ROW=35,	COL=13,	Q=.00000047,	LAYER=4,	QTYPE=24,	\$END	A=24
\$NEWELL	ROW=36,	COL=11,	Q=.00000249,	LAYER=4,	QTYPE=24,	\$END	A=24
\$NEWELL	ROW=36,	COL=12,	Q=.00000249,	LAYER=4,	QTYPE=24,	\$END	A=24
\$NEWELL	ROW=36,	COL=13,	Q=.00000249,	LAYER=4,	QTYPE=24,	\$END	A=24
\$NEWELL	ROW=36,	COL=14,	Q=.00000233,	LAYER=4,	QTYPE=24,	\$END	A=24
\$NEWELL	ROW=35,	COL=11,	Q=.00000090,	LAYER=3,	QTYPE=24,	\$END	A=24
\$NEWELL	ROW=35,	COL=12,	Q=.00000075,	LAYER=3,	QTYPE=24,	\$END	A=24
\$NEWELL	ROW=35,	COL=13,	Q=.00000022,	LAYER=3,	QTYPE=24,	\$END	A=24
\$NEWELL	ROW=36,	COL=11,	Q=.00000120,	LAYER=3,	QTYPE=24,	\$END	A=24
\$NEWELL	ROW=36,	COL=12,	Q=.00000120,	LAYER=3,	QTYPE=24,	\$END	A=24
\$NEWELL	ROW=36,	COL=13,	Q=.00000120,	LAYER=3,	QTYPE=24,	\$END	A=24
\$NEWELL	ROW=36,	COL=14,	Q=.00000112,	LAYER=3,	QTYPE=24,	\$END	A=24
\$NEWELL	ROW=35,	COL=23,	Q=.00000045,	LAYER=7,	QTYPE=25,	\$END	A=25
\$NEWELL	ROW=35,	COL=24,	Q=.00000030,	LAYER=7,	QTYPE=25,	\$END	A=25
\$NEWELL	ROW=35,	COL=25,	Q=.00000045,	LAYER=7,	QTYPE=25,	\$END	A=25
\$NEWELL	ROW=35,	COL=26,	Q=.00000012,	LAYER=7,	QTYPE=25,	\$END	A=25
\$NEWELL	ROW=36,	COL=23,	Q=.00000037,	LAYER=7,	QTYPE=25,	\$END	A=25
\$NEWELL	ROW=36,	COL=24,	Q=.00000147,	LAYER=7,	QTYPE=25,	\$END	A=25
\$NEWELL	ROW=36,	COL=25,	Q=.00000147,	LAYER=7,	QTYPE=25,	\$END	A=25
\$NEWELL	ROW=36,	COL=26,	Q=.00000184,	LAYER=7,	QTYPE=25,	\$END	A=25
\$NEWELL	ROW=36,	COL=27,	Q=.00000122,	LAYER=7,	QTYPE=25,	\$END	A=25
\$NEWELL	ROW=37,	COL=23,	Q=.00000024,	LAYER=7,	QTYPE=25,	\$END	A=25
\$NEWELL	ROW=37,	COL=24,	Q=.00000012,	LAYER=7,	QTYPE=25,	\$END	A=25
\$NEWELL	ROW=37,	COL=25,	Q=.00000122,	LAYER=7,	QTYPE=25,	\$END	A=25
\$NEWELL	ROW=37,	COL=26,	Q=.00000196,	LAYER=7,	QTYPE=25,	\$END	A=25
\$NEWELL	ROW=37,	COL=27,	Q=.00000171,	LAYER=7,	QTYPE=25,	\$END	A=25

## Attachment 2.--Input file for the 1950-79 transient simulation--Continued

\$NEWELL	ROW=38,	COL=23,	Q=.00000012,	LAYER=7,	QTYPE=25,	\$END	A=25
\$NEWELL	ROW=38,	COL=26,	Q=.00000098,	LAYER=7,	QTYPE=25,	\$END	A=25
\$NEWELL	ROW=38,	COL=27,	Q=.00000147,	LAYER=7,	QTYPE=25,	\$END	A=25
\$NEWELL	ROW=38,	COL=28,	Q=.00000024,	LAYER=7,	QTYPE=25,	\$END	A=25
\$NEWELL	ROW=39,	COL=27,	Q=.00000122,	LAYER=7,	QTYPE=25,	\$END	A=25
\$NEWELL	ROW=39,	COL=28,	Q=.00000037,	LAYER=7,	QTYPE=25,	\$END	A=25
\$NEWELL	ROW=35,	COL=23,	Q=.00000045,	LAYER=6,	QTYPE=25,	\$END	A=25
\$NEWELL	ROW=35,	COL=24,	Q=.00000030,	LAYER=6,	QTYPE=25,	\$END	A=25
\$NEWELL	ROW=35,	COL=25,	Q=.00000045,	LAYER=6,	QTYPE=25,	\$END	A=25
\$NEWELL	ROW=35,	COL=26,	Q=.00000015,	LAYER=6,	QTYPE=25,	\$END	A=25
\$NEWELL	ROW=36,	COL=23,	Q=.00000045,	LAYER=6,	QTYPE=25,	\$END	A=25
\$NEWELL	ROW=36,	COL=24,	Q=.00000182,	LAYER=6,	QTYPE=25,	\$END	A=25
\$NEWELL	ROW=36,	COL=25,	Q=.00000182,	LAYER=6,	QTYPE=25,	\$END	A=25
\$NEWELL	ROW=36,	COL=26,	Q=.00000227,	LAYER=6,	QTYPE=25,	\$END	A=25
\$NEWELL	ROW=36,	COL=27,	Q=.00000152,	LAYER=6,	QTYPE=25,	\$END	A=25
\$NEWELL	ROW=37,	COL=23,	Q=.00000030,	LAYER=6,	QTYPE=25,	\$END	A=25
\$NEWELL	ROW=37,	COL=24,	Q=.00000015,	LAYER=6,	QTYPE=25,	\$END	A=25
\$NEWELL	ROW=37,	COL=25,	Q=.00000152,	LAYER=6,	QTYPE=25,	\$END	A=25
\$NEWELL	ROW=37,	COL=26,	Q=.00000242,	LAYER=6,	QTYPE=25,	\$END	A=25
\$NEWELL	ROW=37,	COL=27,	Q=.00000212,	LAYER=6,	QTYPE=25,	\$END	A=25
\$NEWELL	ROW=38,	COL=23,	Q=.00000015,	LAYER=6,	QTYPE=25,	\$END	A=25
\$NEWELL	ROW=38,	COL=26,	Q=.00000121,	LAYER=6,	QTYPE=25,	\$END	A=25
\$NEWELL	ROW=38,	COL=27,	Q=.00000182,	LAYER=6,	QTYPE=25,	\$END	A=25
\$NEWELL	ROW=38,	COL=28,	Q=.00000030,	LAYER=6,	QTYPE=25,	\$END	A=25
\$NEWELL	ROW=39,	COL=27,	Q=.00000152,	LAYER=6,	QTYPE=25,	\$END	A=25
\$NEWELL	ROW=39,	COL=28,	Q=.00000045,	LAYER=6,	QTYPE=25,	\$END	A=25
\$NEWELL	ROW=35,	COL=23,	Q=.00000024,	LAYER=5,	QTYPE=25,	\$END	A=25
\$NEWELL	ROW=35,	COL=24,	Q=.00000016,	LAYER=5,	QTYPE=25,	\$END	A=25
\$NEWELL	ROW=35,	COL=25,	Q=.00000024,	LAYER=5,	QTYPE=25,	\$END	A=25
\$NEWELL	ROW=35,	COL=26,	Q=.00000008,	LAYER=5,	QTYPE=25,	\$END	A=25
\$NEWELL	ROW=36,	COL=23,	Q=.00000024,	LAYER=5,	QTYPE=25,	\$END	A=25
\$NEWELL	ROW=36,	COL=24,	Q=.00000097,	LAYER=5,	QTYPE=25,	\$END	A=25
\$NEWELL	ROW=36,	COL=25,	Q=.00000097,	LAYER=5,	QTYPE=25,	\$END	A=25
\$NEWELL	ROW=36,	COL=26,	Q=.00000121,	LAYER=5,	QTYPE=25,	\$END	A=25
\$NEWELL	ROW=36,	COL=27,	Q=.00000081,	LAYER=5,	QTYPE=25,	\$END	A=25
\$NEWELL	ROW=37,	COL=23,	Q=.00000016,	LAYER=5,	QTYPE=25,	\$END	A=25
\$NEWELL	ROW=37,	COL=24,	Q=.00000008,	LAYER=5,	QTYPE=25,	\$END	A=25
\$NEWELL	ROW=37,	COL=25,	Q=.00000081,	LAYER=5,	QTYPE=25,	\$END	A=25
\$NEWELL	ROW=37,	COL=26,	Q=.00000129,	LAYER=5,	QTYPE=25,	\$END	A=25
\$NEWELL	ROW=37,	COL=27,	Q=.00000113,	LAYER=5,	QTYPE=25,	\$END	A=25
\$NEWELL	ROW=38,	COL=23,	Q=.00000008,	LAYER=5,	QTYPE=25,	\$END	A=25
\$NEWELL	ROW=38,	COL=26,	Q=.00000064,	LAYER=5,	QTYPE=25,	\$END	A=25
\$NEWELL	ROW=38,	COL=27,	Q=.00000097,	LAYER=5,	QTYPE=25,	\$END	A=25
\$NEWELL	ROW=38,	COL=28,	Q=.00000016,	LAYER=5,	QTYPE=25,	\$END	A=25
\$NEWELL	ROW=39,	COL=27,	Q=.00000081,	LAYER=5,	QTYPE=25,	\$END	A=25
\$NEWELL	ROW=39,	COL=28,	Q=.00000024,	LAYER=5,	QTYPE=25,	\$END	A=25
\$NEWELL	ROW=35,	COL=23,	Q=.00000009,	LAYER=4,	QTYPE=25,	\$END	A=25
\$NEWELL	ROW=35,	COL=24,	Q=.00000006,	LAYER=4,	QTYPE=25,	\$END	A=25
\$NEWELL	ROW=35,	COL=25,	Q=.00000009,	LAYER=4,	QTYPE=25,	\$END	A=25
\$NEWELL	ROW=35,	COL=26,	Q=.00000003,	LAYER=4,	QTYPE=25,	\$END	A=25
\$NEWELL	ROW=36,	COL=23,	Q=.00000009,	LAYER=4,	QTYPE=25,	\$END	A=25
\$NEWELL	ROW=36,	COL=24,	Q=.00000037,	LAYER=4,	QTYPE=25,	\$END	A=25

## Attachment 2.--Input file for the 1950-79 transient simulation--Continued

\$NEWELL	ROW=36,	COL=25,	Q=.00000037,	LAYER=4,	QTYPE=25,	\$END	A=25
\$NEWELL	ROW=36,	COL=26,	Q=.00000047,	LAYER=4,	QTYPE=25,	\$END	A=25
\$NEWELL	ROW=36,	COL=27,	Q=.00000031,	LAYER=4,	QTYPE=25,	\$END	A=25
\$NEWELL	ROW=37,	COL=23,	Q=.00000006,	LAYER=4,	QTYPE=25,	\$END	A=25
\$NEWELL	ROW=37,	COL=24,	Q=.00000003,	LAYER=4,	QTYPE=25,	\$END	A=25
\$NEWELL	ROW=37,	COL=25,	Q=.00000031,	LAYER=4,	QTYPE=25,	\$END	A=25
\$NEWELL	ROW=37,	COL=26,	Q=.00000050,	LAYER=4,	QTYPE=25,	\$END	A=25
\$NEWELL	ROW=37,	COL=27,	Q=.00000044,	LAYER=4,	QTYPE=25,	\$END	A=25
\$NEWELL	ROW=38,	COL=23,	Q=.00000033,	LAYER=4,	QTYPE=25,	\$END	A=25
\$NEWELL	ROW=38,	COL=26,	Q=.00000025,	LAYER=4,	QTYPE=25,	\$END	A=25
\$NEWELL	ROW=38,	COL=27,	Q=.00000037,	LAYER=4,	QTYPE=25,	\$END	A=25
\$NEWELL	ROW=38,	COL=28,	Q=.00000006,	LAYER=4,	QTYPE=25,	\$END	A=25
\$NEWELL	ROW=39,	COL=27,	Q=.00000031,	LAYER=4,	QTYPE=25,	\$END	A=25
\$NEWELL	ROW=39,	COL=28,	Q=.00000009,	LAYER=4,	QTYPE=25,	\$END	A=25
\$NEWELL	ROW=35,	COL=23,	Q=.00000003,	LAYER=3,	QTYPE=25,	\$END	A=25
\$NEWELL	ROW=35,	COL=24,	Q=.00000002,	LAYER=3,	QTYPE=25,	\$END	A=25
\$NEWELL	ROW=35,	COL=25,	Q=.00000003,	LAYER=3,	QTYPE=25,	\$END	A=25
\$NEWELL	ROW=35,	COL=26,	Q=.00000001,	LAYER=3,	QTYPE=25,	\$END	A=25
\$NEWELL	ROW=36,	COL=23,	Q=.00000003,	LAYER=3,	QTYPE=25,	\$END	A=25
\$NEWELL	ROW=36,	COL=24,	Q=.00000011,	LAYER=3,	QTYPE=25,	\$END	A=25
\$NEWELL	ROW=36,	COL=25,	Q=.00000011,	LAYER=3,	QTYPE=25,	\$END	A=25
\$NEWELL	ROW=36,	COL=26,	Q=.00000014,	LAYER=3,	QTYPE=25,	\$END	A=25
\$NEWELL	ROW=36,	COL=27,	Q=.00000009,	LAYER=3,	QTYPE=25,	\$END	A=25
\$NEWELL	ROW=37,	COL=23,	Q=.00000002,	LAYER=3,	QTYPE=25,	\$END	A=25
\$NEWELL	ROW=37,	COL=24,	Q=.00000001,	LAYER=3,	QTYPE=25,	\$END	A=25
\$NEWELL	ROW=37,	COL=25,	Q=.00000009,	LAYER=3,	QTYPE=25,	\$END	A=25
\$NEWELL	ROW=37,	COL=26,	Q=.00000015,	LAYER=3,	QTYPE=25,	\$END	A=25
\$NEWELL	ROW=37,	COL=27,	Q=.00000013,	LAYER=3,	QTYPE=25,	\$END	A=25
\$NEWELL	ROW=38,	COL=23,	Q=.00000001,	LAYER=3,	QTYPE=25,	\$END	A=25
\$NEWELL	ROW=38,	COL=26,	Q=.00000007,	LAYER=3,	QTYPE=25,	\$END	A=25
\$NEWELL	ROW=38,	COL=27,	Q=.00000011,	LAYER=3,	QTYPE=25,	\$END	A=25
\$NEWELL	ROW=38,	COL=28,	Q=.00000002,	LAYER=3,	QTYPE=25,	\$END	A=25
\$NEWELL	ROW=39,	COL=27,	Q=.00000009,	LAYER=3,	QTYPE=25,	\$END	A=25
\$NEWELL	ROW=39,	COL=28,	Q=.00000003,	LAYER=3,	QTYPE=25,	\$END	A=25
\$NEWELL	ROW=37,	COL=11,	Q=.00000078,	LAYER=7,	QTYPE=26,	\$END	A=26
\$NEWELL	ROW=37,	COL=12,	Q=.00000073,	LAYER=7,	QTYPE=26,	\$END	A=26
\$NEWELL	ROW=38,	COL=11,	Q=.00000078,	LAYER=7,	QTYPE=26,	\$END	A=26
\$NEWELL	ROW=38,	COL=12,	Q=.00000068,	LAYER=7,	QTYPE=26,	\$END	A=26
\$NEWELL	ROW=39,	COL=11,	Q=.00000078,	LAYER=7,	QTYPE=26,	\$END	A=26
\$NEWELL	ROW=39,	COL=12,	Q=.00000063,	LAYER=7,	QTYPE=26,	\$END	A=26
\$NEWELL	ROW=40,	COL=11,	Q=.00000063,	LAYER=7,	QTYPE=26,	\$END	A=26
\$NEWELL	ROW=40,	COL=12,	Q=.00000078,	LAYER=7,	QTYPE=26,	\$END	A=26
\$NEWELL	ROW=41,	COL=11,	Q=.00000078,	LAYER=7,	QTYPE=26,	\$END	A=26
\$NEWELL	ROW=41,	COL=12,	Q=.00000058,	LAYER=7,	QTYPE=26,	\$END	A=26
\$NEWELL	ROW=41,	COL=13,	Q=.00000049,	LAYER=7,	QTYPE=26,	\$END	A=26
\$NEWELL	ROW=42,	COL=11,	Q=.00000078,	LAYER=7,	QTYPE=26,	\$END	A=26
\$NEWELL	ROW=42,	COL=12,	Q=.00000078,	LAYER=7,	QTYPE=26,	\$END	A=26
\$NEWELL	ROW=42,	COL=13,	Q=.00000078,	LAYER=7,	QTYPE=26,	\$END	A=26
\$NEWELL	ROW=42,	COL=14,	Q=.00000058,	LAYER=7,	QTYPE=26,	\$END	A=26
\$NEWELL	ROW=42,	COL=15,	Q=.00000039,	LAYER=7,	QTYPE=26,	\$END	A=26
\$NEWELL	ROW=43,	COL=11,	Q=.00000078,	LAYER=7,	QTYPE=26,	\$END	A=26
\$NEWELL	ROW=43,	COL=12,	Q=.00000078,	LAYER=7,	QTYPE=26,	\$END	A=26



## Attachment 2.--Input file for the 1950-79 transient simulation--Continued

\$NEWELL	ROW=43,	COL=13,	Q=.00000078,	LAYER=7,	QTYPE=26,	\$END	A=26
\$NEWELL	ROW=43,	COL=14,	Q=.00000073,	LAYER=7,	QTYPE=26,	\$END	A=26
\$NEWELL	ROW=43,	COL=15,	Q=.00000010,	LAYER=7,	QTYPE=26,	\$END	A=26
\$NEWELL	ROW=44,	COL=11,	Q=.00000078,	LAYER=7,	QTYPE=26,	\$END	A=26
\$NEWELL	ROW=44,	COL=12,	Q=.00000078,	LAYER=7,	QTYPE=26,	\$END	A=26
\$NEWELL	ROW=44,	COL=13,	Q=.00000068,	LAYER=7,	QTYPE=26,	\$END	A=26
\$NEWELL	ROW=45,	COL=11,	Q=.00000078,	LAYER=7,	QTYPE=26,	\$END	A=26
\$NEWELL	ROW=45,	COL=12,	Q=.00000078,	LAYER=7,	QTYPE=26,	\$END	A=26
\$NEWELL	ROW=45,	COL=13,	Q=.00000063,	LAYER=7,	QTYPE=26,	\$END	A=26
\$NEWELL	ROW=46,	COL=11,	Q=.00000078,	LAYER=7,	QTYPE=26,	\$END	A=26
\$NEWELL	ROW=37,	COL=11,	Q=.00000171,	LAYER=6,	QTYPE=26,	\$END	A=26
\$NEWELL	ROW=37,	COL=12,	Q=.00000160,	LAYER=6,	QTYPE=26,	\$END	A=26
\$NEWELL	ROW=38,	COL=11,	Q=.00000171,	LAYER=6,	QTYPE=26,	\$END	A=26
\$NEWELL	ROW=38,	COL=12,	Q=.00000150,	LAYER=6,	QTYPE=26,	\$END	A=26
\$NEWELL	ROW=39,	COL=11,	Q=.00000171,	LAYER=6,	QTYPE=26,	\$END	A=26
\$NEWELL	ROW=39,	COL=12,	Q=.00000139,	LAYER=6,	QTYPE=26,	\$END	A=26
\$NEWELL	ROW=40,	COL=11,	Q=.00000139,	LAYER=6,	QTYPE=26,	\$END	A=26
\$NEWELL	ROW=40,	COL=12,	Q=.00000171,	LAYER=6,	QTYPE=26,	\$END	A=26
\$NEWELL	ROW=41,	COL=11,	Q=.00000171,	LAYER=6,	QTYPE=26,	\$END	A=26
\$NEWELL	ROW=41,	COL=12,	Q=.00000128,	LAYER=6,	QTYPE=26,	\$END	A=26
\$NEWELL	ROW=41,	COL=13,	Q=.00000107,	LAYER=6,	QTYPE=26,	\$END	A=26
\$NEWELL	ROW=42,	COL=11,	Q=.00000171,	LAYER=6,	QTYPE=26,	\$END	A=26
\$NEWELL	ROW=42,	COL=12,	Q=.00000171,	LAYER=6,	QTYPE=26,	\$END	A=26
\$NEWELL	ROW=42,	COL=13,	Q=.00000171,	LAYER=6,	QTYPE=26,	\$END	A=26
\$NEWELL	ROW=42,	COL=14,	Q=.00000128,	LAYER=6,	QTYPE=26,	\$END	A=26
\$NEWELL	ROW=42,	COL=15,	Q=.00000086,	LAYER=6,	QTYPE=26,	\$END	A=26
\$NEWELL	ROW=43,	COL=11,	Q=.00000171,	LAYER=6,	QTYPE=26,	\$END	A=26
\$NEWELL	ROW=43,	COL=12,	Q=.00000171,	LAYER=6,	QTYPE=26,	\$END	A=26
\$NEWELL	ROW=43,	COL=13,	Q=.00000171,	LAYER=6,	QTYPE=26,	\$END	A=26
\$NEWELL	ROW=43,	COL=14,	Q=.00000160,	LAYER=6,	QTYPE=26,	\$END	A=26
\$NEWELL	ROW=43,	COL=15,	Q=.00000021,	LAYER=6,	QTYPE=26,	\$END	A=26
\$NEWELL	ROW=44,	COL=11,	Q=.00000171,	LAYER=6,	QTYPE=26,	\$END	A=26
\$NEWELL	ROW=44,	COL=12,	Q=.00000171,	LAYER=6,	QTYPE=26,	\$END	A=26
\$NEWELL	ROW=44,	COL=13,	Q=.00000150,	LAYER=6,	QTYPE=26,	\$END	A=26
\$NEWELL	ROW=45,	COL=11,	Q=.00000171,	LAYER=6,	QTYPE=26,	\$END	A=26
\$NEWELL	ROW=45,	COL=12,	Q=.00000171,	LAYER=6,	QTYPE=26,	\$END	A=26
\$NEWELL	ROW=45,	COL=13,	Q=.00000139,	LAYER=6,	QTYPE=26,	\$END	A=26
\$NEWELL	ROW=46,	COL=11,	Q=.00000171,	LAYER=6,	QTYPE=26,	\$END	A=26
\$NEWELL	ROW=37,	COL=11,	Q=.00000236,	LAYER=5,	QTYPE=26,	\$END	A=26
\$NEWELL	ROW=37,	COL=12,	Q=.00000221,	LAYER=5,	QTYPE=26,	\$END	A=26
\$NEWELL	ROW=38,	COL=11,	Q=.00000236,	LAYER=5,	QTYPE=26,	\$END	A=26
\$NEWELL	ROW=38,	COL=12,	Q=.00000207,	LAYER=5,	QTYPE=26,	\$END	A=26
\$NEWELL	ROW=39,	COL=11,	Q=.00000236,	LAYER=5,	QTYPE=26,	\$END	A=26
\$NEWELL	ROW=39,	COL=12,	Q=.00000192,	LAYER=5,	QTYPE=26,	\$END	A=26
\$NEWELL	ROW=40,	COL=11,	Q=.00000192,	LAYER=5,	QTYPE=26,	\$END	A=26
\$NEWELL	ROW=40,	COL=12,	Q=.00000236,	LAYER=5,	QTYPE=26,	\$END	A=26
\$NEWELL	ROW=41,	COL=11,	Q=.00000236,	LAYER=5,	QTYPE=26,	\$END	A=26
\$NEWELL	ROW=41,	COL=12,	Q=.00000177,	LAYER=5,	QTYPE=26,	\$END	A=26
\$NEWELL	ROW=41,	COL=13,	Q=.00000148,	LAYER=5,	QTYPE=26,	\$END	A=26
\$NEWELL	ROW=42,	COL=11,	Q=.00000236,	LAYER=5,	QTYPE=26,	\$END	A=26
\$NEWELL	ROW=42,	COL=12,	Q=.00000236,	LAYER=5,	QTYPE=26,	\$END	A=26
\$NEWELL	ROW=42,	COL=13,	Q=.00000236,	LAYER=5,	QTYPE=26,	\$END	A=26

Attachment 2.--Input file for the 1950-79 transient simulation--Continued

\$NEWELL	ROW=42,	COL=14,	Q=.00000177,	LAYER=5,	QTYPE=26,	\$END	A=26
\$NEWELL	ROW=42,	COL=15,	Q=.00000118,	LAYER=5,	QTYPE=26,	\$END	A=26
\$NEWELL	ROW=43,	COL=11,	Q=.00000236,	LAYER=5,	QTYPE=26,	\$END	A=26
\$NEWELL	ROW=43,	COL=12,	Q=.00000236,	LAYER=5,	QTYPE=26,	\$END	A=26
\$NEWELL	ROW=43,	COL=13,	Q=.00000236,	LAYER=5,	QTYPE=26,	\$END	A=26
\$NEWELL	ROW=43,	COL=14,	Q=.00000221,	LAYER=5,	QTYPE=26,	\$END	A=26
\$NEWELL	ROW=43,	COL=15,	Q=.00000030,	LAYER=5,	QTYPE=26,	\$END	A=26
\$NEWELL	ROW=44,	COL=11,	Q=.00000236,	LAYER=5,	QTYPE=26,	\$END	A=26
\$NEWELL	ROW=44,	COL=12,	Q=.00000236,	LAYER=5,	QTYPE=26,	\$END	A=26
\$NEWELL	ROW=44,	COL=13,	Q=.00000207,	LAYER=5,	QTYPE=26,	\$END	A=26
\$NEWELL	ROW=45,	COL=11,	Q=.00000236,	LAYER=5,	QTYPE=26,	\$END	A=26
\$NEWELL	ROW=45,	COL=12,	Q=.00000236,	LAYER=5,	QTYPE=26,	\$END	A=26
\$NEWELL	ROW=45,	COL=13,	Q=.00000192,	LAYER=5,	QTYPE=26,	\$END	A=26
\$NEWELL	ROW=46,	COL=11,	Q=.00000236,	LAYER=5,	QTYPE=26,	\$END	A=26
\$NEWELL	ROW=37,	COL=11,	Q=.00000134,	LAYER=4,	QTYPE=26,	\$END	A=26
\$NEWELL	ROW=37,	COL=12,	Q=.00000126,	LAYER=4,	QTYPE=26,	\$END	A=26
\$NEWELL	ROW=38,	COL=11,	Q=.00000134,	LAYER=4,	QTYPE=26,	\$END	A=26
\$NEWELL	ROW=38,	COL=12,	Q=.00000117,	LAYER=4,	QTYPE=26,	\$END	A=26
\$NEWELL	ROW=39,	COL=11,	Q=.00000134,	LAYER=4,	QTYPE=26,	\$END	A=26
\$NEWELL	ROW=39,	COL=12,	Q=.00000109,	LAYER=4,	QTYPE=26,	\$END	A=26
\$NEWELL	ROW=40,	COL=11,	Q=.00000109,	LAYER=4,	QTYPE=26,	\$END	A=26
\$NEWELL	ROW=40,	COL=12,	Q=.00000134,	LAYER=4,	QTYPE=26,	\$END	A=26
\$NEWELL	ROW=41,	COL=11,	Q=.00000134,	LAYER=4,	QTYPE=26,	\$END	A=26
\$NEWELL	ROW=41,	COL=12,	Q=.00000100,	LAYER=4,	QTYPE=26,	\$END	A=26
\$NEWELL	ROW=41,	COL=13,	Q=.00000084,	LAYER=4,	QTYPE=26,	\$END	A=26
\$NEWELL	ROW=42,	COL=11,	Q=.00000134,	LAYER=4,	QTYPE=26,	\$END	A=26
\$NEWELL	ROW=42,	COL=12,	Q=.00000134,	LAYER=4,	QTYPE=26,	\$END	A=26
\$NEWELL	ROW=42,	COL=13,	Q=.00000134,	LAYER=4,	QTYPE=26,	\$END	A=26
\$NEWELL	ROW=42,	COL=14,	Q=.00000100,	LAYER=4,	QTYPE=26,	\$END	A=26
\$NEWELL	ROW=42,	COL=15,	Q=.00000068,	LAYER=4,	QTYPE=26,	\$END	A=26
\$NEWELL	ROW=43,	COL=11,	Q=.00000134,	LAYER=4,	QTYPE=26,	\$END	A=26
\$NEWELL	ROW=43,	COL=12,	Q=.00000134,	LAYER=4,	QTYPE=26,	\$END	A=26
\$NEWELL	ROW=43,	COL=13,	Q=.00000134,	LAYER=4,	QTYPE=26,	\$END	A=26
\$NEWELL	ROW=43,	COL=14,	Q=.00000126,	LAYER=4,	QTYPE=26,	\$END	A=26
\$NEWELL	ROW=43,	COL=15,	Q=.00000017,	LAYER=4,	QTYPE=26,	\$END	A=26
\$NEWELL	ROW=44,	COL=11,	Q=.00000134,	LAYER=4,	QTYPE=26,	\$END	A=26
\$NEWELL	ROW=44,	COL=12,	Q=.00000134,	LAYER=4,	QTYPE=26,	\$END	A=26
\$NEWELL	ROW=44,	COL=13,	Q=.00000117,	LAYER=4,	QTYPE=26,	\$END	A=26
\$NEWELL	ROW=45,	COL=11,	Q=.00000134,	LAYER=4,	QTYPE=26,	\$END	A=26
\$NEWELL	ROW=45,	COL=12,	Q=.00000134,	LAYER=4,	QTYPE=26,	\$END	A=26
\$NEWELL	ROW=45,	COL=13,	Q=.00000109,	LAYER=4,	QTYPE=26,	\$END	A=26
\$NEWELL	ROW=46,	COL=11,	Q=.00000134,	LAYER=4,	QTYPE=26,	\$END	A=26
\$NEWELL	ROW=37,	COL=11,	Q=.00000013,	LAYER=3,	QTYPE=26,	\$END	A=26
\$NEWELL	ROW=37,	COL=12,	Q=.00000012,	LAYER=3,	QTYPE=26,	\$END	A=26
\$NEWELL	ROW=38,	COL=11,	Q=.00000013,	LAYER=3,	QTYPE=26,	\$END	A=26
\$NEWELL	ROW=38,	COL=12,	Q=.00000012,	LAYER=3,	QTYPE=26,	\$END	A=26
\$NEWELL	ROW=39,	COL=11,	Q=.00000013,	LAYER=3,	QTYPE=26,	\$END	A=26
\$NEWELL	ROW=39,	COL=12,	Q=.00000011,	LAYER=3,	QTYPE=26,	\$END	A=26
\$NEWELL	ROW=40,	COL=11,	Q=.00000011,	LAYER=3,	QTYPE=26,	\$END	A=26
\$NEWELL	ROW=40,	COL=12,	Q=.00000013,	LAYER=3,	QTYPE=26,	\$END	A=26
\$NEWELL	ROW=41,	COL=11,	Q=.00000013,	LAYER=3,	QTYPE=26,	\$END	A=26
\$NEWELL	ROW=41,	COL=12,	Q=.00000010,	LAYER=3,	QTYPE=26,	\$END	A=26

Attachment 2.--Input file for the 1950-79 transient simulation--Continued

\$NEWELL	ROW=41,	COL=13,	Q=.00000008,	LAYER=3,	QTYPE=26,	\$END	A=26
\$NEWELL	ROW=42,	COL=11,	Q=.00000013,	LAYER=3,	QTYPE=26,	\$END	A=26
\$NEWELL	ROW=42,	COL=12,	Q=.00000013,	LAYER=3,	QTYPE=26,	\$END	A=26
\$NEWELL	ROW=42,	COL=13,	Q=.00000013,	LAYER=3,	QTYPE=26,	\$END	A=26
\$NEWELL	ROW=42,	COL=14,	Q=.00000010,	LAYER=3,	QTYPE=26,	\$END	A=26
\$NEWELL	ROW=42,	COL=15,	Q=.00000007,	LAYER=3,	QTYPE=26,	\$END	A=26
\$NEWELL	ROW=43,	COL=11,	Q=.00000013,	LAYER=3,	QTYPE=26,	\$END	A=26
\$NEWELL	ROW=43,	COL=12,	Q=.00000013,	LAYER=3,	QTYPE=26,	\$END	A=26
\$NEWELL	ROW=43,	COL=13,	Q=.00000013,	LAYER=3,	QTYPE=26,	\$END	A=26
\$NEWELL	ROW=43,	COL=14,	Q=.00000012,	LAYER=3,	QTYPE=26,	\$END	A=26
\$NEWELL	ROW=43,	COL=15,	Q=.00000002,	LAYER=3,	QTYPE=26,	\$END	A=26
\$NEWELL	ROW=44,	COL=11,	Q=.00000013,	LAYER=3,	QTYPE=26,	\$END	A=26
\$NEWELL	ROW=44,	COL=12,	Q=.00000013,	LAYER=3,	QTYPE=26,	\$END	A=26
\$NEWELL	ROW=44,	COL=13,	Q=.00000012,	LAYER=3,	QTYPE=26,	\$END	A=26
\$NEWELL	ROW=45,	COL=11,	Q=.00000013,	LAYER=3,	QTYPE=26,	\$END	A=26
\$NEWELL	ROW=45,	COL=12,	Q=.00000013,	LAYER=3,	QTYPE=26,	\$END	A=26
\$NEWELL	ROW=45,	COL=13,	Q=.00000011,	LAYER=3,	QTYPE=26,	\$END	A=26
\$NEWELL	ROW=46,	COL=11,	Q=.00000013,	LAYER=3,	QTYPE=26,	\$END	A=26
\$NEWELL	ROW=37,	COL=13,	Q=.00000100,	LAYER=5,	QTYPE=27,	\$END	A=27
\$NEWELL	ROW=37,	COL=14,	Q=.00000134,	LAYER=5,	QTYPE=27,	\$END	A=27
\$NEWELL	ROW=37,	COL=15,	Q=.00000100,	LAYER=5,	QTYPE=27,	\$END	A=27
\$NEWELL	ROW=38,	COL=13,	Q=.00000126,	LAYER=5,	QTYPE=27,	\$END	A=27
\$NEWELL	ROW=38,	COL=14,	Q=.00000134,	LAYER=5,	QTYPE=27,	\$END	A=27
\$NEWELL	ROW=38,	COL=15,	Q=.00000134,	LAYER=5,	QTYPE=27,	\$END	A=27
\$NEWELL	ROW=39,	COL=13,	Q=.00000067,	LAYER=5,	QTYPE=27,	\$END	A=27
\$NEWELL	ROW=39,	COL=14,	Q=.00000134,	LAYER=5,	QTYPE=27,	\$END	A=27
\$NEWELL	ROW=39,	COL=15,	Q=.00000134,	LAYER=5,	QTYPE=27,	\$END	A=27
\$NEWELL	ROW=39,	COL=16,	Q=.00000134,	LAYER=5,	QTYPE=27,	\$END	A=27
\$NEWELL	ROW=40,	COL=13,	Q=.00000134,	LAYER=5,	QTYPE=27,	\$END	A=27
\$NEWELL	ROW=40,	COL=14,	Q=.00000134,	LAYER=5,	QTYPE=27,	\$END	A=27
\$NEWELL	ROW=40,	COL=15,	Q=.00000117,	LAYER=5,	QTYPE=27,	\$END	A=27
\$NEWELL	ROW=40,	COL=16,	Q=.00000067,	LAYER=5,	QTYPE=27,	\$END	A=27
\$NEWELL	ROW=40,	COL=17,	Q=.00000067,	LAYER=5,	QTYPE=27,	\$END	A=27
\$NEWELL	ROW=41,	COL=14,	Q=.00000117,	LAYER=5,	QTYPE=27,	\$END	A=27
\$NEWELL	ROW=41,	COL=15,	Q=.00000117,	LAYER=5,	QTYPE=27,	\$END	A=27
\$NEWELL	ROW=41,	COL=16,	Q=.00000067,	LAYER=5,	QTYPE=27,	\$END	A=27
\$NEWELL	ROW=37,	COL=13,	Q=.00000237,	LAYER=4,	QTYPE=27,	\$END	A=27
\$NEWELL	ROW=37,	COL=14,	Q=.00000316,	LAYER=4,	QTYPE=27,	\$END	A=27
\$NEWELL	ROW=37,	COL=15,	Q=.00000237,	LAYER=4,	QTYPE=27,	\$END	A=27
\$NEWELL	ROW=38,	COL=13,	Q=.00000296,	LAYER=4,	QTYPE=27,	\$END	A=27
\$NEWELL	ROW=38,	COL=14,	Q=.00000316,	LAYER=4,	QTYPE=27,	\$END	A=27
\$NEWELL	ROW=38,	COL=15,	Q=.00000316,	LAYER=4,	QTYPE=27,	\$END	A=27
\$NEWELL	ROW=39,	COL=13,	Q=.00000158,	LAYER=4,	QTYPE=27,	\$END	A=27
\$NEWELL	ROW=39,	COL=14,	Q=.00000316,	LAYER=4,	QTYPE=27,	\$END	A=27
\$NEWELL	ROW=39,	COL=15,	Q=.00000316,	LAYER=4,	QTYPE=27,	\$END	A=27
\$NEWELL	ROW=39,	COL=16,	Q=.00000316,	LAYER=4,	QTYPE=27,	\$END	A=27
\$NEWELL	ROW=40,	COL=13,	Q=.00000316,	LAYER=4,	QTYPE=27,	\$END	A=27
\$NEWELL	ROW=40,	COL=14,	Q=.00000316,	LAYER=4,	QTYPE=27,	\$END	A=27
\$NEWELL	ROW=40,	COL=15,	Q=.00000276,	LAYER=4,	QTYPE=27,	\$END	A=27
\$NEWELL	ROW=40,	COL=16,	Q=.00000158,	LAYER=4,	QTYPE=27,	\$END	A=27
\$NEWELL	ROW=40,	COL=17,	Q=.00000158,	LAYER=4,	QTYPE=27,	\$END	A=27
\$NEWELL	ROW=41,	COL=14,	Q=.00000276,	LAYER=4,	QTYPE=27,	\$END	A=27

Attachment 2.--Input file for the 1950-79 transient simulation--Continued

\$NEWELL	ROW=41,	COL=15,	Q=.00000276,	LAYER=4,	QTYPE=27,	\$END	A=27
\$NEWELL	ROW=41,	COL=16,	Q=.00000158,	LAYER=4,	QTYPE=27,	\$END	A=27
\$NEWELL	ROW=37,	COL=13,	Q=.00000137,	LAYER=3,	QTYPE=27,	\$END	A=27
\$NEWELL	ROW=37,	COL=14,	Q=.00000183,	LAYER=3,	QTYPE=27,	\$END	A=27
\$NEWELL	ROW=37,	COL=15,	Q=.00000137,	LAYER=3,	QTYPE=27,	\$END	A=27
\$NEWELL	ROW=38,	COL=13,	Q=.00000171,	LAYER=3,	QTYPE=27,	\$END	A=27
\$NEWELL	ROW=38,	COL=14,	Q=.00000183,	LAYER=3,	QTYPE=27,	\$END	A=27
\$NEWELL	ROW=38,	COL=15,	Q=.00000183,	LAYER=3,	QTYPE=27,	\$END	A=27
\$NEWELL	ROW=39,	COL=13,	Q=.00000091,	LAYER=3,	QTYPE=27,	\$END	A=27
\$NEWELL	ROW=39,	COL=14,	Q=.00000183,	LAYER=3,	QTYPE=27,	\$END	A=27
\$NEWELL	ROW=39,	COL=15,	Q=.00000183,	LAYER=3,	QTYPE=27,	\$END	A=27
\$NEWELL	ROW=39,	COL=16,	Q=.00000183,	LAYER=3,	QTYPE=27,	\$END	A=27
\$NEWELL	ROW=40,	COL=13,	Q=.00000183,	LAYER=3,	QTYPE=27,	\$END	A=27
\$NEWELL	ROW=40,	COL=14,	Q=.00000183,	LAYER=3,	QTYPE=27,	\$END	A=27
\$NEWELL	ROW=40,	COL=15,	Q=.00000160,	LAYER=3,	QTYPE=27,	\$END	A=27
\$NEWELL	ROW=40,	COL=16,	Q=.00000091,	LAYER=3,	QTYPE=27,	\$END	A=27
\$NEWELL	ROW=40,	COL=17,	Q=.00000091,	LAYER=3,	QTYPE=27,	\$END	A=27
\$NEWELL	ROW=41,	COL=14,	Q=.00000160,	LAYER=3,	QTYPE=27,	\$END	A=27
\$NEWELL	ROW=41,	COL=15,	Q=.00000160,	LAYER=3,	QTYPE=27,	\$END	A=27
\$NEWELL	ROW=41,	COL=16,	Q=.00000091,	LAYER=3,	QTYPE=27,	\$END	A=27
\$NEWELL	ROW=38,	COL=19,	Q=.00000018,	LAYER=7,	QTYPE=28,	\$END	A=28
\$NEWELL	ROW=38,	COL=20,	Q=.00000005,	LAYER=7,	QTYPE=28,	\$END	A=28
\$NEWELL	ROW=38,	COL=21,	Q=.00000005,	LAYER=7,	QTYPE=28,	\$END	A=28
\$NEWELL	ROW=39,	COL=19,	Q=.00000009,	LAYER=7,	QTYPE=28,	\$END	A=28
\$NEWELL	ROW=39,	COL=20,	Q=.00000005,	LAYER=7,	QTYPE=28,	\$END	A=28
\$NEWELL	ROW=39,	COL=21,	Q=.00000046,	LAYER=7,	QTYPE=28,	\$END	A=28
\$NEWELL	ROW=40,	COL=20,	Q=.00000009,	LAYER=7,	QTYPE=28,	\$END	A=28
\$NEWELL	ROW=40,	COL=21,	Q=.00000073,	LAYER=7,	QTYPE=28,	\$END	A=28
\$NEWELL	ROW=41,	COL=21,	Q=.00000009,	LAYER=7,	QTYPE=28,	\$END	A=28
\$NEWELL	ROW=38,	COL=19,	Q=.00000069,	LAYER=6,	QTYPE=28,	\$END	A=28
\$NEWELL	ROW=38,	COL=20,	Q=.00000017,	LAYER=6,	QTYPE=28,	\$END	A=28
\$NEWELL	ROW=38,	COL=21,	Q=.00000017,	LAYER=6,	QTYPE=28,	\$END	A=28
\$NEWELL	ROW=39,	COL=19,	Q=.00000034,	LAYER=6,	QTYPE=28,	\$END	A=28
\$NEWELL	ROW=39,	COL=20,	Q=.00000017,	LAYER=6,	QTYPE=28,	\$END	A=28
\$NEWELL	ROW=39,	COL=21,	Q=.00000172,	LAYER=6,	QTYPE=28,	\$END	A=28
\$NEWELL	ROW=40,	COL=20,	Q=.00000034,	LAYER=6,	QTYPE=28,	\$END	A=28
\$NEWELL	ROW=40,	COL=21,	Q=.00000275,	LAYER=6,	QTYPE=28,	\$END	A=28
\$NEWELL	ROW=41,	COL=21,	Q=.00000034,	LAYER=6,	QTYPE=28,	\$END	A=28
\$NEWELL	ROW=38,	COL=19,	Q=.00000057,	LAYER=5,	QTYPE=28,	\$END	A=28
\$NEWELL	ROW=38,	COL=20,	Q=.00000014,	LAYER=5,	QTYPE=28,	\$END	A=28
\$NEWELL	ROW=38,	COL=21,	Q=.00000014,	LAYER=5,	QTYPE=28,	\$END	A=28
\$NEWELL	ROW=39,	COL=19,	Q=.00000028,	LAYER=5,	QTYPE=28,	\$END	A=28
\$NEWELL	ROW=39,	COL=20,	Q=.00000014,	LAYER=5,	QTYPE=28,	\$END	A=28
\$NEWELL	ROW=39,	COL=21,	Q=.00000142,	LAYER=5,	QTYPE=28,	\$END	A=28
\$NEWELL	ROW=40,	COL=20,	Q=.00000028,	LAYER=5,	QTYPE=28,	\$END	A=28
\$NEWELL	ROW=40,	COL=21,	Q=.00000227,	LAYER=5,	QTYPE=28,	\$END	A=28
\$NEWELL	ROW=41,	COL=21,	Q=.00000028,	LAYER=5,	QTYPE=28,	\$END	A=28
\$NEWELL	ROW=38,	COL=19,	Q=.00000010,	LAYER=4,	QTYPE=28,	\$END	A=28
\$NEWELL	ROW=38,	COL=20,	Q=.00000003,	LAYER=4,	QTYPE=28,	\$END	A=28
\$NEWELL	ROW=38,	COL=21,	Q=.00000003,	LAYER=4,	QTYPE=28,	\$END	A=28
\$NEWELL	ROW=39,	COL=19,	Q=.00000005,	LAYER=4,	QTYPE=28,	\$END	A=28
\$NEWELL	ROW=39,	COL=20,	Q=.00000003,	LAYER=4,	QTYPE=28,	\$END	A=28

Attachment 2.--Input file for the 1950-79 transient simulation--Continued

\$NEWELL	ROW=39,	COL=21,	Q=.00000025,	LAYER=4,	QTYPE=28,	\$END	A=28
\$NEWELL	ROW=40,	COL=20,	Q=.00000005,	LAYER=4,	QTYPE=28,	\$END	A=28
\$NEWELL	ROW=40,	COL=21,	Q=.00000040,	LAYER=4,	QTYPE=28,	\$END	A=28
\$NEWELL	ROW=41,	COL=21,	Q=.00000005,	LAYER=4,	QTYPE=28,	\$END	A=28
\$NEWELL	ROW=38,	COL=19,	Q=.00000004,	LAYER=3,	QTYPE=28,	\$END	A=28
\$NEWELL	ROW=38,	COL=20,	Q=.00000001,	LAYER=3,	QTYPE=28,	\$END	A=28
\$NEWELL	ROW=38,	COL=21,	Q=.00000001,	LAYER=3,	QTYPE=28,	\$END	A=28
\$NEWELL	ROW=39,	COL=19,	Q=.00000002,	LAYER=3,	QTYPE=28,	\$END	A=28
\$NEWELL	ROW=39,	COL=20,	Q=.00000001,	LAYER=3,	QTYPE=28,	\$END	A=28
\$NEWELL	ROW=39,	COL=21,	Q=.00000010,	LAYER=3,	QTYPE=28,	\$END	A=28
\$NEWELL	ROW=40,	COL=20,	Q=.00000002,	LAYER=3,	QTYPE=28,	\$END	A=28
\$NEWELL	ROW=40,	COL=21,	Q=.00000016,	LAYER=3,	QTYPE=28,	\$END	A=28
\$NEWELL	ROW=41,	COL=21,	Q=.00000002,	LAYER=3,	QTYPE=28,	\$END	A=28
\$NEWELL	ROW=47,	COL=12,	Q=.00000069,	LAYER=7,	QTYPE=29,	\$END	A=29
\$NEWELL	ROW=47,	COL=13,	Q=.00000060,	LAYER=7,	QTYPE=29,	\$END	A=29
\$NEWELL	ROW=47,	COL=14,	Q=.00000112,	LAYER=7,	QTYPE=29,	\$END	A=29
\$NEWELL	ROW=47,	COL=15,	Q=.00000034,	LAYER=7,	QTYPE=29,	\$END	A=29
\$NEWELL	ROW=48,	COL=12,	Q=.00000086,	LAYER=7,	QTYPE=29,	\$END	A=29
\$NEWELL	ROW=48,	COL=13,	Q=.00000103,	LAYER=7,	QTYPE=29,	\$END	A=29
\$NEWELL	ROW=48,	COL=14,	Q=.00000095,	LAYER=7,	QTYPE=29,	\$END	A=29
\$NEWELL	ROW=49,	COL=13,	Q=.00000043,	LAYER=7,	QTYPE=29,	\$END	A=29
\$NEWELL	ROW=47,	COL=12,	Q=.00000151,	LAYER=6,	QTYPE=29,	\$END	A=29
\$NEWELL	ROW=47,	COL=13,	Q=.00000132,	LAYER=6,	QTYPE=29,	\$END	A=29
\$NEWELL	ROW=47,	COL=14,	Q=.00000246,	LAYER=6,	QTYPE=29,	\$END	A=29
\$NEWELL	ROW=47,	COL=15,	Q=.00000076,	LAYER=6,	QTYPE=29,	\$END	A=29
\$NEWELL	ROW=48,	COL=12,	Q=.00000189,	LAYER=6,	QTYPE=29,	\$END	A=29
\$NEWELL	ROW=48,	COL=13,	Q=.00000227,	LAYER=6,	QTYPE=29,	\$END	A=29
\$NEWELL	ROW=48,	COL=14,	Q=.00000208,	LAYER=6,	QTYPE=29,	\$END	A=29
\$NEWELL	ROW=49,	COL=13,	Q=.00000095,	LAYER=6,	QTYPE=29,	\$END	A=29
\$NEWELL	ROW=47,	COL=12,	Q=.00000082,	LAYER=5,	QTYPE=29,	\$END	A=29
\$NEWELL	ROW=47,	COL=13,	Q=.00000072,	LAYER=5,	QTYPE=29,	\$END	A=29
\$NEWELL	ROW=47,	COL=14,	Q=.00000134,	LAYER=5,	QTYPE=29,	\$END	A=29
\$NEWELL	ROW=47,	COL=15,	Q=.00000041,	LAYER=5,	QTYPE=29,	\$END	A=29
\$NEWELL	ROW=48,	COL=12,	Q=.00000103,	LAYER=5,	QTYPE=29,	\$END	A=29
\$NEWELL	ROW=48,	COL=13,	Q=.00000124,	LAYER=5,	QTYPE=29,	\$END	A=29
\$NEWELL	ROW=48,	COL=14,	Q=.00000113,	LAYER=5,	QTYPE=29,	\$END	A=29
\$NEWELL	ROW=49,	COL=13,	Q=.00000052,	LAYER=5,	QTYPE=29,	\$END	A=29
\$NEWELL	ROW=47,	COL=12,	Q=.00000007,	LAYER=4,	QTYPE=29,	\$END	A=29
\$NEWELL	ROW=47,	COL=13,	Q=.00000006,	LAYER=4,	QTYPE=29,	\$END	A=29
\$NEWELL	ROW=47,	COL=14,	Q=.00000011,	LAYER=4,	QTYPE=29,	\$END	A=29
\$NEWELL	ROW=47,	COL=15,	Q=.00000003,	LAYER=4,	QTYPE=29,	\$END	A=29
\$NEWELL	ROW=48,	COL=12,	Q=.00000009,	LAYER=4,	QTYPE=29,	\$END	A=29
\$NEWELL	ROW=48,	COL=13,	Q=.00000010,	LAYER=4,	QTYPE=29,	\$END	A=29
\$NEWELL	ROW=48,	COL=14,	Q=.00000010,	LAYER=4,	QTYPE=29,	\$END	A=29
\$NEWELL	ROW=49,	COL=13,	Q=.00000004,	LAYER=4,	QTYPE=29,	\$END	A=29
\$NEWELL	ROW=47,	COL=12,	Q=.00000007,	LAYER=3,	QTYPE=29,	\$END	A=29
\$NEWELL	ROW=47,	COL=13,	Q=.00000006,	LAYER=3,	QTYPE=29,	\$END	A=29
\$NEWELL	ROW=47,	COL=14,	Q=.00000011,	LAYER=3,	QTYPE=29,	\$END	A=29
\$NEWELL	ROW=47,	COL=15,	Q=.00000003,	LAYER=3,	QTYPE=29,	\$END	A=29
\$NEWELL	ROW=48,	COL=12,	Q=.00000009,	LAYER=3,	QTYPE=29,	\$END	A=29
\$NEWELL	ROW=48,	COL=13,	Q=.00000010,	LAYER=3,	QTYPE=29,	\$END	A=29
\$NEWELL	ROW=48,	COL=14,	Q=.00000010,	LAYER=3,	QTYPE=29,	\$END	A=29

Attachment 2.--Input file for the 1950-79 transient simulation--Continued

```

$NEWELL ROW=49, COL=13, Q=.00000004, LAYER=3, QTYPE=29, $END A=29
$NEWELL ROW=28, COL=11, Q=0.111, LAYER=7, QTYPE=30, $END GRVTY RF
$NEWELL ROW=12, COL=13, Q=0.221, LAYER=7, QTYPE=30, $END GRVTY RF
$NEWELL ROW=14, COL=13, Q=0.221, LAYER=7, QTYPE=30, $END GRVTY RF
$NEWELL ROW=14, COL=14, Q=0.221, LAYER=7, QTYPE=30, $END GRVTY RF
$NEWELL ROW=22, COL=11, Q=0.221, LAYER=7, QTYPE=30, $END GRVTY RF
$NEWELL ROW=23, COL= 8, Q=0.221, LAYER=7, QTYPE=30, $END GRVTY RF
$NEWELL ROW=25, COL= 6, Q=0.221, LAYER=7, QTYPE=30, $END GRVTY RF
$NEWELL ROW=27, COL= 6, Q=0.221, LAYER=7, QTYPE=30, $END GRVTY RF
$NEWELL ROW=27, COL= 7, Q=0.221, LAYER=7, QTYPE=30, $END GRVTY RF
$NEWELL ROW=28, COL= 7, Q=0.221, LAYER=7, QTYPE=30, $END GRVTY RF
$NEWELL ROW=28, COL=12, Q=0.221, LAYER=7, QTYPE=30, $END GRVTY RF
$NEWELL ROW=29, COL=11, Q=0.221, LAYER=7, QTYPE=30, $END GRVTY RF
$NEWELL ROW=30, COL=10, Q=0.221, LAYER=7, QTYPE=30, $END GRVTY RF
$NEWELL ROW=33, COL=11, Q=0.221, LAYER=7, QTYPE=30, $END GRVTY RF
$NEWELL ROW=35, COL=24, Q=0.221, LAYER=7, QTYPE=30, $END GRVTY RF
$NEWELL ROW=35, COL=26, Q=0.221, LAYER=7, QTYPE=30, $END GRVTY RF
$NEWELL ROW=38, COL= 9, Q=0.221, LAYER=7, QTYPE=30, $END GRVTY RF
$NEWELL ROW=38, COL=19, Q=0.221, LAYER=7, QTYPE=30, $END GRVTY RF
$NEWELL ROW=38, COL=20, Q=0.221, LAYER=7, QTYPE=30, $END GRVTY RF
$NEWELL ROW=38, COL=21, Q=0.221, LAYER=7, QTYPE=30, $END GRVTY RF
$NEWELL ROW=38, COL=23, Q=0.221, LAYER=7, QTYPE=30, $END GRVTY RF
$NEWELL ROW=38, COL=28, Q=0.221, LAYER=7, QTYPE=30, $END GRVTY RF
$NEWELL ROW=39, COL=21, Q=0.221, LAYER=7, QTYPE=30, $END GRVTY RF
$NEWELL ROW=39, COL=28, Q=0.221, LAYER=7, QTYPE=30, $END GRVTY RF
$NEWELL ROW=23, COL= 6, Q=0.332, LAYER=7, QTYPE=30, $END GRVTY RF
$NEWELL ROW=15, COL=13, Q=0.442, LAYER=7, QTYPE=30, $END GRVTY RF
$NEWELL ROW=16, COL=19, Q=0.442, LAYER=7, QTYPE=30, $END GRVTY RF
$NEWELL ROW=17, COL=12, Q=0.442, LAYER=7, QTYPE=30, $END GRVTY RF
$NEWELL ROW=21, COL= 6, Q=0.442, LAYER=7, QTYPE=30, $END GRVTY RF
$NEWELL ROW=23, COL= 7, Q=0.442, LAYER=7, QTYPE=30, $END GRVTY RF
$NEWELL ROW=23, COL= 9, Q=0.442, LAYER=7, QTYPE=30, $END GRVTY RF
$NEWELL ROW=25, COL= 8, Q=0.442, LAYER=7, QTYPE=30, $END GRVTY RF
$NEWELL ROW=25, COL=14, Q=0.442, LAYER=7, QTYPE=30, $END GRVTY RF
$NEWELL ROW=25, COL=16, Q=0.442, LAYER=7, QTYPE=30, $END GRVTY RF
$NEWELL ROW=26, COL= 6, Q=0.442, LAYER=7, QTYPE=30, $END GRVTY RF
$NEWELL ROW=27, COL= 9, Q=0.442, LAYER=7, QTYPE=30, $END GRVTY RF
$NEWELL ROW=27, COL=10, Q=0.442, LAYER=7, QTYPE=30, $END GRVTY RF
$NEWELL ROW=29, COL=17, Q=0.442, LAYER=7, QTYPE=30, $END GRVTY RF
$NEWELL ROW=34, COL= 8, Q=0.442, LAYER=7, QTYPE=30, $END GRVTY RF
$NEWELL ROW=35, COL=23, Q=0.442, LAYER=7, QTYPE=30, $END GRVTY RF
$NEWELL ROW=36, COL=23, Q=0.442, LAYER=7, QTYPE=30, $END GRVTY RF
$NEWELL ROW=37, COL=23, Q=0.442, LAYER=7, QTYPE=30, $END GRVTY RF
$NEWELL ROW=40, COL=21, Q=0.442, LAYER=7, QTYPE=30, $END GRVTY RF
$NEWELL ROW=41, COL=21, Q=0.442, LAYER=7, QTYPE=30, $END GRVTY RF
$NEWELL ROW=43, COL=15, Q=0.442, LAYER=7, QTYPE=30, $END GRVTY RF
$NEWELL ROW=48, COL=12, Q=0.442, LAYER=7, QTYPE=30, $END GRVTY RF
$NEWELL ROW=25, COL= 9, Q=0.553, LAYER=7, QTYPE=30, $END GRVTY RF
$NEWELL ROW=28, COL= 6, Q=0.553, LAYER=7, QTYPE=30, $END GRVTY RF
$NEWELL ROW= 7, COL=15, Q=0.663, LAYER=7, QTYPE=30, $END GRVTY RF
$NEWELL ROW=11, COL=14, Q=0.663, LAYER=7, QTYPE=30, $END GRVTY RF
$NEWELL ROW=12, COL=14, Q=0.663, LAYER=7, QTYPE=30, $END GRVTY RF

```

Attachment 2.--Input file for the 1950-79 transient simulation--Continued

```

$NEWELL ROW=12, COL=16, Q=0.663, LAYER=7, QTYPE=30, $END GRVTY RF
$NEWELL ROW=16, COL= 7, Q=0.663, LAYER=7, QTYPE=30, $END GRVTY RF
$NEWELL ROW=16, COL=17, Q=0.663, LAYER=7, QTYPE=30, $END GRVTY RF
$NEWELL ROW=22, COL=14, Q=0.663, LAYER=7, QTYPE=30, $END GRVTY RF
$NEWELL ROW=24, COL= 7, Q=0.663, LAYER=7, QTYPE=30, $END GRVTY RF
$NEWELL ROW=24, COL=10, Q=0.663, LAYER=7, QTYPE=30, $END GRVTY RF
$NEWELL ROW=25, COL= 5, Q=0.663, LAYER=7, QTYPE=30, $END GRVTY RF
$NEWELL ROW=26, COL= 7, Q=0.663, LAYER=7, QTYPE=30, $END GRVTY RF
$NEWELL ROW=26, COL=10, Q=0.663, LAYER=7, QTYPE=30, $END GRVTY RF
$NEWELL ROW=26, COL=15, Q=0.663, LAYER=7, QTYPE=30, $END GRVTY RF
$NEWELL ROW=26, COL=16, Q=0.663, LAYER=7, QTYPE=30, $END GRVTY RF
$NEWELL ROW=28, COL=17, Q=0.663, LAYER=7, QTYPE=30, $END GRVTY RF
$NEWELL ROW=29, COL= 8, Q=0.663, LAYER=7, QTYPE=30, $END GRVTY RF
$NEWELL ROW=33, COL=12, Q=0.663, LAYER=7, QTYPE=30, $END GRVTY RF
$NEWELL ROW=34, COL=23, Q=0.663, LAYER=7, QTYPE=30, $END GRVTY RF
$NEWELL ROW=35, COL=25, Q=0.663, LAYER=7, QTYPE=30, $END GRVTY RF
$NEWELL ROW=39, COL=27, Q=0.663, LAYER=7, QTYPE=30, $END GRVTY RF
$NEWELL ROW=23, COL=10, Q=0.774, LAYER=7, QTYPE=30, $END GRVTY RF
$NEWELL ROW=26, COL= 5, Q=0.774, LAYER=7, QTYPE=30, $END GRVTY RF
$NEWELL ROW=12, COL=15, Q=0.884, LAYER=7, QTYPE=30, $END GRVTY RF
$NEWELL ROW=13, COL=14, Q=0.884, LAYER=7, QTYPE=30, $END GRVTY RF
$NEWELL ROW=15, COL= 9, Q=0.884, LAYER=7, QTYPE=30, $END GRVTY RF
$NEWELL ROW=15, COL=14, Q=0.884, LAYER=7, QTYPE=30, $END GRVTY RF
$NEWELL ROW=16, COL= 9, Q=0.884, LAYER=7, QTYPE=30, $END GRVTY RF
$NEWELL ROW=16, COL=18, Q=0.884, LAYER=7, QTYPE=30, $END GRVTY RF
$NEWELL ROW=17, COL=16, Q=0.884, LAYER=7, QTYPE=30, $END GRVTY RF
$NEWELL ROW=21, COL=11, Q=0.884, LAYER=7, QTYPE=30, $END GRVTY RF
$NEWELL ROW=22, COL= 9, Q=0.884, LAYER=7, QTYPE=30, $END GRVTY RF
$NEWELL ROW=24, COL= 9, Q=0.884, LAYER=7, QTYPE=30, $END GRVTY RF
$NEWELL ROW=25, COL= 7, Q=0.884, LAYER=7, QTYPE=30, $END GRVTY RF
$NEWELL ROW=25, COL=11, Q=0.884, LAYER=7, QTYPE=30, $END GRVTY RF
$NEWELL ROW=26, COL= 9, Q=0.884, LAYER=7, QTYPE=30, $END GRVTY RF
$NEWELL ROW=26, COL=11, Q=0.884, LAYER=7, QTYPE=30, $END GRVTY RF
$NEWELL ROW=27, COL= 2, Q=0.884, LAYER=7, QTYPE=30, $END GRVTY RF
$NEWELL ROW=29, COL=10, Q=0.884, LAYER=7, QTYPE=30, $END GRVTY RF
$NEWELL ROW=29, COL=16, Q=0.884, LAYER=7, QTYPE=30, $END GRVTY RF
$NEWELL ROW=38, COL=27, Q=0.884, LAYER=7, QTYPE=30, $END GRVTY RF
$NEWELL ROW=47, COL=12, Q=0.884, LAYER=7, QTYPE=30, $END GRVTY RF
$NEWELL ROW=47, COL=15, Q=0.884, LAYER=7, QTYPE=30, $END GRVTY RF
$NEWELL ROW=36, COL=24, Q=0.995, LAYER=7, QTYPE=30, $END GRVTY RF
$NEWELL ROW=19, COL= 6, Q=1.105, LAYER=7, QTYPE=30, $END GRVTY RF
$NEWELL ROW=22, COL= 5, Q=1.105, LAYER=7, QTYPE=30, $END GRVTY RF
$NEWELL ROW=23, COL=12, Q=1.105, LAYER=7, QTYPE=30, $END GRVTY RF
$NEWELL ROW=24, COL= 6, Q=1.105, LAYER=7, QTYPE=30, $END GRVTY RF
$NEWELL ROW=24, COL= 8, Q=1.105, LAYER=7, QTYPE=30, $END GRVTY RF
$NEWELL ROW=24, COL=13, Q=1.105, LAYER=7, QTYPE=30, $END GRVTY RF
$NEWELL ROW=24, COL=15, Q=1.105, LAYER=7, QTYPE=30, $END GRVTY RF
$NEWELL ROW=25, COL=13, Q=1.105, LAYER=7, QTYPE=30, $END GRVTY RF
$NEWELL ROW=26, COL= 8, Q=1.105, LAYER=7, QTYPE=30, $END GRVTY RF
$NEWELL ROW=27, COL= 5, Q=1.105, LAYER=7, QTYPE=30, $END GRVTY RF
$NEWELL ROW=27, COL=14, Q=1.105, LAYER=7, QTYPE=30, $END GRVTY RF
$NEWELL ROW=31, COL=10, Q=1.105, LAYER=7, QTYPE=30, $END GRVTY RF

```

## Attachment 2.--Input file for the 1950-79 transient simulation--Continued

```

$NEWELL ROW=36, COL= 8, Q=1.105, LAYER=7, QTYPE=30, $END GRVTY RF
$NEWELL ROW=24, COL=11, Q=1.216, LAYER=7, QTYPE=30, $END GRVTY RF
$NEWELL ROW=29, COL=15, Q=1.216, LAYER=7, QTYPE=30, $END GRVTY RF
$NEWELL ROW=30, COL=11, Q=1.216, LAYER=7, QTYPE=30, $END GRVTY RF
$NEWELL ROW= 5, COL=13, Q=1.326, LAYER=7, QTYPE=30, $END GRVTY RF
$NEWELL ROW= 6, COL=14, Q=1.326, LAYER=7, QTYPE=30, $END GRVTY RF
$NEWELL ROW= 7, COL=13, Q=1.326, LAYER=7, QTYPE=30, $END GRVTY RF
$NEWELL ROW=10, COL=15, Q=1.326, LAYER=7, QTYPE=30, $END GRVTY RF
$NEWELL ROW=15, COL=10, Q=1.326, LAYER=7, QTYPE=30, $END GRVTY RF
$NEWELL ROW=16, COL=10, Q=1.326, LAYER=7, QTYPE=30, $END GRVTY RF
$NEWELL ROW=17, COL= 7, Q=1.326, LAYER=7, QTYPE=30, $END GRVTY RF
$NEWELL ROW=17, COL=13, Q=1.326, LAYER=7, QTYPE=30, $END GRVTY RF
$NEWELL ROW=18, COL= 9, Q=1.326, LAYER=7, QTYPE=30, $END GRVTY RF
$NEWELL ROW=20, COL=11, Q=1.326, LAYER=7, QTYPE=30, $END GRVTY RF
$NEWELL ROW=23, COL= 5, Q=1.326, LAYER=7, QTYPE=30, $END GRVTY RF
$NEWELL ROW=28, COL=14, Q=1.326, LAYER=7, QTYPE=30, $END GRVTY RF
$NEWELL ROW=29, COL= 7, Q=1.326, LAYER=7, QTYPE=30, $END GRVTY RF
$NEWELL ROW=30, COL= 6, Q=1.326, LAYER=7, QTYPE=30, $END GRVTY RF
$NEWELL ROW=31, COL=11, Q=1.326, LAYER=7, QTYPE=30, $END GRVTY RF
$NEWELL ROW=33, COL=10, Q=1.326, LAYER=7, QTYPE=30, $END GRVTY RF
$NEWELL ROW=35, COL= 7, Q=1.326, LAYER=7, QTYPE=30, $END GRVTY RF
$NEWELL ROW=35, COL=12, Q=1.326, LAYER=7, QTYPE=30, $END GRVTY RF
$NEWELL ROW=37, COL= 9, Q=1.326, LAYER=7, QTYPE=30, $END GRVTY RF
$NEWELL ROW=10, COL=14, Q=1.547, LAYER=7, QTYPE=30, $END GRVTY RF
$NEWELL ROW=14, COL= 8, Q=1.547, LAYER=7, QTYPE=30, $END GRVTY RF
$NEWELL ROW=14, COL= 9, Q=1.547, LAYER=7, QTYPE=30, $END GRVTY RF
$NEWELL ROW=15, COL=11, Q=1.547, LAYER=7, QTYPE=30, $END GRVTY RF
$NEWELL ROW=20, COL= 6, Q=1.547, LAYER=7, QTYPE=30, $END GRVTY RF
$NEWELL ROW=24, COL=12, Q=1.547, LAYER=7, QTYPE=30, $END GRVTY RF
$NEWELL ROW=25, COL=15, Q=1.547, LAYER=7, QTYPE=30, $END GRVTY RF
$NEWELL ROW=29, COL= 9, Q=1.547, LAYER=7, QTYPE=30, $END GRVTY RF
$NEWELL ROW=32, COL=11, Q=1.547, LAYER=7, QTYPE=30, $END GRVTY RF
$NEWELL ROW=36, COL=13, Q=1.547, LAYER=7, QTYPE=30, $END GRVTY RF
$NEWELL ROW=36, COL=14, Q=1.547, LAYER=7, QTYPE=30, $END GRVTY RF
$NEWELL ROW=37, COL= 8, Q=1.547, LAYER=7, QTYPE=30, $END GRVTY RF
$NEWELL ROW=44, COL=11, Q=1.547, LAYER=7, QTYPE=30, $END GRVTY RF
$NEWELL ROW=47, COL=13, Q=1.547, LAYER=7, QTYPE=30, $END GRVTY RF
$NEWELL ROW=11, COL=15, Q=1.768, LAYER=7, QTYPE=30, $END GRVTY RF
$NEWELL ROW=12, COL= 6, Q=1.768, LAYER=7, QTYPE=30, $END GRVTY RF
$NEWELL ROW=15, COL= 8, Q=1.768, LAYER=7, QTYPE=30, $END GRVTY RF
$NEWELL ROW=16, COL=13, Q=1.768, LAYER=7, QTYPE=30, $END GRVTY RF
$NEWELL ROW=16, COL=15, Q=1.768, LAYER=7, QTYPE=30, $END GRVTY RF
$NEWELL ROW=22, COL= 7, Q=1.768, LAYER=7, QTYPE=30, $END GRVTY RF
$NEWELL ROW=22, COL= 8, Q=1.768, LAYER=7, QTYPE=30, $END GRVTY RF
$NEWELL ROW=22, COL=10, Q=1.768, LAYER=7, QTYPE=30, $END GRVTY RF
$NEWELL ROW=30, COL= 9, Q=1.768, LAYER=7, QTYPE=30, $END GRVTY RF
$NEWELL ROW=33, COL= 7, Q=1.768, LAYER=7, QTYPE=30, $END GRVTY RF
$NEWELL ROW=33, COL= 9, Q=1.768, LAYER=7, QTYPE=30, $END GRVTY RF
$NEWELL ROW=39, COL=10, Q=1.768, LAYER=7, QTYPE=30, $END GRVTY RF
$NEWELL ROW=39, COL=13, Q=1.768, LAYER=7, QTYPE=30, $END GRVTY RF
$NEWELL ROW=40, COL= 9, Q=1.768, LAYER=7, QTYPE=30, $END GRVTY RF
$NEWELL ROW=40, COL=16, Q=1.768, LAYER=7, QTYPE=30, $END GRVTY RF

```



Attachment 2.--Input file for the 1950-79 transient simulation--Continued

\$NEWELL	ROW=40,	COL=17,	Q=1.768,	LAYER=7,	QTYPE=30,	\$END	GRVTY RF
\$NEWELL	ROW=42,	COL=15,	Q=1.768,	LAYER=7,	QTYPE=30,	\$END	GRVTY RF
\$NEWELL	ROW=27,	COL= 3,	Q=1.879,	LAYER=7,	QTYPE=30,	\$END	GRVTY RF
\$NEWELL	ROW=30,	COL=12,	Q=1.875,	LAYER=7,	QTYPE=30,	\$END	GRVTY RF
\$NEWELL	ROW=13,	COL=10,	Q=1.989,	LAYER=7,	QTYPE=30,	\$END	GRVTY RF
\$NEWELL	ROW=26,	COL= 2,	Q=1.989,	LAYER=7,	QTYPE=30,	\$END	GRVTY RF
\$NEWELL	ROW=33,	COL= 8,	Q=1.989,	LAYER=7,	QTYPE=30,	\$END	GRVTY RF
\$NEWELL	ROW=36,	COL=27,	Q=1.989,	LAYER=7,	QTYPE=30,	\$END	GRVTY RF
\$NEWELL	ROW=37,	COL=25,	Q=1.989,	LAYER=7,	QTYPE=30,	\$END	GRVTY RF
\$NEWELL	ROW=41,	COL=16,	Q=1.989,	LAYER=7,	QTYPE=30,	\$END	GRVTY RF
\$NEWELL	ROW=31,	COL= 9,	Q=2.100,	LAYER=7,	QTYPE=30,	\$END	GRVTY RF
\$NEWELL	ROW=12,	COL= 5,	Q=2.210,	LAYER=7,	QTYPE=30,	\$END	GRVTY RF
\$NEWELL	ROW=15,	COL=12,	Q=2.210,	LAYER=7,	QTYPE=30,	\$END	GRVTY RF
\$NEWELL	ROW=16,	COL=12,	Q=2.210,	LAYER=7,	QTYPE=30,	\$END	GRVTY RF
\$NEWELL	ROW=17,	COL= 8,	Q=2.210,	LAYER=7,	QTYPE=30,	\$END	GRVTY RF
\$NEWELL	ROW=22,	COL= 6,	Q=2.210,	LAYER=7,	QTYPE=30,	\$END	GRVTY RF
\$NEWELL	ROW=23,	COL=13,	Q=2.210,	LAYER=7,	QTYPE=30,	\$END	GRVTY RF
\$NEWELL	ROW=26,	COL= 3,	Q=2.210,	LAYER=7,	QTYPE=30,	\$END	GRVTY RF
\$NEWELL	ROW=27,	COL=16,	Q=2.210,	LAYER=7,	QTYPE=30,	\$END	GRVTY RF
\$NEWELL	ROW=28,	COL=15,	Q=2.210,	LAYER=7,	QTYPE=30,	\$END	GRVTY RF
\$NEWELL	ROW=32,	COL= 9,	Q=2.210,	LAYER=7,	QTYPE=30,	\$END	GRVTY RF
\$NEWELL	ROW=32,	COL=10,	Q=2.210,	LAYER=7,	QTYPE=30,	\$END	GRVTY RF
\$NEWELL	ROW=34,	COL= 7,	Q=2.210,	LAYER=7,	QTYPE=30,	\$END	GRVTY RF
\$NEWELL	ROW=35,	COL=11,	Q=2.210,	LAYER=7,	QTYPE=30,	\$END	GRVTY RF
\$NEWELL	ROW=40,	COL=10,	Q=2.210,	LAYER=7,	QTYPE=30,	\$END	GRVTY RF
\$NEWELL	ROW=41,	COL=13,	Q=2.210,	LAYER=7,	QTYPE=30,	\$END	GRVTY RF
\$NEWELL	ROW=48,	COL=13,	Q=2.210,	LAYER=7,	QTYPE=30,	\$END	GRVTY RF
\$NEWELL	ROW= 6,	COL=13,	Q=2.431,	LAYER=7,	QTYPE=30,	\$END	GRVTY RF
\$NEWELL	ROW=13,	COL=15,	Q=2.431,	LAYER=7,	QTYPE=30,	\$END	GRVTY RF
\$NEWELL	ROW=17,	COL=17,	Q=2.431,	LAYER=7,	QTYPE=30,	\$END	GRVTY RF
\$NEWELL	ROW=21,	COL=10,	Q=2.431,	LAYER=7,	QTYPE=30,	\$END	GRVTY RF
\$NEWELL	ROW=23,	COL=14,	Q=2.431,	LAYER=7,	QTYPE=30,	\$END	GRVTY RF
\$NEWELL	ROW=24,	COL=14,	Q=2.431,	LAYER=7,	QTYPE=30,	\$END	GRVTY RF
\$NEWELL	ROW=27,	COL= 4,	Q=2.431,	LAYER=7,	QTYPE=30,	\$END	GRVTY RF
\$NEWELL	ROW=27,	COL=15,	Q=2.431,	LAYER=7,	QTYPE=30,	\$END	GRVTY RF
\$NEWELL	ROW=31,	COL= 7,	Q=2.431,	LAYER=7,	QTYPE=30,	\$END	GRVTY RF
\$NEWELL	ROW=36,	COL= 9,	Q=2.431,	LAYER=7,	QTYPE=30,	\$END	GRVTY RF
\$NEWELL	ROW=36,	COL=12,	Q=2.431,	LAYER=7,	QTYPE=30,	\$END	GRVTY RF
\$NEWELL	ROW=36,	COL=25,	Q=2.431,	LAYER=7,	QTYPE=30,	\$END	GRVTY RF
\$NEWELL	ROW=36,	COL=26,	Q=2.431,	LAYER=7,	QTYPE=30,	\$END	GRVTY RF
\$NEWELL	ROW=37,	COL=13,	Q=2.431,	LAYER=7,	QTYPE=30,	\$END	GRVTY RF
\$NEWELL	ROW=37,	COL=15,	Q=2.431,	LAYER=7,	QTYPE=30,	\$END	GRVTY RF
\$NEWELL	ROW=37,	COL=27,	Q=2.431,	LAYER=7,	QTYPE=30,	\$END	GRVTY RF
\$NEWELL	ROW=38,	COL=11,	Q=2.431,	LAYER=7,	QTYPE=30,	\$END	GRVTY RF
\$NEWELL	ROW=45,	COL=11,	Q=2.431,	LAYER=7,	QTYPE=30,	\$END	GRVTY RF
\$NEWELL	ROW=48,	COL=14,	Q=2.431,	LAYER=7,	QTYPE=30,	\$END	GRVTY RF
\$NEWELL	ROW= 5,	COL=12,	Q=2.652,	LAYER=7,	QTYPE=30,	\$END	GRVTY RF
\$NEWELL	ROW=13,	COL= 6,	Q=2.652,	LAYER=7,	QTYPE=30,	\$END	GRVTY RF
\$NEWELL	ROW=18,	COL= 7,	Q=2.652,	LAYER=7,	QTYPE=30,	\$END	GRVTY RF
\$NEWELL	ROW=19,	COL= 8,	Q=2.652,	LAYER=7,	QTYPE=30,	\$END	GRVTY RF
\$NEWELL	ROW=30,	COL= 8,	Q=2.652,	LAYER=7,	QTYPE=30,	\$END	GRVTY RF
\$NEWELL	ROW=36,	COL=11,	Q=2.652,	LAYER=7,	QTYPE=30,	\$END	GRVTY RF

## Attachment 2.--Input file for the 1950-79 transient simulation--Continued

\$NEWELL	ROW=37,	COL=10,	Q=2.652,	LAYER=7,	QTYPE=30,	\$END	GRVTY	RF
\$NEWELL	ROW=37,	COL=26,	Q=2.652,	LAYER=7,	QTYPE=30,	\$END	GRVTY	RF
\$NEWELL	ROW=38,	COL=10,	Q=2.652,	LAYER=7,	QTYPE=30,	\$END	GRVTY	RF
\$NEWELL	ROW=39,	COL=11,	Q=2.652,	LAYER=7,	QTYPE=30,	\$END	GRVTY	RF
\$NEWELL	ROW=39,	COL=12,	Q=2.652,	LAYER=7,	QTYPE=30,	\$END	GRVTY	RF
\$NEWELL	ROW=41,	COL=12,	Q=2.652,	LAYER=7,	QTYPE=30,	\$END	GRVTY	RF
\$NEWELL	ROW=42,	COL=14,	Q=2.652,	LAYER=7,	QTYPE=30,	\$END	GRVTY	RF
\$NEWELL	ROW=45,	COL=13,	Q=2.652,	LAYER=7,	QTYPE=30,	\$END	GRVTY	RF
\$NEWELL	ROW= 7,	COL=14,	Q=2.727,	LAYER=7,	QTYPE=30,	\$END	GRVTY	RF
\$NEWELL	ROW=19,	COL= 7,	Q=2.873,	LAYER=7,	QTYPE=30,	\$END	GRVTY	RF
\$NEWELL	ROW=32,	COL=15,	Q=2.873,	LAYER=7,	QTYPE=30,	\$END	GRVTY	RF
\$NEWELL	ROW=37,	COL=12,	Q=2.873,	LAYER=7,	QTYPE=30,	\$END	GRVTY	RF
\$NEWELL	ROW=38,	COL=12,	Q=2.873,	LAYER=7,	QTYPE=30,	\$END	GRVTY	RF
\$NEWELL	ROW=40,	COL=11,	Q=2.873,	LAYER=7,	QTYPE=30,	\$END	GRVTY	RF
\$NEWELL	ROW=47,	COL=14,	Q=2.873,	LAYER=7,	QTYPE=30,	\$END	GRVTY	RF
\$NEWELL	ROW=13,	COL= 7,	Q=3.094,	LAYER=7,	QTYPE=30,	\$END	GRVTY	RF
\$NEWELL	ROW=13,	COL= 9,	Q=3.094,	LAYER=7,	QTYPE=30,	\$END	GRVTY	RF
\$NEWELL	ROW=14,	COL=10,	Q=3.094,	LAYER=7,	QTYPE=30,	\$END	GRVTY	RF
\$NEWELL	ROW=21,	COL= 7,	Q=3.094,	LAYER=7,	QTYPE=30,	\$END	GRVTY	RF
\$NEWELL	ROW=28,	COL=16,	Q=3.094,	LAYER=7,	QTYPE=30,	\$END	GRVTY	RF
\$NEWELL	ROW=31,	COL= 8,	Q=3.094,	LAYER=7,	QTYPE=30,	\$END	GRVTY	RF
\$NEWELL	ROW=33,	COL=15,	Q=3.094,	LAYER=7,	QTYPE=30,	\$END	GRVTY	RF
\$NEWELL	ROW=35,	COL= 8,	Q=3.094,	LAYER=7,	QTYPE=30,	\$END	GRVTY	RF
\$NEWELL	ROW=35,	COL=10,	Q=3.094,	LAYER=7,	QTYPE=30,	\$END	GRVTY	RF
\$NEWELL	ROW=37,	COL=14,	Q=3.094,	LAYER=7,	QTYPE=30,	\$END	GRVTY	RF
\$NEWELL	ROW=40,	COL=15,	Q=3.094,	LAYER=7,	QTYPE=30,	\$END	GRVTY	RF
\$NEWELL	ROW=41,	COL=14,	Q=3.094,	LAYER=7,	QTYPE=30,	\$END	GRVTY	RF
\$NEWELL	ROW=41,	COL=15,	Q=3.094,	LAYER=7,	QTYPE=30,	\$END	GRVTY	RF
\$NEWELL	ROW=44,	COL=13,	Q=3.094,	LAYER=7,	QTYPE=30,	\$END	GRVTY	RF
\$NEWELL	ROW=45,	COL=12,	Q=3.094,	LAYER=7,	QTYPE=30,	\$END	GRVTY	RF
\$NEWELL	ROW=46,	COL=11,	Q=3.094,	LAYER=7,	QTYPE=30,	\$END	GRVTY	RF
\$NEWELL	ROW=13,	COL= 8,	Q=3.315,	LAYER=7,	QTYPE=30,	\$END	GRVTY	RF
\$NEWELL	ROW=14,	COL=11,	Q=3.315,	LAYER=7,	QTYPE=30,	\$END	GRVTY	RF
\$NEWELL	ROW=16,	COL= 8,	Q=3.315,	LAYER=7,	QTYPE=30,	\$END	GRVTY	RF
\$NEWELL	ROW=20,	COL= 7,	Q=3.315,	LAYER=7,	QTYPE=30,	\$END	GRVTY	RF
\$NEWELL	ROW=20,	COL=10,	Q=3.315,	LAYER=7,	QTYPE=30,	\$END	GRVTY	RF
\$NEWELL	ROW=30,	COL= 7,	Q=3.315,	LAYER=7,	QTYPE=30,	\$END	GRVTY	RF
\$NEWELL	ROW=32,	COL= 7,	Q=3.315,	LAYER=7,	QTYPE=30,	\$END	GRVTY	RF
\$NEWELL	ROW=35,	COL= 9,	Q=3.315,	LAYER=7,	QTYPE=30,	\$END	GRVTY	RF
\$NEWELL	ROW=36,	COL=10,	Q=3.315,	LAYER=7,	QTYPE=30,	\$END	GRVTY	RF
\$NEWELL	ROW=37,	COL=11,	Q=3.315,	LAYER=7,	QTYPE=30,	\$END	GRVTY	RF
\$NEWELL	ROW=38,	COL=13,	Q=3.315,	LAYER=7,	QTYPE=30,	\$END	GRVTY	RF
\$NEWELL	ROW=38,	COL=14,	Q=3.315,	LAYER=7,	QTYPE=30,	\$END	GRVTY	RF
\$NEWELL	ROW=42,	COL=13,	Q=3.315,	LAYER=7,	QTYPE=30,	\$END	GRVTY	RF
\$NEWELL	ROW=43,	COL=14,	Q=3.315,	LAYER=7,	QTYPE=30,	\$END	GRVTY	RF
\$NEWELL	ROW=18,	COL= 8,	Q=3.536,	LAYER=7,	QTYPE=30,	\$END	GRVTY	RF
\$NEWELL	ROW=20,	COL= 8,	Q=3.536,	LAYER=7,	QTYPE=30,	\$END	GRVTY	RF
\$NEWELL	ROW=20,	COL= 9,	Q=3.536,	LAYER=7,	QTYPE=30,	\$END	GRVTY	RF
\$NEWELL	ROW=21,	COL= 8,	Q=3.536,	LAYER=7,	QTYPE=30,	\$END	GRVTY	RF
\$NEWELL	ROW=21,	COL= 9,	Q=3.536,	LAYER=7,	QTYPE=30,	\$END	GRVTY	RF
\$NEWELL	ROW=32,	COL= 8,	Q=3.536,	LAYER=7,	QTYPE=30,	\$END	GRVTY	RF
\$NEWELL	ROW=38,	COL=15,	Q=3.536,	LAYER=7,	QTYPE=30,	\$END	GRVTY	RF

Attachment 2.--Input file for the 1950-79 transient simulation--Continued

```

$NEWELL ROW=39, COL=14, Q=3.536, LAYER=7, QTYPE=30, $END GRVTY RF
$NEWELL ROW=39, COL=15, Q=3.536, LAYER=7, QTYPE=30, $END GRVTY RF
$NEWELL ROW=39, COL=16, Q=3.536, LAYER=7, QTYPE=30, $END GRVTY RF
$NEWELL ROW=40, COL=12, Q=3.536, LAYER=7, QTYPE=30, $END GRVTY RF
$NEWELL ROW=40, COL=13, Q=3.536, LAYER=7, QTYPE=30, $END GRVTY RF
$NEWELL ROW=40, COL=14, Q=3.536, LAYER=7, QTYPE=30, $END GRVTY RF
$NEWELL ROW=41, COL=11, Q=3.536, LAYER=7, QTYPE=30, $END GRVTY RF
$NEWELL ROW=42, COL=11, Q=3.536, LAYER=7, QTYPE=30, $END GRVTY RF
$NEWELL ROW=42, COL=12, Q=3.536, LAYER=7, QTYPE=30, $END GRVTY RF
$NEWELL ROW=43, COL=11, Q=3.536, LAYER=7, QTYPE=30, $END GRVTY RF
$NEWELL ROW=43, COL=12, Q=3.536, LAYER=7, QTYPE=30, $END GRVTY RF
$NEWELL ROW=43, COL=13, Q=3.536, LAYER=7, QTYPE=30, $END GRVTY RF
$NEWELL ROW=44, COL=12, Q=3.536, LAYER=7, QTYPE=30, $END GRVTY RF
$NEWELL ROW= 7, COL=14, Q=0.111, LAYER=7, QTYPE=40, $END SPKLR RF
$NEWELL ROW= 6, COL=13, Q=0.221, LAYER=7, QTYPE=40, $END SPKLR RF
$NEWELL ROW=12, COL= 7, Q=0.221, LAYER=7, QTYPE=40, $END SPKLR RF
$NEWELL ROW=12, COL= 8, Q=0.221, LAYER=7, QTYPE=40, $END SPKLR RF
$NEWELL ROW=12, COL=12, Q=0.221, LAYER=7, QTYPE=40, $END SPKLR RF
$NEWELL ROW=13, COL=15, Q=0.221, LAYER=7, QTYPE=40, $END SPKLR RF
$NEWELL ROW=14, COL= 9, Q=0.221, LAYER=7, QTYPE=40, $END SPKLR RF
$NEWELL ROW=14, COL=13, Q=0.221, LAYER=7, QTYPE=40, $END SPKLR RF
$NEWELL ROW=14, COL=14, Q=0.221, LAYER=7, QTYPE=40, $END SPKLR RF
$NEWELL ROW=16, COL= 8, Q=0.221, LAYER=7, QTYPE=40, $END SPKLR RF
$NEWELL ROW=16, COL=17, Q=0.221, LAYER=7, QTYPE=40, $END SPKLR RF
$NEWELL ROW=20, COL= 7, Q=0.221, LAYER=7, QTYPE=40, $END SPKLR RF
$NEWELL ROW=20, COL=10, Q=0.221, LAYER=7, QTYPE=40, $END SPKLR RF
$NEWELL ROW=28, COL=17, Q=0.221, LAYER=7, QTYPE=40, $END SPKLR RF
$NEWELL ROW=30, COL= 8, Q=0.221, LAYER=7, QTYPE=40, $END SPKLR RF
$NEWELL ROW=31, COL= 8, Q=0.221, LAYER=7, QTYPE=40, $END SPKLR RF
$NEWELL ROW=33, COL= 8, Q=0.221, LAYER=7, QTYPE=40, $END SPKLR RF
$NEWELL ROW=34, COL= 9, Q=0.221, LAYER=7, QTYPE=40, $END SPKLR RF
$NEWELL ROW=34, COL=22, Q=0.221, LAYER=7, QTYPE=40, $END SPKLR RF
$NEWELL ROW=35, COL= 9, Q=0.221, LAYER=7, QTYPE=40, $END SPKLR RF
$NEWELL ROW=35, COL=10, Q=0.221, LAYER=7, QTYPE=40, $END SPKLR RF
$NEWELL ROW=35, COL=23, Q=0.221, LAYER=7, QTYPE=40, $END SPKLR RF
$NEWELL ROW=35, COL=24, Q=0.221, LAYER=7, QTYPE=40, $END SPKLR RF
$NEWELL ROW=36, COL=10, Q=0.221, LAYER=7, QTYPE=40, $END SPKLR RF
$NEWELL ROW=36, COL=23, Q=0.221, LAYER=7, QTYPE=40, $END SPKLR RF
$NEWELL ROW=36, COL=25, Q=0.221, LAYER=7, QTYPE=40, $END SPKLR RF
$NEWELL ROW=36, COL=27, Q=0.221, LAYER=7, QTYPE=40, $END SPKLR RF
$NEWELL ROW=37, COL= 9, Q=0.221, LAYER=7, QTYPE=40, $END SPKLR RF
$NEWELL ROW=37, COL=11, Q=0.221, LAYER=7, QTYPE=40, $END SPKLR RF
$NEWELL ROW=37, COL=13, Q=0.221, LAYER=7, QTYPE=40, $END SPKLR RF
$NEWELL ROW=37, COL=15, Q=0.221, LAYER=7, QTYPE=40, $END SPKLR RF
$NEWELL ROW=37, COL=25, Q=0.221, LAYER=7, QTYPE=40, $END SPKLR RF
$NEWELL ROW=38, COL=12, Q=0.221, LAYER=7, QTYPE=40, $END SPKLR RF
$NEWELL ROW=38, COL=14, Q=0.221, LAYER=7, QTYPE=40, $END SPKLR RF
$NEWELL ROW=38, COL=28, Q=0.221, LAYER=7, QTYPE=40, $END SPKLR RF
$NEWELL ROW=39, COL=12, Q=0.221, LAYER=7, QTYPE=40, $END SPKLR RF
$NEWELL ROW=40, COL= 9, Q=0.221, LAYER=7, QTYPE=40, $END SPKLR RF
$NEWELL ROW=42, COL=13, Q=0.221, LAYER=7, QTYPE=40, $END SPKLR RF
$NEWELL ROW=45, COL=13, Q=0.221, LAYER=7, QTYPE=40, $END SPKLR RF

```

## Attachment 2.--Input file for the 1950-79 transient simulation--Continued

\$NEWELL	ROW=12,	COL=11,	Q=0.332,	LAYER=7,	QTYPE=40,	\$END	SPKLR RF
\$NEWELL	ROW=27,	COL= 3,	Q=0.332,	LAYER=7,	QTYPE=40,	\$END	SPKLR RF
\$NEWELL	ROW=10,	COL=15,	Q=0.442,	LAYER=7,	QTYPE=40,	\$END	SPKLR RF
\$NEWELL	ROW=15,	COL=13,	Q=0.442,	LAYER=7,	QTYPE=40,	\$END	SPKLR RF
\$NEWELL	ROW=16,	COL=19,	Q=0.442,	LAYER=7,	QTYPE=40,	\$END	SPKLR RF
\$NEWELL	ROW=21,	COL= 7,	Q=0.442,	LAYER=7,	QTYPE=40,	\$END	SPKLR RF
\$NEWELL	ROW=23,	COL= 5,	Q=0.442,	LAYER=7,	QTYPE=40,	\$END	SPKLR RF
\$NEWELL	ROW=25,	COL= 4,	Q=0.442,	LAYER=7,	QTYPE=40,	\$END	SPKLR RF
\$NEWELL	ROW=26,	COL= 3,	Q=0.442,	LAYER=7,	QTYPE=40,	\$END	SPKLR RF
\$NEWELL	ROW=28,	COL=16,	Q=0.442,	LAYER=7,	QTYPE=40,	\$END	SPKLR RF
\$NEWELL	ROW=30,	COL= 6,	Q=0.442,	LAYER=7,	QTYPE=40,	\$END	SPKLR RF
\$NEWELL	ROW=30,	COL= 9,	Q=0.442,	LAYER=7,	QTYPE=40,	\$END	SPKLR RF
\$NEWELL	ROW=30,	COL=15,	Q=0.442,	LAYER=7,	QTYPE=40,	\$END	SPKLR RF
\$NEWELL	ROW=32,	COL=15,	Q=0.442,	LAYER=7,	QTYPE=40,	\$END	SPKLR RF
\$NEWELL	ROW=33,	COL=12,	Q=0.442,	LAYER=7,	QTYPE=40,	\$END	SPKLR RF
\$NEWELL	ROW=35,	COL= 8,	Q=0.442,	LAYER=7,	QTYPE=40,	\$END	SPKLR RF
\$NEWELL	ROW=35,	COL=11,	Q=0.442,	LAYER=7,	QTYPE=40,	\$END	SPKLR RF
\$NEWELL	ROW=37,	COL= 8,	Q=0.442,	LAYER=7,	QTYPE=40,	\$END	SPKLR RF
\$NEWELL	ROW=37,	COL=12,	Q=0.442,	LAYER=7,	QTYPE=40,	\$END	SPKLR RF
\$NEWELL	ROW=37,	COL=14,	Q=0.442,	LAYER=7,	QTYPE=40,	\$END	SPKLR RF
\$NEWELL	ROW=37,	COL=24,	Q=0.442,	LAYER=7,	QTYPE=40,	\$END	SPKLR RF
\$NEWELL	ROW=39,	COL=20,	Q=0.442,	LAYER=7,	QTYPE=40,	\$END	SPKLR RF
\$NEWELL	ROW=39,	COL=28,	Q=0.442,	LAYER=7,	QTYPE=40,	\$END	SPKLR RF
\$NEWELL	ROW=40,	COL=10,	Q=0.442,	LAYER=7,	QTYPE=40,	\$END	SPKLR RF
\$NEWELL	ROW=45,	COL=12,	Q=0.442,	LAYER=7,	QTYPE=40,	\$END	SPKLR RF
\$NEWELL	ROW=46,	COL=11,	Q=0.442,	LAYER=7,	QTYPE=40,	\$END	SPKLR RF
\$NEWELL	ROW=48,	COL=13,	Q=0.442,	LAYER=7,	QTYPE=40,	\$END	SPKLR RF
\$NEWELL	ROW=12,	COL=13,	Q=0.663,	LAYER=7,	QTYPE=40,	\$END	SPKLR RF
\$NEWELL	ROW=12,	COL=16,	Q=0.663,	LAYER=7,	QTYPE=40,	\$END	SPKLR RF
\$NEWELL	ROW=14,	COL=12,	Q=0.663,	LAYER=7,	QTYPE=40,	\$END	SPKLR RF
\$NEWELL	ROW=22,	COL=13,	Q=0.663,	LAYER=7,	QTYPE=40,	\$END	SPKLR RF
\$NEWELL	ROW=24,	COL=14,	Q=0.663,	LAYER=7,	QTYPE=40,	\$END	SPKLR RF
\$NEWELL	ROW=30,	COL=10,	Q=0.663,	LAYER=7,	QTYPE=40,	\$END	SPKLR RF
\$NEWELL	ROW=31,	COL= 7,	Q=0.663,	LAYER=7,	QTYPE=40,	\$END	SPKLR RF
\$NEWELL	ROW=31,	COL=11,	Q=0.663,	LAYER=7,	QTYPE=40,	\$END	SPKLR RF
\$NEWELL	ROW=34,	COL=10,	Q=0.663,	LAYER=7,	QTYPE=40,	\$END	SPKLR RF
\$NEWELL	ROW=35,	COL=13,	Q=0.663,	LAYER=7,	QTYPE=40,	\$END	SPKLR RF
\$NEWELL	ROW=37,	COL=27,	Q=0.663,	LAYER=7,	QTYPE=40,	\$END	SPKLR RF
\$NEWELL	ROW=38,	COL=19,	Q=0.663,	LAYER=7,	QTYPE=40,	\$END	SPKLR RF
\$NEWELL	ROW=39,	COL= 9,	Q=0.663,	LAYER=7,	QTYPE=40,	\$END	SPKLR RF
\$NEWELL	ROW=13,	COL=10,	Q=0.884,	LAYER=7,	QTYPE=40,	\$END	SPKLR RF
\$NEWELL	ROW=19,	COL= 6,	Q=0.884,	LAYER=7,	QTYPE=40,	\$END	SPKLR RF
\$NEWELL	ROW=21,	COL=11,	Q=0.884,	LAYER=7,	QTYPE=40,	\$END	SPKLR RF
\$NEWELL	ROW=21,	COL=14,	Q=0.884,	LAYER=7,	QTYPE=40,	\$END	SPKLR RF
\$NEWELL	ROW=22,	COL=14,	Q=0.884,	LAYER=7,	QTYPE=40,	\$END	SPKLR RF
\$NEWELL	ROW=31,	COL= 6,	Q=0.884,	LAYER=7,	QTYPE=40,	\$END	SPKLR RF
\$NEWELL	ROW=31,	COL=10,	Q=0.884,	LAYER=7,	QTYPE=40,	\$END	SPKLR RF
\$NEWELL	ROW=35,	COL= 7,	Q=0.884,	LAYER=7,	QTYPE=40,	\$END	SPKLR RF
\$NEWELL	ROW=35,	COL=12,	Q=0.884,	LAYER=7,	QTYPE=40,	\$END	SPKLR RF
\$NEWELL	ROW=36,	COL=11,	Q=0.884,	LAYER=7,	QTYPE=40,	\$END	SPKLR RF
\$NEWELL	ROW=36,	COL=26,	Q=0.884,	LAYER=7,	QTYPE=40,	\$END	SPKLR RF
\$NEWELL	ROW=37,	COL=10,	Q=0.884,	LAYER=7,	QTYPE=40,	\$END	SPKLR RF

Attachment 2.--Input file for the 1950-79 transient simulation--Continued

\$NEWELL	ROW=37,	COL=26,	Q=0.884,	LAYER=7,	QTYPE=40,	\$END	SPKLR RF
\$NEWELL	ROW=38,	COL=10,	Q=0.884,	LAYER=7,	QTYPE=40,	\$END	SPKLR RF
\$NEWELL	ROW=39,	COL=11,	Q=0.884,	LAYER=7,	QTYPE=40,	\$END	SPKLR RF
\$NEWELL	ROW=39,	COL=19,	Q=0.884,	LAYER=7,	QTYPE=40,	\$END	SPKLR RF
\$NEWELL	ROW=40,	COL=20,	Q=0.884,	LAYER=7,	QTYPE=40,	\$END	SPKLR RF
\$NEWELL	ROW=47,	COL=12,	Q=0.884,	LAYER=7,	QTYPE=40,	\$END	SPKLR RF
\$NEWELL	ROW=10,	COL=14,	Q=1.105,	LAYER=7,	QTYPE=40,	\$END	SPKLR RF
\$NEWELL	ROW=11,	COL=15,	Q=1.105,	LAYER=7,	QTYPE=40,	\$END	SPKLR RF
\$NEWELL	ROW=13,	COL=11,	Q=1.105,	LAYER=7,	QTYPE=40,	\$END	SPKLR RF
\$NEWELL	ROW=13,	COL=13,	Q=1.105,	LAYER=7,	QTYPE=40,	\$END	SPKLR RF
\$NEWELL	ROW=20,	COL= 6,	Q=1.105,	LAYER=7,	QTYPE=40,	\$END	SPKLR RF
\$NEWELL	ROW=21,	COL=10,	Q=1.105,	LAYER=7,	QTYPE=40,	\$END	SPKLR RF
\$NEWELL	ROW=22,	COL= 5,	Q=1.105,	LAYER=7,	QTYPE=40,	\$END	SPKLR RF
\$NEWELL	ROW=23,	COL=14,	Q=1.105,	LAYER=7,	QTYPE=40,	\$END	SPKLR RF
\$NEWELL	ROW=25,	COL=15,	Q=1.105,	LAYER=7,	QTYPE=40,	\$END	SPKLR RF
\$NEWELL	ROW=27,	COL= 4,	Q=1.105,	LAYER=7,	QTYPE=40,	\$END	SPKLR RF
\$NEWELL	ROW=27,	COL=15,	Q=1.105,	LAYER=7,	QTYPE=40,	\$END	SPKLR RF
\$NEWELL	ROW=32,	COL=11,	Q=1.105,	LAYER=7,	QTYPE=40,	\$END	SPKLR RF
\$NEWELL	ROW=36,	COL= 9,	Q=1.105,	LAYER=7,	QTYPE=40,	\$END	SPKLR RF
\$NEWELL	ROW=36,	COL=12,	Q=1.105,	LAYER=7,	QTYPE=40,	\$END	SPKLR RF
\$NEWELL	ROW=38,	COL= 9,	Q=1.105,	LAYER=7,	QTYPE=40,	\$END	SPKLR RF
\$NEWELL	ROW=38,	COL=11,	Q=1.105,	LAYER=7,	QTYPE=40,	\$END	SPKLR RF
\$NEWELL	ROW=45,	COL=11,	Q=1.105,	LAYER=7,	QTYPE=40,	\$END	SPKLR RF
\$NEWELL	ROW=12,	COL=14,	Q=1.326,	LAYER=7,	QTYPE=40,	\$END	SPKLR RF
\$NEWELL	ROW=21,	COL=13,	Q=1.326,	LAYER=7,	QTYPE=40,	\$END	SPKLR RF
\$NEWELL	ROW=22,	COL= 6,	Q=1.326,	LAYER=7,	QTYPE=40,	\$END	SPKLR RF
\$NEWELL	ROW=23,	COL=13,	Q=1.326,	LAYER=7,	QTYPE=40,	\$END	SPKLR RF
\$NEWELL	ROW=27,	COL=16,	Q=1.326,	LAYER=7,	QTYPE=40,	\$END	SPKLR RF
\$NEWELL	ROW=28,	COL=15,	Q=1.326,	LAYER=7,	QTYPE=40,	\$END	SPKLR RF
\$NEWELL	ROW=29,	COL= 7,	Q=1.326,	LAYER=7,	QTYPE=40,	\$END	SPKLR RF
\$NEWELL	ROW=29,	COL=16,	Q=1.326,	LAYER=7,	QTYPE=40,	\$END	SPKLR RF
\$NEWELL	ROW=32,	COL= 9,	Q=1.326,	LAYER=7,	QTYPE=40,	\$END	SPKLR RF
\$NEWELL	ROW=32,	COL=10,	Q=1.326,	LAYER=7,	QTYPE=40,	\$END	SPKLR RF
\$NEWELL	ROW=49,	COL=13,	Q=1.326,	LAYER=7,	QTYPE=40,	\$END	SPKLR RF
\$NEWELL	ROW=29,	COL=15,	Q=1.437,	LAYER=7,	QTYPE=40,	\$END	SPKLR RF
\$NEWELL	ROW=31,	COL= 9,	Q=1.437,	LAYER=7,	QTYPE=40,	\$END	SPKLR RF
\$NEWELL	ROW=23,	COL=12,	Q=1.547,	LAYER=7,	QTYPE=40,	\$END	SPKLR RF
\$NEWELL	ROW=26,	COL=15,	Q=1.547,	LAYER=7,	QTYPE=40,	\$END	SPKLR RF
\$NEWELL	ROW=28,	COL=13,	Q=1.547,	LAYER=7,	QTYPE=40,	\$END	SPKLR RF
\$NEWELL	ROW=39,	COL=27,	Q=1.547,	LAYER=7,	QTYPE=40,	\$END	SPKLR RF
\$NEWELL	ROW=30,	COL=12,	Q=1.658,	LAYER=7,	QTYPE=40,	\$END	SPKLR RF
\$NEWELL	ROW=36,	COL=24,	Q=1.658,	LAYER=7,	QTYPE=40,	\$END	SPKLR RF
\$NEWELL	ROW=15,	COL= 8,	Q=1.768,	LAYER=7,	QTYPE=40,	\$END	SPKLR RF
\$NEWELL	ROW=15,	COL= 9,	Q=1.768,	LAYER=7,	QTYPE=40,	\$END	SPKLR RF
\$NEWELL	ROW=22,	COL= 7,	Q=1.768,	LAYER=7,	QTYPE=40,	\$END	SPKLR RF
\$NEWELL	ROW=22,	COL= 8,	Q=1.768,	LAYER=7,	QTYPE=40,	\$END	SPKLR RF
\$NEWELL	ROW=22,	COL=10,	Q=1.768,	LAYER=7,	QTYPE=40,	\$END	SPKLR RF
\$NEWELL	ROW=25,	COL=13,	Q=1.768,	LAYER=7,	QTYPE=40,	\$END	SPKLR RF
\$NEWELL	ROW=25,	COL=16,	Q=1.768,	LAYER=7,	QTYPE=40,	\$END	SPKLR RF
\$NEWELL	ROW=26,	COL=16,	Q=1.768,	LAYER=7,	QTYPE=40,	\$END	SPKLR RF
\$NEWELL	ROW=29,	COL=12,	Q=1.768,	LAYER=7,	QTYPE=40,	\$END	SPKLR RF
\$NEWELL	ROW=29,	COL=14,	Q=1.768,	LAYER=7,	QTYPE=40,	\$END	SPKLR RF

## Attachment 2.--Input file for the 1950-79 transient simulation--Continued

```

$NEWELL ROW=36, COL=14, Q=1.768, LAYER=7, QTYPE=40, $END SPKLR RF
$NEWELL ROW=38, COL=26, Q=1.768, LAYER=7, QTYPE=40, $END SPKLR RF
$NEWELL ROW=38, COL=27, Q=1.768, LAYER=7, QTYPE=40, $END SPKLR RF
$NEWELL ROW=39, COL=10, Q=1.768, LAYER=7, QTYPE=40, $END SPKLR RF
$NEWELL ROW=48, COL=12, Q=1.768, LAYER=7, QTYPE=40, $END SPKLR RF
$NEWELL ROW=11, COL=14, Q=1.989, LAYER=7, QTYPE=40, $END SPKLR RF
$NEWELL ROW=14, COL= 8, Q=1.989, LAYER=7, QTYPE=40, $END SPKLR RF
$NEWELL ROW=24, COL=12, Q=1.989, LAYER=7, QTYPE=40, $END SPKLR RF
$NEWELL ROW=25, COL= 5, Q=1.989, LAYER=7, QTYPE=40, $END SPKLR RF
$NEWELL ROW=25, COL=14, Q=1.989, LAYER=7, QTYPE=40, $END SPKLR RF
$NEWELL ROW=29, COL= 9, Q=1.989, LAYER=7, QTYPE=40, $END SPKLR RF
$NEWELL ROW=36, COL=13, Q=1.989, LAYER=7, QTYPE=40, $END SPKLR RF
$NEWELL ROW=39, COL=21, Q=1.989, LAYER=7, QTYPE=40, $END SPKLR RF
$NEWELL ROW=44, COL=11, Q=1.989, LAYER=7, QTYPE=40, $END SPKLR RF
$NEWELL ROW=30, COL=11, Q=2.100, LAYER=7, QTYPE=40, $END SPKLR RF
$NEWELL ROW=24, COL= 8, Q=2.210, LAYER=7, QTYPE=40, $END SPKLR RF
$NEWELL ROW=26, COL= 4, Q=2.210, LAYER=7, QTYPE=40, $END SPKLR RF
$NEWELL ROW=28, COL=14, Q=2.210, LAYER=7, QTYPE=40, $END SPKLR RF
$NEWELL ROW=31, COL=14, Q=2.210, LAYER=7, QTYPE=40, $END SPKLR RF
$NEWELL ROW=24, COL=11, Q=2.321, LAYER=7, QTYPE=40, $END SPKLR RF
$NEWELL ROW=12, COL=15, Q=2.431, LAYER=7, QTYPE=40, $END SPKLR RF
$NEWELL ROW=21, COL= 6, Q=2.431, LAYER=7, QTYPE=40, $END SPKLR RF
$NEWELL ROW=24, COL= 6, Q=2.431, LAYER=7, QTYPE=40, $END SPKLR RF
$NEWELL ROW=24, COL= 9, Q=2.431, LAYER=7, QTYPE=40, $END SPKLR RF
$NEWELL ROW=24, COL=13, Q=2.431, LAYER=7, QTYPE=40, $END SPKLR RF
$NEWELL ROW=26, COL= 8, Q=2.431, LAYER=7, QTYPE=40, $END SPKLR RF
$NEWELL ROW=26, COL=11, Q=2.431, LAYER=7, QTYPE=40, $END SPKLR RF
$NEWELL ROW=27, COL= 5, Q=2.431, LAYER=7, QTYPE=40, $END SPKLR RF
$NEWELL ROW=27, COL=14, Q=2.431, LAYER=7, QTYPE=40, $END SPKLR RF
$NEWELL ROW=29, COL= 8, Q=2.431, LAYER=7, QTYPE=40, $END SPKLR RF
$NEWELL ROW=36, COL= 8, Q=2.431, LAYER=7, QTYPE=40, $END SPKLR RF
$NEWELL ROW=22, COL= 9, Q=2.652, LAYER=7, QTYPE=40, $END SPKLR RF
$NEWELL ROW=24, COL= 5, Q=2.652, LAYER=7, QTYPE=40, $END SPKLR RF
$NEWELL ROW=25, COL= 7, Q=2.652, LAYER=7, QTYPE=40, $END SPKLR RF
$NEWELL ROW=25, COL=11, Q=2.652, LAYER=7, QTYPE=40, $END SPKLR RF
$NEWELL ROW=26, COL= 9, Q=2.652, LAYER=7, QTYPE=40, $END SPKLR RF
$NEWELL ROW=26, COL=12, Q=2.652, LAYER=7, QTYPE=40, $END SPKLR RF
$NEWELL ROW=29, COL=10, Q=2.652, LAYER=7, QTYPE=40, $END SPKLR RF
$NEWELL ROW=30, COL=13, Q=2.652, LAYER=7, QTYPE=40, $END SPKLR RF
$NEWELL ROW=23, COL=10, Q=2.763, LAYER=7, QTYPE=40, $END SPKLR RF
$NEWELL ROW=26, COL= 5, Q=2.763, LAYER=7, QTYPE=40, $END SPKLR RF
$NEWELL ROW=24, COL= 7, Q=2.873, LAYER=7, QTYPE=40, $END SPKLR RF
$NEWELL ROW=24, COL=10, Q=2.873, LAYER=7, QTYPE=40, $END SPKLR RF
$NEWELL ROW=26, COL= 7, Q=2.873, LAYER=7, QTYPE=40, $END SPKLR RF
$NEWELL ROW=26, COL=10, Q=2.873, LAYER=7, QTYPE=40, $END SPKLR RF
$NEWELL ROW=25, COL= 9, Q=2.984, LAYER=7, QTYPE=40, $END SPKLR RF
$NEWELL ROW=28, COL= 6, Q=2.984, LAYER=7, QTYPE=40, $END SPKLR RF
$NEWELL ROW=23, COL= 7, Q=3.094, LAYER=7, QTYPE=40, $END SPKLR RF
$NEWELL ROW=23, COL= 9, Q=3.094, LAYER=7, QTYPE=40, $END SPKLR RF
$NEWELL ROW=25, COL= 8, Q=3.094, LAYER=7, QTYPE=40, $END SPKLR RF
$NEWELL ROW=25, COL=12, Q=3.094, LAYER=7, QTYPE=40, $END SPKLR RF
$NEWELL ROW=26, COL= 6, Q=3.094, LAYER=7, QTYPE=40, $END SPKLR RF

```

Attachment 2.--Input file for the 1950-79 transient simulation--Continued

```

$NEWELL ROW=26, COL=13, Q=3.094, LAYER=7, QTYPE=40, $END SPKLR RF
$NEWELL ROW=26, COL=14, Q=3.094, LAYER=7, QTYPE=40, $END SPKLR RF
$NEWELL ROW=27, COL= 9, Q=3.094, LAYER=7, QTYPE=40, $END SPKLR RF
$NEWELL ROW=27, COL=10, Q=3.094, LAYER=7, QTYPE=40, $END SPKLR RF
$NEWELL ROW=27, COL=13, Q=3.094, LAYER=7, QTYPE=40, $END SPKLR RF
$NEWELL ROW=28, COL=12, Q=3.094, LAYER=7, QTYPE=40, $END SPKLR RF
$NEWELL ROW=40, COL=21, Q=3.094, LAYER=7, QTYPE=40, $END SPKLR RF
$NEWELL ROW=23, COL= 6, Q=3.205, LAYER=7, QTYPE=40, $END SPKLR RF
$NEWELL ROW=22, COL=11, Q=3.315, LAYER=7, QTYPE=40, $END SPKLR RF
$NEWELL ROW=23, COL= 8, Q=3.315, LAYER=7, QTYPE=40, $END SPKLR RF
$NEWELL ROW=25, COL= 6, Q=3.315, LAYER=7, QTYPE=40, $END SPKLR RF
$NEWELL ROW=27, COL= 6, Q=3.315, LAYER=7, QTYPE=40, $END SPKLR RF
$NEWELL ROW=27, COL= 7, Q=3.315, LAYER=7, QTYPE=40, $END SPKLR RF
$NEWELL ROW=28, COL= 7, Q=3.315, LAYER=7, QTYPE=40, $END SPKLR RF
$NEWELL ROW=29, COL=11, Q=3.315, LAYER=7, QTYPE=40, $END SPKLR RF
$NEWELL ROW=30, COL=14, Q=3.315, LAYER=7, QTYPE=40, $END SPKLR RF
$NEWELL ROW=28, COL=11, Q=3.426, LAYER=7, QTYPE=40, $END SPKLR RF
$NEWELL ROW=22, COL=12, Q=3.536, LAYER=7, QTYPE=40, $END SPKLR RF
$NEWELL ROW=23, COL=11, Q=3.536, LAYER=7, QTYPE=40, $END SPKLR RF
$NEWELL ROW=25, COL=10, Q=3.536, LAYER=7, QTYPE=40, $END SPKLR RF
$NEWELL ROW=27, COL= 8, Q=3.536, LAYER=7, QTYPE=40, $END SPKLR RF
$NEWELL ROW=27, COL=11, Q=3.536, LAYER=7, QTYPE=40, $END SPKLR RF
$NEWELL ROW=27, COL=12, Q=3.536, LAYER=7, QTYPE=40, $END SPKLR RF
$NEWELL ROW=28, COL= 8, Q=3.536, LAYER=7, QTYPE=40, $END SPKLR RF
$NEWELL ROW=28, COL= 9, Q=3.536, LAYER=7, QTYPE=40, $END SPKLR RF
$NEWELL ROW=28, COL=10, Q=3.536, LAYER=7, QTYPE=40, $END SPKLR RF
$NEWELL ROW=29, COL=13, Q=3.536, LAYER=7, QTYPE=40, $END SPKLR RF
$NEWELL ROW=0, $END
$NEWRIV
VK(98)= 64*0.0525E-8, 24*0.1051E-8, 11*0.1576E-8, 5*0.2102E-8,
VK(648)= 76*0.1686E-8, 76*0.0525E-8, 75*0.3372E-8, 75*0.1051E-8,
         43*0.5058E-8, 43*0.1576E-8, 97*0.6744E-8, 97*0.2102E-8,
QMXOUT(98)=104*0.0,
QMXOUT(648)=582*0.0,
QMAX(98)= 64*0.2930, 24*0.5860, 11*0.8790, 5*1.1719,
QMAX(648)=76*0.5641, 76*0.4102, 75*1.1281, 75*0.8204,
         43*1.6922, 43*1.2306, 97*2.2562, 97*1.6408,
VK(1242)= 29*1.1574E-9, 6*1.1574E-8, 3*1.1574E-9,
VK(1)= 50*0.0906E-8, 21*0.1812E-8, 16*0.2718E-8, 10*0.3624E-8,
VK(202)=73*0.2907E-8, 73*0.0906E-8, 59*0.5814E-8, 59*0.1812E-8,
        35*0.8721E-8, 35*0.2718E-8, 56*1.1628E-8, 56*0.3624E-8,
VK(1230)=3*0.2907E-8, 3*0.2907E-8, 3*0.0906E-8, 1*0.8721E-8,
        1*0.8721E-8, 1*0.2718E-8,
QMXOUT(1)=97*0.0,
QMXOUT(202)=446*0.0,
QMXOUT(1230)=12*0.0,
QMXOUT(1242)=38*45.0,
QMAX(1)=50*0.5052, 21*1.0103, 16*1.5155, 10*2.0206,
QMAX(202)=73*0.9725, 73*0.7072, 59*1.9450, 59*1.4144,

```

Attachment 2.--Input file for the 1950-79 transient simulation--Continued

```

        35*2.9175, 35*2.1217, 56*3.8900, 56*2.8289,
QMAX(1230)=3*0.9725, 3*0.9725, 3*0.7072,
        1*2.9175, 1*2.9175, 1*2.1217,
QMAX(1242)=38*45.0,
$END
$NEWPP KP=2, TMAX=3650, NUMT=100, CDLT=1.0, DELT=2190,
QFAC=29*-253000,
QFAC(30)=0.14,
QFAC(40)=0.14,
QFAC(58)=-253000,
QFAC(61)=-253000,
QFAC(62)=-253000,
$END
$NEWELL ROW=0, $END
$NEWIRIV
VK(98)= 64*0.0453E-8, 24*0.0906E-8, 11*0.1359E-8, 5*0.1812E-8,
VK(648)=76*0.1454E-8, 76*0.0453E-8, 75*0.2907E-8, 75*0.0906E-8,
        43*0.4361E-8, 43*0.1359E-8, 97*0.5814E-8, 97*0.1812E-8,
QMAX(98)= 64*0.2526, 24*0.5052, 11*0.7578, 5*1.0103,
QMAX(648)=76*0.4863, 76*0.3536, 75*0.9725, 75*0.7072,
        43*1.4588, 43*1.0609, 97*1.9450, 97*1.4145,
$END
*MASS GET WAIT=ON WAITIME=60 CODE:/SLV/CTSS/CODE/B3KWMT
*& BAKIN:/SLV/OCT/BAKMG
*& REDEND2:/GLENN/UTILITY/REDEND2
*LDR BIN=CODE,LIB=METALIB
*XCORE */EXECUTE
*MASS STORE WAIT=ON WAITIME=60 BAKOUT:/SLV/OCT/BAKMK70
*& OUTPUT:/SLV/OCT/OUTMK70
*DESTROY BAKIN
*COPY BAKOUT BAKIN
*TRIXGL */EDIT TO TRIM EXCESS
A
REDEND2
*DISPOSE
DN=NEWOUT,TID=MFARV,FID=GAHMK,SF="CC",WAIT */PRINT OUTPUT
*DESTROY BAKOUT INPUT OUTPUT NEWOUT
*FILE NAME=INPUT
$CONTROL
        PHISET=.TRUE.,
        RESTRT=.TRUE.,
        SELRES=.TRUE.,
        ZRMBAL=.TRUE.,
$END
DUMMY
$INLIST
        NCUBES=0,
        NPER=1,
$END
HEADER

```



Attachment 2.--Input file for the 1950-79 transient simulation--Continued

- - - GROUND-WATER FLOW MODEL OF SAN LUIS VALLEY NORTH OF SAN LUIS HILLS - -  
-OCTOBER 1983 \*\*\* TRANSIENT 1970-79

END

SYMBOLS

ZIP 0

ONE 1

END

OUTPUT CUBES

1 7 DDN LST

END

ENDOF CUBES

\$NEWPP KP=1, TMAX=3650, NUMT=100, CDLT=1.0, DELT=2190,

QFAC(1)=6\*-432100,

QFAC(7)=-617300,

QFAC(8)=-432100, QFAC(58)=-432100,

QFAC(9)=-253000,

QFAC(10)=-617300,

QFAC(11)=-253000, QFAC(61)=-617300,

QFAC(12)=-253000, QFAC(62)=-617300,

QFAC(13)=-253000,

QFAC(14)=-802500,

QFAC(15)=-617300,

QFAC(16)=-253000,

QFAC(17)=-253000,

QFAC(18)=-253000,

QFAC(19)=-253000,

QFAC(20)=-253000,

QFAC(21)=-253000,

QFAC(22)=-253000,

QFAC(23)=-253000,

QFAC(24)=-253000,

QFAC(25)=-253000,

QFAC(26)=-617300, QFAC(76)=-253000,

QFAC(27)=-253000,

QFAC(28)=-1852000,

QFAC(29)=-617300,

QFAC(30)=0.26,

QFAC(40)=-0.34,

\$END

\$NEWELL ROW= 5, COL=12, Q=.00000159, LAYER=7, QTYPE=1, \$END A= 1

\$NEWELL ROW= 5, COL=13, Q=.00000079, LAYER=7, QTYPE=1, \$END A= 1

\$NEWELL ROW= 6, COL=13, Q=.00000159, LAYER=7, QTYPE=1, \$END A= 1

\$NEWELL ROW= 6, COL=14, Q=.00000079, LAYER=7, QTYPE=1, \$END A= 1

\$NEWELL ROW= 7, COL=13, Q=.00000079, LAYER=7, QTYPE=1, \$END A= 1

\$NEWELL ROW= 7, COL=14, Q=.00000171, LAYER=7, QTYPE=1, \$END A= 1

\$NEWELL ROW= 7, COL=15, Q=.00000040, LAYER=7, QTYPE=1, \$END A= 1

\$NEWELL ROW= 5, COL=12, Q=.00000189, LAYER=6, QTYPE=1, \$END A= 1

\$NEWELL ROW= 5, COL=13, Q=.00000095, LAYER=6, QTYPE=1, \$END A= 1

\$NEWELL ROW= 6, COL=13, Q=.00000189, LAYER=6, QTYPE=1, \$END A= 1

\$NEWELL ROW= 6, COL=14, Q=.00000095, LAYER=6, QTYPE=1, \$END A= 1

\$NEWELL ROW= 7, COL=13, Q=.00000095, LAYER=6, QTYPE=1, \$END A= 1

## Attachment 2.--Input file for the 1950-79 transient simulation--Continued

\$NEWELL	ROW= 7,	COL=14,	Q=.00000206,	LAYER=6,	QTYPE=1,	\$END	A= 1
\$NEWELL	ROW= 7,	COL=15,	Q=.00000047,	LAYER=6,	QTYPE=1,	\$END	A= 1
\$NEWELL	ROW= 5,	COL=12,	Q=.00000079,	LAYER=5,	QTYPE=1,	\$END	A= 1
\$NEWELL	ROW= 5,	COL=13,	Q=.00000040,	LAYER=5,	QTYPE=1,	\$END	A= 1
\$NEWELL	ROW= 6,	COL=13,	Q=.00000079,	LAYER=5,	QTYPE=1,	\$END	A= 1
\$NEWELL	ROW= 6,	COL=14,	Q=.00000040,	LAYER=5,	QTYPE=1,	\$END	A= 1
\$NEWELL	ROW= 7,	COL=13,	Q=.00000040,	LAYER=5,	QTYPE=1,	\$END	A= 1
\$NEWELL	ROW= 7,	COL=14,	Q=.00000086,	LAYER=5,	QTYPE=1,	\$END	A= 1
\$NEWELL	ROW= 7,	COL=15,	Q=.00000019,	LAYER=5,	QTYPE=1,	\$END	A= 1
\$NEWELL	ROW= 5,	COL=12,	Q=.00000047,	LAYER=4,	QTYPE=1,	\$END	A= 1
\$NEWELL	ROW= 5,	COL=13,	Q=.00000023,	LAYER=4,	QTYPE=1,	\$END	A= 1
\$NEWELL	ROW= 6,	COL=13,	Q=.00000047,	LAYER=4,	QTYPE=1,	\$END	A= 1
\$NEWELL	ROW= 6,	COL=14,	Q=.00000023,	LAYER=4,	QTYPE=1,	\$END	A= 1
\$NEWELL	ROW= 7,	COL=13,	Q=.00000023,	LAYER=4,	QTYPE=1,	\$END	A= 1
\$NEWELL	ROW= 7,	COL=14,	Q=.00000051,	LAYER=4,	QTYPE=1,	\$END	A= 1
\$NEWELL	ROW= 7,	COL=15,	Q=.00000012,	LAYER=4,	QTYPE=1,	\$END	A= 1
\$NEWELL	ROW=10,	COL=14,	Q=.00000235,	LAYER=7,	QTYPE=2,	\$END	A= 2
\$NEWELL	ROW=10,	COL=15,	Q=.00000156,	LAYER=7,	QTYPE=2,	\$END	A= 2
\$NEWELL	ROW=11,	COL=14,	Q=.00000235,	LAYER=7,	QTYPE=2,	\$END	A= 2
\$NEWELL	ROW=11,	COL=15,	Q=.00000254,	LAYER=7,	QTYPE=2,	\$END	A= 2
\$NEWELL	ROW=12,	COL=13,	Q=.00000079,	LAYER=7,	QTYPE=2,	\$END	A= 2
\$NEWELL	ROW=12,	COL=14,	Q=.00000175,	LAYER=7,	QTYPE=2,	\$END	A= 2
\$NEWELL	ROW=12,	COL=15,	Q=.00000293,	LAYER=7,	QTYPE=2,	\$END	A= 2
\$NEWELL	ROW=12,	COL=16,	Q=.00000117,	LAYER=7,	QTYPE=2,	\$END	A= 2
\$NEWELL	ROW=13,	COL=13,	Q=.00000039,	LAYER=7,	QTYPE=2,	\$END	A= 2
\$NEWELL	ROW=13,	COL=14,	Q=.00000079,	LAYER=7,	QTYPE=2,	\$END	A= 2
\$NEWELL	ROW=13,	COL=15,	Q=.00000235,	LAYER=7,	QTYPE=2,	\$END	A= 2
\$NEWELL	ROW=14,	COL=13,	Q=.00000039,	LAYER=7,	QTYPE=2,	\$END	A= 2
\$NEWELL	ROW=14,	COL=14,	Q=.00000039,	LAYER=7,	QTYPE=2,	\$END	A= 2
\$NEWELL	ROW=15,	COL=13,	Q=.00000079,	LAYER=7,	QTYPE=2,	\$END	A= 2
\$NEWELL	ROW=10,	COL=14,	Q=.00000188,	LAYER=6,	QTYPE=2,	\$END	A= 2
\$NEWELL	ROW=10,	COL=15,	Q=.00000126,	LAYER=6,	QTYPE=2,	\$END	A= 2
\$NEWELL	ROW=11,	COL=14,	Q=.00000188,	LAYER=6,	QTYPE=2,	\$END	A= 2
\$NEWELL	ROW=11,	COL=15,	Q=.00000203,	LAYER=6,	QTYPE=2,	\$END	A= 2
\$NEWELL	ROW=12,	COL=13,	Q=.00000062,	LAYER=6,	QTYPE=2,	\$END	A= 2
\$NEWELL	ROW=12,	COL=14,	Q=.00000141,	LAYER=6,	QTYPE=2,	\$END	A= 2
\$NEWELL	ROW=12,	COL=15,	Q=.00000235,	LAYER=6,	QTYPE=2,	\$END	A= 2
\$NEWELL	ROW=12,	COL=16,	Q=.00000094,	LAYER=6,	QTYPE=2,	\$END	A= 2
\$NEWELL	ROW=13,	COL=13,	Q=.00000032,	LAYER=6,	QTYPE=2,	\$END	A= 2
\$NEWELL	ROW=13,	COL=14,	Q=.00000062,	LAYER=6,	QTYPE=2,	\$END	A= 2
\$NEWELL	ROW=13,	COL=15,	Q=.00000188,	LAYER=6,	QTYPE=2,	\$END	A= 2
\$NEWELL	ROW=14,	COL=13,	Q=.00000032,	LAYER=6,	QTYPE=2,	\$END	A= 2
\$NEWELL	ROW=14,	COL=14,	Q=.00000032,	LAYER=6,	QTYPE=2,	\$END	A= 2
\$NEWELL	ROW=15,	COL=13,	Q=.00000062,	LAYER=6,	QTYPE=2,	\$END	A= 2
\$NEWELL	ROW=10,	COL=14,	Q=.00000040,	LAYER=5,	QTYPE=2,	\$END	A= 2
\$NEWELL	ROW=10,	COL=15,	Q=.00000026,	LAYER=5,	QTYPE=2,	\$END	A= 2
\$NEWELL	ROW=11,	COL=14,	Q=.00000040,	LAYER=5,	QTYPE=2,	\$END	A= 2
\$NEWELL	ROW=11,	COL=15,	Q=.00000043,	LAYER=5,	QTYPE=2,	\$END	A= 2
\$NEWELL	ROW=12,	COL=13,	Q=.00000014,	LAYER=5,	QTYPE=2,	\$END	A= 2

Attachment 2.--Input file for the 1950-79 transient simulation--Continued

\$NEWELL	ROW=12,	COL=14,	Q=.00000030,	LAYER=5,	QTYPE=2,	\$END	A= 2
\$NEWELL	ROW=12,	COL=15,	Q=.00000050,	LAYER=5,	QTYPE=2,	\$END	A= 2
\$NEWELL	ROW=12,	COL=16,	Q=.00000019,	LAYER=5,	QTYPE=2,	\$END	A= 2
\$NEWELL	ROW=13,	COL=13,	Q=.00000007,	LAYER=5,	QTYPE=2,	\$END	A= 2
\$NEWELL	ROW=13,	COL=14,	Q=.00000014,	LAYER=5,	QTYPE=2,	\$END	A= 2
\$NEWELL	ROW=13,	COL=15,	Q=.00000040,	LAYER=5,	QTYPE=2,	\$END	A= 2
\$NEWELL	ROW=14,	COL=13,	Q=.00000007,	LAYER=5,	QTYPE=2,	\$END	A= 2
\$NEWELL	ROW=14,	COL=14,	Q=.00000007,	LAYER=5,	QTYPE=2,	\$END	A= 2
\$NEWELL	ROW=15,	COL=13,	Q=.00000014,	LAYER=5,	QTYPE=2,	\$END	A= 2
\$NEWELL	ROW=10,	COL=14,	Q=.00000010,	LAYER=4,	QTYPE=2,	\$END	A= 2
\$NEWELL	ROW=10,	COL=15,	Q=.00000007,	LAYER=4,	QTYPE=2,	\$END	A= 2
\$NEWELL	ROW=11,	COL=14,	Q=.00000010,	LAYER=4,	QTYPE=2,	\$END	A= 2
\$NEWELL	ROW=11,	COL=15,	Q=.00000011,	LAYER=4,	QTYPE=2,	\$END	A= 2
\$NEWELL	ROW=12,	COL=13,	Q=.00000003,	LAYER=4,	QTYPE=2,	\$END	A= 2
\$NEWELL	ROW=12,	COL=14,	Q=.00000007,	LAYER=4,	QTYPE=2,	\$END	A= 2
\$NEWELL	ROW=12,	COL=15,	Q=.00000012,	LAYER=4,	QTYPE=2,	\$END	A= 2
\$NEWELL	ROW=12,	COL=16,	Q=.00000006,	LAYER=4,	QTYPE=2,	\$END	A= 2
\$NEWELL	ROW=13,	COL=13,	Q=.00000001,	LAYER=4,	QTYPE=2,	\$END	A= 2
\$NEWELL	ROW=13,	COL=14,	Q=.00000003,	LAYER=4,	QTYPE=2,	\$END	A= 2
\$NEWELL	ROW=13,	COL=15,	Q=.00000010,	LAYER=4,	QTYPE=2,	\$END	A= 2
\$NEWELL	ROW=14,	COL=13,	Q=.00000001,	LAYER=4,	QTYPE=2,	\$END	A= 2
\$NEWELL	ROW=14,	COL=14,	Q=.00000001,	LAYER=4,	QTYPE=2,	\$END	A= 2
\$NEWELL	ROW=15,	COL=13,	Q=.00000003,	LAYER=4,	QTYPE=2,	\$END	A= 2
\$NEWELL	ROW=10,	COL=14,	Q=.00000003,	LAYER=3,	QTYPE=2,	\$END	A= 2
\$NEWELL	ROW=10,	COL=15,	Q=.00000003,	LAYER=3,	QTYPE=2,	\$END	A= 2
\$NEWELL	ROW=11,	COL=14,	Q=.00000003,	LAYER=3,	QTYPE=2,	\$END	A= 2
\$NEWELL	ROW=11,	COL=15,	Q=.00000004,	LAYER=3,	QTYPE=2,	\$END	A= 2
\$NEWELL	ROW=12,	COL=13,	Q=.00000001,	LAYER=3,	QTYPE=2,	\$END	A= 2
\$NEWELL	ROW=12,	COL=14,	Q=.00000003,	LAYER=3,	QTYPE=2,	\$END	A= 2
\$NEWELL	ROW=12,	COL=15,	Q=.00000004,	LAYER=3,	QTYPE=2,	\$END	A= 2
\$NEWELL	ROW=12,	COL=16,	Q=.00000001,	LAYER=3,	QTYPE=2,	\$END	A= 2
\$NEWELL	ROW=13,	COL=13,	Q=.00000001,	LAYER=3,	QTYPE=2,	\$END	A= 2
\$NEWELL	ROW=13,	COL=14,	Q=.00000001,	LAYER=3,	QTYPE=2,	\$END	A= 2
\$NEWELL	ROW=13,	COL=15,	Q=.00000003,	LAYER=3,	QTYPE=2,	\$END	A= 2
\$NEWELL	ROW=14,	COL=13,	Q=.00000001,	LAYER=3,	QTYPE=2,	\$END	A= 2
\$NEWELL	ROW=14,	COL=14,	Q=.00000001,	LAYER=3,	QTYPE=2,	\$END	A= 2
\$NEWELL	ROW=15,	COL=13,	Q=.00000001,	LAYER=3,	QTYPE=2,	\$END	A= 2
\$NEWELL	ROW=12,	COL= 7,	Q=.00000021,	LAYER=7,	QTYPE=3,	\$END	A= 3
\$NEWELL	ROW=12,	COL= 8,	Q=.00000021,	LAYER=7,	QTYPE=3,	\$END	A= 3
\$NEWELL	ROW=12,	COL=11,	Q=.00000021,	LAYER=7,	QTYPE=3,	\$END	A= 3
\$NEWELL	ROW=12,	COL=12,	Q=.00000021,	LAYER=7,	QTYPE=3,	\$END	A= 3
\$NEWELL	ROW=13,	COL= 7,	Q=.00000288,	LAYER=7,	QTYPE=3,	\$END	A= 3
\$NEWELL	ROW=13,	COL= 8,	Q=.00000309,	LAYER=7,	QTYPE=3,	\$END	A= 3
\$NEWELL	ROW=13,	COL= 9,	Q=.00000288,	LAYER=7,	QTYPE=3,	\$END	A= 3
\$NEWELL	ROW=13,	COL=10,	Q=.00000268,	LAYER=7,	QTYPE=3,	\$END	A= 3
\$NEWELL	ROW=13,	COL=11,	Q=.00000083,	LAYER=7,	QTYPE=3,	\$END	A= 3
\$NEWELL	ROW=12,	COL= 7,	Q=.00000015,	LAYER=6,	QTYPE=3,	\$END	A= 3
\$NEWELL	ROW=12,	COL= 8,	Q=.00000015,	LAYER=6,	QTYPE=3,	\$END	A= 3
\$NEWELL	ROW=12,	COL=11,	Q=.00000015,	LAYER=6,	QTYPE=3,	\$END	A= 3
\$NEWELL	ROW=12,	COL=12,	Q=.00000015,	LAYER=6,	QTYPE=3,	\$END	A= 3
\$NEWELL	ROW=13,	COL= 7,	Q=.00000217,	LAYER=6,	QTYPE=3,	\$END	A= 3

## Attachment 2.--Input file for the 1950-79 transient simulation--Continued

\$NEWELL	ROW=13,	COL= 8,	Q=.00000232,	LAYER=6,	QTYPE=3,	\$END	A= 3
\$NEWELL	ROW=13,	COL= 9,	Q=.00000217,	LAYER=6,	QTYPE=3,	\$END	A= 3
\$NEWELL	ROW=13,	COL=10,	Q=.00000201,	LAYER=6,	QTYPE=3,	\$END	A= 3
\$NEWELL	ROW=13,	COL=11,	Q=.00000062,	LAYER=6,	QTYPE=3,	\$END	A= 3
\$NEWELL	ROW=12,	COL= 7,	Q=.00000003,	LAYER=5,	QTYPE=3,	\$END	A= 3
\$NEWELL	ROW=12,	COL= 8,	Q=.00000003,	LAYER=5,	QTYPE=3,	\$END	A= 3
\$NEWELL	ROW=12,	COL=11,	Q=.00000003,	LAYER=5,	QTYPE=3,	\$END	A= 3
\$NEWELL	ROW=12,	COL=12,	Q=.00000003,	LAYER=5,	QTYPE=3,	\$END	A= 3
\$NEWELL	ROW=13,	COL= 7,	Q=.00000036,	LAYER=5,	QTYPE=3,	\$END	A= 3
\$NEWELL	ROW=13,	COL= 8,	Q=.00000039,	LAYER=5,	QTYPE=3,	\$END	A= 3
\$NEWELL	ROW=13,	COL= 9,	Q=.00000036,	LAYER=5,	QTYPE=3,	\$END	A= 3
\$NEWELL	ROW=13,	COL=10,	Q=.00000035,	LAYER=5,	QTYPE=3,	\$END	A= 3
\$NEWELL	ROW=13,	COL=11,	Q=.00000011,	LAYER=5,	QTYPE=3,	\$END	A= 3
\$NEWELL	ROW=12,	COL= 7,	Q=.00000001,	LAYER=4,	QTYPE=3,	\$END	A= 3
\$NEWELL	ROW=12,	COL= 8,	Q=.00000001,	LAYER=4,	QTYPE=3,	\$END	A= 3
\$NEWELL	ROW=12,	COL=11,	Q=.00000001,	LAYER=4,	QTYPE=3,	\$END	A= 3
\$NEWELL	ROW=12,	COL=12,	Q=.00000001,	LAYER=4,	QTYPE=3,	\$END	A= 3
\$NEWELL	ROW=13,	COL= 7,	Q=.00000012,	LAYER=4,	QTYPE=3,	\$END	A= 3
\$NEWELL	ROW=13,	COL= 8,	Q=.00000012,	LAYER=4,	QTYPE=3,	\$END	A= 3
\$NEWELL	ROW=13,	COL= 9,	Q=.00000012,	LAYER=4,	QTYPE=3,	\$END	A= 3
\$NEWELL	ROW=13,	COL=10,	Q=.00000011,	LAYER=4,	QTYPE=3,	\$END	A= 3
\$NEWELL	ROW=13,	COL=11,	Q=.00000004,	LAYER=4,	QTYPE=3,	\$END	A= 3
\$NEWELL	ROW=14,	COL= 8,	Q=.00000270,	LAYER=7,	QTYPE=4,	\$END	A= 4
\$NEWELL	ROW=14,	COL= 9,	Q=.00000135,	LAYER=7,	QTYPE=4,	\$END	A= 4
\$NEWELL	ROW=15,	COL= 8,	Q=.00000270,	LAYER=7,	QTYPE=4,	\$END	A= 4
\$NEWELL	ROW=15,	COL= 9,	Q=.00000203,	LAYER=7,	QTYPE=4,	\$END	A= 4
\$NEWELL	ROW=14,	COL= 8,	Q=.00000277,	LAYER=6,	QTYPE=4,	\$END	A= 4
\$NEWELL	ROW=14,	COL= 9,	Q=.00000139,	LAYER=6,	QTYPE=4,	\$END	A= 4
\$NEWELL	ROW=15,	COL= 8,	Q=.00000277,	LAYER=6,	QTYPE=4,	\$END	A= 4
\$NEWELL	ROW=15,	COL= 9,	Q=.00000208,	LAYER=6,	QTYPE=4,	\$END	A= 4
\$NEWELL	ROW=14,	COL= 8,	Q=.00000052,	LAYER=5,	QTYPE=4,	\$END	A= 4
\$NEWELL	ROW=14,	COL= 9,	Q=.00000026,	LAYER=5,	QTYPE=4,	\$END	A= 4
\$NEWELL	ROW=15,	COL= 8,	Q=.00000052,	LAYER=5,	QTYPE=4,	\$END	A= 4
\$NEWELL	ROW=15,	COL= 9,	Q=.00000040,	LAYER=5,	QTYPE=4,	\$END	A= 4
\$NEWELL	ROW=14,	COL= 8,	Q=.00000022,	LAYER=4,	QTYPE=4,	\$END	A= 4
\$NEWELL	ROW=14,	COL= 9,	Q=.00000011,	LAYER=4,	QTYPE=4,	\$END	A= 4
\$NEWELL	ROW=15,	COL= 8,	Q=.00000022,	LAYER=4,	QTYPE=4,	\$END	A= 4
\$NEWELL	ROW=15,	COL= 9,	Q=.00000017,	LAYER=4,	QTYPE=4,	\$END	A= 4
\$NEWELL	ROW=14,	COL= 8,	Q=.00000007,	LAYER=3,	QTYPE=4,	\$END	A= 4
\$NEWELL	ROW=14,	COL= 9,	Q=.00000004,	LAYER=3,	QTYPE=4,	\$END	A= 4
\$NEWELL	ROW=15,	COL= 8,	Q=.00000007,	LAYER=3,	QTYPE=4,	\$END	A= 4
\$NEWELL	ROW=15,	COL= 9,	Q=.00000006,	LAYER=3,	QTYPE=4,	\$END	A= 4
\$NEWELL	ROW=14,	COL=10,	Q=.00000112,	LAYER=7,	QTYPE=5,	\$END	A= 5
\$NEWELL	ROW=14,	COL=11,	Q=.00000120,	LAYER=7,	QTYPE=5,	\$END	A= 5
\$NEWELL	ROW=15,	COL=10,	Q=.00000048,	LAYER=7,	QTYPE=5,	\$END	A= 5
\$NEWELL	ROW=15,	COL=11,	Q=.00000055,	LAYER=7,	QTYPE=5,	\$END	A= 5
\$NEWELL	ROW=15,	COL=12,	Q=.00000080,	LAYER=7,	QTYPE=5,	\$END	A= 5
\$NEWELL	ROW=15,	COL=14,	Q=.00000032,	LAYER=7,	QTYPE=5,	\$END	A= 5
\$NEWELL	ROW=16,	COL= 7,	Q=.00000023,	LAYER=7,	QTYPE=5,	\$END	A= 5
\$NEWELL	ROW=16,	COL= 8,	Q=.00000127,	LAYER=7,	QTYPE=5,	\$END	A= 5
\$NEWELL	ROW=16,	COL= 9,	Q=.00000032,	LAYER=7,	QTYPE=5,	\$END	A= 5

## Attachment 2.--Input file for the 1950-79 transient simulation--Continued

\$NEWELL	ROW=16,	COL=10,	Q=.00000048,	LAYER=7,	QTYPE=5,	\$END	A= 5
\$NEWELL	ROW=16,	COL=12,	Q=.00000080,	LAYER=7,	QTYPE=5,	\$END	A= 5
\$NEWELL	ROW=16,	COL=13,	Q=.00000063,	LAYER=7,	QTYPE=5,	\$END	A= 5
\$NEWELL	ROW=16,	COL=15,	Q=.00000063,	LAYER=7,	QTYPE=5,	\$END	A= 5
\$NEWELL	ROW=17,	COL= 7,	Q=.00000048,	LAYER=7,	QTYPE=5,	\$END	A= 5
\$NEWELL	ROW=17,	COL= 8,	Q=.00000080,	LAYER=7,	QTYPE=5,	\$END	A= 5
\$NEWELL	ROW=17,	COL=12,	Q=.00000017,	LAYER=7,	QTYPE=5,	\$END	A= 5
\$NEWELL	ROW=17,	COL=13,	Q=.00000048,	LAYER=7,	QTYPE=5,	\$END	A= 5
\$NEWELL	ROW=18,	COL= 7,	Q=.00000095,	LAYER=7,	QTYPE=5,	\$END	A= 5
\$NEWELL	ROW=18,	COL= 8,	Q=.00000127,	LAYER=7,	QTYPE=5,	\$END	A= 5
\$NEWELL	ROW=18,	COL= 9,	Q=.00000048,	LAYER=7,	QTYPE=5,	\$END	A= 5
\$NEWELL	ROW=19,	COL= 7,	Q=.00000104,	LAYER=7,	QTYPE=5,	\$END	A= 5
\$NEWELL	ROW=19,	COL= 8,	Q=.00000095,	LAYER=7,	QTYPE=5,	\$END	A= 5
\$NEWELL	ROW=14,	COL=10,	Q=.00000119,	LAYER=6,	QTYPE=5,	\$END	A= 5
\$NEWELL	ROW=14,	COL=11,	Q=.00000127,	LAYER=6,	QTYPE=5,	\$END	A= 5
\$NEWELL	ROW=15,	COL=10,	Q=.00000051,	LAYER=6,	QTYPE=5,	\$END	A= 5
\$NEWELL	ROW=15,	COL=11,	Q=.00000059,	LAYER=6,	QTYPE=5,	\$END	A= 5
\$NEWELL	ROW=15,	COL=12,	Q=.00000084,	LAYER=6,	QTYPE=5,	\$END	A= 5
\$NEWELL	ROW=15,	COL=14,	Q=.00000035,	LAYER=6,	QTYPE=5,	\$END	A= 5
\$NEWELL	ROW=16,	COL= 7,	Q=.00000025,	LAYER=6,	QTYPE=5,	\$END	A= 5
\$NEWELL	ROW=16,	COL= 8,	Q=.00000135,	LAYER=6,	QTYPE=5,	\$END	A= 5
\$NEWELL	ROW=16,	COL= 9,	Q=.00000035,	LAYER=6,	QTYPE=5,	\$END	A= 5
\$NEWELL	ROW=16,	COL=10,	Q=.00000051,	LAYER=6,	QTYPE=5,	\$END	A= 5
\$NEWELL	ROW=16,	COL=12,	Q=.00000084,	LAYER=6,	QTYPE=5,	\$END	A= 5
\$NEWELL	ROW=16,	COL=13,	Q=.00000068,	LAYER=6,	QTYPE=5,	\$END	A= 5
\$NEWELL	ROW=16,	COL=15,	Q=.00000068,	LAYER=6,	QTYPE=5,	\$END	A= 5
\$NEWELL	ROW=17,	COL= 7,	Q=.00000051,	LAYER=6,	QTYPE=5,	\$END	A= 5
\$NEWELL	ROW=17,	COL= 8,	Q=.00000084,	LAYER=6,	QTYPE=5,	\$END	A= 5
\$NEWELL	ROW=17,	COL=12,	Q=.00000017,	LAYER=6,	QTYPE=5,	\$END	A= 5
\$NEWELL	ROW=17,	COL=13,	Q=.00000051,	LAYER=6,	QTYPE=5,	\$END	A= 5
\$NEWELL	ROW=18,	COL= 7,	Q=.00000102,	LAYER=6,	QTYPE=5,	\$END	A= 5
\$NEWELL	ROW=18,	COL= 8,	Q=.00000135,	LAYER=6,	QTYPE=5,	\$END	A= 5
\$NEWELL	ROW=18,	COL= 9,	Q=.00000051,	LAYER=6,	QTYPE=5,	\$END	A= 5
\$NEWELL	ROW=19,	COL= 7,	Q=.00000110,	LAYER=6,	QTYPE=5,	\$END	A= 5
\$NEWELL	ROW=19,	COL= 8,	Q=.00000102,	LAYER=6,	QTYPE=5,	\$END	A= 5
\$NEWELL	ROW=14,	COL=10,	Q=.00000105,	LAYER=5,	QTYPE=5,	\$END	A= 5
\$NEWELL	ROW=14,	COL=11,	Q=.00000112,	LAYER=5,	QTYPE=5,	\$END	A= 5
\$NEWELL	ROW=15,	COL=10,	Q=.00000044,	LAYER=5,	QTYPE=5,	\$END	A= 5
\$NEWELL	ROW=15,	COL=11,	Q=.00000052,	LAYER=5,	QTYPE=5,	\$END	A= 5
\$NEWELL	ROW=15,	COL=12,	Q=.00000090,	LAYER=5,	QTYPE=5,	\$END	A= 5
\$NEWELL	ROW=15,	COL=14,	Q=.00000030,	LAYER=5,	QTYPE=5,	\$END	A= 5
\$NEWELL	ROW=16,	COL= 7,	Q=.00000022,	LAYER=5,	QTYPE=5,	\$END	A= 5
\$NEWELL	ROW=16,	COL= 8,	Q=.00000119,	LAYER=5,	QTYPE=5,	\$END	A= 5
\$NEWELL	ROW=16,	COL= 9,	Q=.00000030,	LAYER=5,	QTYPE=5,	\$END	A= 5
\$NEWELL	ROW=16,	COL=10,	Q=.00000044,	LAYER=5,	QTYPE=5,	\$END	A= 5
\$NEWELL	ROW=16,	COL=12,	Q=.00000075,	LAYER=5,	QTYPE=5,	\$END	A= 5
\$NEWELL	ROW=16,	COL=13,	Q=.00000059,	LAYER=5,	QTYPE=5,	\$END	A= 5
\$NEWELL	ROW=16,	COL=15,	Q=.00000059,	LAYER=5,	QTYPE=5,	\$END	A= 5
\$NEWELL	ROW=17,	COL= 7,	Q=.00000044,	LAYER=5,	QTYPE=5,	\$END	A= 5

## Attachment 2.--Input file for the 1950-79 transient simulation--Continued

\$NEWELL	ROW=17,	COL= 8,	Q=.00000075,	LAYER=5,	QTYPE=5,	\$END	A= 5
\$NEWELL	ROW=17,	COL=12,	Q=.00000015,	LAYER=5,	QTYPE=5,	\$END	A= 5
\$NEWELL	ROW=17,	COL=13,	Q=.00000044,	LAYER=5,	QTYPE=5,	\$END	A= 5
\$NEWELL	ROW=18,	COL= 7,	Q=.00000090,	LAYER=5,	QTYPE=5,	\$END	A= 5
\$NEWELL	ROW=18,	COL= 8,	Q=.00000119,	LAYER=5,	QTYPE=5,	\$END	A= 5
\$NEWELL	ROW=18,	COL= 9,	Q=.00000044,	LAYER=5,	QTYPE=5,	\$END	A= 5
\$NEWELL	ROW=19,	COL= 7,	Q=.00000097,	LAYER=5,	QTYPE=5,	\$END	A= 5
\$NEWELL	ROW=19,	COL= 8,	Q=.00000090,	LAYER=5,	QTYPE=5,	\$END	A= 5
\$NEWELL	ROW=14,	COL=10,	Q=.00000155,	LAYER=4,	QTYPE=5,	\$END	A= 5
\$NEWELL	ROW=14,	COL=11,	Q=.00000166,	LAYER=4,	QTYPE=5,	\$END	A= 5
\$NEWELL	ROW=15,	COL=10,	Q=.00000066,	LAYER=4,	QTYPE=5,	\$END	A= 5
\$NEWELL	ROW=15,	COL=11,	Q=.00000177,	LAYER=4,	QTYPE=5,	\$END	A= 5
\$NEWELL	ROW=15,	COL=12,	Q=.00000132,	LAYER=4,	QTYPE=5,	\$END	A= 5
\$NEWELL	ROW=15,	COL=14,	Q=.00000044,	LAYER=4,	QTYPE=5,	\$END	A= 5
\$NEWELL	ROW=16,	COL= 7,	Q=.00000033,	LAYER=4,	QTYPE=5,	\$END	A= 5
\$NEWELL	ROW=16,	COL= 8,	Q=.00000177,	LAYER=4,	QTYPE=5,	\$END	A= 5
\$NEWELL	ROW=16,	COL= 9,	Q=.00000044,	LAYER=4,	QTYPE=5,	\$END	A= 5
\$NEWELL	ROW=16,	COL=10,	Q=.00000066,	LAYER=4,	QTYPE=5,	\$END	A= 5
\$NEWELL	ROW=16,	COL=12,	Q=.00000110,	LAYER=4,	QTYPE=5,	\$END	A= 5
\$NEWELL	ROW=16,	COL=13,	Q=.00000088,	LAYER=4,	QTYPE=5,	\$END	A= 5
\$NEWELL	ROW=16,	COL=15,	Q=.00000088,	LAYER=4,	QTYPE=5,	\$END	A= 5
\$NEWELL	ROW=17,	COL= 7,	Q=.00000066,	LAYER=4,	QTYPE=5,	\$END	A= 5
\$NEWELL	ROW=17,	COL= 8,	Q=.00000110,	LAYER=4,	QTYPE=5,	\$END	A= 5
\$NEWELL	ROW=17,	COL=12,	Q=.00000022,	LAYER=4,	QTYPE=5,	\$END	A= 5
\$NEWELL	ROW=17,	COL=13,	Q=.00000066,	LAYER=4,	QTYPE=5,	\$END	A= 5
\$NEWELL	ROW=18,	COL= 7,	Q=.00000132,	LAYER=4,	QTYPE=5,	\$END	A= 5
\$NEWELL	ROW=18,	COL= 8,	Q=.00000177,	LAYER=4,	QTYPE=5,	\$END	A= 5
\$NEWELL	ROW=18,	COL= 9,	Q=.00000066,	LAYER=4,	QTYPE=5,	\$END	A= 5
\$NEWELL	ROW=19,	COL= 7,	Q=.00000144,	LAYER=4,	QTYPE=5,	\$END	A= 5
\$NEWELL	ROW=19,	COL= 8,	Q=.00000132,	LAYER=4,	QTYPE=5,	\$END	A= 5
\$NEWELL	ROW=14,	COL=10,	Q=.00000065,	LAYER=3,	QTYPE=5,	\$END	A= 5
\$NEWELL	ROW=14,	COL=11,	Q=.00000069,	LAYER=3,	QTYPE=5,	\$END	A= 5
\$NEWELL	ROW=15,	COL=10,	Q=.00000028,	LAYER=3,	QTYPE=5,	\$END	A= 5
\$NEWELL	ROW=15,	COL=11,	Q=.00000032,	LAYER=3,	QTYPE=5,	\$END	A= 5
\$NEWELL	ROW=15,	COL=12,	Q=.00000046,	LAYER=3,	QTYPE=5,	\$END	A= 5
\$NEWELL	ROW=15,	COL=14,	Q=.00000018,	LAYER=3,	QTYPE=5,	\$END	A= 5
\$NEWELL	ROW=16,	COL= 7,	Q=.00000014,	LAYER=3,	QTYPE=5,	\$END	A= 5
\$NEWELL	ROW=16,	COL= 8,	Q=.00000075,	LAYER=3,	QTYPE=5,	\$END	A= 5
\$NEWELL	ROW=16,	COL= 9,	Q=.00000018,	LAYER=3,	QTYPE=5,	\$END	A= 5
\$NEWELL	ROW=16,	COL=10,	Q=.00000028,	LAYER=3,	QTYPE=5,	\$END	A= 5
\$NEWELL	ROW=16,	COL=12,	Q=.00000046,	LAYER=3,	QTYPE=5,	\$END	A= 5
\$NEWELL	ROW=16,	COL=13,	Q=.00000037,	LAYER=3,	QTYPE=5,	\$END	A= 5
\$NEWELL	ROW=16,	COL=15,	Q=.00000037,	LAYER=3,	QTYPE=5,	\$END	A= 5
\$NEWELL	ROW=17,	COL= 7,	Q=.00000028,	LAYER=3,	QTYPE=5,	\$END	A= 5
\$NEWELL	ROW=17,	COL= 8,	Q=.00000046,	LAYER=3,	QTYPE=5,	\$END	A= 5
\$NEWELL	ROW=17,	COL=12,	Q=.00000010,	LAYER=3,	QTYPE=5,	\$END	A= 5
\$NEWELL	ROW=17,	COL=13,	Q=.00000028,	LAYER=3,	QTYPE=5,	\$END	A= 5
\$NEWELL	ROW=18,	COL= 7,	Q=.00000055,	LAYER=3,	QTYPE=5,	\$END	A= 5
\$NEWELL	ROW=18,	COL= 8,	Q=.00000075,	LAYER=3,	QTYPE=5,	\$END	A= 5
\$NEWELL	ROW=18,	COL= 9,	Q=.00000028,	LAYER=3,	QTYPE=5,	\$END	A= 5

## Attachment 2.--Input file for the 1950-79 transient simulation--Continued

\$NEWELL	ROW=19,	COL= 7,	Q=.00000061,	LAYER=3,	QTYPE=5,	\$END	A= 5
\$NEWELL	ROW=19,	COL= 8,	Q=.00000055,	LAYER=3,	QTYPE=5,	\$END	A= 5
\$NEWELL	ROW=16,	COL=17,	Q=.00000102,	LAYER=7,	QTYPE=6,	\$END	A= 6
\$NEWELL	ROW=16,	COL=18,	Q=.00000102,	LAYER=7,	QTYPE=6,	\$END	A= 6
\$NEWELL	ROW=16,	COL=19,	Q=.00000102,	LAYER=7,	QTYPE=6,	\$END	A= 6
\$NEWELL	ROW=17,	COL=16,	Q=.00000102,	LAYER=7,	QTYPE=6,	\$END	A= 6
\$NEWELL	ROW=17,	COL=17,	Q=.00000315,	LAYER=7,	QTYPE=6,	\$END	A= 6
\$NEWELL	ROW=16,	COL=17,	Q=.00000057,	LAYER=6,	QTYPE=6,	\$END	A= 6
\$NEWELL	ROW=16,	COL=18,	Q=.00000057,	LAYER=6,	QTYPE=6,	\$END	A= 6
\$NEWELL	ROW=16,	COL=19,	Q=.00000057,	LAYER=6,	QTYPE=6,	\$END	A= 6
\$NEWELL	ROW=17,	COL=16,	Q=.00000057,	LAYER=6,	QTYPE=6,	\$END	A= 6
\$NEWELL	ROW=17,	COL=17,	Q=.00000155,	LAYER=6,	QTYPE=6,	\$END	A= 6
\$NEWELL	ROW=19,	COL= 6,	Q=.00000063,	LAYER=7,	QTYPE=7,	\$END	A= 7
\$NEWELL	ROW=20,	COL= 6,	Q=.00000084,	LAYER=7,	QTYPE=7,	\$END	A= 7
\$NEWELL	ROW=21,	COL= 6,	Q=.00000092,	LAYER=7,	QTYPE=7,	\$END	A= 7
\$NEWELL	ROW=22,	COL= 5,	Q=.00000070,	LAYER=7,	QTYPE=7,	\$END	A= 7
\$NEWELL	ROW=19,	COL= 6,	Q=.00000178,	LAYER=6,	QTYPE=7,	\$END	A= 7
\$NEWELL	ROW=20,	COL= 6,	Q=.00000237,	LAYER=6,	QTYPE=7,	\$END	A= 7
\$NEWELL	ROW=21,	COL= 6,	Q=.00000257,	LAYER=6,	QTYPE=7,	\$END	A= 7
\$NEWELL	ROW=22,	COL= 5,	Q=.00000197,	LAYER=6,	QTYPE=7,	\$END	A= 7
\$NEWELL	ROW=19,	COL= 6,	Q=.00000115,	LAYER=5,	QTYPE=7,	\$END	A= 7
\$NEWELL	ROW=20,	COL= 6,	Q=.00000153,	LAYER=5,	QTYPE=7,	\$END	A= 7
\$NEWELL	ROW=21,	COL= 6,	Q=.00000166,	LAYER=5,	QTYPE=7,	\$END	A= 7
\$NEWELL	ROW=22,	COL= 5,	Q=.00000127,	LAYER=5,	QTYPE=7,	\$END	A= 7
\$NEWELL	ROW=20,	COL= 7,	Q=.00000072,	LAYER=7,	QTYPE=58,	\$END	A= 8
\$NEWELL	ROW=20,	COL= 8,	Q=.00000072,	LAYER=7,	QTYPE=8,	\$END	A= 8
\$NEWELL	ROW=20,	COL= 9,	Q=.00000072,	LAYER=7,	QTYPE=8,	\$END	A= 8
\$NEWELL	ROW=20,	COL=10,	Q=.00000072,	LAYER=7,	QTYPE=8,	\$END	A= 8
\$NEWELL	ROW=20,	COL=11,	Q=.00000028,	LAYER=7,	QTYPE=8,	\$END	A= 8
\$NEWELL	ROW=21,	COL= 7,	Q=.00000072,	LAYER=7,	QTYPE=58,	\$END	A= 8
\$NEWELL	ROW=21,	COL= 8,	Q=.00000072,	LAYER=7,	QTYPE=8,	\$END	A= 8
\$NEWELL	ROW=21,	COL= 9,	Q=.00000072,	LAYER=7,	QTYPE=8,	\$END	A= 8
\$NEWELL	ROW=21,	COL=10,	Q=.00000072,	LAYER=7,	QTYPE=8,	\$END	A= 8
\$NEWELL	ROW=21,	COL=11,	Q=.00000036,	LAYER=7,	QTYPE=8,	\$END	A= 8
\$NEWELL	ROW=20,	COL= 7,	Q=.00000046,	LAYER=6,	QTYPE=58,	\$END	A= 8
\$NEWELL	ROW=20,	COL= 8,	Q=.00000046,	LAYER=6,	QTYPE=8,	\$END	A= 8
\$NEWELL	ROW=20,	COL= 9,	Q=.00000046,	LAYER=6,	QTYPE=8,	\$END	A= 8
\$NEWELL	ROW=20,	COL=10,	Q=.00000046,	LAYER=6,	QTYPE=8,	\$END	A= 8
\$NEWELL	ROW=20,	COL=11,	Q=.00000017,	LAYER=6,	QTYPE=8,	\$END	A= 8
\$NEWELL	ROW=21,	COL= 7,	Q=.00000046,	LAYER=6,	QTYPE=58,	\$END	A= 8
\$NEWELL	ROW=21,	COL= 8,	Q=.00000046,	LAYER=6,	QTYPE=8,	\$END	A= 8
\$NEWELL	ROW=21,	COL= 9,	Q=.00000046,	LAYER=6,	QTYPE=8,	\$END	A= 8
\$NEWELL	ROW=21,	COL=10,	Q=.00000046,	LAYER=6,	QTYPE=8,	\$END	A= 8
\$NEWELL	ROW=21,	COL=11,	Q=.00000022,	LAYER=6,	QTYPE=8,	\$END	A= 8
\$NEWELL	ROW=20,	COL= 7,	Q=.00000145,	LAYER=5,	QTYPE=58,	\$END	A= 8
\$NEWELL	ROW=20,	COL= 8,	Q=.00000145,	LAYER=5,	QTYPE=8,	\$END	A= 8
\$NEWELL	ROW=20,	COL= 9,	Q=.00000145,	LAYER=5,	QTYPE=8,	\$END	A= 8
\$NEWELL	ROW=20,	COL=10,	Q=.00000145,	LAYER=5,	QTYPE=8,	\$END	A= 8
\$NEWELL	ROW=20,	COL=11,	Q=.00000054,	LAYER=5,	QTYPE=8,	\$END	A= 8
\$NEWELL	ROW=21,	COL= 7,	Q=.00000145,	LAYER=5,	QTYPE=58,	\$END	A= 8
\$NEWELL	ROW=21,	COL= 8,	Q=.00000145,	LAYER=5,	QTYPE=8,	\$END	A= 8

## Attachment 2.--Input file for the 1950-79 transient simulation--Continued

\$NEWELL	ROW=21,	COL= 9,	Q=.00000145,	LAYER=5,	QTYPE=8,	\$END	A= 8
\$NEWELL	ROW=21,	COL=10,	Q=.00000145,	LAYER=5,	QTYPE=8,	\$END	A= 8
\$NEWELL	ROW=21,	COL=11,	Q=.00000072,	LAYER=5,	QTYPE=8,	\$END	A= 8
\$NEWELL	ROW=20,	COL= 7,	Q=.00000253,	LAYER=4,	QTYPE=58,	\$END	A= 8
\$NEWELL	ROW=20,	COL= 8,	Q=.00000253,	LAYER=4,	QTYPE=8,	\$END	A= 8
\$NEWELL	ROW=20,	COL= 9,	Q=.00000253,	LAYER=4,	QTYPE=8,	\$END	A= 8
\$NEWELL	ROW=20,	COL=10,	Q=.00000253,	LAYER=4,	QTYPE=8,	\$END	A= 8
\$NEWELL	ROW=20,	COL=11,	Q=.00000095,	LAYER=4,	QTYPE=8,	\$END	A= 8
\$NEWELL	ROW=21,	COL= 7,	Q=.00000253,	LAYER=4,	QTYPE=58,	\$END	A= 8
\$NEWELL	ROW=21,	COL= 8,	Q=.00000253,	LAYER=4,	QTYPE=8,	\$END	A= 8
\$NEWELL	ROW=21,	COL= 9,	Q=.00000253,	LAYER=4,	QTYPE=8,	\$END	A= 8
\$NEWELL	ROW=21,	COL=10,	Q=.00000253,	LAYER=4,	QTYPE=8,	\$END	A= 8
\$NEWELL	ROW=21,	COL=11,	Q=.00000127,	LAYER=4,	QTYPE=8,	\$END	A= 8
\$NEWELL	ROW=20,	COL= 7,	Q=.00000117,	LAYER=3,	QTYPE=58,	\$END	A= 8
\$NEWELL	ROW=20,	COL= 8,	Q=.00000117,	LAYER=3,	QTYPE=8,	\$END	A= 8
\$NEWELL	ROW=20,	COL= 9,	Q=.00000117,	LAYER=3,	QTYPE=8,	\$END	A= 8
\$NEWELL	ROW=20,	COL=10,	Q=.00000117,	LAYER=3,	QTYPE=8,	\$END	A= 8
\$NEWELL	ROW=20,	COL=11,	Q=.00000044,	LAYER=3,	QTYPE=8,	\$END	A= 8
\$NEWELL	ROW=21,	COL= 7,	Q=.00000117,	LAYER=3,	QTYPE=58,	\$END	A= 8
\$NEWELL	ROW=21,	COL= 8,	Q=.00000117,	LAYER=3,	QTYPE=8,	\$END	A= 8
\$NEWELL	ROW=21,	COL= 9,	Q=.00000117,	LAYER=3,	QTYPE=8,	\$END	A= 8
\$NEWELL	ROW=21,	COL=10,	Q=.00000117,	LAYER=3,	QTYPE=8,	\$END	A= 8
\$NEWELL	ROW=21,	COL=11,	Q=.00000059,	LAYER=3,	QTYPE=8,	\$END	A= 8
\$NEWELL	ROW=21,	COL=13,	Q=.00000121,	LAYER=7,	QTYPE=9,	\$END	A= 9
\$NEWELL	ROW=21,	COL=14,	Q=.00000091,	LAYER=7,	QTYPE=9,	\$END	A= 9
\$NEWELL	ROW=22,	COL=12,	Q=.00000363,	LAYER=7,	QTYPE=9,	\$END	A= 9
\$NEWELL	ROW=22,	COL=13,	Q=.00000061,	LAYER=7,	QTYPE=9,	\$END	A= 9
\$NEWELL	ROW=22,	COL=14,	Q=.00000211,	LAYER=7,	QTYPE=9,	\$END	A= 9
\$NEWELL	ROW=23,	COL=14,	Q=.00000483,	LAYER=7,	QTYPE=9,	\$END	A= 9
\$NEWELL	ROW=24,	COL=14,	Q=.00000483,	LAYER=7,	QTYPE=9,	\$END	A= 9
\$NEWELL	ROW=24,	COL=15,	Q=.00000150,	LAYER=7,	QTYPE=9,	\$END	A= 9
\$NEWELL	ROW=25,	COL=14,	Q=.00000333,	LAYER=7,	QTYPE=9,	\$END	A= 9
\$NEWELL	ROW=25,	COL=15,	Q=.00000363,	LAYER=7,	QTYPE=9,	\$END	A= 9
\$NEWELL	ROW=25,	COL=16,	Q=.00000302,	LAYER=7,	QTYPE=9,	\$END	A= 9
\$NEWELL	ROW=26,	COL=12,	Q=.00000302,	LAYER=7,	QTYPE=9,	\$END	A= 9
\$NEWELL	ROW=26,	COL=13,	Q=.00000363,	LAYER=7,	QTYPE=9,	\$END	A= 9
\$NEWELL	ROW=26,	COL=14,	Q=.00000422,	LAYER=7,	QTYPE=9,	\$END	A= 9
\$NEWELL	ROW=26,	COL=15,	Q=.00000181,	LAYER=7,	QTYPE=9,	\$END	A= 9
\$NEWELL	ROW=26,	COL=16,	Q=.00000272,	LAYER=7,	QTYPE=9,	\$END	A= 9
\$NEWELL	ROW=27,	COL=12,	Q=.00000483,	LAYER=7,	QTYPE=9,	\$END	A= 9
\$NEWELL	ROW=27,	COL=13,	Q=.00000302,	LAYER=7,	QTYPE=9,	\$END	A= 9
\$NEWELL	ROW=27,	COL=14,	Q=.00000483,	LAYER=7,	QTYPE=9,	\$END	A= 9
\$NEWELL	ROW=28,	COL=12,	Q=.00000453,	LAYER=7,	QTYPE=9,	\$END	A= 9
\$NEWELL	ROW=28,	COL=13,	Q=.00000211,	LAYER=7,	QTYPE=9,	\$END	A= 9
\$NEWELL	ROW=28,	COL=14,	Q=.00000483,	LAYER=7,	QTYPE=9,	\$END	A= 9
\$NEWELL	ROW=29,	COL=12,	Q=.00000242,	LAYER=7,	QTYPE=9,	\$END	A= 9
\$NEWELL	ROW=29,	COL=13,	Q=.00000483,	LAYER=7,	QTYPE=9,	\$END	A= 9
\$NEWELL	ROW=29,	COL=14,	Q=.00000242,	LAYER=7,	QTYPE=9,	\$END	A= 9
\$NEWELL	ROW=29,	COL=15,	Q=.00000363,	LAYER=7,	QTYPE=9,	\$END	A= 9
\$NEWELL	ROW=29,	COL=16,	Q=.00000302,	LAYER=7,	QTYPE=9,	\$END	A= 9
\$NEWELL	ROW=30,	COL=12,	Q=.00000483,	LAYER=7,	QTYPE=9,	\$END	A= 9



Attachment 2.--Input file for the 1950-79 transient simulation--Continued

\$NEWELL	ROW=30,	COL=13,	Q=.00000302,	LAYER=7,	QTYPE=9,	\$END	A= 9
\$NEWELL	ROW=30,	COL=14,	Q=.00000363,	LAYER=7,	QTYPE=9,	\$END	A= 9
\$NEWELL	ROW=31,	COL=14,	Q=.00000030,	LAYER=7,	QTYPE=9,	\$END	A= 9
\$NEWELL	ROW=21,	COL=13,	Q=.00000033,	LAYER=6,	QTYPE=9,	\$END	A= 9
\$NEWELL	ROW=21,	COL=14,	Q=.00000025,	LAYER=6,	QTYPE=9,	\$END	A= 9
\$NEWELL	ROW=22,	COL=12,	Q=.00000131,	LAYER=6,	QTYPE=9,	\$END	A= 9
\$NEWELL	ROW=22,	COL=13,	Q=.00000017,	LAYER=6,	QTYPE=9,	\$END	A= 9
\$NEWELL	ROW=22,	COL=14,	Q=.00000057,	LAYER=6,	QTYPE=9,	\$END	A= 9
\$NEWELL	ROW=23,	COL=14,	Q=.00000131,	LAYER=6,	QTYPE=9,	\$END	A= 9
\$NEWELL	ROW=24,	COL=14,	Q=.00000131,	LAYER=6,	QTYPE=9,	\$END	A= 9
\$NEWELL	ROW=24,	COL=15,	Q=.00000041,	LAYER=6,	QTYPE=9,	\$END	A= 9
\$NEWELL	ROW=25,	COL=14,	Q=.00000090,	LAYER=6,	QTYPE=9,	\$END	A= 9
\$NEWELL	ROW=25,	COL=15,	Q=.00000098,	LAYER=6,	QTYPE=9,	\$END	A= 9
\$NEWELL	ROW=25,	COL=16,	Q=.00000081,	LAYER=6,	QTYPE=9,	\$END	A= 9
\$NEWELL	ROW=26,	COL=12,	Q=.00000081,	LAYER=6,	QTYPE=9,	\$END	A= 9
\$NEWELL	ROW=26,	COL=13,	Q=.00000098,	LAYER=6,	QTYPE=9,	\$END	A= 9
\$NEWELL	ROW=26,	COL=14,	Q=.00000115,	LAYER=6,	QTYPE=9,	\$END	A= 9
\$NEWELL	ROW=26,	COL=15,	Q=.00000050,	LAYER=6,	QTYPE=9,	\$END	A= 9
\$NEWELL	ROW=26,	COL=16,	Q=.00000073,	LAYER=6,	QTYPE=9,	\$END	A= 9
\$NEWELL	ROW=27,	COL=12,	Q=.00000131,	LAYER=6,	QTYPE=9,	\$END	A= 9
\$NEWELL	ROW=27,	COL=13,	Q=.00000081,	LAYER=6,	QTYPE=9,	\$END	A= 9
\$NEWELL	ROW=27,	COL=14,	Q=.00000131,	LAYER=6,	QTYPE=9,	\$END	A= 9
\$NEWELL	ROW=28,	COL=12,	Q=.00000123,	LAYER=6,	QTYPE=9,	\$END	A= 9
\$NEWELL	ROW=28,	COL=13,	Q=.00000057,	LAYER=6,	QTYPE=9,	\$END	A= 9
\$NEWELL	ROW=28,	COL=14,	Q=.00000131,	LAYER=6,	QTYPE=9,	\$END	A= 9
\$NEWELL	ROW=29,	COL=12,	Q=.00000065,	LAYER=6,	QTYPE=9,	\$END	A= 9
\$NEWELL	ROW=29,	COL=13,	Q=.00000131,	LAYER=6,	QTYPE=9,	\$END	A= 9
\$NEWELL	ROW=29,	COL=14,	Q=.00000065,	LAYER=6,	QTYPE=9,	\$END	A= 9
\$NEWELL	ROW=29,	COL=15,	Q=.00000098,	LAYER=6,	QTYPE=9,	\$END	A= 9
\$NEWELL	ROW=29,	COL=16,	Q=.00000081,	LAYER=6,	QTYPE=9,	\$END	A= 9
\$NEWELL	ROW=30,	COL=12,	Q=.00000131,	LAYER=6,	QTYPE=9,	\$END	A= 9
\$NEWELL	ROW=30,	COL=13,	Q=.00000081,	LAYER=6,	QTYPE=9,	\$END	A= 9
\$NEWELL	ROW=30,	COL=14,	Q=.00000098,	LAYER=6,	QTYPE=9,	\$END	A= 9
\$NEWELL	ROW=31,	COL=14,	Q=.00000008,	LAYER=6,	QTYPE=9,	\$END	A= 9
\$NEWELL	ROW=21,	COL=13,	Q=.00000001,	LAYER=5,	QTYPE=9,	\$END	A= 9
\$NEWELL	ROW=21,	COL=14,	Q=.00000001,	LAYER=5,	QTYPE=9,	\$END	A= 9
\$NEWELL	ROW=22,	COL=12,	Q=.00000004,	LAYER=5,	QTYPE=9,	\$END	A= 9
\$NEWELL	ROW=22,	COL=13,	Q=.00000001,	LAYER=5,	QTYPE=9,	\$END	A= 9
\$NEWELL	ROW=22,	COL=14,	Q=.00000001,	LAYER=5,	QTYPE=9,	\$END	A= 9
\$NEWELL	ROW=23,	COL=14,	Q=.00000004,	LAYER=5,	QTYPE=9,	\$END	A= 9
\$NEWELL	ROW=24,	COL=14,	Q=.00000004,	LAYER=5,	QTYPE=9,	\$END	A= 9
\$NEWELL	ROW=24,	COL=15,	Q=.00000001,	LAYER=5,	QTYPE=9,	\$END	A= 9
\$NEWELL	ROW=25,	COL=14,	Q=.00000003,	LAYER=5,	QTYPE=9,	\$END	A= 9
\$NEWELL	ROW=25,	COL=15,	Q=.00000003,	LAYER=5,	QTYPE=9,	\$END	A= 9
\$NEWELL	ROW=25,	COL=16,	Q=.00000003,	LAYER=5,	QTYPE=9,	\$END	A= 9
\$NEWELL	ROW=26,	COL=12,	Q=.00000003,	LAYER=5,	QTYPE=9,	\$END	A= 9
\$NEWELL	ROW=26,	COL=13,	Q=.00000003,	LAYER=5,	QTYPE=9,	\$END	A= 9
\$NEWELL	ROW=26,	COL=14,	Q=.00000004,	LAYER=5,	QTYPE=9,	\$END	A= 9
\$NEWELL	ROW=26,	COL=15,	Q=.00000001,	LAYER=5,	QTYPE=9,	\$END	A= 9
\$NEWELL	ROW=26,	COL=16,	Q=.00000003,	LAYER=5,	QTYPE=9,	\$END	A= 9
\$NEWELL	ROW=27,	COL=12,	Q=.00000004,	LAYER=5,	QTYPE=9,	\$END	A= 9

## Attachment 2.--Input file for the 1950-79 transient simulation--Continued

\$NEWELL	ROW=27,	COL=13,	Q=.00000003,	LAYER=5,	QTYPE=9,	\$END	A= 9
\$NEWELL	ROW=27,	COL=14,	Q=.00000004,	LAYER=5,	QTYPE=9,	\$END	A= 9
\$NEWELL	ROW=28,	COL=12,	Q=.00000004,	LAYER=5,	QTYPE=9,	\$END	A= 9
\$NEWELL	ROW=28,	COL=13,	Q=.00000001,	LAYER=5,	QTYPE=9,	\$END	A= 9
\$NEWELL	ROW=28,	COL=14,	Q=.00000004,	LAYER=5,	QTYPE=9,	\$END	A= 9
\$NEWELL	ROW=29,	COL=12,	Q=.00000003,	LAYER=5,	QTYPE=9,	\$END	A= 9
\$NEWELL	ROW=29,	COL=13,	Q=.00000004,	LAYER=5,	QTYPE=9,	\$END	A= 9
\$NEWELL	ROW=29,	COL=14,	Q=.00000003,	LAYER=5,	QTYPE=9,	\$END	A= 9
\$NEWELL	ROW=29,	COL=15,	Q=.00000003,	LAYER=5,	QTYPE=9,	\$END	A= 9
\$NEWELL	ROW=29,	COL=16,	Q=.00000003,	LAYER=5,	QTYPE=9,	\$END	A= 9
\$NEWELL	ROW=30,	COL=12,	Q=.00000004,	LAYER=5,	QTYPE=9,	\$END	A= 9
\$NEWELL	ROW=30,	COL=13,	Q=.00000003,	LAYER=5,	QTYPE=9,	\$END	A= 9
\$NEWELL	ROW=30,	COL=14,	Q=.00000003,	LAYER=5,	QTYPE=9,	\$END	A= 9
\$NEWELL	ROW=21,	COL=13,	Q=.00000001,	LAYER=4,	QTYPE=9,	\$END	A= 9
\$NEWELL	ROW=21,	COL=14,	Q=.00000001,	LAYER=4,	QTYPE=9,	\$END	A= 9
\$NEWELL	ROW=22,	COL=12,	Q=.00000007,	LAYER=4,	QTYPE=9,	\$END	A= 9
\$NEWELL	ROW=22,	COL=13,	Q=.00000001,	LAYER=4,	QTYPE=9,	\$END	A= 9
\$NEWELL	ROW=22,	COL=14,	Q=.00000003,	LAYER=4,	QTYPE=9,	\$END	A= 9
\$NEWELL	ROW=23,	COL=14,	Q=.00000007,	LAYER=4,	QTYPE=9,	\$END	A= 9
\$NEWELL	ROW=24,	COL=14,	Q=.00000007,	LAYER=4,	QTYPE=9,	\$END	A= 9
\$NEWELL	ROW=24,	COL=15,	Q=.00000003,	LAYER=4,	QTYPE=9,	\$END	A= 9
\$NEWELL	ROW=25,	COL=14,	Q=.00000006,	LAYER=4,	QTYPE=9,	\$END	A= 9
\$NEWELL	ROW=25,	COL=15,	Q=.00000006,	LAYER=4,	QTYPE=9,	\$END	A= 9
\$NEWELL	ROW=25,	COL=16,	Q=.00000004,	LAYER=4,	QTYPE=9,	\$END	A= 9
\$NEWELL	ROW=26,	COL=12,	Q=.00000004,	LAYER=4,	QTYPE=9,	\$END	A= 9
\$NEWELL	ROW=26,	COL=13,	Q=.00000006,	LAYER=4,	QTYPE=9,	\$END	A= 9
\$NEWELL	ROW=26,	COL=14,	Q=.00000007,	LAYER=4,	QTYPE=9,	\$END	A= 9
\$NEWELL	ROW=26,	COL=15,	Q=.00000003,	LAYER=4,	QTYPE=9,	\$END	A= 9
\$NEWELL	ROW=26,	COL=16,	Q=.00000004,	LAYER=4,	QTYPE=9,	\$END	A= 9
\$NEWELL	ROW=27,	COL=12,	Q=.00000007,	LAYER=4,	QTYPE=9,	\$END	A= 9
\$NEWELL	ROW=27,	COL=13,	Q=.00000004,	LAYER=4,	QTYPE=9,	\$END	A= 9
\$NEWELL	ROW=27,	COL=14,	Q=.00000007,	LAYER=4,	QTYPE=9,	\$END	A= 9
\$NEWELL	ROW=28,	COL=12,	Q=.00000007,	LAYER=4,	QTYPE=9,	\$END	A= 9
\$NEWELL	ROW=28,	COL=13,	Q=.00000003,	LAYER=4,	QTYPE=9,	\$END	A= 9
\$NEWELL	ROW=28,	COL=14,	Q=.00000007,	LAYER=4,	QTYPE=9,	\$END	A= 9
\$NEWELL	ROW=29,	COL=12,	Q=.00000004,	LAYER=4,	QTYPE=9,	\$END	A= 9
\$NEWELL	ROW=29,	COL=13,	Q=.00000007,	LAYER=4,	QTYPE=9,	\$END	A= 9
\$NEWELL	ROW=29,	COL=14,	Q=.00000004,	LAYER=4,	QTYPE=9,	\$END	A= 9
\$NEWELL	ROW=29,	COL=15,	Q=.00000006,	LAYER=4,	QTYPE=9,	\$END	A= 9
\$NEWELL	ROW=29,	COL=16,	Q=.00000004,	LAYER=4,	QTYPE=9,	\$END	A= 9
\$NEWELL	ROW=30,	COL=12,	Q=.00000007,	LAYER=4,	QTYPE=9,	\$END	A= 9
\$NEWELL	ROW=30,	COL=13,	Q=.00000004,	LAYER=4,	QTYPE=9,	\$END	A= 9
\$NEWELL	ROW=30,	COL=14,	Q=.00000006,	LAYER=4,	QTYPE=9,	\$END	A= 9
\$NEWELL	ROW=21,	COL=13,	Q=.00000001,	LAYER=3,	QTYPE=9,	\$END	A= 9
\$NEWELL	ROW=21,	COL=14,	Q=.00000001,	LAYER=3,	QTYPE=9,	\$END	A= 9
\$NEWELL	ROW=22,	COL=12,	Q=.00000007,	LAYER=3,	QTYPE=9,	\$END	A= 9
\$NEWELL	ROW=22,	COL=13,	Q=.00000001,	LAYER=3,	QTYPE=9,	\$END	A= 9
\$NEWELL	ROW=22,	COL=14,	Q=.00000003,	LAYER=3,	QTYPE=9,	\$END	A= 9
\$NEWELL	ROW=23,	COL=14,	Q=.00000007,	LAYER=3,	QTYPE=9,	\$END	A= 9
\$NEWELL	ROW=24,	COL=14,	Q=.00000007,	LAYER=3,	QTYPE=9,	\$END	A= 9

Attachment 2.--Input file for the 1950-79 transient simulation--Continued

\$NEWELL	ROW=24,	COL=15,	Q=.00000003,	LAYER=3,	QTYPE=9,	\$END	A= 9
\$NEWELL	ROW=25,	COL=14,	Q=.00000004,	LAYER=3,	QTYPE=9,	\$END	A= 9
\$NEWELL	ROW=25,	COL=15,	Q=.00000006,	LAYER=3,	QTYPE=9,	\$END	A= 9
\$NEWELL	ROW=25,	COL=16,	Q=.00000004,	LAYER=3,	QTYPE=9,	\$END	A= 9
\$NEWELL	ROW=26,	COL=12,	Q=.00000004,	LAYER=3,	QTYPE=9,	\$END	A= 9
\$NEWELL	ROW=26,	COL=13,	Q=.00000006,	LAYER=3,	QTYPE=9,	\$END	A= 9
\$NEWELL	ROW=26,	COL=14,	Q=.00000006,	LAYER=3,	QTYPE=9,	\$END	A= 9
\$NEWELL	ROW=26,	COL=15,	Q=.00000003,	LAYER=3,	QTYPE=9,	\$END	A= 9
\$NEWELL	ROW=26,	COL=16,	Q=.00000004,	LAYER=3,	QTYPE=9,	\$END	A= 9
\$NEWELL	ROW=27,	COL=12,	Q=.00000007,	LAYER=3,	QTYPE=9,	\$END	A= 9
\$NEWELL	ROW=27,	COL=13,	Q=.00000004,	LAYER=3,	QTYPE=9,	\$END	A= 9
\$NEWELL	ROW=27,	COL=14,	Q=.00000007,	LAYER=3,	QTYPE=9,	\$END	A= 9
\$NEWELL	ROW=28,	COL=12,	Q=.00000007,	LAYER=3,	QTYPE=9,	\$END	A= 9
\$NEWELL	ROW=28,	COL=13,	Q=.00000003,	LAYER=3,	QTYPE=9,	\$END	A= 9
\$NEWELL	ROW=28,	COL=14,	Q=.00000007,	LAYER=3,	QTYPE=9,	\$END	A= 9
\$NEWELL	ROW=29,	COL=12,	Q=.00000004,	LAYER=3,	QTYPE=9,	\$END	A= 9
\$NEWELL	ROW=29,	COL=13,	Q=.00000007,	LAYER=3,	QTYPE=9,	\$END	A= 9
\$NEWELL	ROW=29,	COL=14,	Q=.00000004,	LAYER=3,	QTYPE=9,	\$END	A= 9
\$NEWELL	ROW=29,	COL=15,	Q=.00000006,	LAYER=3,	QTYPE=9,	\$END	A= 9
\$NEWELL	ROW=29,	COL=16,	Q=.00000004,	LAYER=3,	QTYPE=9,	\$END	A= 9
\$NEWELL	ROW=30,	COL=12,	Q=.00000007,	LAYER=3,	QTYPE=9,	\$END	A= 9
\$NEWELL	ROW=30,	COL=13,	Q=.00000004,	LAYER=3,	QTYPE=9,	\$END	A= 9
\$NEWELL	ROW=30,	COL=14,	Q=.00000006,	LAYER=3,	QTYPE=9,	\$END	A= 9
\$NEWELL	ROW=22,	COL= 6,	Q=.00000413,	LAYER=7,	QTYPE=10,	\$END	A=10
\$NEWELL	ROW=23,	COL= 5,	Q=.00000206,	LAYER=7,	QTYPE=10,	\$END	A=10
\$NEWELL	ROW=23,	COL= 6,	Q=.00000413,	LAYER=7,	QTYPE=10,	\$END	A=10
\$NEWELL	ROW=24,	COL= 5,	Q=.00000232,	LAYER=7,	QTYPE=10,	\$END	A=10
\$NEWELL	ROW=24,	COL= 6,	Q=.00000413,	LAYER=7,	QTYPE=10,	\$END	A=10
\$NEWELL	ROW=25,	COL= 5,	Q=.00000310,	LAYER=7,	QTYPE=10,	\$END	A=10
\$NEWELL	ROW=25,	COL= 6,	Q=.00000413,	LAYER=7,	QTYPE=10,	\$END	A=10
\$NEWELL	ROW=26,	COL= 2,	Q=.00000232,	LAYER=7,	QTYPE=10,	\$END	A=10
\$NEWELL	ROW=26,	COL= 3,	Q=.00000310,	LAYER=7,	QTYPE=10,	\$END	A=10
\$NEWELL	ROW=26,	COL= 4,	Q=.00000258,	LAYER=7,	QTYPE=10,	\$END	A=10
\$NEWELL	ROW=26,	COL= 5,	Q=.00000413,	LAYER=7,	QTYPE=10,	\$END	A=10
\$NEWELL	ROW=27,	COL= 2,	Q=.00000103,	LAYER=7,	QTYPE=10,	\$END	A=10
\$NEWELL	ROW=27,	COL= 3,	Q=.00000258,	LAYER=7,	QTYPE=10,	\$END	A=10
\$NEWELL	ROW=27,	COL= 4,	Q=.00000413,	LAYER=7,	QTYPE=10,	\$END	A=10
\$NEWELL	ROW=22,	COL= 6,	Q=.00000202,	LAYER=6,	QTYPE=10,	\$END	A=10
\$NEWELL	ROW=23,	COL= 5,	Q=.00000101,	LAYER=6,	QTYPE=10,	\$END	A=10
\$NEWELL	ROW=23,	COL= 6,	Q=.00000202,	LAYER=6,	QTYPE=10,	\$END	A=10
\$NEWELL	ROW=24,	COL= 5,	Q=.00000114,	LAYER=6,	QTYPE=10,	\$END	A=10
\$NEWELL	ROW=24,	COL= 6,	Q=.00000202,	LAYER=6,	QTYPE=10,	\$END	A=10
\$NEWELL	ROW=25,	COL= 5,	Q=.00000152,	LAYER=6,	QTYPE=10,	\$END	A=10
\$NEWELL	ROW=25,	COL= 6,	Q=.00000202,	LAYER=6,	QTYPE=10,	\$END	A=10
\$NEWELL	ROW=26,	COL= 2,	Q=.00000114,	LAYER=6,	QTYPE=10,	\$END	A=10
\$NEWELL	ROW=26,	COL= 3,	Q=.00000152,	LAYER=6,	QTYPE=10,	\$END	A=10
\$NEWELL	ROW=26,	COL= 4,	Q=.00000126,	LAYER=6,	QTYPE=10,	\$END	A=10
\$NEWELL	ROW=26,	COL= 5,	Q=.00000202,	LAYER=6,	QTYPE=10,	\$END	A=10
\$NEWELL	ROW=27,	COL= 2,	Q=.00000051,	LAYER=6,	QTYPE=10,	\$END	A=10
\$NEWELL	ROW=27,	COL= 3,	Q=.00000126,	LAYER=6,	QTYPE=10,	\$END	A=10
\$NEWELL	ROW=27,	COL= 4,	Q=.00000202,	LAYER=6,	QTYPE=10,	\$END	A=10

Attachment 2.--Input file for the 1950-79 transient simulation--Continued

\$NEWELL	ROW=22,	COL= 6,	Q=.00000015,	LAYER=5,	QTYPE=10,	\$END	A=10
\$NEWELL	ROW=23,	COL= 5,	Q=.00000008,	LAYER=5,	QTYPE=10,	\$END	A=10
\$NEWELL	ROW=23,	COL= 6,	Q=.00000015,	LAYER=5,	QTYPE=10,	\$END	A=10
\$NEWELL	ROW=24,	COL= 5,	Q=.00000009,	LAYER=5,	QTYPE=10,	\$END	A=10
\$NEWELL	ROW=24,	COL= 6,	Q=.00000015,	LAYER=5,	QTYPE=10,	\$END	A=10
\$NEWELL	ROW=25,	COL= 5,	Q=.00000011,	LAYER=5,	QTYPE=10,	\$END	A=10
\$NEWELL	ROW=25,	COL= 6,	Q=.00000015,	LAYER=5,	QTYPE=10,	\$END	A=10
\$NEWELL	ROW=26,	COL= 2,	Q=.00000009,	LAYER=5,	QTYPE=10,	\$END	A=10
\$NEWELL	ROW=26,	COL= 3,	Q=.00000011,	LAYER=5,	QTYPE=10,	\$END	A=10
\$NEWELL	ROW=26,	COL= 4,	Q=.00000009,	LAYER=5,	QTYPE=10,	\$END	A=10
\$NEWELL	ROW=26,	COL= 5,	Q=.00000015,	LAYER=5,	QTYPE=10,	\$END	A=10
\$NEWELL	ROW=27,	COL= 2,	Q=.00000004,	LAYER=5,	QTYPE=10,	\$END	A=10
\$NEWELL	ROW=27,	COL= 3,	Q=.00000009,	LAYER=5,	QTYPE=10,	\$END	A=10
\$NEWELL	ROW=27,	COL= 4,	Q=.00000015,	LAYER=5,	QTYPE=10,	\$END	A=10
\$NEWELL	ROW=22,	COL= 6,	Q=.00000001,	LAYER=4,	QTYPE=10,	\$END	A=10
\$NEWELL	ROW=23,	COL= 5,	Q=.00000001,	LAYER=4,	QTYPE=10,	\$END	A=10
\$NEWELL	ROW=23,	COL= 6,	Q=.00000001,	LAYER=4,	QTYPE=10,	\$END	A=10
\$NEWELL	ROW=24,	COL= 5,	Q=.00000001,	LAYER=4,	QTYPE=10,	\$END	A=10
\$NEWELL	ROW=24,	COL= 6,	Q=.00000001,	LAYER=4,	QTYPE=10,	\$END	A=10
\$NEWELL	ROW=25,	COL= 5,	Q=.00000001,	LAYER=4,	QTYPE=10,	\$END	A=10
\$NEWELL	ROW=25,	COL= 6,	Q=.00000001,	LAYER=4,	QTYPE=10,	\$END	A=10
\$NEWELL	ROW=26,	COL= 2,	Q=.00000001,	LAYER=4,	QTYPE=10,	\$END	A=10
\$NEWELL	ROW=26,	COL= 3,	Q=.00000001,	LAYER=4,	QTYPE=10,	\$END	A=10
\$NEWELL	ROW=26,	COL= 4,	Q=.00000001,	LAYER=4,	QTYPE=10,	\$END	A=10
\$NEWELL	ROW=26,	COL= 5,	Q=.00000001,	LAYER=4,	QTYPE=10,	\$END	A=10
\$NEWELL	ROW=27,	COL= 2,	Q=.00000004,	LAYER=4,	QTYPE=10,	\$END	A=10
\$NEWELL	ROW=27,	COL= 3,	Q=.00000001,	LAYER=4,	QTYPE=10,	\$END	A=10
\$NEWELL	ROW=27,	COL= 4,	Q=.00000001,	LAYER=4,	QTYPE=10,	\$END	A=10
\$NEWELL	ROW=22,	COL= 7,	Q=.00000604,	LAYER=7,	QTYPE=61,	\$END	A=11
\$NEWELL	ROW=22,	COL= 8,	Q=.00000604,	LAYER=7,	QTYPE=11,	\$END	A=11
\$NEWELL	ROW=22,	COL= 9,	Q=.00000604,	LAYER=7,	QTYPE=11,	\$END	A=11
\$NEWELL	ROW=22,	COL=10,	Q=.00000604,	LAYER=7,	QTYPE=11,	\$END	A=11
\$NEWELL	ROW=23,	COL= 9,	Q=.00000604,	LAYER=7,	QTYPE=11,	\$END	A=11
\$NEWELL	ROW=23,	COL=10,	Q=.00000604,	LAYER=7,	QTYPE=11,	\$END	A=11
\$NEWELL	ROW=22,	COL= 7,	Q=.00000028,	LAYER=6,	QTYPE=61,	\$END	A=11
\$NEWELL	ROW=22,	COL= 8,	Q=.00000028,	LAYER=6,	QTYPE=11,	\$END	A=11
\$NEWELL	ROW=22,	COL= 9,	Q=.00000028,	LAYER=6,	QTYPE=11,	\$END	A=11
\$NEWELL	ROW=22,	COL=10,	Q=.00000028,	LAYER=6,	QTYPE=11,	\$END	A=11
\$NEWELL	ROW=23,	COL= 9,	Q=.00000028,	LAYER=6,	QTYPE=11,	\$END	A=11
\$NEWELL	ROW=23,	COL=10,	Q=.00000028,	LAYER=6,	QTYPE=11,	\$END	A=11
\$NEWELL	ROW=22,	COL=11,	Q=.00000538,	LAYER=7,	QTYPE=12,	\$END	A=12
\$NEWELL	ROW=23,	COL= 7,	Q=.00000538,	LAYER=7,	QTYPE=62,	\$END	A=12
\$NEWELL	ROW=23,	COL= 8,	Q=.00000538,	LAYER=7,	QTYPE=12,	\$END	A=12
\$NEWELL	ROW=23,	COL=11,	Q=.00000538,	LAYER=7,	QTYPE=12,	\$END	A=12
\$NEWELL	ROW=24,	COL= 7,	Q=.00000538,	LAYER=7,	QTYPE=62,	\$END	A=12
\$NEWELL	ROW=24,	COL= 8,	Q=.00000504,	LAYER=7,	QTYPE=12,	\$END	A=12
\$NEWELL	ROW=24,	COL= 9,	Q=.00000504,	LAYER=7,	QTYPE=12,	\$END	A=12
\$NEWELL	ROW=24,	COL=10,	Q=.00000538,	LAYER=7,	QTYPE=12,	\$END	A=12
\$NEWELL	ROW=24,	COL=11,	Q=.00000538,	LAYER=7,	QTYPE=12,	\$END	A=12
\$NEWELL	ROW=25,	COL= 7,	Q=.00000538,	LAYER=7,	QTYPE=62,	\$END	A=12
\$NEWELL	ROW=25,	COL= 8,	Q=.00000538,	LAYER=7,	QTYPE=62,	\$END	A=12

Attachment 2.--Input file for the 1950-79 transient simulation--Continued

\$NEWELL	ROW=25,	COL= 9,	Q=.00000538,	LAYER=7,	QTYPE=12,	\$END	A=12
\$NEWELL	ROW=25,	COL=10,	Q=.00000538,	LAYER=7,	QTYPE=12,	\$END	A=12
\$NEWELL	ROW=25,	COL=11,	Q=.00000538,	LAYER=7,	QTYPE=12,	\$END	A=12
\$NEWELL	ROW=26,	COL= 9,	Q=.00000538,	LAYER=7,	QTYPE=62,	\$END	A=12
\$NEWELL	ROW=26,	COL=10,	Q=.00000538,	LAYER=7,	QTYPE=12,	\$END	A=12
\$NEWELL	ROW=27,	COL= 9,	Q=.00000538,	LAYER=7,	QTYPE=62,	\$END	A=12
\$NEWELL	ROW=27,	COL=10,	Q=.00000538,	LAYER=7,	QTYPE=12,	\$END	A=12
\$NEWELL	ROW=28,	COL= 8,	Q=.00000538,	LAYER=7,	QTYPE=62,	\$END	A=12
\$NEWELL	ROW=28,	COL= 9,	Q=.00000538,	LAYER=7,	QTYPE=12,	\$END	A=12
\$NEWELL	ROW=28,	COL=10,	Q=.00000538,	LAYER=7,	QTYPE=12,	\$END	A=12
\$NEWELL	ROW=22,	COL=11,	Q=.00000089,	LAYER=6,	QTYPE=12,	\$END	A=12
\$NEWELL	ROW=23,	COL= 7,	Q=.00000089,	LAYER=6,	QTYPE=62,	\$END	A=12
\$NEWELL	ROW=23,	COL= 8,	Q=.00000089,	LAYER=6,	QTYPE=12,	\$END	A=12
\$NEWELL	ROW=23,	COL=11,	Q=.00000089,	LAYER=6,	QTYPE=12,	\$END	A=12
\$NEWELL	ROW=24,	COL= 7,	Q=.00000089,	LAYER=6,	QTYPE=62,	\$END	A=12
\$NEWELL	ROW=24,	COL= 8,	Q=.00000083,	LAYER=6,	QTYPE=12,	\$END	A=12
\$NEWELL	ROW=24,	COL= 9,	Q=.00000083,	LAYER=6,	QTYPE=12,	\$END	A=12
\$NEWELL	ROW=24,	COL=10,	Q=.00000089,	LAYER=6,	QTYPE=12,	\$END	A=12
\$NEWELL	ROW=24,	COL=11,	Q=.00000089,	LAYER=6,	QTYPE=12,	\$END	A=12
\$NEWELL	ROW=25,	COL= 7,	Q=.00000089,	LAYER=6,	QTYPE=62,	\$END	A=12
\$NEWELL	ROW=25,	COL= 8,	Q=.00000089,	LAYER=6,	QTYPE=62,	\$END	A=12
\$NEWELL	ROW=25,	COL= 9,	Q=.00000089,	LAYER=6,	QTYPE=12,	\$END	A=12
\$NEWELL	ROW=25,	COL=10,	Q=.00000089,	LAYER=6,	QTYPE=12,	\$END	A=12
\$NEWELL	ROW=25,	COL=11,	Q=.00000089,	LAYER=6,	QTYPE=12,	\$END	A=12
\$NEWELL	ROW=26,	COL= 9,	Q=.00000089,	LAYER=6,	QTYPE=62,	\$END	A=12
\$NEWELL	ROW=26,	COL=10,	Q=.00000089,	LAYER=6,	QTYPE=12,	\$END	A=12
\$NEWELL	ROW=27,	COL= 9,	Q=.00000089,	LAYER=6,	QTYPE=62,	\$END	A=12
\$NEWELL	ROW=27,	COL=10,	Q=.00000089,	LAYER=6,	QTYPE=12,	\$END	A=12
\$NEWELL	ROW=28,	COL= 8,	Q=.00000089,	LAYER=6,	QTYPE=62,	\$END	A=12
\$NEWELL	ROW=28,	COL= 9,	Q=.00000089,	LAYER=6,	QTYPE=12,	\$END	A=12
\$NEWELL	ROW=28,	COL=10,	Q=.00000089,	LAYER=6,	QTYPE=12,	\$END	A=12
\$NEWELL	ROW=22,	COL=11,	Q=.00000002,	LAYER=5,	QTYPE=12,	\$END	A=12
\$NEWELL	ROW=23,	COL= 7,	Q=.00000002,	LAYER=5,	QTYPE=62,	\$END	A=12
\$NEWELL	ROW=23,	COL= 8,	Q=.00000002,	LAYER=5,	QTYPE=12,	\$END	A=12
\$NEWELL	ROW=23,	COL=11,	Q=.00000002,	LAYER=5,	QTYPE=12,	\$END	A=12
\$NEWELL	ROW=24,	COL= 7,	Q=.00000002,	LAYER=5,	QTYPE=62,	\$END	A=12
\$NEWELL	ROW=24,	COL= 8,	Q=.00000002,	LAYER=5,	QTYPE=12,	\$END	A=12
\$NEWELL	ROW=24,	COL= 9,	Q=.00000002,	LAYER=5,	QTYPE=12,	\$END	A=12
\$NEWELL	ROW=24,	COL=10,	Q=.00000002,	LAYER=5,	QTYPE=12,	\$END	A=12
\$NEWELL	ROW=24,	COL=11,	Q=.00000002,	LAYER=5,	QTYPE=12,	\$END	A=12
\$NEWELL	ROW=25,	COL= 7,	Q=.00000002,	LAYER=5,	QTYPE=62,	\$END	A=12
\$NEWELL	ROW=25,	COL= 8,	Q=.00000002,	LAYER=5,	QTYPE=62,	\$END	A=12
\$NEWELL	ROW=25,	COL= 9,	Q=.00000002,	LAYER=5,	QTYPE=12,	\$END	A=12
\$NEWELL	ROW=25,	COL=10,	Q=.00000002,	LAYER=5,	QTYPE=12,	\$END	A=12
\$NEWELL	ROW=25,	COL=11,	Q=.00000002,	LAYER=5,	QTYPE=12,	\$END	A=12
\$NEWELL	ROW=26,	COL= 9,	Q=.00000002,	LAYER=5,	QTYPE=62,	\$END	A=12
\$NEWELL	ROW=26,	COL=10,	Q=.00000002,	LAYER=5,	QTYPE=12,	\$END	A=12
\$NEWELL	ROW=27,	COL= 9,	Q=.00000002,	LAYER=5,	QTYPE=62,	\$END	A=12
\$NEWELL	ROW=27,	COL=10,	Q=.00000002,	LAYER=5,	QTYPE=12,	\$END	A=12
\$NEWELL	ROW=28,	COL= 8,	Q=.00000002,	LAYER=5,	QTYPE=62,	\$END	A=12
\$NEWELL	ROW=28,	COL= 9,	Q=.00000002,	LAYER=5,	QTYPE=12,	\$END	A=12

## Attachment 2.--Input file for the 1950-79 transient simulation--Continued

\$NEWELL	ROW=28,	COL=10,	Q=.00000002,	LAYER=5,	QTYPE=12,	\$END	A=12
\$NEWELL	ROW=22,	COL=11,	Q=.00000003,	LAYER=4,	QTYPE=12,	\$END	A=12
\$NEWELL	ROW=23,	COL= 7,	Q=.00000003,	LAYER=4,	QTYPE=62,	\$END	A=12
\$NEWELL	ROW=23,	COL= 8,	Q=.00000003,	LAYER=4,	QTYPE=12,	\$END	A=12
\$NEWELL	ROW=23,	COL=11,	Q=.00000003,	LAYER=4,	QTYPE=12,	\$END	A=12
\$NEWELL	ROW=24,	COL= 7,	Q=.00000003,	LAYER=4,	QTYPE=62,	\$END	A=12
\$NEWELL	ROW=24,	COL= 8,	Q=.00000002,	LAYER=4,	QTYPE=12,	\$END	A=12
\$NEWELL	ROW=24,	COL= 9,	Q=.00000002,	LAYER=4,	QTYPE=12,	\$END	A=12
\$NEWELL	ROW=24,	COL=10,	Q=.00000003,	LAYER=4,	QTYPE=12,	\$END	A=12
\$NEWELL	ROW=24,	COL=11,	Q=.00000003,	LAYER=4,	QTYPE=12,	\$END	A=12
\$NEWELL	ROW=25,	COL= 7,	Q=.00000003,	LAYER=4,	QTYPE=62,	\$END	A=12
\$NEWELL	ROW=25,	COL= 8,	Q=.00000003,	LAYER=4,	QTYPE=62,	\$END	A=12
\$NEWELL	ROW=25,	COL= 9,	Q=.00000003,	LAYER=4,	QTYPE=12,	\$END	A=12
\$NEWELL	ROW=25,	COL=10,	Q=.00000003,	LAYER=4,	QTYPE=12,	\$END	A=12
\$NEWELL	ROW=25,	COL=11,	Q=.00000003,	LAYER=4,	QTYPE=12,	\$END	A=12
\$NEWELL	ROW=26,	COL= 9,	Q=.00000003,	LAYER=4,	QTYPE=62,	\$END	A=12
\$NEWELL	ROW=26,	COL=10,	Q=.00000003,	LAYER=4,	QTYPE=12,	\$END	A=12
\$NEWELL	ROW=27,	COL= 9,	Q=.00000003,	LAYER=4,	QTYPE=62,	\$END	A=12
\$NEWELL	ROW=27,	COL=10,	Q=.00000003,	LAYER=4,	QTYPE=12,	\$END	A=12
\$NEWELL	ROW=28,	COL= 8,	Q=.00000003,	LAYER=4,	QTYPE=62,	\$END	A=12
\$NEWELL	ROW=28,	COL= 9,	Q=.00000003,	LAYER=4,	QTYPE=12,	\$END	A=12
\$NEWELL	ROW=28,	COL=10,	Q=.00000003,	LAYER=4,	QTYPE=12,	\$END	A=12
\$NEWELL	ROW=22,	COL=11,	Q=.00000001,	LAYER=3,	QTYPE=12,	\$END	A=12
\$NEWELL	ROW=23,	COL= 7,	Q=.00000001,	LAYER=3,	QTYPE=62,	\$END	A=12
\$NEWELL	ROW=23,	COL= 8,	Q=.00000001,	LAYER=3,	QTYPE=12,	\$END	A=12
\$NEWELL	ROW=23,	COL=11,	Q=.00000001,	LAYER=3,	QTYPE=12,	\$END	A=12
\$NEWELL	ROW=24,	COL= 7,	Q=.00000001,	LAYER=3,	QTYPE=62,	\$END	A=12
\$NEWELL	ROW=24,	COL= 8,	Q=.00000001,	LAYER=3,	QTYPE=12,	\$END	A=12
\$NEWELL	ROW=24,	COL= 9,	Q=.00000001,	LAYER=3,	QTYPE=12,	\$END	A=12
\$NEWELL	ROW=24,	COL=10,	Q=.00000001,	LAYER=3,	QTYPE=12,	\$END	A=12
\$NEWELL	ROW=24,	COL=11,	Q=.00000001,	LAYER=3,	QTYPE=12,	\$END	A=12
\$NEWELL	ROW=25,	COL= 7,	Q=.00000001,	LAYER=3,	QTYPE=62,	\$END	A=12
\$NEWELL	ROW=25,	COL= 8,	Q=.00000001,	LAYER=3,	QTYPE=62,	\$END	A=12
\$NEWELL	ROW=25,	COL= 9,	Q=.00000001,	LAYER=3,	QTYPE=12,	\$END	A=12
\$NEWELL	ROW=25,	COL=10,	Q=.00000001,	LAYER=3,	QTYPE=12,	\$END	A=12
\$NEWELL	ROW=25,	COL=11,	Q=.00000001,	LAYER=3,	QTYPE=12,	\$END	A=12
\$NEWELL	ROW=26,	COL= 9,	Q=.00000001,	LAYER=3,	QTYPE=62,	\$END	A=12
\$NEWELL	ROW=26,	COL=10,	Q=.00000001,	LAYER=3,	QTYPE=12,	\$END	A=12
\$NEWELL	ROW=27,	COL= 9,	Q=.00000001,	LAYER=3,	QTYPE=62,	\$END	A=12
\$NEWELL	ROW=27,	COL=10,	Q=.00000001,	LAYER=3,	QTYPE=12,	\$END	A=12
\$NEWELL	ROW=28,	COL= 8,	Q=.00000001,	LAYER=3,	QTYPE=62,	\$END	A=12
\$NEWELL	ROW=28,	COL= 9,	Q=.00000001,	LAYER=3,	QTYPE=12,	\$END	A=12
\$NEWELL	ROW=28,	COL=10,	Q=.00000001,	LAYER=3,	QTYPE=12,	\$END	A=12
\$NEWELL	ROW=23,	COL=12,	Q=.00000357,	LAYER=7,	QTYPE=13,	\$END	A=13
\$NEWELL	ROW=23,	COL=13,	Q=.00000476,	LAYER=7,	QTYPE=13,	\$END	A=13
\$NEWELL	ROW=24,	COL=12,	Q=.00000476,	LAYER=7,	QTYPE=13,	\$END	A=13
\$NEWELL	ROW=24,	COL=13,	Q=.00000476,	LAYER=7,	QTYPE=13,	\$END	A=13
\$NEWELL	ROW=25,	COL=12,	Q=.00000297,	LAYER=7,	QTYPE=13,	\$END	A=13
\$NEWELL	ROW=25,	COL=13,	Q=.00000357,	LAYER=7,	QTYPE=13,	\$END	A=13
\$NEWELL	ROW=23,	COL=12,	Q=.00000069,	LAYER=6,	QTYPE=13,	\$END	A=13
\$NEWELL	ROW=23,	COL=13,	Q=.00000092,	LAYER=6,	QTYPE=13,	\$END	A=13

## Attachment 2.--Input file for the 1950-79 transient simulation--Continued

```

$NEWELL ROW=24, COL=12, Q=.00000092, LAYER=6, QTYPE=13, $END A=13
$NEWELL ROW=24, COL=13, Q=.00000092, LAYER=6, QTYPE=13, $END A=13
$NEWELL ROW=25, COL=12, Q=.00000058, LAYER=6, QTYPE=13, $END A=13
$NEWELL ROW=25, COL=13, Q=.00000069, LAYER=6, QTYPE=13, $END A=13
$NEWELL ROW=23, COL=12, Q=.00000024, LAYER=4, QTYPE=13, $END A=13
$NEWELL ROW=23, COL=13, Q=.00000032, LAYER=4, QTYPE=13, $END A=13
$NEWELL ROW=24, COL=12, Q=.00000032, LAYER=4, QTYPE=13, $END A=13
$NEWELL ROW=24, COL=13, Q=.00000032, LAYER=4, QTYPE=13, $END A=13
$NEWELL ROW=25, COL=12, Q=.00000020, LAYER=4, QTYPE=13, $END A=13
$NEWELL ROW=25, COL=13, Q=.00000024, LAYER=4, QTYPE=13, $END A=13
$NEWELL ROW=23, COL=12, Q=.00000024, LAYER=3, QTYPE=13, $END A=13
$NEWELL ROW=23, COL=13, Q=.00000032, LAYER=3, QTYPE=13, $END A=13
$NEWELL ROW=24, COL=12, Q=.00000032, LAYER=3, QTYPE=13, $END A=13
$NEWELL ROW=24, COL=13, Q=.00000032, LAYER=3, QTYPE=13, $END A=13
$NEWELL ROW=25, COL=12, Q=.00000020, LAYER=3, QTYPE=13, $END A=13
$NEWELL ROW=25, COL=13, Q=.00000024, LAYER=3, QTYPE=13, $END A=13
$NEWELL ROW=26, COL= 6, Q=.00000380, LAYER=7, QTYPE=14, $END A=14
$NEWELL ROW=27, COL= 5, Q=.00000380, LAYER=7, QTYPE=14, $END A=14
$NEWELL ROW=27, COL= 6, Q=.00000380, LAYER=7, QTYPE=14, $END A=14
$NEWELL ROW=28, COL= 6, Q=.00000380, LAYER=7, QTYPE=14, $END A=14
$NEWELL ROW=26, COL= 6, Q=.00000237, LAYER=6, QTYPE=14, $END A=14
$NEWELL ROW=27, COL= 5, Q=.00000237, LAYER=6, QTYPE=14, $END A=14
$NEWELL ROW=27, COL= 6, Q=.00000237, LAYER=6, QTYPE=14, $END A=14
$NEWELL ROW=28, COL= 6, Q=.00000237, LAYER=6, QTYPE=14, $END A=14
$NEWELL ROW=26, COL= 6, Q=.00000008, LAYER=5, QTYPE=14, $END A=14
$NEWELL ROW=27, COL= 5, Q=.00000008, LAYER=5, QTYPE=14, $END A=14
$NEWELL ROW=27, COL= 6, Q=.00000008, LAYER=5, QTYPE=14, $END A=14
$NEWELL ROW=28, COL= 6, Q=.00000008, LAYER=5, QTYPE=14, $END A=14
$NEWELL ROW=26, COL= 6, Q=.00000005, LAYER=4, QTYPE=14, $END A=14
$NEWELL ROW=27, COL= 5, Q=.00000005, LAYER=4, QTYPE=14, $END A=14
$NEWELL ROW=27, COL= 6, Q=.00000005, LAYER=4, QTYPE=14, $END A=14
$NEWELL ROW=28, COL= 6, Q=.00000005, LAYER=4, QTYPE=14, $END A=14
$NEWELL ROW=26, COL= 6, Q=.00000002, LAYER=3, QTYPE=14, $END A=14
$NEWELL ROW=27, COL= 5, Q=.00000002, LAYER=3, QTYPE=14, $END A=14
$NEWELL ROW=27, COL= 6, Q=.00000002, LAYER=3, QTYPE=14, $END A=14
$NEWELL ROW=28, COL= 6, Q=.00000002, LAYER=3, QTYPE=14, $END A=14
$NEWELL ROW=26, COL= 7, Q=.00000503, LAYER=7, QTYPE=15, $END A=15
$NEWELL ROW=26, COL= 8, Q=.00000503, LAYER=7, QTYPE=15, $END A=15
$NEWELL ROW=27, COL= 7, Q=.00000503, LAYER=7, QTYPE=15, $END A=15
$NEWELL ROW=27, COL= 8, Q=.00000503, LAYER=7, QTYPE=15, $END A=15
$NEWELL ROW=28, COL= 7, Q=.00000503, LAYER=7, QTYPE=15, $END A=15
$NEWELL ROW=26, COL= 7, Q=.00000123, LAYER=6, QTYPE=15, $END A=15
$NEWELL ROW=26, COL= 8, Q=.00000123, LAYER=6, QTYPE=15, $END A=15
$NEWELL ROW=27, COL= 7, Q=.00000123, LAYER=6, QTYPE=15, $END A=15
$NEWELL ROW=27, COL= 8, Q=.00000123, LAYER=6, QTYPE=15, $END A=15
$NEWELL ROW=28, COL= 7, Q=.00000123, LAYER=6, QTYPE=15, $END A=15
$NEWELL ROW=26, COL= 7, Q=.00000008, LAYER=5, QTYPE=15, $END A=15
$NEWELL ROW=26, COL= 8, Q=.00000008, LAYER=5, QTYPE=15, $END A=15
$NEWELL ROW=27, COL= 7, Q=.00000008, LAYER=5, QTYPE=15, $END A=15

```

Attachment 2.--Input file for the 1950-79 transient simulation--Continued

\$NEWELL	ROW=27,	COL= 8,	Q=.00000008,	LAYER=5,	QTYPE=15,	\$END	A=15
\$NEWELL	ROW=28,	COL= 7,	Q=.00000008,	LAYER=5,	QTYPE=15,	\$END	A=15
\$NEWELL	ROW=27,	COL=15,	Q=.00000431,	LAYER=7,	QTYPE=16,	\$END	A=16
\$NEWELL	ROW=27,	COL=16,	Q=.00000431,	LAYER=7,	QTYPE=16,	\$END	A=16
\$NEWELL	ROW=28,	COL=15,	Q=.00000431,	LAYER=7,	QTYPE=16,	\$END	A=16
\$NEWELL	ROW=28,	COL=16,	Q=.00000431,	LAYER=7,	QTYPE=16,	\$END	A=16
\$NEWELL	ROW=28,	COL=17,	Q=.00000108,	LAYER=7,	QTYPE=16,	\$END	A=16
\$NEWELL	ROW=29,	COL=17,	Q=.00000054,	LAYER=7,	QTYPE=16,	\$END	A=16
\$NEWELL	ROW=27,	COL=15,	Q=.00000121,	LAYER=6,	QTYPE=16,	\$END	A=16
\$NEWELL	ROW=27,	COL=16,	Q=.00000121,	LAYER=6,	QTYPE=16,	\$END	A=16
\$NEWELL	ROW=28,	COL=15,	Q=.00000121,	LAYER=6,	QTYPE=16,	\$END	A=16
\$NEWELL	ROW=28,	COL=16,	Q=.00000121,	LAYER=6,	QTYPE=16,	\$END	A=16
\$NEWELL	ROW=28,	COL=17,	Q=.00000030,	LAYER=6,	QTYPE=16,	\$END	A=16
\$NEWELL	ROW=29,	COL=17,	Q=.00000015,	LAYER=6,	QTYPE=16,	\$END	A=16
\$NEWELL	ROW=27,	COL=15,	Q=.00000040,	LAYER=4,	QTYPE=16,	\$END	A=16
\$NEWELL	ROW=27,	COL=16,	Q=.00000040,	LAYER=4,	QTYPE=16,	\$END	A=16
\$NEWELL	ROW=28,	COL=15,	Q=.00000040,	LAYER=4,	QTYPE=16,	\$END	A=16
\$NEWELL	ROW=28,	COL=16,	Q=.00000040,	LAYER=4,	QTYPE=16,	\$END	A=16
\$NEWELL	ROW=28,	COL=17,	Q=.00000010,	LAYER=4,	QTYPE=16,	\$END	A=16
\$NEWELL	ROW=29,	COL=17,	Q=.00000005,	LAYER=4,	QTYPE=16,	\$END	A=16
\$NEWELL	ROW=27,	COL=15,	Q=.00000040,	LAYER=3,	QTYPE=16,	\$END	A=16
\$NEWELL	ROW=27,	COL=16,	Q=.00000040,	LAYER=3,	QTYPE=16,	\$END	A=16
\$NEWELL	ROW=28,	COL=15,	Q=.00000040,	LAYER=3,	QTYPE=16,	\$END	A=16
\$NEWELL	ROW=28,	COL=16,	Q=.00000040,	LAYER=3,	QTYPE=16,	\$END	A=16
\$NEWELL	ROW=28,	COL=17,	Q=.00000010,	LAYER=3,	QTYPE=16,	\$END	A=16
\$NEWELL	ROW=29,	COL=17,	Q=.00000005,	LAYER=3,	QTYPE=16,	\$END	A=16
\$NEWELL	ROW=26,	COL=11,	Q=.00000566,	LAYER=7,	QTYPE=17,	\$END	A=17
\$NEWELL	ROW=27,	COL=11,	Q=.00000604,	LAYER=7,	QTYPE=17,	\$END	A=17
\$NEWELL	ROW=28,	COL=11,	Q=.00000604,	LAYER=7,	QTYPE=17,	\$END	A=17
\$NEWELL	ROW=29,	COL= 7,	Q=.00000453,	LAYER=7,	QTYPE=17,	\$END	A=17
\$NEWELL	ROW=29,	COL= 8,	Q=.00000528,	LAYER=7,	QTYPE=17,	\$END	A=17
\$NEWELL	ROW=29,	COL= 9,	Q=.00000604,	LAYER=7,	QTYPE=17,	\$END	A=17
\$NEWELL	ROW=29,	COL=10,	Q=.00000604,	LAYER=7,	QTYPE=17,	\$END	A=17
\$NEWELL	ROW=29,	COL=11,	Q=.00000604,	LAYER=7,	QTYPE=17,	\$END	A=17
\$NEWELL	ROW=30,	COL=10,	Q=.00000151,	LAYER=7,	QTYPE=17,	\$END	A=17
\$NEWELL	ROW=30,	COL=11,	Q=.00000566,	LAYER=7,	QTYPE=17,	\$END	A=17
\$NEWELL	ROW=26,	COL=11,	Q=.00000020,	LAYER=6,	QTYPE=17,	\$END	A=17
\$NEWELL	ROW=27,	COL=11,	Q=.00000021,	LAYER=6,	QTYPE=17,	\$END	A=17
\$NEWELL	ROW=28,	COL=11,	Q=.00000021,	LAYER=6,	QTYPE=17,	\$END	A=17
\$NEWELL	ROW=29,	COL= 7,	Q=.00000016,	LAYER=6,	QTYPE=17,	\$END	A=17
\$NEWELL	ROW=29,	COL= 8,	Q=.00000018,	LAYER=6,	QTYPE=17,	\$END	A=17
\$NEWELL	ROW=29,	COL= 9,	Q=.00000021,	LAYER=6,	QTYPE=17,	\$END	A=17
\$NEWELL	ROW=29,	COL=10,	Q=.00000021,	LAYER=6,	QTYPE=17,	\$END	A=17
\$NEWELL	ROW=29,	COL=11,	Q=.00000021,	LAYER=6,	QTYPE=17,	\$END	A=17
\$NEWELL	ROW=30,	COL=10,	Q=.00000005,	LAYER=6,	QTYPE=17,	\$END	A=17
\$NEWELL	ROW=30,	COL=11,	Q=.00000021,	LAYER=6,	QTYPE=17,	\$END	A=17
\$NEWELL	ROW=26,	COL=11,	Q=.00000001,	LAYER=5,	QTYPE=17,	\$END	A=17
\$NEWELL	ROW=27,	COL=11,	Q=.00000001,	LAYER=5,	QTYPE=17,	\$END	A=17
\$NEWELL	ROW=28,	COL=11,	Q=.00000001,	LAYER=5,	QTYPE=17,	\$END	A=17
\$NEWELL	ROW=29,	COL= 7,	Q=.00000001,	LAYER=5,	QTYPE=17,	\$END	A=17
\$NEWELL	ROW=29,	COL= 8,	Q=.00000001,	LAYER=5,	QTYPE=17,	\$END	A=17



## Attachment 2.--Input file for the 1950-79 transient simulation--Continued

\$NEWELL	ROW=29,	COL= 9,	Q=.00000001,	LAYER=5,	QTYPE=17,	\$END	A=17
\$NEWELL	ROW=29,	COL=10,	Q=.00000001,	LAYER=5,	QTYPE=17,	\$END	A=17
\$NEWELL	ROW=29,	COL=11,	Q=.00000001,	LAYER=5,	QTYPE=17,	\$END	A=17
\$NEWELL	ROW=30,	COL=11,	Q=.00000001,	LAYER=5,	QTYPE=17,	\$END	A=17
\$NEWELL	ROW=26,	COL=11,	Q=.00000003,	LAYER=4,	QTYPE=17,	\$END	A=17
\$NEWELL	ROW=27,	COL=11,	Q=.00000003,	LAYER=4,	QTYPE=17,	\$END	A=17
\$NEWELL	ROW=28,	COL=11,	Q=.00000003,	LAYER=4,	QTYPE=17,	\$END	A=17
\$NEWELL	ROW=29,	COL= 7,	Q=.00000002,	LAYER=4,	QTYPE=17,	\$END	A=17
\$NEWELL	ROW=29,	COL= 8,	Q=.00000003,	LAYER=4,	QTYPE=17,	\$END	A=17
\$NEWELL	ROW=29,	COL= 9,	Q=.00000003,	LAYER=4,	QTYPE=17,	\$END	A=17
\$NEWELL	ROW=29,	COL=10,	Q=.00000003,	LAYER=4,	QTYPE=17,	\$END	A=17
\$NEWELL	ROW=29,	COL=11,	Q=.00000003,	LAYER=4,	QTYPE=17,	\$END	A=17
\$NEWELL	ROW=30,	COL=10,	Q=.00000001,	LAYER=4,	QTYPE=17,	\$END	A=17
\$NEWELL	ROW=30,	COL=11,	Q=.00000003,	LAYER=4,	QTYPE=17,	\$END	A=17
\$NEWELL	ROW=26,	COL=11,	Q=.00000003,	LAYER=3,	QTYPE=17,	\$END	A=17
\$NEWELL	ROW=27,	COL=11,	Q=.00000003,	LAYER=3,	QTYPE=17,	\$END	A=17
\$NEWELL	ROW=28,	COL=11,	Q=.00000003,	LAYER=3,	QTYPE=17,	\$END	A=17
\$NEWELL	ROW=29,	COL= 7,	Q=.00000002,	LAYER=3,	QTYPE=17,	\$END	A=17
\$NEWELL	ROW=29,	COL= 8,	Q=.00000003,	LAYER=3,	QTYPE=17,	\$END	A=17
\$NEWELL	ROW=29,	COL= 9,	Q=.00000003,	LAYER=3,	QTYPE=17,	\$END	A=17
\$NEWELL	ROW=29,	COL=10,	Q=.00000003,	LAYER=3,	QTYPE=17,	\$END	A=17
\$NEWELL	ROW=29,	COL=11,	Q=.00000003,	LAYER=3,	QTYPE=17,	\$END	A=17
\$NEWELL	ROW=30,	COL=10,	Q=.00000001,	LAYER=3,	QTYPE=17,	\$END	A=17
\$NEWELL	ROW=30,	COL=11,	Q=.00000003,	LAYER=3,	QTYPE=17,	\$END	A=17
\$NEWELL	ROW=29,	COL= 6,	Q=.00000351,	LAYER=7,	QTYPE=18,	\$END	A=18
\$NEWELL	ROW=30,	COL= 6,	Q=.00000281,	LAYER=7,	QTYPE=18,	\$END	A=18
\$NEWELL	ROW=30,	COL= 7,	Q=.00000562,	LAYER=7,	QTYPE=18,	\$END	A=18
\$NEWELL	ROW=30,	COL= 8,	Q=.00000455,	LAYER=7,	QTYPE=18,	\$END	A=18
\$NEWELL	ROW=30,	COL= 9,	Q=.00000351,	LAYER=7,	QTYPE=18,	\$END	A=18
\$NEWELL	ROW=31,	COL= 6,	Q=.00000105,	LAYER=7,	QTYPE=18,	\$END	A=18
\$NEWELL	ROW=31,	COL= 7,	Q=.00000527,	LAYER=7,	QTYPE=18,	\$END	A=18
\$NEWELL	ROW=31,	COL= 8,	Q=.00000562,	LAYER=7,	QTYPE=18,	\$END	A=18
\$NEWELL	ROW=29,	COL= 6,	Q=.00000039,	LAYER=6,	QTYPE=18,	\$END	A=18
\$NEWELL	ROW=30,	COL= 6,	Q=.00000032,	LAYER=6,	QTYPE=18,	\$END	A=18
\$NEWELL	ROW=30,	COL= 7,	Q=.00000063,	LAYER=6,	QTYPE=18,	\$END	A=18
\$NEWELL	ROW=30,	COL= 8,	Q=.00000051,	LAYER=6,	QTYPE=18,	\$END	A=18
\$NEWELL	ROW=30,	COL= 9,	Q=.00000039,	LAYER=6,	QTYPE=18,	\$END	A=18
\$NEWELL	ROW=31,	COL= 6,	Q=.00000012,	LAYER=6,	QTYPE=18,	\$END	A=18
\$NEWELL	ROW=31,	COL= 7,	Q=.00000059,	LAYER=6,	QTYPE=18,	\$END	A=18
\$NEWELL	ROW=31,	COL= 6,	Q=.00000001,	LAYER=5,	QTYPE=18,	\$END	A=18
\$NEWELL	ROW=31,	COL= 7,	Q=.00000007,	LAYER=5,	QTYPE=18,	\$END	A=18
\$NEWELL	ROW=31,	COL= 8,	Q=.00000007,	LAYER=5,	QTYPE=18,	\$END	A=18
\$NEWELL	ROW=31,	COL= 9,	Q=.00000519,	LAYER=7,	QTYPE=19,	\$END	A=19
\$NEWELL	ROW=31,	COL=10,	Q=.00000292,	LAYER=7,	QTYPE=19,	\$END	A=19
\$NEWELL	ROW=31,	COL=11,	Q=.00000292,	LAYER=7,	QTYPE=19,	\$END	A=19
\$NEWELL	ROW=32,	COL= 9,	Q=.00000519,	LAYER=7,	QTYPE=19,	\$END	A=19
\$NEWELL	ROW=32,	COL=10,	Q=.00000519,	LAYER=7,	QTYPE=19,	\$END	A=19
\$NEWELL	ROW=32,	COL=11,	Q=.00000389,	LAYER=7,	QTYPE=19,	\$END	A=19
\$NEWELL	ROW=33,	COL=11,	Q=.00000032,	LAYER=7,	QTYPE=19,	\$END	A=19

Attachment 2.--Input file for the 1950-79 transient simulation--Continued

\$NEWELL	ROW=33,	COL=12,	Q=.00000162,	LAYER=7,	QTYPE=19,	\$END	A=19
\$NEWELL	ROW=31,	COL= 9,	Q=.00000009,	LAYER=6,	QTYPE=19,	\$END	A=19
\$NEWELL	ROW=31,	COL=10,	Q=.00000005,	LAYER=6,	QTYPE=19,	\$END	A=19
\$NEWELL	ROW=31,	COL=11,	Q=.00000005,	LAYER=6,	QTYPE=19,	\$END	A=19
\$NEWELL	ROW=32,	COL= 9,	Q=.00000009,	LAYER=6,	QTYPE=19,	\$END	A=19
\$NEWELL	ROW=32,	COL=10,	Q=.00000009,	LAYER=6,	QTYPE=19,	\$END	A=19
\$NEWELL	ROW=32,	COL=11,	Q=.00000007,	LAYER=6,	QTYPE=19,	\$END	A=19
\$NEWELL	ROW=33,	COL=11,	Q=.00000001,	LAYER=6,	QTYPE=19,	\$END	A=19
\$NEWELL	ROW=33,	COL=12,	Q=.00000003,	LAYER=6,	QTYPE=19,	\$END	A=19
\$NEWELL	ROW=31,	COL= 9,	Q=.00000015,	LAYER=5,	QTYPE=19,	\$END	A=19
\$NEWELL	ROW=31,	COL=10,	Q=.00000008,	LAYER=5,	QTYPE=19,	\$END	A=19
\$NEWELL	ROW=31,	COL=11,	Q=.00000008,	LAYER=5,	QTYPE=19,	\$END	A=19
\$NEWELL	ROW=32,	COL= 9,	Q=.00000015,	LAYER=5,	QTYPE=19,	\$END	A=19
\$NEWELL	ROW=32,	COL=10,	Q=.00000015,	LAYER=5,	QTYPE=19,	\$END	A=19
\$NEWELL	ROW=32,	COL=11,	Q=.00000011,	LAYER=5,	QTYPE=19,	\$END	A=19
\$NEWELL	ROW=33,	COL=11,	Q=.00000001,	LAYER=5,	QTYPE=19,	\$END	A=19
\$NEWELL	ROW=33,	COL=12,	Q=.00000005,	LAYER=5,	QTYPE=19,	\$END	A=19
\$NEWELL	ROW=31,	COL= 9,	Q=.00000051,	LAYER=4,	QTYPE=19,	\$END	A=19
\$NEWELL	ROW=31,	COL=10,	Q=.00000029,	LAYER=4,	QTYPE=19,	\$END	A=19
\$NEWELL	ROW=31,	COL=11,	Q=.00000029,	LAYER=4,	QTYPE=19,	\$END	A=19
\$NEWELL	ROW=32,	COL= 9,	Q=.00000051,	LAYER=4,	QTYPE=19,	\$END	A=19
\$NEWELL	ROW=32,	COL=10,	Q=.00000051,	LAYER=4,	QTYPE=19,	\$END	A=19
\$NEWELL	ROW=32,	COL=11,	Q=.00000038,	LAYER=4,	QTYPE=19,	\$END	A=19
\$NEWELL	ROW=33,	COL=11,	Q=.00000003,	LAYER=4,	QTYPE=19,	\$END	A=19
\$NEWELL	ROW=33,	COL=12,	Q=.00000016,	LAYER=4,	QTYPE=19,	\$END	A=19
\$NEWELL	ROW=31,	COL= 9,	Q=.00000040,	LAYER=3,	QTYPE=19,	\$END	A=19
\$NEWELL	ROW=31,	COL=10,	Q=.00000022,	LAYER=3,	QTYPE=19,	\$END	A=19
\$NEWELL	ROW=31,	COL=11,	Q=.00000022,	LAYER=3,	QTYPE=19,	\$END	A=19
\$NEWELL	ROW=32,	COL= 9,	Q=.00000040,	LAYER=3,	QTYPE=19,	\$END	A=19
\$NEWELL	ROW=32,	COL=10,	Q=.00000040,	LAYER=3,	QTYPE=19,	\$END	A=19
\$NEWELL	ROW=32,	COL=11,	Q=.00000030,	LAYER=3,	QTYPE=19,	\$END	A=19
\$NEWELL	ROW=33,	COL=11,	Q=.00000002,	LAYER=3,	QTYPE=19,	\$END	A=19
\$NEWELL	ROW=33,	COL=12,	Q=.00000012,	LAYER=3,	QTYPE=19,	\$END	A=19
\$NEWELL	ROW=32,	COL= 7,	Q=.00000135,	LAYER=7,	QTYPE=20,	\$END	A=20
\$NEWELL	ROW=32,	COL= 8,	Q=.00000144,	LAYER=7,	QTYPE=20,	\$END	A=20
\$NEWELL	ROW=33,	COL= 7,	Q=.00000072,	LAYER=7,	QTYPE=20,	\$END	A=20
\$NEWELL	ROW=33,	COL= 8,	Q=.00000090,	LAYER=7,	QTYPE=20,	\$END	A=20
\$NEWELL	ROW=33,	COL= 9,	Q=.00000072,	LAYER=7,	QTYPE=20,	\$END	A=20
\$NEWELL	ROW=33,	COL=10,	Q=.00000054,	LAYER=7,	QTYPE=20,	\$END	A=20
\$NEWELL	ROW=32,	COL= 7,	Q=.00000027,	LAYER=6,	QTYPE=20,	\$END	A=20
\$NEWELL	ROW=32,	COL= 8,	Q=.00000029,	LAYER=6,	QTYPE=20,	\$END	A=20
\$NEWELL	ROW=33,	COL= 7,	Q=.00000015,	LAYER=6,	QTYPE=20,	\$END	A=20
\$NEWELL	ROW=33,	COL= 8,	Q=.00000018,	LAYER=6,	QTYPE=20,	\$END	A=20
\$NEWELL	ROW=33,	COL= 9,	Q=.00000015,	LAYER=6,	QTYPE=20,	\$END	A=20
\$NEWELL	ROW=33,	COL=10,	Q=.00000011,	LAYER=6,	QTYPE=20,	\$END	A=20
\$NEWELL	ROW=32,	COL= 7,	Q=.00000108,	LAYER=5,	QTYPE=20,	\$END	A=20
\$NEWELL	ROW=32,	COL= 8,	Q=.00000115,	LAYER=5,	QTYPE=20,	\$END	A=20
\$NEWELL	ROW=33,	COL= 7,	Q=.00000057,	LAYER=5,	QTYPE=20,	\$END	A=20
\$NEWELL	ROW=33,	COL= 8,	Q=.00000072,	LAYER=5,	QTYPE=20,	\$END	A=20
\$NEWELL	ROW=33,	COL= 9,	Q=.00000057,	LAYER=5,	QTYPE=20,	\$END	A=20
\$NEWELL	ROW=33,	COL=10,	Q=.00000043,	LAYER=5,	QTYPE=20,	\$END	A=20

Attachment 2.--Input file for the 1950-79 transient simulation--Continued

\$NEWELL	ROW=32,	COL= 7,	Q=.00000215,	LAYER=4,	QTYPE=20,	\$END	A=20
\$NEWELL	ROW=32,	COL= 8,	Q=.00000230,	LAYER=4,	QTYPE=20,	\$END	A=20
\$NEWELL	ROW=33,	COL= 7,	Q=.00000115,	LAYER=4,	QTYPE=20,	\$END	A=20
\$NEWELL	ROW=33,	COL= 8,	Q=.00000144,	LAYER=4,	QTYPE=20,	\$END	A=20
\$NEWELL	ROW=33,	COL= 9,	Q=.00000115,	LAYER=4,	QTYPE=20,	\$END	A=20
\$NEWELL	ROW=33,	COL=10,	Q=.00000086,	LAYER=4,	QTYPE=20,	\$END	A=20
\$NEWELL	ROW=32,	COL= 7,	Q=.00000108,	LAYER=3,	QTYPE=20,	\$END	A=20
\$NEWELL	ROW=32,	COL= 8,	Q=.00000115,	LAYER=3,	QTYPE=20,	\$END	A=20
\$NEWELL	ROW=33,	COL= 7,	Q=.00000057,	LAYER=3,	QTYPE=20,	\$END	A=20
\$NEWELL	ROW=33,	COL= 8,	Q=.00000072,	LAYER=3,	QTYPE=20,	\$END	A=20
\$NEWELL	ROW=33,	COL= 9,	Q=.00000057,	LAYER=3,	QTYPE=20,	\$END	A=20
\$NEWELL	ROW=33,	COL=10,	Q=.00000043,	LAYER=3,	QTYPE=20,	\$END	A=20
\$NEWELL	ROW=32,	COL=15,	Q=.00000114,	LAYER=7,	QTYPE=21,	\$END	A=21
\$NEWELL	ROW=33,	COL=15,	Q=.00000107,	LAYER=7,	QTYPE=21,	\$END	A=21
\$NEWELL	ROW=32,	COL=15,	Q=.00000046,	LAYER=6,	QTYPE=21,	\$END	A=21
\$NEWELL	ROW=33,	COL=15,	Q=.00000043,	LAYER=6,	QTYPE=21,	\$END	A=21
\$NEWELL	ROW=32,	COL=15,	Q=.00000023,	LAYER=5,	QTYPE=21,	\$END	A=21
\$NEWELL	ROW=33,	COL=15,	Q=.00000022,	LAYER=5,	QTYPE=21,	\$END	A=21
\$NEWELL	ROW=32,	COL=15,	Q=.00000205,	LAYER=4,	QTYPE=21,	\$END	A=21
\$NEWELL	ROW=33,	COL=15,	Q=.00000191,	LAYER=4,	QTYPE=21,	\$END	A=21
\$NEWELL	ROW=32,	COL=15,	Q=.00000205,	LAYER=3,	QTYPE=21,	\$END	A=21
\$NEWELL	ROW=33,	COL=15,	Q=.00000191,	LAYER=3,	QTYPE=21,	\$END	A=21
\$NEWELL	ROW=34,	COL= 7,	Q=.00000130,	LAYER=7,	QTYPE=22,	\$END	A=22
\$NEWELL	ROW=34,	COL= 8,	Q=.00000026,	LAYER=7,	QTYPE=22,	\$END	A=22
\$NEWELL	ROW=35,	COL= 7,	Q=.00000130,	LAYER=7,	QTYPE=22,	\$END	A=22
\$NEWELL	ROW=35,	COL= 8,	Q=.00000208,	LAYER=7,	QTYPE=22,	\$END	A=22
\$NEWELL	ROW=36,	COL= 8,	Q=.00000208,	LAYER=7,	QTYPE=22,	\$END	A=22
\$NEWELL	ROW=37,	COL= 8,	Q=.00000117,	LAYER=7,	QTYPE=22,	\$END	A=22
\$NEWELL	ROW=34,	COL= 7,	Q=.00000160,	LAYER=6,	QTYPE=22,	\$END	A=22
\$NEWELL	ROW=34,	COL= 8,	Q=.00000032,	LAYER=6,	QTYPE=22,	\$END	A=22
\$NEWELL	ROW=35,	COL= 7,	Q=.00000160,	LAYER=6,	QTYPE=22,	\$END	A=22
\$NEWELL	ROW=35,	COL= 8,	Q=.00000256,	LAYER=6,	QTYPE=22,	\$END	A=22
\$NEWELL	ROW=36,	COL= 8,	Q=.00000256,	LAYER=6,	QTYPE=22,	\$END	A=22
\$NEWELL	ROW=37,	COL= 8,	Q=.00000144,	LAYER=6,	QTYPE=22,	\$END	A=22
\$NEWELL	ROW=34,	COL= 7,	Q=.00000075,	LAYER=5,	QTYPE=22,	\$END	A=22
\$NEWELL	ROW=34,	COL= 8,	Q=.00000015,	LAYER=5,	QTYPE=22,	\$END	A=22
\$NEWELL	ROW=35,	COL= 7,	Q=.00000075,	LAYER=5,	QTYPE=22,	\$END	A=22
\$NEWELL	ROW=35,	COL= 8,	Q=.00000119,	LAYER=5,	QTYPE=22,	\$END	A=22
\$NEWELL	ROW=36,	COL= 8,	Q=.00000119,	LAYER=5,	QTYPE=22,	\$END	A=22
\$NEWELL	ROW=37,	COL= 8,	Q=.00000067,	LAYER=5,	QTYPE=22,	\$END	A=22
\$NEWELL	ROW=34,	COL= 7,	Q=.00000019,	LAYER=4,	QTYPE=22,	\$END	A=22
\$NEWELL	ROW=34,	COL= 8,	Q=.00000004,	LAYER=4,	QTYPE=22,	\$END	A=22
\$NEWELL	ROW=35,	COL= 7,	Q=.00000019,	LAYER=4,	QTYPE=22,	\$END	A=22
\$NEWELL	ROW=35,	COL= 8,	Q=.00000030,	LAYER=4,	QTYPE=22,	\$END	A=22
\$NEWELL	ROW=36,	COL= 8,	Q=.00000030,	LAYER=4,	QTYPE=22,	\$END	A=22
\$NEWELL	ROW=37,	COL= 8,	Q=.00000017,	LAYER=4,	QTYPE=22,	\$END	A=22
\$NEWELL	ROW=34,	COL= 7,	Q=.00000011,	LAYER=3,	QTYPE=22,	\$END	A=22
\$NEWELL	ROW=34,	COL= 8,	Q=.00000002,	LAYER=3,	QTYPE=22,	\$END	A=22
\$NEWELL	ROW=35,	COL= 7,	Q=.00000011,	LAYER=3,	QTYPE=22,	\$END	A=22
\$NEWELL	ROW=35,	COL= 8,	Q=.00000013,	LAYER=3,	QTYPE=22,	\$END	A=22
\$NEWELL	ROW=36,	COL= 8,	Q=.00000018,	LAYER=3,	QTYPE=22,	\$END	A=22

Attachment 2.--Input file for the 1950-79 transient simulation--Continued

\$NEWELL	ROW=37,	COL= 8,	Q=.00000010,	LAYER=3,	QTYPE=22,	\$END	A=22
\$NEWELL	ROW=34,	COL=10,	Q=.00000022,	LAYER=7,	QTYPE=23,	\$END	A=23
\$NEWELL	ROW=35,	COL= 9,	Q=.00000175,	LAYER=7,	QTYPE=23,	\$END	A=23
\$NEWELL	ROW=35,	COL=10,	Q=.00000164,	LAYER=7,	QTYPE=23,	\$END	A=23
\$NEWELL	ROW=36,	COL= 9,	Q=.00000175,	LAYER=7,	QTYPE=23,	\$END	A=23
\$NEWELL	ROW=36,	COL=10,	Q=.00000175,	LAYER=7,	QTYPE=23,	\$END	A=23
\$NEWELL	ROW=37,	COL= 9,	Q=.00000077,	LAYER=7,	QTYPE=23,	\$END	A=23
\$NEWELL	ROW=37,	COL=10,	Q=.00000175,	LAYER=7,	QTYPE=23,	\$END	A=23
\$NEWELL	ROW=38,	COL= 9,	Q=.00000066,	LAYER=7,	QTYPE=23,	\$END	A=23
\$NEWELL	ROW=38,	COL=10,	Q=.00000175,	LAYER=7,	QTYPE=23,	\$END	A=23
\$NEWELL	ROW=39,	COL= 9,	Q=.00000022,	LAYER=7,	QTYPE=23,	\$END	A=23
\$NEWELL	ROW=39,	COL=10,	Q=.00000175,	LAYER=7,	QTYPE=23,	\$END	A=23
\$NEWELL	ROW=40,	COL= 9,	Q=.00000098,	LAYER=7,	QTYPE=23,	\$END	A=23
\$NEWELL	ROW=40,	COL=10,	Q=.00000131,	LAYER=7,	QTYPE=23,	\$END	A=23
\$NEWELL	ROW=34,	COL=10,	Q=.00000015,	LAYER=6,	QTYPE=23,	\$END	A=23
\$NEWELL	ROW=35,	COL= 9,	Q=.00000118,	LAYER=6,	QTYPE=23,	\$END	A=23
\$NEWELL	ROW=35,	COL=10,	Q=.00000111,	LAYER=6,	QTYPE=23,	\$END	A=23
\$NEWELL	ROW=36,	COL= 9,	Q=.00000118,	LAYER=6,	QTYPE=23,	\$END	A=23
\$NEWELL	ROW=36,	COL=10,	Q=.00000118,	LAYER=6,	QTYPE=23,	\$END	A=23
\$NEWELL	ROW=37,	COL= 9,	Q=.00000052,	LAYER=6,	QTYPE=23,	\$END	A=23
\$NEWELL	ROW=37,	COL=10,	Q=.00000118,	LAYER=6,	QTYPE=23,	\$END	A=23
\$NEWELL	ROW=38,	COL= 9,	Q=.00000044,	LAYER=6,	QTYPE=23,	\$END	A=23
\$NEWELL	ROW=38,	COL=10,	Q=.00000118,	LAYER=6,	QTYPE=23,	\$END	A=23
\$NEWELL	ROW=39,	COL= 9,	Q=.00000015,	LAYER=6,	QTYPE=23,	\$END	A=23
\$NEWELL	ROW=39,	COL=10,	Q=.00000118,	LAYER=6,	QTYPE=23,	\$END	A=23
\$NEWELL	ROW=40,	COL= 9,	Q=.00000066,	LAYER=6,	QTYPE=23,	\$END	A=23
\$NEWELL	ROW=40,	COL=10,	Q=.00000089,	LAYER=6,	QTYPE=23,	\$END	A=23
\$NEWELL	ROW=34,	COL=10,	Q=.00000021,	LAYER=5,	QTYPE=23,	\$END	A=23
\$NEWELL	ROW=35,	COL= 9,	Q=.00000169,	LAYER=5,	QTYPE=23,	\$END	A=23
\$NEWELL	ROW=35,	COL=10,	Q=.00000158,	LAYER=5,	QTYPE=23,	\$END	A=23
\$NEWELL	ROW=36,	COL= 9,	Q=.00000169,	LAYER=5,	QTYPE=23,	\$END	A=23
\$NEWELL	ROW=36,	COL=10,	Q=.00000169,	LAYER=5,	QTYPE=23,	\$END	A=23
\$NEWELL	ROW=37,	COL= 9,	Q=.00000074,	LAYER=5,	QTYPE=23,	\$END	A=23
\$NEWELL	ROW=37,	COL=10,	Q=.00000169,	LAYER=5,	QTYPE=23,	\$END	A=23
\$NEWELL	ROW=38,	COL= 9,	Q=.00000063,	LAYER=5,	QTYPE=23,	\$END	A=23
\$NEWELL	ROW=38,	COL=10,	Q=.00000169,	LAYER=5,	QTYPE=23,	\$END	A=23
\$NEWELL	ROW=39,	COL= 9,	Q=.00000021,	LAYER=5,	QTYPE=23,	\$END	A=23
\$NEWELL	ROW=39,	COL=10,	Q=.00000169,	LAYER=5,	QTYPE=23,	\$END	A=23
\$NEWELL	ROW=40,	COL= 9,	Q=.00000095,	LAYER=5,	QTYPE=23,	\$END	A=23
\$NEWELL	ROW=40,	COL=10,	Q=.00000126,	LAYER=5,	QTYPE=23,	\$END	A=23
\$NEWELL	ROW=34,	COL=10,	Q=.00000016,	LAYER=4,	QTYPE=23,	\$END	A=23
\$NEWELL	ROW=35,	COL= 9,	Q=.00000128,	LAYER=4,	QTYPE=23,	\$END	A=23
\$NEWELL	ROW=35,	COL=10,	Q=.00000120,	LAYER=4,	QTYPE=23,	\$END	A=23
\$NEWELL	ROW=36,	COL= 9,	Q=.00000128,	LAYER=4,	QTYPE=23,	\$END	A=23
\$NEWELL	ROW=36,	COL=10,	Q=.00000128,	LAYER=4,	QTYPE=23,	\$END	A=23
\$NEWELL	ROW=37,	COL= 9,	Q=.00000056,	LAYER=4,	QTYPE=23,	\$END	A=23
\$NEWELL	ROW=37,	COL=10,	Q=.00000128,	LAYER=4,	QTYPE=23,	\$END	A=23
\$NEWELL	ROW=38,	COL= 9,	Q=.00000048,	LAYER=4,	QTYPE=23,	\$END	A=23
\$NEWELL	ROW=38,	COL=10,	Q=.00000128,	LAYER=4,	QTYPE=23,	\$END	A=23
\$NEWELL	ROW=39,	COL= 9,	Q=.00000016,	LAYER=4,	QTYPE=23,	\$END	A=23
\$NEWELL	ROW=39,	COL=10,	Q=.00000128,	LAYER=4,	QTYPE=23,	\$END	A=23

## Attachment 2.--Input file for the 1950-79 transient simulation--Continued

\$NEWELL	ROW=40,	COL= 9,	Q=.00000072,	LAYER=4,	QTYPE=23,	\$END	A=23
\$NEWELL	ROW=40,	COL=10,	Q=.00000096,	LAYER=4,	QTYPE=23,	\$END	A=23
\$NEWELL	ROW=34,	COL=10,	Q=.00000005,	LAYER=3,	QTYPE=23,	\$END	A=23
\$NEWELL	ROW=35,	COL= 9,	Q=.00000044,	LAYER=3,	QTYPE=23,	\$END	A=23
\$NEWELL	ROW=35,	COL=10,	Q=.00000041,	LAYER=3,	QTYPE=23,	\$END	A=23
\$NEWELL	ROW=36,	COL= 9,	Q=.00000044,	LAYER=3,	QTYPE=23,	\$END	A=23
\$NEWELL	ROW=36,	COL=10,	Q=.00000044,	LAYER=3,	QTYPE=23,	\$END	A=23
\$NEWELL	ROW=37,	COL= 9,	Q=.00000019,	LAYER=3,	QTYPE=23,	\$END	A=23
\$NEWELL	ROW=37,	COL=10,	Q=.00000044,	LAYER=3,	QTYPE=23,	\$END	A=23
\$NEWELL	ROW=38,	COL= 9,	Q=.00000016,	LAYER=3,	QTYPE=23,	\$END	A=23
\$NEWELL	ROW=38,	COL=10,	Q=.00000044,	LAYER=3,	QTYPE=23,	\$END	A=23
\$NEWELL	ROW=39,	COL= 9,	Q=.00000005,	LAYER=3,	QTYPE=23,	\$END	A=23
\$NEWELL	ROW=39,	COL=10,	Q=.00000044,	LAYER=3,	QTYPE=23,	\$END	A=23
\$NEWELL	ROW=40,	COL= 9,	Q=.00000025,	LAYER=3,	QTYPE=23,	\$END	A=23
\$NEWELL	ROW=40,	COL=10,	Q=.00000033,	LAYER=3,	QTYPE=23,	\$END	A=23
\$NEWELL	ROW=35,	COL=11,	Q=.00000050,	LAYER=6,	QTYPE=24,	\$END	A=24
\$NEWELL	ROW=35,	COL=12,	Q=.00000042,	LAYER=6,	QTYPE=24,	\$END	A=24
\$NEWELL	ROW=35,	COL=13,	Q=.00000013,	LAYER=6,	QTYPE=24,	\$END	A=24
\$NEWELL	ROW=36,	COL=11,	Q=.00000067,	LAYER=6,	QTYPE=24,	\$END	A=24
\$NEWELL	ROW=36,	COL=12,	Q=.00000067,	LAYER=6,	QTYPE=24,	\$END	A=24
\$NEWELL	ROW=36,	COL=13,	Q=.00000067,	LAYER=6,	QTYPE=24,	\$END	A=24
\$NEWELL	ROW=36,	COL=14,	Q=.00000063,	LAYER=6,	QTYPE=24,	\$END	A=24
\$NEWELL	ROW=35,	COL=11,	Q=.00000147,	LAYER=5,	QTYPE=24,	\$END	A=24
\$NEWELL	ROW=35,	COL=12,	Q=.00000123,	LAYER=5,	QTYPE=24,	\$END	A=24
\$NEWELL	ROW=35,	COL=13,	Q=.00000037,	LAYER=5,	QTYPE=24,	\$END	A=24
\$NEWELL	ROW=36,	COL=11,	Q=.00000196,	LAYER=5,	QTYPE=24,	\$END	A=24
\$NEWELL	ROW=36,	COL=12,	Q=.00000196,	LAYER=5,	QTYPE=24,	\$END	A=24
\$NEWELL	ROW=36,	COL=13,	Q=.00000196,	LAYER=5,	QTYPE=24,	\$END	A=24
\$NEWELL	ROW=36,	COL=14,	Q=.00000184,	LAYER=5,	QTYPE=24,	\$END	A=24
\$NEWELL	ROW=35,	COL=11,	Q=.00000187,	LAYER=4,	QTYPE=24,	\$END	A=24
\$NEWELL	ROW=35,	COL=12,	Q=.00000156,	LAYER=4,	QTYPE=24,	\$END	A=24
\$NEWELL	ROW=35,	COL=13,	Q=.00000047,	LAYER=4,	QTYPE=24,	\$END	A=24
\$NEWELL	ROW=36,	COL=11,	Q=.00000249,	LAYER=4,	QTYPE=24,	\$END	A=24
\$NEWELL	ROW=36,	COL=12,	Q=.00000249,	LAYER=4,	QTYPE=24,	\$END	A=24
\$NEWELL	ROW=36,	COL=13,	Q=.00000249,	LAYER=4,	QTYPE=24,	\$END	A=24
\$NEWELL	ROW=36,	COL=14,	Q=.00000233,	LAYER=4,	QTYPE=24,	\$END	A=24
\$NEWELL	ROW=35,	COL=11,	Q=.00000090,	LAYER=3,	QTYPE=24,	\$END	A=24
\$NEWELL	ROW=35,	COL=12,	Q=.00000075,	LAYER=3,	QTYPE=24,	\$END	A=24
\$NEWELL	ROW=35,	COL=13,	Q=.00000022,	LAYER=3,	QTYPE=24,	\$END	A=24
\$NEWELL	ROW=36,	COL=11,	Q=.00000120,	LAYER=3,	QTYPE=24,	\$END	A=24
\$NEWELL	ROW=36,	COL=12,	Q=.00000120,	LAYER=3,	QTYPE=24,	\$END	A=24
\$NEWELL	ROW=36,	COL=13,	Q=.00000120,	LAYER=3,	QTYPE=24,	\$END	A=24
\$NEWELL	ROW=36,	COL=14,	Q=.00000112,	LAYER=3,	QTYPE=24,	\$END	A=24
\$NEWELL	ROW=35,	COL=23,	Q=.00000045,	LAYER=7,	QTYPE=25,	\$END	A=25
\$NEWELL	ROW=35,	COL=24,	Q=.00000030,	LAYER=7,	QTYPE=25,	\$END	A=25
\$NEWELL	ROW=35,	COL=25,	Q=.00000045,	LAYER=7,	QTYPE=25,	\$END	A=25
\$NEWELL	ROW=35,	COL=26,	Q=.00000012,	LAYER=7,	QTYPE=25,	\$END	A=25
\$NEWELL	ROW=36,	COL=23,	Q=.00000037,	LAYER=7,	QTYPE=25,	\$END	A=25
\$NEWELL	ROW=36,	COL=24,	Q=.00000147,	LAYER=7,	QTYPE=25,	\$END	A=25
\$NEWELL	ROW=36,	COL=25,	Q=.00000147,	LAYER=7,	QTYPE=25,	\$END	A=25
\$NEWELL	ROW=36,	COL=26,	Q=.00000184,	LAYER=7,	QTYPE=25,	\$END	A=25

## Attachment 2.--Input file for the 1950-79 transient simulation--Continued

\$NEWELL	ROW=36,	COL=27,	Q=.00000122,	LAYER=7,	QTYPE=25,	\$END	A=25
\$NEWELL	ROW=37,	COL=23,	Q=.00000024,	LAYER=7,	QTYPE=25,	\$END	A=25
\$NEWELL	ROW=37,	COL=24,	Q=.00000012,	LAYER=7,	QTYPE=25,	\$END	A=25
\$NEWELL	ROW=37,	COL=25,	Q=.00000122,	LAYER=7,	QTYPE=25,	\$END	A=25
\$NEWELL	ROW=37,	COL=26,	Q=.00000196,	LAYER=7,	QTYPE=25,	\$END	A=25
\$NEWELL	ROW=37,	COL=27,	Q=.00000171,	LAYER=7,	QTYPE=25,	\$END	A=25
\$NEWELL	ROW=38,	COL=23,	Q=.00000012,	LAYER=7,	QTYPE=25,	\$END	A=25
\$NEWELL	ROW=38,	COL=26,	Q=.00000098,	LAYER=7,	QTYPE=25,	\$END	A=25
\$NEWELL	ROW=38,	COL=27,	Q=.00000147,	LAYER=7,	QTYPE=25,	\$END	A=25
\$NEWELL	ROW=38,	COL=28,	Q=.00000024,	LAYER=7,	QTYPE=25,	\$END	A=25
\$NEWELL	ROW=39,	COL=27,	Q=.00000122,	LAYER=7,	QTYPE=25,	\$END	A=25
\$NEWELL	ROW=39,	COL=28,	Q=.00000037,	LAYER=7,	QTYPE=25,	\$END	A=25
\$NEWELL	ROW=35,	COL=23,	Q=.00000045,	LAYER=6,	QTYPE=25,	\$END	A=25
\$NEWELL	ROW=35,	COL=24,	Q=.00000030,	LAYER=6,	QTYPE=25,	\$END	A=25
\$NEWELL	ROW=35,	COL=25,	Q=.00000045,	LAYER=6,	QTYPE=25,	\$END	A=25
\$NEWELL	ROW=35,	COL=26,	Q=.00000015,	LAYER=6,	QTYPE=25,	\$END	A=25
\$NEWELL	ROW=36,	COL=23,	Q=.00000045,	LAYER=6,	QTYPE=25,	\$END	A=25
\$NEWELL	ROW=36,	COL=24,	Q=.00000182,	LAYER=6,	QTYPE=25,	\$END	A=25
\$NEWELL	ROW=36,	COL=25,	Q=.00000182,	LAYER=6,	QTYPE=25,	\$END	A=25
\$NEWELL	ROW=36,	COL=26,	Q=.00000227,	LAYER=6,	QTYPE=25,	\$END	A=25
\$NEWELL	ROW=36,	COL=27,	Q=.00000152,	LAYER=6,	QTYPE=25,	\$END	A=25
\$NEWELL	ROW=37,	COL=23,	Q=.00000030,	LAYER=6,	QTYPE=25,	\$END	A=25
\$NEWELL	ROW=37,	COL=24,	Q=.00000015,	LAYER=6,	QTYPE=25,	\$END	A=25
\$NEWELL	ROW=37,	COL=25,	Q=.00000152,	LAYER=6,	QTYPE=25,	\$END	A=25
\$NEWELL	ROW=37,	COL=26,	Q=.00000242,	LAYER=6,	QTYPE=25,	\$END	A=25
\$NEWELL	ROW=37,	COL=27,	Q=.00000212,	LAYER=6,	QTYPE=25,	\$END	A=25
\$NEWELL	ROW=38,	COL=23,	Q=.00000015,	LAYER=6,	QTYPE=25,	\$END	A=25
\$NEWELL	ROW=38,	COL=26,	Q=.00000121,	LAYER=6,	QTYPE=25,	\$END	A=25
\$NEWELL	ROW=38,	COL=27,	Q=.00000182,	LAYER=6,	QTYPE=25,	\$END	A=25
\$NEWELL	ROW=38,	COL=28,	Q=.00000030,	LAYER=6,	QTYPE=25,	\$END	A=25
\$NEWELL	ROW=39,	COL=27,	Q=.00000152,	LAYER=6,	QTYPE=25,	\$END	A=25
\$NEWELL	ROW=39,	COL=28,	Q=.00000045,	LAYER=6,	QTYPE=25,	\$END	A=25
\$NEWELL	ROW=35,	COL=23,	Q=.00000024,	LAYER=5,	QTYPE=25,	\$END	A=25
\$NEWELL	ROW=35,	COL=24,	Q=.00000016,	LAYER=5,	QTYPE=25,	\$END	A=25
\$NEWELL	ROW=35,	COL=25,	Q=.00000024,	LAYER=5,	QTYPE=25,	\$END	A=25
\$NEWELL	ROW=35,	COL=26,	Q=.00000008,	LAYER=5,	QTYPE=25,	\$END	A=25
\$NEWELL	ROW=36,	COL=23,	Q=.00000024,	LAYER=5,	QTYPE=25,	\$END	A=25
\$NEWELL	ROW=36,	COL=24,	Q=.00000097,	LAYER=5,	QTYPE=25,	\$END	A=25
\$NEWELL	ROW=36,	COL=25,	Q=.00000097,	LAYER=5,	QTYPE=25,	\$END	A=25
\$NEWELL	ROW=36,	COL=26,	Q=.00000121,	LAYER=5,	QTYPE=25,	\$END	A=25
\$NEWELL	ROW=36,	COL=27,	Q=.00000081,	LAYER=5,	QTYPE=25,	\$END	A=25
\$NEWELL	ROW=37,	COL=23,	Q=.00000016,	LAYER=5,	QTYPE=25,	\$END	A=25
\$NEWELL	ROW=37,	COL=24,	Q=.00000008,	LAYER=5,	QTYPE=25,	\$END	A=25
\$NEWELL	ROW=37,	COL=25,	Q=.00000081,	LAYER=5,	QTYPE=25,	\$END	A=25
\$NEWELL	ROW=37,	COL=26,	Q=.00000129,	LAYER=5,	QTYPE=25,	\$END	A=25
\$NEWELL	ROW=37,	COL=27,	Q=.00000113,	LAYER=5,	QTYPE=25,	\$END	A=25
\$NEWELL	ROW=38,	COL=23,	Q=.00000008,	LAYER=5,	QTYPE=25,	\$END	A=25
\$NEWELL	ROW=38,	COL=26,	Q=.00000064,	LAYER=5,	QTYPE=25,	\$END	A=25
\$NEWELL	ROW=38,	COL=27,	Q=.00000097,	LAYER=5,	QTYPE=25,	\$END	A=25
\$NEWELL	ROW=38,	COL=28,	Q=.00000016,	LAYER=5,	QTYPE=25,	\$END	A=25
\$NEWELL	ROW=39,	COL=27,	Q=.00000081,	LAYER=5,	QTYPE=25,	\$END	A=25

Attachment 2.--Input file for the 1950-79 transient simulation--Continued

\$NEWELL	ROW=39,	COL=28,	Q=.00000024,	LAYER=5,	QTYPE=25,	\$END	A=25
\$NEWELL	ROW=35,	COL=23,	Q=.00000009,	LAYER=4,	QTYPE=25,	\$END	A=25
\$NEWELL	ROW=35,	COL=24,	Q=.00000006,	LAYER=4,	QTYPE=25,	\$END	A=25
\$NEWELL	ROW=35,	COL=25,	Q=.00000009,	LAYER=4,	QTYPE=25,	\$END	A=25
\$NEWELL	ROW=35,	COL=26,	Q=.00000003,	LAYER=4,	QTYPE=25,	\$END	A=25
\$NEWELL	ROW=36,	COL=23,	Q=.00000009,	LAYER=4,	QTYPE=25,	\$END	A=25
\$NEWELL	ROW=36,	COL=24,	Q=.00000037,	LAYER=4,	QTYPE=25,	\$END	A=25
\$NEWELL	ROW=36,	COL=25,	Q=.00000037,	LAYER=4,	QTYPE=25,	\$END	A=25
\$NEWELL	ROW=36,	COL=26,	Q=.00000047,	LAYER=4,	QTYPE=25,	\$END	A=25
\$NEWELL	ROW=36,	COL=27,	Q=.00000031,	LAYER=4,	QTYPE=25,	\$END	A=25
\$NEWELL	ROW=37,	COL=23,	Q=.00000006,	LAYER=4,	QTYPE=25,	\$END	A=25
\$NEWELL	ROW=37,	COL=24,	Q=.00000003,	LAYER=4,	QTYPE=25,	\$END	A=25
\$NEWELL	ROW=37,	COL=25,	Q=.00000031,	LAYER=4,	QTYPE=25,	\$END	A=25
\$NEWELL	ROW=37,	COL=26,	Q=.00000050,	LAYER=4,	QTYPE=25,	\$END	A=25
\$NEWELL	ROW=37,	COL=27,	Q=.00000044,	LAYER=4,	QTYPE=25,	\$END	A=25
\$NEWELL	ROW=38,	COL=23,	Q=.00000033,	LAYER=4,	QTYPE=25,	\$END	A=25
\$NEWELL	ROW=38,	COL=26,	Q=.00000025,	LAYER=4,	QTYPE=25,	\$END	A=25
\$NEWELL	ROW=38,	COL=27,	Q=.00000037,	LAYER=4,	QTYPE=25,	\$END	A=25
\$NEWELL	ROW=38,	COL=28,	Q=.00000006,	LAYER=4,	QTYPE=25,	\$END	A=25
\$NEWELL	ROW=39,	COL=27,	Q=.00000031,	LAYER=4,	QTYPE=25,	\$END	A=25
\$NEWELL	ROW=39,	COL=28,	Q=.00000009,	LAYER=4,	QTYPE=25,	\$END	A=25
\$NEWELL	ROW=35,	COL=23,	Q=.00000003,	LAYER=3,	QTYPE=25,	\$END	A=25
\$NEWELL	ROW=35,	COL=24,	Q=.00000002,	LAYER=3,	QTYPE=25,	\$END	A=25
\$NEWELL	ROW=35,	COL=25,	Q=.00000003,	LAYER=3,	QTYPE=25,	\$END	A=25
\$NEWELL	ROW=35,	COL=26,	Q=.00000001,	LAYER=3,	QTYPE=25,	\$END	A=25
\$NEWELL	ROW=36,	COL=23,	Q=.00000003,	LAYER=3,	QTYPE=25,	\$END	A=25
\$NEWELL	ROW=36,	COL=24,	Q=.00000011,	LAYER=3,	QTYPE=25,	\$END	A=25
\$NEWELL	ROW=36,	COL=25,	Q=.00000011,	LAYER=3,	QTYPE=25,	\$END	A=25
\$NEWELL	ROW=36,	COL=26,	Q=.00000014,	LAYER=3,	QTYPE=25,	\$END	A=25
\$NEWELL	ROW=36,	COL=27,	Q=.00000009,	LAYER=3,	QTYPE=25,	\$END	A=25
\$NEWELL	ROW=37,	COL=23,	Q=.00000002,	LAYER=3,	QTYPE=25,	\$END	A=25
\$NEWELL	ROW=37,	COL=24,	Q=.00000001,	LAYER=3,	QTYPE=25,	\$END	A=25
\$NEWELL	ROW=37,	COL=25,	Q=.00000009,	LAYER=3,	QTYPE=25,	\$END	A=25
\$NEWELL	ROW=37,	COL=26,	Q=.00000015,	LAYER=3,	QTYPE=25,	\$END	A=25
\$NEWELL	ROW=37,	COL=27,	Q=.00000013,	LAYER=3,	QTYPE=25,	\$END	A=25
\$NEWELL	ROW=38,	COL=23,	Q=.00000001,	LAYER=3,	QTYPE=25,	\$END	A=25
\$NEWELL	ROW=38,	COL=26,	Q=.00000007,	LAYER=3,	QTYPE=25,	\$END	A=25
\$NEWELL	ROW=38,	COL=27,	Q=.00000011,	LAYER=3,	QTYPE=25,	\$END	A=25
\$NEWELL	ROW=38,	COL=28,	Q=.00000002,	LAYER=3,	QTYPE=25,	\$END	A=25
\$NEWELL	ROW=39,	COL=27,	Q=.00000009,	LAYER=3,	QTYPE=25,	\$END	A=25
\$NEWELL	ROW=39,	COL=28,	Q=.00000003,	LAYER=3,	QTYPE=25,	\$END	A=25
\$NEWELL	ROW=37,	COL=11,	Q=.00000078,	LAYER=7,	QTYPE=76,	\$END	A=26
\$NEWELL	ROW=37,	COL=12,	Q=.00000073,	LAYER=7,	QTYPE=76,	\$END	A=26
\$NEWELL	ROW=38,	COL=11,	Q=.00000078,	LAYER=7,	QTYPE=76,	\$END	A=26
\$NEWELL	ROW=38,	COL=12,	Q=.00000068,	LAYER=7,	QTYPE=76,	\$END	A=26
\$NEWELL	ROW=39,	COL=11,	Q=.00000078,	LAYER=7,	QTYPE=76,	\$END	A=26
\$NEWELL	ROW=39,	COL=12,	Q=.00000063,	LAYER=7,	QTYPE=76,	\$END	A=26
\$NEWELL	ROW=40,	COL=11,	Q=.00000063,	LAYER=7,	QTYPE=76,	\$END	A=26
\$NEWELL	ROW=40,	COL=12,	Q=.00000078,	LAYER=7,	QTYPE=76,	\$END	A=26
\$NEWELL	ROW=41,	COL=11,	Q=.00000078,	LAYER=7,	QTYPE=26,	\$END	A=26
\$NEWELL	ROW=41,	COL=12,	Q=.00000058,	LAYER=7,	QTYPE=26,	\$END	A=26

Attachment 2.--Input file for the 1950-79 transient simulation--Continued

\$NEWELL	ROW=41,	COL=13,	Q=.00000049,	LAYER=7,	QTYPE=26,	\$END	A=26
\$NEWELL	ROW=42,	COL=11,	Q=.00000078,	LAYER=7,	QTYPE=26,	\$END	A=26
\$NEWELL	ROW=42,	COL=12,	Q=.00000078,	LAYER=7,	QTYPE=26,	\$END	A=26
\$NEWELL	ROW=42,	COL=13,	Q=.00000078,	LAYER=7,	QTYPE=26,	\$END	A=26
\$NEWELL	ROW=42,	COL=14,	Q=.00000058,	LAYER=7,	QTYPE=26,	\$END	A=26
\$NEWELL	ROW=42,	COL=15,	Q=.00000039,	LAYER=7,	QTYPE=26,	\$END	A=26
\$NEWELL	ROW=43,	COL=11,	Q=.00000078,	LAYER=7,	QTYPE=26,	\$END	A=26
\$NEWELL	ROW=43,	COL=12,	Q=.00000078,	LAYER=7,	QTYPE=26,	\$END	A=26
\$NEWELL	ROW=43,	COL=13,	Q=.00000078,	LAYER=7,	QTYPE=26,	\$END	A=26
\$NEWELL	ROW=43,	COL=14,	Q=.00000073,	LAYER=7,	QTYPE=26,	\$END	A=26
\$NEWELL	ROW=43,	COL=15,	Q=.00000010,	LAYER=7,	QTYPE=26,	\$END	A=26
\$NEWELL	ROW=44,	COL=11,	Q=.00000078,	LAYER=7,	QTYPE=26,	\$END	A=26
\$NEWELL	ROW=44,	COL=12,	Q=.00000078,	LAYER=7,	QTYPE=26,	\$END	A=26
\$NEWELL	ROW=44,	COL=13,	Q=.00000068,	LAYER=7,	QTYPE=26,	\$END	A=26
\$NEWELL	ROW=45,	COL=11,	Q=.00000078,	LAYER=7,	QTYPE=26,	\$END	A=26
\$NEWELL	ROW=45,	COL=12,	Q=.00000078,	LAYER=7,	QTYPE=26,	\$END	A=26
\$NEWELL	ROW=45,	COL=13,	Q=.00000063,	LAYER=7,	QTYPE=26,	\$END	A=26
\$NEWELL	ROW=46,	COL=11,	Q=.00000078,	LAYER=7,	QTYPE=26,	\$END	A=26
\$NEWELL	ROW=37,	COL=11,	Q=.00000171,	LAYER=6,	QTYPE=76,	\$END	A=26
\$NEWELL	ROW=37,	COL=12,	Q=.00000160,	LAYER=6,	QTYPE=76,	\$END	A=26
\$NEWELL	ROW=38,	COL=11,	Q=.00000171,	LAYER=6,	QTYPE=76,	\$END	A=26
\$NEWELL	ROW=38,	COL=12,	Q=.00000150,	LAYER=6,	QTYPE=76,	\$END	A=26
\$NEWELL	ROW=39,	COL=11,	Q=.00000171,	LAYER=6,	QTYPE=76,	\$END	A=26
\$NEWELL	ROW=39,	COL=12,	Q=.00000139,	LAYER=6,	QTYPE=76,	\$END	A=26
\$NEWELL	ROW=40,	COL=11,	Q=.00000139,	LAYER=6,	QTYPE=76,	\$END	A=26
\$NEWELL	ROW=40,	COL=12,	Q=.00000171,	LAYER=6,	QTYPE=76,	\$END	A=26
\$NEWELL	ROW=41,	COL=11,	Q=.00000171,	LAYER=6,	QTYPE=26,	\$END	A=26
\$NEWELL	ROW=41,	COL=12,	Q=.00000128,	LAYER=6,	QTYPE=26,	\$END	A=26
\$NEWELL	ROW=41,	COL=13,	Q=.00000107,	LAYER=6,	QTYPE=26,	\$END	A=26
\$NEWELL	ROW=42,	COL=11,	Q=.00000171,	LAYER=6,	QTYPE=26,	\$END	A=26
\$NEWELL	ROW=42,	COL=12,	Q=.00000171,	LAYER=6,	QTYPE=26,	\$END	A=26
\$NEWELL	ROW=42,	COL=13,	Q=.00000171,	LAYER=6,	QTYPE=26,	\$END	A=26
\$NEWELL	ROW=42,	COL=14,	Q=.00000128,	LAYER=6,	QTYPE=26,	\$END	A=26
\$NEWELL	ROW=42,	COL=15,	Q=.00000086,	LAYER=6,	QTYPE=26,	\$END	A=26
\$NEWELL	ROW=43,	COL=11,	Q=.00000171,	LAYER=6,	QTYPE=26,	\$END	A=26
\$NEWELL	ROW=43,	COL=12,	Q=.00000171,	LAYER=6,	QTYPE=26,	\$END	A=26
\$NEWELL	ROW=43,	COL=13,	Q=.00000171,	LAYER=6,	QTYPE=26,	\$END	A=26
\$NEWELL	ROW=43,	COL=14,	Q=.00000160,	LAYER=6,	QTYPE=26,	\$END	A=26
\$NEWELL	ROW=43,	COL=15,	Q=.00000021,	LAYER=6,	QTYPE=26,	\$END	A=26
\$NEWELL	ROW=44,	COL=11,	Q=.00000171,	LAYER=6,	QTYPE=26,	\$END	A=26
\$NEWELL	ROW=44,	COL=12,	Q=.00000171,	LAYER=6,	QTYPE=26,	\$END	A=26
\$NEWELL	ROW=44,	COL=13,	Q=.00000150,	LAYER=6,	QTYPE=26,	\$END	A=26
\$NEWELL	ROW=45,	COL=11,	Q=.00000171,	LAYER=6,	QTYPE=26,	\$END	A=26
\$NEWELL	ROW=45,	COL=12,	Q=.00000171,	LAYER=6,	QTYPE=26,	\$END	A=26
\$NEWELL	ROW=45,	COL=13,	Q=.00000139,	LAYER=6,	QTYPE=26,	\$END	A=26
\$NEWELL	ROW=46,	COL=11,	Q=.00000171,	LAYER=6,	QTYPE=26,	\$END	A=26
\$NEWELL	ROW=37,	COL=11,	Q=.00000236,	LAYER=5,	QTYPE=76,	\$END	A=26
\$NEWELL	ROW=37,	COL=12,	Q=.00000221,	LAYER=5,	QTYPE=76,	\$END	A=26
\$NEWELL	ROW=38,	COL=11,	Q=.00000236,	LAYER=5,	QTYPE=76,	\$END	A=26
\$NEWELL	ROW=38,	COL=12,	Q=.00000207,	LAYER=5,	QTYPE=76,	\$END	A=26
\$NEWELL	ROW=39,	COL=11,	Q=.00000236,	LAYER=5,	QTYPE=76,	\$END	A=26



Attachment 2.--Input file for the 1950-79 transient simulation--Continued

\$NEWELL	ROW=39,	COL=12,	Q=.00000192,	LAYER=5,	QTYPE=76,	\$END	A=26
\$NEWELL	ROW=40,	COL=11,	Q=.00000192,	LAYER=5,	QTYPE=76,	\$END	A=26
\$NEWELL	ROW=40,	COL=12,	Q=.00000236,	LAYER=5,	QTYPE=76,	\$END	A=26
\$NEWELL	ROW=41,	COL=11,	Q=.00000236,	LAYER=5,	QTYPE=26,	\$END	A=26
\$NEWELL	ROW=41,	COL=12,	Q=.00000177,	LAYER=5,	QTYPE=26,	\$END	A=26
\$NEWELL	ROW=41,	COL=13,	Q=.00000148,	LAYER=5,	QTYPE=26,	\$END	A=26
\$NEWELL	ROW=42,	COL=11,	Q=.00000236,	LAYER=5,	QTYPE=26,	\$END	A=26
\$NEWELL	ROW=42,	COL=12,	Q=.00000236,	LAYER=5,	QTYPE=26,	\$END	A=26
\$NEWELL	ROW=42,	COL=13,	Q=.00000236,	LAYER=5,	QTYPE=26,	\$END	A=26
\$NEWELL	ROW=42,	COL=14,	Q=.00000177,	LAYER=5,	QTYPE=26,	\$END	A=26
\$NEWELL	ROW=42,	COL=15,	Q=.00000118,	LAYER=5,	QTYPE=26,	\$END	A=26
\$NEWELL	ROW=43,	COL=11,	Q=.00000236,	LAYER=5,	QTYPE=26,	\$END	A=26
\$NEWELL	ROW=43,	COL=12,	Q=.00000236,	LAYER=5,	QTYPE=26,	\$END	A=26
\$NEWELL	ROW=43,	COL=13,	Q=.00000236,	LAYER=5,	QTYPE=26,	\$END	A=26
\$NEWELL	ROW=43,	COL=14,	Q=.00000221,	LAYER=5,	QTYPE=26,	\$END	A=26
\$NEWELL	ROW=43,	COL=15,	Q=.00000030,	LAYER=5,	QTYPE=26,	\$END	A=26
\$NEWELL	ROW=44,	COL=11,	Q=.00000236,	LAYER=5,	QTYPE=26,	\$END	A=26
\$NEWELL	ROW=44,	COL=12,	Q=.00000236,	LAYER=5,	QTYPE=26,	\$END	A=26
\$NEWELL	ROW=44,	COL=13,	Q=.00000207,	LAYER=5,	QTYPE=26,	\$END	A=26
\$NEWELL	ROW=45,	COL=11,	Q=.00000236,	LAYER=5,	QTYPE=26,	\$END	A=26
\$NEWELL	ROW=45,	COL=12,	Q=.00000236,	LAYER=5,	QTYPE=26,	\$END	A=26
\$NEWELL	ROW=45,	COL=13,	Q=.00000192,	LAYER=5,	QTYPE=26,	\$END	A=26
\$NEWELL	ROW=46,	COL=11,	Q=.00000236,	LAYER=5,	QTYPE=26,	\$END	A=26
\$NEWELL	ROW=37,	COL=11,	Q=.00000134,	LAYER=4,	QTYPE=76,	\$END	A=26
\$NEWELL	ROW=37,	COL=12,	Q=.00000126,	LAYER=4,	QTYPE=76,	\$END	A=26
\$NEWELL	ROW=38,	COL=11,	Q=.00000134,	LAYER=4,	QTYPE=76,	\$END	A=26
\$NEWELL	ROW=38,	COL=12,	Q=.00000117,	LAYER=4,	QTYPE=76,	\$END	A=26
\$NEWELL	ROW=39,	COL=11,	Q=.00000134,	LAYER=4,	QTYPE=76,	\$END	A=26
\$NEWELL	ROW=39,	COL=12,	Q=.00000109,	LAYER=4,	QTYPE=76,	\$END	A=26
\$NEWELL	ROW=40,	COL=11,	Q=.00000109,	LAYER=4,	QTYPE=76,	\$END	A=26
\$NEWELL	ROW=40,	COL=12,	Q=.00000134,	LAYER=4,	QTYPE=76,	\$END	A=26
\$NEWELL	ROW=41,	COL=11,	Q=.00000134,	LAYER=4,	QTYPE=26,	\$END	A=26
\$NEWELL	ROW=41,	COL=12,	Q=.00000100,	LAYER=4,	QTYPE=26,	\$END	A=26
\$NEWELL	ROW=41,	COL=13,	Q=.00000084,	LAYER=4,	QTYPE=26,	\$END	A=26
\$NEWELL	ROW=42,	COL=11,	Q=.00000134,	LAYER=4,	QTYPE=26,	\$END	A=26
\$NEWELL	ROW=42,	COL=12,	Q=.00000134,	LAYER=4,	QTYPE=26,	\$END	A=26
\$NEWELL	ROW=42,	COL=13,	Q=.00000134,	LAYER=4,	QTYPE=26,	\$END	A=26
\$NEWELL	ROW=42,	COL=14,	Q=.00000100,	LAYER=4,	QTYPE=26,	\$END	A=26
\$NEWELL	ROW=42,	COL=15,	Q=.00000068,	LAYER=4,	QTYPE=26,	\$END	A=26
\$NEWELL	ROW=43,	COL=11,	Q=.00000134,	LAYER=4,	QTYPE=26,	\$END	A=26
\$NEWELL	ROW=43,	COL=12,	Q=.00000134,	LAYER=4,	QTYPE=26,	\$END	A=26
\$NEWELL	ROW=43,	COL=13,	Q=.00000134,	LAYER=4,	QTYPE=26,	\$END	A=26
\$NEWELL	ROW=43,	COL=14,	Q=.00000126,	LAYER=4,	QTYPE=26,	\$END	A=26
\$NEWELL	ROW=43,	COL=15,	Q=.00000017,	LAYER=4,	QTYPE=26,	\$END	A=26
\$NEWELL	ROW=44,	COL=11,	Q=.00000134,	LAYER=4,	QTYPE=26,	\$END	A=26
\$NEWELL	ROW=44,	COL=12,	Q=.00000134,	LAYER=4,	QTYPE=26,	\$END	A=26
\$NEWELL	ROW=44,	COL=13,	Q=.00000117,	LAYER=4,	QTYPE=26,	\$END	A=26
\$NEWELL	ROW=45,	COL=11,	Q=.00000134,	LAYER=4,	QTYPE=26,	\$END	A=26
\$NEWELL	ROW=45,	COL=12,	Q=.00000134,	LAYER=4,	QTYPE=26,	\$END	A=26
\$NEWELL	ROW=45,	COL=13,	Q=.00000109,	LAYER=4,	QTYPE=26,	\$END	A=26
\$NEWELL	ROW=46,	COL=11,	Q=.00000134,	LAYER=4,	QTYPE=26,	\$END	A=26

Attachment 2.--Input file for the 1950-79 transient simulation--Continued

\$NEWELL	ROW=37,	COL=11,	Q=.00000013,	LAYER=3,	QTYPE=76,	\$END	A=26
\$NEWELL	ROW=37,	COL=12,	Q=.00000012,	LAYER=3,	QTYPE=76,	\$END	A=26
\$NEWELL	ROW=38,	COL=11,	Q=.00000013,	LAYER=3,	QTYPE=76,	\$END	A=26
\$NEWELL	ROW=38,	COL=12,	Q=.00000012,	LAYER=3,	QTYPE=76,	\$END	A=26
\$NEWELL	ROW=39,	COL=11,	Q=.00000013,	LAYER=3,	QTYPE=76,	\$END	A=26
\$NEWELL	ROW=39,	COL=12,	Q=.00000011,	LAYER=3,	QTYPE=76,	\$END	A=26
\$NEWELL	ROW=40,	COL=11,	Q=.00000011,	LAYER=3,	QTYPE=76,	\$END	A=26
\$NEWELL	ROW=40,	COL=12,	Q=.00000013,	LAYER=3,	QTYPE=76,	\$END	A=26
\$NEWELL	ROW=41,	COL=11,	Q=.00000013,	LAYER=3,	QTYPE=26,	\$END	A=26
\$NEWELL	ROW=41,	COL=12,	Q=.00000010,	LAYER=3,	QTYPE=26,	\$END	A=26
\$NEWELL	ROW=41,	COL=13,	Q=.00000008,	LAYER=3,	QTYPE=26,	\$END	A=26
\$NEWELL	ROW=42,	COL=11,	Q=.00000013,	LAYER=3,	QTYPE=26,	\$END	A=26
\$NEWELL	ROW=42,	COL=12,	Q=.00000013,	LAYER=3,	QTYPE=26,	\$END	A=26
\$NEWELL	ROW=42,	COL=13,	Q=.00000013,	LAYER=3,	QTYPE=26,	\$END	A=26
\$NEWELL	ROW=42,	COL=14,	Q=.00000010,	LAYER=3,	QTYPE=26,	\$END	A=26
\$NEWELL	ROW=42,	COL=15,	Q=.00000007,	LAYER=3,	QTYPE=26,	\$END	A=26
\$NEWELL	ROW=43,	COL=11,	Q=.00000013,	LAYER=3,	QTYPE=26,	\$END	A=26
\$NEWELL	ROW=43,	COL=12,	Q=.00000013,	LAYER=3,	QTYPE=26,	\$END	A=26
\$NEWELL	ROW=43,	COL=13,	Q=.00000013,	LAYER=3,	QTYPE=26,	\$END	A=26
\$NEWELL	ROW=43,	COL=14,	Q=.00000012,	LAYER=3,	QTYPE=26,	\$END	A=26
\$NEWELL	ROW=43,	COL=15,	Q=.00000002,	LAYER=3,	QTYPE=26,	\$END	A=26
\$NEWELL	ROW=44,	COL=11,	Q=.00000013,	LAYER=3,	QTYPE=26,	\$END	A=26
\$NEWELL	ROW=44,	COL=12,	Q=.00000013,	LAYER=3,	QTYPE=26,	\$END	A=26
\$NEWELL	ROW=44,	COL=13,	Q=.00000012,	LAYER=3,	QTYPE=26,	\$END	A=26
\$NEWELL	ROW=45,	COL=11,	Q=.00000013,	LAYER=3,	QTYPE=26,	\$END	A=26
\$NEWELL	ROW=45,	COL=12,	Q=.00000013,	LAYER=3,	QTYPE=26,	\$END	A=26
\$NEWELL	ROW=45,	COL=13,	Q=.00000011,	LAYER=3,	QTYPE=26,	\$END	A=26
\$NEWELL	ROW=46,	COL=11,	Q=.00000013,	LAYER=3,	QTYPE=26,	\$END	A=26
\$NEWELL	ROW=37,	COL=13,	Q=.00000100,	LAYER=5,	QTYPE=27,	\$END	A=27
\$NEWELL	ROW=37,	COL=14,	Q=.00000134,	LAYER=5,	QTYPE=27,	\$END	A=27
\$NEWELL	ROW=37,	COL=15,	Q=.00000100,	LAYER=5,	QTYPE=27,	\$END	A=27
\$NEWELL	ROW=38,	COL=13,	Q=.00000126,	LAYER=5,	QTYPE=27,	\$END	A=27
\$NEWELL	ROW=38,	COL=14,	Q=.00000134,	LAYER=5,	QTYPE=27,	\$END	A=27
\$NEWELL	ROW=38,	COL=15,	Q=.00000134,	LAYER=5,	QTYPE=27,	\$END	A=27
\$NEWELL	ROW=39,	COL=13,	Q=.00000067,	LAYER=5,	QTYPE=27,	\$END	A=27
\$NEWELL	ROW=39,	COL=14,	Q=.00000134,	LAYER=5,	QTYPE=27,	\$END	A=27
\$NEWELL	ROW=39,	COL=15,	Q=.00000134,	LAYER=5,	QTYPE=27,	\$END	A=27
\$NEWELL	ROW=39,	COL=16,	Q=.00000134,	LAYER=5,	QTYPE=27,	\$END	A=27
\$NEWELL	ROW=40,	COL=13,	Q=.00000134,	LAYER=5,	QTYPE=27,	\$END	A=27
\$NEWELL	ROW=40,	COL=14,	Q=.00000134,	LAYER=5,	QTYPE=27,	\$END	A=27
\$NEWELL	ROW=40,	COL=15,	Q=.00000117,	LAYER=5,	QTYPE=27,	\$END	A=27
\$NEWELL	ROW=40,	COL=16,	Q=.00000067,	LAYER=5,	QTYPE=27,	\$END	A=27
\$NEWELL	ROW=40,	COL=17,	Q=.00000067,	LAYER=5,	QTYPE=27,	\$END	A=27
\$NEWELL	ROW=41,	COL=14,	Q=.00000117,	LAYER=5,	QTYPE=27,	\$END	A=27
\$NEWELL	ROW=41,	COL=15,	Q=.00000117,	LAYER=5,	QTYPE=27,	\$END	A=27
\$NEWELL	ROW=41,	COL=16,	Q=.00000067,	LAYER=5,	QTYPE=27,	\$END	A=27
\$NEWELL	ROW=37,	COL=13,	Q=.00000237,	LAYER=4,	QTYPE=27,	\$END	A=27
\$NEWELL	ROW=37,	COL=14,	Q=.00000316,	LAYER=4,	QTYPE=27,	\$END	A=27
\$NEWELL	ROW=37,	COL=15,	Q=.00000237,	LAYER=4,	QTYPE=27,	\$END	A=27
\$NEWELL	ROW=38,	COL=13,	Q=.00000296,	LAYER=4,	QTYPE=27,	\$END	A=27
\$NEWELL	ROW=38,	COL=14,	Q=.00000316,	LAYER=4,	QTYPE=27,	\$END	A=27

Attachment 2.--Input file for the 1950-79 transient simulation--Continued

\$NEWELL	ROW=38,	COL=15,	Q=.00000316,	LAYER=4,	QTYPE=27,	\$END	A=27
\$NEWELL	ROW=39,	COL=13,	Q=.00000158,	LAYER=4,	QTYPE=27,	\$END	A=27
\$NEWELL	ROW=39,	COL=14,	Q=.00000316,	LAYER=4,	QTYPE=27,	\$END	A=27
\$NEWELL	ROW=39,	COL=15,	Q=.00000316,	LAYER=4,	QTYPE=27,	\$END	A=27
\$NEWELL	ROW=39,	COL=16,	Q=.00000316,	LAYER=4,	QTYPE=27,	\$END	A=27
\$NEWELL	ROW=40,	COL=13,	Q=.00000316,	LAYER=4,	QTYPE=27,	\$END	A=27
\$NEWELL	ROW=40,	COL=14,	Q=.00000316,	LAYER=4,	QTYPE=27,	\$END	A=27
\$NEWELL	ROW=40,	COL=15,	Q=.00000276,	LAYER=4,	QTYPE=27,	\$END	A=27
\$NEWELL	ROW=40,	COL=16,	Q=.00000158,	LAYER=4,	QTYPE=27,	\$END	A=27
\$NEWELL	ROW=40,	COL=17,	Q=.00000158,	LAYER=4,	QTYPE=27,	\$END	A=27
\$NEWELL	ROW=41,	COL=14,	Q=.00000276,	LAYER=4,	QTYPE=27,	\$END	A=27
\$NEWELL	ROW=41,	COL=15,	Q=.00000276,	LAYER=4,	QTYPE=27,	\$END	A=27
\$NEWELL	ROW=41,	COL=16,	Q=.00000158,	LAYER=4,	QTYPE=27,	\$END	A=27
\$NEWELL	ROW=37,	COL=13,	Q=.00000137,	LAYER=3,	QTYPE=27,	\$END	A=27
\$NEWELL	ROW=37,	COL=14,	Q=.00000183,	LAYER=3,	QTYPE=27,	\$END	A=27
\$NEWELL	ROW=37,	COL=15,	Q=.00000137,	LAYER=3,	QTYPE=27,	\$END	A=27
\$NEWELL	ROW=38,	COL=13,	Q=.00000171,	LAYER=3,	QTYPE=27,	\$END	A=27
\$NEWELL	ROW=38,	COL=14,	Q=.00000183,	LAYER=3,	QTYPE=27,	\$END	A=27
\$NEWELL	ROW=38,	COL=15,	Q=.00000183,	LAYER=3,	QTYPE=27,	\$END	A=27
\$NEWELL	ROW=39,	COL=13,	Q=.00000091,	LAYER=3,	QTYPE=27,	\$END	A=27
\$NEWELL	ROW=39,	COL=14,	Q=.00000183,	LAYER=3,	QTYPE=27,	\$END	A=27
\$NEWELL	ROW=39,	COL=15,	Q=.00000183,	LAYER=3,	QTYPE=27,	\$END	A=27
\$NEWELL	ROW=39,	COL=16,	Q=.00000183,	LAYER=3,	QTYPE=27,	\$END	A=27
\$NEWELL	ROW=40,	COL=13,	Q=.00000183,	LAYER=3,	QTYPE=27,	\$END	A=27
\$NEWELL	ROW=40,	COL=14,	Q=.00000183,	LAYER=3,	QTYPE=27,	\$END	A=27
\$NEWELL	ROW=40,	COL=15,	Q=.00000160,	LAYER=3,	QTYPE=27,	\$END	A=27
\$NEWELL	ROW=40,	COL=16,	Q=.00000091,	LAYER=3,	QTYPE=27,	\$END	A=27
\$NEWELL	ROW=40,	COL=17,	Q=.00000091,	LAYER=3,	QTYPE=27,	\$END	A=27
\$NEWELL	ROW=41,	COL=14,	Q=.00000160,	LAYER=3,	QTYPE=27,	\$END	A=27
\$NEWELL	ROW=41,	COL=15,	Q=.00000160,	LAYER=3,	QTYPE=27,	\$END	A=27
\$NEWELL	ROW=41,	COL=16,	Q=.00000091,	LAYER=3,	QTYPE=27,	\$END	A=27
\$NEWELL	ROW=38,	COL=19,	Q=.00000018,	LAYER=7,	QTYPE=28,	\$END	A=28
\$NEWELL	ROW=38,	COL=20,	Q=.00000005,	LAYER=7,	QTYPE=28,	\$END	A=28
\$NEWELL	ROW=38,	COL=21,	Q=.00000005,	LAYER=7,	QTYPE=28,	\$END	A=28
\$NEWELL	ROW=39,	COL=19,	Q=.00000009,	LAYER=7,	QTYPE=28,	\$END	A=28
\$NEWELL	ROW=39,	COL=20,	Q=.00000005,	LAYER=7,	QTYPE=28,	\$END	A=28
\$NEWELL	ROW=39,	COL=21,	Q=.00000046,	LAYER=7,	QTYPE=28,	\$END	A=28
\$NEWELL	ROW=40,	COL=20,	Q=.00000009,	LAYER=7,	QTYPE=28,	\$END	A=28
\$NEWELL	ROW=40,	COL=21,	Q=.00000073,	LAYER=7,	QTYPE=28,	\$END	A=28
\$NEWELL	ROW=41,	COL=21,	Q=.00000009,	LAYER=7,	QTYPE=28,	\$END	A=28
\$NEWELL	ROW=38,	COL=19,	Q=.00000069,	LAYER=6,	QTYPE=28,	\$END	A=28
\$NEWELL	ROW=38,	COL=20,	Q=.00000017,	LAYER=6,	QTYPE=28,	\$END	A=28
\$NEWELL	ROW=38,	COL=21,	Q=.00000017,	LAYER=6,	QTYPE=28,	\$END	A=28
\$NEWELL	ROW=39,	COL=19,	Q=.00000034,	LAYER=6,	QTYPE=28,	\$END	A=28
\$NEWELL	ROW=39,	COL=20,	Q=.00000017,	LAYER=6,	QTYPE=28,	\$END	A=28
\$NEWELL	ROW=39,	COL=21,	Q=.00000172,	LAYER=6,	QTYPE=28,	\$END	A=28
\$NEWELL	ROW=40,	COL=20,	Q=.00000034,	LAYER=6,	QTYPE=28,	\$END	A=28
\$NEWELL	ROW=40,	COL=21,	Q=.00000275,	LAYER=6,	QTYPE=28,	\$END	A=28
\$NEWELL	ROW=41,	COL=21,	Q=.00000034,	LAYER=6,	QTYPE=28,	\$END	A=28
\$NEWELL	ROW=38,	COL=19,	Q=.00000057,	LAYER=5,	QTYPE=28,	\$END	A=28
\$NEWELL	ROW=38,	COL=20,	Q=.00000014,	LAYER=5,	QTYPE=28,	\$END	A=28

## Attachment 2.--Input file for the 1950-79 transient simulation--Continued

\$NEWELL	ROW=38,	COL=21,	Q=.00000014,	LAYER=5,	QTYPE=28,	\$END	A=28
\$NEWELL	ROW=39,	COL=19,	Q=.00000028,	LAYER=5,	QTYPE=28,	\$END	A=28
\$NEWELL	ROW=39,	COL=20,	Q=.00000014,	LAYER=5,	QTYPE=28,	\$END	A=28
\$NEWELL	ROW=39,	COL=21,	Q=.000000142,	LAYER=5,	QTYPE=28,	\$END	A=28
\$NEWELL	ROW=40,	COL=20,	Q=.00000028,	LAYER=5,	QTYPE=28,	\$END	A=28
\$NEWELL	ROW=40,	COL=21,	Q=.000000227,	LAYER=5,	QTYPE=28,	\$END	A=28
\$NEWELL	ROW=41,	COL=21,	Q=.00000028,	LAYER=5,	QTYPE=28,	\$END	A=28
\$NEWELL	ROW=38,	COL=19,	Q=.00000010,	LAYER=4,	QTYPE=28,	\$END	A=28
\$NEWELL	ROW=38,	COL=20,	Q=.00000003,	LAYER=4,	QTYPE=28,	\$END	A=28
\$NEWELL	ROW=38,	COL=21,	Q=.00000003,	LAYER=4,	QTYPE=28,	\$END	A=28
\$NEWELL	ROW=39,	COL=19,	Q=.00000005,	LAYER=4,	QTYPE=28,	\$END	A=28
\$NEWELL	ROW=39,	COL=20,	Q=.00000003,	LAYER=4,	QTYPE=28,	\$END	A=28
\$NEWELL	ROW=39,	COL=21,	Q=.00000025,	LAYER=4,	QTYPE=28,	\$END	A=28
\$NEWELL	ROW=40,	COL=20,	Q=.00000005,	LAYER=4,	QTYPE=28,	\$END	A=28
\$NEWELL	ROW=40,	COL=21,	Q=.00000040,	LAYER=4,	QTYPE=28,	\$END	A=28
\$NEWELL	ROW=41,	COL=21,	Q=.00000005,	LAYER=4,	QTYPE=28,	\$END	A=28
\$NEWELL	ROW=38,	COL=19,	Q=.00000004,	LAYER=3,	QTYPE=28,	\$END	A=28
\$NEWELL	ROW=38,	COL=20,	Q=.00000001,	LAYER=3,	QTYPE=28,	\$END	A=28
\$NEWELL	ROW=38,	COL=21,	Q=.00000001,	LAYER=3,	QTYPE=28,	\$END	A=28
\$NEWELL	ROW=39,	COL=19,	Q=.00000002,	LAYER=3,	QTYPE=28,	\$END	A=28
\$NEWELL	ROW=39,	COL=20,	Q=.00000001,	LAYER=3,	QTYPE=28,	\$END	A=28
\$NEWELL	ROW=39,	COL=21,	Q=.00000010,	LAYER=3,	QTYPE=28,	\$END	A=28
\$NEWELL	ROW=40,	COL=20,	Q=.00000002,	LAYER=3,	QTYPE=28,	\$END	A=28
\$NEWELL	ROW=40,	COL=21,	Q=.00000016,	LAYER=3,	QTYPE=28,	\$END	A=28
\$NEWELL	ROW=41,	COL=21,	Q=.00000002,	LAYER=3,	QTYPE=28,	\$END	A=28
\$NEWELL	ROW=47,	COL=12,	Q=.00000069,	LAYER=7,	QTYPE=29,	\$END	A=29
\$NEWELL	ROW=47,	COL=13,	Q=.00000060,	LAYER=7,	QTYPE=29,	\$END	A=29
\$NEWELL	ROW=47,	COL=14,	Q=.00000112,	LAYER=7,	QTYPE=29,	\$END	A=29
\$NEWELL	ROW=47,	COL=15,	Q=.00000034,	LAYER=7,	QTYPE=29,	\$END	A=29
\$NEWELL	ROW=48,	COL=12,	Q=.00000086,	LAYER=7,	QTYPE=29,	\$END	A=29
\$NEWELL	ROW=48,	COL=13,	Q=.00000103,	LAYER=7,	QTYPE=29,	\$END	A=29
\$NEWELL	ROW=48,	COL=14,	Q=.00000095,	LAYER=7,	QTYPE=29,	\$END	A=29
\$NEWELL	ROW=49,	COL=13,	Q=.00000043,	LAYER=7,	QTYPE=29,	\$END	A=29
\$NEWELL	ROW=47,	COL=12,	Q=.00000151,	LAYER=6,	QTYPE=29,	\$END	A=29
\$NEWELL	ROW=47,	COL=13,	Q=.00000132,	LAYER=6,	QTYPE=29,	\$END	A=29
\$NEWELL	ROW=47,	COL=14,	Q=.00000246,	LAYER=6,	QTYPE=29,	\$END	A=29
\$NEWELL	ROW=47,	COL=15,	Q=.00000076,	LAYER=6,	QTYPE=29,	\$END	A=29
\$NEWELL	ROW=48,	COL=12,	Q=.00000189,	LAYER=6,	QTYPE=29,	\$END	A=29
\$NEWELL	ROW=48,	COL=13,	Q=.00000227,	LAYER=6,	QTYPE=29,	\$END	A=29
\$NEWELL	ROW=48,	COL=14,	Q=.00000208,	LAYER=6,	QTYPE=29,	\$END	A=29
\$NEWELL	ROW=49,	COL=13,	Q=.00000095,	LAYER=6,	QTYPE=29,	\$END	A=29
\$NEWELL	ROW=47,	COL=12,	Q=.00000082,	LAYER=5,	QTYPE=29,	\$END	A=29
\$NEWELL	ROW=47,	COL=13,	Q=.00000072,	LAYER=5,	QTYPE=29,	\$END	A=29
\$NEWELL	ROW=47,	COL=14,	Q=.00000134,	LAYER=5,	QTYPE=29,	\$END	A=29
\$NEWELL	ROW=47,	COL=15,	Q=.00000041,	LAYER=5,	QTYPE=29,	\$END	A=29
\$NEWELL	ROW=48,	COL=12,	Q=.00000103,	LAYER=5,	QTYPE=29,	\$END	A=29
\$NEWELL	ROW=48,	COL=13,	Q=.00000124,	LAYER=5,	QTYPE=29,	\$END	A=29
\$NEWELL	ROW=48,	COL=14,	Q=.00000113,	LAYER=5,	QTYPE=29,	\$END	A=29
\$NEWELL	ROW=49,	COL=13,	Q=.00000052,	LAYER=5,	QTYPE=29,	\$END	A=29
\$NEWELL	ROW=47,	COL=12,	Q=.00000007,	LAYER=4,	QTYPE=29,	\$END	A=29
\$NEWELL	ROW=47,	COL=13,	Q=.00000006,	LAYER=4,	QTYPE=29,	\$END	A=29

## Attachment 2.--Input file for the 1950-79 transient simulation--Continued

```

$NEWELL ROW=47, COL=14, Q=.00000011, LAYER=4, QTYPE=29, $END A=29
$NEWELL ROW=47, COL=15, Q=.00000003, LAYER=4, QTYPE=29, $END A=29
$NEWELL ROW=48, COL=12, Q=.00000009, LAYER=4, QTYPE=29, $END A=29
$NEWELL ROW=48, COL=13, Q=.00000010, LAYER=4, QTYPE=29, $END A=29
$NEWELL ROW=48, COL=14, Q=.00000010, LAYER=4, QTYPE=29, $END A=29
$NEWELL ROW=49, COL=13, Q=.00000004, LAYER=4, QTYPE=29, $END A=29
$NEWELL ROW=47, COL=12, Q=.00000007, LAYER=3, QTYPE=29, $END A=29
$NEWELL ROW=47, COL=13, Q=.00000006, LAYER=3, QTYPE=29, $END A=29
$NEWELL ROW=47, COL=14, Q=.00000011, LAYER=3, QTYPE=29, $END A=29
$NEWELL ROW=47, COL=15, Q=.00000003, LAYER=3, QTYPE=29, $END A=29
$NEWELL ROW=48, COL=12, Q=.00000009, LAYER=3, QTYPE=29, $END A=29
$NEWELL ROW=48, COL=13, Q=.00000010, LAYER=3, QTYPE=29, $END A=29
$NEWELL ROW=48, COL=14, Q=.00000010, LAYER=3, QTYPE=29, $END A=29
$NEWELL ROW=49, COL=13, Q=.00000004, LAYER=3, QTYPE=29, $END A=29
$NEWELL ROW=28, COL=11, Q=0.111, LAYER=7, QTYPE=30, $END GRVTY RF
$NEWELL ROW=12, COL=13, Q=0.221, LAYER=7, QTYPE=30, $END GRVTY RF
$NEWELL ROW=14, COL=13, Q=0.221, LAYER=7, QTYPE=30, $END GRVTY RF
$NEWELL ROW=14, COL=14, Q=0.221, LAYER=7, QTYPE=30, $END GRVTY RF
$NEWELL ROW=22, COL=11, Q=0.221, LAYER=7, QTYPE=30, $END GRVTY RF
$NEWELL ROW=23, COL= 8, Q=0.221, LAYER=7, QTYPE=30, $END GRVTY RF
$NEWELL ROW=25, COL= 6, Q=0.221, LAYER=7, QTYPE=30, $END GRVTY RF
$NEWELL ROW=27, COL= 6, Q=0.221, LAYER=7, QTYPE=30, $END GRVTY RF
$NEWELL ROW=27, COL= 7, Q=0.221, LAYER=7, QTYPE=30, $END GRVTY RF
$NEWELL ROW=28, COL= 7, Q=0.221, LAYER=7, QTYPE=30, $END GRVTY RF
$NEWELL ROW=28, COL=12, Q=0.221, LAYER=7, QTYPE=30, $END GRVTY RF
$NEWELL ROW=29, COL=11, Q=0.221, LAYER=7, QTYPE=30, $END GRVTY RF
$NEWELL ROW=30, COL=10, Q=0.221, LAYER=7, QTYPE=30, $END GRVTY RF
$NEWELL ROW=33, COL=11, Q=0.221, LAYER=7, QTYPE=30, $END GRVTY RF
$NEWELL ROW=35, COL=24, Q=0.221, LAYER=7, QTYPE=30, $END GRVTY RF
$NEWELL ROW=35, COL=26, Q=0.221, LAYER=7, QTYPE=30, $END GRVTY RF
$NEWELL ROW=38, COL= 9, Q=0.221, LAYER=7, QTYPE=30, $END GRVTY RF
$NEWELL ROW=38, COL=19, Q=0.221, LAYER=7, QTYPE=30, $END GRVTY RF
$NEWELL ROW=38, COL=20, Q=0.221, LAYER=7, QTYPE=30, $END GRVTY RF
$NEWELL ROW=38, COL=21, Q=0.221, LAYER=7, QTYPE=30, $END GRVTY RF
$NEWELL ROW=38, COL=23, Q=0.221, LAYER=7, QTYPE=30, $END GRVTY RF
$NEWELL ROW=38, COL=28, Q=0.221, LAYER=7, QTYPE=30, $END GRVTY RF
$NEWELL ROW=39, COL=21, Q=0.221, LAYER=7, QTYPE=30, $END GRVTY RF
$NEWELL ROW=39, COL=28, Q=0.221, LAYER=7, QTYPE=30, $END GRVTY RF
$NEWELL ROW=23, COL= 6, Q=0.332, LAYER=7, QTYPE=30, $END GRVTY RF
$NEWELL ROW=15, COL=13, Q=0.442, LAYER=7, QTYPE=30, $END GRVTY RF
$NEWELL ROW=16, COL=19, Q=0.442, LAYER=7, QTYPE=30, $END GRVTY RF
$NEWELL ROW=17, COL=12, Q=0.442, LAYER=7, QTYPE=30, $END GRVTY RF
$NEWELL ROW=21, COL= 6, Q=0.442, LAYER=7, QTYPE=30, $END GRVTY RF
$NEWELL ROW=23, COL= 7, Q=0.442, LAYER=7, QTYPE=30, $END GRVTY RF
$NEWELL ROW=23, COL= 9, Q=0.442, LAYER=7, QTYPE=30, $END GRVTY RF
$NEWELL ROW=25, COL= 8, Q=0.442, LAYER=7, QTYPE=30, $END GRVTY RF
$NEWELL ROW=25, COL=14, Q=0.442, LAYER=7, QTYPE=30, $END GRVTY RF
$NEWELL ROW=25, COL=16, Q=0.442, LAYER=7, QTYPE=30, $END GRVTY RF
$NEWELL ROW=26, COL= 6, Q=0.442, LAYER=7, QTYPE=30, $END GRVTY RF
$NEWELL ROW=27, COL= 9, Q=0.442, LAYER=7, QTYPE=30, $END GRVTY RF
$NEWELL ROW=27, COL=10, Q=0.442, LAYER=7, QTYPE=30, $END GRVTY RF

```

Attachment 2.--Input file for the 1950-79 transient simulation--Continued

\$NEWELL	ROW=29,	COL=17,	Q=0.442,	LAYER=7,	QTYPE=30,	\$END	GRVTY	RF
\$NEWELL	ROW=34,	COL= 8,	Q=0.442,	LAYER=7,	QTYPE=30,	\$END	GRVTY	RF
\$NEWELL	ROW=35,	COL=23,	Q=0.442,	LAYER=7,	QTYPE=30,	\$END	GRVTY	RF
\$NEWELL	ROW=36,	COL=23,	Q=0.442,	LAYER=7,	QTYPE=30,	\$END	GRVTY	RF
\$NEWELL	ROW=37,	COL=23,	Q=0.442,	LAYER=7,	QTYPE=30,	\$END	GRVTY	RF
\$NEWELL	ROW=40,	COL=21,	Q=0.442,	LAYER=7,	QTYPE=30,	\$END	GRVTY	RF
\$NEWELL	ROW=41,	COL=21,	Q=0.442,	LAYER=7,	QTYPE=30,	\$END	GRVTY	RF
\$NEWELL	ROW=43,	COL=15,	Q=0.442,	LAYER=7,	QTYPE=30,	\$END	GRVTY	RF
\$NEWELL	ROW=48,	COL=12,	Q=0.442,	LAYER=7,	QTYPE=30,	\$END	GRVTY	RF
\$NEWELL	ROW=25,	COL= 9,	Q=0.553,	LAYER=7,	QTYPE=30,	\$END	GRVTY	RF
\$NEWELL	ROW=28,	COL= 6,	Q=0.553,	LAYER=7,	QTYPE=30,	\$END	GRVTY	RF
\$NEWELL	ROW= 7,	COL=15,	Q=0.663,	LAYER=7,	QTYPE=30,	\$END	GRVTY	RF
\$NEWELL	ROW=11,	COL=14,	Q=0.663,	LAYER=7,	QTYPE=30,	\$END	GRVTY	RF
\$NEWELL	ROW=12,	COL=14,	Q=0.663,	LAYER=7,	QTYPE=30,	\$END	GRVTY	RF
\$NEWELL	ROW=12,	COL=16,	Q=0.663,	LAYER=7,	QTYPE=30,	\$END	GRVTY	RF
\$NEWELL	ROW=16,	COL= 7,	Q=0.663,	LAYER=7,	QTYPE=30,	\$END	GRVTY	RF
\$NEWELL	ROW=16,	COL=17,	Q=0.663,	LAYER=7,	QTYPE=30,	\$END	GRVTY	RF
\$NEWELL	ROW=22,	COL=14,	Q=0.663,	LAYER=7,	QTYPE=30,	\$END	GRVTY	RF
\$NEWELL	ROW=24,	COL= 7,	Q=0.663,	LAYER=7,	QTYPE=30,	\$END	GRVTY	RF
\$NEWELL	ROW=24,	COL=10,	Q=0.663,	LAYER=7,	QTYPE=30,	\$END	GRVTY	RF
\$NEWELL	ROW=25,	COL= 5,	Q=0.663,	LAYER=7,	QTYPE=30,	\$END	GRVTY	RF
\$NEWELL	ROW=26,	COL= 7,	Q=0.663,	LAYER=7,	QTYPE=30,	\$END	GRVTY	RF
\$NEWELL	ROW=26,	COL=10,	Q=0.663,	LAYER=7,	QTYPE=30,	\$END	GRVTY	RF
\$NEWELL	ROW=26,	COL=15,	Q=0.663,	LAYER=7,	QTYPE=30,	\$END	GRVTY	RF
\$NEWELL	ROW=26,	COL=16,	Q=0.663,	LAYER=7,	QTYPE=30,	\$END	GRVTY	RF
\$NEWELL	ROW=28,	COL=17,	Q=0.663,	LAYER=7,	QTYPE=30,	\$END	GRVTY	RF
\$NEWELL	ROW=29,	COL= 8,	Q=0.663,	LAYER=7,	QTYPE=30,	\$END	GRVTY	RF
\$NEWELL	ROW=33,	COL=12,	Q=0.663,	LAYER=7,	QTYPE=30,	\$END	GRVTY	RF
\$NEWELL	ROW=34,	COL=23,	Q=0.663,	LAYER=7,	QTYPE=30,	\$END	GRVTY	RF
\$NEWELL	ROW=35,	COL=25,	Q=0.663,	LAYER=7,	QTYPE=30,	\$END	GRVTY	RF
\$NEWELL	ROW=39,	COL=27,	Q=0.663,	LAYER=7,	QTYPE=30,	\$END	GRVTY	RF
\$NEWELL	ROW=23,	COL=10,	Q=0.774,	LAYER=7,	QTYPE=30,	\$END	GRVTY	RF
\$NEWELL	ROW=26,	COL= 5,	Q=0.774,	LAYER=7,	QTYPE=30,	\$END	GRVTY	RF
\$NEWELL	ROW=12,	COL=15,	Q=0.884,	LAYER=7,	QTYPE=30,	\$END	GRVTY	RF
\$NEWELL	ROW=13,	COL=14,	Q=0.884,	LAYER=7,	QTYPE=30,	\$END	GRVTY	RF
\$NEWELL	ROW=15,	COL= 9,	Q=0.884,	LAYER=7,	QTYPE=30,	\$END	GRVTY	RF
\$NEWELL	ROW=15,	COL=14,	Q=0.884,	LAYER=7,	QTYPE=30,	\$END	GRVTY	RF
\$NEWELL	ROW=16,	COL= 9,	Q=0.884,	LAYER=7,	QTYPE=30,	\$END	GRVTY	RF
\$NEWELL	ROW=16,	COL=18,	Q=0.884,	LAYER=7,	QTYPE=30,	\$END	GRVTY	RF
\$NEWELL	ROW=17,	COL=16,	Q=0.884,	LAYER=7,	QTYPE=30,	\$END	GRVTY	RF
\$NEWELL	ROW=21,	COL=11,	Q=0.884,	LAYER=7,	QTYPE=30,	\$END	GRVTY	RF
\$NEWELL	ROW=22,	COL= 9,	Q=0.884,	LAYER=7,	QTYPE=30,	\$END	GRVTY	RF
\$NEWELL	ROW=24,	COL= 9,	Q=0.884,	LAYER=7,	QTYPE=30,	\$END	GRVTY	RF
\$NEWELL	ROW=25,	COL= 7,	Q=0.884,	LAYER=7,	QTYPE=30,	\$END	GRVTY	RF
\$NEWELL	ROW=25,	COL=11,	Q=0.884,	LAYER=7,	QTYPE=30,	\$END	GRVTY	RF
\$NEWELL	ROW=26,	COL= 9,	Q=0.884,	LAYER=7,	QTYPE=30,	\$END	GRVTY	RF
\$NEWELL	ROW=26,	COL=11,	Q=0.884,	LAYER=7,	QTYPE=30,	\$END	GRVTY	RF
\$NEWELL	ROW=27,	COL= 2,	Q=0.884,	LAYER=7,	QTYPE=30,	\$END	GRVTY	RF
\$NEWELL	ROW=29,	COL=10,	Q=0.884,	LAYER=7,	QTYPE=30,	\$END	GRVTY	RF
\$NEWELL	ROW=29,	COL=16,	Q=0.884,	LAYER=7,	QTYPE=30,	\$END	GRVTY	RF
\$NEWELL	ROW=38,	COL=27,	Q=0.884,	LAYER=7,	QTYPE=30,	\$END	GRVTY	RF

## Attachment 2.--Input file for the 1950-79 transient simulation--Continued

\$NEWELL	ROW=47,	COL=12,	Q=0.884,	LAYER=7,	QTYPE=30,	\$END	GRVTY RF
\$NEWELL	ROW=47,	COL=15,	Q=0.884,	LAYER=7,	QTYPE=30,	\$END	GRVTY RF
\$NEWELL	ROW=36,	COL=24,	Q=0.995,	LAYER=7,	QTYPE=30,	\$END	GRVTY RF
\$NEWELL	ROW=19,	COL= 6,	Q=1.105,	LAYER=7,	QTYPE=30,	\$END	GRVTY RF
\$NEWELL	ROW=22,	COL= 5,	Q=1.105,	LAYER=7,	QTYPE=30,	\$END	GRVTY RF
\$NEWELL	ROW=23,	COL=12,	Q=1.105,	LAYER=7,	QTYPE=30,	\$END	GRVTY RF
\$NEWELL	ROW=24,	COL= 6,	Q=1.105,	LAYER=7,	QTYPE=30,	\$END	GRVTY RF
\$NEWELL	ROW=24,	COL= 8,	Q=1.105,	LAYER=7,	QTYPE=30,	\$END	GRVTY RF
\$NEWELL	ROW=24,	COL=13,	Q=1.105,	LAYER=7,	QTYPE=30,	\$END	GRVTY RF
\$NEWELL	ROW=24,	COL=15,	Q=1.105,	LAYER=7,	QTYPE=30,	\$END	GRVTY RF
\$NEWELL	ROW=25,	COL=13,	Q=1.105,	LAYER=7,	QTYPE=30,	\$END	GRVTY RF
\$NEWELL	ROW=26,	COL= 8,	Q=1.105,	LAYER=7,	QTYPE=30,	\$END	GRVTY RF
\$NEWELL	ROW=27,	COL= 5,	Q=1.105,	LAYER=7,	QTYPE=30,	\$END	GRVTY RF
\$NEWELL	ROW=27,	COL=14,	Q=1.105,	LAYER=7,	QTYPE=30,	\$END	GRVTY RF
\$NEWELL	ROW=31,	COL=10,	Q=1.105,	LAYER=7,	QTYPE=30,	\$END	GRVTY RF
\$NEWELL	ROW=36,	COL= 8,	Q=1.105,	LAYER=7,	QTYPE=30,	\$END	GRVTY RF
\$NEWELL	ROW=24,	COL=11,	Q=1.216,	LAYER=7,	QTYPE=30,	\$END	GRVTY RF
\$NEWELL	ROW=29,	COL=15,	Q=1.216,	LAYER=7,	QTYPE=30,	\$END	GRVTY RF
\$NEWELL	ROW=30,	COL=11,	Q=1.216,	LAYER=7,	QTYPE=30,	\$END	GRVTY RF
\$NEWELL	ROW= 5,	COL=13,	Q=1.326,	LAYER=7,	QTYPE=30,	\$END	GRVTY RF
\$NEWELL	ROW= 6,	COL=14,	Q=1.326,	LAYER=7,	QTYPE=30,	\$END	GRVTY RF
\$NEWELL	ROW= 7,	COL=13,	Q=1.326,	LAYER=7,	QTYPE=30,	\$END	GRVTY RF
\$NEWELL	ROW=10,	COL=15,	Q=1.326,	LAYER=7,	QTYPE=30,	\$END	GRVTY RF
\$NEWELL	ROW=15,	COL=10,	Q=1.326,	LAYER=7,	QTYPE=30,	\$END	GRVTY RF
\$NEWELL	ROW=16,	COL=10,	Q=1.326,	LAYER=7,	QTYPE=30,	\$END	GRVTY RF
\$NEWELL	ROW=17,	COL= 7,	Q=1.326,	LAYER=7,	QTYPE=30,	\$END	GRVTY RF
\$NEWELL	ROW=17,	COL=13,	Q=1.326,	LAYER=7,	QTYPE=30,	\$END	GRVTY RF
\$NEWELL	ROW=18,	COL= 9,	Q=1.326,	LAYER=7,	QTYPE=30,	\$END	GRVTY RF
\$NEWELL	ROW=20,	COL=11,	Q=1.326,	LAYER=7,	QTYPE=30,	\$END	GRVTY RF
\$NEWELL	ROW=23,	COL= 5,	Q=1.326,	LAYER=7,	QTYPE=30,	\$END	GRVTY RF
\$NEWELL	ROW=28,	COL=14,	Q=1.326,	LAYER=7,	QTYPE=30,	\$END	GRVTY RF
\$NEWELL	ROW=29,	COL= 7,	Q=1.326,	LAYER=7,	QTYPE=30,	\$END	GRVTY RF
\$NEWELL	ROW=30,	COL= 6,	Q=1.326,	LAYER=7,	QTYPE=30,	\$END	GRVTY RF
\$NEWELL	ROW=31,	COL=11,	Q=1.326,	LAYER=7,	QTYPE=30,	\$END	GRVTY RF
\$NEWELL	ROW=33,	COL=10,	Q=1.326,	LAYER=7,	QTYPE=30,	\$END	GRVTY RF
\$NEWELL	ROW=35,	COL= 7,	Q=1.326,	LAYER=7,	QTYPE=30,	\$END	GRVTY RF
\$NEWELL	ROW=35,	COL=12,	Q=1.326,	LAYER=7,	QTYPE=30,	\$END	GRVTY RF
\$NEWELL	ROW=37,	COL= 9,	Q=1.326,	LAYER=7,	QTYPE=30,	\$END	GRVTY RF
\$NEWELL	ROW=10,	COL=14,	Q=1.547,	LAYER=7,	QTYPE=30,	\$END	GRVTY RF
\$NEWELL	ROW=14,	COL= 8,	Q=1.547,	LAYER=7,	QTYPE=30,	\$END	GRVTY RF
\$NEWELL	ROW=14,	COL= 9,	Q=1.547,	LAYER=7,	QTYPE=30,	\$END	GRVTY RF
\$NEWELL	ROW=15,	COL=11,	Q=1.547,	LAYER=7,	QTYPE=30,	\$END	GRVTY RF
\$NEWELL	ROW=20,	COL= 6,	Q=1.547,	LAYER=7,	QTYPE=30,	\$END	GRVTY RF
\$NEWELL	ROW=24,	COL=12,	Q=1.547,	LAYER=7,	QTYPE=30,	\$END	GRVTY RF
\$NEWELL	ROW=25,	COL=15,	Q=1.547,	LAYER=7,	QTYPE=30,	\$END	GRVTY RF
\$NEWELL	ROW=29,	COL= 9,	Q=1.547,	LAYER=7,	QTYPE=30,	\$END	GRVTY RF
\$NEWELL	ROW=32,	COL=11,	Q=1.547,	LAYER=7,	QTYPE=30,	\$END	GRVTY RF
\$NEWELL	ROW=36,	COL=13,	Q=1.547,	LAYER=7,	QTYPE=30,	\$END	GRVTY RF
\$NEWELL	ROW=36,	COL=14,	Q=1.547,	LAYER=7,	QTYPE=30,	\$END	GRVTY RF
\$NEWELL	ROW=37,	COL= 8,	Q=1.547,	LAYER=7,	QTYPE=30,	\$END	GRVTY RF
\$NEWELL	ROW=44,	COL=11,	Q=1.547,	LAYER=7,	QTYPE=30,	\$END	GRVTY RF

## Attachment 2.--Input file for the 1950-79 transient simulation--Continued

```

$NEWELL ROW=29, COL=17, Q=0.442, LAYER=7, QTYPE=30, $END GRVTY RF
$NEWELL ROW=34, COL= 8, Q=0.442, LAYER=7, QTYPE=30, $END GRVTY RF
$NEWELL ROW=47, COL=13, Q=1.547, LAYER=7, QTYPE=30, $END GRVTY RF
$NEWELL ROW=11, COL=15, Q=1.768, LAYER=7, QTYPE=30, $END GRVTY RF
$NEWELL ROW=12, COL= 6, Q=1.768, LAYER=7, QTYPE=30, $END GRVTY RF
$NEWELL ROW=15, COL= 8, Q=1.768, LAYER=7, QTYPE=30, $END GRVTY RF
$NEWELL ROW=16, COL=13, Q=1.768, LAYER=7, QTYPE=30, $END GRVTY RF
$NEWELL ROW=16, COL=15, Q=1.768, LAYER=7, QTYPE=30, $END GRVTY RF
$NEWELL ROW=22, COL= 7, Q=1.768, LAYER=7, QTYPE=30, $END GRVTY RF
$NEWELL ROW=22, COL= 8, Q=1.768, LAYER=7, QTYPE=30, $END GRVTY RF
$NEWELL ROW=22, COL=10, Q=1.768, LAYER=7, QTYPE=30, $END GRVTY RF
$NEWELL ROW=30, COL= 9, Q=1.768, LAYER=7, QTYPE=30, $END GRVTY RF
$NEWELL ROW=33, COL= 7, Q=1.768, LAYER=7, QTYPE=30, $END GRVTY RF
$NEWELL ROW=33, COL= 9, Q=1.768, LAYER=7, QTYPE=30, $END GRVTY RF
$NEWELL ROW=39, COL=10, Q=1.768, LAYER=7, QTYPE=30, $END GRVTY RF
$NEWELL ROW=39, COL=13, Q=1.768, LAYER=7, QTYPE=30, $END GRVTY RF
$NEWELL ROW=40, COL= 9, Q=1.768, LAYER=7, QTYPE=30, $END GRVTY RF
$NEWELL ROW=40, COL=16, Q=1.768, LAYER=7, QTYPE=30, $END GRVTY RF
$NEWELL ROW=40, COL=17, Q=1.768, LAYER=7, QTYPE=30, $END GRVTY RF
$NEWELL ROW=42, COL=15, Q=1.768, LAYER=7, QTYPE=30, $END GRVTY RF
$NEWELL ROW=27, COL= 3, Q=1.879, LAYER=7, QTYPE=30, $END GRVTY RF
$NEWELL ROW=30, COL=12, Q=1.875, LAYER=7, QTYPE=30, $END GRVTY RF
$NEWELL ROW=13, COL=10, Q=1.989, LAYER=7, QTYPE=30, $END GRVTY RF
$NEWELL ROW=26, COL= 2, Q=1.989, LAYER=7, QTYPE=30, $END GRVTY RF
$NEWELL ROW=33, COL= 8, Q=1.989, LAYER=7, QTYPE=30, $END GRVTY RF
$NEWELL ROW=36, COL=27, Q=1.989, LAYER=7, QTYPE=30, $END GRVTY RF
$NEWELL ROW=37, COL=25, Q=1.989, LAYER=7, QTYPE=30, $END GRVTY RF
$NEWELL ROW=41, COL=16, Q=1.989, LAYER=7, QTYPE=30, $END GRVTY RF
$NEWELL ROW=31, COL= 9, Q=2.100, LAYER=7, QTYPE=30, $END GRVTY RF
$NEWELL ROW=12, COL= 5, Q=2.210, LAYER=7, QTYPE=30, $END GRVTY RF
$NEWELL ROW=15, COL=12, Q=2.210, LAYER=7, QTYPE=30, $END GRVTY RF
$NEWELL ROW=16, COL=12, Q=2.210, LAYER=7, QTYPE=30, $END GRVTY RF
$NEWELL ROW=17, COL= 8, Q=2.210, LAYER=7, QTYPE=30, $END GRVTY RF
$NEWELL ROW=22, COL= 6, Q=2.210, LAYER=7, QTYPE=30, $END GRVTY RF
$NEWELL ROW=23, COL=13, Q=2.210, LAYER=7, QTYPE=30, $END GRVTY RF
$NEWELL ROW=26, COL= 3, Q=2.210, LAYER=7, QTYPE=30, $END GRVTY RF
$NEWELL ROW=27, COL=16, Q=2.210, LAYER=7, QTYPE=30, $END GRVTY RF
$NEWELL ROW=28, COL=15, Q=2.210, LAYER=7, QTYPE=30, $END GRVTY RF
$NEWELL ROW=32, COL= 9, Q=2.210, LAYER=7, QTYPE=30, $END GRVTY RF
$NEWELL ROW=32, COL=10, Q=2.210, LAYER=7, QTYPE=30, $END GRVTY RF
$NEWELL ROW=34, COL= 7, Q=2.210, LAYER=7, QTYPE=30, $END GRVTY RF
$NEWELL ROW=35, COL=11, Q=2.210, LAYER=7, QTYPE=30, $END GRVTY RF
$NEWELL ROW=40, COL=10, Q=2.210, LAYER=7, QTYPE=30, $END GRVTY RF
$NEWELL ROW=41, COL=13, Q=2.210, LAYER=7, QTYPE=30, $END GRVTY RF
$NEWELL ROW=48, COL=13, Q=2.210, LAYER=7, QTYPE=30, $END GRVTY RF
$NEWELL ROW= 6, COL=13, Q=2.431, LAYER=7, QTYPE=30, $END GRVTY RF
$NEWELL ROW=13, COL=15, Q=2.431, LAYER=7, QTYPE=30, $END GRVTY RF
$NEWELL ROW=17, COL=17, Q=2.431, LAYER=7, QTYPE=30, $END GRVTY RF
$NEWELL ROW=21, COL=10, Q=2.431, LAYER=7, QTYPE=30, $END GRVTY RF
$NEWELL ROW=23, COL=14, Q=2.431, LAYER=7, QTYPE=30, $END GRVTY RF
$NEWELL ROW=24, COL=14, Q=2.431, LAYER=7, QTYPE=30, $END GRVTY RF

```



Attachment 2.--Input file for the 1950-79 transient simulation--Continued

\$NEWELL	ROW=27,	COL= 4,	Q=2.431,	LAYER=7,	QTYPE=30,	\$END	GRVTY RF
\$NEWELL	ROW=27,	COL=15,	Q=2.431,	LAYER=7,	QTYPE=30,	\$END	GRVTY RF
\$NEWELL	ROW=31,	COL= 7,	Q=2.431,	LAYER=7,	QTYPE=30,	\$END	GRVTY RF
\$NEWELL	ROW=36,	COL= 9,	Q=2.431,	LAYER=7,	QTYPE=30,	\$END	GRVTY RF
\$NEWELL	ROW=36,	COL=12,	Q=2.431,	LAYER=7,	QTYPE=30,	\$END	GRVTY RF
\$NEWELL	ROW=36,	COL=25,	Q=2.431,	LAYER=7,	QTYPE=30,	\$END	GRVTY RF
\$NEWELL	ROW=36,	COL=26,	Q=2.431,	LAYER=7,	QTYPE=30,	\$END	GRVTY RF
\$NEWELL	ROW=37,	COL=13,	Q=2.431,	LAYER=7,	QTYPE=30,	\$END	GRVTY RF
\$NEWELL	ROW=37,	COL=15,	Q=2.431,	LAYER=7,	QTYPE=30,	\$END	GRVTY RF
\$NEWELL	ROW=37,	COL=27,	Q=2.431,	LAYER=7,	QTYPE=30,	\$END	GRVTY RF
\$NEWELL	ROW=38,	COL=11,	Q=2.431,	LAYER=7,	QTYPE=30,	\$END	GRVTY RF
\$NEWELL	ROW=45,	COL=11,	Q=2.431,	LAYER=7,	QTYPE=30,	\$END	GRVTY RF
\$NEWELL	ROW=48,	COL=14,	Q=2.431,	LAYER=7,	QTYPE=30,	\$END	GRVTY RF
\$NEWELL	ROW= 5,	COL=12,	Q=2.652,	LAYER=7,	QTYPE=30,	\$END	GRVTY RF
\$NEWELL	ROW=13,	COL= 6,	Q=2.652,	LAYER=7,	QTYPE=30,	\$END	GRVTY RF
\$NEWELL	ROW=18,	COL= 7,	Q=2.652,	LAYER=7,	QTYPE=30,	\$END	GRVTY RF
\$NEWELL	ROW=19,	COL= 8,	Q=2.652,	LAYER=7,	QTYPE=30,	\$END	GRVTY RF
\$NEWELL	ROW=30,	COL= 8,	Q=2.652,	LAYER=7,	QTYPE=30,	\$END	GRVTY RF
\$NEWELL	ROW=36,	COL=11,	Q=2.652,	LAYER=7,	QTYPE=30,	\$END	GRVTY RF
\$NEWELL	ROW=37,	COL=10,	Q=2.652,	LAYER=7,	QTYPE=30,	\$END	GRVTY RF
\$NEWELL	ROW=37,	COL=26,	Q=2.652,	LAYER=7,	QTYPE=30,	\$END	GRVTY RF
\$NEWELL	ROW=38,	COL=10,	Q=2.652,	LAYER=7,	QTYPE=30,	\$END	GRVTY RF
\$NEWELL	ROW=39,	COL=11,	Q=2.652,	LAYER=7,	QTYPE=30,	\$END	GRVTY RF
\$NEWELL	ROW=39,	COL=12,	Q=2.652,	LAYER=7,	QTYPE=30,	\$END	GRVTY RF
\$NEWELL	ROW=41,	COL=12,	Q=2.652,	LAYER=7,	QTYPE=30,	\$END	GRVTY RF
\$NEWELL	ROW=42,	COL=14,	Q=2.652,	LAYER=7,	QTYPE=30,	\$END	GRVTY RF
\$NEWELL	ROW=45,	COL=13,	Q=2.652,	LAYER=7,	QTYPE=30,	\$END	GRVTY RF
\$NEWELL	ROW= 7,	COL=14,	Q=2.727,	LAYER=7,	QTYPE=30,	\$END	GRVTY RF
\$NEWELL	ROW=19,	COL= 7,	Q=2.873,	LAYER=7,	QTYPE=30,	\$END	GRVTY RF
\$NEWELL	ROW=32,	COL=15,	Q=2.873,	LAYER=7,	QTYPE=30,	\$END	GRVTY RF
\$NEWELL	ROW=37,	COL=12,	Q=2.873,	LAYER=7,	QTYPE=30,	\$END	GRVTY RF
\$NEWELL	ROW=38,	COL=12,	Q=2.873,	LAYER=7,	QTYPE=30,	\$END	GRVTY RF
\$NEWELL	ROW=40,	COL=11,	Q=2.873,	LAYER=7,	QTYPE=30,	\$END	GRVTY RF
\$NEWELL	ROW=47,	COL=14,	Q=2.873,	LAYER=7,	QTYPE=30,	\$END	GRVTY RF
\$NEWELL	ROW=13,	COL= 7,	Q=3.094,	LAYER=7,	QTYPE=30,	\$END	GRVTY RF
\$NEWELL	ROW=13,	COL= 9,	Q=3.094,	LAYER=7,	QTYPE=30,	\$END	GRVTY RF
\$NEWELL	ROW=14,	COL=10,	Q=3.094,	LAYER=7,	QTYPE=30,	\$END	GRVTY RF
\$NEWELL	ROW=21,	COL= 7,	Q=3.094,	LAYER=7,	QTYPE=30,	\$END	GRVTY RF
\$NEWELL	ROW=28,	COL=16,	Q=3.094,	LAYER=7,	QTYPE=30,	\$END	GRVTY RF
\$NEWELL	ROW=31,	COL= 8,	Q=3.094,	LAYER=7,	QTYPE=30,	\$END	GRVTY RF
\$NEWELL	ROW=33,	COL=15,	Q=3.094,	LAYER=7,	QTYPE=30,	\$END	GRVTY RF
\$NEWELL	ROW=35,	COL= 8,	Q=3.094,	LAYER=7,	QTYPE=30,	\$END	GRVTY RF
\$NEWELL	ROW=35,	COL=10,	Q=3.094,	LAYER=7,	QTYPE=30,	\$END	GRVTY RF
\$NEWELL	ROW=37,	COL=14,	Q=3.094,	LAYER=7,	QTYPE=30,	\$END	GRVTY RF
\$NEWELL	ROW=40,	COL=15,	Q=3.094,	LAYER=7,	QTYPE=30,	\$END	GRVTY RF
\$NEWELL	ROW=41,	COL=14,	Q=3.094,	LAYER=7,	QTYPE=30,	\$END	GRVTY RF
\$NEWELL	ROW=41,	COL=15,	Q=3.094,	LAYER=7,	QTYPE=30,	\$END	GRVTY RF
\$NEWELL	ROW=44,	COL=13,	Q=3.094,	LAYER=7,	QTYPE=30,	\$END	GRVTY RF
\$NEWELL	ROW=45,	COL=12,	Q=3.094,	LAYER=7,	QTYPE=30,	\$END	GRVTY RF
\$NEWELL	ROW=46,	COL=11,	Q=3.094,	LAYER=7,	QTYPE=30,	\$END	GRVTY RF
\$NEWELL	ROW=13,	COL= 8,	Q=3.315,	LAYER=7,	QTYPE=30,	\$END	GRVTY RF

## Attachment 2.--Input file for the 1950-79 transient simulation--Continued

```

$NEWELL ROW=14, COL=11, Q=3.315, LAYER=7, QTYPE=30, $END GRVTY RF
$NEWELL ROW=16, COL= 8, Q=3.315, LAYER=7, QTYPE=30, $END GRVTY RF
$NEWELL ROW=20, COL= 7, Q=3.315, LAYER=7, QTYPE=30, $END GRVTY RF
$NEWELL ROW=20, COL=10, Q=3.315, LAYER=7, QTYPE=30, $END GRVTY RF
$NEWELL ROW=30, COL= 7, Q=3.315, LAYER=7, QTYPE=30, $END GRVTY RF
$NEWELL ROW=32, COL= 7, Q=3.315, LAYER=7, QTYPE=30, $END GRVTY RF
$NEWELL ROW=35, COL= 9, Q=3.315, LAYER=7, QTYPE=30, $END GRVTY RF
$NEWELL ROW=36, COL=10, Q=3.315, LAYER=7, QTYPE=30, $END GRVTY RF
$NEWELL ROW=37, COL=11, Q=3.315, LAYER=7, QTYPE=30, $END GRVTY RF
$NEWELL ROW=38, COL=13, Q=3.315, LAYER=7, QTYPE=30, $END GRVTY RF
$NEWELL ROW=38, COL=14, Q=3.315, LAYER=7, QTYPE=30, $END GRVTY RF
$NEWELL ROW=42, COL=13, Q=3.315, LAYER=7, QTYPE=30, $END GRVTY RF
$NEWELL ROW=43, COL=14, Q=3.315, LAYER=7, QTYPE=30, $END GRVTY RF
$NEWELL ROW=18, COL= 8, Q=3.536, LAYER=7, QTYPE=30, $END GRVTY RF
$NEWELL ROW=20, COL= 8, Q=3.536, LAYER=7, QTYPE=30, $END GRVTY RF
$NEWELL ROW=20, COL= 9, Q=3.536, LAYER=7, QTYPE=30, $END GRVTY RF
$NEWELL ROW=21, COL= 8, Q=3.536, LAYER=7, QTYPE=30, $END GRVTY RF
$NEWELL ROW=21, COL= 9, Q=3.536, LAYER=7, QTYPE=30, $END GRVTY RF
$NEWELL ROW=32, COL= 8, Q=3.536, LAYER=7, QTYPE=30, $END GRVTY RF
$NEWELL ROW=38, COL=15, Q=3.536, LAYER=7, QTYPE=30, $END GRVTY RF
$NEWELL ROW=39, COL=14, Q=3.536, LAYER=7, QTYPE=30, $END GRVTY RF
$NEWELL ROW=39, COL=15, Q=3.536, LAYER=7, QTYPE=30, $END GRVTY RF
$NEWELL ROW=39, COL=16, Q=3.536, LAYER=7, QTYPE=30, $END GRVTY RF
$NEWELL ROW=40, COL=12, Q=3.536, LAYER=7, QTYPE=30, $END GRVTY RF
$NEWELL ROW=40, COL=13, Q=3.536, LAYER=7, QTYPE=30, $END GRVTY RF
$NEWELL ROW=40, COL=14, Q=3.536, LAYER=7, QTYPE=30, $END GRVTY RF
$NEWELL ROW=41, COL=11, Q=3.536, LAYER=7, QTYPE=30, $END GRVTY RF
$NEWELL ROW=42, COL=11, Q=3.536, LAYER=7, QTYPE=30, $END GRVTY RF
$NEWELL ROW=42, COL=12, Q=3.536, LAYER=7, QTYPE=30, $END GRVTY RF
$NEWELL ROW=43, COL=11, Q=3.536, LAYER=7, QTYPE=30, $END GRVTY RF
$NEWELL ROW=43, COL=12, Q=3.536, LAYER=7, QTYPE=30, $END GRVTY RF
$NEWELL ROW=43, COL=13, Q=3.536, LAYER=7, QTYPE=30, $END GRVTY RF
$NEWELL ROW=44, COL=12, Q=3.536, LAYER=7, QTYPE=30, $END GRVTY RF
$NEWELL ROW= 7, COL=14, Q=0.111, LAYER=7, QTYPE=40, $END SPKLR RF
$NEWELL ROW= 6, COL=13, Q=0.221, LAYER=7, QTYPE=40, $END SPKLR RF
$NEWELL ROW=12, COL= 7, Q=0.221, LAYER=7, QTYPE=40, $END SPKLR RF
$NEWELL ROW=12, COL= 8, Q=0.221, LAYER=7, QTYPE=40, $END SPKLR RF
$NEWELL ROW=12, COL=12, Q=0.221, LAYER=7, QTYPE=40, $END SPKLR RF
$NEWELL ROW=13, COL=15, Q=0.221, LAYER=7, QTYPE=40, $END SPKLR RF
$NEWELL ROW=14, COL= 9, Q=0.221, LAYER=7, QTYPE=40, $END SPKLR RF
$NEWELL ROW=14, COL=13, Q=0.221, LAYER=7, QTYPE=40, $END SPKLR RF
$NEWELL ROW=14, COL=14, Q=0.221, LAYER=7, QTYPE=40, $END SPKLR RF
$NEWELL ROW=16, COL= 8, Q=0.221, LAYER=7, QTYPE=40, $END SPKLR RF
$NEWELL ROW=16, COL=17, Q=0.221, LAYER=7, QTYPE=40, $END SPKLR RF
$NEWELL ROW=20, COL= 7, Q=0.221, LAYER=7, QTYPE=40, $END SPKLR RF
$NEWELL ROW=20, COL=10, Q=0.221, LAYER=7, QTYPE=40, $END SPKLR RF
$NEWELL ROW=28, COL=17, Q=0.221, LAYER=7, QTYPE=40, $END SPKLR RF
$NEWELL ROW=30, COL= 8, Q=0.221, LAYER=7, QTYPE=40, $END SPKLR RF
$NEWELL ROW=31, COL= 8, Q=0.221, LAYER=7, QTYPE=40, $END SPKLR RF
$NEWELL ROW=33, COL= 8, Q=0.221, LAYER=7, QTYPE=40, $END SPKLR RF
$NEWELL ROW=34, COL= 9, Q=0.221, LAYER=7, QTYPE=40, $END SPKLR RF

```

Attachment 2.--Input file for the 1950-79 transient simulation--Continued

\$NEWELL	ROW=34,	COL=22,	Q=0.221,	LAYER=7,	QTYPE=40,	\$END	SPKLR RF
\$NEWELL	ROW=35,	COL= 9,	Q=0.221,	LAYER=7,	QTYPE=40,	\$END	SPKLR RF
\$NEWELL	ROW=35,	COL=10,	Q=0.221,	LAYER=7,	QTYPE=40,	\$END	SPKLR RF
\$NEWELL	ROW=35,	COL=23,	Q=0.221,	LAYER=7,	QTYPE=40,	\$END	SPKLR RF
\$NEWELL	ROW=35,	COL=24,	Q=0.221,	LAYER=7,	QTYPE=40,	\$END	SPKLR RF
\$NEWELL	ROW=36,	COL=10,	Q=0.221,	LAYER=7,	QTYPE=40,	\$END	SPKLR RF
\$NEWELL	ROW=36,	COL=23,	Q=0.221,	LAYER=7,	QTYPE=40,	\$END	SPKLR RF
\$NEWELL	ROW=36,	COL=25,	Q=0.221,	LAYER=7,	QTYPE=40,	\$END	SPKLR RF
\$NEWELL	ROW=36,	COL=27,	Q=0.221,	LAYER=7,	QTYPE=40,	\$END	SPKLR RF
\$NEWELL	ROW=37,	COL= 9,	Q=0.221,	LAYER=7,	QTYPE=40,	\$END	SPKLR RF
\$NEWELL	ROW=37,	COL=11,	Q=0.221,	LAYER=7,	QTYPE=40,	\$END	SPKLR RF
\$NEWELL	ROW=37,	COL=13,	Q=0.221,	LAYER=7,	QTYPE=40,	\$END	SPKLR RF
\$NEWELL	ROW=37,	COL=15,	Q=0.221,	LAYER=7,	QTYPE=40,	\$END	SPKLR RF
\$NEWELL	ROW=37,	COL=25,	Q=0.221,	LAYER=7,	QTYPE=40,	\$END	SPKLR RF
\$NEWELL	ROW=38,	COL=12,	Q=0.221,	LAYER=7,	QTYPE=40,	\$END	SPKLR RF
\$NEWELL	ROW=38,	COL=14,	Q=0.221,	LAYER=7,	QTYPE=40,	\$END	SPKLR RF
\$NEWELL	ROW=38,	COL=28,	Q=0.221,	LAYER=7,	QTYPE=40,	\$END	SPKLR RF
\$NEWELL	ROW=39,	COL=12,	Q=0.221,	LAYER=7,	QTYPE=40,	\$END	SPKLR RF
\$NEWELL	ROW=40,	COL= 9,	Q=0.221,	LAYER=7,	QTYPE=40,	\$END	SPKLR RF
\$NEWELL	ROW=42,	COL=13,	Q=0.221,	LAYER=7,	QTYPE=40,	\$END	SPKLR RF
\$NEWELL	ROW=45,	COL=13,	Q=0.221,	LAYER=7,	QTYPE=40,	\$END	SPKLR RF
\$NEWELL	ROW=12,	COL=11,	Q=0.332,	LAYER=7,	QTYPE=40,	\$END	SPKLR RF
\$NEWELL	ROW=27,	COL= 3,	Q=0.332,	LAYER=7,	QTYPE=40,	\$END	SPKLR RF
\$NEWELL	ROW=10,	COL=15,	Q=0.442,	LAYER=7,	QTYPE=40,	\$END	SPKLR RF
\$NEWELL	ROW=15,	COL=13,	Q=0.442,	LAYER=7,	QTYPE=40,	\$END	SPKLR RF
\$NEWELL	ROW=16,	COL=19,	Q=0.442,	LAYER=7,	QTYPE=40,	\$END	SPKLR RF
\$NEWELL	ROW=21,	COL= 7,	Q=0.442,	LAYER=7,	QTYPE=40,	\$END	SPKLR RF
\$NEWELL	ROW=23,	COL= 5,	Q=0.442,	LAYER=7,	QTYPE=40,	\$END	SPKLR RF
\$NEWELL	ROW=25,	COL= 4,	Q=0.442,	LAYER=7,	QTYPE=40,	\$END	SPKLR RF
\$NEWELL	ROW=26,	COL= 3,	Q=0.442,	LAYER=7,	QTYPE=40,	\$END	SPKLR RF
\$NEWELL	ROW=28,	COL=16,	Q=0.442,	LAYER=7,	QTYPE=40,	\$END	SPKLR RF
\$NEWELL	ROW=30,	COL= 6,	Q=0.442,	LAYER=7,	QTYPE=40,	\$END	SPKLR RF
\$NEWELL	ROW=30,	COL= 9,	Q=0.442,	LAYER=7,	QTYPE=40,	\$END	SPKLR RF
\$NEWELL	ROW=30,	COL=15,	Q=0.442,	LAYER=7,	QTYPE=40,	\$END	SPKLR RF
\$NEWELL	ROW=32,	COL=15,	Q=0.442,	LAYER=7,	QTYPE=40,	\$END	SPKLR RF
\$NEWELL	ROW=33,	COL=12,	Q=0.442,	LAYER=7,	QTYPE=40,	\$END	SPKLR RF
\$NEWELL	ROW=35,	COL= 8,	Q=0.442,	LAYER=7,	QTYPE=40,	\$END	SPKLR RF
\$NEWELL	ROW=35,	COL=11,	Q=0.442,	LAYER=7,	QTYPE=40,	\$END	SPKLR RF
\$NEWELL	ROW=37,	COL= 8,	Q=0.442,	LAYER=7,	QTYPE=40,	\$END	SPKLR RF
\$NEWELL	ROW=37,	COL=12,	Q=0.442,	LAYER=7,	QTYPE=40,	\$END	SPKLR RF
\$NEWELL	ROW=37,	COL=14,	Q=0.442,	LAYER=7,	QTYPE=40,	\$END	SPKLR RF
\$NEWELL	ROW=37,	COL=24,	Q=0.442,	LAYER=7,	QTYPE=40,	\$END	SPKLR RF
\$NEWELL	ROW=39,	COL=20,	Q=0.442,	LAYER=7,	QTYPE=40,	\$END	SPKLR RF
\$NEWELL	ROW=39,	COL=28,	Q=0.442,	LAYER=7,	QTYPE=40,	\$END	SPKLR RF
\$NEWELL	ROW=40,	COL=10,	Q=0.442,	LAYER=7,	QTYPE=40,	\$END	SPKLR RF
\$NEWELL	ROW=45,	COL=12,	Q=0.442,	LAYER=7,	QTYPE=40,	\$END	SPKLR RF
\$NEWELL	ROW=46,	COL=11,	Q=0.442,	LAYER=7,	QTYPE=40,	\$END	SPKLR RF
\$NEWELL	ROW=48,	COL=13,	Q=0.442,	LAYER=7,	QTYPE=40,	\$END	SPKLR RF
\$NEWELL	ROW=12,	COL=13,	Q=0.663,	LAYER=7,	QTYPE=40,	\$END	SPKLR RF
\$NEWELL	ROW=12,	COL=16,	Q=0.663,	LAYER=7,	QTYPE=40,	\$END	SPKLR RF
\$NEWELL	ROW=14,	COL=12,	Q=0.663,	LAYER=7,	QTYPE=40,	\$END	SPKLR RF

Attachment 2.--Input file for the 1950-79 transient simulation--Continued

\$NEWELL	ROW=22,	COL=13,	Q=0.663,	LAYER=7,	QTYPE=40,	\$END	SPKLR	RF
\$NEWELL	ROW=24,	COL=14,	Q=0.663,	LAYER=7,	QTYPE=40,	\$END	SPKLR	RF
\$NEWELL	ROW=30,	COL=10,	Q=0.663,	LAYER=7,	QTYPE=40,	\$END	SPKLR	RF
\$NEWELL	ROW=31,	COL= 7,	Q=0.663,	LAYER=7,	QTYPE=40,	\$END	SPKLR	RF
\$NEWELL	ROW=31,	COL=11,	Q=0.663,	LAYER=7,	QTYPE=40,	\$END	SPKLR	RF
\$NEWELL	ROW=34,	COL=10,	Q=0.663,	LAYER=7,	QTYPE=40,	\$END	SPKLR	RF
\$NEWELL	ROW=35,	COL=13,	Q=0.663,	LAYER=7,	QTYPE=40,	\$END	SPKLR	RF
\$NEWELL	ROW=37,	COL=27,	Q=0.663,	LAYER=7,	QTYPE=40,	\$END	SPKLR	RF
\$NEWELL	ROW=38,	COL=19,	Q=0.663,	LAYER=7,	QTYPE=40,	\$END	SPKLR	RF
\$NEWELL	ROW=39,	COL= 9,	Q=0.663,	LAYER=7,	QTYPE=40,	\$END	SPKLR	RF
\$NEWELL	ROW=13,	COL=10,	Q=0.884,	LAYER=7,	QTYPE=40,	\$END	SPKLR	RF
\$NEWELL	ROW=19,	COL= 6,	Q=0.884,	LAYER=7,	QTYPE=40,	\$END	SPKLR	RF
\$NEWELL	ROW=21,	COL=11,	Q=0.884,	LAYER=7,	QTYPE=40,	\$END	SPKLR	RF
\$NEWELL	ROW=21,	COL=14,	Q=0.884,	LAYER=7,	QTYPE=40,	\$END	SPKLR	RF
\$NEWELL	ROW=22,	COL=14,	Q=0.884,	LAYER=7,	QTYPE=40,	\$END	SPKLR	RF
\$NEWELL	ROW=31,	COL= 6,	Q=0.884,	LAYER=7,	QTYPE=40,	\$END	SPKLR	RF
\$NEWELL	ROW=31,	COL=10,	Q=0.884,	LAYER=7,	QTYPE=40,	\$END	SPKLR	RF
\$NEWELL	ROW=35,	COL= 7,	Q=0.884,	LAYER=7,	QTYPE=40,	\$END	SPKLR	RF
\$NEWELL	ROW=35,	COL=12,	Q=0.884,	LAYER=7,	QTYPE=40,	\$END	SPKLR	RF
\$NEWELL	ROW=36,	COL=11,	Q=0.884,	LAYER=7,	QTYPE=40,	\$END	SPKLR	RF
\$NEWELL	ROW=36,	COL=26,	Q=0.884,	LAYER=7,	QTYPE=40,	\$END	SPKLR	RF
\$NEWELL	ROW=37,	COL=10,	Q=0.884,	LAYER=7,	QTYPE=40,	\$END	SPKLR	RF
\$NEWELL	ROW=37,	COL=26,	Q=0.884,	LAYER=7,	QTYPE=40,	\$END	SPKLR	RF
\$NEWELL	ROW=38,	COL=10,	Q=0.884,	LAYER=7,	QTYPE=40,	\$END	SPKLR	RF
\$NEWELL	ROW=39,	COL=11,	Q=0.884,	LAYER=7,	QTYPE=40,	\$END	SPKLR	RF
\$NEWELL	ROW=39,	COL=19,	Q=0.884,	LAYER=7,	QTYPE=40,	\$END	SPKLR	RF
\$NEWELL	ROW=40,	COL=20,	Q=0.884,	LAYER=7,	QTYPE=40,	\$END	SPKLR	RF
\$NEWELL	ROW=47,	COL=12,	Q=0.884,	LAYER=7,	QTYPE=40,	\$END	SPKLR	RF
\$NEWELL	ROW=10,	COL=14,	Q=1.105,	LAYER=7,	QTYPE=40,	\$END	SPKLR	RF
\$NEWELL	ROW=11,	COL=15,	Q=1.105,	LAYER=7,	QTYPE=40,	\$END	SPKLR	RF
\$NEWELL	ROW=13,	COL=11,	Q=1.105,	LAYER=7,	QTYPE=40,	\$END	SPKLR	RF
\$NEWELL	ROW=13,	COL=13,	Q=1.105,	LAYER=7,	QTYPE=40,	\$END	SPKLR	RF
\$NEWELL	ROW=20,	COL= 6,	Q=1.105,	LAYER=7,	QTYPE=40,	\$END	SPKLR	RF
\$NEWELL	ROW=21,	COL=10,	Q=1.105,	LAYER=7,	QTYPE=40,	\$END	SPKLR	RF
\$NEWELL	ROW=22,	COL= 5,	Q=1.105,	LAYER=7,	QTYPE=40,	\$END	SPKLR	RF
\$NEWELL	ROW=23,	COL=14,	Q=1.105,	LAYER=7,	QTYPE=40,	\$END	SPKLR	RF
\$NEWELL	ROW=25,	COL=15,	Q=1.105,	LAYER=7,	QTYPE=40,	\$END	SPKLR	RF
\$NEWELL	ROW=27,	COL= 4,	Q=1.105,	LAYER=7,	QTYPE=40,	\$END	SPKLR	RF
\$NEWELL	ROW=27,	COL=15,	Q=1.105,	LAYER=7,	QTYPE=40,	\$END	SPKLR	RF
\$NEWELL	ROW=32,	COL=11,	Q=1.105,	LAYER=7,	QTYPE=40,	\$END	SPKLR	RF
\$NEWELL	ROW=36,	COL= 9,	Q=1.105,	LAYER=7,	QTYPE=40,	\$END	SPKLR	RF
\$NEWELL	ROW=36,	COL=12,	Q=1.105,	LAYER=7,	QTYPE=40,	\$END	SPKLR	RF
\$NEWELL	ROW=38,	COL= 9,	Q=1.105,	LAYER=7,	QTYPE=40,	\$END	SPKLR	RF
\$NEWELL	ROW=38,	COL=11,	Q=1.105,	LAYER=7,	QTYPE=40,	\$END	SPKLR	RF
\$NEWELL	ROW=45,	COL=11,	Q=1.105,	LAYER=7,	QTYPE=40,	\$END	SPKLR	RF
\$NEWELL	ROW=12,	COL=14,	Q=1.326,	LAYER=7,	QTYPE=40,	\$END	SPKLR	RF
\$NEWELL	ROW=21,	COL=13,	Q=1.326,	LAYER=7,	QTYPE=40,	\$END	SPKLR	RF
\$NEWELL	ROW=22,	COL= 6,	Q=1.326,	LAYER=7,	QTYPE=40,	\$END	SPKLR	RF
\$NEWELL	ROW=23,	COL=13,	Q=1.326,	LAYER=7,	QTYPE=40,	\$END	SPKLR	RF
\$NEWELL	ROW=27,	COL=16,	Q=1.326,	LAYER=7,	QTYPE=40,	\$END	SPKLR	RF
\$NEWELL	ROW=28,	COL=15,	Q=1.326,	LAYER=7,	QTYPE=40,	\$END	SPKLR	RF

Attachment 2.--Input file for the 1950-79 transient simulation--Continued

\$NEWELL	ROW=29,	COL= 7,	Q=1.326,	LAYER=7,	QTYPE=40,	\$END	SPKLR RF
\$NEWELL	ROW=29,	COL=16,	Q=1.326,	LAYER=7,	QTYPE=40,	\$END	SPKLR RF
\$NEWELL	ROW=32,	COL= 9,	Q=1.326,	LAYER=7,	QTYPE=40,	\$END	SPKLR RF
\$NEWELL	ROW=32,	COL=10,	Q=1.326,	LAYER=7,	QTYPE=40,	\$END	SPKLR RF
\$NEWELL	ROW=49,	COL=13,	Q=1.326,	LAYER=7,	QTYPE=40,	\$END	SPKLR RF
\$NEWELL	ROW=29,	COL=15,	Q=1.437,	LAYER=7,	QTYPE=40,	\$END	SPKLR RF
\$NEWELL	ROW=31,	COL= 9,	Q=1.437,	LAYER=7,	QTYPE=40,	\$END	SPKLR RF
\$NEWELL	ROW=23,	COL=12,	Q=1.547,	LAYER=7,	QTYPE=40,	\$END	SPKLR RF
\$NEWELL	ROW=26,	COL=15,	Q=1.547,	LAYER=7,	QTYPE=40,	\$END	SPKLR RF
\$NEWELL	ROW=28,	COL=13,	Q=1.547,	LAYER=7,	QTYPE=40,	\$END	SPKLR RF
\$NEWELL	ROW=39,	COL=27,	Q=1.547,	LAYER=7,	QTYPE=40,	\$END	SPKLR RF
\$NEWELL	ROW=30,	COL=12,	Q=1.658,	LAYER=7,	QTYPE=40,	\$END	SPKLR RF
\$NEWELL	ROW=36,	COL=24,	Q=1.658,	LAYER=7,	QTYPE=40,	\$END	SPKLR RF
\$NEWELL	ROW=15,	COL= 8,	Q=1.768,	LAYER=7,	QTYPE=40,	\$END	SPKLR RF
\$NEWELL	ROW=15,	COL= 9,	Q=1.768,	LAYER=7,	QTYPE=40,	\$END	SPKLR RF
\$NEWELL	ROW=22,	COL= 7,	Q=1.768,	LAYER=7,	QTYPE=40,	\$END	SPKLR RF
\$NEWELL	ROW=22,	COL= 8,	Q=1.768,	LAYER=7,	QTYPE=40,	\$END	SPKLR RF
\$NEWELL	ROW=22,	COL=10,	Q=1.768,	LAYER=7,	QTYPE=40,	\$END	SPKLR RF
\$NEWELL	ROW=25,	COL=13,	Q=1.768,	LAYER=7,	QTYPE=40,	\$END	SPKLR RF
\$NEWELL	ROW=25,	COL=16,	Q=1.768,	LAYER=7,	QTYPE=40,	\$END	SPKLR RF
\$NEWELL	ROW=26,	COL=16,	Q=1.768,	LAYER=7,	QTYPE=40,	\$END	SPKLR RF
\$NEWELL	ROW=29,	COL=12,	Q=1.768,	LAYER=7,	QTYPE=40,	\$END	SPKLR RF
\$NEWELL	ROW=29,	COL=14,	Q=1.768,	LAYER=7,	QTYPE=40,	\$END	SPKLR RF
\$NEWELL	ROW=36,	COL=14,	Q=1.768,	LAYER=7,	QTYPE=40,	\$END	SPKLR RF
\$NEWELL	ROW=38,	COL=26,	Q=1.768,	LAYER=7,	QTYPE=40,	\$END	SPKLR RF
\$NEWELL	ROW=38,	COL=27,	Q=1.768,	LAYER=7,	QTYPE=40,	\$END	SPKLR RF
\$NEWELL	ROW=39,	COL=10,	Q=1.768,	LAYER=7,	QTYPE=40,	\$END	SPKLR RF
\$NEWELL	ROW=48,	COL=12,	Q=1.768,	LAYER=7,	QTYPE=40,	\$END	SPKLR RF
\$NEWELL	ROW=11,	COL=14,	Q=1.989,	LAYER=7,	QTYPE=40,	\$END	SPKLR RF
\$NEWELL	ROW=14,	COL= 8,	Q=1.989,	LAYER=7,	QTYPE=40,	\$END	SPKLR RF
\$NEWELL	ROW=24,	COL=12,	Q=1.989,	LAYER=7,	QTYPE=40,	\$END	SPKLR RF
\$NEWELL	ROW=25,	COL= 5,	Q=1.989,	LAYER=7,	QTYPE=40,	\$END	SPKLR RF
\$NEWELL	ROW=25,	COL=14,	Q=1.989,	LAYER=7,	QTYPE=40,	\$END	SPKLR RF
\$NEWELL	ROW=29,	COL= 9,	Q=1.989,	LAYER=7,	QTYPE=40,	\$END	SPKLR RF
\$NEWELL	ROW=36,	COL=13,	Q=1.989,	LAYER=7,	QTYPE=40,	\$END	SPKLR RF
\$NEWELL	ROW=39,	COL=21,	Q=1.989,	LAYER=7,	QTYPE=40,	\$END	SPKLR RF
\$NEWELL	ROW=44,	COL=11,	Q=1.989,	LAYER=7,	QTYPE=40,	\$END	SPKLR RF
\$NEWELL	ROW=30,	COL=11,	Q=2.100,	LAYER=7,	QTYPE=40,	\$END	SPKLR RF
\$NEWELL	ROW=24,	COL= 8,	Q=2.210,	LAYER=7,	QTYPE=40,	\$END	SPKLR RF
\$NEWELL	ROW=26,	COL= 4,	Q=2.210,	LAYER=7,	QTYPE=40,	\$END	SPKLR RF
\$NEWELL	ROW=28,	COL=14,	Q=2.210,	LAYER=7,	QTYPE=40,	\$END	SPKLR RF
\$NEWELL	ROW=31,	COL=14,	Q=2.210,	LAYER=7,	QTYPE=40,	\$END	SPKLR RF
\$NEWELL	ROW=24,	COL=11,	Q=2.321,	LAYER=7,	QTYPE=40,	\$END	SPKLR RF
\$NEWELL	ROW=12,	COL=15,	Q=2.431,	LAYER=7,	QTYPE=40,	\$END	SPKLR RF
\$NEWELL	ROW=21,	COL= 6,	Q=2.431,	LAYER=7,	QTYPE=40,	\$END	SPKLR RF
\$NEWELL	ROW=24,	COL= 6,	Q=2.431,	LAYER=7,	QTYPE=40,	\$END	SPKLR RF
\$NEWELL	ROW=24,	COL= 9,	Q=2.431,	LAYER=7,	QTYPE=40,	\$END	SPKLR RF
\$NEWELL	ROW=24,	COL=13,	Q=2.431,	LAYER=7,	QTYPE=40,	\$END	SPKLR RF
\$NEWELL	ROW=26,	COL= 8,	Q=2.431,	LAYER=7,	QTYPE=40,	\$END	SPKLR RF
\$NEWELL	ROW=26,	COL=11,	Q=2.431,	LAYER=7,	QTYPE=40,	\$END	SPKLR RF
\$NEWELL	ROW=27,	COL= 5,	Q=2.431,	LAYER=7,	QTYPE=40,	\$END	SPKLR RF
\$NEWELL	ROW=27,	COL=14,	Q=2.431,	LAYER=7,	QTYPE=40,	\$END	SPKLR RF

Attachment 2.--Input file for the 1950-79 transient simulation--Continued

```

$NEWELL ROW=29, COL= 8, Q=2.431, LAYER=7, QTYPE=40, $END SPKLR RF
$NEWELL ROW=36, COL= 8, Q=2.431, LAYER=7, QTYPE=40, $END SPKLR RF
$NEWELL ROW=22, COL= 9, Q=2.652, LAYER=7, QTYPE=40, $END SPKLR RF
$NEWELL ROW=24, COL= 5, Q=2.652, LAYER=7, QTYPE=40, $END SPKLR RF
$NEWELL ROW=25, COL= 7, Q=2.652, LAYER=7, QTYPE=40, $END SPKLR RF
$NEWELL ROW=25, COL=11, Q=2.652, LAYER=7, QTYPE=40, $END SPKLR RF
$NEWELL ROW=26, COL= 9, Q=2.652, LAYER=7, QTYPE=40, $END SPKLR RF
$NEWELL ROW=26, COL=12, Q=2.652, LAYER=7, QTYPE=40, $END SPKLR RF
$NEWELL ROW=29, COL=10, Q=2.652, LAYER=7, QTYPE=40, $END SPKLR RF
$NEWELL ROW=30, COL=13, Q=2.652, LAYER=7, QTYPE=40, $END SPKLR RF
$NEWELL ROW=23, COL=10, Q=2.763, LAYER=7, QTYPE=40, $END SPKLR RF
$NEWELL ROW=26, COL= 5, Q=2.763, LAYER=7, QTYPE=40, $END SPKLR RF
$NEWELL ROW=24, COL= 7, Q=2.873, LAYER=7, QTYPE=40, $END SPKLR RF
$NEWELL ROW=24, COL=10, Q=2.873, LAYER=7, QTYPE=40, $END SPKLR RF
$NEWELL ROW=26, COL= 7, Q=2.873, LAYER=7, QTYPE=40, $END SPKLR RF
$NEWELL ROW=26, COL=10, Q=2.873, LAYER=7, QTYPE=40, $END SPKLR RF
$NEWELL ROW=25, COL= 9, Q=2.984, LAYER=7, QTYPE=40, $END SPKLR RF
$NEWELL ROW=28, COL= 6, Q=2.984, LAYER=7, QTYPE=40, $END SPKLR RF
$NEWELL ROW=23, COL= 7, Q=3.094, LAYER=7, QTYPE=40, $END SPKLR RF
$NEWELL ROW=23, COL= 9, Q=3.094, LAYER=7, QTYPE=40, $END SPKLR RF
$NEWELL ROW=25, COL= 8, Q=3.094, LAYER=7, QTYPE=40, $END SPKLR RF
$NEWELL ROW=25, COL=12, Q=3.094, LAYER=7, QTYPE=40, $END SPKLR RF
$NEWELL ROW=26, COL= 6, Q=3.094, LAYER=7, QTYPE=40, $END SPKLR RF
$NEWELL ROW=26, COL=13, Q=3.094, LAYER=7, QTYPE=40, $END SPKLR RF
$NEWELL ROW=26, COL=14, Q=3.094, LAYER=7, QTYPE=40, $END SPKLR RF
$NEWELL ROW=27, COL= 9, Q=3.094, LAYER=7, QTYPE=40, $END SPKLR RF
$NEWELL ROW=27, COL=10, Q=3.094, LAYER=7, QTYPE=40, $END SPKLR RF
$NEWELL ROW=27, COL=13, Q=3.094, LAYER=7, QTYPE=40, $END SPKLR RF
$NEWELL ROW=28, COL=12, Q=3.094, LAYER=7, QTYPE=40, $END SPKLR RF
$NEWELL ROW=40, COL=21, Q=3.094, LAYER=7, QTYPE=40, $END SPKLR RF
$NEWELL ROW=23, COL= 6, Q=3.205, LAYER=7, QTYPE=40, $END SPKLR RF
$NEWELL ROW=22, COL=11, Q=3.315, LAYER=7, QTYPE=40, $END SPKLR RF
$NEWELL ROW=23, COL= 8, Q=3.315, LAYER=7, QTYPE=40, $END SPKLR RF
$NEWELL ROW=25, COL= 6, Q=3.315, LAYER=7, QTYPE=40, $END SPKLR RF
$NEWELL ROW=27, COL= 6, Q=3.315, LAYER=7, QTYPE=40, $END SPKLR RF
$NEWELL ROW=27, COL= 7, Q=3.315, LAYER=7, QTYPE=40, $END SPKLR RF
$NEWELL ROW=28, COL= 7, Q=3.315, LAYER=7, QTYPE=40, $END SPKLR RF
$NEWELL ROW=29, COL=11, Q=3.315, LAYER=7, QTYPE=40, $END SPKLR RF
$NEWELL ROW=30, COL=14, Q=3.315, LAYER=7, QTYPE=40, $END SPKLR RF
$NEWELL ROW=28, COL=11, Q=3.426, LAYER=7, QTYPE=40, $END SPKLR RF
$NEWELL ROW=22, COL=12, Q=3.536, LAYER=7, QTYPE=40, $END SPKLR RF
$NEWELL ROW=23, COL=11, Q=3.536, LAYER=7, QTYPE=40, $END SPKLR RF
$NEWELL ROW=25, COL=10, Q=3.536, LAYER=7, QTYPE=40, $END SPKLR RF
$NEWELL ROW=27, COL= 8, Q=3.536, LAYER=7, QTYPE=40, $END SPKLR RF
$NEWELL ROW=27, COL=11, Q=3.536, LAYER=7, QTYPE=40, $END SPKLR RF
$NEWELL ROW=27, COL=12, Q=3.536, LAYER=7, QTYPE=40, $END SPKLR RF
$NEWELL ROW=28, COL= 8, Q=3.536, LAYER=7, QTYPE=40, $END SPKLR RF
$NEWELL ROW=28, COL= 9, Q=3.536, LAYER=7, QTYPE=40, $END SPKLR RF
$NEWELL ROW=28, COL=10, Q=3.536, LAYER=7, QTYPE=40, $END SPKLR RF
$NEWELL ROW=29, COL=13, Q=3.536, LAYER=7, QTYPE=40, $END SPKLR RF
$NEWELL ROW=0, $END

```

Attachment 2.--Input file for the 1950-79 transient simulation--Continued

\$NEWRIV

VK(98)=64*0.0399E-8,	24*0.0797E-8,	11*0.1196E-8,	5*0.1595E-8,
VK(648)=76*0.1279E-8,	76*0.0399E-8,	75*0.2558E-8,	75*0.0797E-8,
43*0.3837E-8,	43*0.1196E-8,	97*0.5116E-8,	97*0.1595E-8,
QMAX(98)=64*0.2223,	24*0.4445,	11*0.6668,	5*0.8891,
QMAX(648)=76*0.4279,	76*0.3112,	75*0.8558,	75*0.6223,
43*1.2837,	43*0.9335,	97*1.7116,	97*1.2447,

\$END

\*XCODE

\*/EXECUTE

\*MASS STORE WAIT=ON WAITIME=60 BAKOUT:/SLV/OCT/BAKMK80

\*&

OUTPUT:/SLV/OCT/OUTMK80

\*TRIXGL

\*/EDIT TO TRIM EXCESS

A

REDEND2

\*DISPOSE DN=NEWOUT,TID=MFARV,FID=GAHMK,SF="CC",WAIT \*/PRINT OUTPUT

\*ENDJOB: